THE ASSESSMENT OF DEEP EXCAVATION PERFORMANCE OF A HIGH
RISE RESIDENTIAL COMPLEX, IN BAYRAKLI, IZMIR

A THESIS SUBMITTED TO
THE GRADUATE SCHOOL OF NATURAL AND APPLIED SCIENCES
OF
MIDDLE EAST TECHNICAL UNIVERSITY

BY

ATALAY MERT TURGUT

IN PARTIAL FULFILLMENT OF THE REQUIREMENTS
FOR
THE DEGREE OF MASTER OF SCIENCE
IN
CIVIL ENGINEERING

JUNE 2022

Approval of the thesis:

THE ASSESSMENT OF DEEP EXCAVATION PERFORMANCE OF A HIGH RISE RESIDENTIAL COMPLEX, IN BAYRAKLI, IZMIR

submitted by **ATALAY MERT TURGUT** in partial fulfillment of the requirements for the degree of **Master of Science in Civil Engineering, Middle East Technical University** by,

Prof. Dr. Halil KALIPÇILAR
Dean, Graduate School of **Natural and Applied Sciences**   _____

Prof. Dr. Erdem CANBAY
Head of Department, **Civil Engineering**   _____

Prof. Dr. Kemal Önder ÇETİN
Supervisor, **Civil Engineering, METU**   _____

Examining Committee Members:

Prof. Dr. Berna UNUTMAZ
Civil Engineering, Hacettepe University   _____

Prof. Dr. Kemal Önder ÇETİN
Civil Engineering, METU   _____

Assoc. Prof. Dr. Nejan Huvaj SARIHAN
Civil Engineering, METU   _____

Assoc. Prof. Dr. Nabi Kartal TOKER
Civil Engineering, METU   _____

Assoc. Prof. Dr. Onur PEKCAN
Civil Engineering, METU   _____

Date: 10.06.2022

I hereby declare that all information in this document has been obtained and presented in accordance with academic rules and ethical conduct. I also declare that, as required by these rules and conduct, I have fully cited and referenced all material and results that are not original to this work.

Name, Last Name: Atalay Mert Turgut

Signature:

ABSTRACT

THE ASSESSMENT OF DEEP EXCAVATION PERFORMANCE OF A HIGH RISE RESIDENTIAL COMPLEX, IN BAYRAKLI, IZMIR

Turgut, Atalay Mert
Master of Science, Civil Engineering
Supervisor: Prof. Dr. Kemal Önder Çetin

June 2022, 453 pages

The need to deep excavation projects is increasing with urbanization. Consistently the excavation depths are also increasing. Therefore, the optimum design of the excavation system becomes more important. An optimum design of an excavation system can be developed with the selection of a suitable excavation system in terms of quality, duration, and cost and with the estimation of representative soil properties. On the other hand, the cost of the deep excavation systems has become a significant portion of the overall project budget. The Single Bore Multiple Anchor (SBMA) system is an important development in the ground anchor industry to make the optimum design.

A deep excavation system of a high-rise building constructed in Bayraklı, İzmir, is examined in this study. The high-rise building consists of three blocks: A, B, and C. A total of 20 cone penetration tests (CPT) and 25 boreholes were performed for the site investigation. The deep excavation system was monitored with 18 inclinometers and 9 load cells. The construction area is divided into seven regions, and each region is studied separately for the estimation of soil parameters and the finite element analysis with Plaxis 2D. Each inclinometer reading is compared with analysis results. Estimated soil parameters are calibrated through scaling of the stiffness separately for

cohesionless and cohesive soil layers. As a result, it is shown that the adopted assessment scheme provides reasonable agreement with field inclinometer readings; which are also concluded to be consistent with recommendations available in the literature.

ÖZ

BAYRAKLI İZMİRDE ÇOK KATLI BİR KONUT PROJESİNE AİT DERİN KAZININ PERFORMANS DEĞERLENDİRMESİ

Turgut, Atalay Mert

Yüksek Lisans, İnşaat Mühendisliği

Tez Yöneticisi: Prof. Dr. Kemal Önder Çetin

Haziran 2022, 453 sayfa

Derin kazı projelerine olan ihtiyaç her geçen gün artmaktadır. Aynı zamanda kazı derinlikleri de artmaktadır. Bu yüzden optimum derin kazı sistemlerinin tasarımı ön plana çıkmaktadır. Optimum kazı sisteminin tasarımı, kalite, süre ve maliyeti göz önünde bulundurarak uygun kazı sisteminin seçilmesi ve makul zemin parametrelerinin tahkiki ile yapılabilir. Bu uygun kazı sisteminin seçilmesi ve zeminin özelliklerinin tahkiki ile mümkündür. Öte yandan derin kazı sistemlerinin maliyeti proje bütçelerinde önemli bir yer edinmektedir. Optimum tasarım yapılabilmesi için tek delik çoklu ankraj (SBMA) sistemi ankraj endüstrisindeki önemli gelişmelerden biridir.

Çalışma kapsamında Bayraklı, İzmir'de inşa edilen çok katlı yapının derin kazı sistemi incelenmiştir. Çok katlı yapı A, B ve C şeklinde 3 adet bloktan oluşmaktadır. Zemin araştırmaları kapsamında toplam 20 adet konik penetrasyon deneyi (CPT) ve 25 adet sondaj açılmıştır. Derin kazı sistemi 18 adet inklinometre ve 9 adet yük hücresi ile izlenmiştir. İnşa alanı 7 farklı bölgeye ayrılmış ve her bölgenin zemin parametre tahkiki ve Plaxis 2D ile sonlu elemanlar için ayrı ayrı çalışma yapılmıştır. Her inklinometre okuması analiz sonuçlarıyla karşılaştırılmıştır. Zeminin rijitlik modülleri

kohezyonsuz ve kohezyonlu zeminler için ayrı ayrı kalibre edilmiştir. Sonuç olarak analiz sonuçlarının, inklinometre okumaları ve literatürde önerilen performans metrikleri ile ortalamada uyumlu olduğu anlaşılmıştır.

Anahtar Kelimeler: Derin Kazı, Sonlu Elemanlar Yöntemi, Geri Analiz, SBMA, Plaxis 2D

To my family…

ACKNOWLEDGMENTS

First of all, I would like to express my sincere thanks and appreciation to my supervisor Prof. Dr. Kemal Önder Çetin, for his guidance, encouragement, and patience throughout my study. This thesis would not have been possible without his endless support.

I would also like to express my gratitude to my mother Nuray Turgut and, my father Bülent Turgut. They always trust and support me not just only in this study but also in each part of my life. I would like to thank them for everything. They are my luck in this life.

I would like to thank Kasktaş family for their support throughout my thesis study. They always provided me with the required time for my study. Also, they helped me with their experience and knowledge.

TABLE OF CONTENTS

LIST OF TABLES

LIST OF FIGURES

FIGURES

LIST OF ABBREVIATIONS

ABBREVIATIONS

ASTM	:	American Society for Testing and Materials
CPT	:	Cone Penetration Test
ER	:	Energy Ratio
F8OS	:	Factor of safety
GWT	:	Ground Water Table
INK	:	Inclinometer
LL	:	Liquid limit
LI	:	Liquidity index
HS	:	Hardening soil
PI	:	Plasticity index
PL	:	Plastic limit
RD	:	Relative Density
SBMA	:	Single Bore Multiple Anchor
SMTS	:	Specified Minimum Tensile Strength
SPT	:	Standard Penetration Test
USCS	:	Unified Soil Classification System

LIST OF SYMBOLS

SYMBOLS

A	:	Area
B_q	:	Normalized pore pressure parameter
c	:	Cohesion
c'	:	Effective cohesion
C_B	:	Borehole diameter correction factor
C_N	:	Overburden correction factor
C_R	:	Rod length correction factor
C_S	:	Sampling method correction factor
c_u	:	Undrained shear strength
D	:	Diameter
e_0	:	Initial void ratio
E	:	Young's modulus
E_0	:	The initial slope of the stress-strain curve
E_{50}	:	Confining stress-dependent stiffness modulus for primary loading
E_{50}^{ref}	:	Stiffness modulus at the reference confining pressure, p^{ref}
E_{conc}	:	Elastic modulus of concrete
E_i	:	Initial stiffness modulus
E_{oed}	:	Oedometer modulus
E_{oed}^{ref}	:	Oedometer modulus for reference pressure
E_{ur}	:	Unloading/reloading stiffness modulus
E_{ur}^{ref}	:	Unloading/reloading stiffness modulus for reference pressure
f_1	:	Stroud's (1974) variable related to plasticity index
f_2	:	Stroud's (1974) variable related to plasticity index
f_{eff}	:	Efficiency factor for anchor fixed length

$F_{max,comp}$	:	Maximum compression capacity of node-to-node anchor element in Plaxis 2D
$F_{max,tens}$	:	Maximum tension capacity of node-to-node anchor element in Plaxis 2D
f_s	:	Sleeve friction of soil
H	:	Depth of Excavation
I	:	Moment of inertia
K_0	:	Coefficient of earth pressure at rest
K_0^{nc}	:	Coefficient of lateral earth pressure for a normally consolidated stress state
K_A	:	Coefficient of active earth pressure
K_P	:	Coefficient of passive earth pressure
$L_{spacing}$	:	Horizontal spacing of support element in Plaxis 2D
M_{max}	:	Maximum bending moment
m	:	Power in stress dependency
m_v	:	Coefficient of volume compressibility
N_{kt}	:	Preliminary cone factor
N_{max}	:	Maximum normal force
N	:	SPT-N value measured from the field
$(N_1)_{60}$	:	Corrected SPT-N value according to field conditions, energy efficiency, overburden pressure
N_{60}	:	Corrected SPT-N value according to field conditions and energy efficiency
p_a	:	Atmospheric pressure
p^{ref}	:	Reference pressure
q_a	:	The asymptotic value of the shear strength
q_c, q_t	:	Tip resistance of soil
Q_{tn}	:	Normalized and corrected CPT resistance
R_f	:	Friction ratio of f_s to q_t %
R_f	:	Failure ratio of HS Model

S_h	:	Horizontal spacing of support element
V_{max}	:	Maximum shear force
w_n	:	The water content of the soil
z_0	:	Depth of tension crack
γ_w	:	Unit weight of water
γ_{dry}	:	Dry unit weight of soil
γ_{sat}	:	Saturated unit weight of soil
$\delta_{h,m}$	:	Maximum horizontal wall displacement
$\delta_{v,m}$	:	Maximum soil settlement
λ	:	Standard Cam-Clay compression index
λ^*	:	Modified compression index
ν	:	Poisson's ratio
ν_{ur}	:	Unloading/reloading Poisson's ratio
ϕ	:	Friction angle
ψ	:	Dilatancy angle

CHAPTER 1

1. INTRODUCTION

1.1. Research Statement

As a result of the development of cities and the increase in population, high-rise buildings are required to be constructed. Excavation depths are increasing day by day to meet these requirements. On the other hand, most of the time, the surrounding historical structures, utilities, and buildings are close to the excavation site. The main risk of a deep excavation system is excessive horizontal displacements, which can trigger the failure of the system.

The study aims back-analysis of a shoring system consisting of diaphragm wall and single bore multiple anchor (SBMA) constructed in Bayraklı, İzmir. The project consistes of 3 different excavation areas named Block A, Block B, and Block C. They can be seen in Figure 1.1. 20 cone penetration tests (CPT) and 25 boreholes were performed within the scope of site investigations. The deep excavation system was monitored with 18 nclinometers and 9 load cells. The deep excavation system was analyzed by using the finite element software, PLAXIS 2D. By using monitoring data and analysis results, soil parameters are calibrated. Then, these calibrated results are compared with recommended typical displacement estimation methods in the literature.

1.2. Research Objectives

The research objectives of this study are explained below;
   a) Comparison of the measured and predicted displacements
   b) Calibration of estimated soil parameters according to finite element analysis results and monitoring data

1.3. Scope of the Thesis

This thesis consists of five chapters. It starts with the introduction in Chapter 1.

In Chapter 2, a summary of the deep excavation systems used worldwide is demonstrated. Furthermore, recommended methods in the literature to estimate the displacements of the excavation system are collected.

In Chapter 3, soil parameters estimation methodologies are explained. Monitoring data were presented for INK-11 as an example.

In Chapter 4, finite element modeling and analysis with Plaxis 2D are explained. Estimated soil parameters are calibrated by comparing predicted and measured results. These results were discussed and also compared with the available methods in the literature.

In Chapter 5, a summary of this thesis is presented. Conclusions and recommendations of the research are explained.

Figure 1.1. Project Site

CHAPTER 2

2. LITERATURE REVIEW

2.1. Introduction

In this chapter, the deep excavation systems are described. Furthermore, a brief description of methodologies to predict the displacement of the excavation system is presented.

2.2. Deep Excavation Systems

The design of a deep excavation system depends on multiple criteria. Some of them are listed below;

- Project Location
- Soil Stratigraphy
- Groundwater Condition
- Excavation Depth
- The Geometry of Project Area
- Project Budget and Deadline
- Surrounding Structures
- Design tolerances and criteria
- The Lifetime of the Excavation System
- Availability of Equipment and Materials
- Special Requirements of the Project

The above-listed issues are considered as a starting point. An appropriate excavation system is chosen by considering the project requirement and necessities. Types of deep excavations are listed as open excavations, cantilever type retaining walls, anchored walls, braced cut strut walls, and top-down construction. For these systems, possible vertical elements are secant piles, contiguous piles, tangent piles, diaphragm walls, soldier piles, sheet piles, jet grout columns, and deep soil mixing columns. The

selection of vertical elements of the shoring system is also wholly dependent on the criteria discussed earlier.

2.2.1. Open Excavations

Open excavations are preferred where any major vertical or lateral elements are not needed to support the excavation. Excavations are performed with appropriate slope angles, heights, and surfaceprotectionn such as shotcrete cover. However, if the depth of excavation increases, the excavated area increases considerably. Therefore, deep excavation cannot be made as open excavations, especially in an urban area. Deep sloped excavations are usually preferred in open-pit mines as shown in Figure 2.1.

Figure 2.1. Open-Pit Mine Excavation

(Source: https://www.911metallurgist.com/blog/open-cast-mining)

2.2.2. Cantilever Type Retaining Walls

Lateral support elements are not used for cantilever systems (Figures 2.2 and 2.3). The crucial point is that the wall has to be socketed at the excavation base, and the active and passive earth pressures have to be in equilibrium to maintain stability given in Figure 2.4. The passive earth pressure is considered as a resistance force. However, considerable displacement is required to mobilize the passive resistance fully (Figure 2.5). Therefore, cantilever-type retaining walls are not recommended if surrounding structures are close to the excavation area. Moreover, this type of excavation is mainly preferred when the excavation depth is lower than 6 m. On the other hand, one of the main advantages is that construction time is relatively short compared to other excavation systems.

Figure 2.2. Cantilever Bored Pile Excavation System

(Source: https://www.constrofacilitator.com/retaining-wall-design-and-its-types-used-on-construction/)
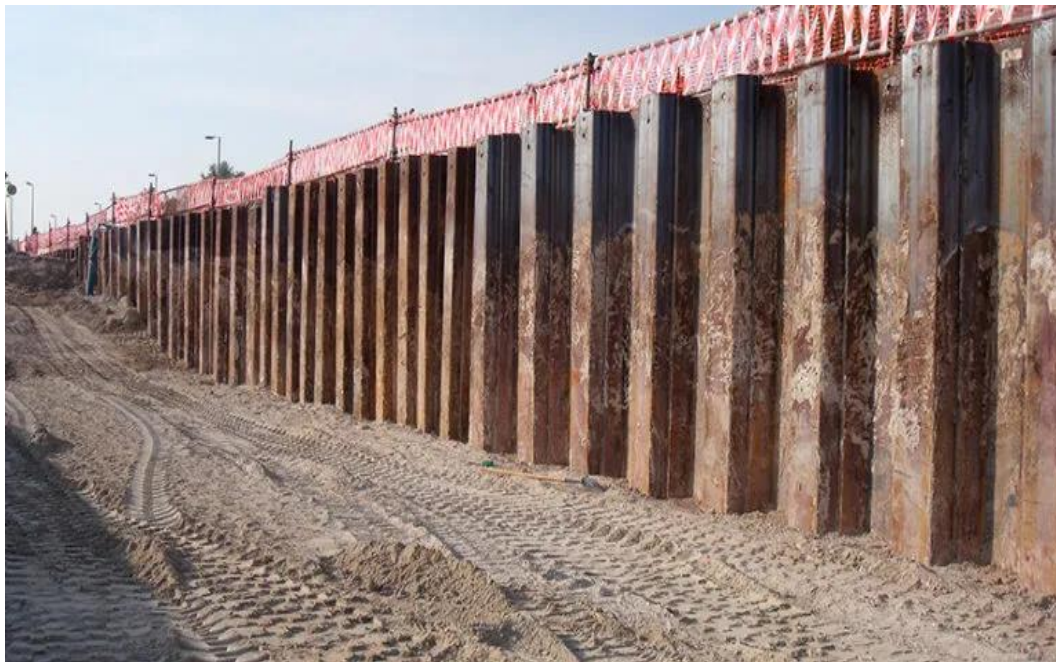
Figure 2.3. Cantilever Sheet Pile Excavation System

(Source: https://www.civilclick.com/sheet-piling-2/)
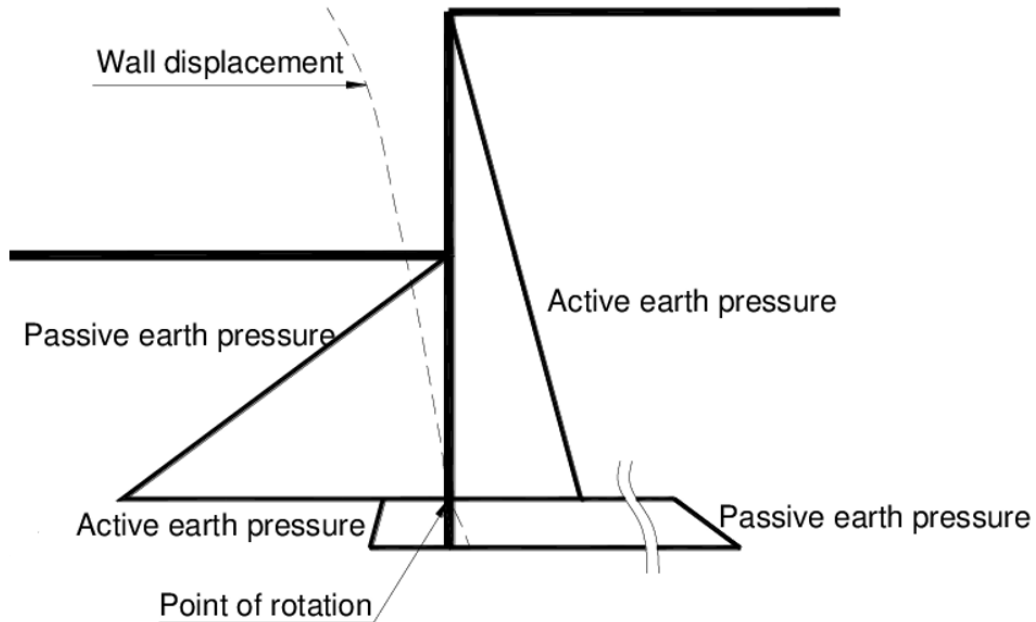
Figure 2.4. Schematic Sketch of Active and Passive Earth Pressures (FHWA-IF-99-015, 1999)
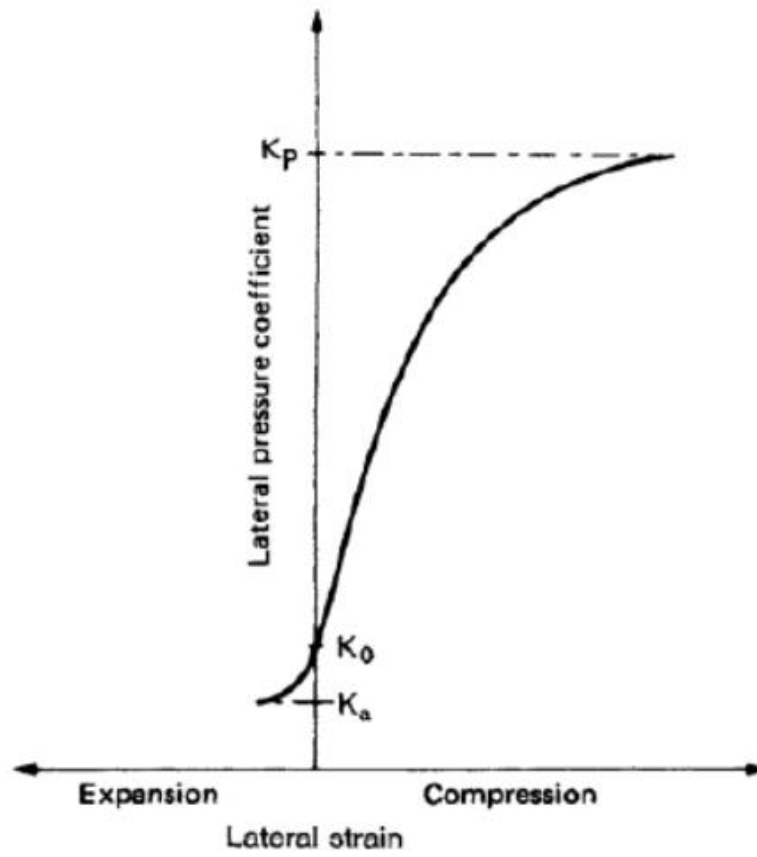
Figure 2.5. Lateral Strain vs. Pressure Coefficients (FHWA-IF-99-015, 1999)

2.2.3. Anchored Walls

The anchored wall is an excavation system composed of a piled wall, diaphragm wall, or soldier pile supported by ground anchors (Figure 2.6). They are used as temporary and permanent support. The free and bond anchor lengths are designed by taking into account the estimated potential failure surfaces. Tensile lateral loads are transferred to the bearing layer by this mechanism.

Figure 2.6. Multi-layered Anchored Wall System

(Source: Kasktaş Database)

General Information

Ground anchors consist of 3 parts: anchorage, free stressing (unbonded) length, and bond length in Figure 2.7. The anchorage has three parts: the anchor head, bearing plate, and trumpet. With the help of the anchorage, prestressing force of the strands is transferred to the bearing layer. The portion of the unbonded length works as a transmitter and is free to elongate elastically. The unbonded length enables to transfer of driving forces to the bond length. These forces are transmitted into the ground with the help of the bond length.
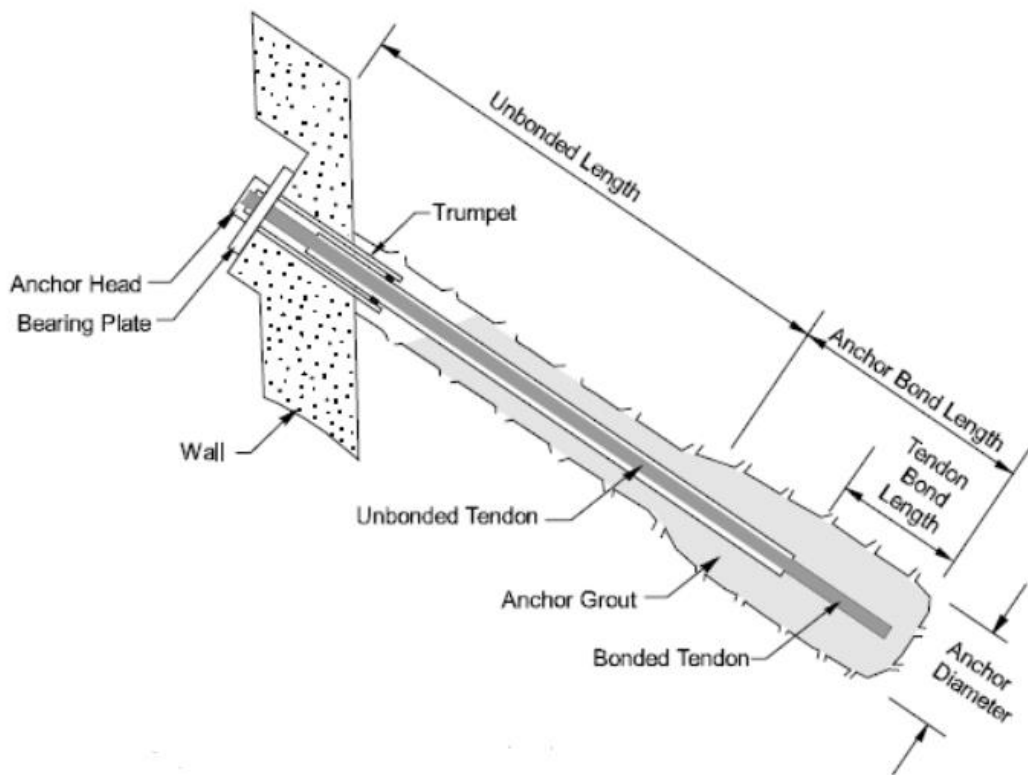
Figure 2.7. Typical Ground Anchor (FHWA-IF-99-015, 1999)

Types of Tie-backs

Types of ground anchors are straight shaft gravity-grouted ground anchors (Type A), straight shaft pressure-grouted ground anchors (Type B), post-grouted ground anchors (Type C), and the underreamed anchor (Type D). Their schematic drawings can be seen in Figure 2.8. Types A, B, and. C are mostly preferred worldwide, but Type D is not common in practice.

Type A: They are typically used in rock and very stiff to hard cohesive soils. Rotary drilling or hollow-stem auger methods are preferred as a construction technique. The diameter of the anchor of the bond length and the diameter of free length are the same. An injection is made with the help of gravity without pressure. The pull-out capacity of the anchor is directly related to the mobilized shear resistance of the root.

Type B: This type of anchor is preferred in fine-grained cohesionless soils, coarse granular soils, and weak fissured rock. The same construction technique can be used in Type A. However, casings are required during the drilling. The injection of the bond

length is made with pressure. As a result, the diameter of the grouted zone is increased, and higher resistance can be obtained.

Type C: Post-grouted anchors are installed by grouting multiple times. After the first injection, a second high-pressure injection is applied. The first injection body is broken with high pressure, and the anchor root is expanded in a fringed manner. The anchor bearing capacity is increased. This type of anchor is used chiefly in cohesionless soils or stiff clay.

Type D: This type of anchor is preferred for a firm to hard cohesive soils. The grouted body consists of underreams and enlargement bells. In addition to shear resistance, tip resistance occurring due to enlargement bells is mobilized under the tension. Therefore, higher anchor capacity can be obtained.
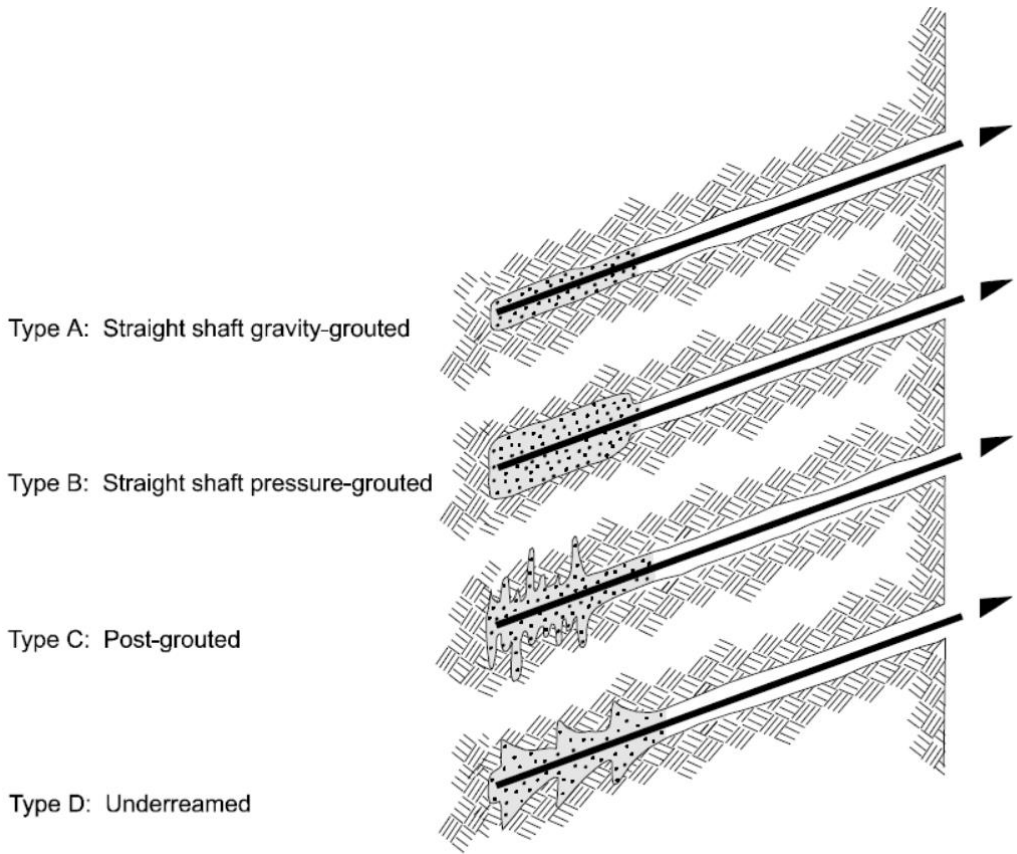
Figure 2.8. Types of Grouted Anchors (FHWA-IF-99-015, 1999)

Bond Length of Anchors

The bond length is determined by considering the required force, spacing, and soil type. The ultimate load-bearing capacity depends on the relative density/consistency of soil. According to FHWA-IF-99-015 (1999), corrected SPT values (N_1) can be used for gravity-grouted anchors. According to the soil type, the average ultimate bond stress can be selected for pressure grouted anchors. The recommended ultimate transfer load and bond stresses can be seen below for straight shaft gravity-grouted and pressure grouted anchors, respectively in Table 2.1 and 2.2;

Table 2.1. Ultimate Transfer Load of Straight Shaft Gravity-Grouted Ground Anchors in Soil (FHWA-IF-99-015, 1999)

Soil type	Relative density/Consistency (SPT range)	Estimated ultimate transfer load (kN/m)
Sand and Gravel	Loose (4-10)	145
	Medium dense (11-30)	220
	Dense (31-50)	290
Sand	Loose (4-10)	100
	Medium dense (11-30)	145
	Dense (31-50)	190
Sand and Silt	Loose (4-10)	70
	Medium dense (11-30)	100
	Dense (31-50)	130
Silt-clay mixture with low plasticity or fine micaceous sand or silt mixtures	Stiff (10-20)	30
	Hard (21-40)	60

Table 2.2. Average Ultimate Bond Stresses for Pressure Grouted Anchors (FHWA-IF-99-015, 1999)

Rock		Cohesive Soil		Cohesionless Soil	
Rock type	Average ultimate bond stress (MPa)	Anchor type	Average ultimate bond stress (MPa)	Anchor type	Average ultimate bond stress (MPa)
Granite and basalt	1.7 - 3.1	Gravity-grouted anchors (straight shaft)	0.03 - 0.07	Gravity-grouted anchors (straight shaft)	0.07 - 0.14
Dolomitic limestone	1.4 - 2.1	Pressure-grouted anchors (straight shaft)		Pressure-grouted anchors (straight shaft)	
Soft limestone	1.0 - 1.4	• Soft silty clay	0.03 - 0.07	• Fine-med. sand, med. dense – dense	0.08 - 0.38
Slates and hard shales	0.8 - 1.4	• Silty clay	0.03 - 0.07	• Med.–coarse sand (w/gravel), med. dense	0.11 - 0.66
Soft shales	0.2 - 0.8	• Stiff clay, med. to high plasticity	0.03 - 0.10	• Med.–coarse sand (w/gravel), dense - very dense	0.25 - 0.97
Sandstones	0.8 - 1.7	• Very stiff clay, med. to high plasticity	0.07 - 0.17	• Silty sands	0.17 - 0.41
Weathered Sandstones	0.7 - 0.8	• Stiff clay, med. plasticity	0.10 - 0.25	• Dense glacial till	0.30 - 0.52
Chalk	0.2 - 1.1	• Very stiff clay, med. plasticity	0.14 - 0.35	• Sandy gravel, med. dense-dense	0.21 - 1.38
Weathered Marl	0.15 - 0.25	• Very stiff sandy silt, med. plasticity	0.28 - 0.38	• Sandy gravel, dense-very dense	0.28 - 1.38
Concrete	1.4 - 2.8				

Anchor bond lengths change between 4.5 m to 12 m. However, a bond length longer than 12 m is not recommended by FHWA-IF-99-015 (1999) and Ostermayer et al. (1977) since the load cannot be transferred from the top of the bond length to the end. The resulting strain exceeds the peak strain, and progressive failure begins in the upper grout body before the capacity is fully mobilized. The graph of bond stress mobilization of the anchor can be seen in Figure 2.9.
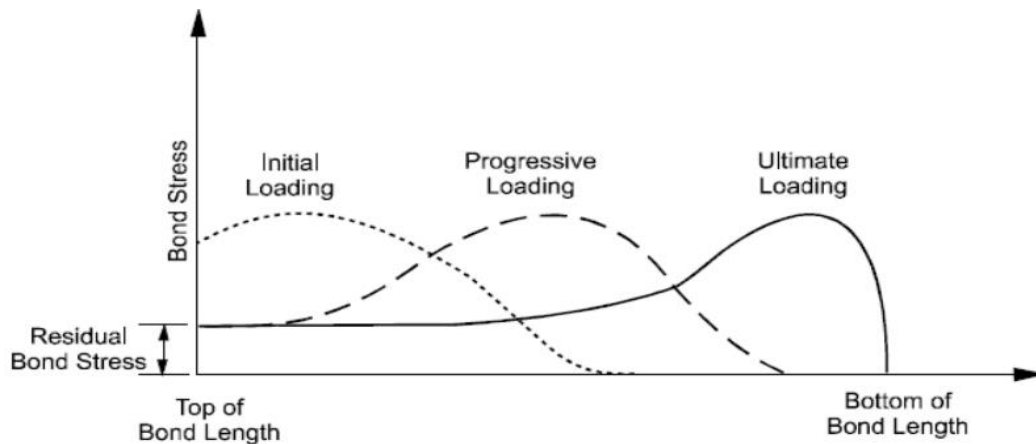
Figure 2.9. Bond Stress Mobilization of Anchors (FHWA-IF-99-015, 1999)

Free Length of Anchors

The unbonded length of anchors is determined by assuming a potential failure surface. This failure surface can be drawn with an angle of $45+\varphi/2$ relative to the horizontal plane. Typically, the inclination of ground anchors changes in between 10 and 45 degrees. The most common installation is at angles of 15 to 30 degrees. The inclination of anchors is important because the bond length should be behind the failure surface. The recommended by FHWA-IF-99-015 criteria can be listed below also can be seen in Figure 2.10;

- The top of the bond length should be shifted 1.5 m or 0.2 H (excavation depth) from the potential failure surface.
- The bond length of the first anchor row should be below 4.5 m from the ground surface at least.
- The minimum unbonded length is 3 m and 4.5 m for bar and strand, respectively.
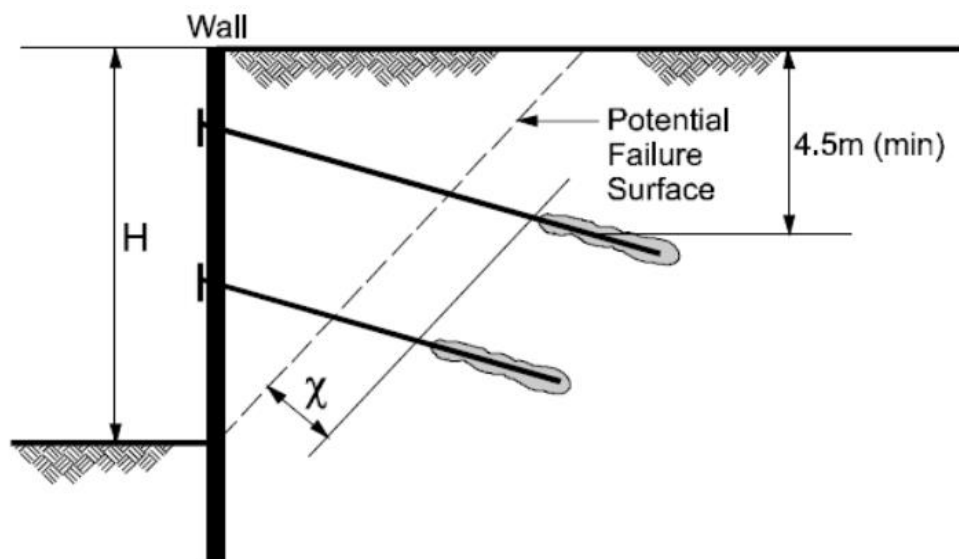
Minimum unbonded length = 3m (bar)
4.5m (strand)

χ = 1.5m or 0.2H, whichever is greater

Figure 2.10. Wall Cross Section to Estimate Unbonded Length of Anchors (FHWA-IF-99-015, 1999)

Spacing of Anchors

S_h > 1.2m
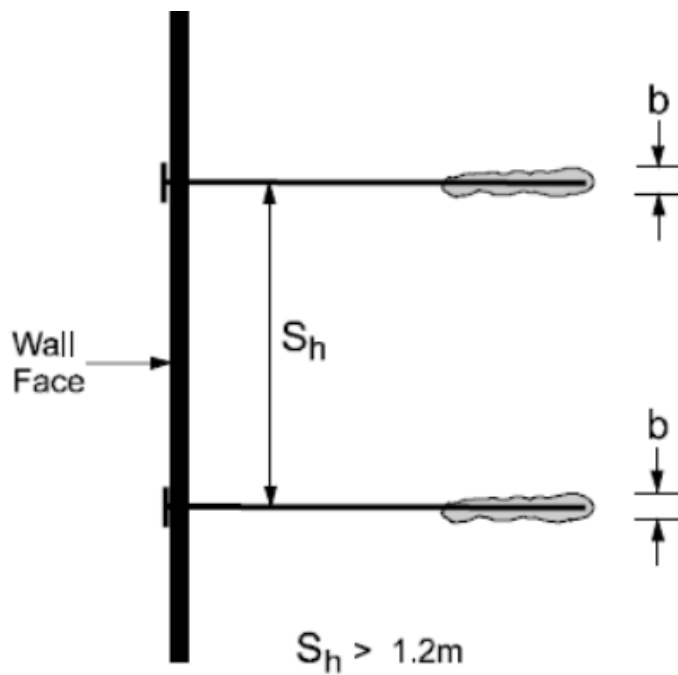
Figure 2.11. Wall Plan View (FHWA-IF-99-015, 1999)

The maximum horizontal spacing is determined by considering the allowable axial capacity of ground anchors and the flexural capacity of the vertical supporting element. Furthermore, minimum spacing should be more than 1.2 m as recommended by FHWA-IF-99-015 (1999) in Figure 2.11. Since group effects must be considered in two aspects: constructability and loading mechanisms. If anchors are too close, the load-carrying capacity of anchors decreases due to the over-loading of soil. Moreover, intersection problems can be encountered due to deviations during the drilling process.

Selection of Prestressing Steel Element

The tendon should have enough capacity to transfer the load to the bond zone without failure. The different factors of safety values are used for design load and lock-off load, respectively. According to FHWA-IF-99-015 (1999), the design load should not be higher than 60% of the tendon's specified minimum tensile strength (SMTS). Moreover, lock-off and test loads are limited to 70% and 80% of the SMTS.

For instance, if the test load is 133% of the design load, the tendon's SMTS is preferred by controlling the 0.6 SMTS value. In Table 2.3, recommendations of ASTM A416 for the properties of 15 mm diameter strands such as cross-section areas, ultimate strengths, and prestressing forces are given;

Table 2.3. 15 mm Dia. Prestressing Tendon Properties (ASTM A416)

Number of 15-mm diameter strands	Cross section area		Ultimate strength		Prestressing force					
					0.8 $f_{pu}A_{ps}$		0.7 $f_{pu}A_{ps}$		0.6 $f_{pu}A_{ps}$	
	(in.^{2})	(mm^2)	(kips)	(kN)	(kips)	(kN)	(kips)	(kN)	(kips)	(kN)
1	0.217	140	58.6	260.7	46.9	209	41.0	182	35.2	156
3	0.651	420	175.8	782.1	140.6	626	123.1	547	105.5	469
4	0.868	560	234.4	1043	187.5	834	164.1	730	140.6	626
5	1.085	700	293.0	1304	234.4	1043	205.1	912	175.8	782
7	1.519	980	410.2	1825	328.2	1460	287.1	1277	246.1	1095
9	1.953	1260	527.4	2346	421.9	1877	369.2	1642	316.4	1408
12	2.604	1680	703.2	3128	562.6	2503	492.2	2190	421.9	1877
15	3.255	2100	879.0	3911	703.2	3128	615.3	2737	527.4	2346
19	4.123	2660	1113.4	4953	890.7	3963	779.4	3467	668.0	2972

Failure Mechanisms of Anchored Walls

There are several failure mechanisms. They can be seen in Figure 2.12. They are listed below:

    a) Tendon failure due to tension

    b) Pullout failure of grout/soil bond

    c) Pullout failure of tendon/grout bond

    d) Bending failure of the wall

    e) Insufficient passive capacity

    f) Insufficient axial capacity

    g) Overturning

    h) Sliding

    i) Global rotational failure

a) Tendon failure due to tension   b) Pullout failure of grout/soil bond
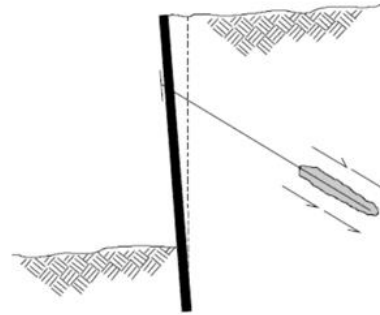
c) Pullout failure of tendon/grout bond   d) Bending failure of the wall

e) Insufficient passive capacity

f) Insufficient axial capacity

g) Overturning

h) Sliding

i) Global rotational failure
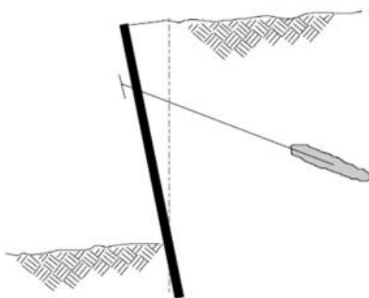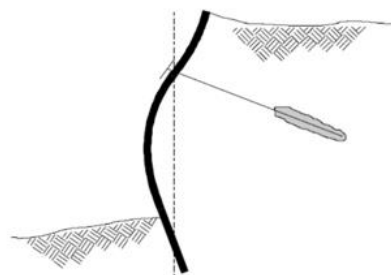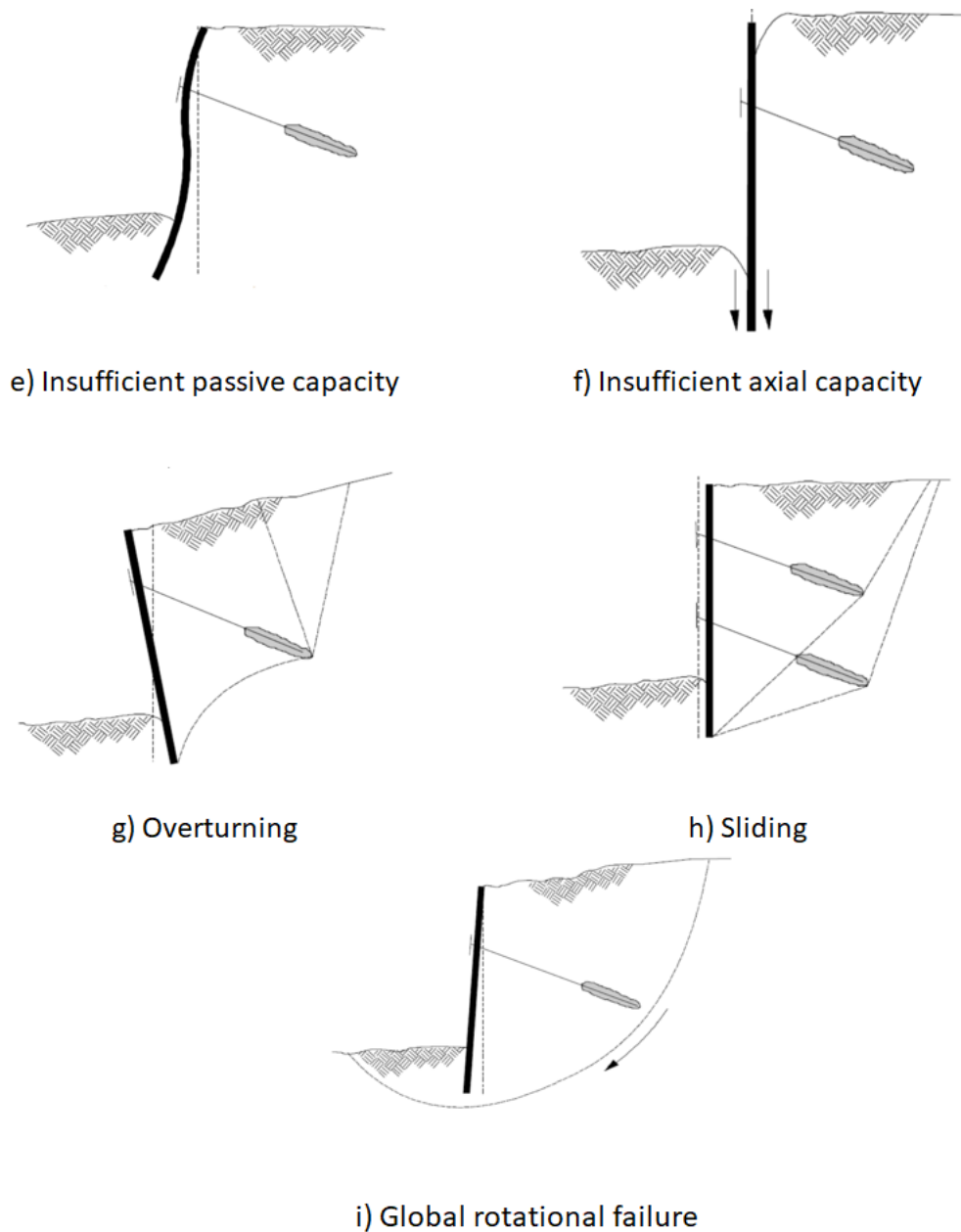
Figure 2.12. Failure Mechanisms of Anchored Walls (FHWA-IF-99-015, 1999)

2.2.4. Braced Cuts

Strut elements are used in braced cuts in Figure 2.13. In contrast to the anchored system, strut elements work as compression members. They are usually made of materials which are steel beam sections and pipes. One of the most important criteria for this type of system is that the width of excavation cannot be wide. The maximum

recommended width is approximately 40 m. If the excavations are wide, inclined struts also known as rakers can be used (Figure 2.14). The advantages of braced cuts with struts are that construction time is quicker. Besides, strut elements are recyclable so they are much cheaper. They can be disassembled for temporary excavations. On the other hand, placement and removal of struts are not easy. Moreover, the working area for machines and employees becomes limited.

Figure 2.13. Excavation Supported with Struts

(Source: Kasktaş Database)

Figure 2.14. Excavation Supported with Rakers

(Source: Kasktaş Database)

The spacing of struts in both horizontal and vertical directions should be as large as possible. It changes between 4 m to 5m in general since open spaces have to be provided for workability. Section types or pipe diameter and thickness are determined according to the required load capacity. Buckling failure is one of the most critical design criteria for struts which work as compression members.

2.2.5. Top-Down Construction

Considering the required excavation dimensions and environmental factors, the top-down construction method has become more popular. Contrary to traditional applications, the structure is constructed from top to bottom in this construction system (Figure 2.15). The constructed support systems are also used as permanent structural elements.

Figure 2.15. Top-Down Excavation System

(Source: Kasktaş Database)

Superstructure and substructure constructions are continued at the same time. For this reason, time savings can be achieved. Displacements are minimized due to the rigid support elements used. Also, since permanently manufactured floors and beams are used as horizontal support elements, the requirements for elements such as anchors and soil nails are eliminated. Less construction area is required, and so, earthworks are decreased. As a result, environmental pollution can be minimized.

It is expected that the displacements in the support system should be less than those of temporary systems. Displacements of the excavation systems are equivalent to the displacements of the structural members since the support system will also be used as permanent structural members. It is more expensive due to the preferred support system. Moreover, there is no chance of waterproofing outside of the walls. Therefore, there is a possibility of water leaking from the joints. Also, access restriction to the excavated area is the most common problem encountered during construction. Furthermore, the connections between the support elements and the floors are more complex.

2.3.   Single Bore Multiple Anchor (SBMA) System

Traditional ground anchors have been used for decades to support the excavation system. Over the years, required excavation depths have been increasing. Therefore, higher anchor capacities are required, which affects the project's budget. SBMA type of anchors is a significant development in geotechnical engineering to eliminate the above problems.

Multiple unit anchors are installed into a single borehole.   Each of them has an individual fixed length. Pre-stressing is applied with separete jacks (Figure 2.16). After that, unit anchors are loaded with synchronized jacks at the same time since loads of unit anchors are required to be the same.

Anchor capacities increase with increasing bond length. However, Barley (1995) figured out that a traditional anchor's load capacity does not increase if the bond length is greater than 8 to 10 m. The reason for this is related to the load transfer mechanism. The whole bond length cannot be mobilized uniformly. The resulting strain exceeds the peak strain, and failure begins in the upper grout body before the capacity is fully mobilized as in Figure 2.17.

Barley (1995) and Ostermayer and Barley (2003) demonstrated that 2 to 3 m bond lengths are more efficient than 4 to 8 m bond lengths. This idea is the most important feature of SBMA.

Vukotić et al. (2013) performed a comparison test of SBMA and conventional anchors in different soil types. They are gravelly sands, stiff silty clays and stiff to very stiff clayey marl. They figured out that SBMA anchors are almost two times efficient than conventional acnhors.

Figure 2.16. Hydraulic Jacks of SBMAs (Duzceer 2014)
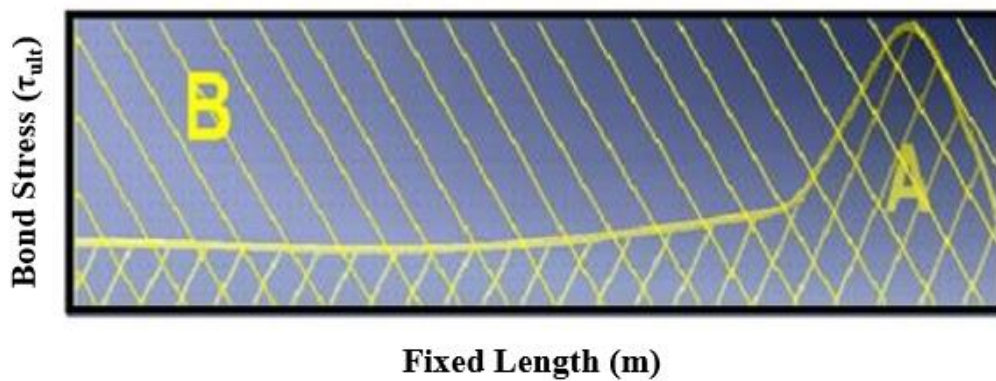
Figure 2.17. Bond Stress vs. Fixed Length (Mothersille 2011 Presentation)

The efficiency factor can be calculated by using Eqn. 2.1;

$$f_{eff} = \frac{AREA\ A}{AREA\ B} = 1.6L^{-0.57} \qquad \text{Eqn. 2-1}$$
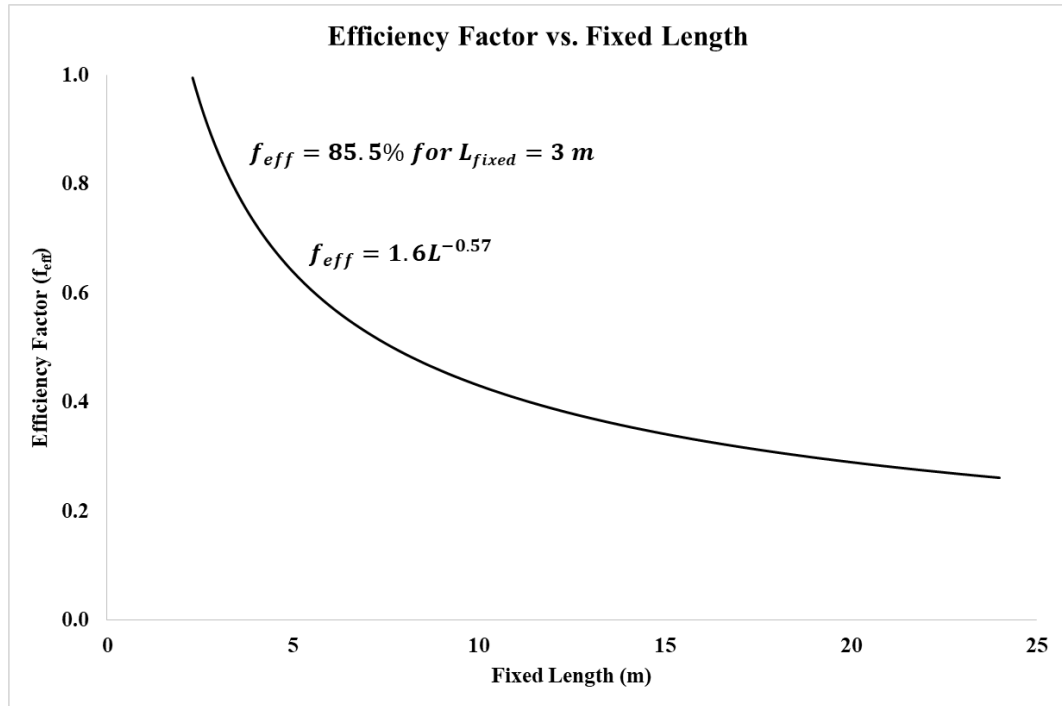
Figure 2.18. Efficiency Factor versus Fixed Length

According to Figure 2.18, the capacity of an SBMA system with 3 unit anchors having a 3 m bond length is 87% higher than the capacity of a conventional anchor with a 9 m bond length. Furthermore, Mothersille et al. (2015) and Duzceer et al. (2018) demonstrated that 1200 – 1250 kN anchor capacities could be obtained in soft soils by using SBMA technology. Comparison of traditional ground anchor and SBMA can be seen in Figure 2.19.
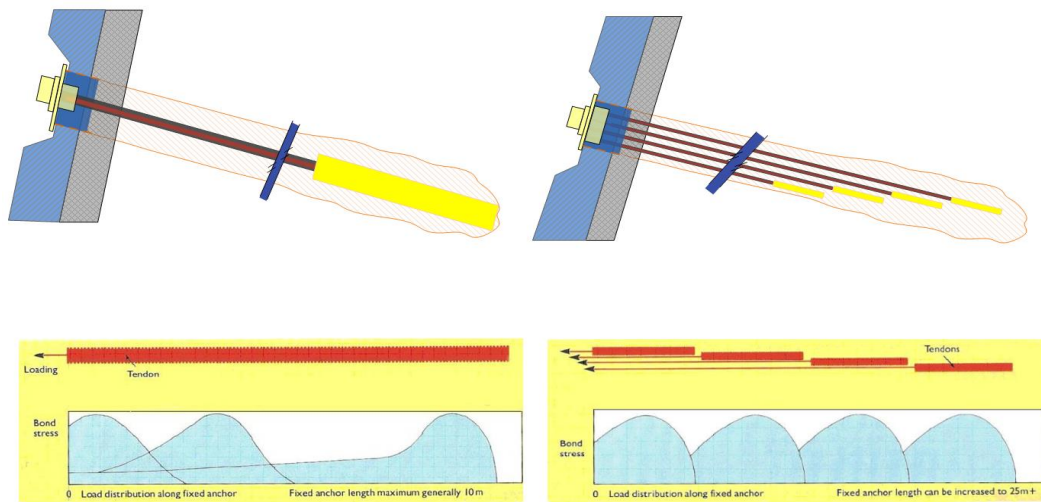
Figure 2.19. Comparison of Traditional Ground Anchor and SBMA (Mothersille 2011 Presentation)

2.4. Earth Pressures

Various numerical and analytical methods are used in the design of a retaining system. The purpose of a wall system is to carry the lateral earth pressures, water pressures, and surcharge loads. Determination of lateral earth pressures is related to the type of wall movement, the shear strength parameters of the soil, the unit weight of the soil, and drainage conditions (Das and Sivakugan, 2019). There exist different lateral earth pressure conditions, which are active, passive, and at rest. Rankine, Coulomb's theories, and the log-spiral method for estimating earth pressures are commonly recommended in the literature.

At rest earth pressure is the condition of vertical loading with no lateral displacement in the horizontal directions. Furthermore, the wall can move towards the excavation direction. Due to this movement, the soil behind the wall will expand, and eventually, the shear failures will occur. For this condition, lateral pressure is called active earth pressure. Moreover, the wall can move towards the opposite direction of the excavation. The soil behind the wall will be compressed, and failure will occur. The lateral pressure for this condition is known as passive earth pressure.

24

2.4.1. Rankine's Theory

Rankine's theory enables designers to determine the magnitude and distribution of active and passive pressures. Pressure zones can be seen in Figure 2.20. Active earth pressure is working as a driving force. Therefore, estimation of this pressure accurately plays an important role in the design of the excavation system. There is a comparative study to determine the compatibility of active pressure estimation with the finite element results. According to Yap et al. (2012), the highest compatibility was obtained from the analysis of Rankine's theory.

Pressure diagrams are assumed as linear and considerable simplifications are made according to the assumptions listed below,

- Soil is homogenous and isotropic
- Lateral earth pressure acts on a vertical plane
- Active thrust acts parallel to the ground surface
- There is no friction between wall and soil, which means that the wall surface is assumed as smooth.
- A potential failure surface is a plane.
- The wall is accepted as infinitely long. The problem is considered a plane strain.
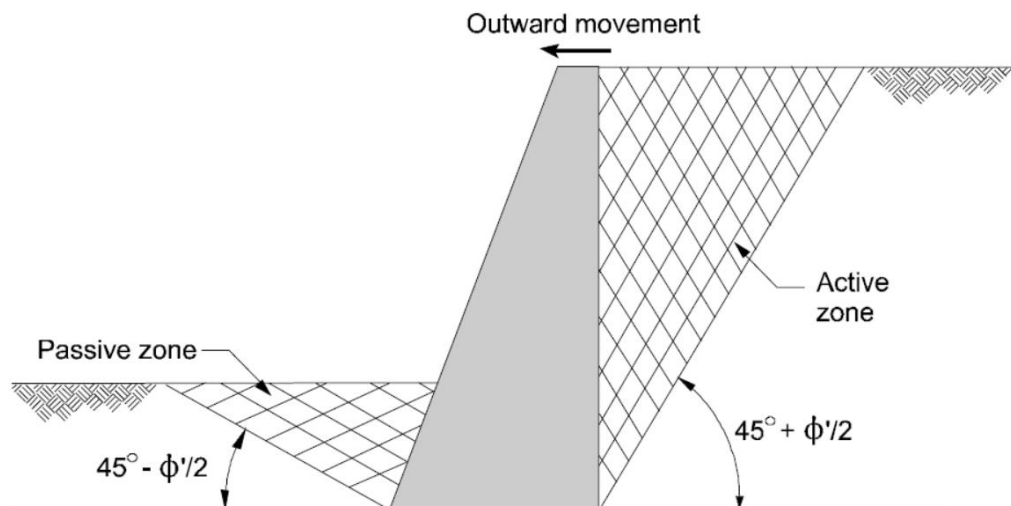
Figure 2.20. Active and Passive Zone of Retaining System (FHWA-IF-99-015, 1999)
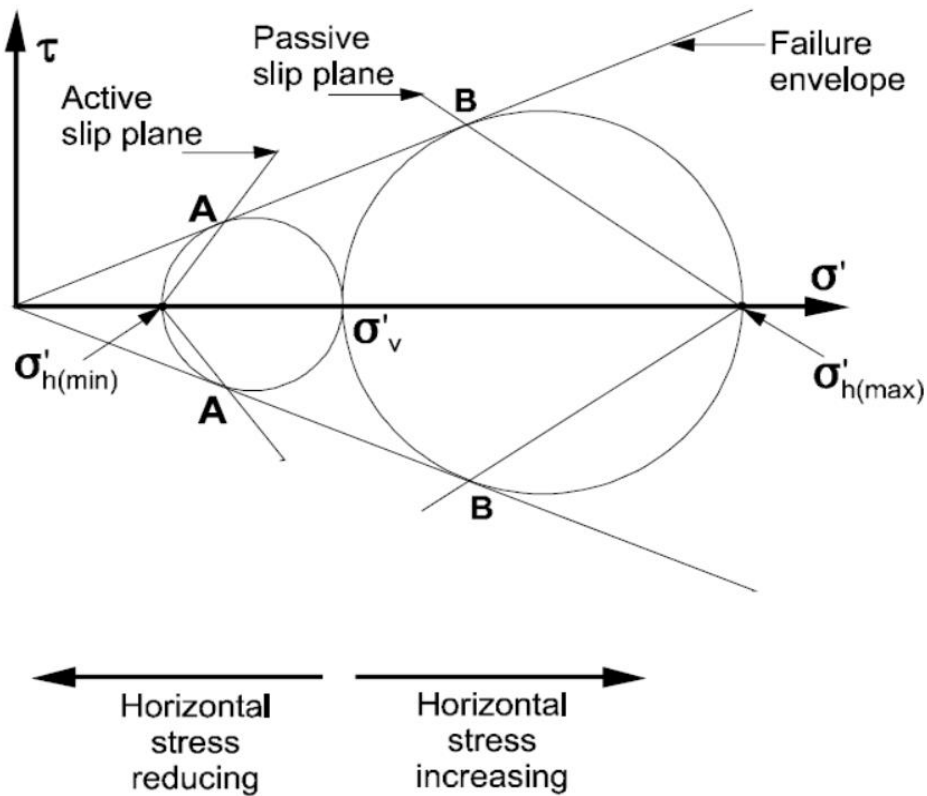
Figure 2.21. Mohr-Coulomb Failure Envelope (FHWA-IF-99-015, 1999)

For cohesionless soils, the following Eqn. 2-2 and 2-3 are derived from Figure 2.21;

$$\frac{\sigma'_{h\,(min)}}{\sigma'_v} = K_A = \frac{1 - \sin\phi'}{1 + \sin\phi'} = \tan(45 - \frac{\phi'}{2})^2 \qquad \text{Eqn. 2-2}$$

$$\frac{\sigma'_{h\,(max)}}{\sigma'_v} = K_p = \frac{1 + \sin\phi'}{1 - \sin\phi'} = \tan(45 + \frac{\phi'}{2})^2 \qquad \text{Eqn. 2-3}$$

where K_A and K_P are the coefficients of the active and passive earth pressures respectively. σ_v' is the total effective stress. Equations 2-2 and 2-3 are derived by assuming as cohesionless soil (c=0).

For cohesive soils, the following relations are used by considering effective stress strength parameters (c' and φ');

26

$$K_A = \tan(45 - \frac{\phi'}{2})^2 - \frac{2c'}{\sigma_v'}\tan(45 - \frac{\phi'}{2}) \qquad \text{Eqn. 2-4}$$

$$K_P = \tan(45 + \frac{\phi'}{2})^2 + \frac{2c'}{\sigma_v'}\tan(45 + \frac{\phi'}{2}) \qquad \text{Eqn. 2-5}$$

For the undrained case of cohesive soils, Equations (Eqn. 2-6 and 2-7) can be simplified by taking as $c = c_u$ and $\varphi = 0$.

$$K_A = 1 - \frac{2c_u}{\sigma_v} \qquad \text{Eqn. 2-6}$$

$$K_P = 1 + \frac{2c_u}{\sigma_v} \qquad \text{Eqn. 2-7}$$

where σ_v is the total vertical stress.

For cohesionless and cohesive soils, the following relation can be used at rest conditions;

$$K_0 = \frac{\sigma_h'}{\sigma_v'} = 1 - \sin\phi' \qquad \text{Eqn. 2-8}$$

where K_0 is the earth pressure coefficient at rest.

It can be seen in Figure 2.5 that the K_0 coefficient is used in the case of no lateral deformation. This condition is not appropriate for retaining wall systems practically.

2.4.2. Coulomb's Theory

The overall stability of the soil wedge is considered in Coulomb's theory (1776). The soil wedge is in between the retaining wall and the failure surface. Soil-wall and soil-soil reaction forces and the weight of the soil wedge are taken into account. These forces should be in equilibrium.

In Figures 2.22 – 2.23, demonstrates the forces, which are resisting and driving forces, acting on the soil wedge for cohesionless soils (c=0).
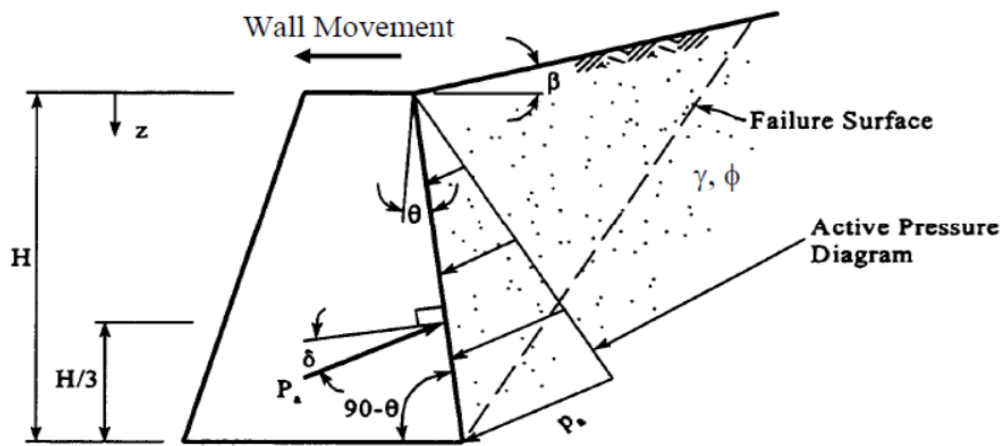
Figure 2.22. Forces Acting on A Soil Body For Active Case (FHWA NHI-06-089 (2006))
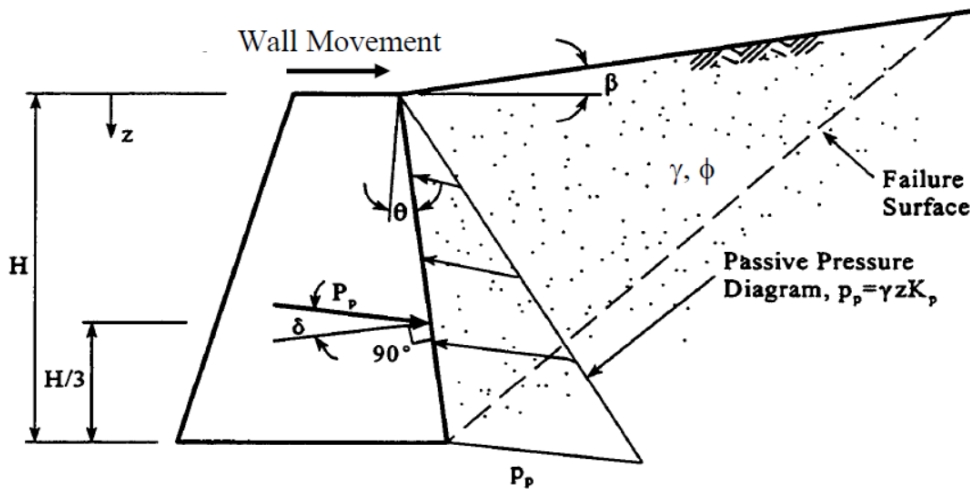
Figure 2.23. Forces Acting on A Soil Body For Passive Case (FHWA NHI-06-089 (2006))

$$K_a = \left(\frac{(\cos\theta + \varphi)^2}{(\cos\theta)^2 \cos(\theta - \delta)\left(1 - \sqrt{\left[\frac{\sin(\varphi + \delta)\sin(\varphi - \beta)}{\cos(\theta - \delta)\cos(\theta - \beta)}\right]}\right)^2} \right)^2 \qquad \text{Eqn. 2-9}$$

$$K_a = \left(\frac{(\cos\theta + \varphi)^2}{(\cos\theta)^2 \cos(\theta - \delta)\left(1 - \sqrt{\left[\frac{\sin(\varphi + \delta)\sin(\varphi - \beta)}{\cos(\theta - \delta)\cos(\theta - \beta)}\right]}\right)^2} \right)^2 \qquad \text{Eqn.2-10}$$

Coulomb's theory's passive earth pressure estimation is unconservative and not reliable because the failure surface is assumed as planar. Therefore, it is not recommended by FHWA-IF-99-015 (1999) and Liu et al. (2018).

2.4.3. Terzaghi Model (Log-Spiral Method)

Rankine's and Coulomb's potential failure surfaces are planar and unrealistic. Planar failure surface can be significant. Moreover, Coulomb's theory overestimated the passive earth pressure, which results in an unsafe design. Furthermore, the wall friction value is not considered in Rankine's theory. These drawbacks of both theories can be eliminated by using the Log-Spiral method. Design chart for log-spiral method is given in Figure 2.24.

$$r = r_0 \, e^{\theta \, \tan\varphi'} \qquad \text{Eqn. 2-11}$$

where

r is the radius of the spiral

r_0 is the starting radius at $\theta = 0$

φ' is the angle of friction of soil

θ is the angle between r and r_0
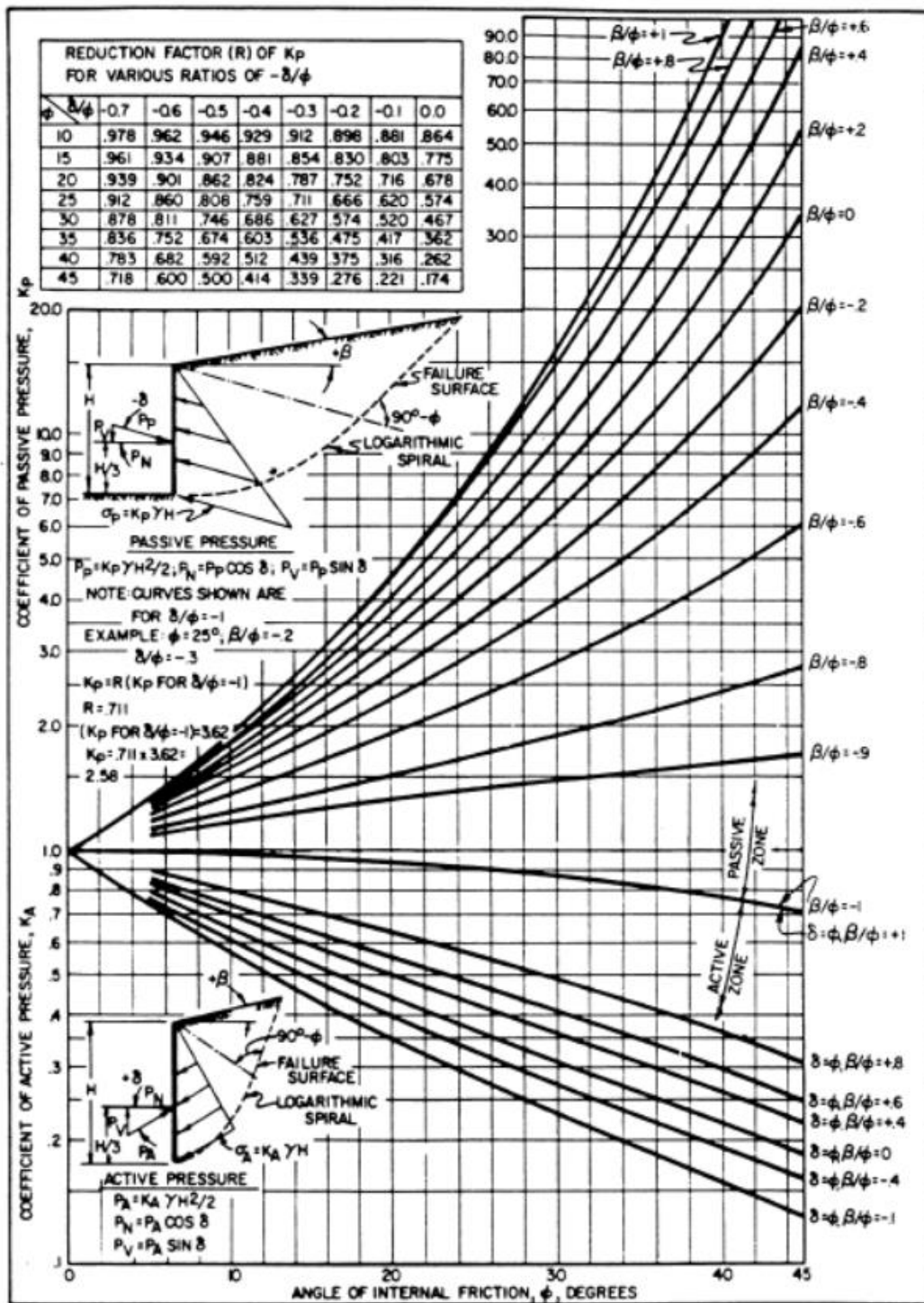
Figure 2.24. Coefficients of Active and Passive Pressure for Inclined Backslope
(FHWA-IF-99-015, 1999)

2.5. Displacements

Estimation of the displacement behavior of the excavation and stress analysis is required to design retaining structures and system elements. Various empirical, analytical and numerical modeling methods are used for the stress-strain analysis of deep excavations.

After the excavation, wall elements have a tendency to move in both the horizontal and vertical directions with the removal of soil. Clough et al. (1990) states that displacements of wall elements depend on several factors. These factors are the wall installation processes and techniques, the stiffness of the excavation system such as wall element, a support element, etc., soil conditions, groundwater level, dewatering, and surcharge loads.

In the literature, researchers study the displacement estimation of the excavation by considering the soil type, excavation depth, excavation system, etc. In this part of Chapter 2, available recommendations in the literature will be summarized.

Maximum Displacements in Stiff Clays, Residual Soils, and Sands

Peck (1969) states that displacements of vertical support elements were restricted to 1 % of the excavation depth.

The study of Peck (1969) given in Figure 2.25 is common and preferred practically in the design. The study consisted of soldier and sheet piles. Its graph is relatively simple. It includes Zone I, Zone II, and Zone III.

- Zone I is for sand/soft to hard clay
- Zone II is very soft to soft clay with a limited or significant depth of soft clay. However, there should have a high margin of a factor of safety for base heave
- Zone III is very soft to soft clay with a low margin of a factor of safety for base heave

Peck (1969) states that displacements of vertical support elements were restricted to 1 % of the excavation depth.
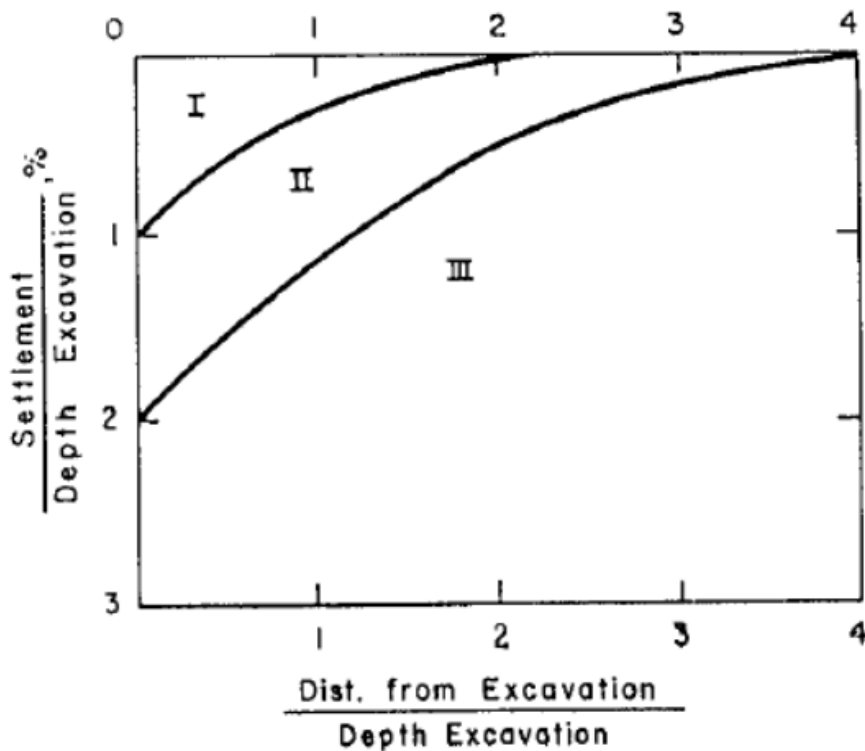
I - Sand and Soft to Hard Clay, Avg. Workmanship

II - Very Soft to Soft Clay
    1. Limited Depth of Clay Below Bott. Exc.
    2. Significant Depth of Clay Below Bott. Exc.,
       But $N_b < N_{cb}$*

III - Very Soft to Soft Clay to a Significant Depth
    Below Exc. Bott. and $N_b > N_{cb}$

    * N_b = Stability No. Using C "Below Base Level" = $\dfrac{\gamma H}{C_b}$
    N_{cb} = Critical Stab No. for Basal Heave

Figure 2.25. Maximum Soil Settlement vs. Depth of Excavation (Peck, 1969)

On the other hand, by using the available case histories in the literature, Goldberg et al. (1976) demonstrates that the maximum horizontal and vertical displacements of elements are less than 0.5 % of H. Clough et al. (1990) by adding to data of Goldberg et al. suggested that the average horizontal and vertical movements are 0.2 % of H and 0.15 % of H respectively. Figures 2.26 – 2.27 were plotted.

32
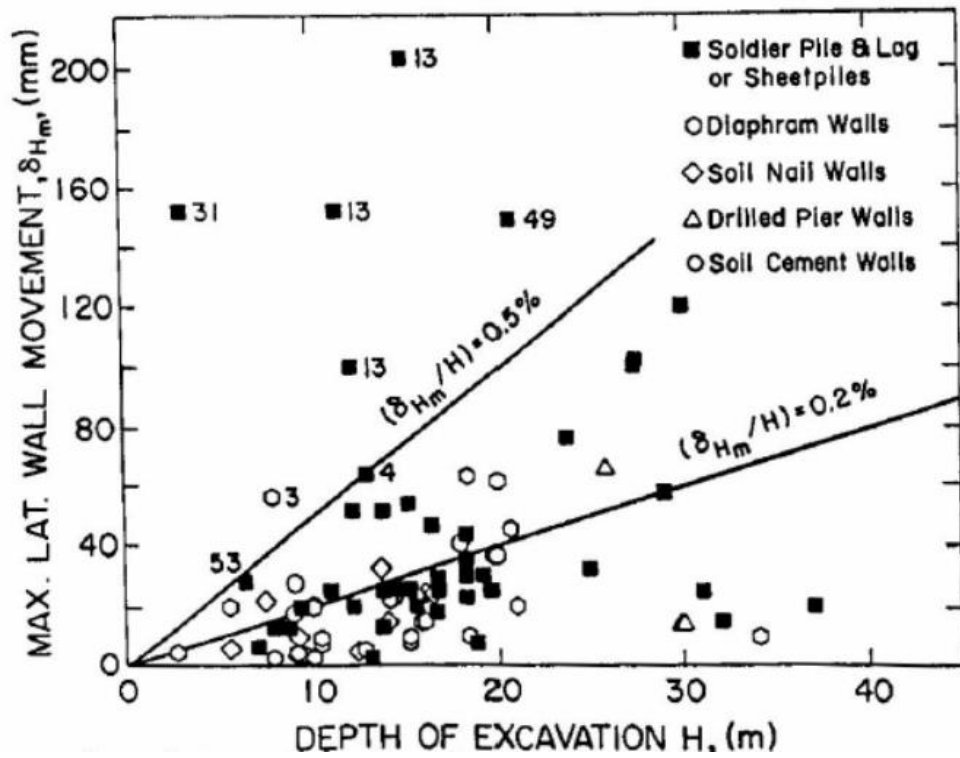
Figure 2.26. Maximum Lateral Wall Movement vs. Depth of Excavation (Clough et al. 1990)
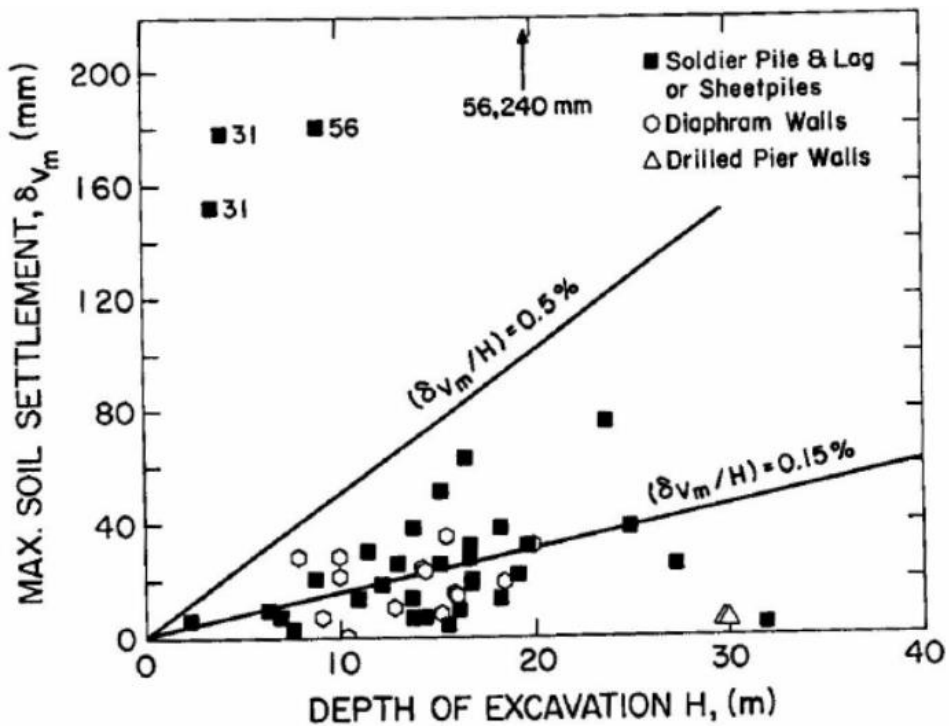
Figure 2.27. Maximum Soil Settlement vs. Depth of Excavation (Clough et al. 1990)

By considering the linear relation of the above graphs, Clough et al. (1990) suggested that the behavior of the soil masses can be defined as elastic. To confirm this suggestion, parametric finite element analysis was made by considering elastic modulus, coefficient of lateral earth pressure, wall type, and strut spacing. This parametric study shows that maximum lateral displacements are around the trend line of 0.2 % of H. It is similar to the average response obtained in the case studies. Plotted maximum lateral wall movement against depth is given below in Figure 2.28.
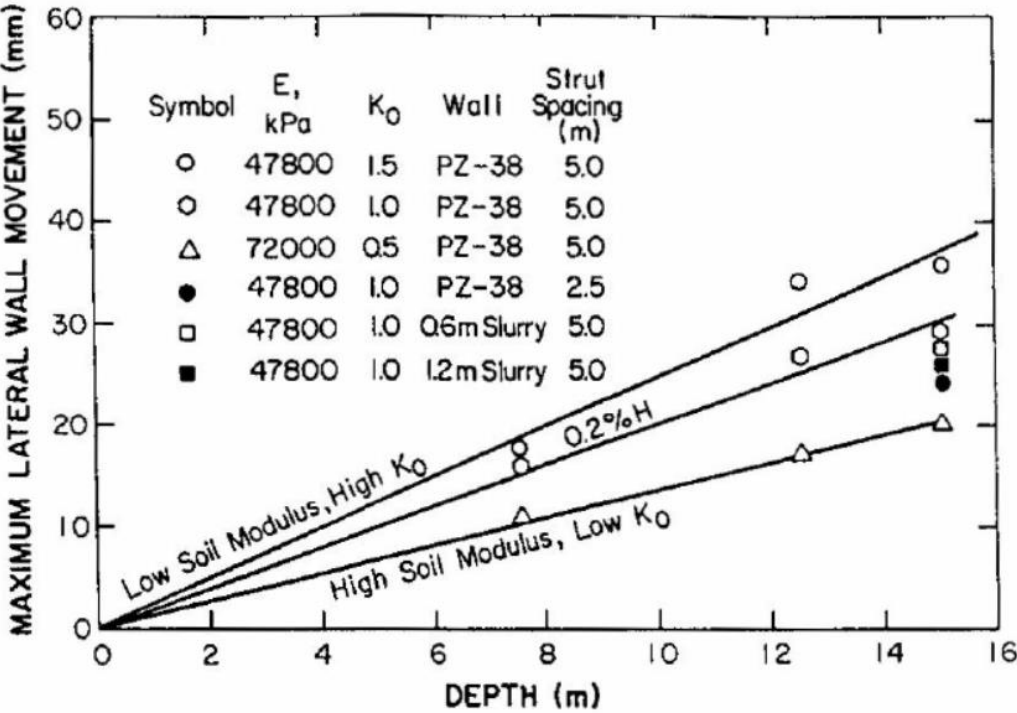
Figure 2.28. Maximum Lateral Wall Movement vs. Depth of Excavation for Parametric Finite Element Analysis (Clough et al. 1990)

Long (2001) proposed a study including 300 case histories of lateral wall displacements of deep excavations in the literature. The author subcategorized the database into 4 sets as in Figure 2.29. H, h, and s are the excavation depth, the thickness of the soft soil layer from the ground, and vertical spacing, respectively. However, s is the sum of retained and fixity depth for Set 4.

34
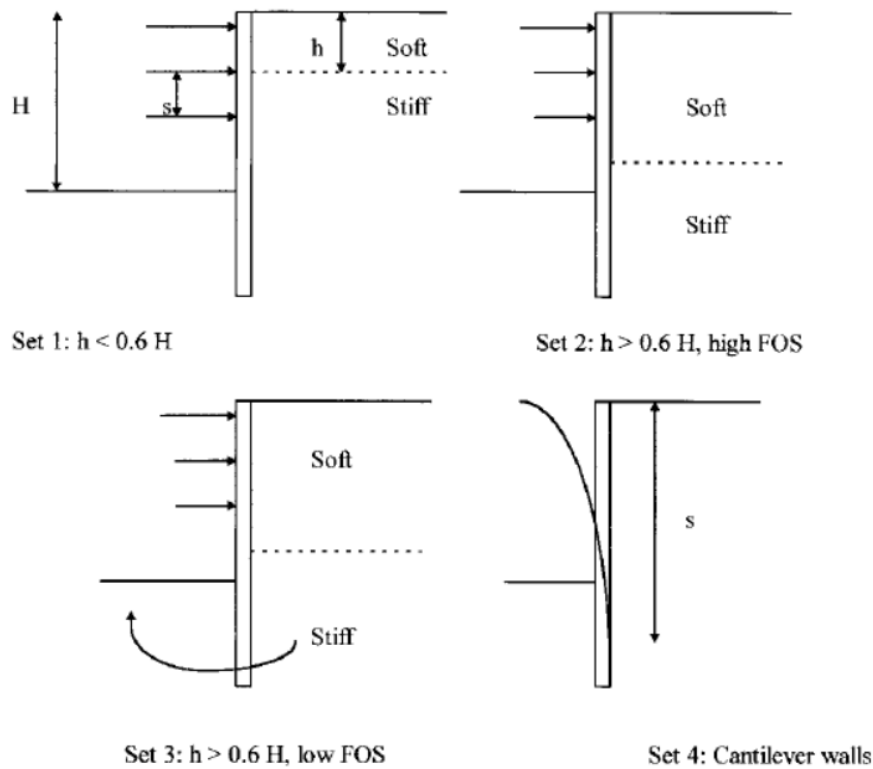
Figure 2.29. Subcategories of the Database (Long 2001)

Set 1 consisted of mostly stiff/medium dense soils, and the thickness of the soft soil, which is less than the % 60 of the excavation depth. Different $\delta_{h, max}$ values were obtained for propped, anchored, and top-down excavation systems. These are respectively 0.17 % H, 0.19 % H, 0.16 % H. When the data, which includes site problem and displacements, are higher than 0.3%H they are eliminated, then displacement values decrease to 0.13 % H, 0.14 % H, and 0.16 % H respectively. Normalized maximum lateral wall movement and settlement versus excavation depth according to Long (2001) are given in Figures 2.30 and 2.31. The summary of the results is given in Table 2.4.
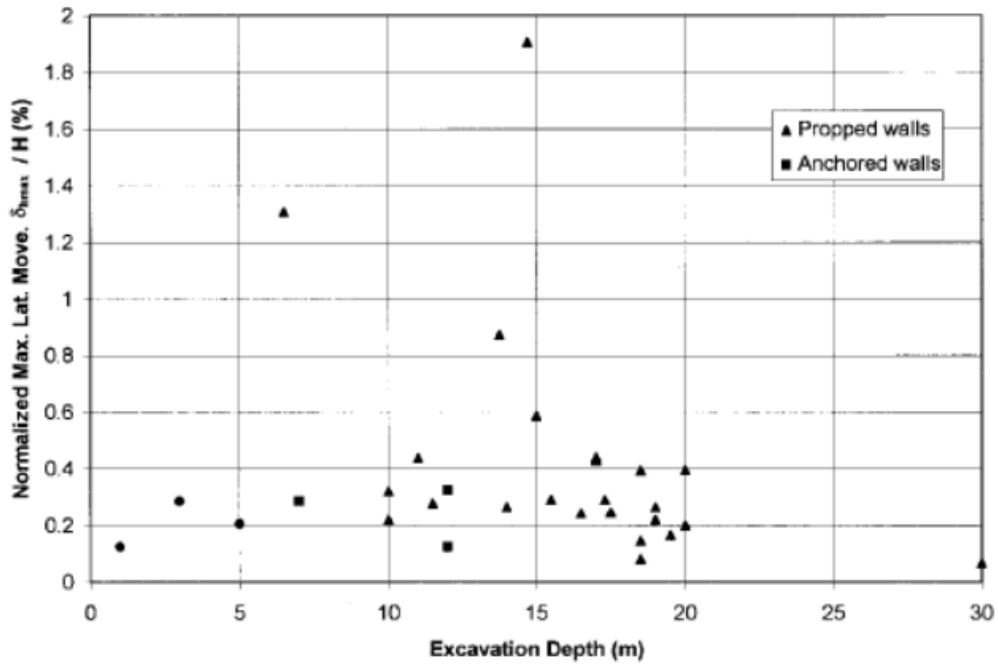
Figure 2.30. Normalized Maximum Lateral Wall Movement vs. Depth of Excavation (Long 2001)
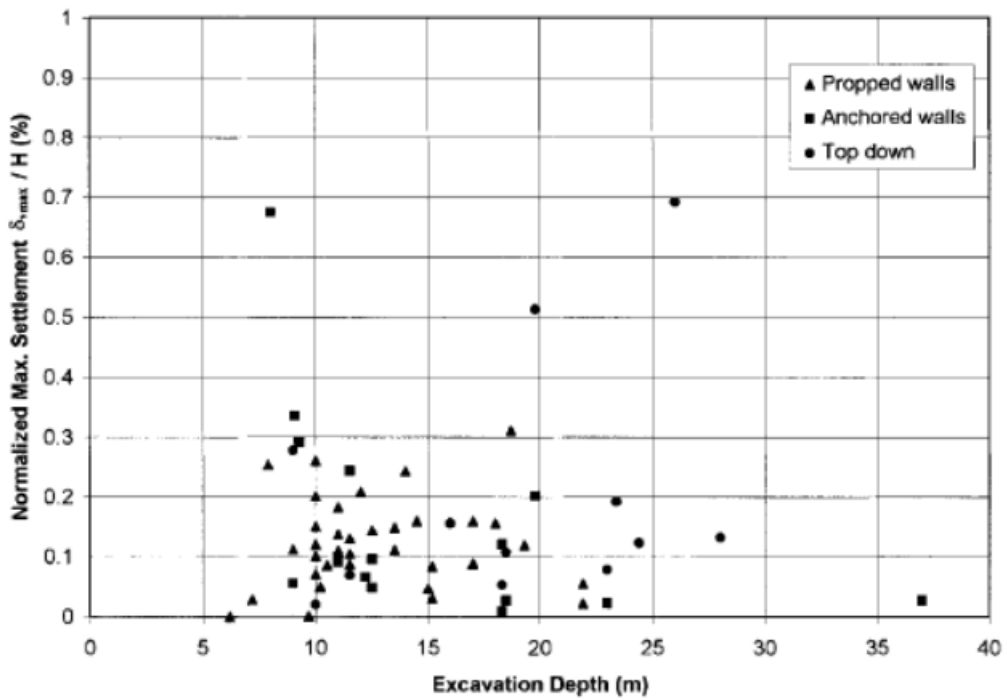
Figure 2.31. Normalized Maximum Settlement vs. Depth of Excavation (Long 2001)

36

Table 2.4. Summary of the Results (Long 2001)

Data set (1)	Cases considered (2)	$\delta_{h\,max}/H$ (%)			$\delta_{v\,max}/H$ (%)		
		Propped[a] (3)	Anchors (4)	Top down (5)	Propped[a] (6)	Anchors (7)	Top down (8)
$h < 0.6H$	All cases	0.17 (96)	0.19 (57)	0.16 (16)	0.12 (37)	0.15 (19)	0.20 (12)
$h > 0.6H$ (stiff at dredge)	All cases	0.39 (25)	0.15 (3)	No cases	0.50 (15)	0.14 (1)	No cases
$h > 0.6H$ (soft at dredge)	All cases	0.84 (35)	0.91 (3)	0.60 (4)	0.80 (13)	6.25 (1)	0.79 (4)
$h < 0.6H$	$\Delta h/H < 0.3\%$ only	0.13 (81)	0.14 (50)	0.16 (16)	0.11 (35)	0.12 (15)	0.20 (12)
$h > 0.6H$ (stiff at dredge)	$\Delta h/H < 0.3\%$ only	0.21 (14)	0.21 (2)	No cases	0.39 (7)	0.14 (1)	No cases
$h > 0.6H$ (soft at dredge)	$\Delta h/H < 0.3\%$ only	Not relevant			Not relevant		

[a]Number of relevant cases are in parentheses.

In Figure 2.32, $\delta_{h,max}/H$ data versus system stiffness graph were plotted to emphasize the effect of system stiffness which was also investigated by Clough et al. (1989). It can be said that system stiffness is not a controlling mechanism of displacements. For example, displacement can be decreased from only 0.22 % H to 0.17 % H by increasing the system stiffness 10 times. The explanation of the author for this condition is that displacements are controlled by the base heave.
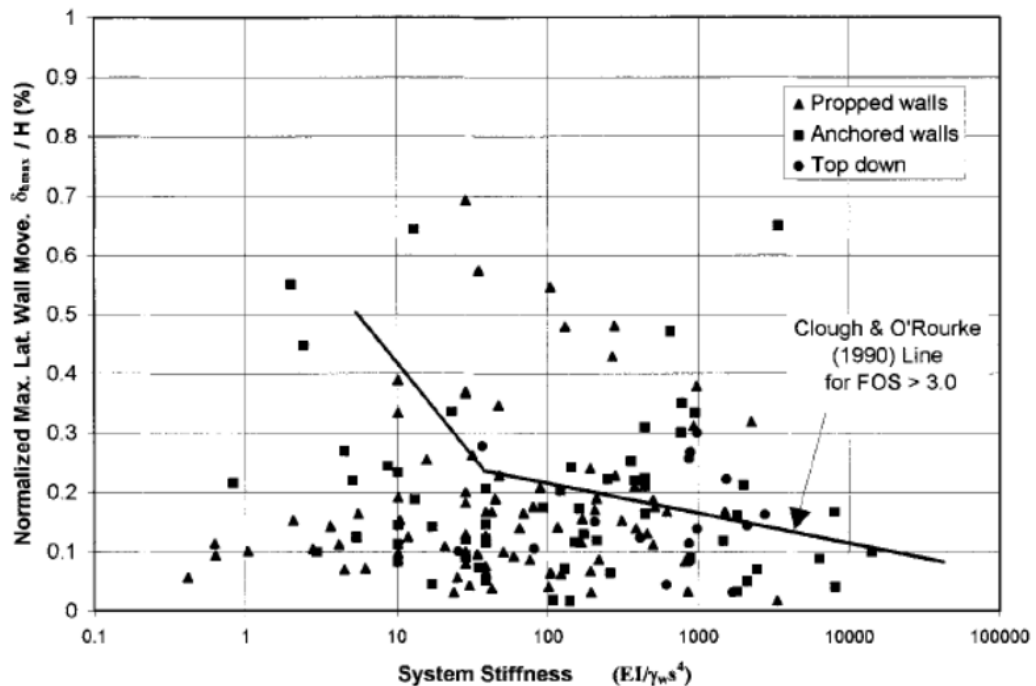
Figure 2.32. Normalized Maximum Lateral Movement vs. System Stiffness (Clough et al. 1989)

Set 2 includes a similar type of soil in Set 1. In addition to this, the wall element is socketed into a stiff layer, so the safety factor against the base heave should be high. It is approximately higher than 3.0, according to studies by Bjerrum and Eide (1956) and Clough and O'Rourke (1990). In this set, the propped and the anchored system gave the same result, which is 0.21 % H when the data having $\delta_{h,max}/H > 0.3$ % was removed.

Set 3 is similar to Set 2 except for FOS against base heave. For Set 3, the factor of safety against the base heave is low. Therefore, significant displacements were observed. Normalized maximum lateral displacement was plotted against FOS of base heave and also system stiffness. It can be seen in Figure 2.33 that displacements have a tendency to decrease after FOS=1.5. However, FOS and displacements behave independently between 1.0 and 1.5.
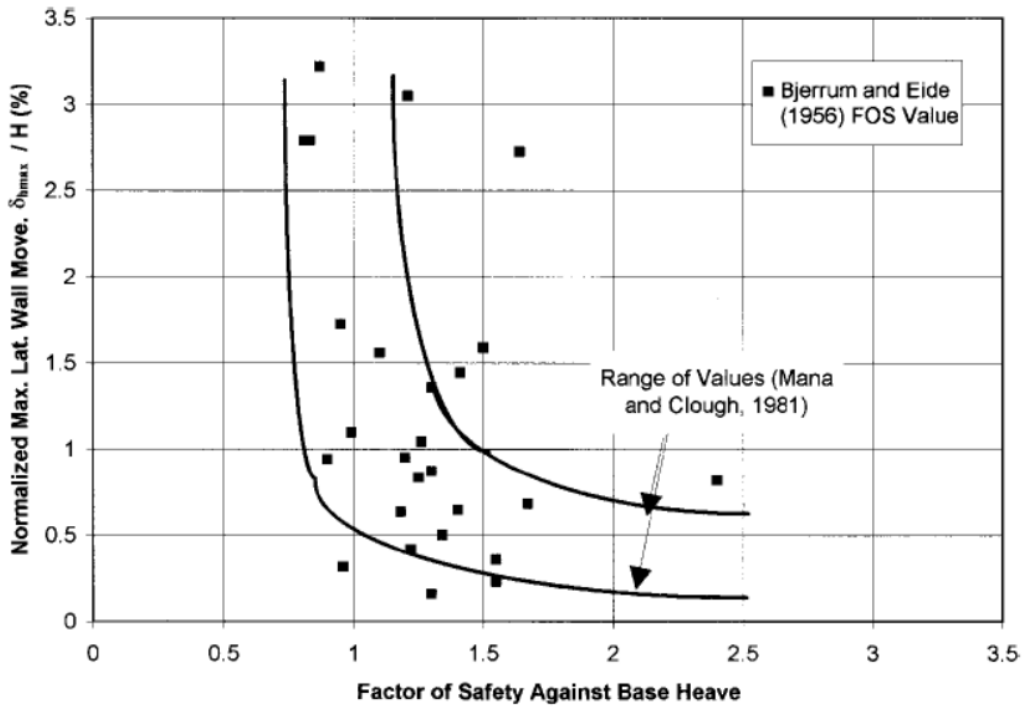
Figure 2.33. Normalized Maximum Lateral Movement vs. FOS of Base Heave (Long 2001)

Set 4 consisted of cantilever-type walls. The average value of the displacements is 0.36 % H. Normalized maximum lateral movement was plotted against the excavation depth in Figure 2.34. It can be seen that most of the cases are in between 0 – 0.5%H
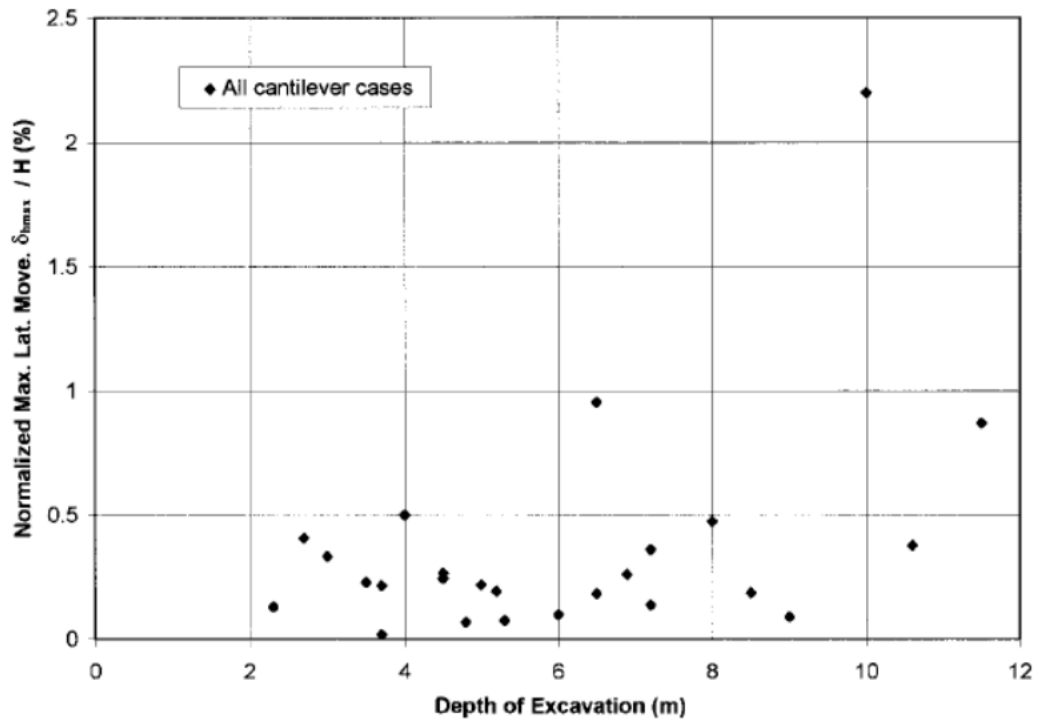
Figure 2.34. Normalized Maximum Lateral Movement vs. Depth of Excavation
(Long 2001)

In Table 2.5, the estimation of Long (2001) and Clough and O'Rourke (1990) for maximum lateral and vertical displacements of strut and anchor support systems were summarized by Ergun (2008).

Table 2.5. The Maximum Lateral and Vertical Displacements of Strut and Anchor Support Systems (Ergun 2008)

Reference	Long, 2001				Clough and O'Rourke (1990)	
Type of soil	Maximum lateral wall movements normalized by excavation height, δ_{hmax}/H (%)		Maximum vertical settlements normalized by excavation height, δ_{vmax}/H (%)		Maximum lateral wall movements normalized by excavation height, δ_{hmax}/H (%)	Maximum vertical settlements normalized by excavation height, δ_{vmax}/H (%)
Supporting system	Strut support	Anchor support	Strut support	Anchor support	Not relevant	
Stiff soils, high factor of safety of base heave	0.13 (81)*	0.14 (50)	0.11 (35)	0.12 (15)	0.20	0.15
Soft soils, high factor of safety of base heave, stiff soil at dredge level	0.21 (14)	0.21 (2)	0.39 (7)	0.14 (1)	<0.5	
Soft soils, high factor of safety of base heave, soft soil at dredge level	0.84 (35)	0.91 (3)	0.80 (13)	6.25 (1)		
Soft soils, low factor of safety of base heave	Values as high as 3.2 % have been recorded for the factor of safety on the order of 0.9				>2.0	

(81)* number of cases studied

Furthermore, FHWA-IF-99-015 (1999) states that the lateral displacement of the anchored wall is 0.2% of H on average and the maximum value can be 0.5% of H for sands and stiff clays. Also for vertical settlements, the average and the maximum values are 0.15% and 0.5% of H respectively.

2.6. Soil Parameter Estimations

SPT-N values should be corrected for very fine or silty sand below the GWT, overburden, energy efficiency, and field procedures (borehole diameter, sampler, and rod length).

To make corrections for very fine or silty sand below the GWT, eqn. 2-12 is given below;

$$N' = 15 + \frac{1}{2}(N - 15) \qquad \text{Eqn. 2-12}$$

This correction is applied when very fine sand or silt sand layer is below the GWT and also, SPT-N values should be smaller than 15. Overestimated resistance due to negative excess pore pressure is corrected.

Moreover, overburden correction, which includes the effective stress effects, is one of the most important corrections. Since it has a considerable effect on SPT-N value. The reason for this correction is that a higher SPT-N value is obtained in the same soil when the test is performed at a deeper level. Recommended relation by Birand et al. (1999) for overburden correction is given in Figure 2.35.
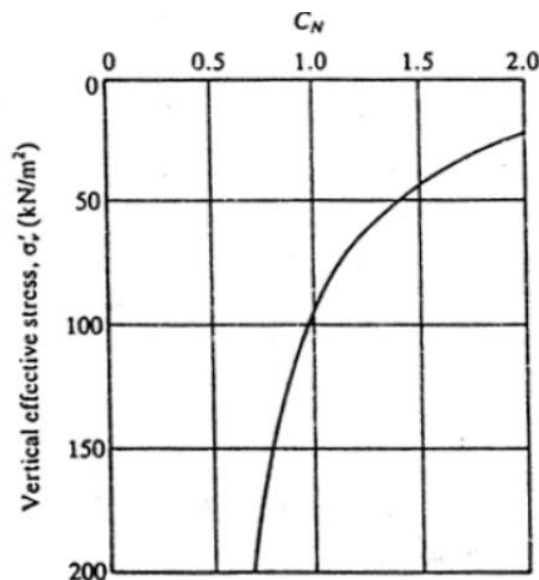
Figure 2.35. Relation of C_N and σ_V' (Birand et al. 1999)

Different hammers and methods are used during the standard penetration test. Their efficiency is changing between 0.43 and 0.85 depending on the hammer type, friction of the system vs. The efficiency of the hammer is corrected by accepting the reference efficiency as 60%. In Eqn. 2-13 and 2-14, correction formulations were given.

$$N_{60} = N \ x \ \frac{ER}{0.6} \ x \ C_B \ x \ C_S \ x \ C_R \qquad \text{Eqn. 2-13}$$

$$(N_1)_{60} = N_{60} \ x \ C_N \qquad \text{Eqn. 2-14}$$

Where;

N = SPT-N value measured from the field

N_{60} = Corrected SPT-N value according to field conditions and energy efficiency

$(N_1)_{60}$ = Corrected SPT-N value according to field conditions, energy efficiency, overburden

ER = Energy ratio for hammer type

C_B = Borehole diameter correction

C_S = Samplers with and without liners correction

C_R = Rod length correction

Table 2.6. The Efficiency of Hammers (Çetin et al., 2018)

Hammer Type	Hammer Efficiency
Safety Hammer[1]	0.40 - 0.75
Donut Hammer[1]	0.30 - 0.60
Donut Hammer[2]	0.70 - 0.85
Automatic-Trip Hammer (Donut or Safety Type)	0.50 - 0.80

(1) Rope and cathead system (Two turns of rope and normal release)
(2) Rope and cathead system (Japanese throw)

Table 2.7. SPT Correction Factors (Robertson and Wride, NCEER 1997 Workshop)

Factor	Equipment Variables	Correction
Borehole diameter factor, C_B	65 - 115 mm	1.00
	150 mm	1.05
	200 mm	1.15
Sampling method factor, C_S	Standard sampler	1.00
	Sampler without liner	1.20
Rod length factor, C_R	3 m to 4 m	0.75
	4 m to 6 m	0.85
	6 m to 10 m	0.95
	10 m to 30 m	1.00
	>30 m	<1.00

Undrained Shear Strength (c_u)

The undrained shear strength (c_u) of cohesive soils was estimated using Stroud's formulation (1974). A database of this formulation includes 1200 SPT-N values at 42 different sites in England. Undisturbed samples were taken and undrained unconsolidated triaxial tests were performed on these samples. As a result of these studies, Stroud (1974) figured out a valid correlation between N_{60} and c_u values. (Equation 2-15);

$$c_u = f_1 \ x \ N_{60}$$

Eqn. 2-15

f_1 is a variable that is related to the plasticity index of the clay layer. It changes between 4 and 7. Recommended equation and chart are given in Eqn. 2-16 and Figure 2.36.

$$c_u = \begin{cases} (6-7)N_{60} & for \ PI < 20 \\ (4-5)N_{60} & for \ 20 < PI < 30 \\ 4.2 \ N_{60} & for \ PI > 30 \end{cases}$$

Eqn. 2-16
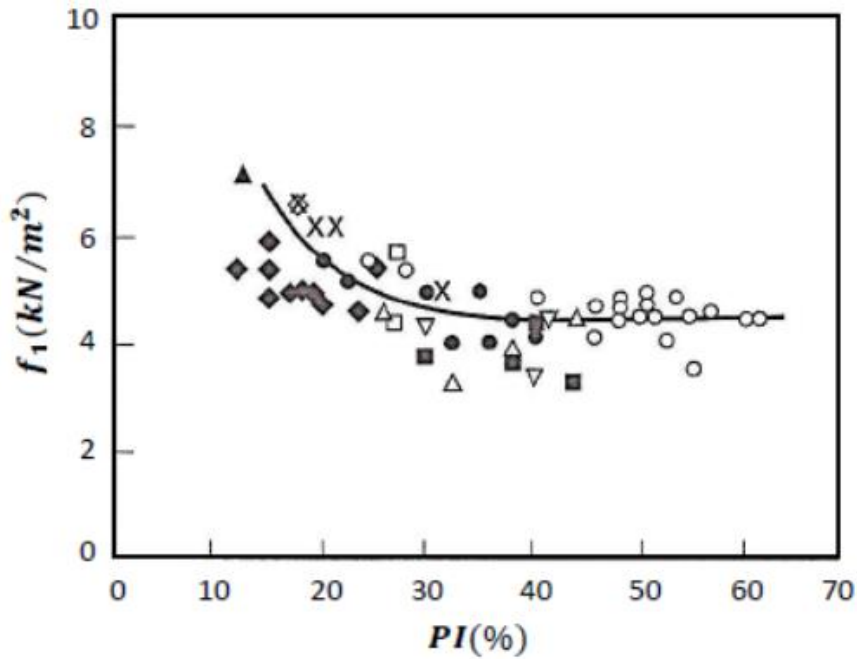
Figure 2.36. Correlation of f_1 and PI (%) (Stround, 1974)

Undrained shear strength can be estimated by using the cone penetration test (CPT) results according to CPT Guide (2012) as in Eqn. 2-17;

$$c_u = \frac{q_t - \sigma_v}{N_{kt}}$$

Eqn. 2-17

where

N_{kt} is the preliminary cone factor value changing between 10 to 18. N_{kt} is proportional to plasticity and inversely proportional to soil sensitivity.

Coefficient of Volume Compressibility (m_v)

The odometric deformation modulus of the soil loaded on a single axis is defined as the ratio of a stress deformation to an axial unit deformation. It is based on the assumption of zero deformation in the direction perpendicular to the direction of axial stress due to loading. It is obtained from the odometer experiment in the laboratory. The odometric module represents the long-term modulus of deformation of cohesive soils. Stroud (1974) figured out a correlation between m_v and SPT values (Eqn. 2-18). The relation between PI and f_2 is given in Figure 2.37.

$$\frac{1}{m_v} = f_2 \; x \; N_{60} \qquad\qquad \text{Eqn. 2-18}$$
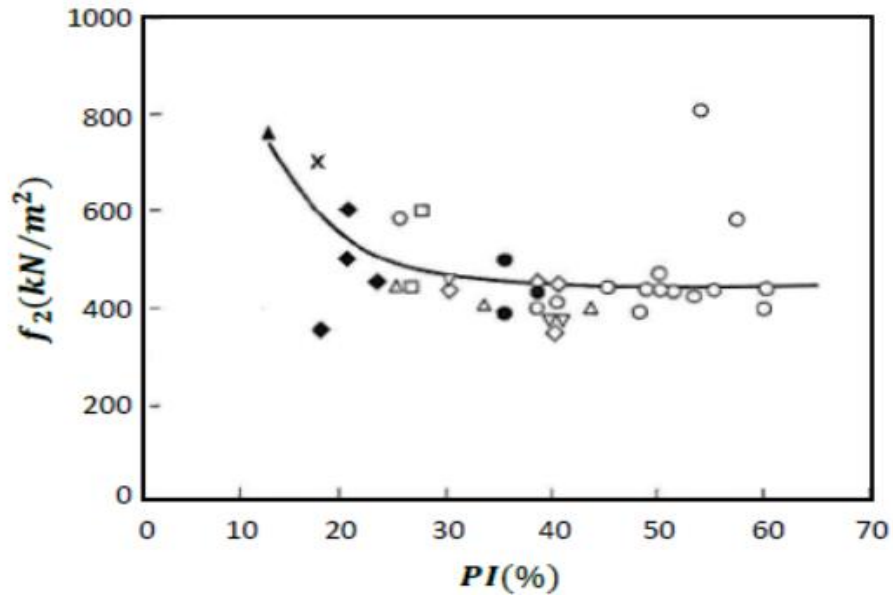
Figure 2.37. Correlation of PI and f_2 (Stroud, 1974)

Cohesion (c')

Effective cohesion of cohesive layers was estimated by using the below formulation in Eqn. 2-19, which is proposed by Sorensen and Okkels (2013);

$$c' = \sim \frac{c_u}{10} \qquad\qquad \text{Eqn. 2-19}$$

Friction Angle (φ)

Terzaghi et al. (1996) suggest an empirical correlation between $(N_1)_{60}$ and Φ' by considering several proposals of researchers, which are Peck et al. (1953), De Mello (1971), Schmertmann (1979), and Stroud (1988). It also includes two different suggestions for $q_c / (N_1)_{60} = 400$ and 500 kPa in Figure 2.38.
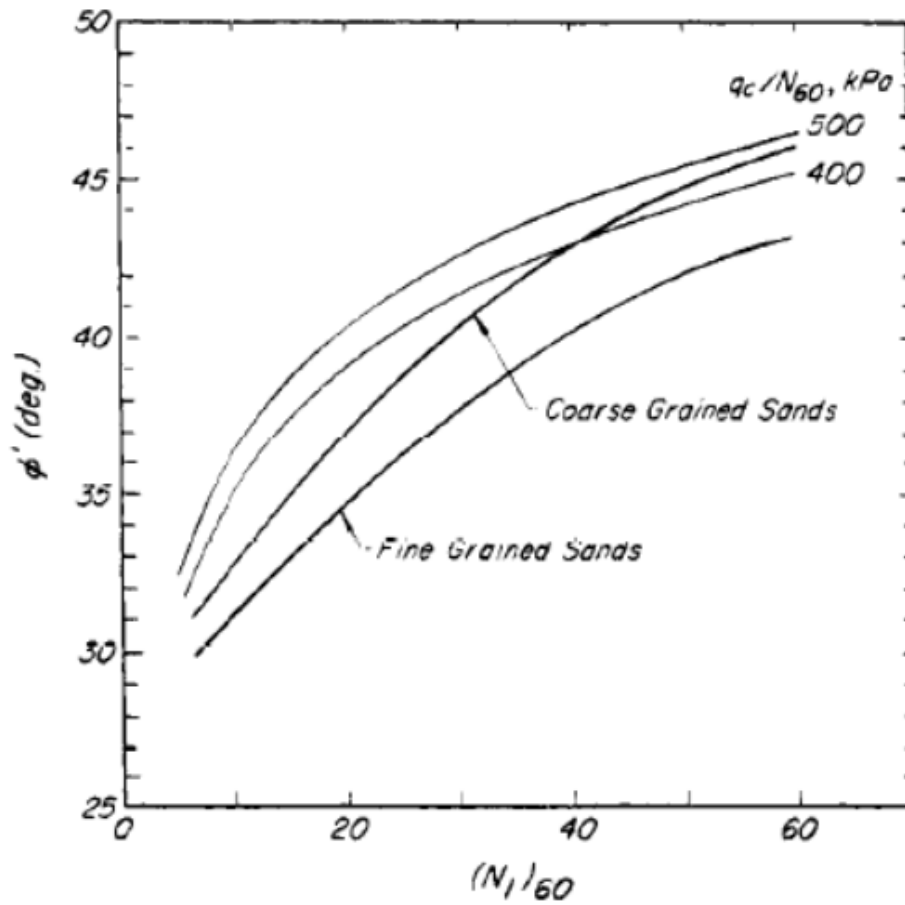
Figure 2.38. Correlation Between Friction Angle and $(N_1)_{60}$ (Terzaghi et al. 1996)

Gibson et al. (1953) figured out a correlation between plasticity index and friction angle in Figure 2.39. Also, two types of friction angles which are drained shear and residual, can be estimated.
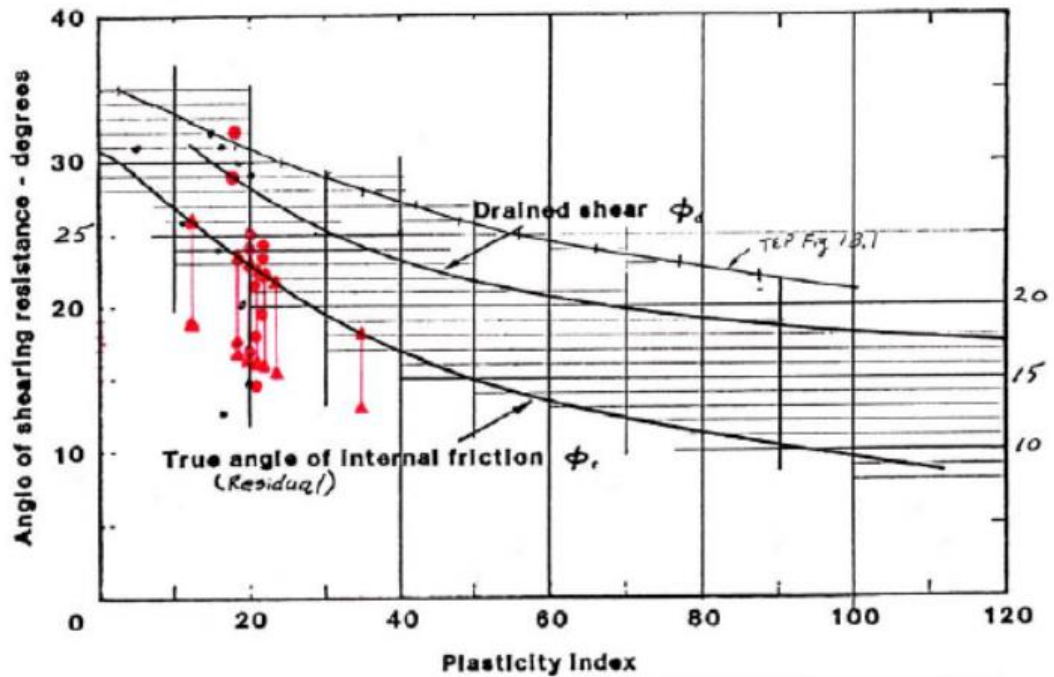
Figure 2.39. Plasticity Index vs. Friction Angle (Gibson 1953)

Terzaghi et al. (1996) conducted research on Mexico City clay to determine the relation between friction angle and plasticity index. Mexico City clay exhibits large friction angles unexpectedly when subjected to a large amount of water. Moreover, for the same plasticity index, there exists a variation in friction angle due to the clay size fraction of soils. Friction angles of soft and stiff clays change from 25^0 to 35^0 and 20^0 to 35^0, respectively. The recommended chart can be seen in Figure 2.40.
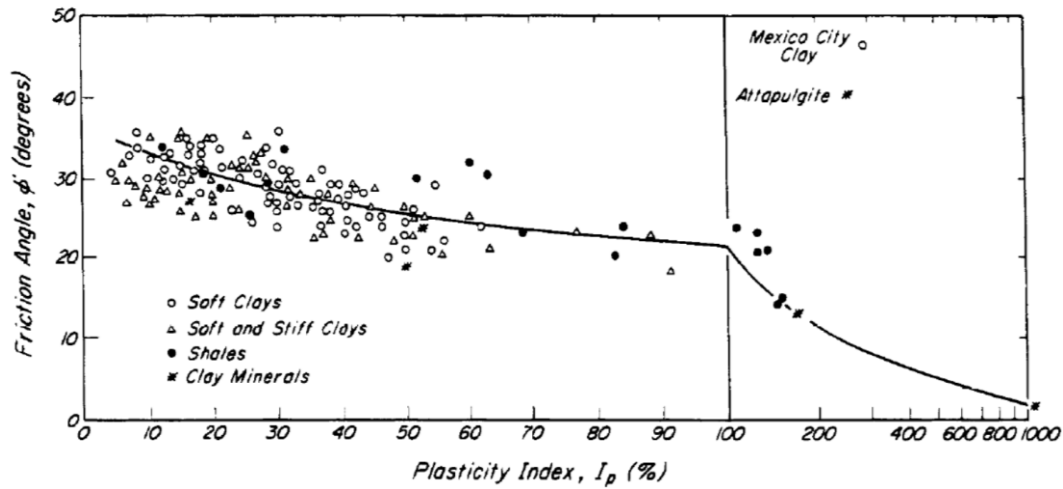
Figure 2.40. Plasticity Index vs. Friction Angle (Terzaghi et al. 1996)

Furthermore, the friction angle of sands can be estimated by using the cone resistance of the soil. Robertson and Campanella (1983) figured out a relation for the peak friction angle in Eqn. 2-20.

$$\tan \phi' = \frac{1}{2.68}\left[\log\left(\frac{q_t}{\sigma'_{vo}}\right) + 0.29\right]$$ Eqn. 2-20

Furthermore, Kulhawy and Mayne (1990) stated an alternative correlation for sand in Eqn. 2-21 and 2-22. High-quality field data taken from 16 different locations were studied.

$$\phi' = 17.6 + 11 \, \log(Q_{tn})$$ Eqn. 2-21

$$Q_{tn} = \frac{(q_c/p_a)}{(\sigma'_{vo}/p_a)^{0.5}}$$ Eqn. 2-22

Where

Q_{tn} is the normalized and corrected CPT resistance for overburden pressure

In addition, the friction angles of cohesive soils can be calculated by using the relation suggested by Senneset et al. (1989) in Eqn 2-23. It is also referred to as Norwegian

48

Institute of Technology (NTH) solution. This relation can be used if $20^0 \leq \Phi' \leq 40^0$ and $0.1 \leq B_q \leq 1.0$, according to Mayne (2006).

$$\phi' = 29.5^\circ \, B_q^{0.121}\left[0.256 + 0.336 \, B_q + \log Q_t\right] \qquad \text{Eqn. 2-23}$$

where

B_q is the normalized pore pressure parameter which is the ratio of $\Delta u / q_n$

Excess pore pressure, $\Delta u = u_2 - u_0$

Net cone resistance, $q_n = q_t - \sigma_{v0}$

Dilatancy Angle (ψ)

Dilatancy angle was estimated by using the proposal of Brinkgreve (2008) for both cohesionless and also cohesive soils (Eqn. 2-24);

$$\psi = \phi - 30^\circ \qquad \text{Eqn. 2-24}$$

Unit Weight

Unit weight of soils was estimated using the recommended correlation of Çetin et al. (2016) is given in Table 2.8.

Table 2.8. SPT N_{60} - Unit Weight Correlation (Çetin et al. 2016)

Coarse-grained soil layers		
SPT-N_{60} (blows/ft)	γ_{moist} (kN/m^3)	γ_{sat} (kN/m3)
0-4	16.0	17.6
5-10	17.6	19.2
11-30	19.2	20.0
30-50	20.0	21.6
Fine-grained soil layers		
0-4	16.0	17.6
5-8	17.6	19.2
9-16	18.4	20.0

Furthermore, the unit weight of the soil can be calculated by using the cone penetration test (CPT) results. Robertson (2010) figured out the following correlation in Eqn 2-25 and Figure 2.41;

$$\frac{\gamma}{\gamma_w} = 0.27\left[\log R_f\right] + 0.36\left[\log\frac{q_t}{p_a}\right] + 1.236 \qquad \text{Eqn. 2-25}$$

Where

f_s is the sleeve friction of the soil

q_t is the tip resistance of the soil

R_f is the friction ratio of f_s to q_t %

γ_w is the unit weight of water

p_a is the atmospheric pressure
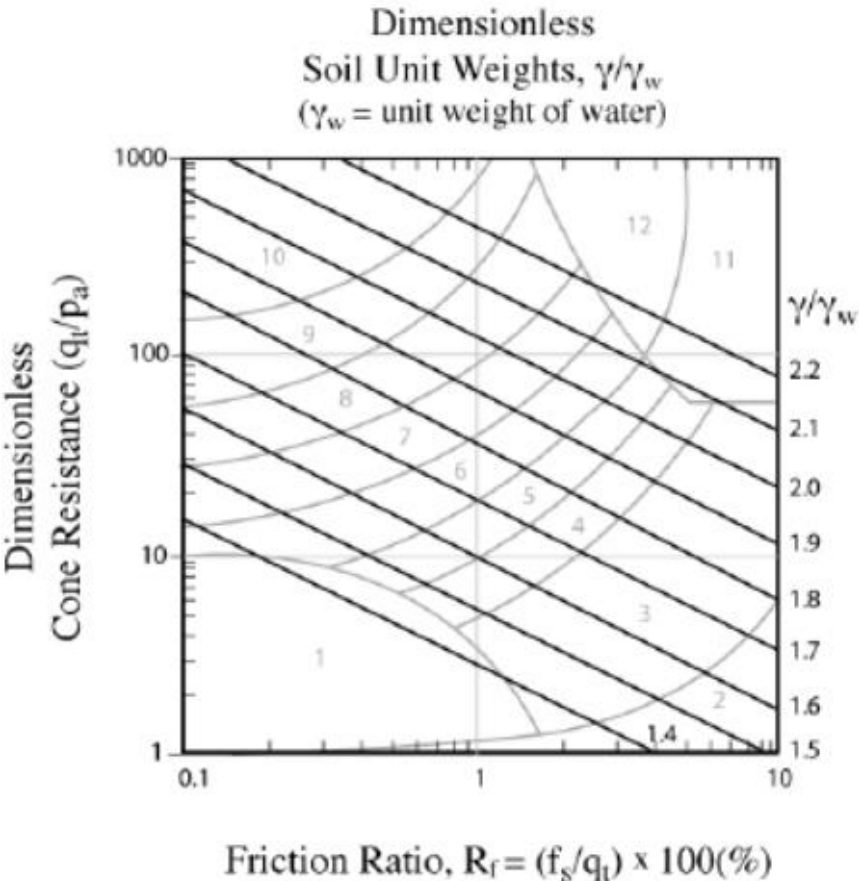
Figure 2.41. Estimation of Soil Unit Weight (Robertson 2010)

The Hardening Soil (HS) Model Parameters

The Theory of the HS Model

The Hardening Soil (HS) model was used as a material model in this study. Soft and stiff soils can be simulated by the HS Model developed by Schanz (1998) and Shanz et al. (1999). Decreasing stiffness and increasing plastic strains at the same time, which are irreversible, are observed in soil under the primary deviatoric loading. Kondner (1963) modeled these types of relationships, and after that, they were used in the hyperbolic model (Duncan & Chang, 1970). The main features of the hardening soil model are that plasticity theory is used instead of elasticity theory, and soil dilatancy and yield cap are considered.

Stress dependency, power, m

Plastic straining due to primary deviatoric loading, E_{50}^{ref}

Plastic straining due to primary compression, E_{oed}^{ref}

Elastic unloading/reloading, E_{ur}^{ref}

In the HS model, the soil stiffness is stress-dependent and is calculated by using Eqn. 2-26 ;

$$E_{oed} = E_{oed}^{ref} \left(\frac{\sigma}{p^{ref}} \right)^m \qquad \text{Eqn. 2-26}$$

The basic relationship between reference pressure in Eqn. 2-27, p^{ref}, and the modified compression index, λ^*, is used for soft soils and is given by the Eqn. 2-28;

$$E_{oed}^{red} = \frac{p^{ref}}{\lambda^*} \qquad \text{Eqn. 2-27}$$

$$\lambda^* = \frac{\lambda}{(1 + e_0)} \qquad \text{Eqn. 2-28}$$

where

p^{ref}: reference pressure

λ^*: the modified compression index

λ: the standard Cam-Clay compression index

e_0: initial void ratio

The hyperbolic relation of the vertical strain, ε_1, and the deviatoric stress, q, is used basically to formulate the hardening soil model as Eqn. 2-29.

$$-\varepsilon_1 = \frac{1}{E_i} \frac{q}{1 - \dfrac{q}{q_a}} \quad for\ q < q_f$$

Eqn. 2-29

Where

q_a: Asymptotic value of the shear strength

E_i: Initial stiffness modulus

There exists a relation between E_i and E_{50}. Formulation and chart (Figure 2.42 and Eqn. 2-30) can be seen below;

$$E_i = \frac{2\ E_{50}}{2 - R_f}$$

Eqn. 2-30
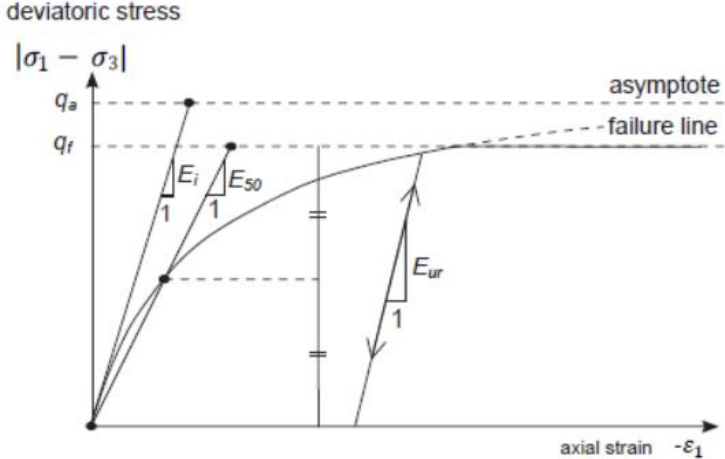
Figure 2.42. Hyperbolic stress-strain relation (Plaxis 2D Material Manuels 2021)

E_{50} is dependent on the confining stress for primary loading. The relationship is given in Eqn. 2-31;

$$E_{50} = E_{50}^{ref} \left(\frac{c * \cos \phi - \sigma_3' \sin \phi}{c * \cos \phi + p^{ref}\ \sin \phi} \right)^m$$

Eqn. 2-31

Where

E_{50}^{ref}: Reference stiffness modulus at p^{ref}

Stress dependency, m, varies between 0.5 and 1.0, according to Von Soos (1990). The asymptotical shear strength, q_a, and the ultimate deviatoric stress, q_f, are calculated by Eqn. 2-32 and 2-33;

$$q_f = (c \, \cot \phi - \sigma_3') \frac{2 \sin \phi}{1 - \sin \phi} \qquad \text{Eqn. 2-32}$$

$$q_a = \frac{q_f}{R_f} \qquad \text{Eqn. 2-33}$$

Eqn. 2-32, which includes shear strength parameters, c, and φ, comes from the Mohr-Coulomb failure criterion. When stress level reaches q=q_f, perfectly plastic yielding occurs, known as a Mohr-Coulomb Model.

R_f is defined as a failure ratio. It is the ratio of q_f to q_a. $R_f = 0.9$ is recommended by Plaxis Material Models Manuel (2021) as a default setting.

Elastic unloading/reloading stress-dependent stiffness modulus is defined as;

$$E_{ur} = E_{ur}^{ref} \left(\frac{c * \cos \phi - \sigma_3' \, \sin \phi}{c * \cos \phi + p^{ref} \, \sin \phi} \right)^m \qquad \text{Eqn. 2-34}$$

Where

E_{ur}^{ref}: Reference elastic unloading/reloading stiffness modulus at p^{ref}

Estimation of Parameters

The reference stiffness parameters of cohesionless layers were estimated by using Brinkgreve et al. (2010). The stiffness of sand changes linearly with relative density (RD) by considering $p_{ref} = 100$ kPa in Eqn. 2-35 – 2-38;

$$E_{50}^{ref} = 60000 \, RD / 100 \qquad \text{Eqn. 2-35}$$

$$E_{oed}^{ref} = 60000 \, RD / 100 \qquad \text{Eqn. 2-36}$$

$$E_{ur}^{ref} = 180000 \, RD / 100 \qquad \text{Eqn. 2-37}$$

$$G_0^{ref} = 60000 + 68000 \, RD / 100 \qquad \text{Eqn. 2-38}$$

The stiffness depends on the stress. The stress dependency, m, is inversely related to the relative density of sand in Eqn. 2-39.

$$m = 0.7 - RD / 320 \qquad \text{Eqn. 2-39}$$

Brinkgreve (2005) recommended that cohesive soils are more stress-dependent than cohesionless soil. Therefore, the power (m) value can be taken as 1.0 for cohesive soils. On the other hand, it changes between 0.4 and 0.7 for cohesionless soils. m=0.5 is reasonable for cohesionless soils.

Oedometer modules are the inverse of the coefficient of volume compressibility in Eqn. 2-40.

$$E_{oed} = \frac{1}{m_v} \qquad \text{Eqn. 2-40}$$

The relation to estimating the oedometer stiffness for normally consolidated clays in Eqn. 2-41 (Brinkgreve, 2005);

$$E_{oed}^{ref} = \frac{1}{2} E_{50}^{ref} \qquad \text{Eqn. 2-41}$$

E_{ur}^{ref} value varies 2 to 6 times of E_{50}^{ref} value according to Azzouz et al. (1976). Furthermore, $E_{ur}^{ref} = 3 \, E_{50}^{ref}$ is recommended by Plaxis Material Models Manuel (2021).

Relative Density (RD)

Gibbs and Holtz (1957) conducted research to investigate the relative density of fine and coarse sand. By controlling the soil density and moisture, the effect of overburden pressure, rod length, and rod weight were evaluated. Tests were performed on a steel tank including springs to control overburden pressure, and then, standard penetration tests were made, and following Figure 2.43 was obtained.
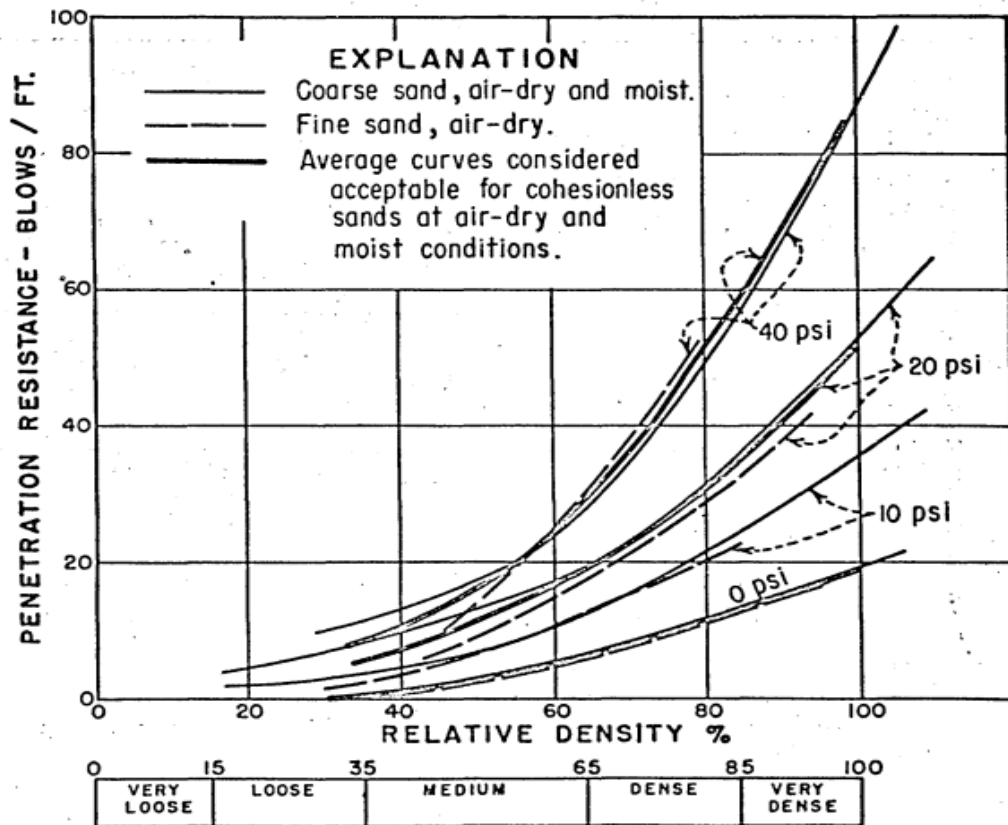
Figure 2.43. SPT-N versus Relative Density for Different Effective Stress Values
(Gibbs and Holtz 1957)

Furthermore, Plaxis 2D Material Manuels (2021) recommended the relation of $N_{1,60}$ and relative density in Eqn. 2-42.

$$(N_1)_{60} = \frac{RD^2}{15^2} \qquad \text{Eqn. 2-42}$$

Baldi et al. (1986) performed calibration chamber testing on the sand and recommended a relation to estimate relative density. A modified formula can be seen below (Eqn. 2-43):

$$RD = \left(\frac{1}{C_2}\right) \ln\left(\frac{Q_{tn}}{C_0}\right) \qquad \text{Eqn. 2-43}$$

Where

The constants C_0 and C_2 are 15.7 and 2.41, respectively, for moderately compressible, normally consolidated sand.

CHAPTER 3

3. GEOTECHNICAL CHARACTERIZATION OF THE STUDY AREA

3.1. Introduction

A new high-rise building was built in Bayraklı, İzmir. The project was constructed in an area of 45,000 m^2. The complex consists of 3 blocks named A, B, and C. Satellite view of the project can be seen in Figure 3.1. There exists a historical Bomonti Beer Fabricate between Block B and C. Block A has a 15-floor podium area and a 57-floor tower on top of it, which will be the highest building in the city. Blocks B and C consist of 3-4 storey commercial and office areas. A deep excavation system with the diaphragm wall + single bore multiple anchors was constructed. At the corner of the excavation area, steel struts were also used. Excavation depths of blocks vary between 13.30 m and 17.80 m.

In the scope of the soil investigation, 20 cone penetration tests (CPT) and 25 boreholes were performed to define the engineering properties and types of soils. Furthermore, laboratory tests were conducted on undisturbed and disturbed samples. The excavation system was monitored with inclinometers and load cell measurements.

In this chapter, site investigation results are summarized, and soil parameters are estimated by using the recommended methods in the literature. Moreover, the selected section's inclinometers and load cell readings are presented. Soil parameters and monitoring readings of other sections are included in Appendix A.
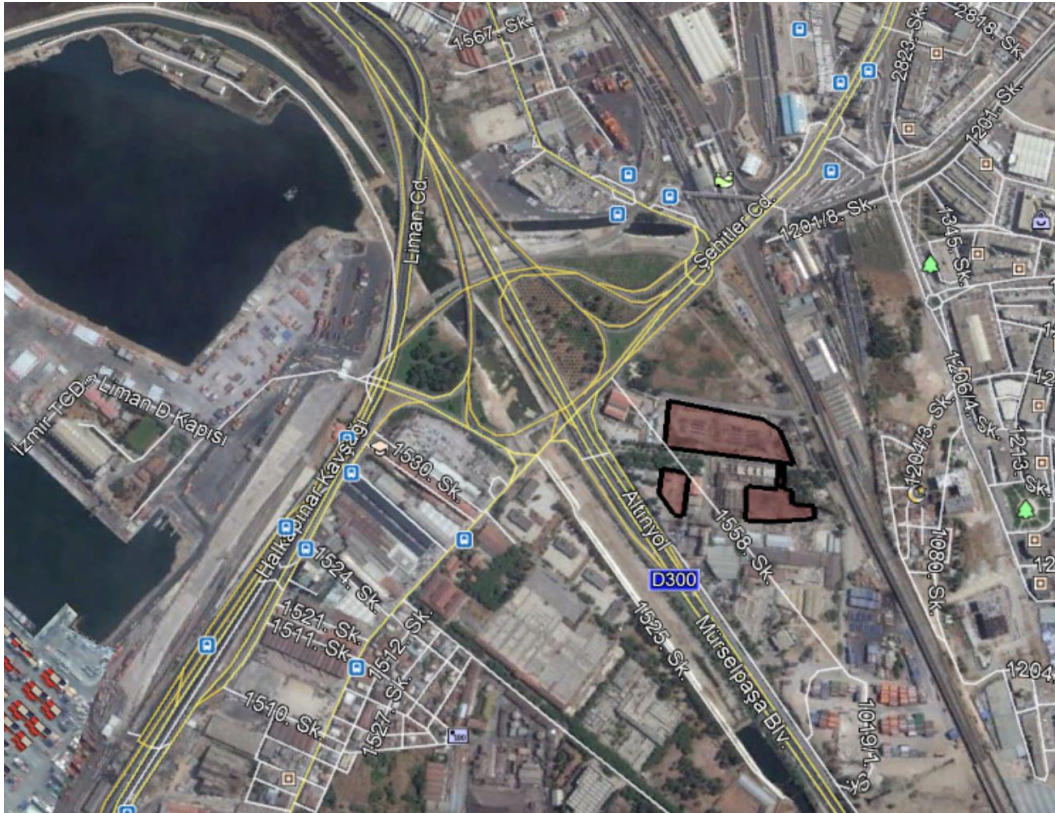
Figure 3.1. Satellite View of the Project

3.2. General Properties of the Excavation System

The elevation of the site is between +1.320 m and +2.323 m. The groundwater level is 1.25 m to 3.60 m below the surface. The thickness of the diaphragm wall is 80 cm. SBMA length of the system is between 18 m and 28 m. The design load of anchors is 650 kN. Moreover, struts with a diameter of 914 mm and a thickness of 13 mm were installed in Block A and Block C. Strut elements are close to inclinometers in Block C. It can be seen in Figure 3.2. Dimension of Block A, B and C are approximately 65m x 205m, 40m x 65m and 65m x 120m respectively. However, their geometries are irregular, which can be seen in Figure 3.2.
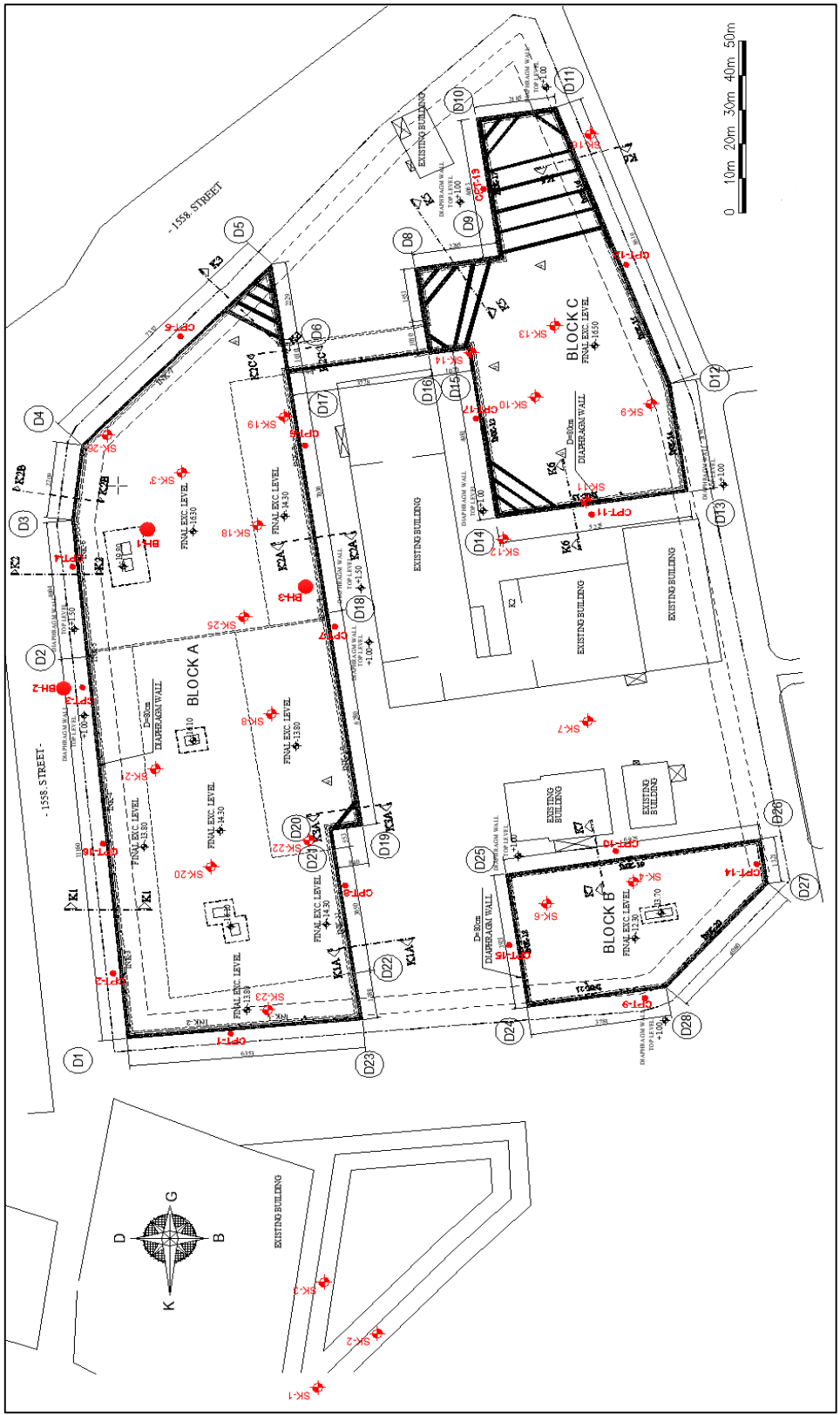
Figure 3.2. Plan View

59

As it can be seen in Figure 3.3, the project site was divided into 7 areas by considering excavation depths, inclinometers, and borehole locations. Soil profiles and parameters were estimated separately for each area. In Chapter 3, soil parameters estimation and monitoring results of area A1/INK-11 are demonstrated. The rest of them are summarized in Appendix A.
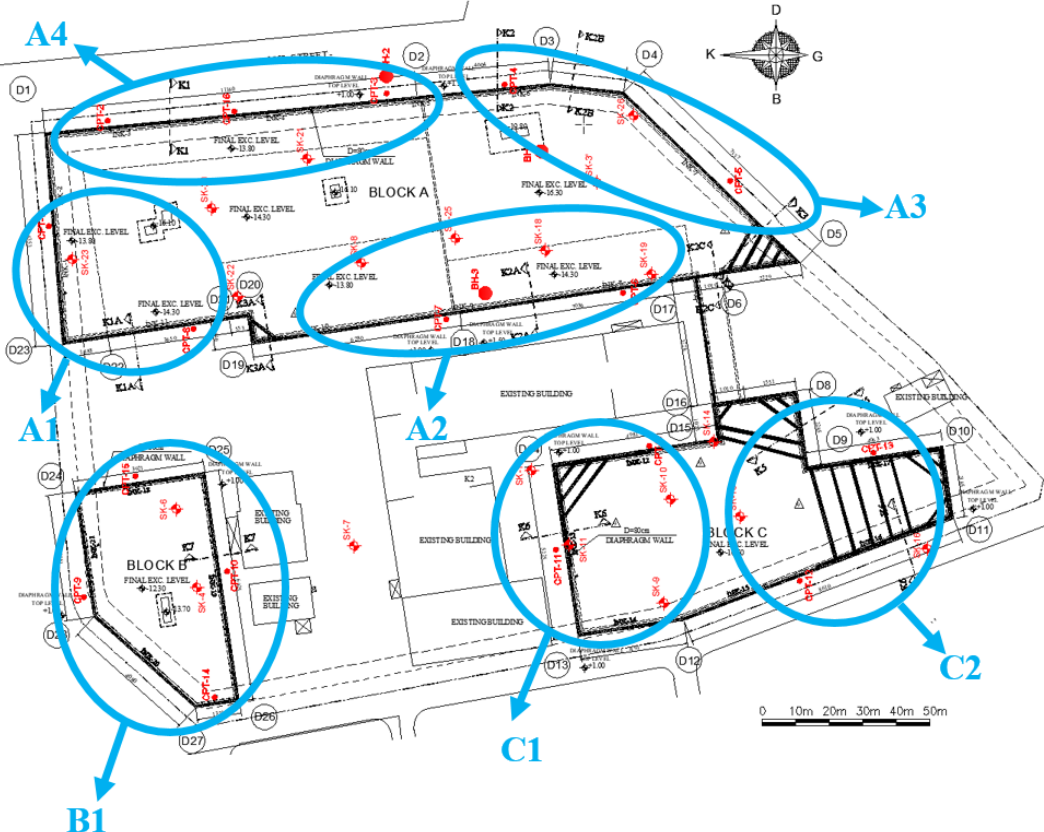
Figure 3.3. Divided Plan View

In Figure 3.4 and 3.5, SPT-N and $N_{1,60}$ versus depth are given. Also, Variation of LL, PL, PI, and w_n versus depth for Area A1 can be seen in Figure 3.6. Cone pentration test results, q_c and f_s versus depth are presented in Figure 3.7 and 3.8.

Area A1
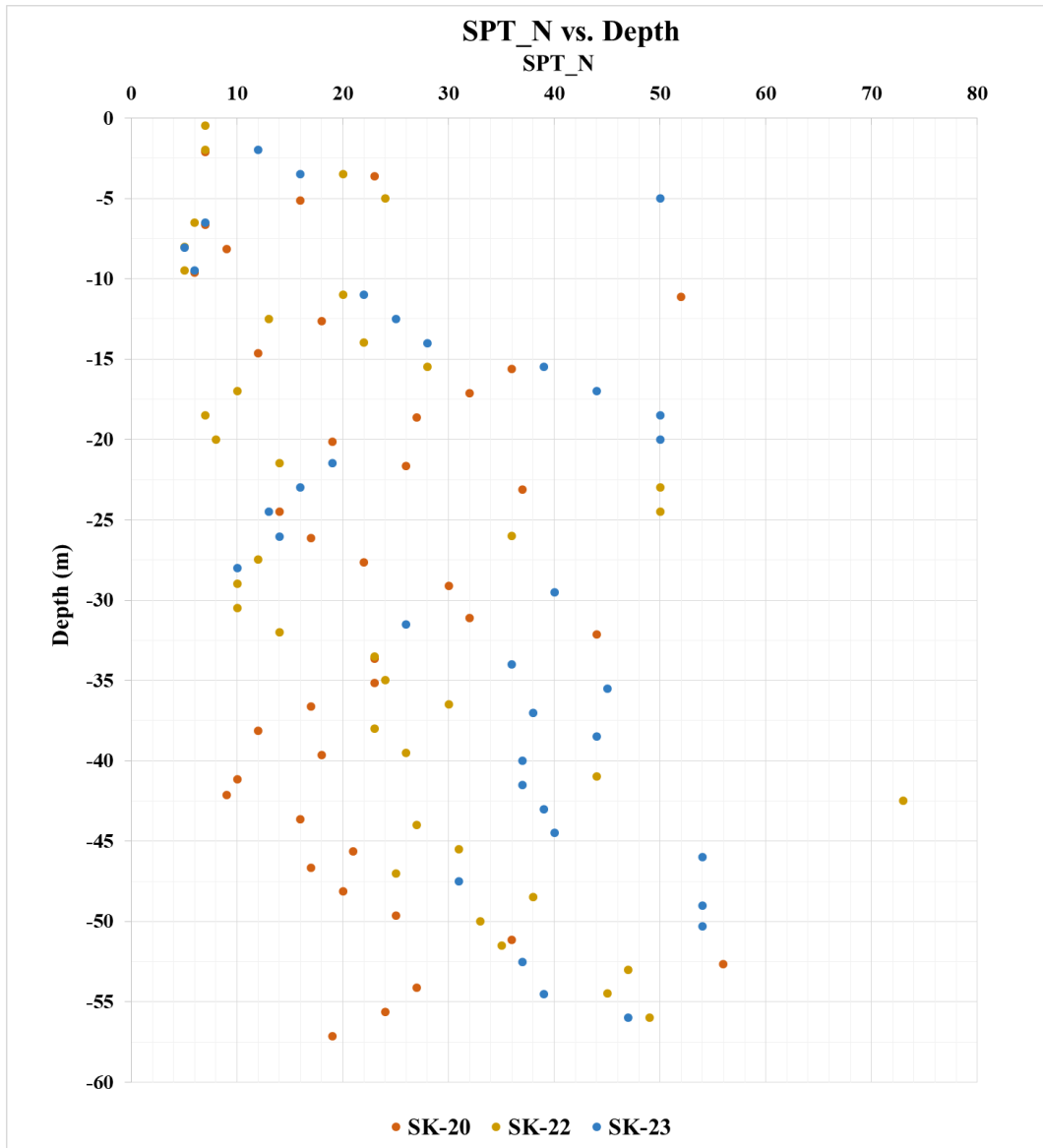
Figure 3.4. SPT-N vs. Depth for Area A1
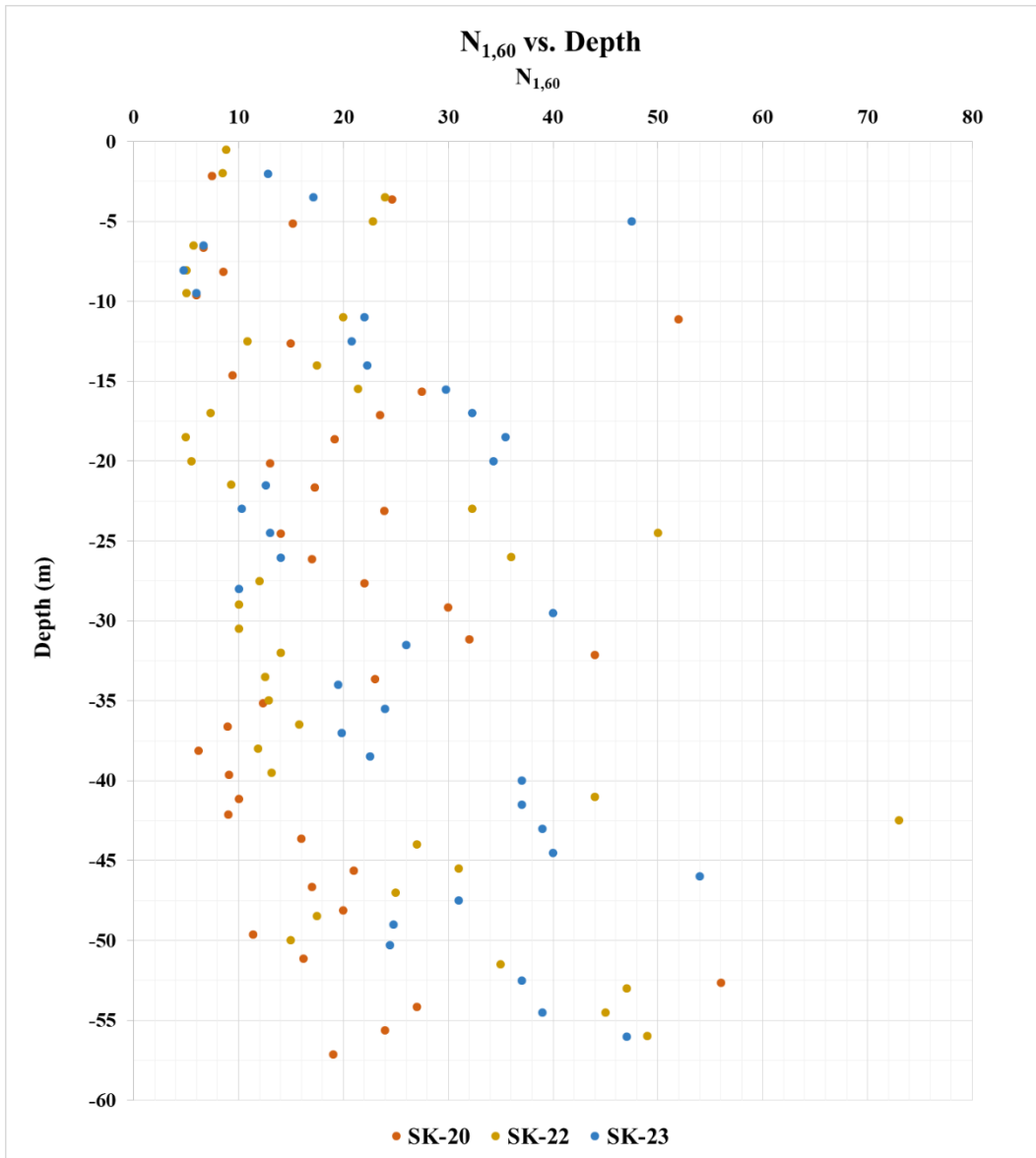
Figure 3.5. SPT-$N_{1,60}$ vs. Depth for Area A1
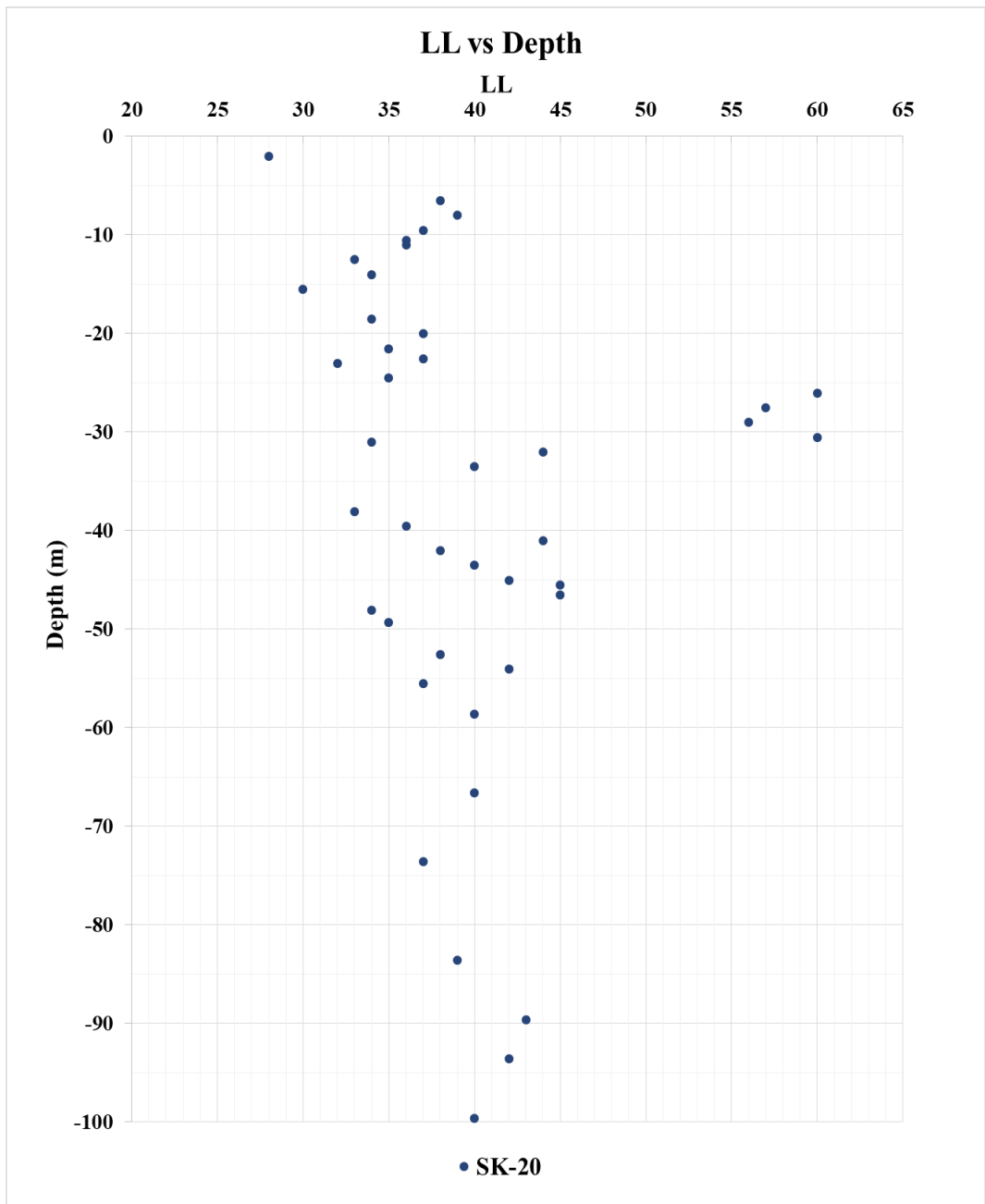
Figure 3.6. LL vs. Depth or Area A1
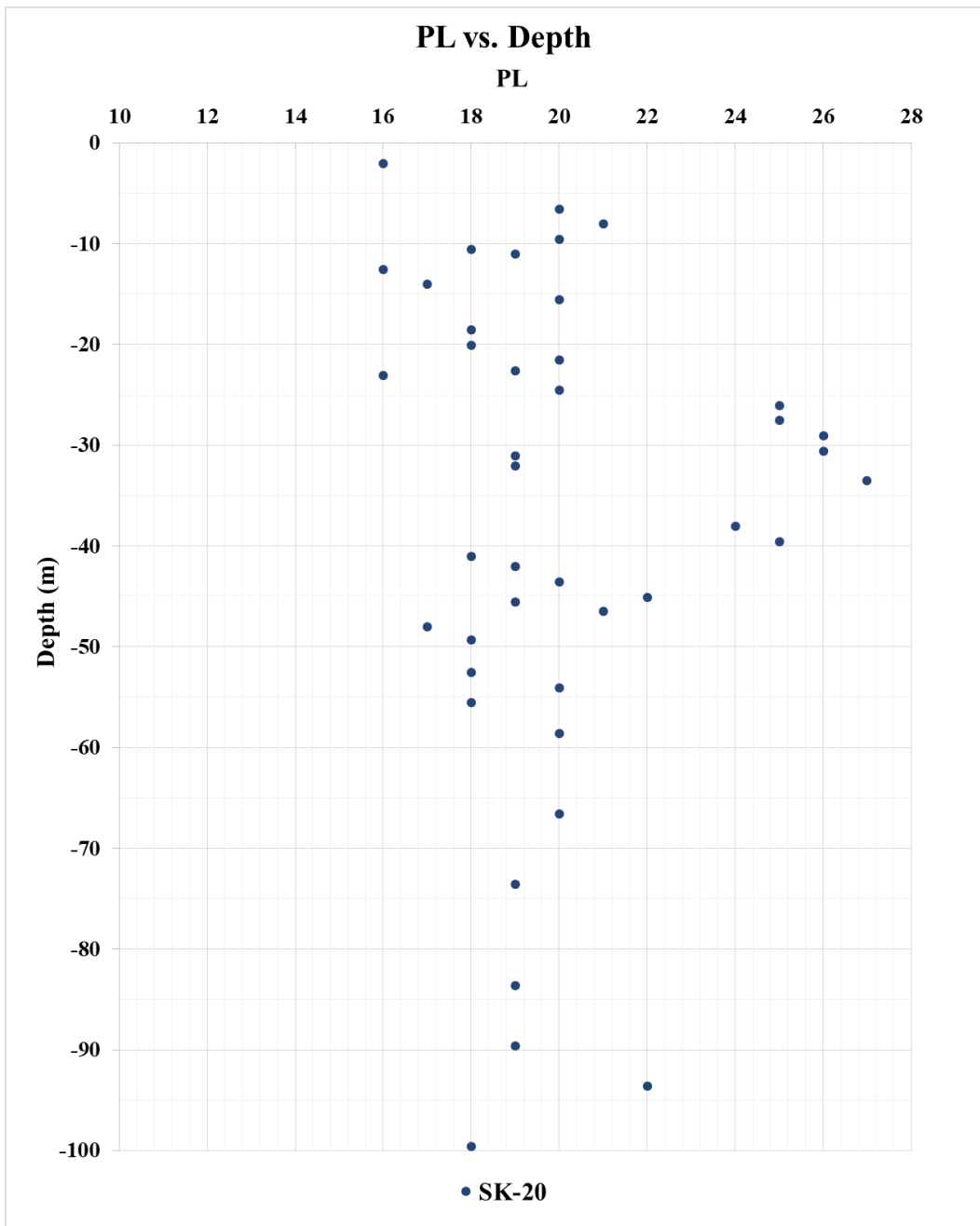
Figure 3.7. PL vs. Depth for Area A1
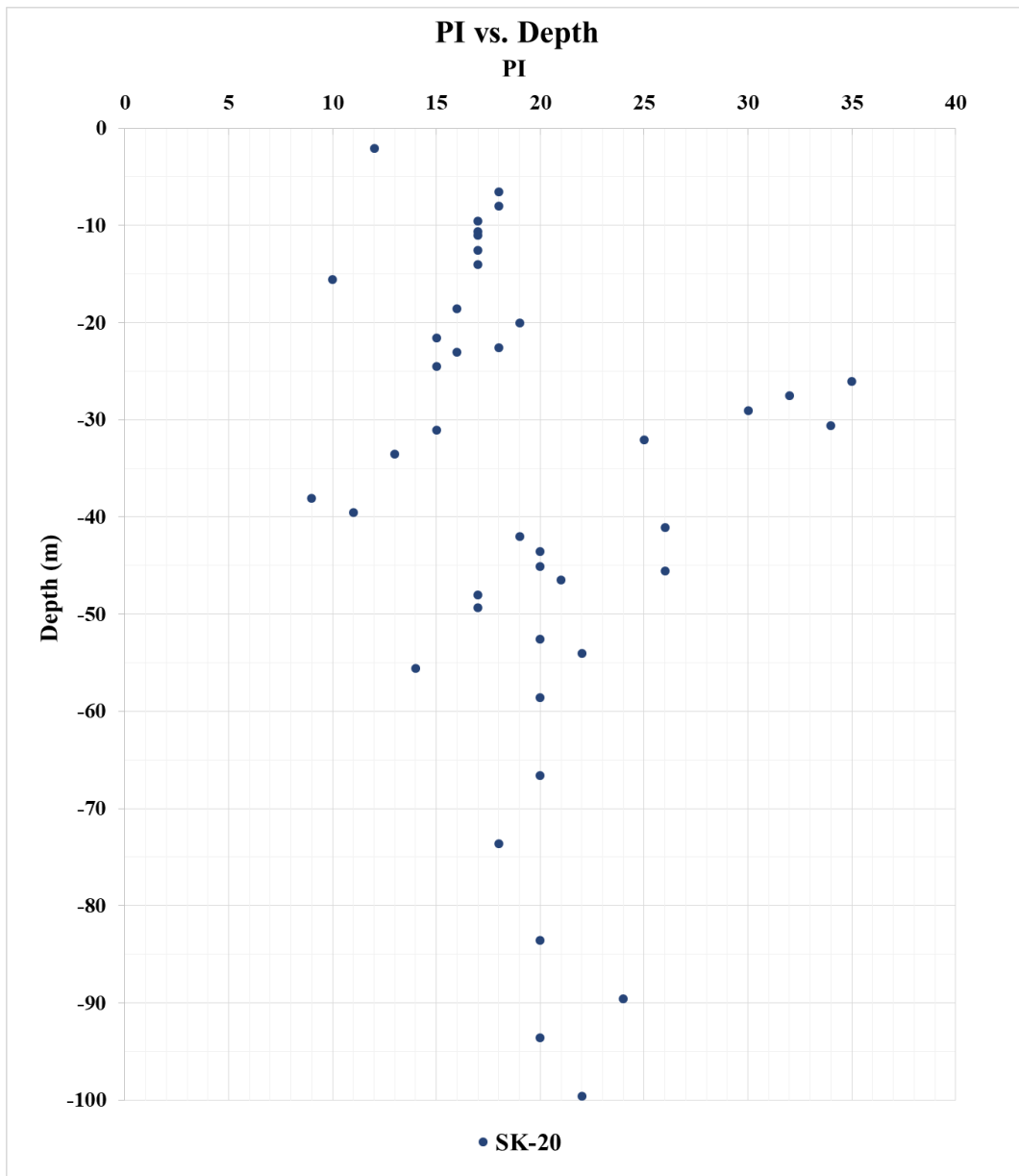
Figure 3.8. PI vs. Depth for Area A1
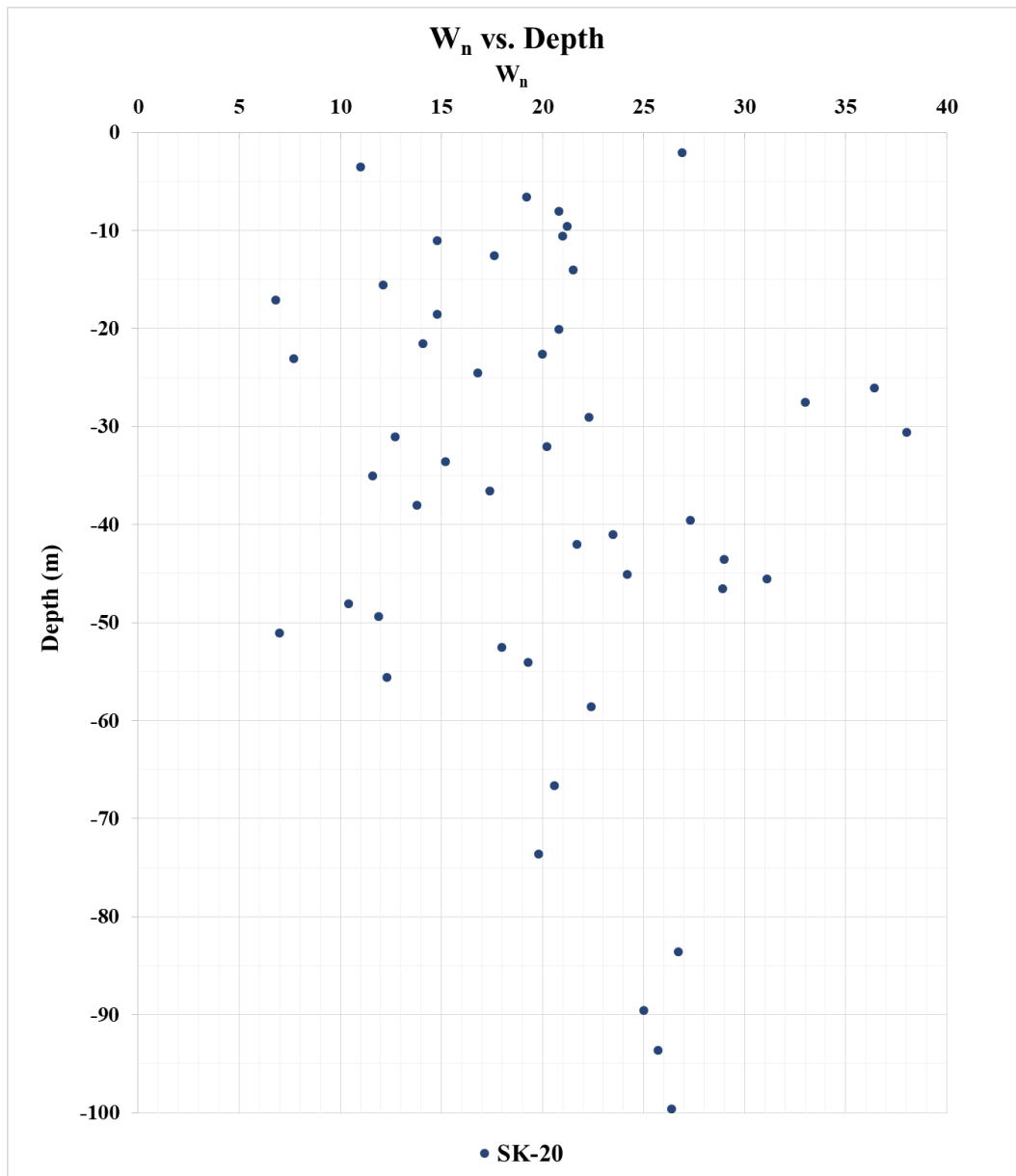
Figure 3.9. w_n vs. Depth for Area A1
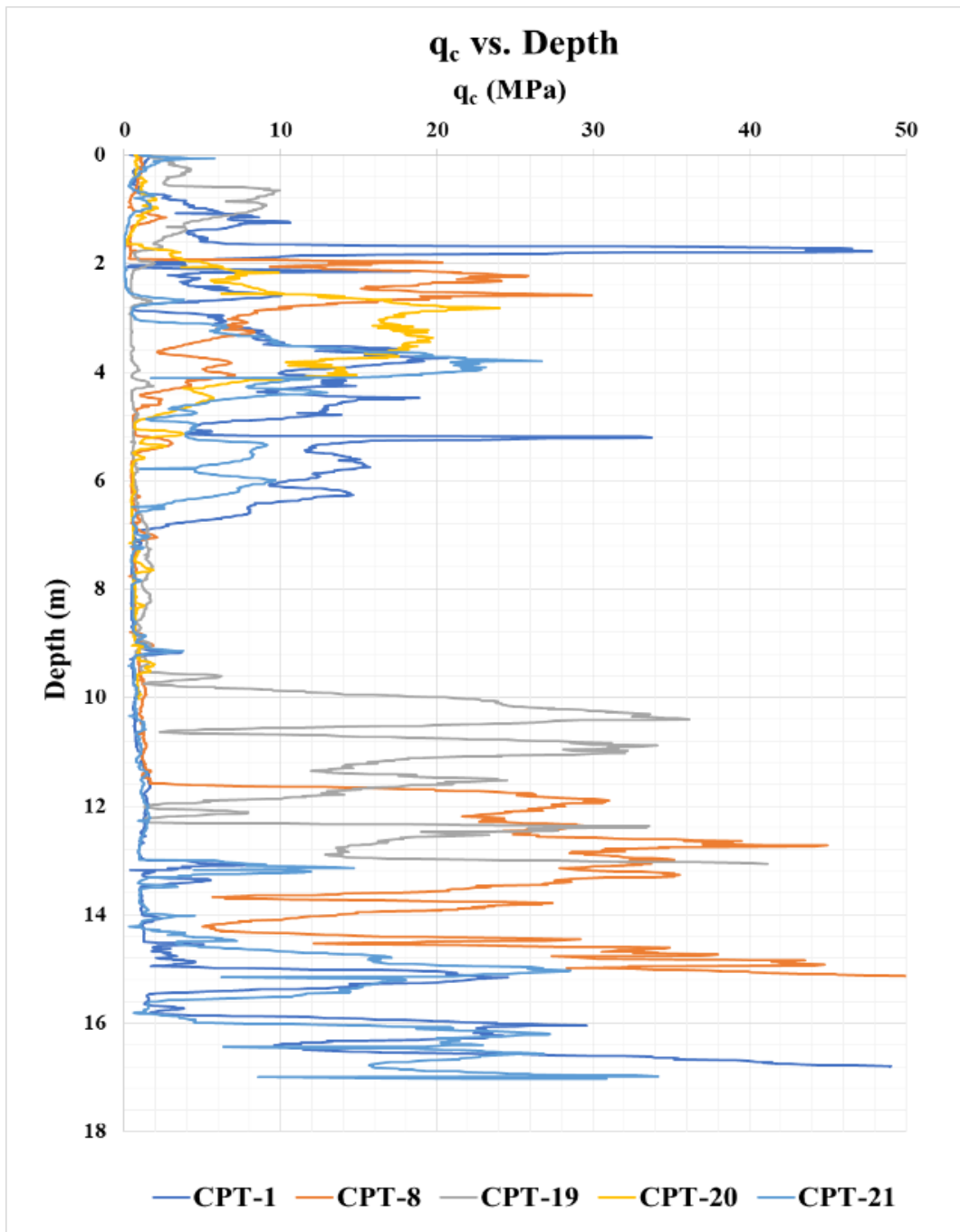
Figure 3.10. Variation of q_c along with the Depth for Area A1
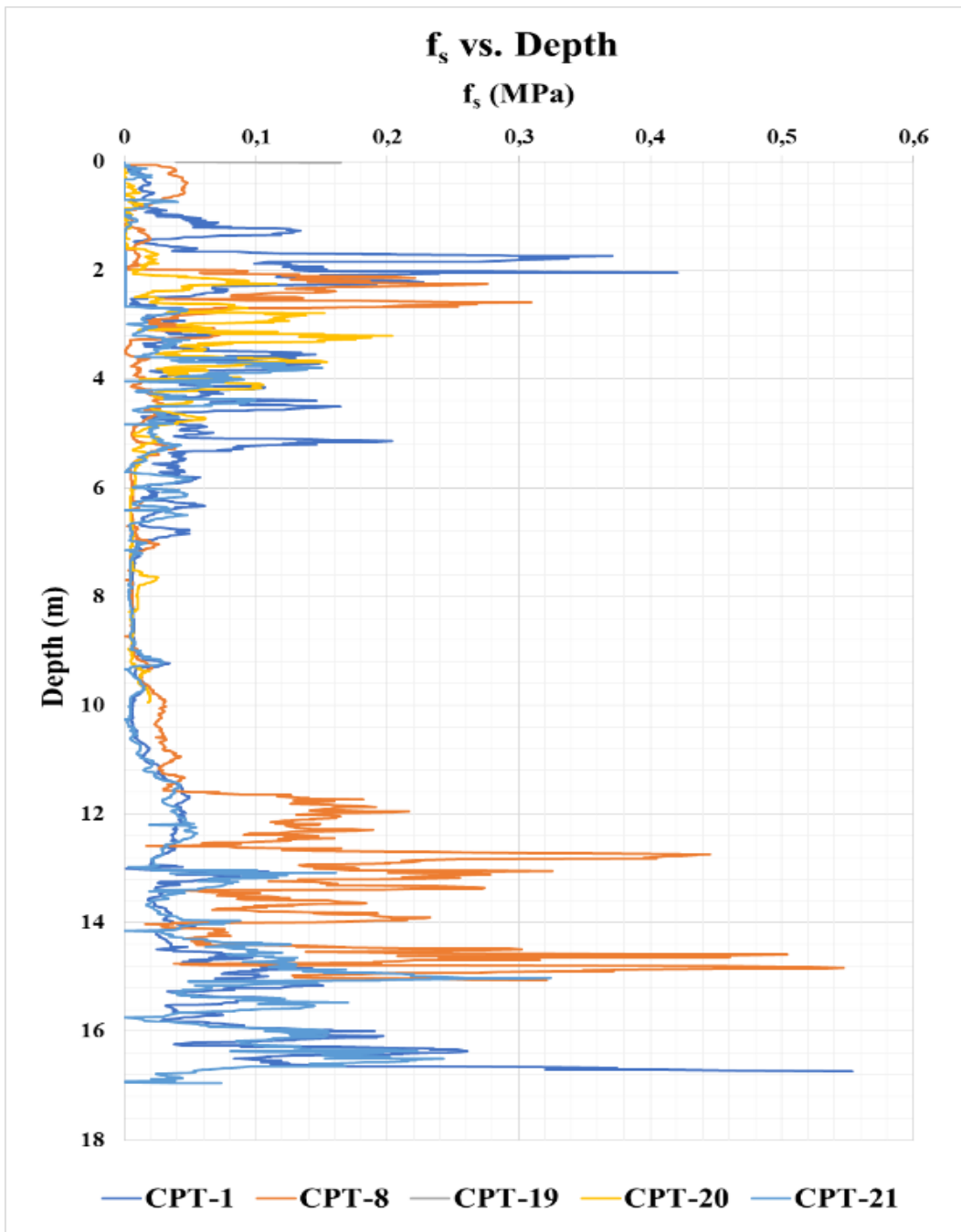
Figure 3.11. Variation of f_s along with the Depth for Area A1

Three boreholes (SK-20, SK-22, and SK-23) and 5 CPT (CPT-1, CPT-8, CPT-19, CPT-20, and CPT-21) were considered. The depths of boreholes change between 50 m to 100 m. Depths of CPT change between 10 m to 17 m. The total depth of boreholes and CPTs is 210 m and 72 m, respectively. Atterberg limit tests were performed on the samples taken from SK-20.

- LL: 28 – 60 % (avg. 39.6 %)
- PL: 16 – 27 % (avg. 20 %)
- PI: 9 – 35 % (avg. 19.3 %)
- w_n: 6.8 – 38 % (avg. 20 %)

Unified soil classification (USCS) was performed for each sample. By considering USCS, SPT $N_{1,60}$ values, and CPT results, the thickness of soil layers were determined. Consolidated Undrained (CU) Triaxial test, Unconsolidated Undrained (UU) Triaxial test, Direct Shear Test, Uniaxial Compression test were performed on soil samples. Test results are summarized in Table 3-1 – 3-4. It can be seen that the depth of most of samples are higher than 40 m. Unfortunately, after close inspection of the available laboratory test, some unrealistic combinations of cohesion and friction were observed (e.g.: non-zero friction angle values in undrained testing reaching to as high as 10 degrees; cohesion in excess of 250 kPa for depths with SPT 20-25 blows/30 cm). Hence field test results were given priority to assess the modeling parameters.

Table 3.1. Triaxial Test (CU) Results

Borehole No	Elevation (m)			Triaxial Test (CU)	
				c (kPa)	φ (°)
BH-01	-33.90	-	-34.40	268	7
	-60.90	-	-61.40	199	10
	-89.40	-	-89.90	222	13
BH-02	-41.50	-	-42.00	76	10
	-70.00	-	-70.50	206	11
BH-03	-30.50	-	-31.00	26	18
	-35.20	-	-35.70	75	15
	-45.70	-	-46.20	87	11
	-65.20	-	-65.70	179	11
	-80.20	-	-80.70	217	6
	-90.20	-	-90.70	29	16

Table 3.2. Direct Shear Test Results

Borehole No	Elevation (m)			Direct Shear	
				c (kPa)	φ (°)
BH-1	-27.90	-	-28.40	222	17
	-72.35	-	-73.40	183	13
	-74.98	-	-76.40	86	13
	-78.35	-	-79.40	139	16
	-91.85	-	-92.90	74	20
	-99.35	-	-100.40	42	21
	-102.35	-	-103.40	194	15
BH-02	-22.00	-	-22.50	71	22
	-36.45	-	-37.00	21	22
	-61.00	-	-62.50	15	22
	-76.00	-	-76.50	339	15
	-106.45	-	-107.50	141	19
	-127.00	-	-128.00	327	20
BH-03	-33.15	-	-34.20	30.3	26.1
	-48.15	-	-49.20	63.7	20
	-116.97	-	-118.20	87	11

Table 3.3. Triaxial Test (UU) Results

Borehole No	Elevation (m)			Triaxial Test (UU)	
				c (kPa)	φ (⁰)
BH-01	-63.35	-	-64.40	226	0
	-72.35	-	-73.40	967	0
	-74.98	-	-76.40	752	0
	-85.85	-	-86.90	375	0
	-88.85	-	-89.40	403	0
	-94.44	-	-95.90	518	0
	-97.85	-	-98.90	988	0
	-102.35	-	-103.40	734	0
BH-02	-32.50	-	-34.00	115	0
	-37.00	-	-38.50	132	0
	-59.50	-	-61.00	315	0
	-62.50	-	-64.00	196	0
	-67.00	-	-68.50	143	0
	-71.50	-	-73.00	214	0
	-74.50	-	-76.00	297	0
	-77.50	-	-79.00	144	0
	-83.50	-	-85.00	159	0
	-85.00	-	-86.50	270	0
	-86.50	-	-88.00	256	0
	-91.00	-	-92.50	201	0
	-103.00	-	-104.50	276	0
BH-03	-9.15	-	-10.20	37	0
	-10.65	-	-11.70	47	0
	-28.65	-	-29.60	123	0
	-31.65	-	-32.70	79	0
	-34.65	-	-35.20	218	0
	-45.15	-	-45.70	178	0
	-48.15	-	-49.20	69	0
	-58.65	-	-59.70	143	0
	-69.15	-	-70.20	331	0
	-76.65	-	-77.70	248	0
	-79.20	-	-80.20	186	0
	-88.65	-	-89.70	224	0
	-91.65	-	-92.70	115	0
	-116.97	-	-118.20	347	0
	-120.15	-	-121.20	97	0

Table 3.4. Uniaxial Test Results

Borehole No	Elevation (m)			Uniaxial Test c_u (kPa)
BH-02	-27.50	-	-28.00	52
	-31.00	-	-32.50	51
	-70.50	-	-71.50	120
	-89.50	-	-91.00	161
	-93.00	-	-94.00	46
	-100.50	-	-101.50	94
	-125.95	-	-127.00	214
BH-03	-12.15	-	-13.20	74
	-20.20	-	-20.70	53
	-30.15	-	-30.70	72
	-33.15	-	-34.20	20
	-36.15	-	-37.20	55
	-46.65	-	-47.70	91
	-49.65	-	-50.70	94
	-61.65	-	-62.70	97
	-64.65	-	-65.20	125
	-82.65	-	-83.70	148
	-118.41	-	-119.70	300
	-121.65	-	-122.7	85
SK-02	-6.55	-	-7.05	24
	-12.55	-	-13.05	60
	-23.05	-	-24.05	31
SK-06	-6.95	-	-7.95	21
	-26.45	-	-27.45	89
	-28.95	-	-29.45	92

Table 3.4. Uniaxial Test Results (Cont'd)

Borehole No	Elevation (m)			Uniaxial Test c_u (kPa)
SK-08	-7.25	-	-7.75	42
	-13.75	-	-14.75	90
	-34.25	-	-34.75	88
	-60.25	-	-61.25	130
	-61.25	-	-64.25	135
	-67.25	-	-70.25	141
	-85.25	-	-86.25	142
	-88.25	-	-89.25	153
SK-16	-27.70	-	-28.20	25
SK-18	-13.70	-	-14.20	39
	-23.20	-	-23.70	92
	-27.70	-	-28.20	67
	-31.70	-	-32.20	85
	-54.20	-	-55.20	109
	-58.20	-	-59.20	115
	-66.70	-	-67.20	120
	-76.20	-	-77.20	130
	-88.20	-	-89.20	158
	-113.20	-	-114.20	132
	-138.20	-	-139.20	178
	-149.20	-	-150.20	144
SK-20	-30.20	-	-30.70	90
	-57.70	-	-58.70	110
	-65.70	-	-66.70	120
	-72.70	-	-73.70	132
	-82.70	-	-83.70	140
	-92.70	-	-93.70	162
	-98.70	-	-99.70	170

Cohesionless Layers

SPT-N values of cohesionless layers change between 14 and 38 blows/30 cm. Furthermore, $(N_1)_{60}$ and N_{60} values of the cohesionless layer are 15 to 19 blows/30 cm and 11 to 38 blows/30 cm, respectively.

According to Çetin et al. (2016) recommendation given in Table 2.8, wet and saturated unit weight of cohesionless soil changes from 19.2 to 20 kN/m³ and from 20 to 21.6 kN/m³, respectively, by considering N_{60}.

For the estimation of the friction angle of cohesionless layers, Peck et al. (1974) and Osaki's (2002) recommendations, which are based on $(N_1)_{60}$ and N_{60} values, are used. Furthermore, Robertson and Campanella (1983) and Kulhawy and Mayne (1990) figured out correlations to estimate friction angle with cone penetration test results. The depth of cone penetration tests can be used only to characterize the first cohesionless layer. For this layer, the friction angle is between 39.5º and 43.4º. Due to the depth of CPTs, soil layers are characterized by using the standard penetration test results. According to the SPT results, recommended friction angles are from 29.8º to 42.6º. The selected friction angles are between 31 and 36º.

Dilatancy angles of cohesionless soils can be calculated by extracting 30 from the friction angles by using the proposal of Brinkgreve (2008) in Eqn. 2-24. They change between 1º and 6º. Effective cohesion values are taken as 2 to 3 kPa by considering the fines content and plasticity index.

Stiffness parameters of the hardening soil model are estimated using the relation of Brinkgreve et al. (2010) given in Eqn. 2-35, 2-36 and, 2-38. For these equations, the relative densities of soil are required. The suggestion of Plaxis 2D Material Manuels (2021) is used to estimate relative density. RD of soils is in between 58 % and 65 %.

For these values of RD, E_{50}^{ref} and E_{oed}^{ref} can be estimated as between 35 MPa and 40 MPa. E_{ur}^{ref} values are there times of E_{50}^{ref}. They change from 105 MPa to 120 MPa.

Brinkgreve (2005) recommended that power (m) can be taken as 0.5 for cohesionless soils. Furthermore, ν_{ur} and R_f are adopted as 0.2 and 0.9 falling in commonly used range, respectively.

Cohesive Layers

SPT-N values of cohesive layers change between 16 and 39 blows/30 cm. Furthermore, N_{60} values of the cohesionless layer are 16 to 39 blows/30 cm.

The wet and saturated unit weights of soils are selected as 18.4 and 20 kN/m^3, respectively, according to Çetin et al. (2016).

Stroud (1974) figured out a chart to estimate a constant related to PI value. Also, this constant can be used to calculate the undrained shear strength of soils. According to Stroud (1974), undrained shear strength change between 95 kPa and 217 kPa. Furthermore, according to Osaki (2002), undrained shear strength values are 100 to 244 kPa. The selected values are from 100 kPa to 230 kPa as an average. Effective cohesion can be found by dividing undrained shear strength by 10, according to Sorensen and Okkels (2013).

Terzaghi et al. (1996) and Gibson (1953) figured out charts to estimate the friction angle of cohesive soil depending on the plasticity index. According to Gibson (1953), friction angles are from 28.3º to 29.5º. Moreover, according to Terzaghi et al. (1996), friction angles are from 30.5º to 37.5º. The selected values are between 29.9º and 30.5º.

Diltancy angles can be calculated similarly to cohesionless soils. They are from 0 to 0.5º.

Furthermore, Stroud (1974) figured out another chart for the estimation of the coefficient of volume compressibility. Estimated parameters are between 0.442×10^{-4} and 1.040×10^{-4}. E_{oed} can be calculated by taking the inverse of the m_v in Eqn. 2-40. In addition, the E_{50} value can be chosen as two times of E_{oed} in Eqn. 2-41, according to Brinkgreve (2005). As similar to cohesionless soils, E_{ur} can be selected as $3 \times E_{50}$. As a result, E_{50} values are from 19.2 MPa to 45.2 MPa. E_{oed} values are between 9.6 MPa and 22.6 MPa. E_{ur} values are selected between 57.6 MPa and 135.7 MPa.

Brinkgreve (2005) recommended that power (m) can be taken as 1.0 for cohesive soils. Furthermore, ν_{ur} and R_f are 0.2 and 0.9 as a default, respectively.

The summarized soil parameters of Area 1 are given in Table 3.5. Also, idealized soil profile is presented in Figure 3.12.

Table 3.5. Soil Profile of Area 1 (A1)

Layer No	Elevation (m)		USCS	Type	Thickness (m)	N	$N_{1,60}$	N_{60}	PI	y_{wet} (kN/m³)	y_{sat} (kN/m³)	c_u (kPa)	c (kPa)	φ (°)	ψ (°)	ν	E_{50}^{ref} (MPa)	E_{oed}^{ref} (MPa)	E_{ur}^{ref} (MPa)	m	ν_{ur}	p_{ref} (kPa)	R_f
1	1.4	-3.6	SC-SM	Cohesionless	5.0	14.0	15.0	11.0	6.0	19.2	20.0	-	2.0	31.0	1.0	0.33	35.0	35.0	105.0	0.5	0.2	100.0	0.9
2	-3.6	-13.0	CL	Cohesive	8.0	16.0	16.0	16.0	17.3	18.4	20.0	100.0	10.0	30.5	0.5	0.33	19.2	9.6	57.6	1.0	0.2	106.1	0.9
3	-13.0	-24.5	GC-SC	Cohesionless	11.5	27.0	19.0	27.0	13.4	19.2	20.0	-	3.0	35.0	5.0	0.30	40.0	40.0	120.0	0.5	0.2	100.0	0.9
4	-24.5	-27.5	CL-ML	Cohesive	3.0	25.0	25.0	25.0	21.0	18.4	20.0	140.0	14.0	30.0	0.0	0.33	27.2	13.6	81.6	1.0	0.2	276.1	0.9
5	-27.5	-33.5	SM-ML	Cohesionless	6.0	28.0	15.0	28.0	5.0	19.2	20.0	-	3.0	33.0	3.0	0.31	35.0	35.0	105.0	0.5	0.2	100.0	0.9
6	-33.5	-42.0	CL	Cohesive	8.5	32.0	32.0	32.0	21.3	18.4	20.0	180.0	18.0	29.9	0.0	0.33	36.8	18.4	110.4	1.0	0.2	393.6	0.9
7	-42.0	-45.0	GP-GC	Cohesionless	3.0	38.0	19.0	38.0	8.5	20.0	21.6	-	3.0	36.0	6.0	0.29	40.0	40.0	120.0	0.5	0.2	100.0	0.9
8	-45.0	-52.5	CL	Cohesive	7.5	39.0	39.0	39.0	19.0	18.4	20.0	230.0	23.0	30.1	0.1	0.33	45.2	22.6	135.7	1.0	0.2	508.4	0.9

Figure 3.12. Idealized Soil Profile of A1

CHAPTER 4

4. AVAILABLE MONITORING DATA

Inclinometer

Inclinometer measurements are made with the inclinometer probe shown in Figure 4.1. There are two wheels opposite each other on the upper and lower parts of the probe. These wheels are supported by springs and provide adaptation according to the diameter of the well and the narrowing condition. Inclinometer tube; As seen in Figure 4.2, it is a plastic tube with a plus sign inside, grooved for the probe rollers to descend easily at every 90°.
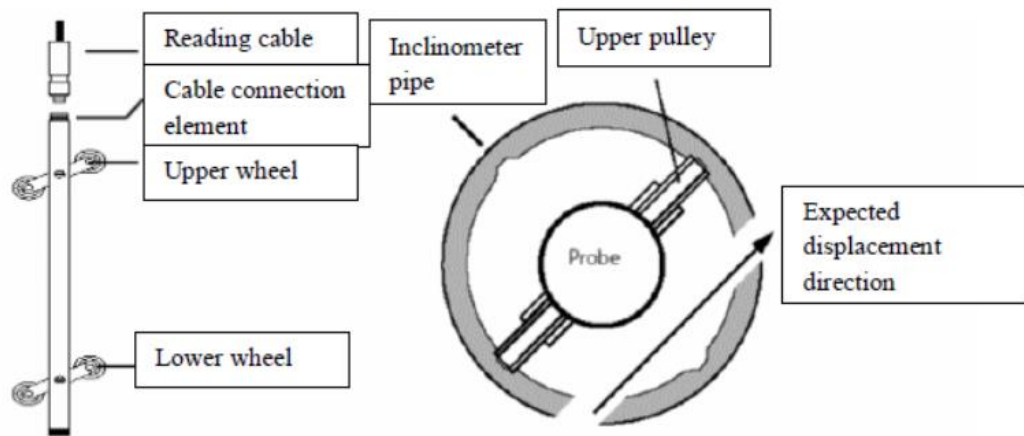
Figure 4.1. Inclinometer Probe
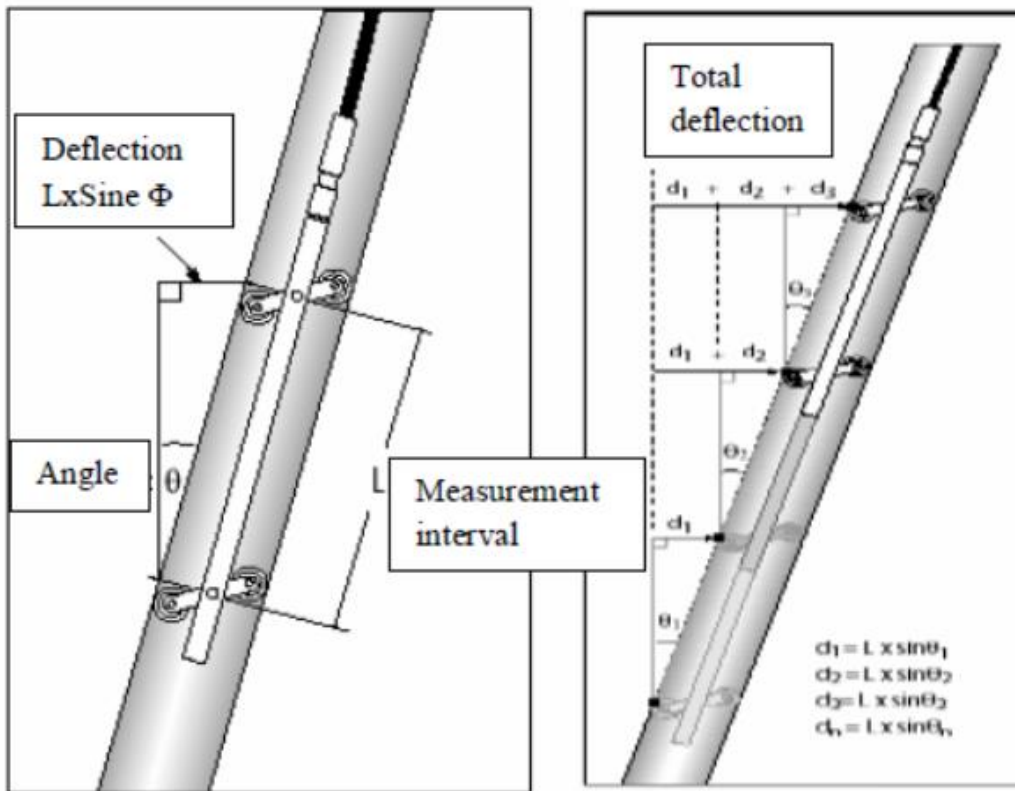
Figure 4.2. Plastic Tube of Inclinometer

Four devices are used for inclinometer monitoring. These are listed below;

- Reading unit (Probe/Sensor)

- Recording unit

- Cables transferring data from reading unit to recording unit

- The pulley system enables the cable to move in upward and downward directions

Locked caps prevent inclinometer casings from damage. In addition, for the installation of inclinometer pipes, drilling is done with drilling equipment up to 5 meters below the toe level of the diaphragm wall. Schematic sketch of the section of the diaphragm wall can be seen in Figure 4.3.
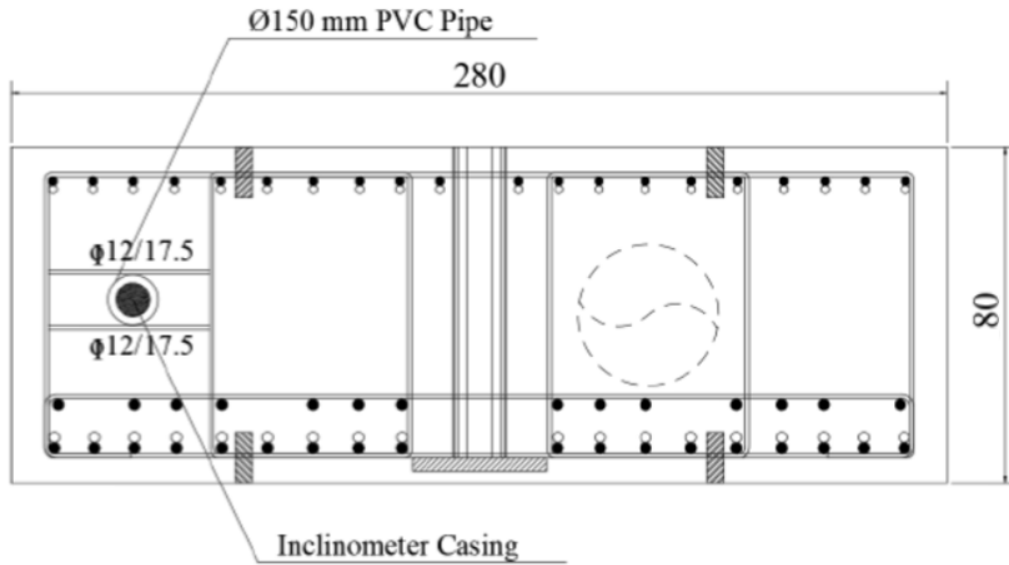
Figure 4.3. Schematic Sketch of Diaphragm Wall

A cable connection is made with the inclinometer reader unit. One of the readers is inserted into the pipe by passing through the pipe grooves with the upper wheels facing forward. With the help of the pulley, the cable is lowered to the reading depth.

Project name, inclinometer number, sensor number, sensor type, unit system, sensor constant, measurement starting and end depth, and an interval of measurement are entered into the recorder. Starting from the measurement starting depth, the sensor is pulled up at the determined measurement intervals, and the readings are recorded until the end.

This reading is known as an A_0 (A zero) direction reading. After taking the zero reading, the sensor is removed from the pipe, rotated 180°, and inserted into the pipe by passing it through the pipe grooves with the lower wheels coming forward, the measurement is lowered to the starting depth, and the readings are recorded until the measurement end depth by pulling it up again at the determined measuring intervals. This reading is named as A_{180} reading. After the A_{180} reading, the measurement process is completed. Readings are evaluated by transferring them to the software.

Load Cell

The measurement of anchor loads is made by using the system given in Figure 4.4. The load cell consists of eight numbers of high-strength cylindrical steel and a winding roll. To minimize eccentricity and non-uniform loads, 8 high-strength steels are mounted at a 45-degree angle to each other. For the accuracy of the readings, it is installed above the anchor plate which distributes the load. The surface of the anchor plate must be smooth in order to take precise readings during the pre-stressing. In the project, nine load cells were used. All of them were placed on the top anchors.
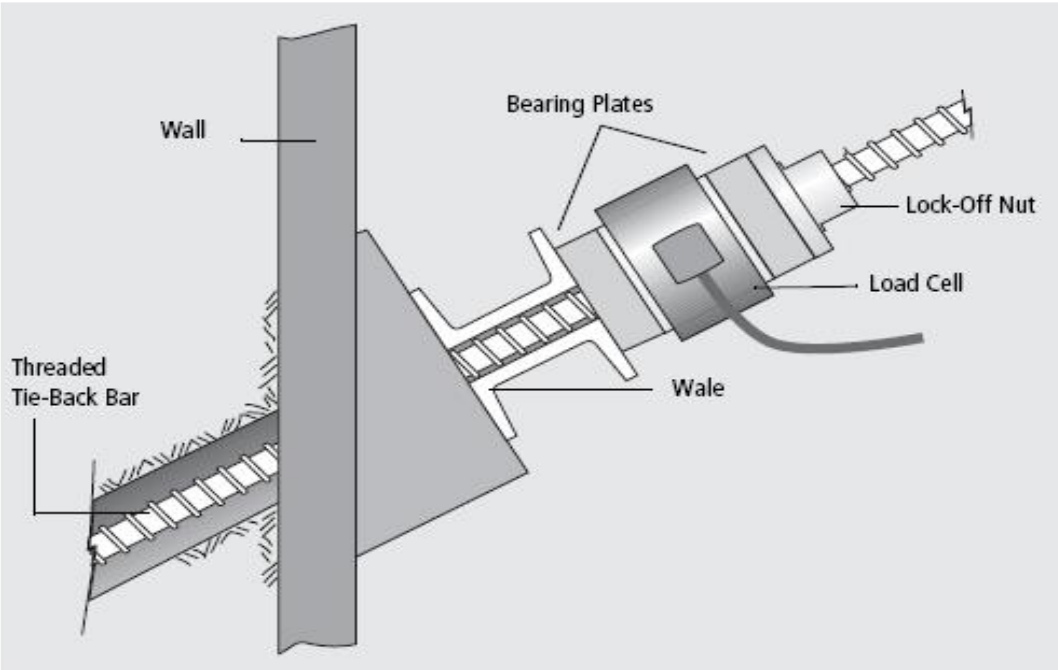
Figure 4.4. Schematic View of Load Cell System

The section view of 1A-1A is given in Figure 4.5 and section properties are summarized in Table 4.1. Measurements of INK-11 are presented in Figures 4.6 – 4.10 for each excavation stage. Load cell measurements can be shown in Figure 4.11.

The quality of the inclinometer readings was examined by controlling the displacement in transverse direction. It is assumed that all readings are correct. Also, three inclinometers were extracted from the data set. The reasons for extraction are broken, clogging, or the quality of readings.
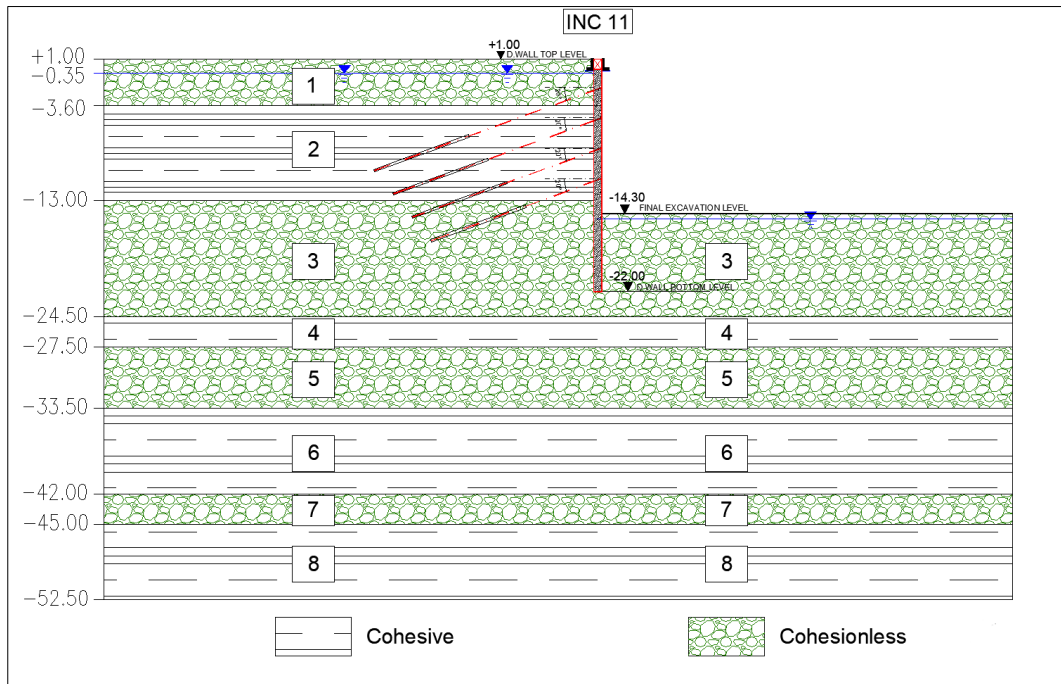
Figure 4.5. Section 1A – 1A

Table 4.1. Section Properties of 1A – 1A

SECTION 1A - 1A									
Diaphragm Wall			SBMA Type Anchor				Excavation Properties		
Top Level (m)	Bottom Level (m)	Length (m)	Anchor No	Anchor Level (m)	Anchor Length (m)	Horizontal Spacing (m)	Top Level (m)	Bottom Level (m)	Depth (m)
1.00	-22.00	23.00	1	-1.80	24.00	2.00	1.00	-14.30	15.30
			2	-4.80	22.00	2.00			
			3	-7.80	20.00	2.00			
			4	-10.80	18.00	2.00			

4.1. Measured Displacements of INK-11
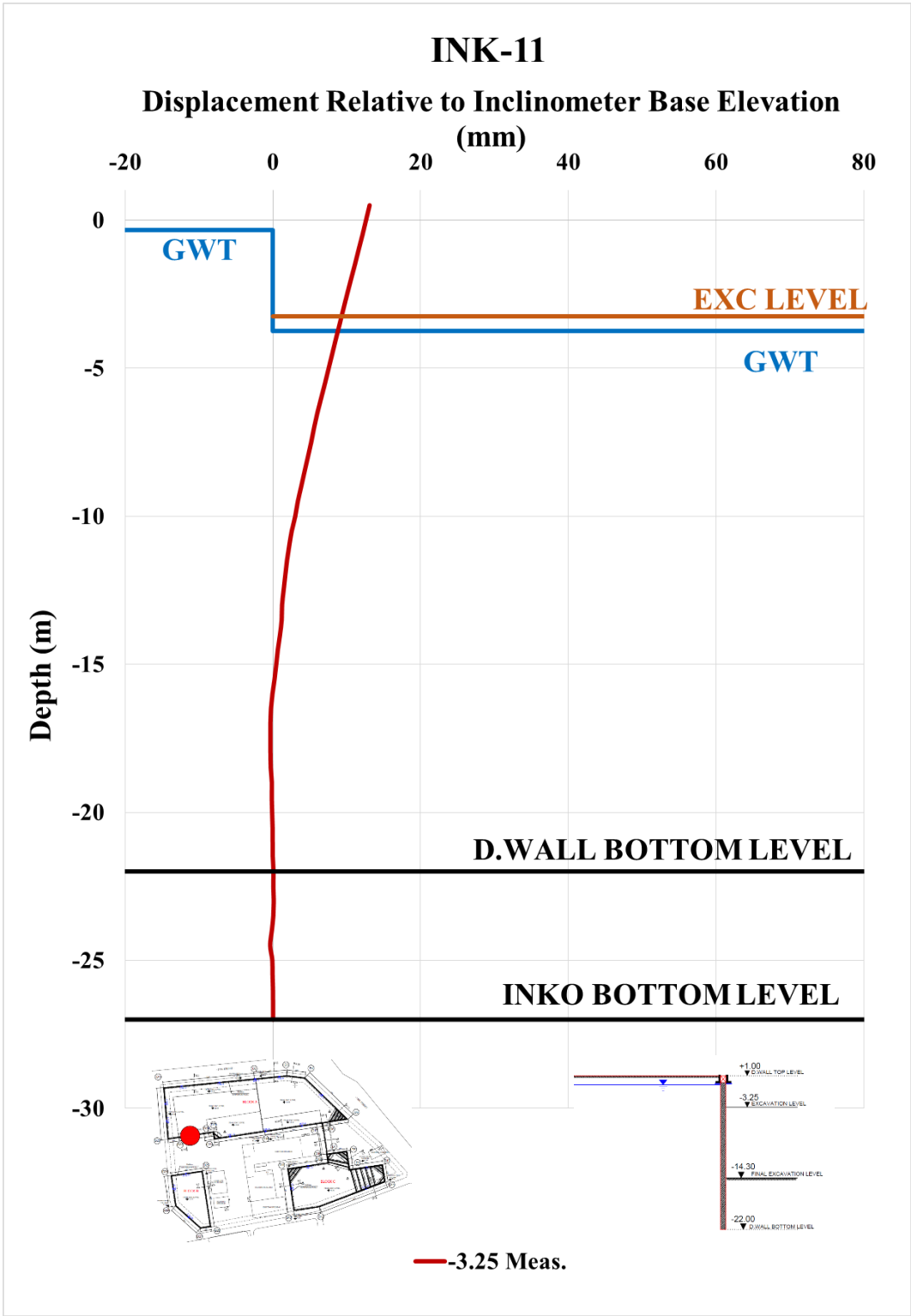
Figure 4.6. Measured Displ. Rel. Inc. Base Elev. At -3.25 m
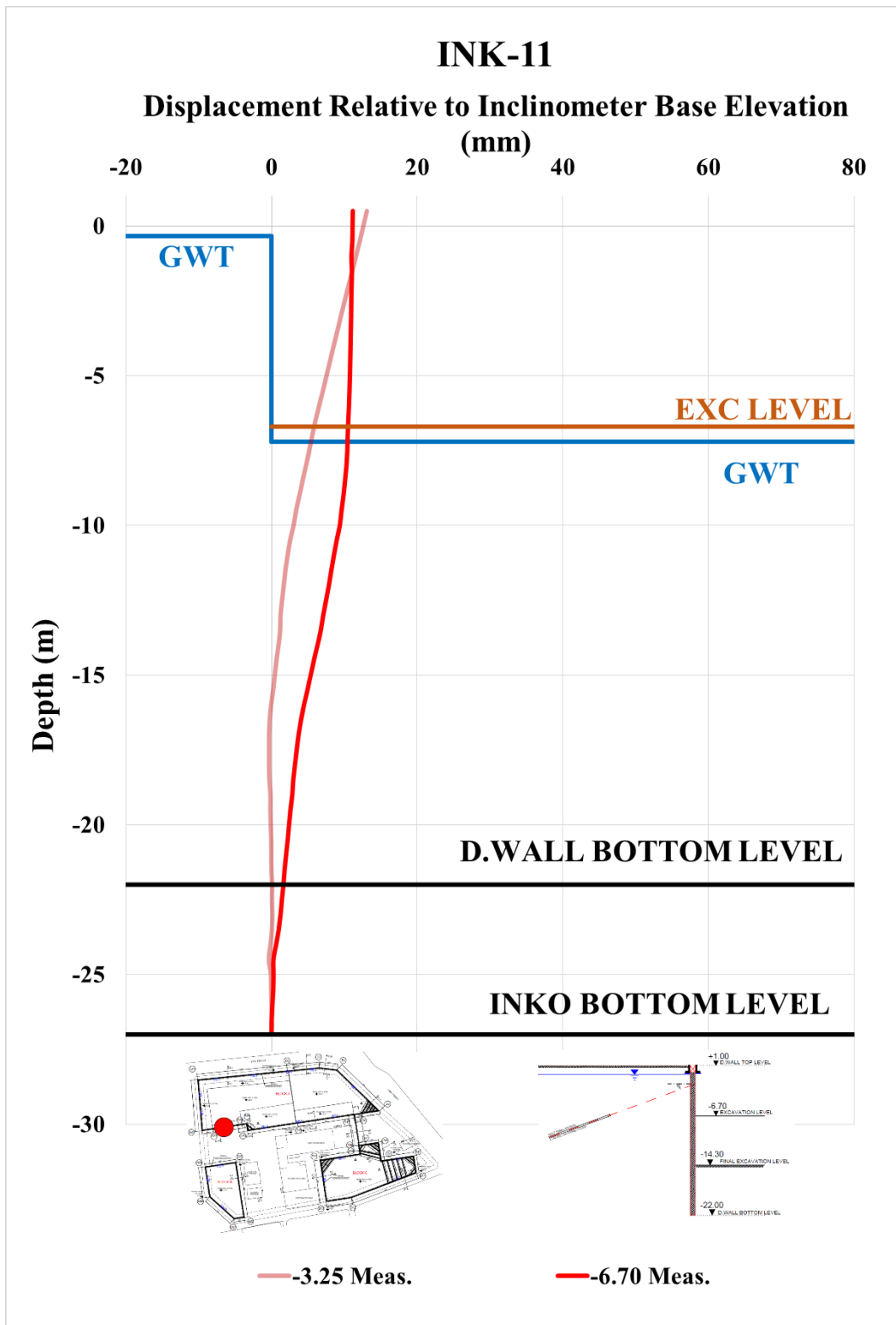
Figure 4.7. Measured Displ. Rel. Inc. Base Elev. At -6.70 m
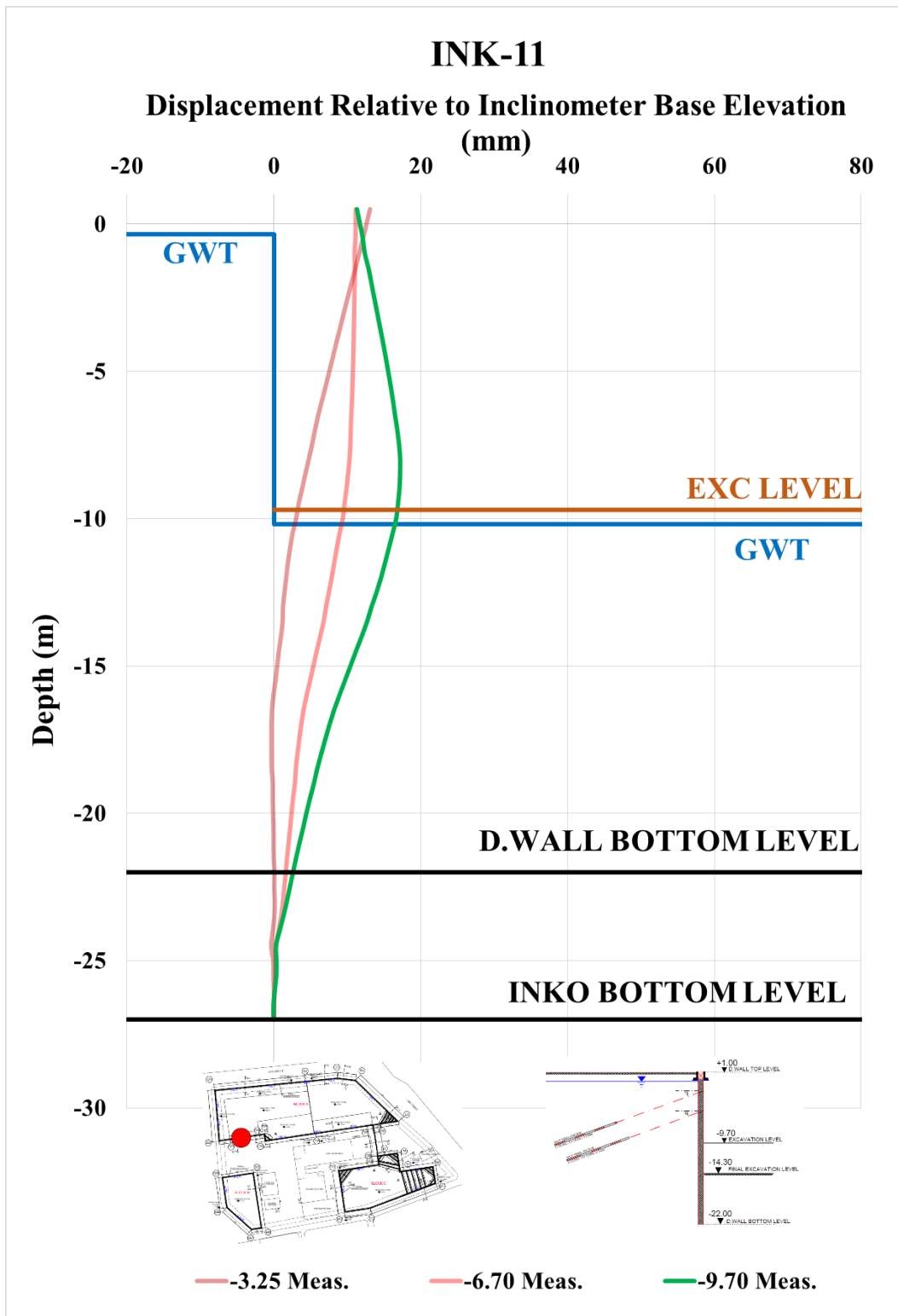
Figure 4.8. Measured Displ. Rel. Inc. Base Elev. At -9.70 m
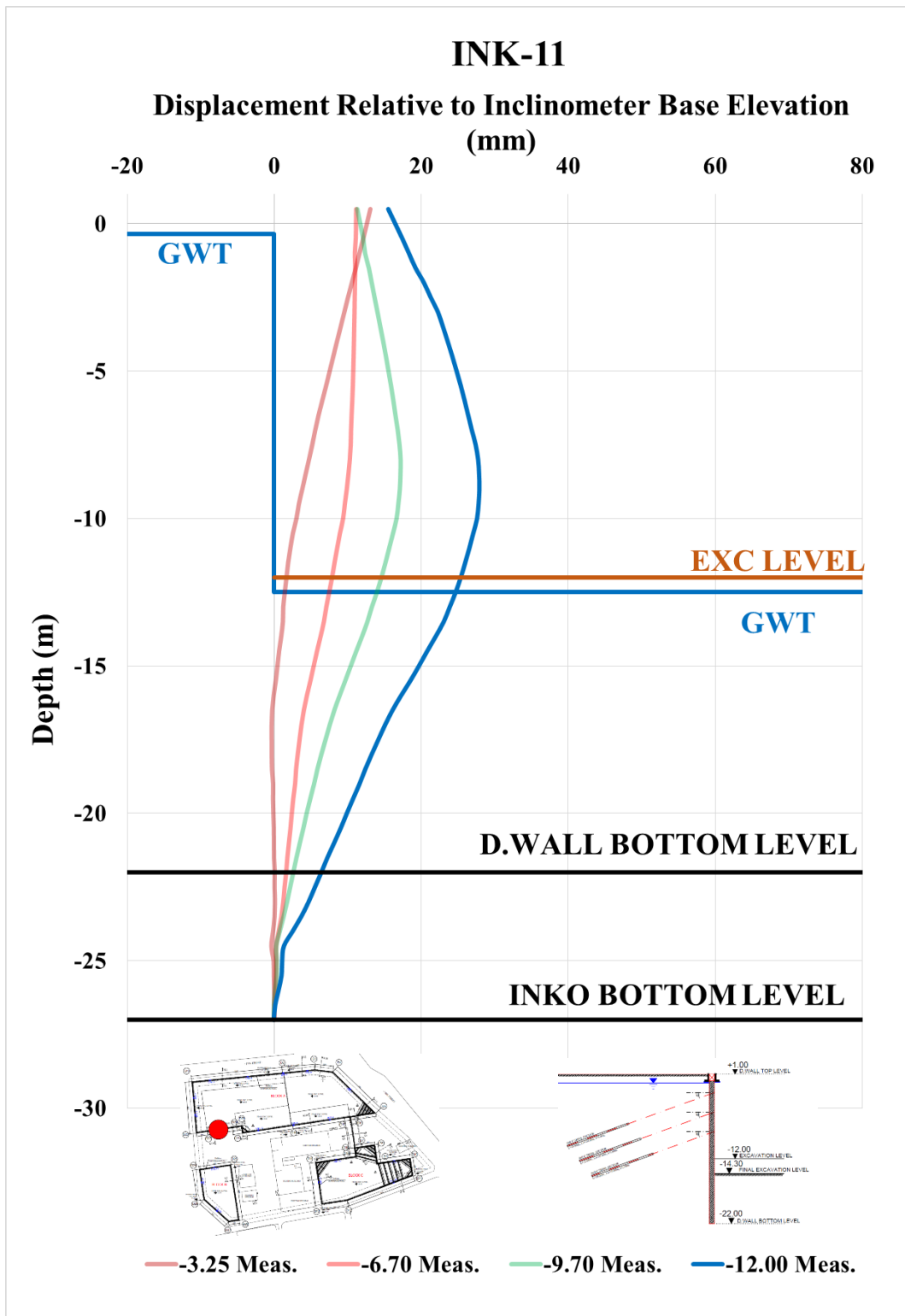
Figure 4.9. Measured Displ. Rel. Inc. Base Elev. At -12.00 m
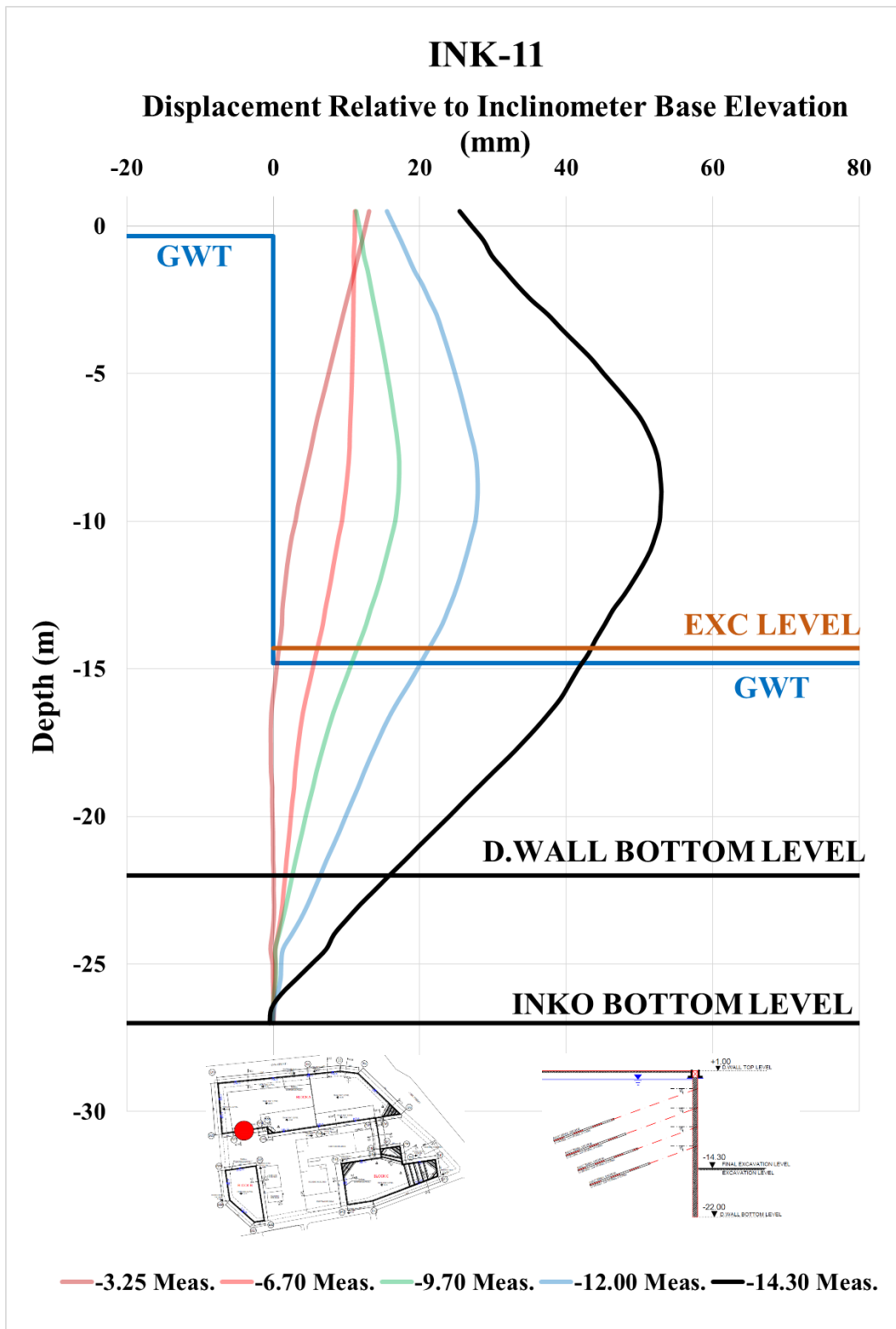
Figure 4.10. Measured Displ. Rel. Inc. Base Elev. At -14.30 m

INK - 11 / Section 1A-1A

Anchor Load vs Stage

Legend	Excavation Stage	1. Anchor Level	2. Excavation Level	2. Anchor Level	3. Excavation Level	3. Anchor Level	4. Excavation Level	4. Anchor Level	Final Excavation Level
——	Measured Load of 1. Anchor Row (kN)	664.65	681.97	669.46	667.62	665.86	657.25	643.13	649.31

Figure 4.11. Load Cell 17 (LC 17) Measurements

CHAPTER 5

5. ANALYSIS, CALIBRATION, AND DISCUSSION

Plaxis 2D is a finite element analysis software to estimate stress, strain, and deformations in geotechnical engineering problems. Fourteen different material models such as Mohr-Coulomb, Hardening Soil, hardening soil with small strain stiffness, Hoek Brown, etc., can be used. Modeling tools and elements are explained in this chapter.

In the scope of the thesis, a back analysis of the excavation system is performed. There exist 7 soil profiles, 18 inclinometers, and 8 different sections. Finite element models are created in Plaxis 2D software corresponding to cross-sections at inclinometer locations. Analysis results are compared with monitoring data, and estimated soil parameters are calibrated.

Finite element analyses were performed for all inclinometers by using Plaxis 2D software. Section 1A-1A / INK-11 is shown in this Chapter as an example. Other results are given in Appendix A. In the first step, soil parameters estimated by using recommended charts, relations, etc., by the literature were used. This analysis results will be called estimated results in the rest of the study. In the second step, calibration study was performed. The stiffness parameters were chosen for calibration purposes as opposed to shear strength parameters since they govern the deformation response. The main reason is that stiffness parameters are majar parameters for calibration study based on displacements of excavation system. Stiffness parameters (E_{50}^{ref}, E_{oed}^{ref}, E_{ur}^{ref}) were scaled by different constants for cohesive and cohesionless soils, and displacements of the excavation system were tried to match with the measured results. The results after calibration will be referred to as "calibrated results" in the rest of the study.

5.1. Plaxis 2D – Finite Element Modeling

Plaxis 2D has two parts: on for input and on for output. Modeling starts with defining general model properties. They are models and elements types. There exist two types of models which are plane strain and axisymmetric. The plane strain model is mostly preferred for geometries having uniform cross-sections. Displacements and strains are accepted as zero but, stresses in the z-direction are completely considered. The dynamic loading earthquake problems can be modeled with plane strain. On the other hand, an axisymmetric model is used in the case of circular structures having approximately uniform radial cross-sections. Stress and deformations for any radial direction are accepted as the same. It is also preferred for single-source vibration problems.

In the second part, the type of elements is required to be selected. They are a 6-noded triangle and a 15-noded triangle in Figure 5.1. The main difference is that the 15-noded triangle option makes a fourth-order interpolation when calculating stresses and strains.

However, a second-order interpolation is made if the 6-noded triangle is preferred. By using the 15-noded option, more complex problems can be modeled and more accurate results can be obtained. 15-noded element is also the default element in Plaxis 2D. Moreover, the contours of the soil model are also defined in this section. These contours are related to the requirements of a problem that will be modeled.

nodes

stress points

a. 15-node triangle

nodes

stress points
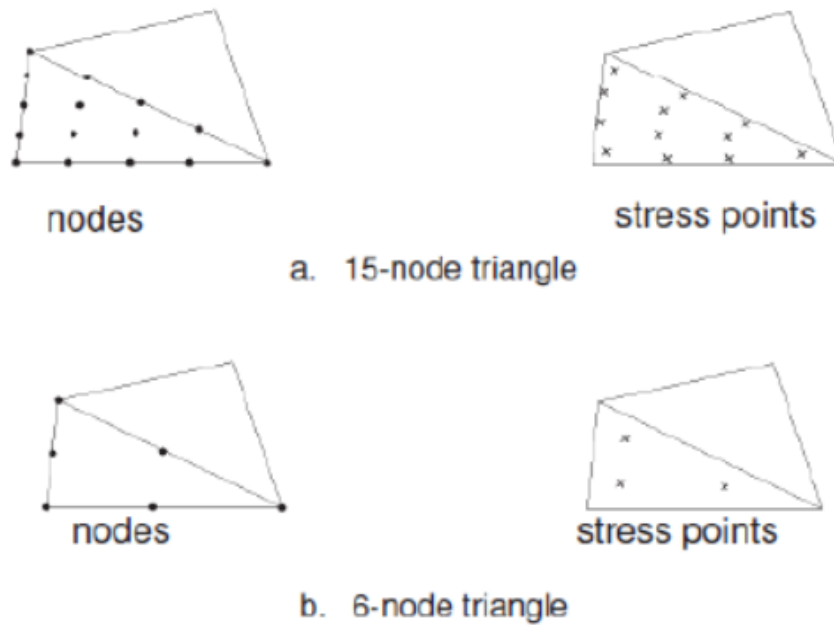
b. 6-node triangle

Figure 5.1. 15-Noded and 6-Noded Triangles (Plaxis 2D Reference Manuel, 2021)

The input program of Plaxis 2D consists of 5 subsections which are soil, structures, mesh, flow conditions, and staged construction. In the soil section, the ground model can be modeled by using boreholes to create non-horizontal soil layers or it can be simply modeled as a horizontal soil layer. In the second structures section, the model of the problem is created. Especially for deep excavation projects, the plate element is used to define the vertical element. Any type of vertical element such as diaphragm wall, secant pile, tangent pile, soldier pile, etc., is modeled as a plate since the vertical element is simplified by considering spacing, thickness, stiffness, and then EA and EI values are entered into the software as plate properties. To consider the soil-structure interaction, the interface is defined around the plate element.

Furthermore, anchor elements are modeled in two parts. They are free length and bond length. Free length and bond length are modeled as a node-to-node anchor and geogrid, respectively. A node-to-node anchor is simply an elastic spring having constant stiffness all over its length. EA and $L_{spacing}$ values are defined if an anchor is modeled as elastic. Also, elastoplastic modeling is possible. In addition, $F_{max, tens}$ and $F_{max, comp}$

values are required to be defined. When modeling the bond length of anchors as a geogrid, stiffness of grout body, EA, value is described. The geogrid option can only be used if it sustains tensile forces. There are two options to model the lateral support element struts. They are node-to-node or fixed-end anchors. The decision of this depends on the model condition, which means that if two facades of the excavation are modeled, the node-to-node anchor can be used. However, the counter facade of the excavation is not considered, fixed-end anchors are used. Properties of fixed-end anchors are similar to node-to-node anchors. Point load and line load options are used to model surcharge load. Surrounding structures can be defined as a line load. Moreover, in this section, soil polygons are divided into layers since it is required in the staged construction section to be able to model the excavation stages. Example geometry at the structures section is given in Figure 5.2.

SBMA systems have three different fixed lengths. Each of them is 3 m. However, in finite element modeling, the whole fixed length was modeled as asingle 9 m long geogrid. A comparative study was performed elsewhere for conventional (single 9 m long) anchors vs. SBMA (3 sets of achors with multiple root configurations). It was seen that the special configuration in SBMA can not be reliably modeled in finite element assessments as anchors with multiple roots. For simplicity the joint effect of the SBMA is modeled through a single root geogrid element in Plaxis. The special response of SBMA is incorporated through field tests which provide a good idea about root stiffness, which is used to select the geogrid root parameters in Plaxis.
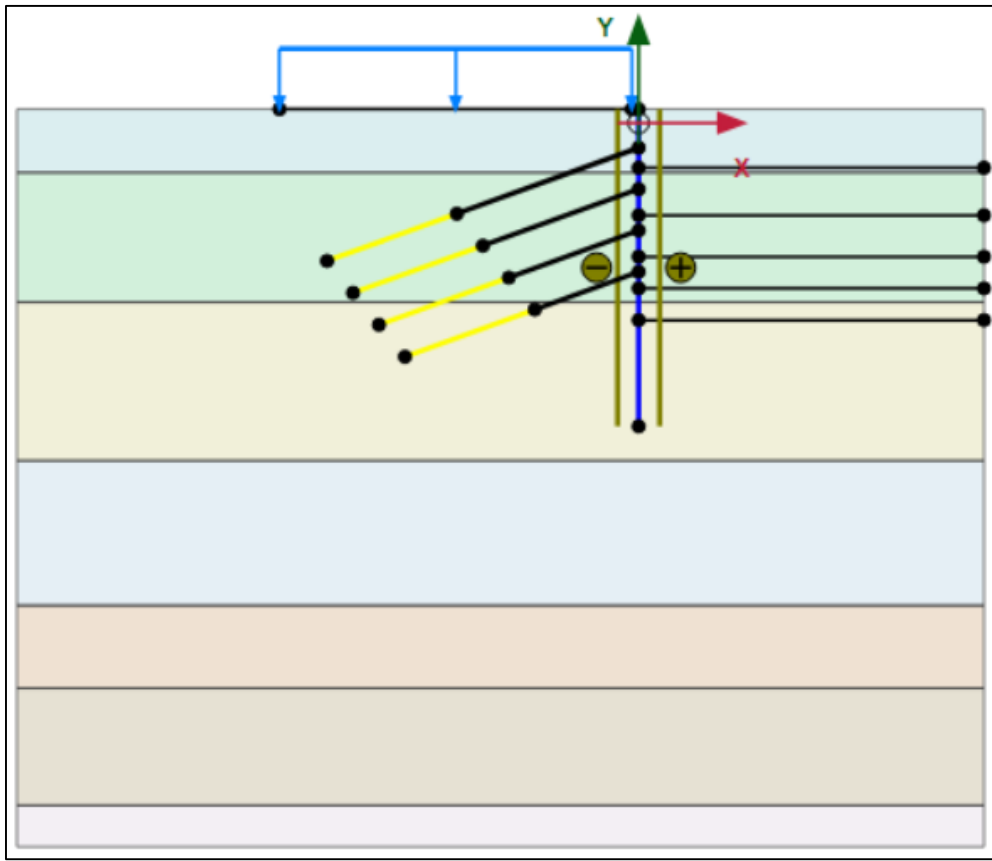
Figure 5.2. Example Geometry at Structures Section

In the mesh section, the geometry of the model is required to be completed. After that, the whole body is divided into finite elements (Figure 5.3). Meshing can be performed automatically by selecting types of element distribution which are very coarse, coarse, medium, fine, and, very fine. There are also expert settings. Relative element size and element dimensions can be determined by users. Selecting finer element distribution lead to an increase in calculation times.
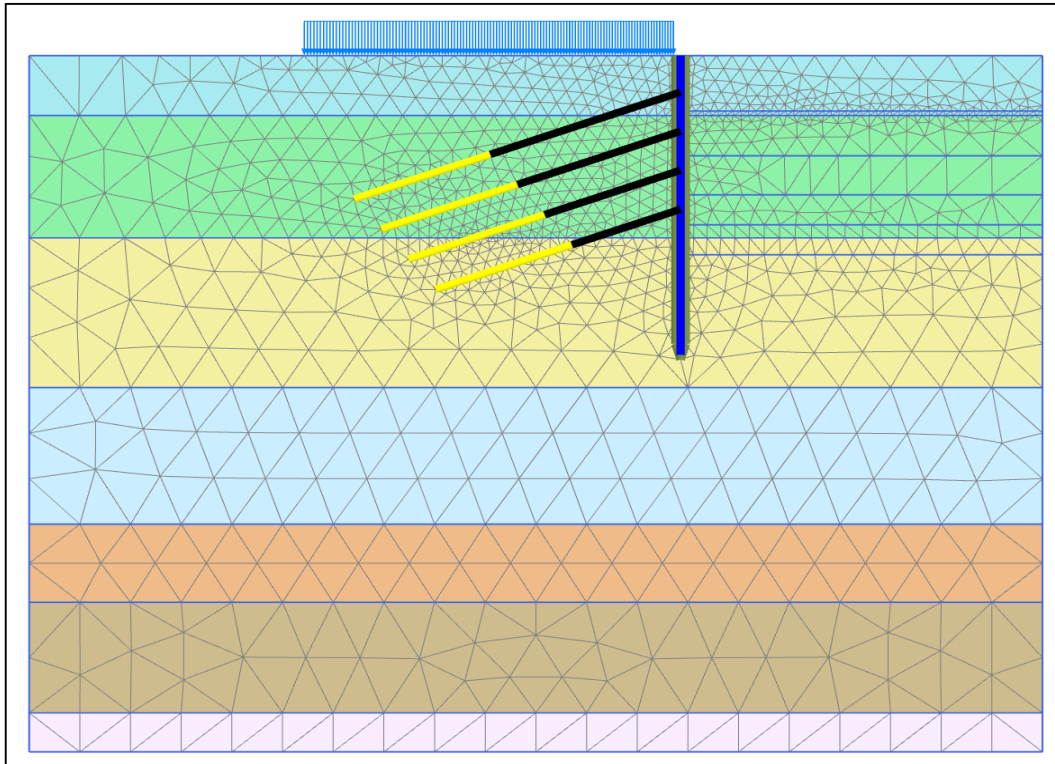
Figure 5.3. Meshed Geometry

In the Flow Conditions section, the groundwater level is defined for each stage of excavation. This is important for modeling the lowering of groundwater level stage by stage.

Staged Construction is the last part of the modeling. Excavation progress such as pile installation, first excavation stage, construction of first stage anchors, application of pre-stressing, etc., can be arranged. Progress of the excavation system as in real practice is simulated for analysis. There are three calculation types which are plastic, consolidation, and safety. Elastoplastic drained or undrained analysis can be performed without considering consolidatıın. On the other hand, time-dependent analysis can be made for deformations and excess pore pressures. Furthermore, the strength reduction method is used in Safety analysis to estimate the global factor of safety of the system. Moreover, pore pressure calculation types should be selected.

There are phreatic, use pressures from the previous phase, and steady-state groundwater flow. For deep excavation projects, plastic analysis is recommended.

Finally, the created model is analyzed with the Input program of Plaxis 2D. Stress, strain, and deformations can be interpreted in the Output program. Also, normal forces, shear forces, bending moments, and deformations of the structural element can be obtained.

5.2.   Material Parameters

In this study, the hardening soil model (HS) is used as a constitutive model for soils. Cohesive and cohesionless soils exist in the excavation area. Pore pressure behaviors are modeled as drained for both of them since long-term behavior is more critical for cohesive soils.

Hardening soil parameters of soils were estimated in Chapter 3. In this part, parameters of horizontal and vertical support elements will be selected. A diaphragm wall with a thickness of 80 cm is modeled as a plate element. Furthermore, 6x0.6 inches consisting of 7-wire strands anchorages was modeled as a node-to-node anchor. The properties of the plate element and node-to-node anchor were calculated as follows in Table 5.1 and 5.2.

Table 5.1. The Properties of The Plate Element

E_{conc} (kPa)	D (m)	A (m^2/m)	I (m^4/m)	EA (kN/m)	EI (kNm^2/m)	w (kN/m/m)
3.00E+07	0.8	0.8	0.04267	2.40E+07	1.28E+06	5.0

Table 5.2. The Properties of The Node-To-Node Anchor

E_{steel} (kPa)	A (mm²)	Tendon Steel Class (MPa)	Spacing (m)	EA (kN)	$F_{max,tens}$ (kN)	$F_{max,comp}$ (kN)
1.95E+08	140.0	1860.0	2.0	1.64E+05	960.0	960.0

5.3. Construction Sequence

The following construction sequences were used to assess the INK-11; INK-11 is close to Section 1A-1A. The staging of the model can be seen in Table 5.3.

Table 5.3. Construction Sequence

INK - 11 / Section 1A-1A	
Stage	**Description**
1	Definition of Soil Model
2	Construction of L=23 m and D=80 cm Diaphragm Wall
3	Lowering the groundwater level to -3.75 m
4	Excavation to -3.25 m
5	Construction of 1. row anchor at -1.80 m
6	Lowering the groundwater level to -7.20 m
7	Excavation to -6.70 m
8	Construction of 2. row anchor at -4.80 m
9	Lowering the groundwater level to -10.20 m
10	Excavation to -9.70 m
11	Construction of 3. row anchor at -7.80 m
12	Lowering the groundwater level to -12.50 m
13	Excavation to -12.00 m
14	Construction of 4. row anchor at -10.80 m
15	Lowering the groundwater level to -14.80 m
16	Excavation to -14.30 m

In Figure 5.4, Plaxis model of Section 1-1 is given. Estimated and Measured displacements are provided in Figure 5.5 – 5.10. Internal forces of diaphragm wall can be seen in Table 5.4.
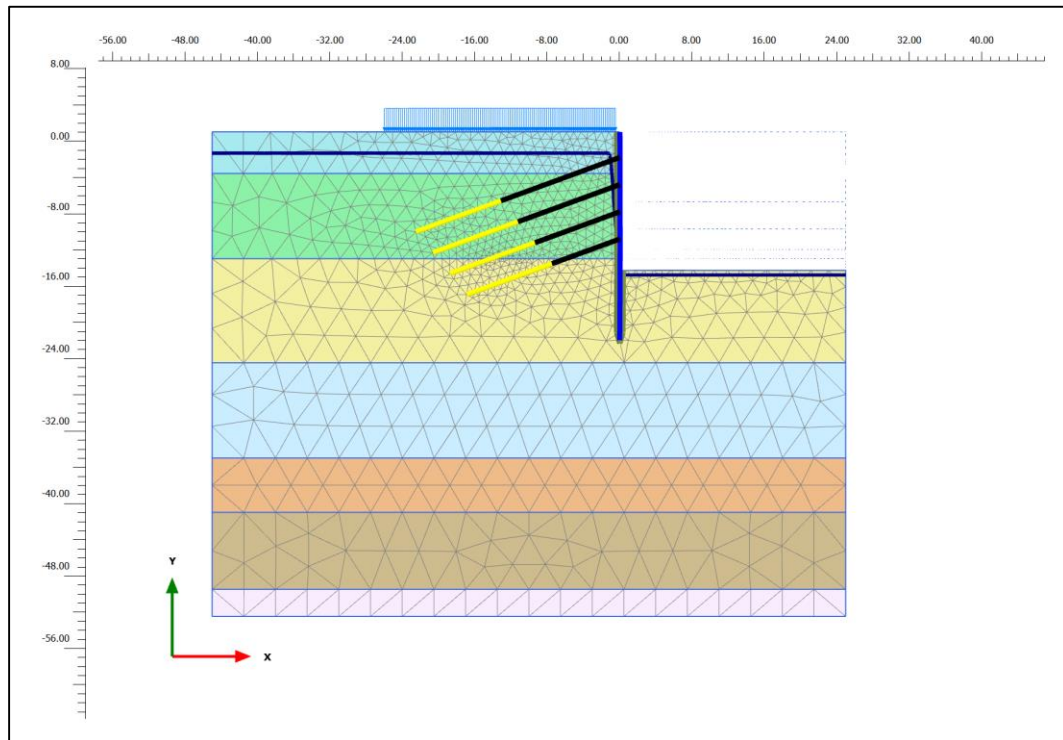
Figure 5.4. Plaxis Model of Section 1-1/INK-11

The envelope of internal forces is given as a software output in Figure 5.11 – 5.13 for -14.30 m. They are plotted for each excavation stage in Figures 5.14 – 5.16. In Figure 5.17, Estimated and Measured anchor loads are presented.

5.4. Estimated Displacements of INK-11

The excavation was modeled in five stages. For each stage, the groundwater level was lowered 0.50 m below to excavation level. In these stages, inclinometer readings were taken. Elevations of these stages are -3.25 m, -6.70 m, -9.70 m, -12.00 m, and -14.30 m respectively. The maximum measured displacements are 13.08 mm, 11.16 mm, 17.20 mm, 27.92 mm, and 52.99 mm in Figures 5.5 – 5.9. On the other hand, the maximum estimated displacements are 16.98 mm, 8.36 mm, 12.44 mm 20.48 mm, and 44.93 mm in Figures 5.5 – 5.9.
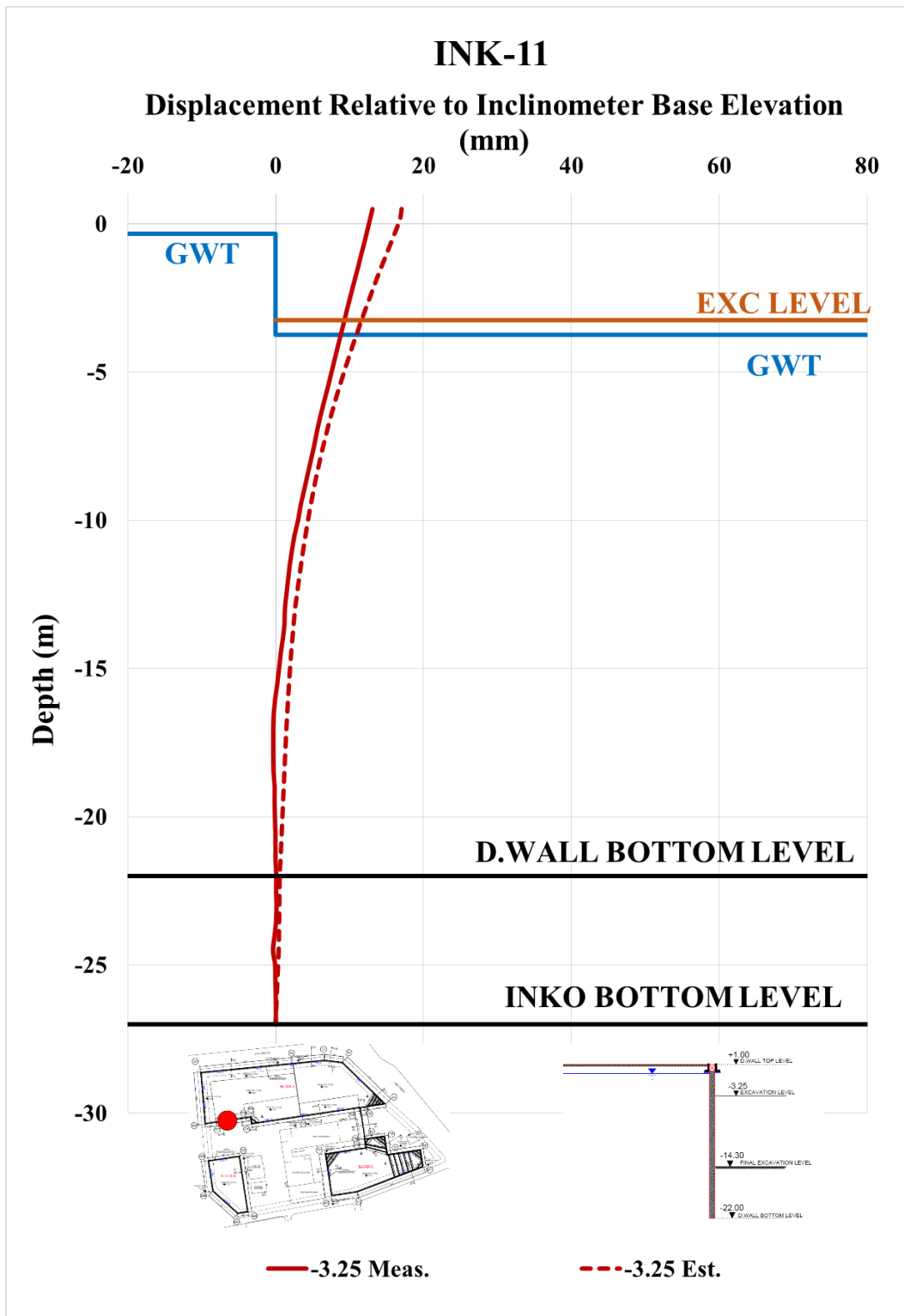
Figure 5.5. Estimated and Measured Displ. Rel. to Inc. Base Elev. at -3.25 m
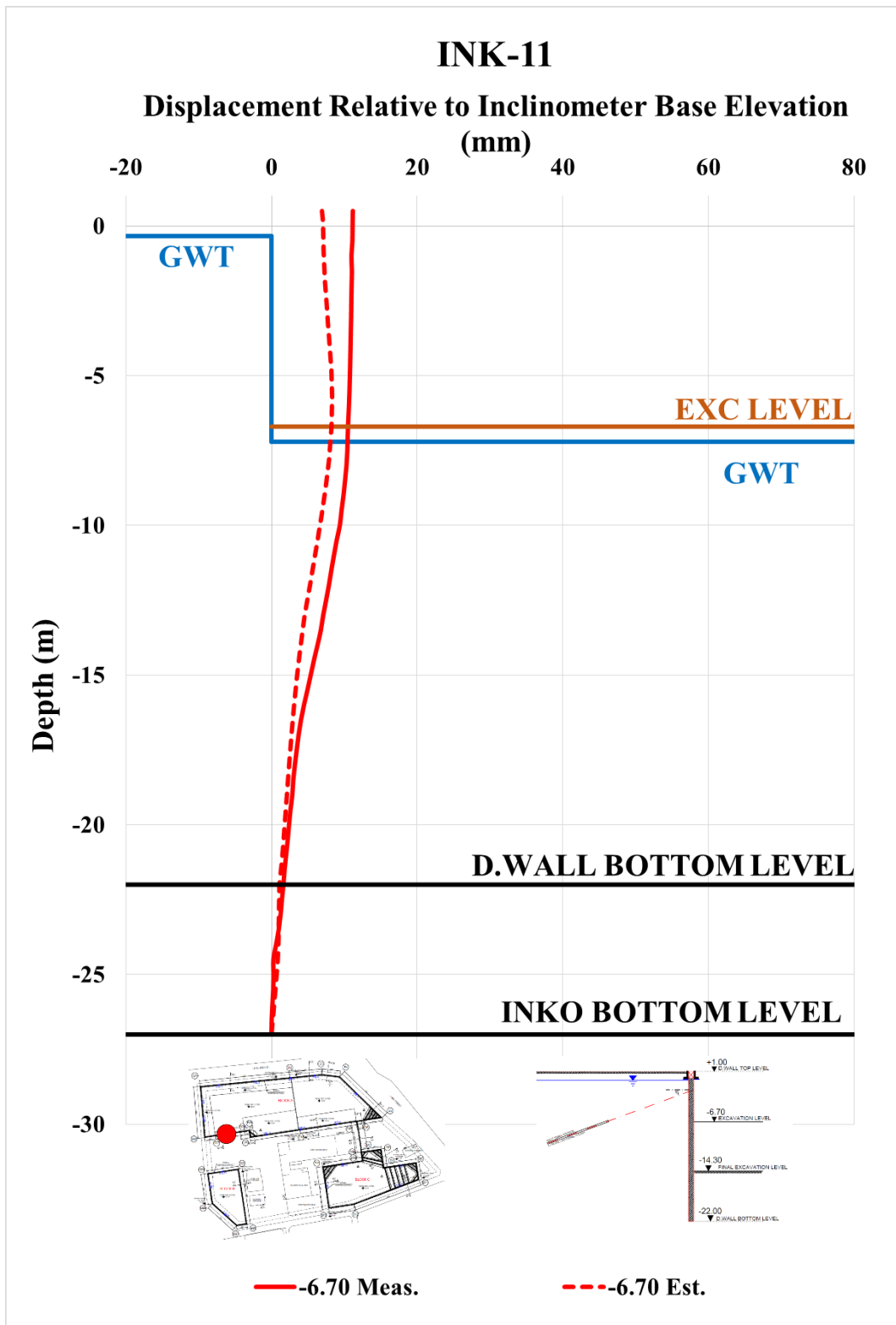
Figure 5.6. Estimated and Measured Displ. Rel. to Inc. Base Elev. at -6.70 m
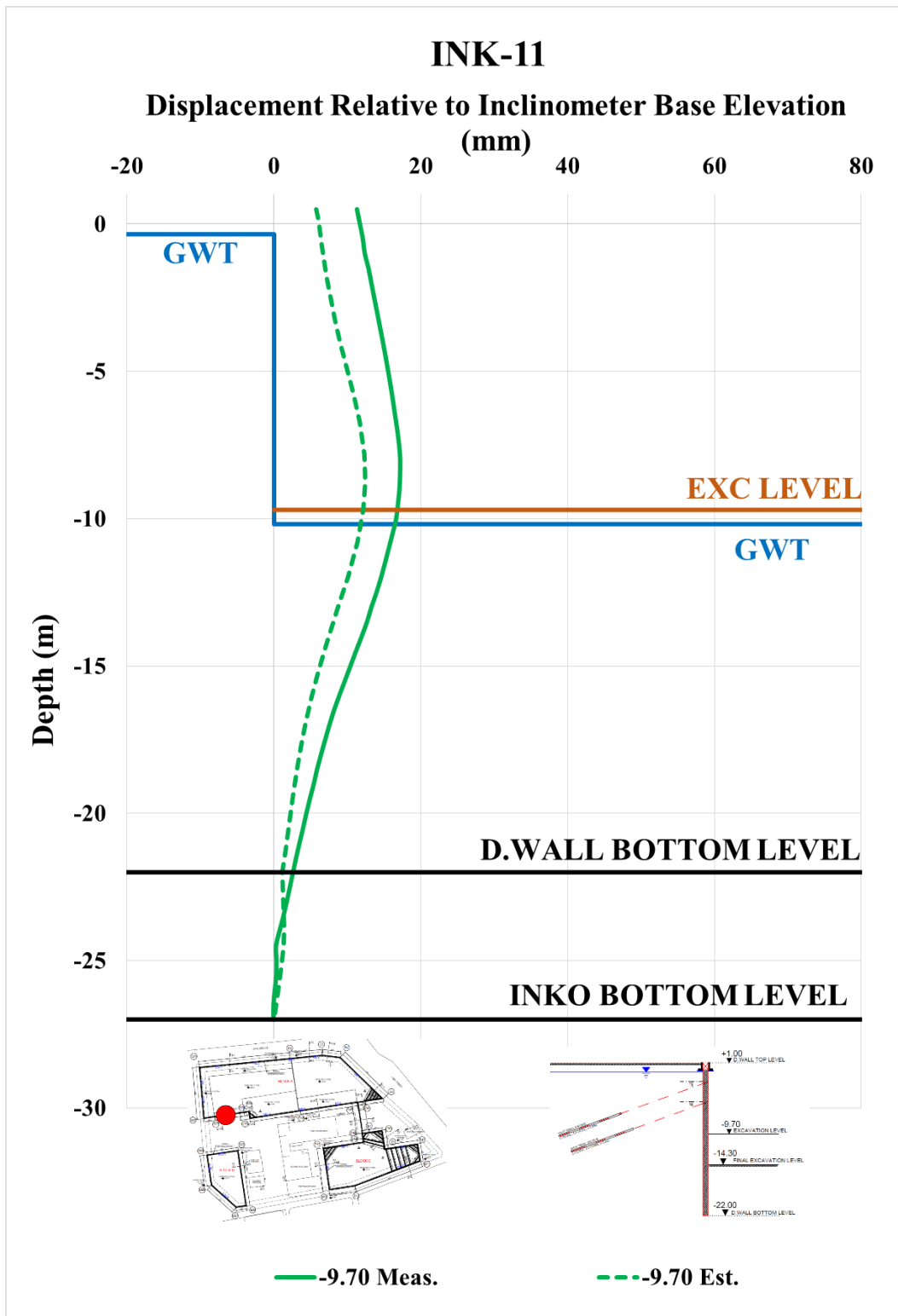
Figure 5.7. Estimated and Measured Displ. Rel. to Inc. Base Elev. at -9.70 m
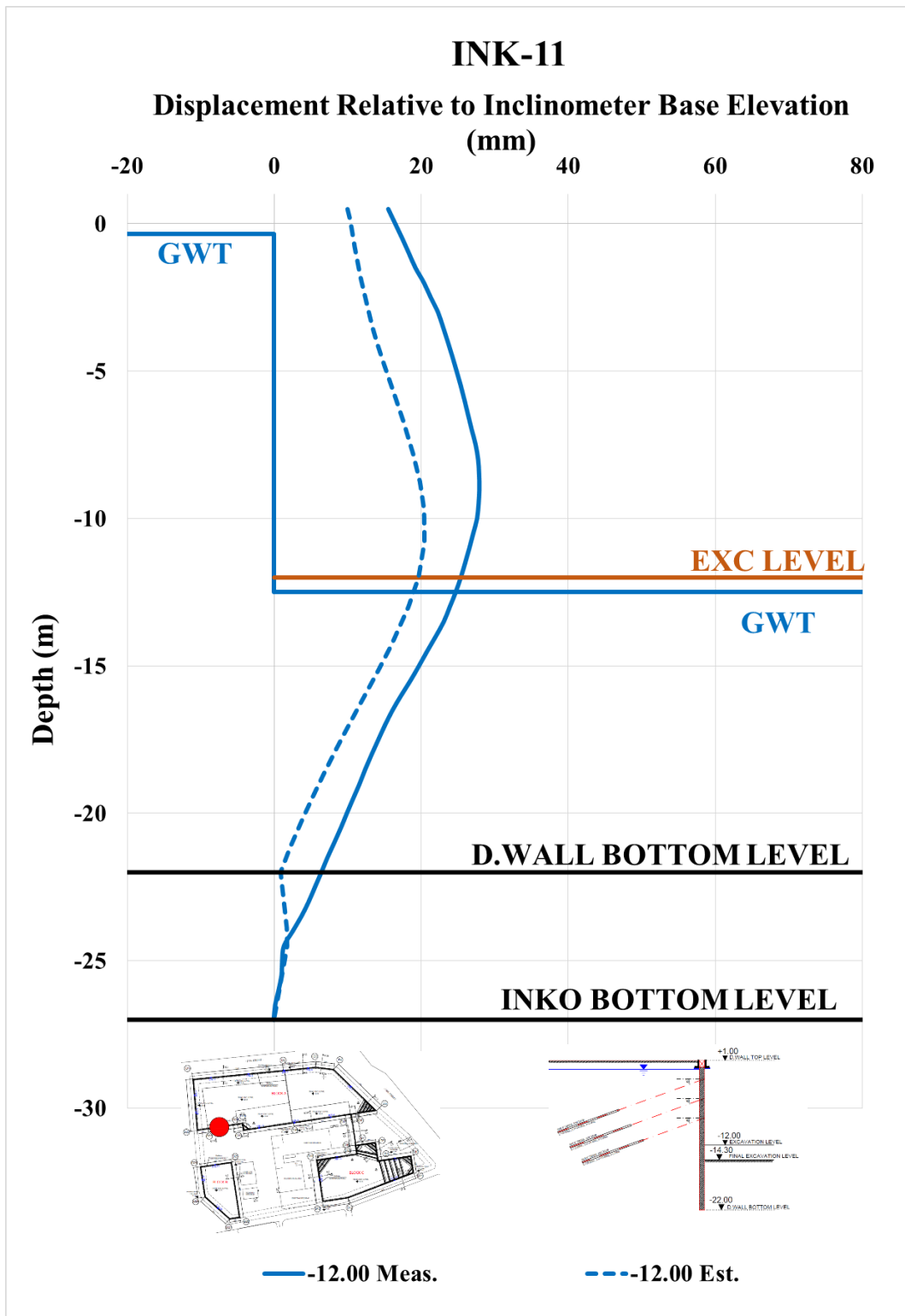
Figure 5.8. Estimated and Measured Displ. Rel. to Inc. Base Elev. at -12.00 m
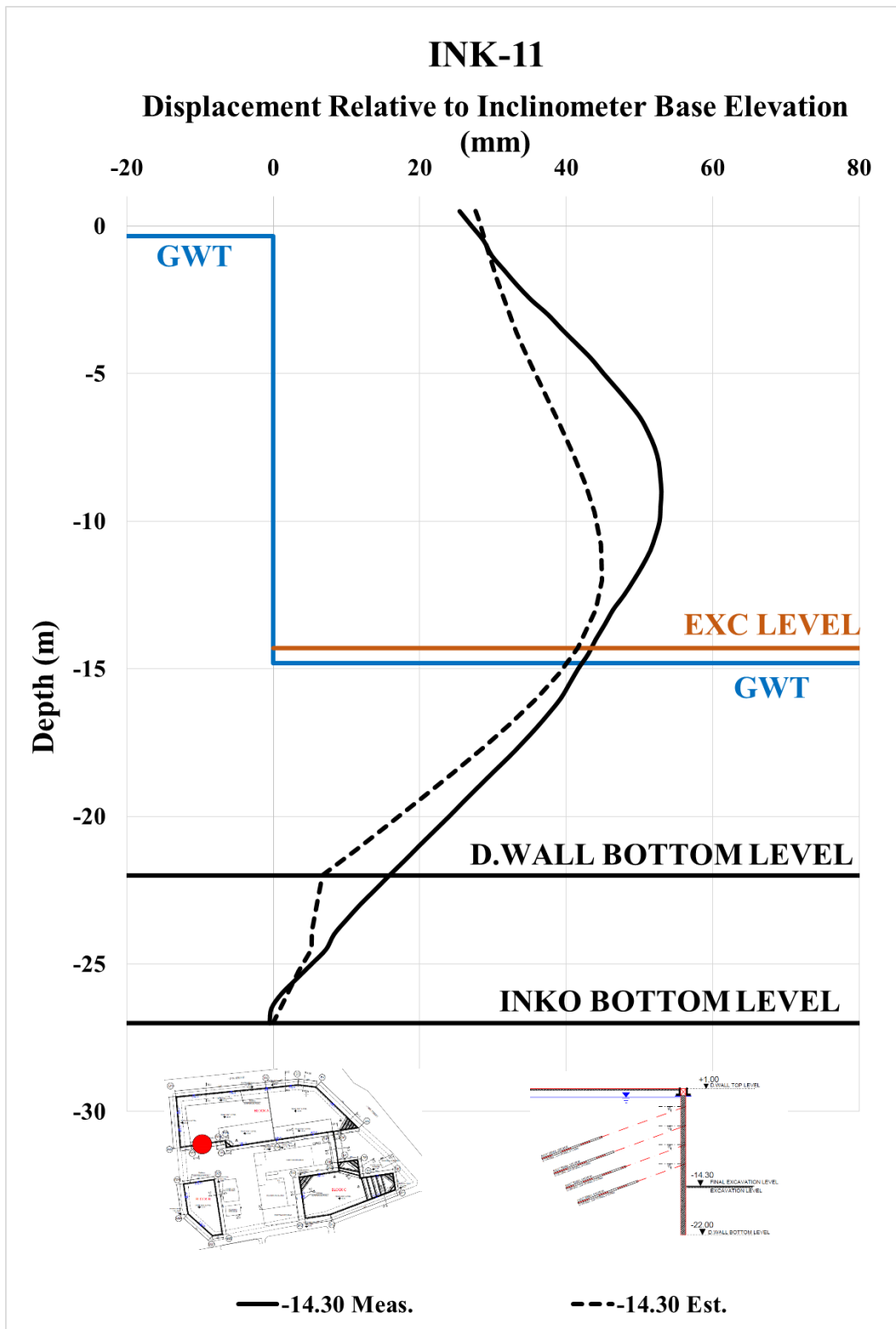
Figure 5.9. Estimated and Measured Displ. Rel. to Inc. Base Elev. at -14.30 m
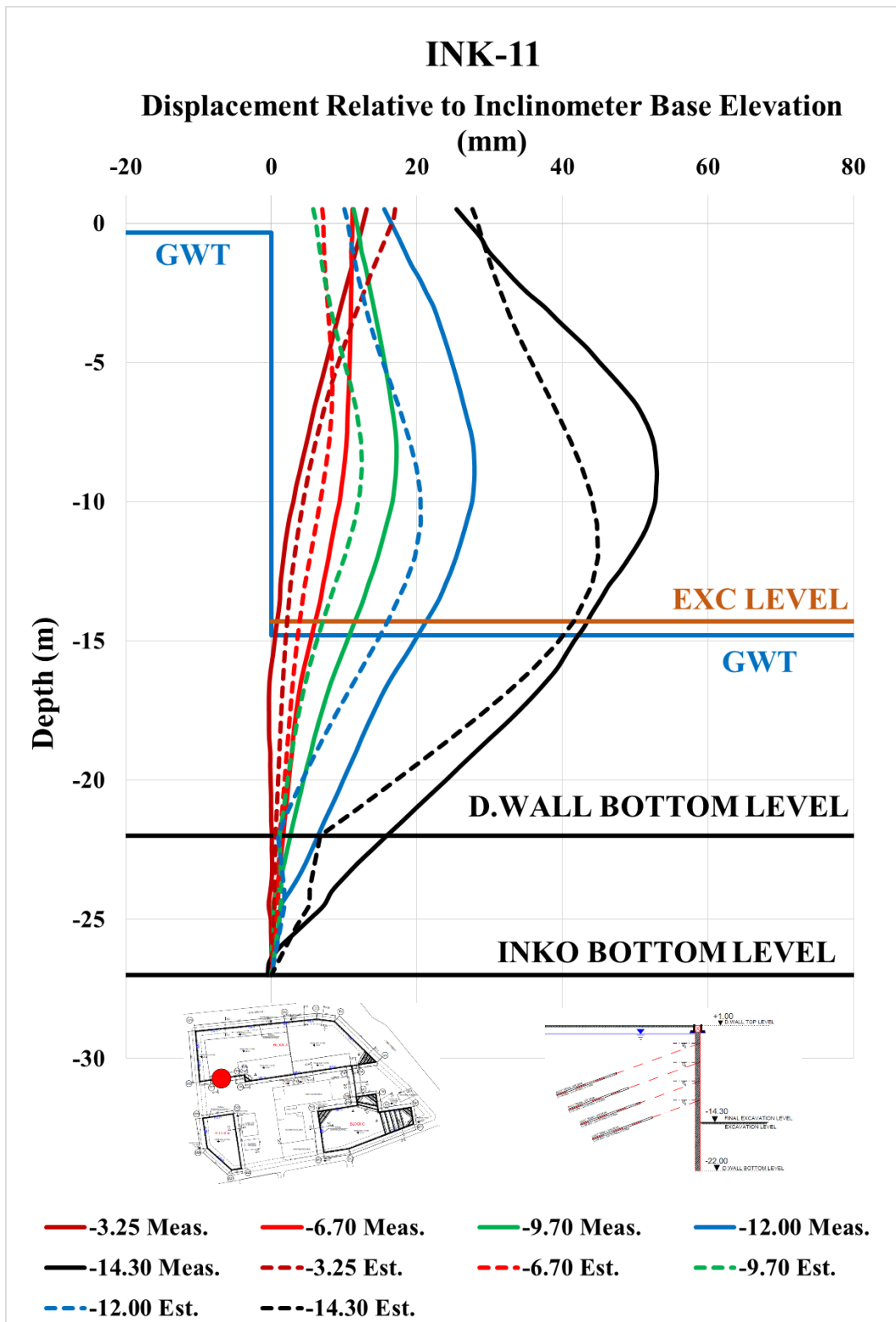
Figure 5.10. Estimated and Measured Displ. Rel. to Inc. Base Elev.

Table 5.4. Internal Forces of Diaphragm Wall Section 1A-1A for Estimated Parameters

INK - 11 / Section 1A-1A					
Excvation Stage	1	2	3	4	5
Excavation Level (m)	-3.25	-6.70	-9.70	-12.00	-14.30
N_{max} (kN/m)	95.64	246.10	430.80	601.00	775.70
V_{max} (kN/m)	57.72	212.10	306.80	344.60	374.70
M_{max} (kN.m/m)	145.70	316.10	622.30	833.10	1272.00

Envelope of Axial forces N (scaled up 5.00*10⁻³ times)
Maximum value = 19.30 kN/m (Element 22 at Node 5823)
Minimum value = -775.7 kN/m
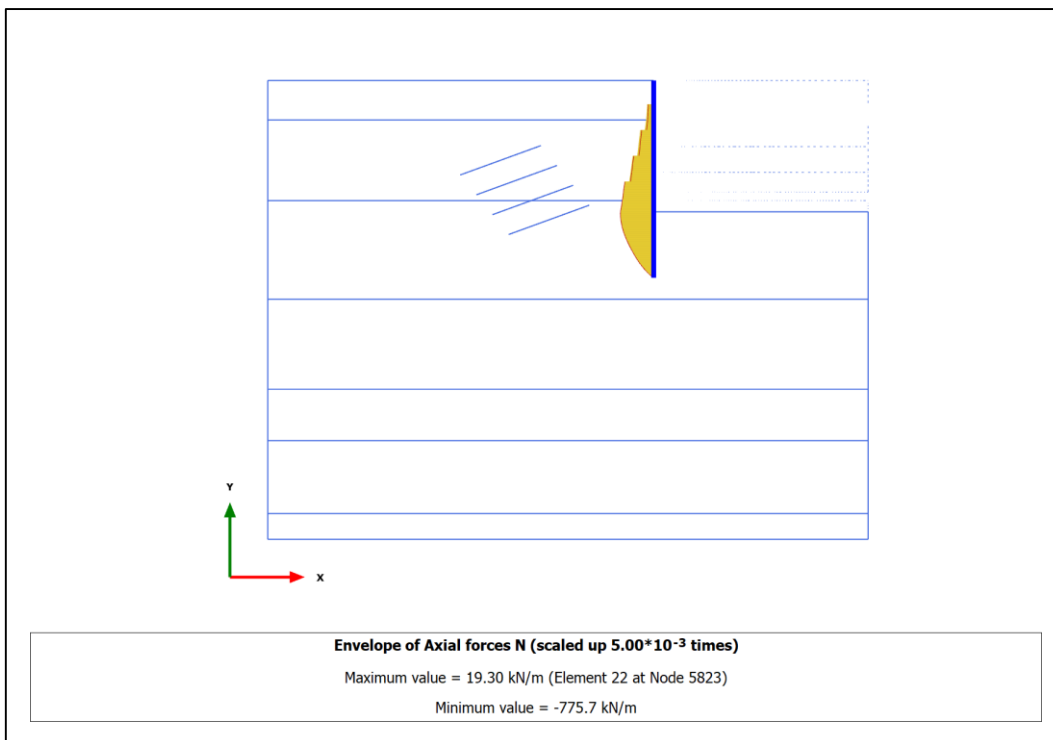
Figure 5.11. Envelope of Axial Forces of Section 1-1/INK-11 at -14.30 m
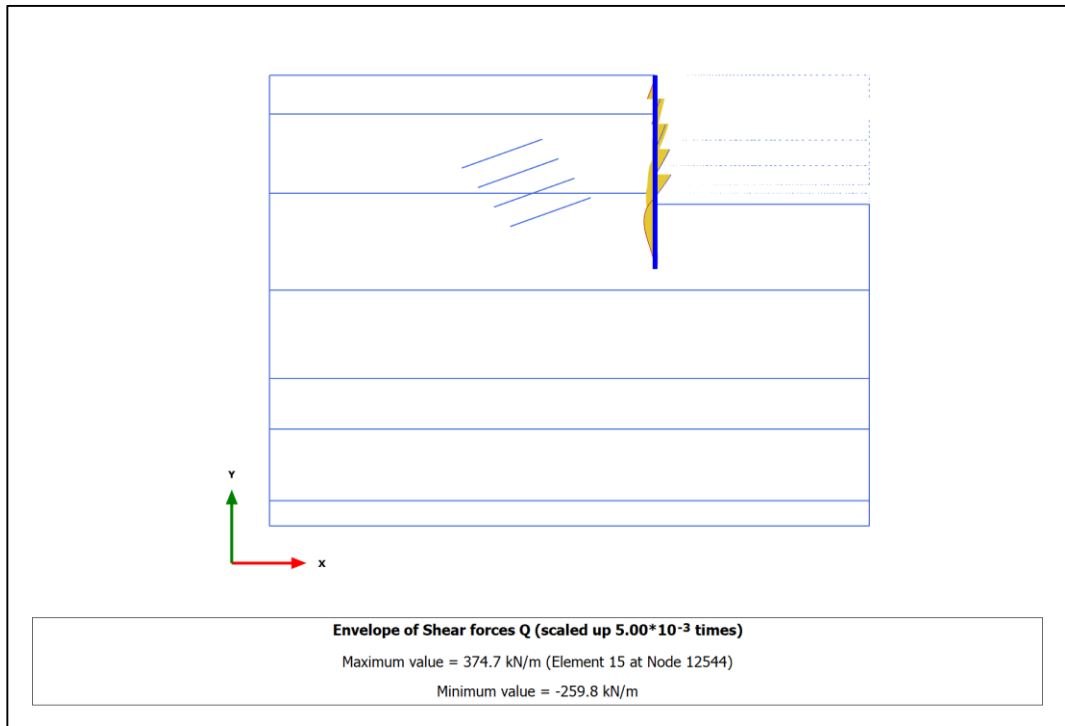
Figure 5.12. Envelope of Shear Forces of Section 1-1/INK-11 at -14.30 m
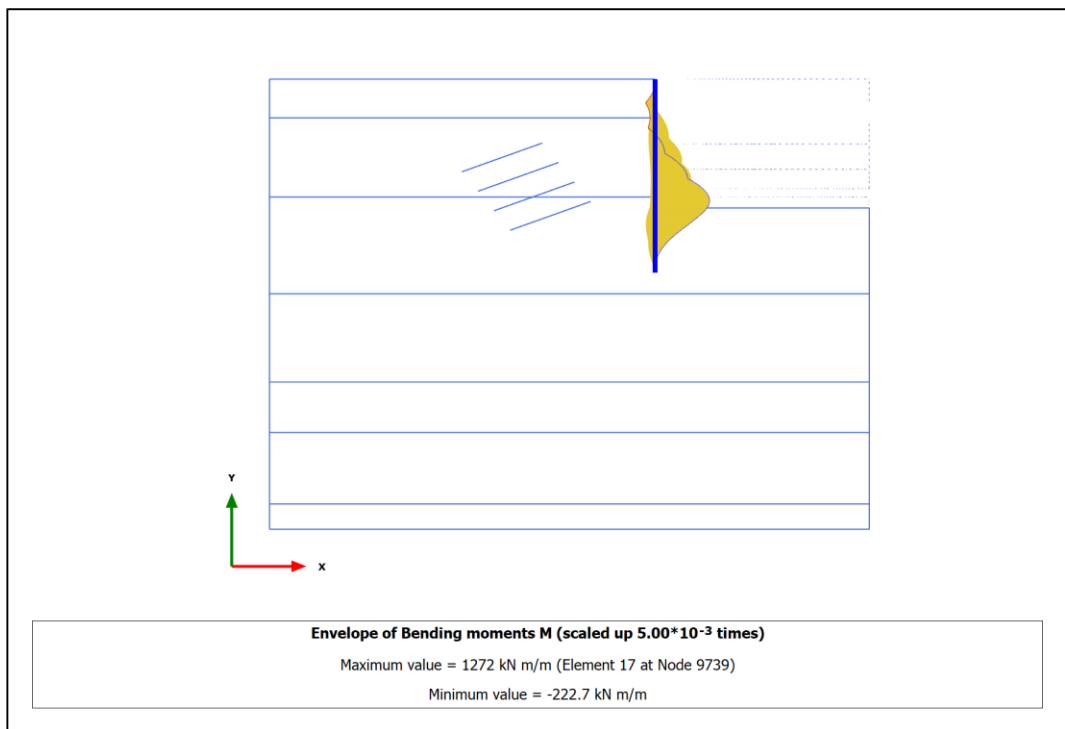
Figure 5.13. Envelope of Bending Moments of Section 1-1/INK-11 at -14.30 m
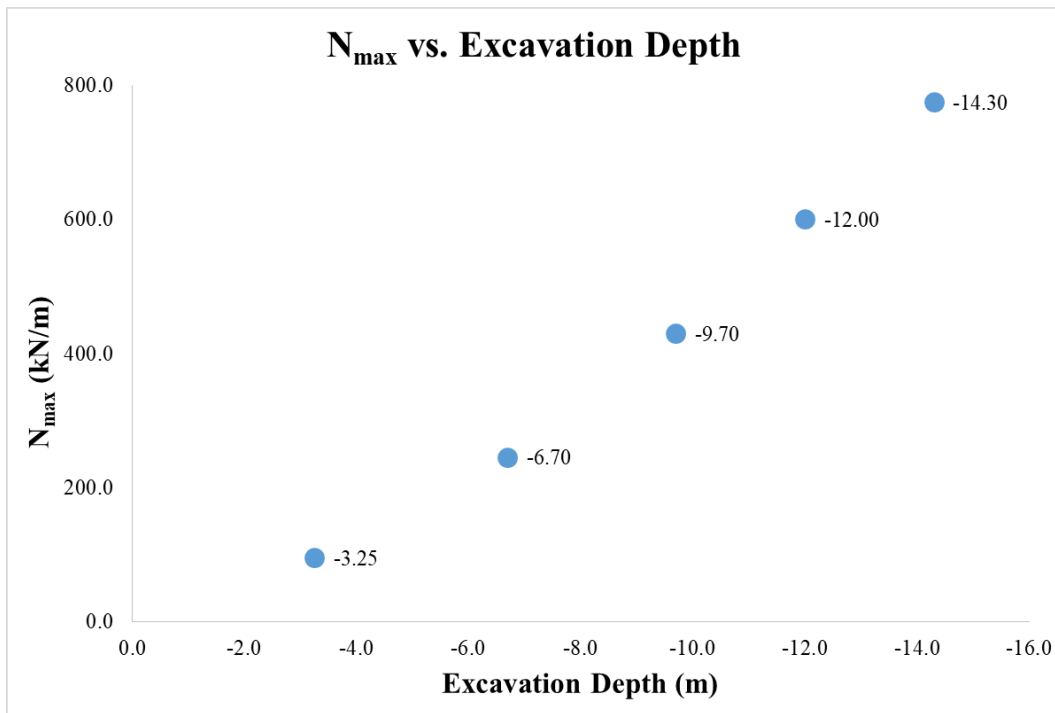
Figure 5.14. Normal Forces of Diaphragm Wall for Each Excavation Stage
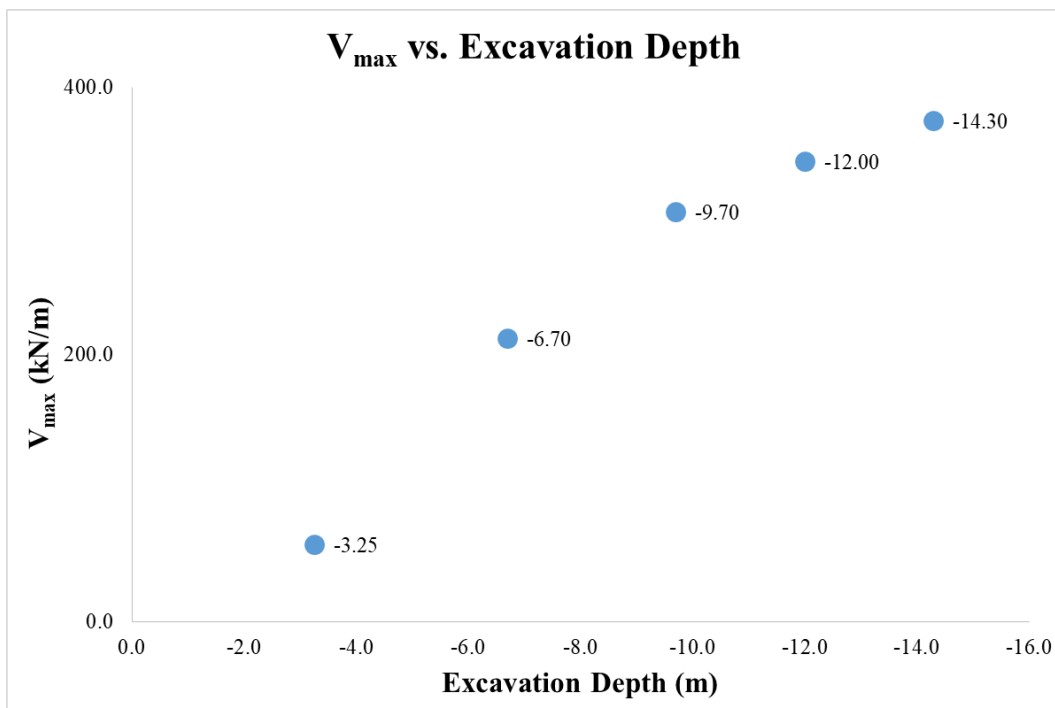
Figure 5.15. Shear Forces of Diaphragm Wall for Each Excavation Stage
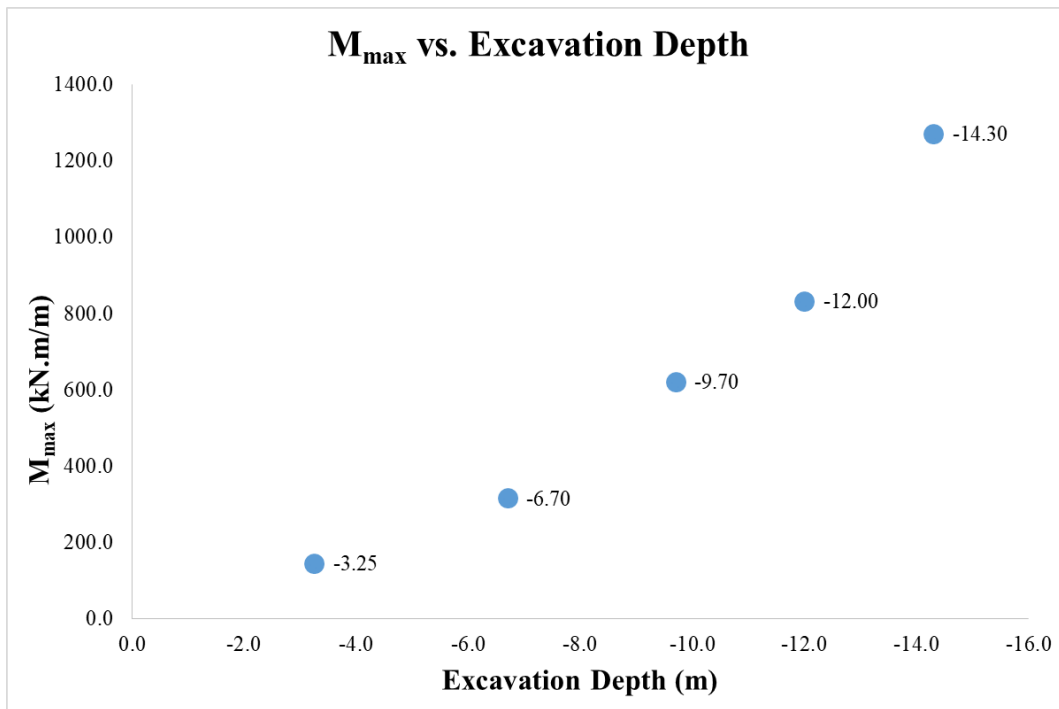
Figure 5.16. Bending Moments of Diaphragm Wall for Each Excavation Stage

INK - 11 / Section 1A-1A

Anchor Load vs Stage

Legend	Excavation Stage	1. Anchor Level	2. Excavation Level	2. Anchor Level	3. Excavation Level	3. Anchor Level	4. Excavation Level	4. Anchor Level	Final Excavation Level
	Measured Load of 1. Anchor Row (kN)	664.65	681.97	669.46	667.62	665.86	657.25	643.13	649.31
	Estimated Load of 1. Anchor Row (kN)	650.00	696.83	626.23	654.43	625.96	638.35	630.13	646.40
	Estimated Load of 2. Anchor Row (kN)	-	-	650.00	708.81	646.54	677.30	651.69	677.42
	Estimated Load of 3. Anchor Row (kN)	-	-	-	-	650.00	718.61	663.78	724.13
	Estimated Load of 4. Anchor Row (kN)	-	-	-	-	-	-	650.00	778.37

Figure 5.17. Anchor Loads of INK-11 for Estimated Soil Parameters

5.5. Calibrated Displacements of INK-11

For the calibration of obtained displacements in Chapter 5.4, the stiffness of cohesionless and cohesive layers was multiplied by 0.75 and 1.25, respectively. When determining these calibration coefficients, a trial and error procedure were followed. For each pairs of coefficients, the plots given in Figure 6.1 and 6.2 were drawn. The best fit was obtained when 0.75 and 1.25 were used for cohesionless and cohesive layers, respectively. Moreover, appropriateness of calibrated stiffness parameters was checked according to literature. They are still in the acceptable range.

The maximum calibrated displacements are 13.92 mm, 8.27 mm, 15.05 mm, 26.89 mm, and 54.76 mm in Figures 5.18 – 5.22.

Calibrated and Measured displacements are provided in Figure 5.18 – 5.23. Internal forces of diaphragm wall can be seen in Table 5.5. They are plotted for each excavation stage in Figure 5.24 – 5.26. In Figure 5.27, Estimated and Measured anchor loads are presented.
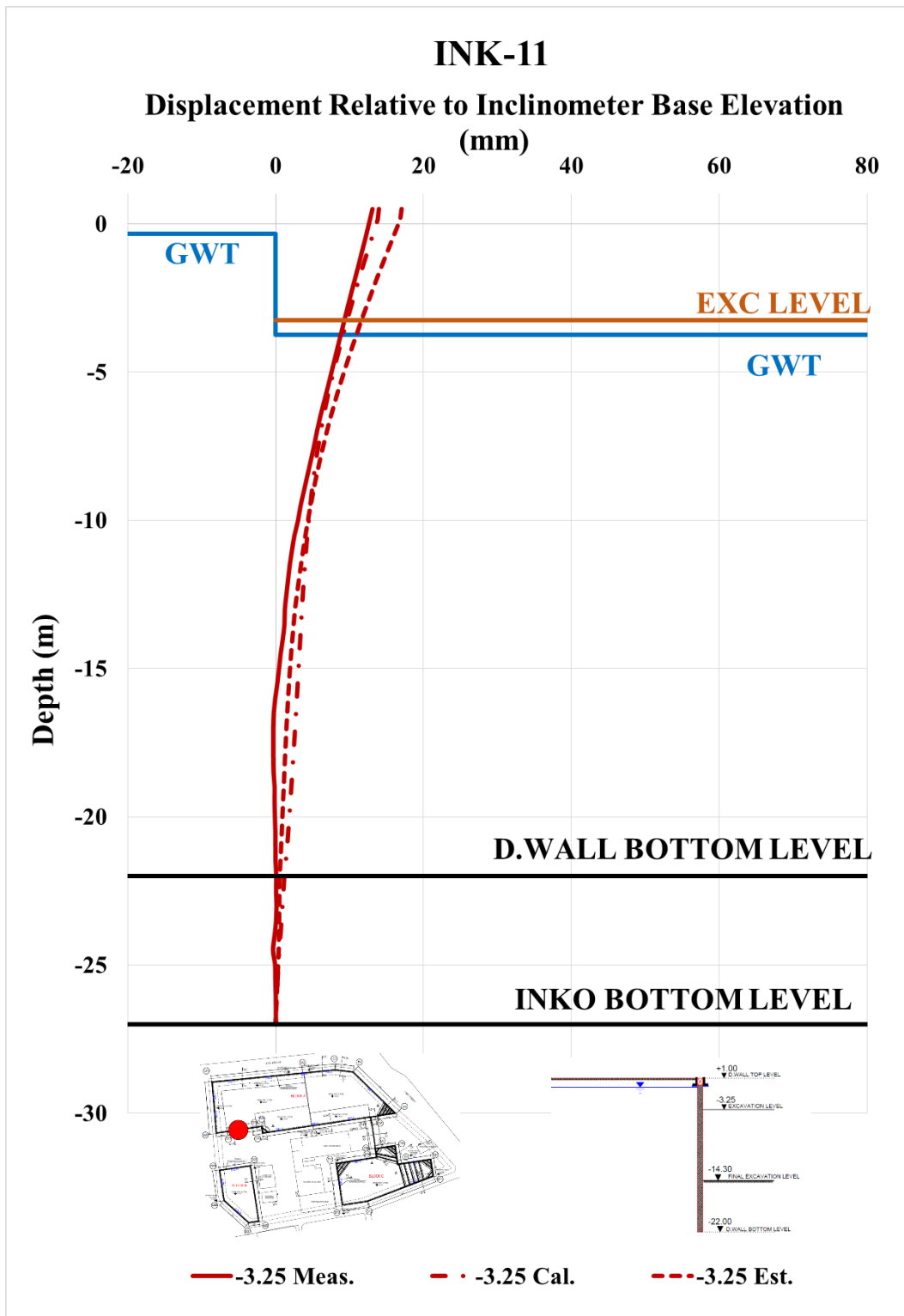
Figure 5.18. Calibrated and Measured Displ. Rel. to Inc. Base Elev. at -3.25 m
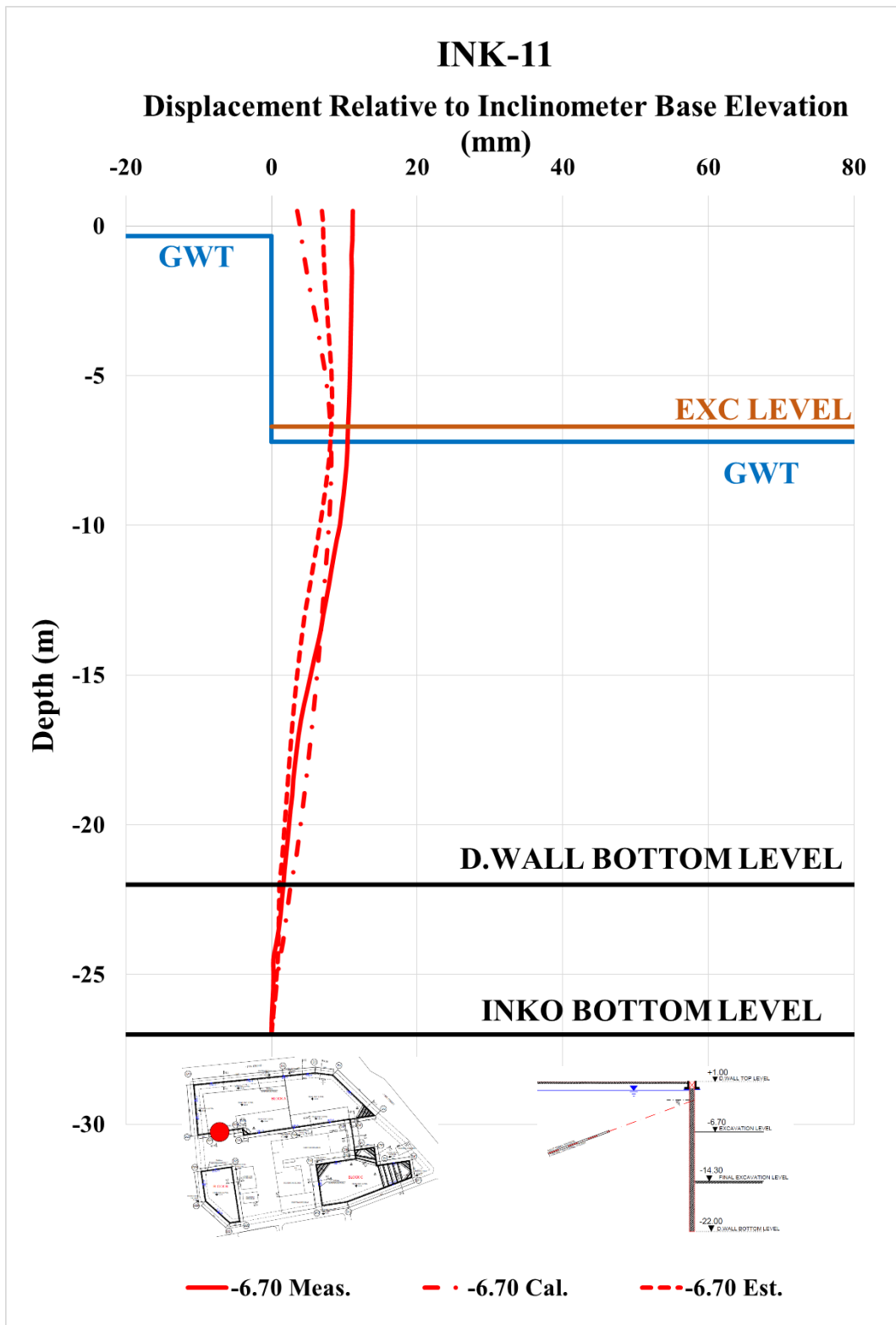
Figure 5.19. Calibrated and Measured Displ. Rel. to Inc. Base Elev. at -6.70 m
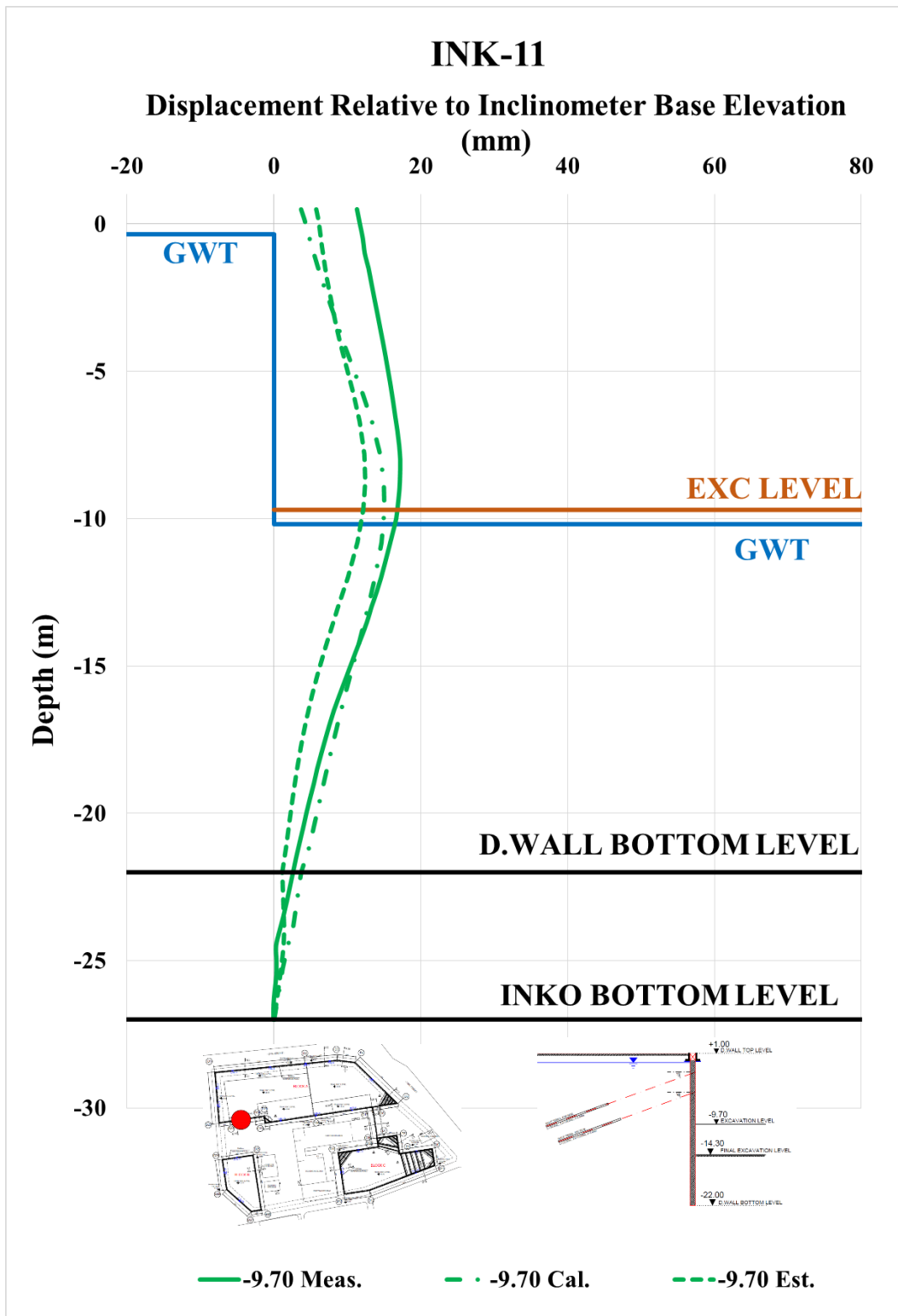
Figure 5.20. Calibrated and Measured Displ. Rel. to Inc. Base Elev. at -9.70 m
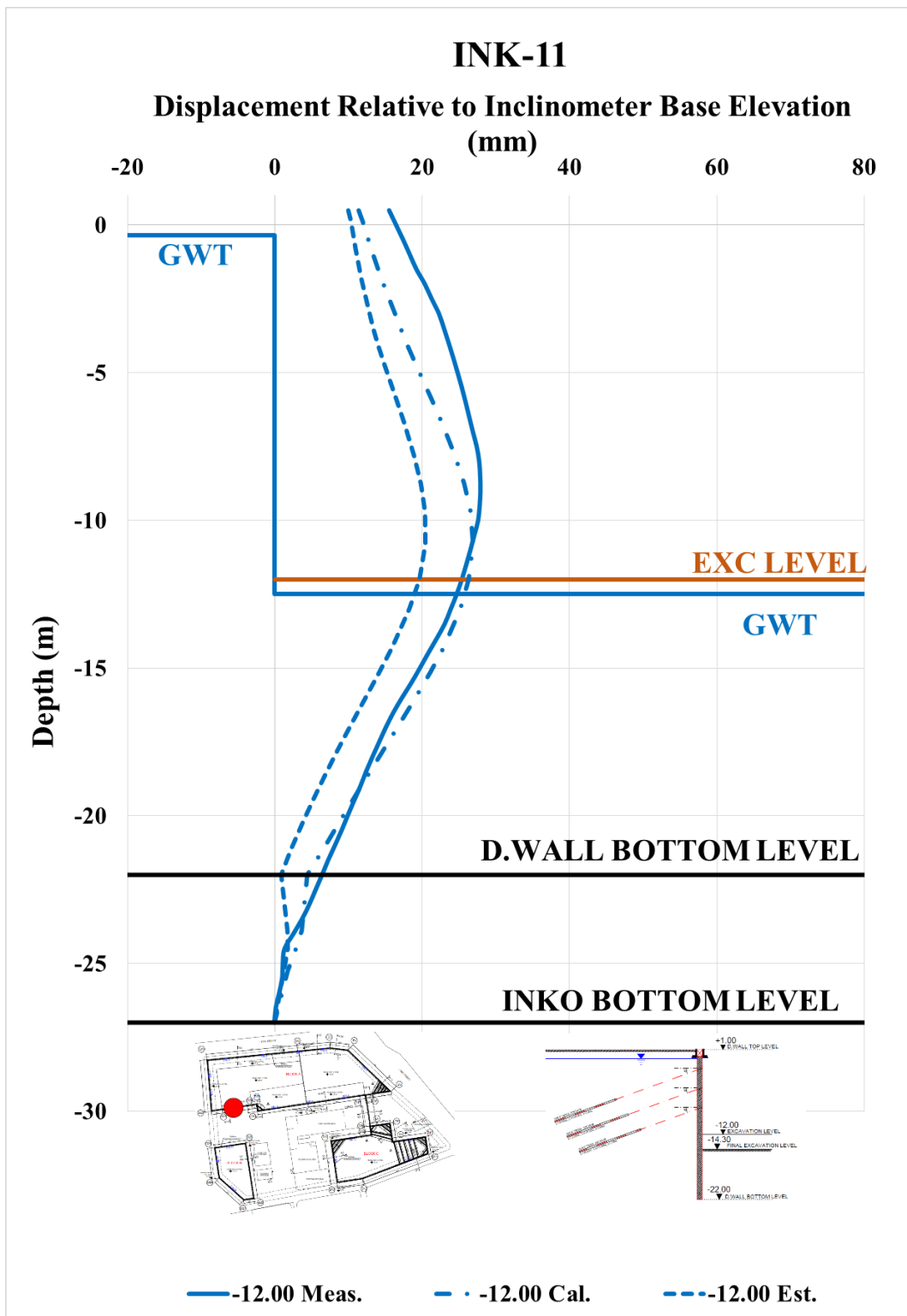
Figure 5.21. Calibrated and Measured Displ. Rel. to Inc. Base Elev. at -12.00 m
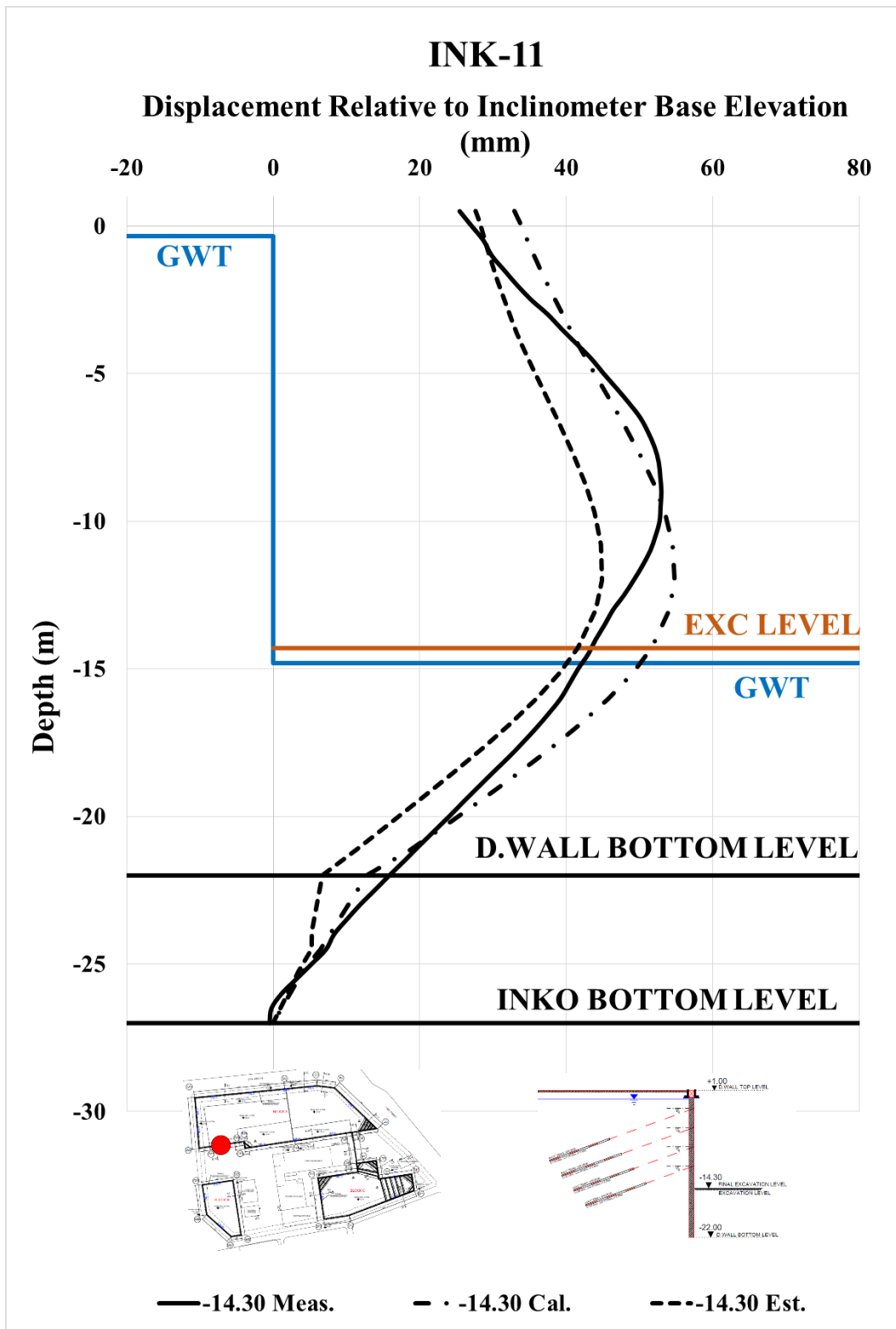
Figure 5.22. Calibrated and Measured Displ. Rel. to Inc. Base Elev. at -14.30 m
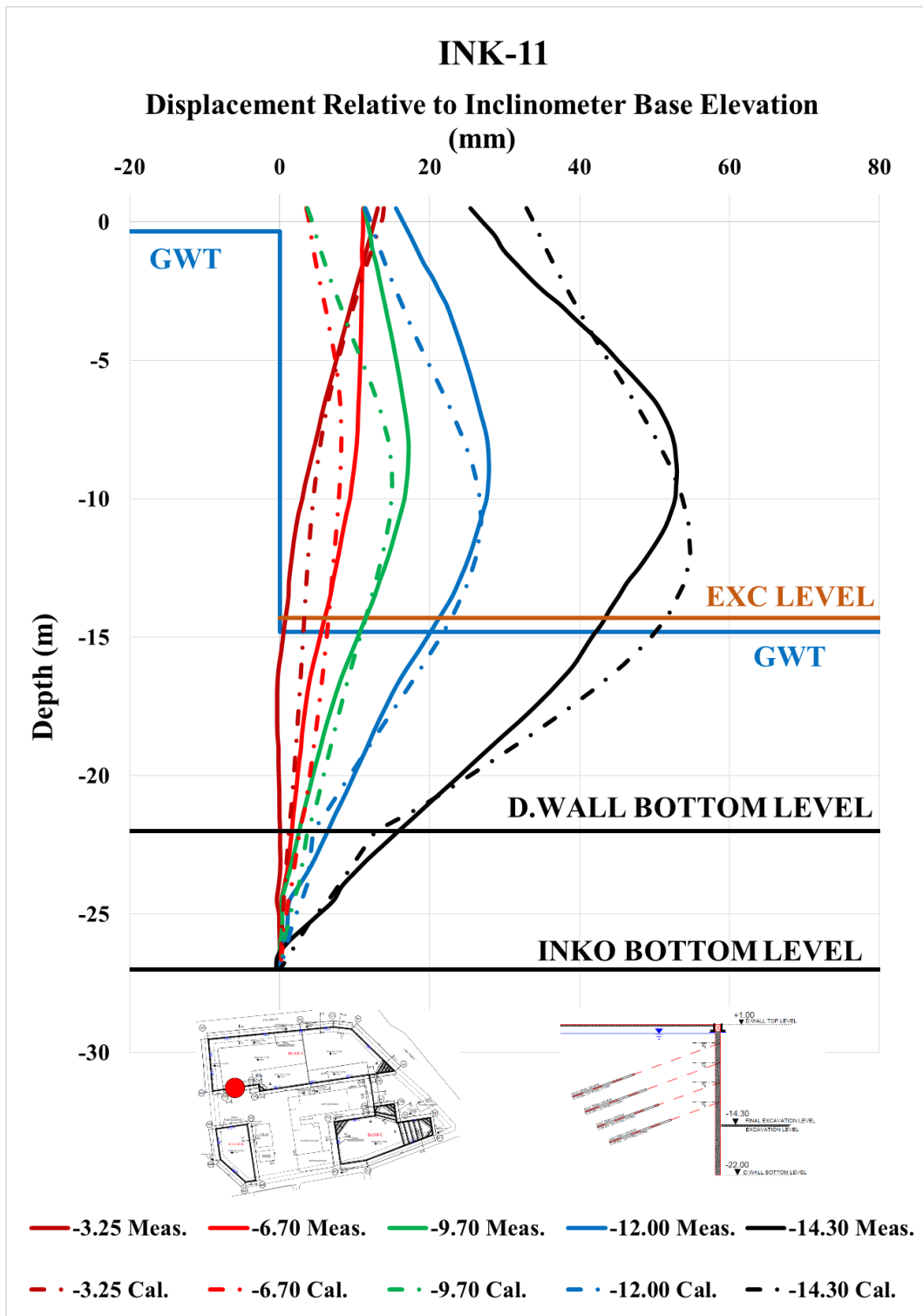
Figure 5.23. Calibrated and Measured Displ. Rel. to Inc. Base Elev.

Measured, estimated and calibrated maximum displacements of the excavation system and also recommendations of the literature are given in Table 5.6. Estimated versus measured and calibrated versus measured displacements are given in Figure 5.28 and 5.29.

Table 5.5. Internal Forces of Diaphragm Wall for Section 1A-1A for Calibrated Parameters

INK - 11 / Section 1A-1A					
Excvation Stage	1	2	3	4	5
Excavation Level (m)	-3.25	-6.70	-9.70	-12.00	-14.30
N_{max} (kN/m)	86.33	249.80	440.10	608.40	765.00
V_{max} (kN/m)	62.29	218.10	304.30	348.80	381.10
M_{max} (kN.m/m)	157.80	326.10	647.70	912.70	1374.00
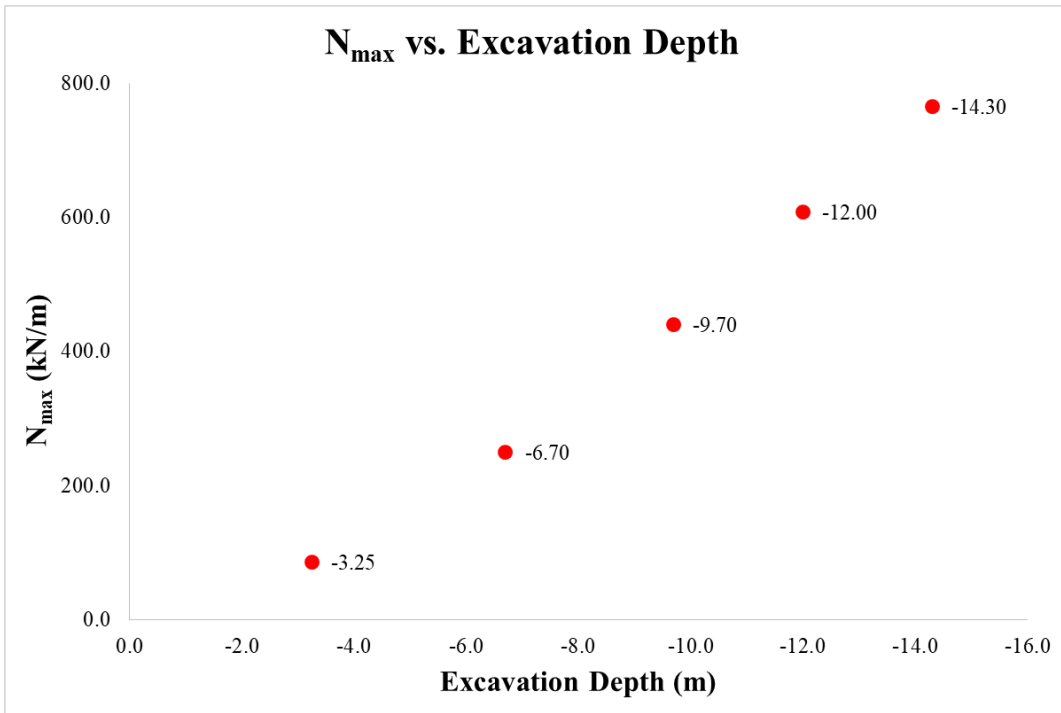
Figure 5.24. Normal Forces of Diaphragm Wall for Each Excavation Stage
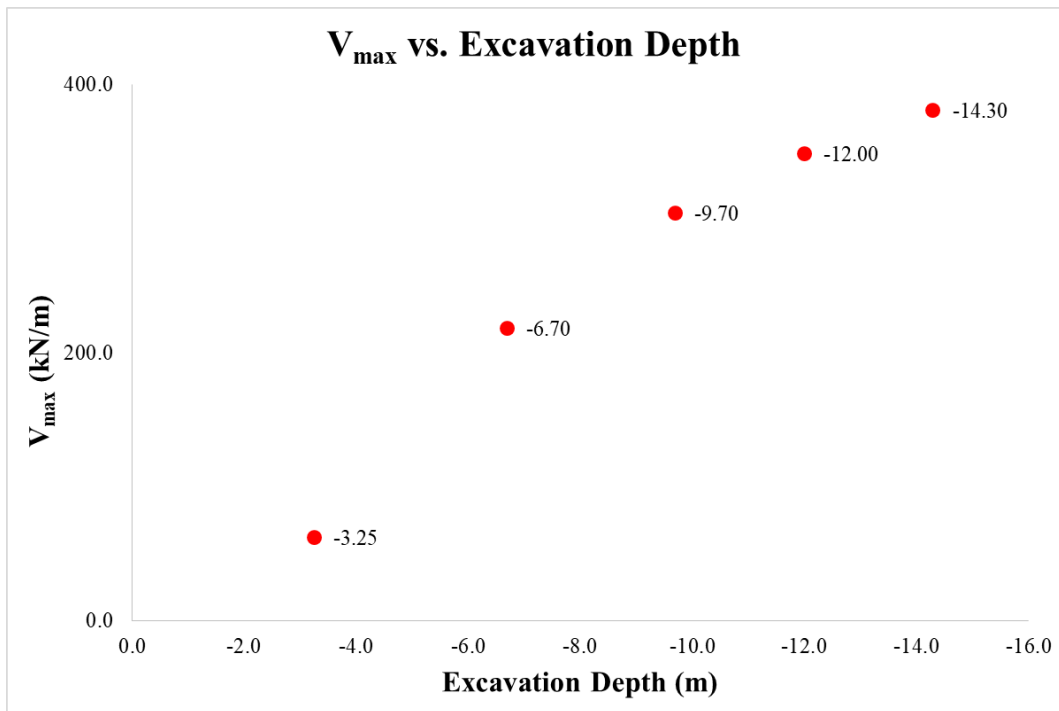
Figure 5.25. Shear Forces of Diaphragm Wall for Each Excavation Stage
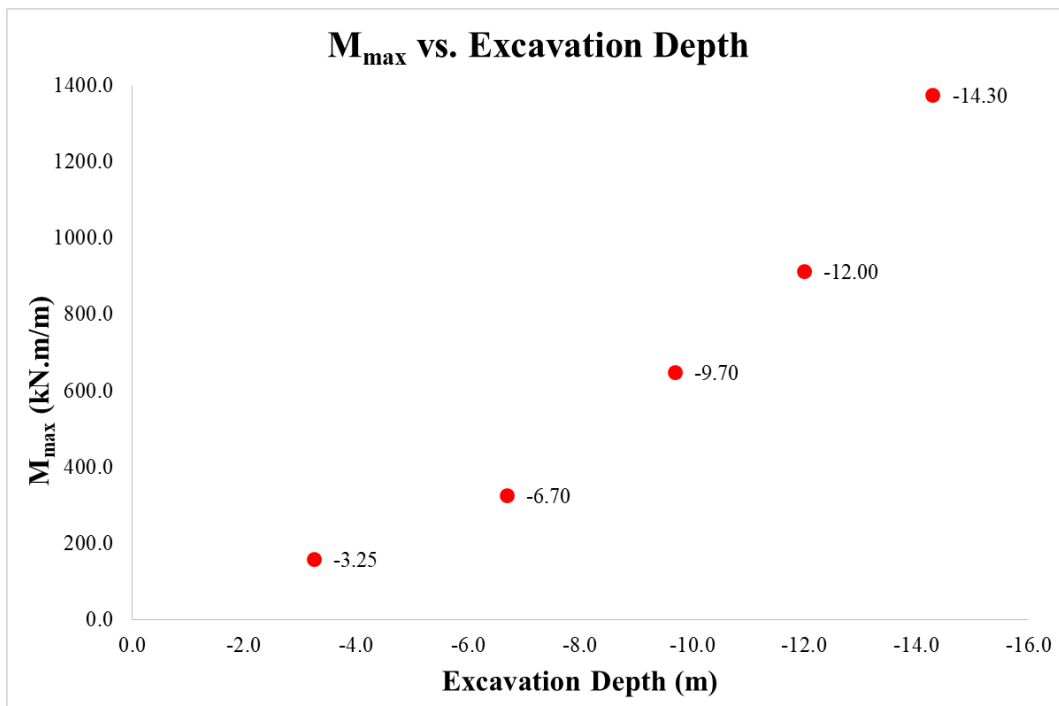
Figure 5.26. Bending Moments of Diaphragm Wall for Each Excavation Stage
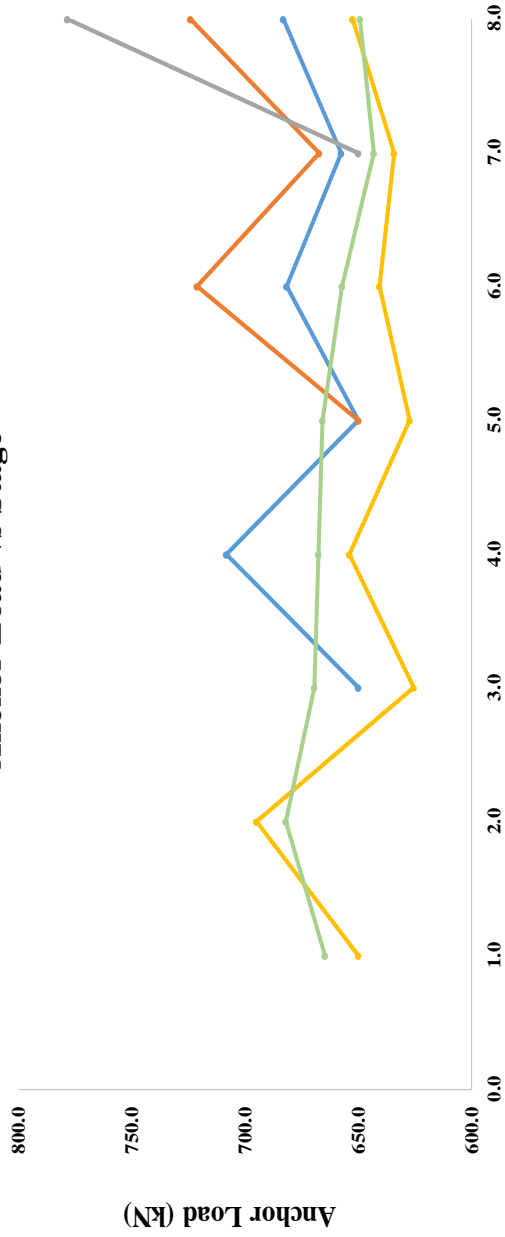
Figure 5.27. Achor Loads of INK-11 for Calibrated Soil Parameters

Legend	Excavation Stage	1. Anchor Level	2. Excavation Level	2. Anchor Level	3. Excavation Level	3. Anchor Level	4. Excavation Level	4. Anchor Level	Final Excavation Level
	Measured Load of 1. Anchor Row (kN)	664.65	681.97	669.46	667.62	665.86	657.25	643.13	649.31
	Estimated Load of 1. Anchor Row (kN)	650.00	694.94	625.45	653.84	627.45	640.80	634.30	652.62
	Estimated Load of 2. Anchor Row (kN)	-	-	650.00	708.30	649.84	681.48	657.45	683.00
	Estimated Load of 3. Anchor Row (kN)	-	-	-	-	650.00	721.18	667.12	724.13
	Estimated Load of 4. Anchor Row (kN)	-	-	-	-	-	-	650.00	778.37

Table 5.6. Summary of Displacement Results

INK - 11 / SECTION 1A - 1A

Excvation Level (m)	Excvation Depth (m)	u_{meas} (mm) Inclinometer Measurements	u_{est} (mm) Estimation with Plaxis 2D Analysis	u_{cal} (mm) Calibration with Plaxis 2D Analysis	$u_{literature}$ (mm) FHWA-IF-99-015 (1999) - Maksimum	$u_{literature}$ (mm) FHWA-IF-99-015 (1999) - Average	$u_{literature}$ (mm) Goldberg et al. (1976)	$u_{literature}$ (mm) Clough et al. (1990) - Maksimum	$u_{literature}$ (mm) Clough et al. (1990) - Average	$u_{literature}$ (mm) Long (2001)	$u_{literature}$ (mm) Long (2001) (Extraordinary cases eliminated)	$u_{literature}$ (mm) Long (2001) Cantilever System
-3,25	4,25	13,08	16,98	13,92	21,25	8,50	21,25	21,25	8,50	8,08	5,95	15,3
-6,70	7,70	11,16	8,36	8,27	38,50	15,40	38,50	38,50	15,40	14,63	10,78	-
-9,70	10,70	17,20	12,44	15,05	53,50	21,40	53,50	53,50	21,40	20,33	14,98	-
-12,00	13,00	27,92	20,48	26,89	65,00	26,00	65,00	65,00	26,00	24,70	18,20	-
-14,30	15,30	52,99	44,93	54,76	76,50	30,60	76,50	76,50	30,60	29,07	21,42	-
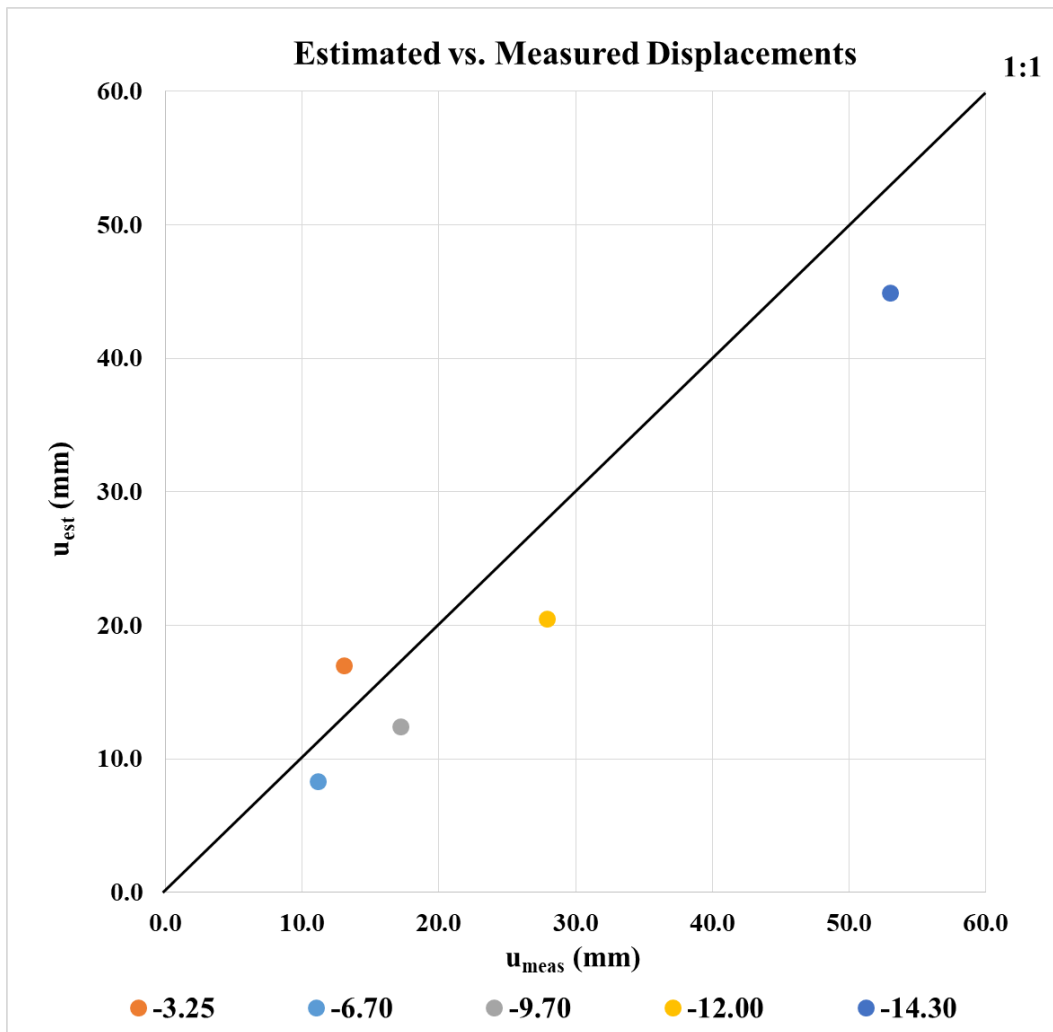
Figure 5.28. Estimated vs. Measured Displacements of INK - 11

Calibrated vs. Measured Displacements
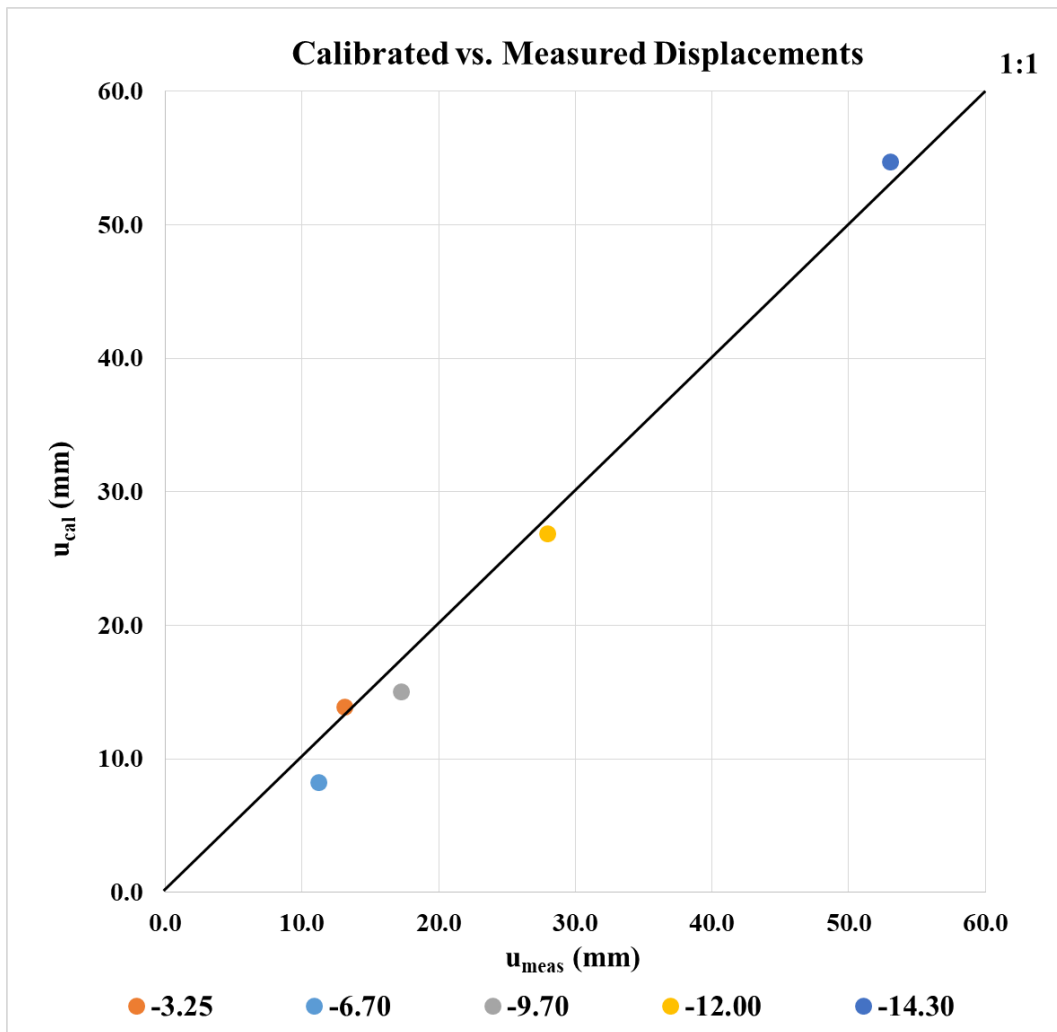
Figure 5.29. Calibrated vs. Measured Displacements of INK – 11

The maximum displacement of Section 1A-1A is 52.99 mm by examining the inclinometer readings. However, according to estimated results from FEM analysis, the maximum displacement is 44.93 mm. It means that lateral displacement of the diaphragm wall was underestimated by approximately 15%. After that, the stiffness of cohesionless and cohesive layers was multiplied by 0.75 and 1.25, respectively. As a result, the maximum displacement of the wall was obtained as 54.76 mm. The error percentage of the analysis was decreased to 3.3%.

Moreover, error percentages between the measured and estimated results increase with the increasing excavation depth. Pre-stressing anchor load is 650 kN. This value is a considerable anchor load, so it prevents the displacement of the wall in finite element analysis.

There is a significant amount of recommendations in the literature related to the lateral displacement of excavation systems. Some of them were summarized in Chapter 2. Goldberg et al. (1976) state that the maximum horizontal displacement is around 0.5 % of H. For Section 1A-1A, the excavation depth is 15.3 m. According to Goldberg et al. (1976), lateral displacement is about 76.5 mm. On the other hand, Clough et al. (1990) suggested that the average and the maximum horizontal displacement are 0.2 % and 0.5 % of H. If 0.35 % of H is considered an average value of 0.2% and 0.5% of H, horizontal displacement is approximately 53.55 mm. Moreover, Long (2001) figured out that the maximum lateral displacements of the anchored wall system are 0.19 % of H by considering the 57 case histories in Table 2-3. According to this recommendation, the maximum displacement is 29.07 mm. Long (2001) eliminated the case whose displacements are higher than 0.3 % of H due to extraordinary conditions and suggests that the maximum lateral wall movement is 0.14 % of H for stiff soils with high FOS of base heave. Fort this suggestion, the maximum wall movement is 21.42 mm. Furthermore, FHWA-IF-99-015 (1999) suggests that the lateral displacement of the anchored wall is 0.2% of H on average, and the maximum value can be 0.5% of H for sands and stiff clays. The average and the maximum displacements are 30.6 mm and 76.5 mm, respectively.

Most researchers classify displacements into two categories. They are average and maximum displacements. Section 1A-1A consists of five excavation stages. When the excavation depth was at -3.25 m, first row anchors had not been pre-stressed yet. Therefore, the diaphragm wall was working as a cantilever system. For the estimation of the displacement of the cantilever system, Long (2001) recommended that the displacement value is 0.36% of H. The wall displacement is 15.30 mm. Furthermore,

displacements at the excavation stages of -6.70 m and -9.70 m are consistent with the recommendation of Long (2001) that extraordinary cases are eliminated. For the excavation stage at-12.00 m, displacement is consistent with the average recommendation of FHWA-IF-99-015 (1999), Clough et al. (1990) and, Long (2001). Also, the displacement at the final excavation level is mean of the average and the maximum recommendation of FHWA-IF-99-015 (1999) and Clough et al. (1990).

When the maximum displacement recommendation of FHWA-IF-99-015 (1999), Clough et al. (1990,) and Goldberg et al. (1976) are considered, the deep excavation system behaved as more rigid than the expected. It can be explained with the quality of the construction. Also, the SBMA technique is more rigid than the conventional ground anchor so less displacements were observed.

Internal forces of the diaphragm wall were summarized in Tables 4-2 and 4-3 for estimated and calibrated FEM results. Maximum normal and shear forces are 775.70 kN/m and 374.70 kN/m, respectively. These forces are calculated as 765.00 kN/m and 381.10 kN/m with calibrated soil parameters. It can be understood that the normal and shear forces are similar in both cases since anchor loads have a significant effect on the normal and shear forces. Also, the weight of the wall is related to normal forces. However, bending moments of estimated and calibrated analysis are 1272 and 1374 kN.m/m, respectively, which means that the maximum bending moment value increased by 8 % in the calibration analysis. This increase can be explained by the increase of lateral displacement.

In Figure 4.17, anchor forces were given for each stage of analysis. Especially for 3. and 4. anchor rows, calculated anchor loads are 10 % to 20 % higher than the pre-stressing forces, which can be explained by the additional displacements of the diaphragm wall.

CHAPTER 6

6. SUMMARY AND CONCLUSIONS

The demand to deep excavation support systems has been increasing due to urbanization. The human population is growing dramatically all over the world and also, most of the people migrate to megacities. On the other hand, deep excavations have been located more closely in the vicinity of existing buildings, utilities, etc. Therefore, the importance of a deep excavation system is realized for the construction of high-rise buildings' basements and subway stations, etc. At the same time, the requirement for deeper excavation depth is also significantly increasing. To meet these demands, single bore multiple anchors (SBMA) technology is advancing. Deeper excavation can be performed with more economical solutions by using SBMA technology.

In the scope of this study, excavation systems including diaphragm wall, SBMA, and struts are examined. The project area was divided into 7 regions to make a more precise and accurate analysis. 18 inclinometers and 9 load cells measurements were compared with finite element analysis results and also, literature recommendations. Furthermore, finite element analysis results are calibrated by decreasing the stiffness parameters of cohesionless layers by 25 % and increasing the stiffness parameters of cohesive layers by 25 %. Examination of INK-11 is presented in Chapters 3, 4, and 5 as an example. Other inclinometers and analysis results are given in Appendix A.

The excavation depth of Section 1A-1A is 15.30 m including a 23 m diaphragm wall and 4 row anchors with a horizontal spacing of 2 m. Measured, estimated, and calibrated maximum displacements of the excavation system are given in Figure 6.1 and 6.2 for 18 inclinometers. Two boundaries which are ±5 mm and ±10 mm were drawn on Figures 6.1 and 6.2. For estimated results, %81.1 of them are between ±10 mm. Also, %47.4 of them are between ±5 mm. After the calibration, %95.8 of them are between ±10 mm. Also, %76.8 of them are between ±5 mm.
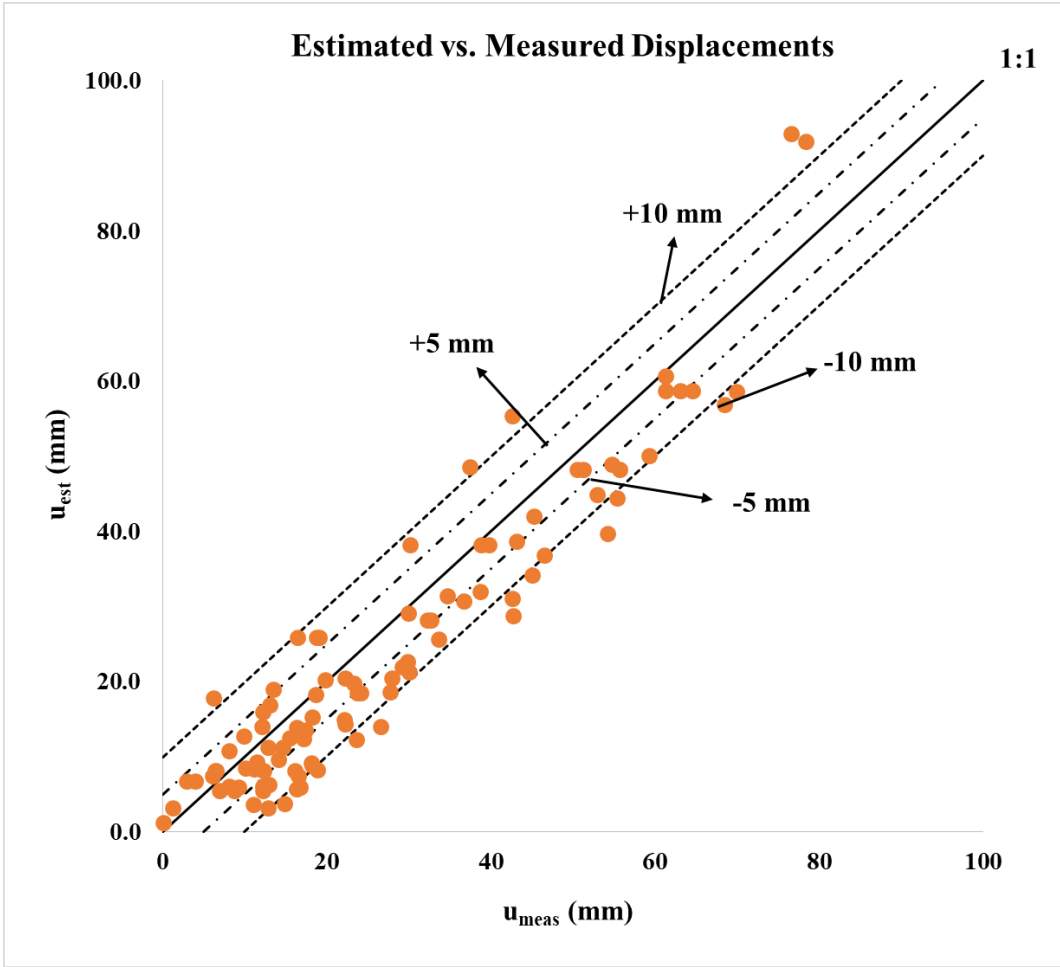
Figure 6.1. Estimated vs. Measured Maximum Displacements Relative To Inclinometer Base Elevation
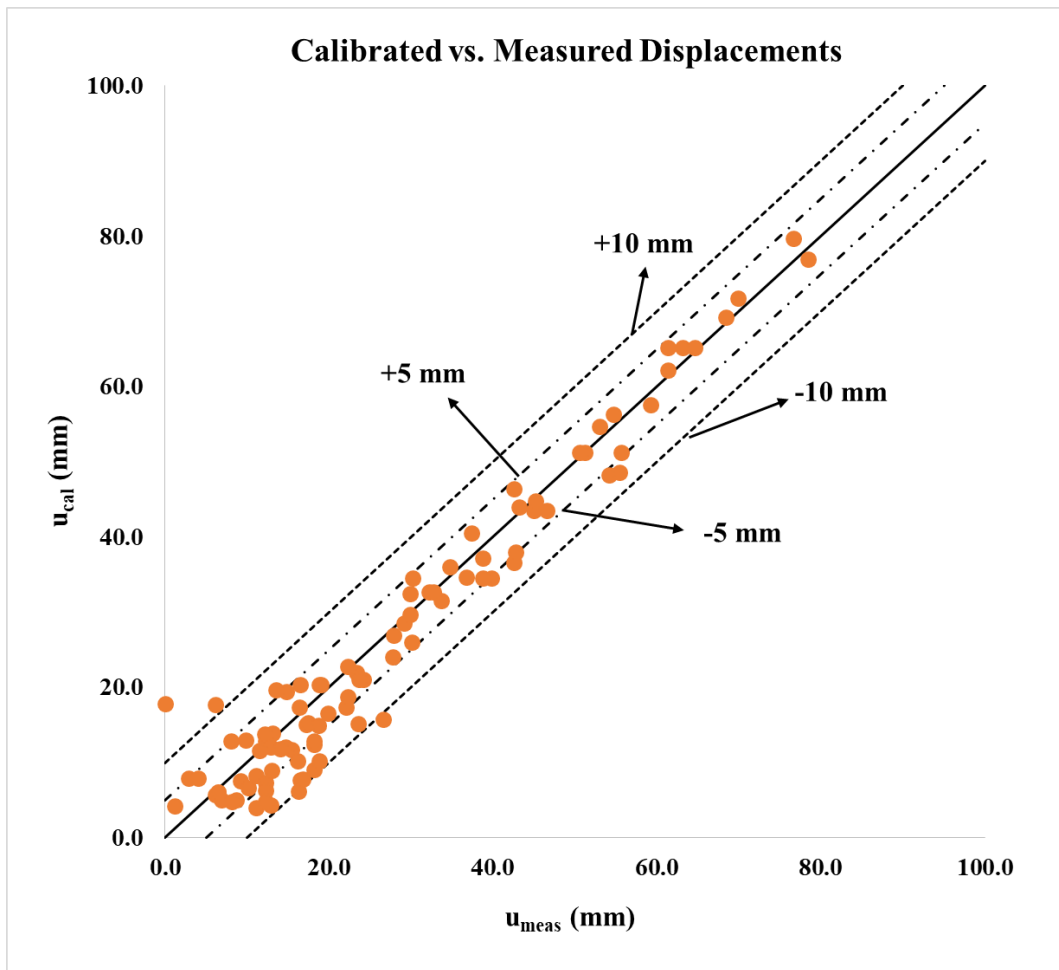
Figure 6.2. Calibrated vs. Measured Maximum Displacements Relative To Inclinometer Base Elevation
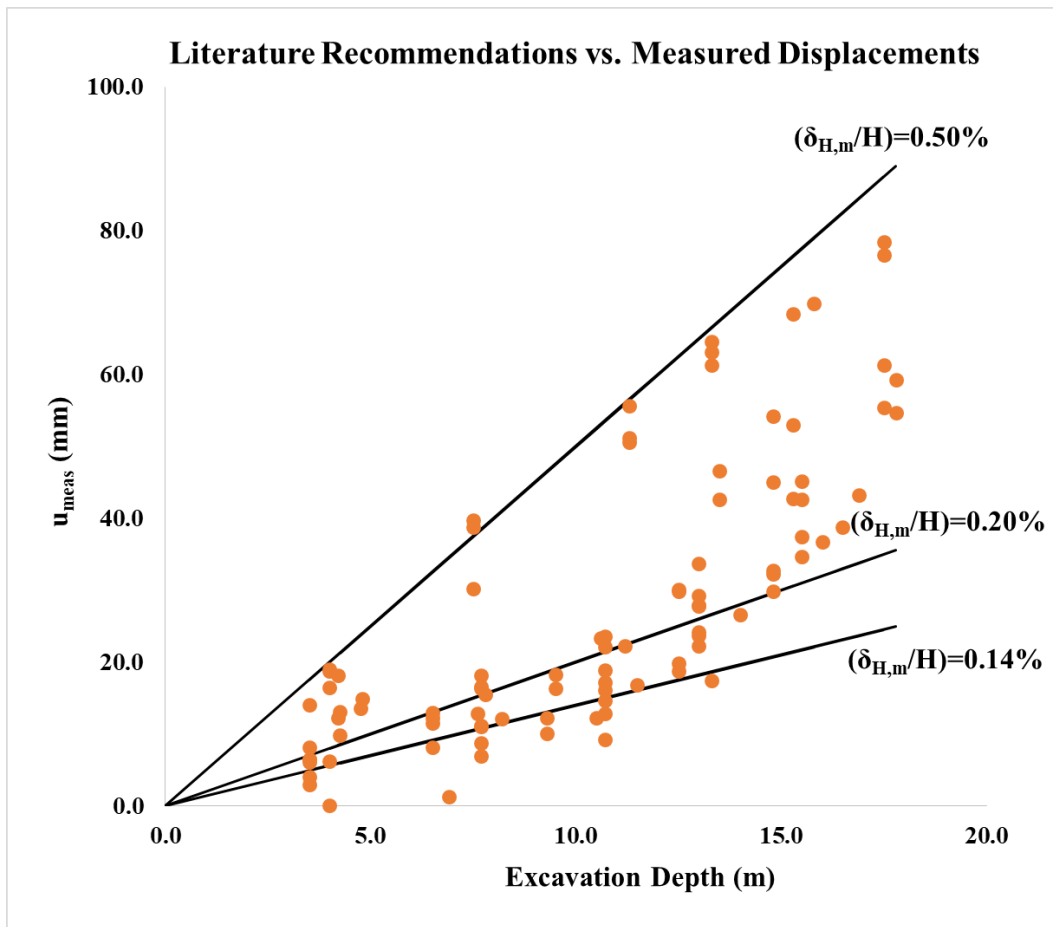
Figure 6.3. Literature Average Recommendations vs. Calibrated Displacements
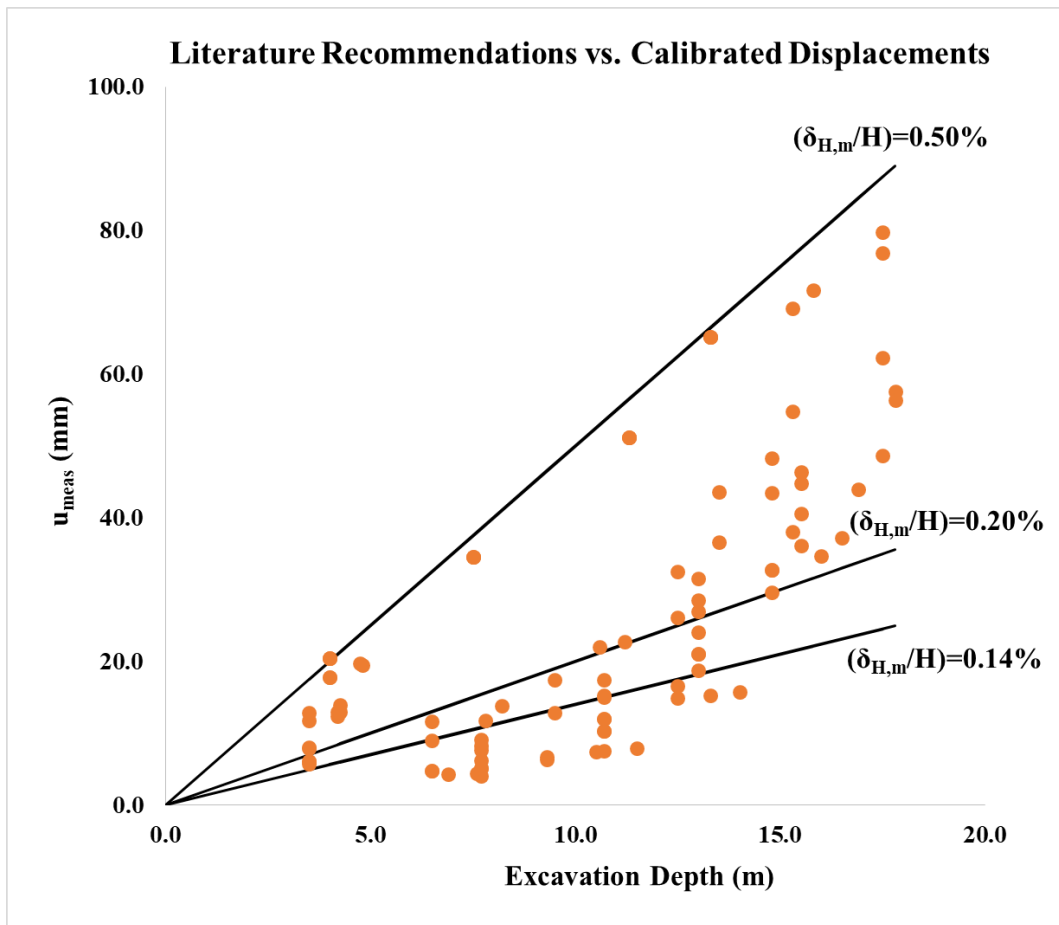
Figure 6.4. Literature Maximum Recommendations vs. Calibrated Displacements

As revealed by the calibration efforts, the predictive average modulus values of 35 MPa overestimated the in-situ stiffnesses, and a calibration coefficient of 0.75 and 1.25 are recommended to be used for cohesionless and cohesive soils respectively. Additionally, the estimated displacements are in conformance with the recommendations of the literature as shown in Figures 6.3 – 6.4. Maximum recommedations of literature is $\delta_{H,m}$/H=0.50% according to FHWA-IF-99-015 (1999), Goldberg et al. (1976) and, Clough et al. (1990). Approximately %97 of all displacements are below this boundary. Until to the excavation depth of 13 m, displacements are mostly close to the average recommendations ($(\delta_{H,m}$/H)=0.20% & $(\delta_{H,m}$/H)=0.14%) of the literature. Displacements are mostly in between the average and the maximum values of recommended literature displacements, especially after the excavation depth of 13 m. The main reason for the increase in displacement is that the waiting time between the excavation stages is higher than expected. Moreover, a gap in between the diaphragm wall and soil cannot be modeled with the finite element analysis software. Moreover, studied excavation system was supported by using single bore multiple anchors (SBMA) but displacements recommendation are for traditional anchored systems. It can be understood that calibrated displacements are close to measured displacements when stiffness parameters are multiplied by calibration coefficients.

.

REFERENCES

Azzouz, A. S., Krizek, R. J., & Corotis, R. B. (1976). Regression analysis of soil compressibility. *Soils and Foundations*, *16*(2), 19-29.

Baldi, G., Bellotti, R., Ghionna, V.N., Jamiolkowski, M., and Lo Presti, D.F.C., 1989. Modulus of sands from CPTs and DMTs. *In Proceedings of the 12th International Conference on Soil Mechanics and Foundation Engineering*. Rio de Janeiro. Balkema Pub., Rotterdam, Vol.1, pp. 165-170.

Barley, A.D. 1995. *Theory and Practice of the Single Bore Multiple Anchor System. International Symposium on Anchors in Theory and Practice,*. Saltzburg, Austria. pp 293-301

Brinkgreve, R. B. (2005). *Selection of Soil Models and Parameters For Geotechnical Engineering Application*

Brinkgreve, R. B. J., Engin, E., & Engin, H. K. (2010). Validation of empirical formulas to derive model parameters for sands. *Numerical methods in geotechnical engineering*, *137*, 142.

Clough, G. W., Smith, E. M., & Sweeney, B. P. (1989). Movement control of excavation support systems by iterative design. In *Foundation engineering: current principles and practices* (pp. 869-884). ASCE.

lough, G. W., and O'Rourke, T. D. (1990). ''Construction induced movements of in situ walls.''Proc., ASCE Conf. on Des. and Perf. Of Earth Retaining Struct., Geotech. Spec. Publ. No. 25, ASCE, NewYork, 439–470.

Cetin, K. O., Seed, R. B., Kayen, R. E., Moss, R. E., Bilge, H. T., Ilgac, M., & Chowdhury, K. (2018). The use of the SPT-based seismic soil liquefaction triggering evaluation methodology in engineering hazard assessments. *MethodsX*, *5*, 1556-1575.

Das, B. M., and Sivakugan, N. (2019). *Principles of Foundation Engineering. Boston: Cengage Learning*.

Duncan, J.M. and Chang, C.Y. (1970). Nonlinear analysis of stress and strain in soils. Journal of Soil Mech. and Foundation Division, ASCE, pp. 1629-1653.

Ergun, M. U. (2008). Deep excavations. *Electronic Journal of Geotechnical Engineering, Available at: www. ejge. com/Bouquet08/UfukErgun_ppr. pdf*.

Goldberg, D. T., Jaworski, W. E., and Gordon, M. D. _1976_. Lateral support systems and underpinning. Rep. No. FHWA-RD-75-129, Federal Highway Administration, Washington, D.C.

Gibbs KJ and Holtz WG (1957) Research on determining the density of sands by spoon penetration testing. Proceedings of the 4th International Conference on Soil Mechanics and Foundation Engineering, London, 35–39

Gibson, R. E., & Lumb, P. (1953). NUMERICAL SOLUTION OF SOME PROBLEMS IN THE CONSOLIDATION OF CLAY. *Proceedings of the Institution of Civil Engineers*, *2*(2), 182-198.

Ilgaç, M., & Çetin, K. Ö., (2016). SPT-Based Seismic Soil Liquefaction Triggering Assessment.

Kondner, R.L. (1963). Hyperbolic Stress-Strain Response: Cohesive Soils. ASCE Journal of the Soil Mechanics and Foundation Division., Vol.89, 115-143

Kulhawy, F.H., and Mayne, P.H., (1990). Manual on estimating soil properties for foundation design, Report EL-6800 Electric Power Research Institute, EPRI, August 1990.

Long, M. (2001). Database for Retaining Wall and Ground Movements Due to Deep Excavations. Journal of Geotechnical and Geoenvironmental Engineering, 203-224.

Mothersille D, Duzceer R, Gokalp A, Okumusoglu B. (2015) Support of 25m deep excavation using SBMA technology in Russia. XVI European Conference on Soil Mechanics and Geotechnical Engineering, Edinburg.

Ostermayer H. & Barley A.D. (2003). Fixed anchor design guidelines, Geotechnical Engineering Handbook Volume 2, 189-205. Pub Ernst and Sohn, Berlin, Germany

Ostermayer H (1977) Detailed design of anchorages. Review of Diaphragm Walls, I.C.E., London pp. 55 - 61.

Peck, R. B. (1969). Deep Excavations and Tunneling in Soft Ground," Proceedings". In *7th International Conference on Soil Mechanics and Foundation Engineering, Mexico City, Mexico, State-of-the-Art* (Vol. 1, pp. 225-290).

Plaxis (2021). Plaxis 2D Material Models Manual.

Plaxis (2021). Plaxis 2D Reference Manual.

Robertson, P.K., and Campanella, R.G., 1983a. Interpretation of cone penetration tests – Part I (sand). *Canadian Geotechnical Journal*, 20(4): 718-733.

Robertson, P. K. (2010, May). Estimating in-situ state parameter and friction angle in sandy soils from CPT. In *2nd International Symposium on Cone Penetration Testing* (pp. 2-43).

Sabatini, P. J., Pass, D. G., & Bachus, R. C. (1999). *Geotechnical engineering circular No. 4: ground anchors and anchored systems* (No. FHWA-IF-99-015).

Samtani, N. C., Nowatzki, E. A., Bryan, R. S., & NCS GeoResources, L. L. C. (2006). Soils and Foundations Reference Manual-Volume II (No. FHWA-NHI–06-089). Federal Highway Administration (US).

Schanz, T. (1998). Zur Modellierung des Mechanischen Verhaltens von Reibungsmaterialen. Habilitation. Stuttgart University.

Schanz, T., & Vermmer, P. A. (1999). The hardening soil model: Formulation and verification. Beyond 2000 in Computational Geotechnics-10 Years of Plaxis.

Senneset, K., Sandven, R., & Janbu, N. (1989). Evaluation of soil parameters from piezocone tests. *Transportation research record*, (1235).

Sorensen, K. K., & Okkels, N. (2013, September). Correlation between drained shear strength and plasticity index of undisturbed overconsolidated clays. In *Proceedings of the 18th International Conference on Soil Mechanics and Geotechnical Engineering, Paris* (Vol. 1, pp. 423-428).

Stroud, M.A. (1974). The Standard Penetration Test in Insensitive Clays and Soft Rocks. Proceedings, First European Conference on Penetration Testing, Stockholm, Vol.1, 367-375.

Terzaghi, K., Peck, R., and Mesri, G. (1996). Soil Mechanics in Engineering Practice (3. b.). New York: John Wiley & Sons, Inc.

Von Soos, P. (1990). Properties of soil and rock (in german). In In: Grundbautaschenbuch Part 4. Ernst & Sohn, Berlin.

Vukotić, G., González, J. G., & Peña, A. S. (2013). The influence of bond stress distribution on ground anchor fixed length design. Field trial results and proposal for design methodology. Proceedings of the 18th ICSMCE, Paris.

Yap, S. P., Salman, F. A., & Shirazi, S. M. (2012). Comparative study of different theories on active earth pressure. *Journal of Central South University*, *19*(10), 2933-2939.

APPENDICES

A. Analysis and Calibration Results

Area A1
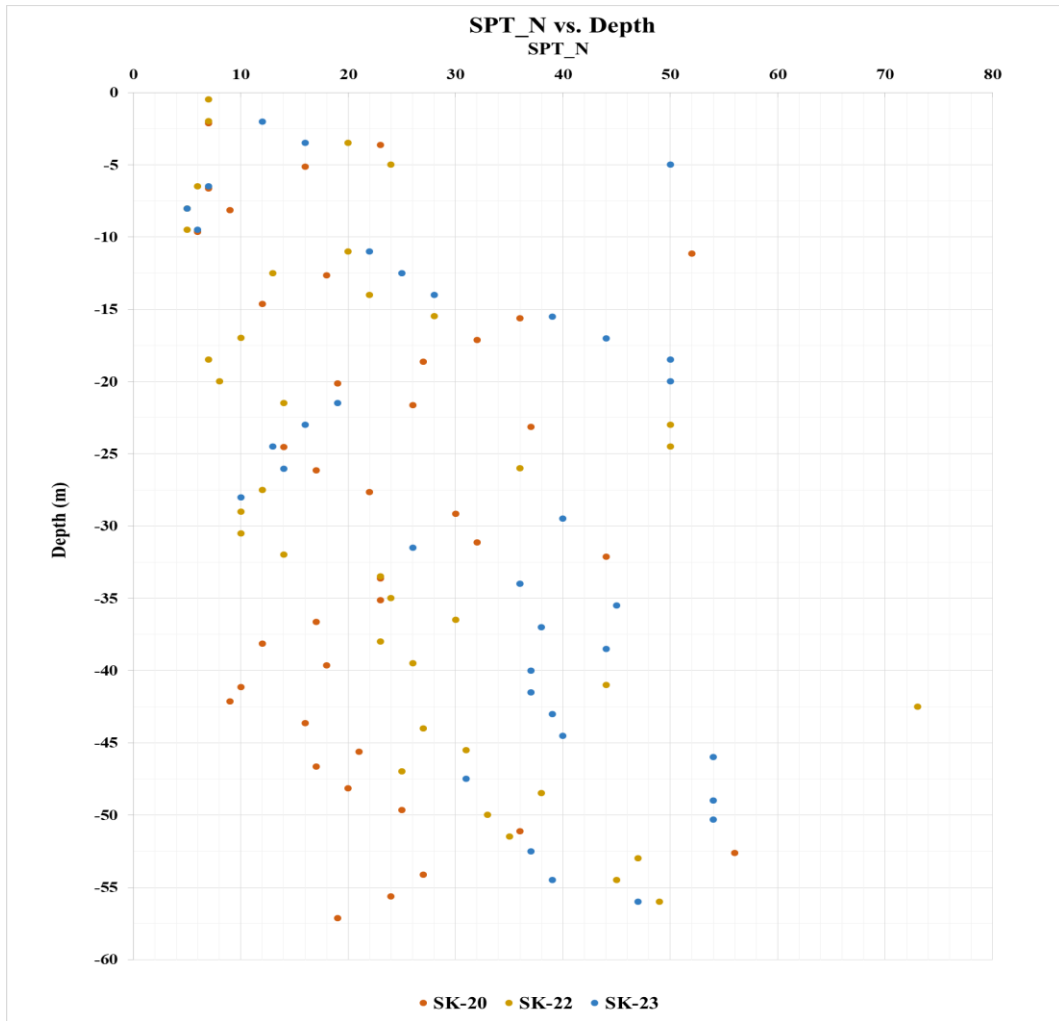
Figure A. 1. SPT-N vs. Depth for Area A1
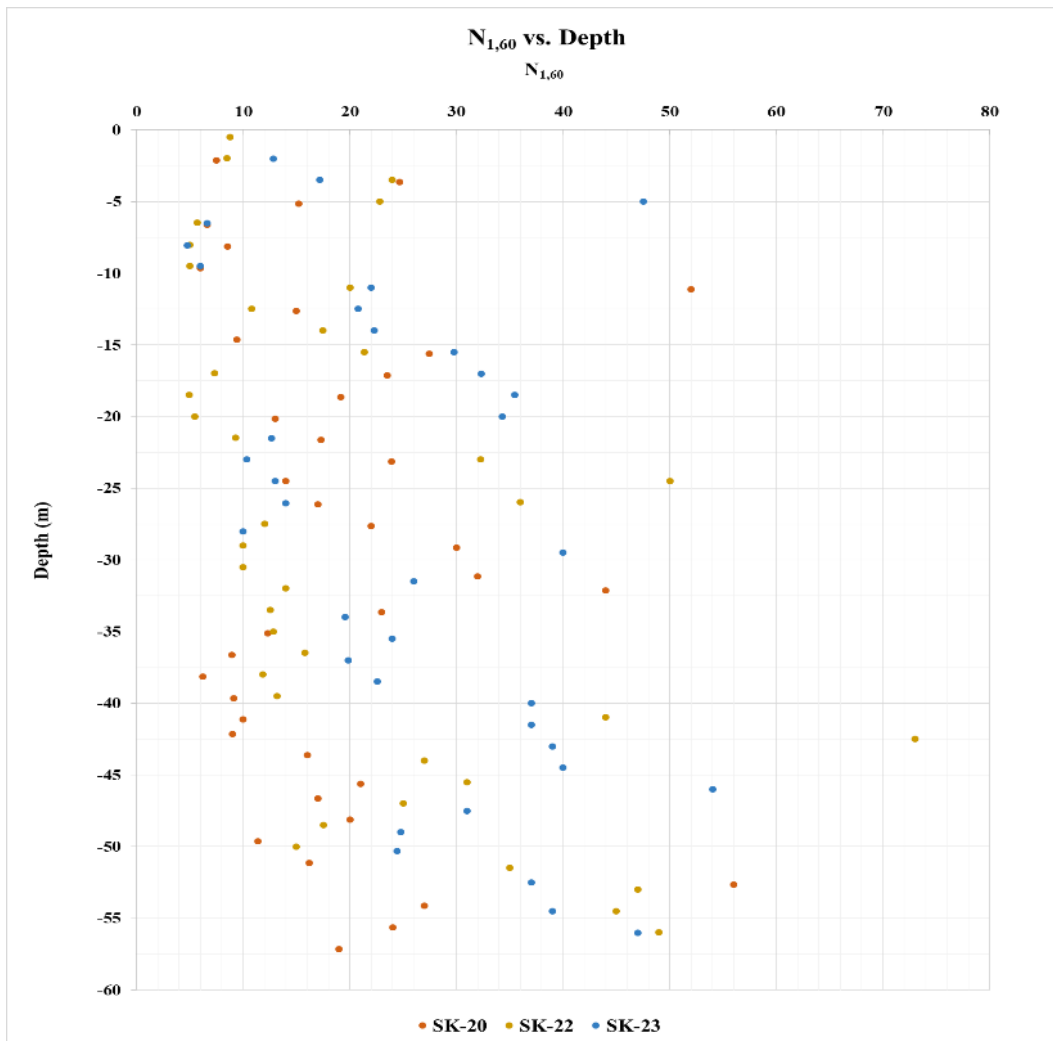
Figure A. 2. SPT-N$_{1,60}$ vs. Depth for Area A1
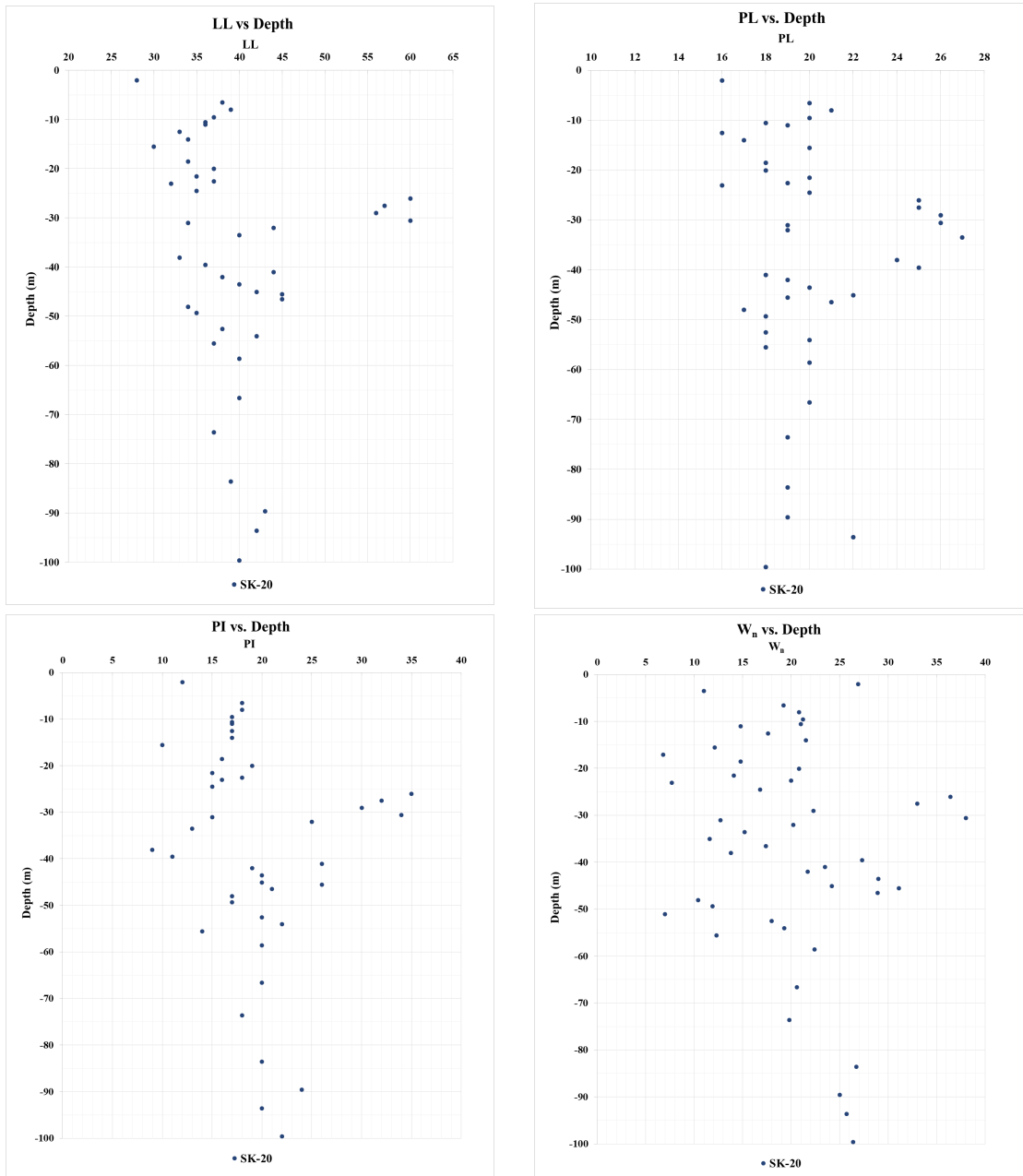
Figure A. 3. Variation of LL, PL, PI, and w_n for Area A1
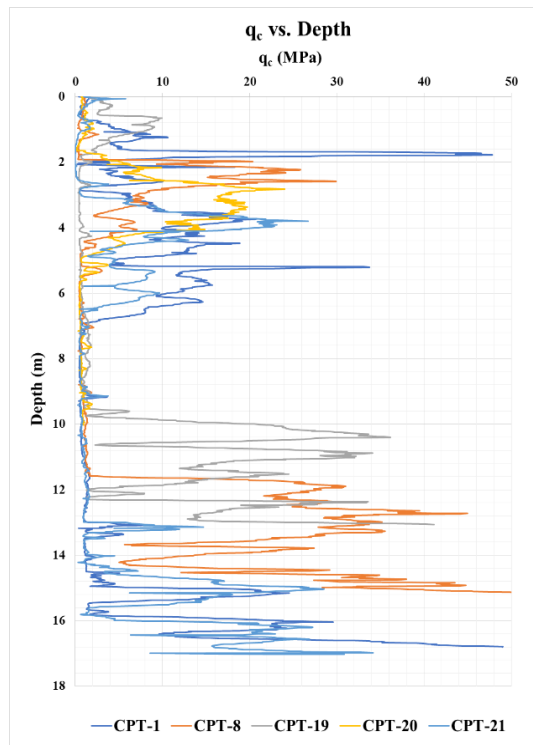
Figure A. 4. Variation of q_c along with the Depth for Area A1
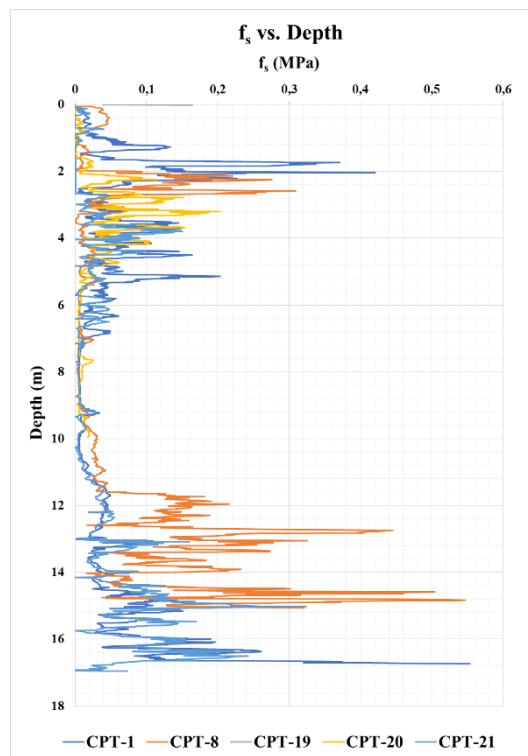
Figure A. 5. Variation of f_s along with the Depth for Area A1

140

3 boreholes (SK-20, SK-22, and SK-23) and 5 CPTs (CPT-1, CPT-8, CPT-19, CPT-20, and CPT-21) were considered. The depths of boreholes are changing between 50 m to 100 m. Depths of CPT are changing between 10 m to 17 m. The total depth of boreholes and CPTs is 210 m and 72 m respectively. Atterberg limit tests were performed on the samples taken from SK-20. LL, PL, PI, and w_n vary in 28 – 60 % (avg. 39.6 %), 16 – 27 % (avg. 20 %), 9 – 35 % (avg. 19.3 %), and 6.8 – 38 % (avg. 20 %) respectively. Unified soil classification (USCS) was performed for each sample. By considering USCS, SPT $N_{1,60}$ values, and CPT results, the thickness of soil layers was determined. Detailed soil parameters are given in below table;

- Boreholes: SK-20, SK-22, and SK-23 (Change in between 50 m to 100 m. 210 m in total)
- CPTs: CPT-1, CPT-8, CPT-19, CPT-20, and CPT-21 (Change in between 10 m to 17 m. 72 m in total)
- LL: 28 – 60 % (avg. 39.6 %)
- PL: 16 – 27 % (avg. 20 %)
- PI: 9 – 35 % (avg. 19.3 %)
- w_n: 6.8 – 38 % (avg. 20 %)

Table A. 1. Soil Profile of Area 1 (A1)

Layer No	Elevation (m)		USCS	Type	Thickness (m)	N	$N_{1,60}$	N_{60}	PI	γ_{wet} (kN/m³)	γ_{sat} (kN/m³)	c_u (kPa)	c (kPa)	φ (°)	ψ (°)	ν	E_{50}^{ref} (MPa)	E_{oed}^{ref} (MPa)	E_{ur}^{ref} (MPa)	m	ν_{ur}	p_{ref} (kPa)	R_f
1	1.4	-3.6	SC-SM	Cohesionless	5.0	14.0	15.0	11.0	6.0	19.2	20.0	-	2.0	31.0	1.0	0.33	35.0	35.0	105.0	0.5	0.2	100.0	0.9
2	-3.6	-13.0	CL	Cohesive	8.0	16.0	16.0	16.0	17.3	18.4	20.0	100.0	10.0	30.5	0.5	0.33	19.2	9.6	57.6	1.0	0.2	106.1	0.9
3	-13.0	-24.5	GC-SC	Cohesionless	11.5	27.0	19.0	27.0	13.4	19.2	20.0	-	3.0	35.0	5.0	0.30	40.0	40.0	120.0	0.5	0.2	100.0	0.9
4	-24.5	-27.5	CL-ML	Cohesive	3.0	25.0	25.0	25.0	21.0	18.4	20.0	140.0	14.0	30.0	0.0	0.33	27.2	13.6	81.6	1.0	0.2	276.1	0.9
5	-27.5	-33.5	SM-ML	Cohesionless	6.0	28.0	15.0	28.0	5.0	19.2	20.0	-	3.0	33.0	3.0	0.31	35.0	35.0	105.0	0.5	0.2	100.0	0.9
6	-33.5	-42.0	CL	Cohesive	8.5	32.0	32.0	32.0	21.3	18.4	20.0	180.0	18.0	29.9	0.0	0.33	36.8	18.4	110.4	1.0	0.2	393.6	0.9
7	-42.0	-45.0	GP-GC	Cohesionless	3.0	38.0	19.0	38.0	8.5	20.0	21.6	-	3.0	36.0	6.0	0.29	40.0	40.0	120.0	0.5	0.2	100.0	0.9
8	-45.0	-52.5	CL	Cohesive	7.5	39.0	39.0	39.0	19.0	18.4	20.0	230.0	23.0	30.1	0.1	0.33	45.2	22.6	135.7	1.0	0.2	508.4	0.9

Figure A. 6. Section 1 – 1

,

Table A. 2. Section Properties of 1 – 1

SECTION 1 - 1									
Diaphragm Wall			SBMA Type Anchor				Excavation Properties		
Top Level (m)	Bottom Level (m)	Length (m)	Anchor No	Anchor Level (m)	Anchor Length (m)	Horizontal Spacing (m)	Top Level (m)	Bottom Level (m)	Depth (m)
1.00	-22.00	23.00	1	-1.80	24.00	2.00	1.00	-13.80	14.80
			2	-4.80	22.00	2.00			
			3	-7.80	20.00	2.00			
			4	-10.80	18.00	2.00			

INK-1 – Estimated and Measured Displacements
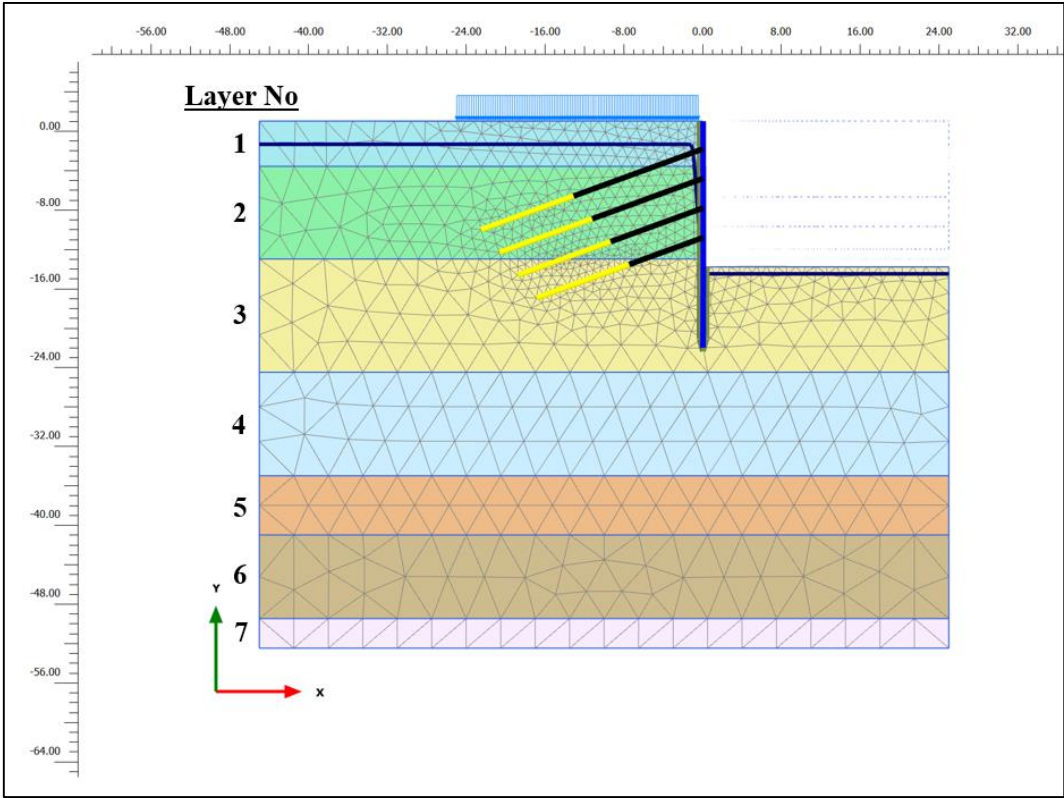
Figure A. 7. Meshed Model for INK-1
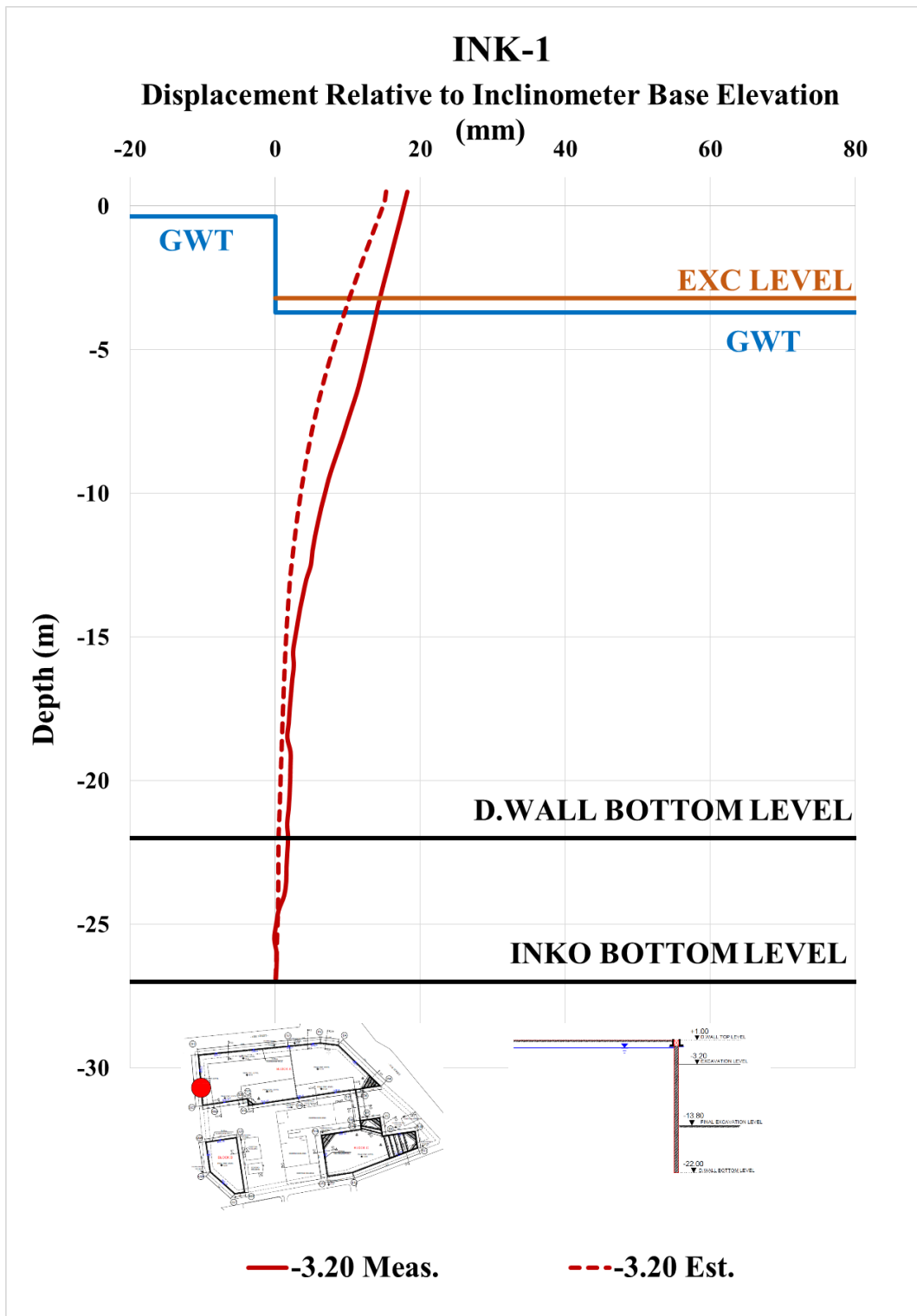
Figure A. 8. Estimated and Measured Displ. Rel. to Inc. Base Elev. at -3.20 m
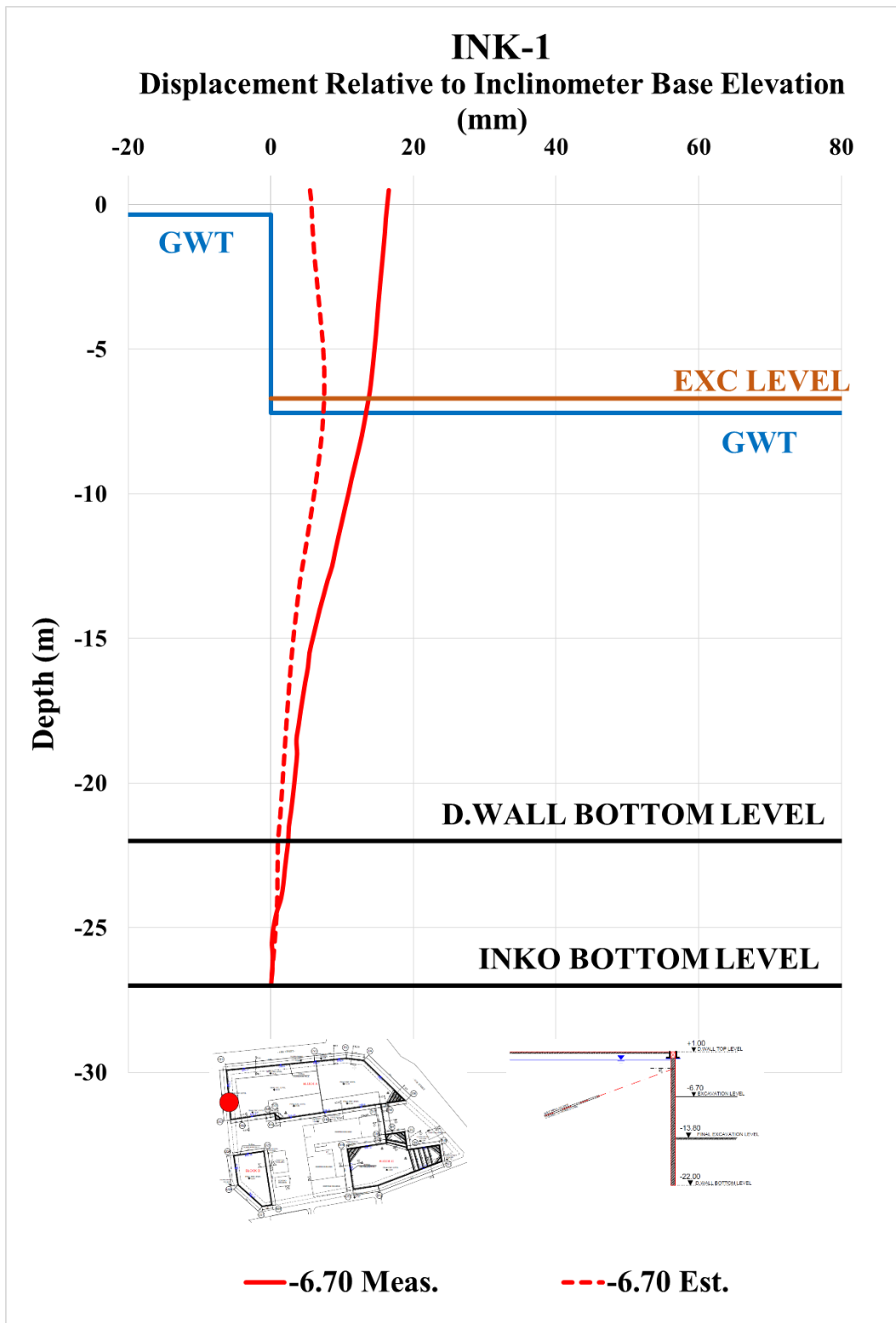
Figure A. 9. Estimated and Measured Displ. Rel. to Inc. Base Elev. at -6.70 m
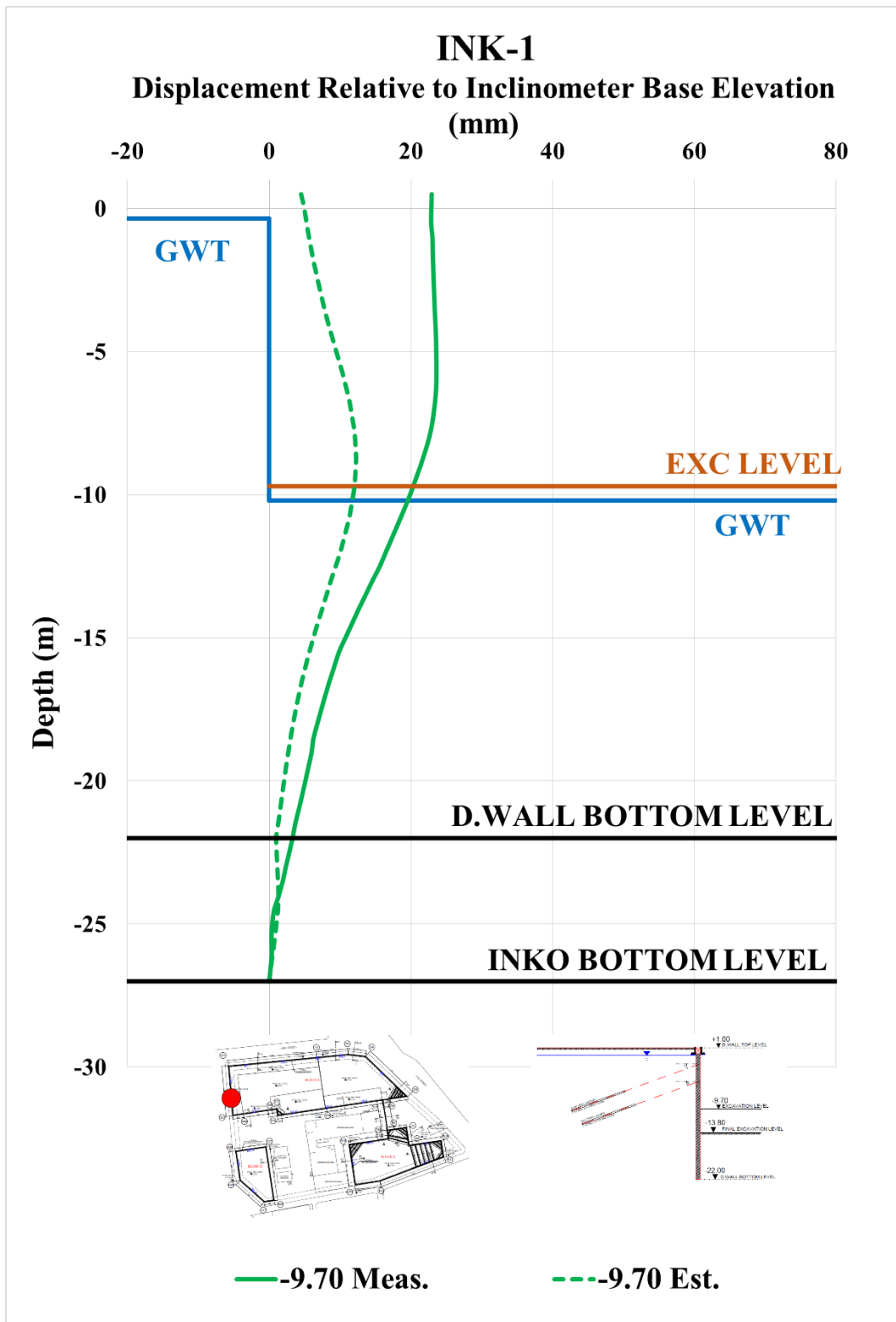
Figure A. 10. Estimated and Measured Displ. Rel. to Inc. Base Elev. at -9.70 m
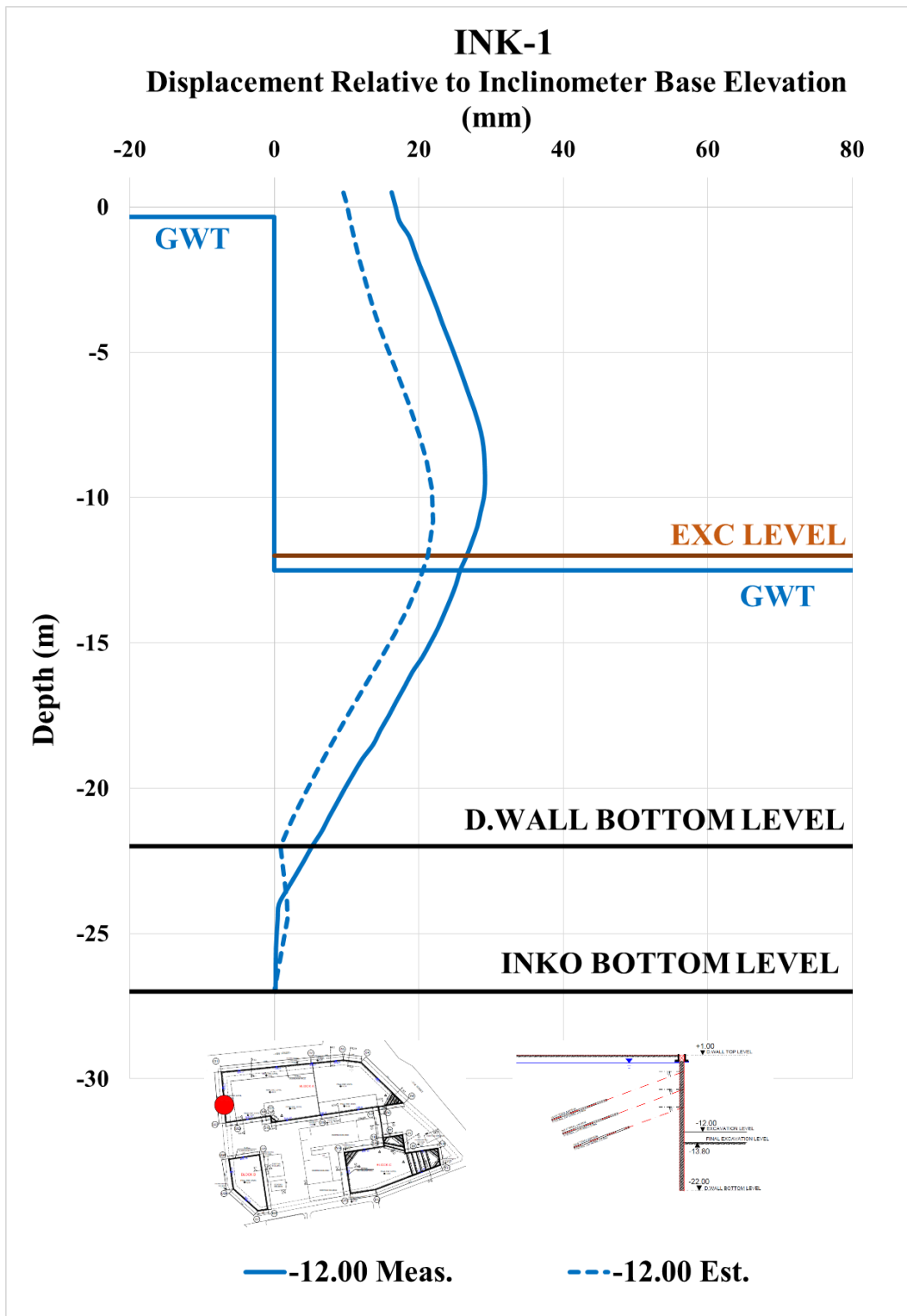
Figure A. 11. Estimated and Measured Displ. Rel. to Inc. Base Elev. at -12.00 m
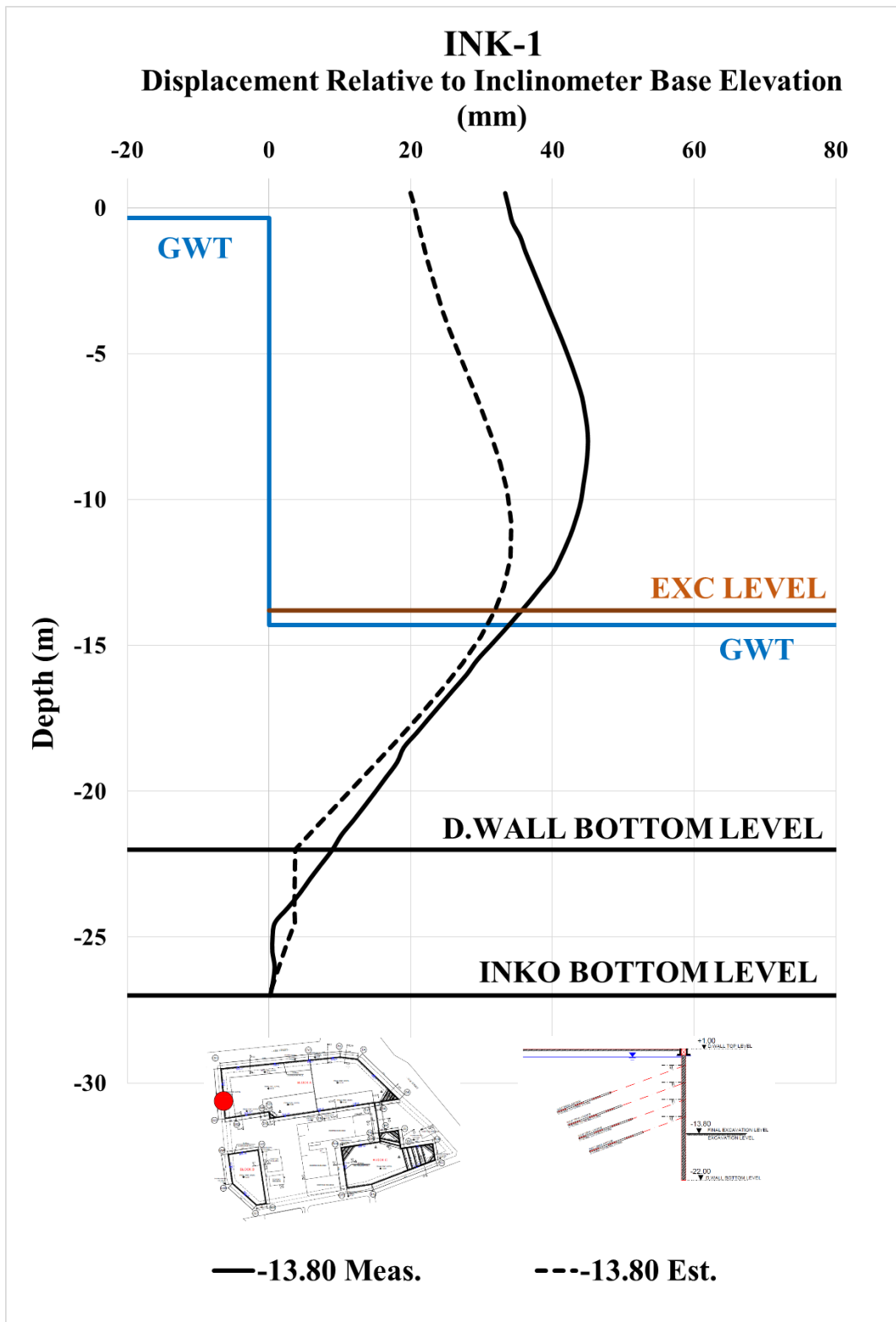
Figure A. 12. Estimated and Measured Displ. Rel. to Inc. Base Elev. at -13.80 m

Table A. 3. Internal Forces of Diaphragm Wall

INK - 1 / Section 1-1					
Excvation Stage	1	2	3	4	5
Excavation Level (m)	-3,20	-6,70	-9,70	-12,00	-13,80
N_{max} (kN/m)	95,78	245,00	429,60	604,30	733,20
V_{max} (kN/m)	57,01	214,30	310,10	353,40	353,40
M_{max} (kN.m/m)	147,40	328,00	642,60	882,70	1034,00

Legend	Excvation Stage	1. Anchor Level	2. Excavation Level	2. Anchor Level	3. Excavation Level	3. Anchor Level	4. Excavation Level	4. Anchor Level	Final Excavation Level
	Measured Load of 1. Anchor Row (kN)	709.36	643.40	635.94	631.86	634.18	627.22	621.16	600.65
	Estimated Load of 1. Anchor Row (kN)	650.00	699.21	628.74	657.50	628.98	641.70	633.42	643.48
	Estimated Load of 2. Anchor Row (kN)	-	-	650.00	710.86	648.50	681.27	655.47	669.28
	Estimated Load of 3. Anchor Row (kN)	-	-	-	-	650.00	725.27	670.08	701.06
	Estimated Load of 4. Anchor Row (kN)	-	-	-	-	-	-	650.00	716.12
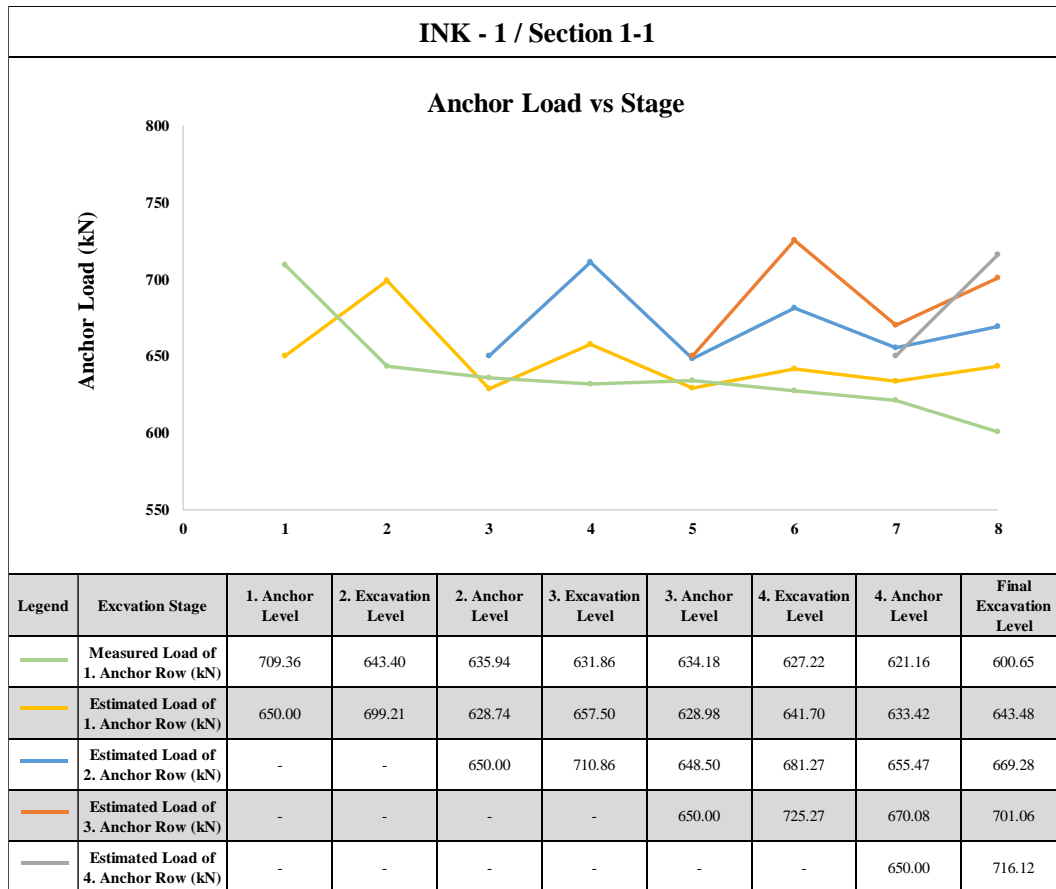
Figure A. 13. Measured and Estimated Anchor Loads

INK-2 – Estimated and Measured Displacements
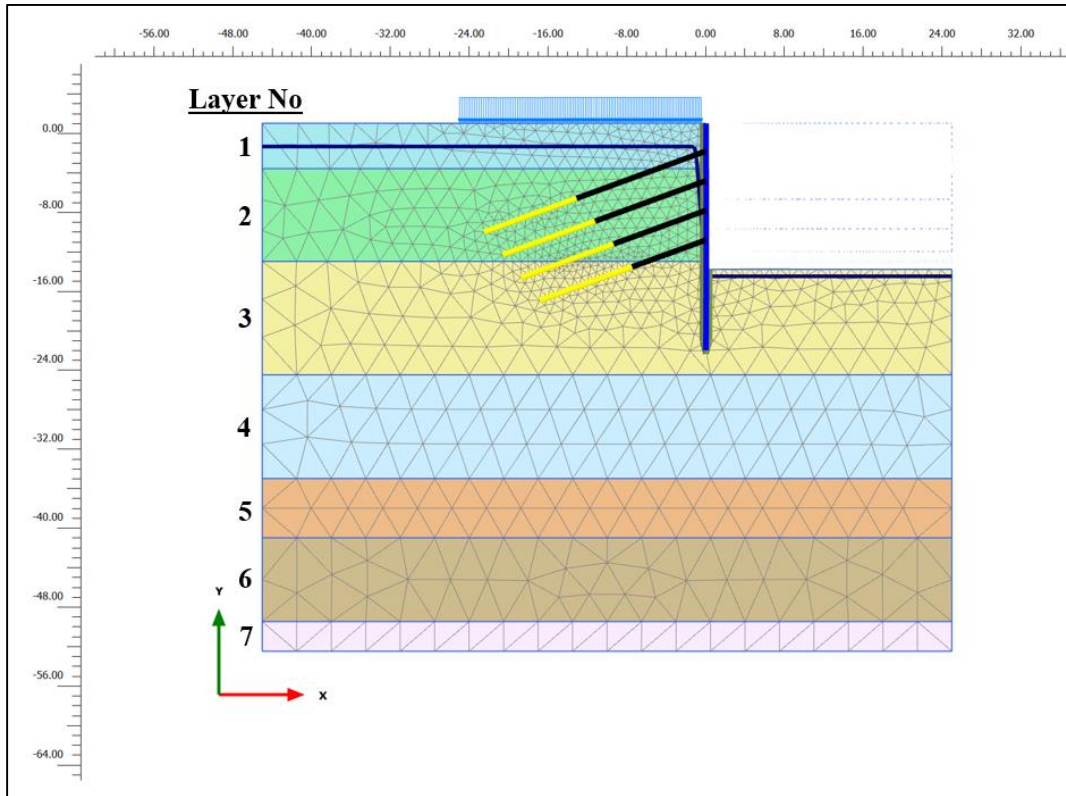
Figure A. 14. Meshed Model for INK-2
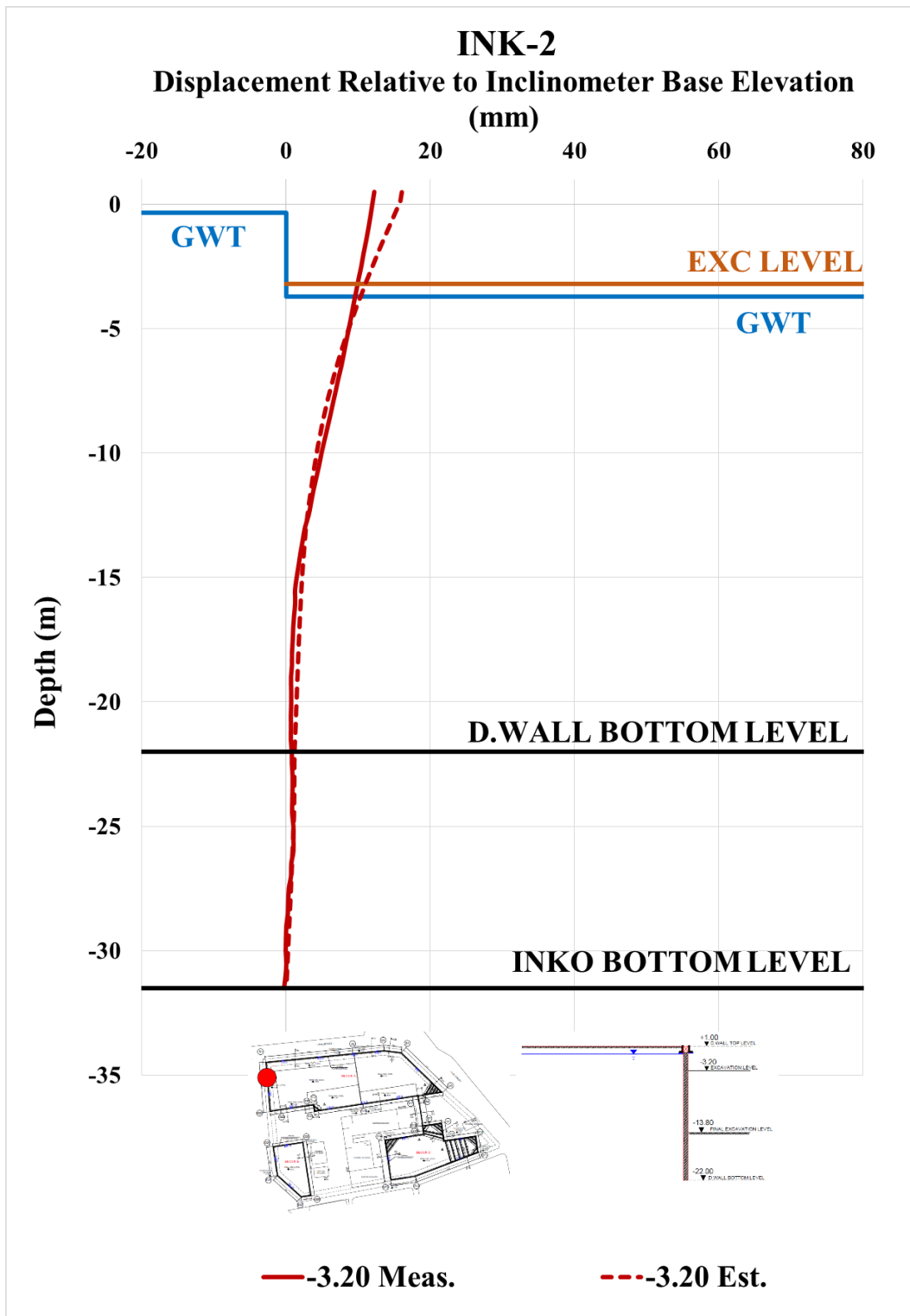
Figure A. 15. Estimated and Measured Displ. Rel. to Inc. Base Elev. at -3.20 m
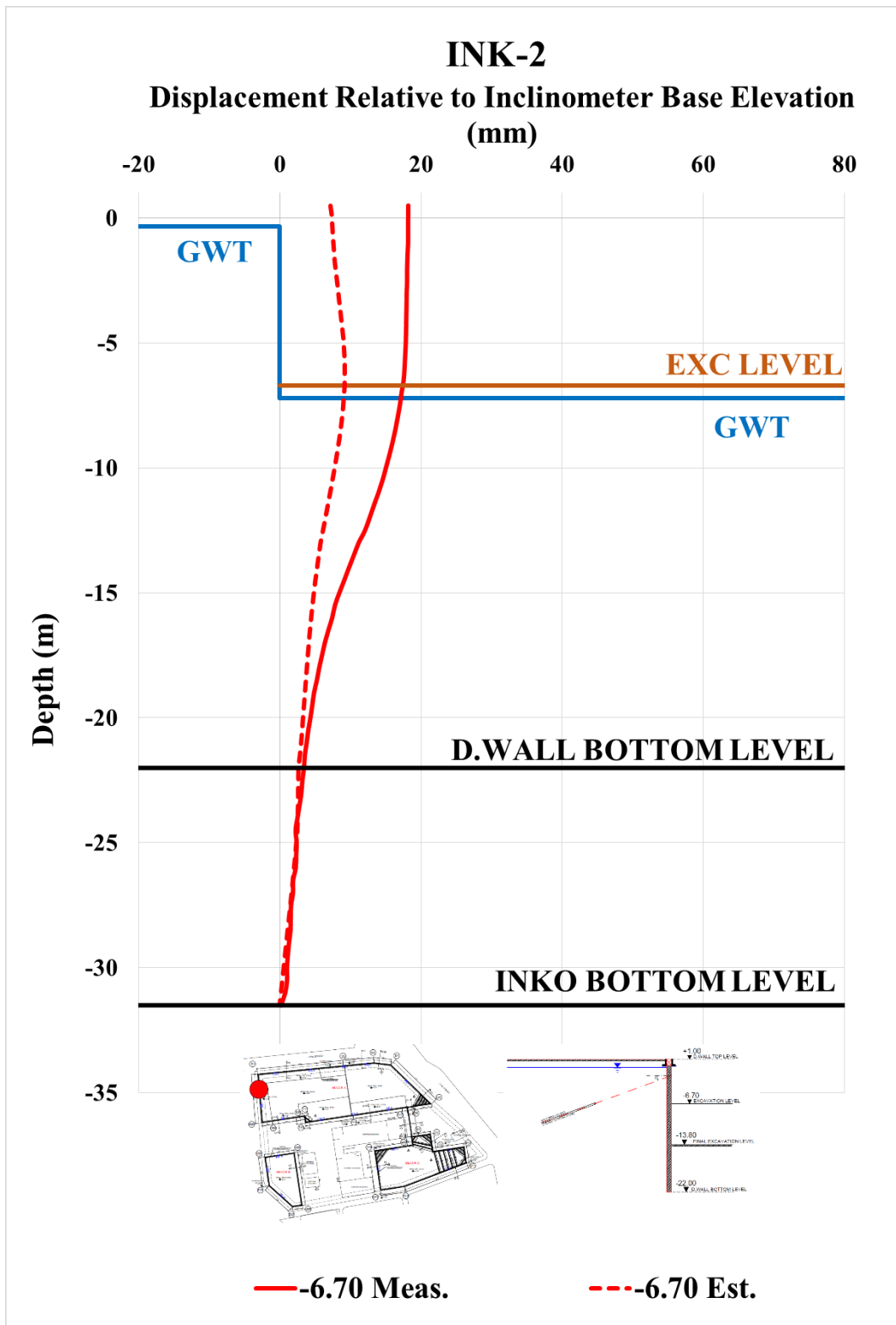
Figure A. 16. Estimated and Measured Displ. Rel. to Inc. Base Elev. at -6.70 m
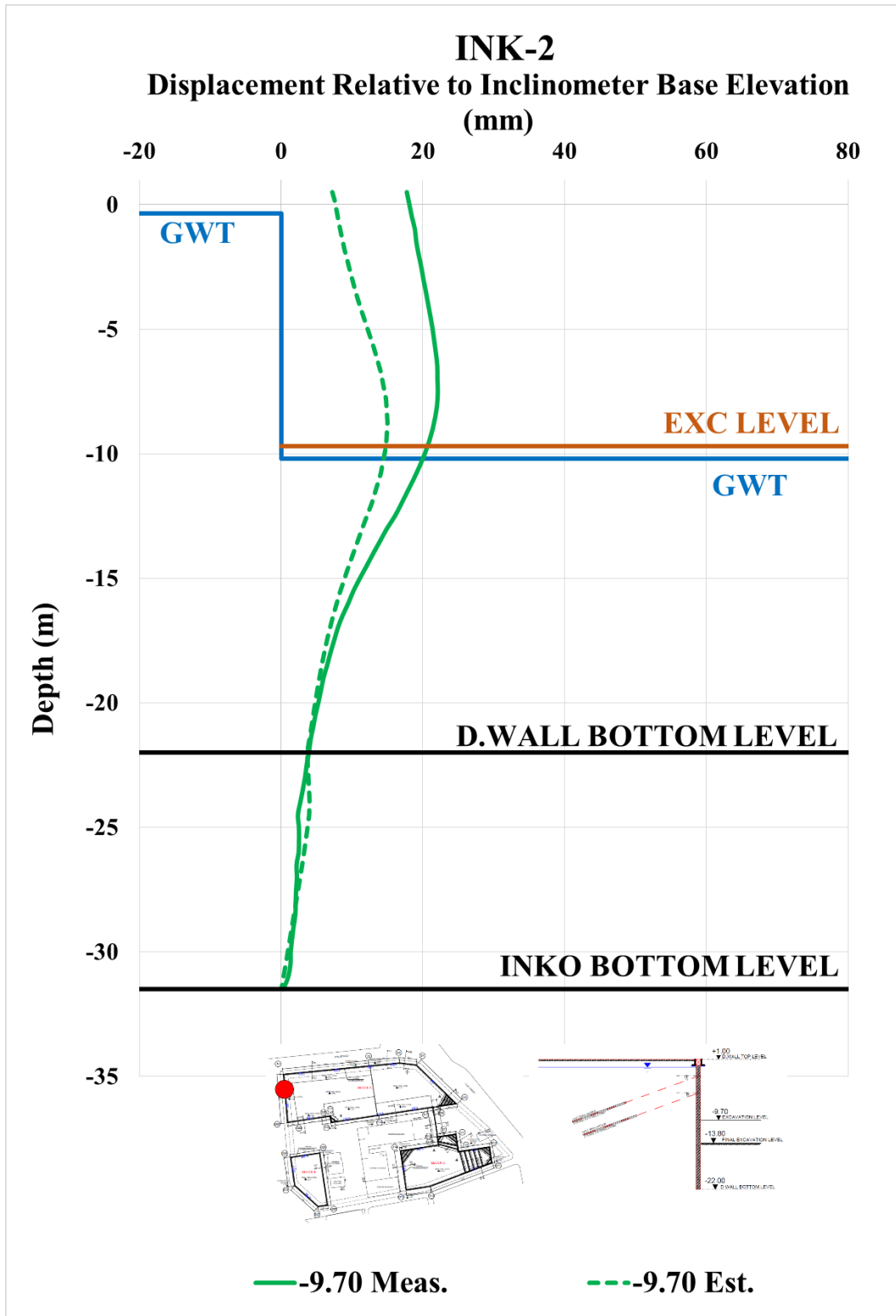
Figure A. 17. Estimated and Measured Displ. Rel. to Inc. Base Elev. at -9.70 m
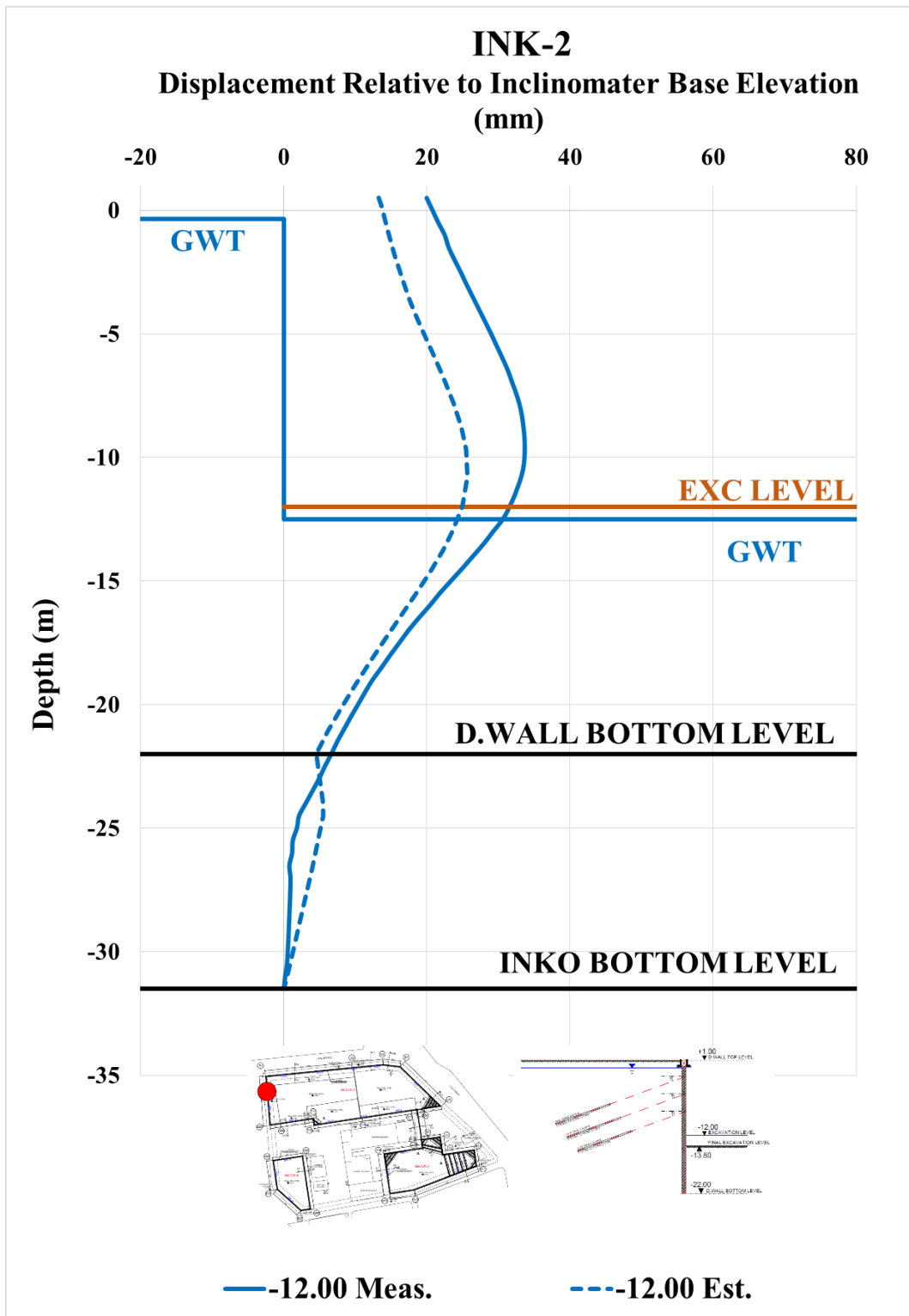
Figure A. 18. Estimated and Measured Displ. Rel. to Inc. Base Elev. at -12.00 m
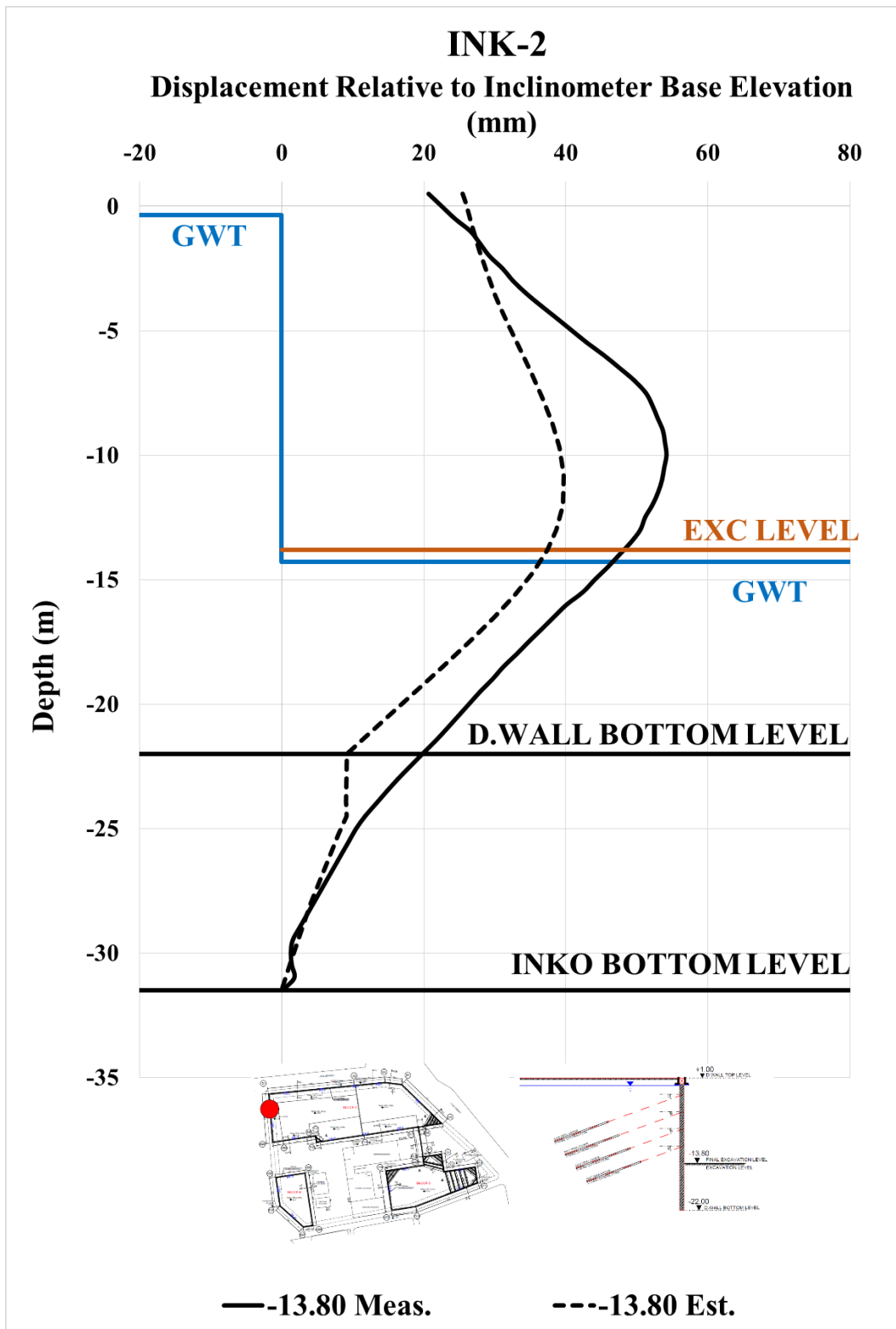
Figure A. 19. Estimated and Measured Displ. Rel. to Inc. Base Elev. at -13.80 m

Table A. 4. Internal Forces of Diaphragm Wall

INK - 2 / Section 1-1					
Excvation Stage	1	2	3	4	5
Excavation Level (m)	-3,20	-6,70	-9,70	-12,00	-13,80
N_{max} (kN/m)	95,78	245,00	429,60	604,30	733,20
V_{max} (kN/m)	57,01	214,30	310,10	353,40	353,40
M_{max} (kN.m/m)	147,40	328,00	642,60	882,70	1034,00

Legend	Excvation Stage	1. Anchor Level	2. Excavation Level	2. Anchor Level	3. Excavation Level	3. Anchor Level	4. Excavation Level	4. Anchor Level	Final Excavation Level
	Measured Load of 1. Anchor Row (kN)	689.654	648.59	651.75	653.68	656.38	656.63	646.50	642.97
	Estimated Load of 1. Anchor Row (kN)	650	699.21	628.74	657.50	628.98	641.70	633.42	643.48
	Estimated Load of 2. Anchor Row (kN)	-	-	650.00	710.86	648.50	681.27	655.47	669.28
	Estimated Load of 3. Anchor Row (kN)	-	-	-	-	650.00	725.27	670.08	701.06
	Estimated Load of 4. Anchor Row (kN)	-	-	-	-	-	-	650.00	716.12
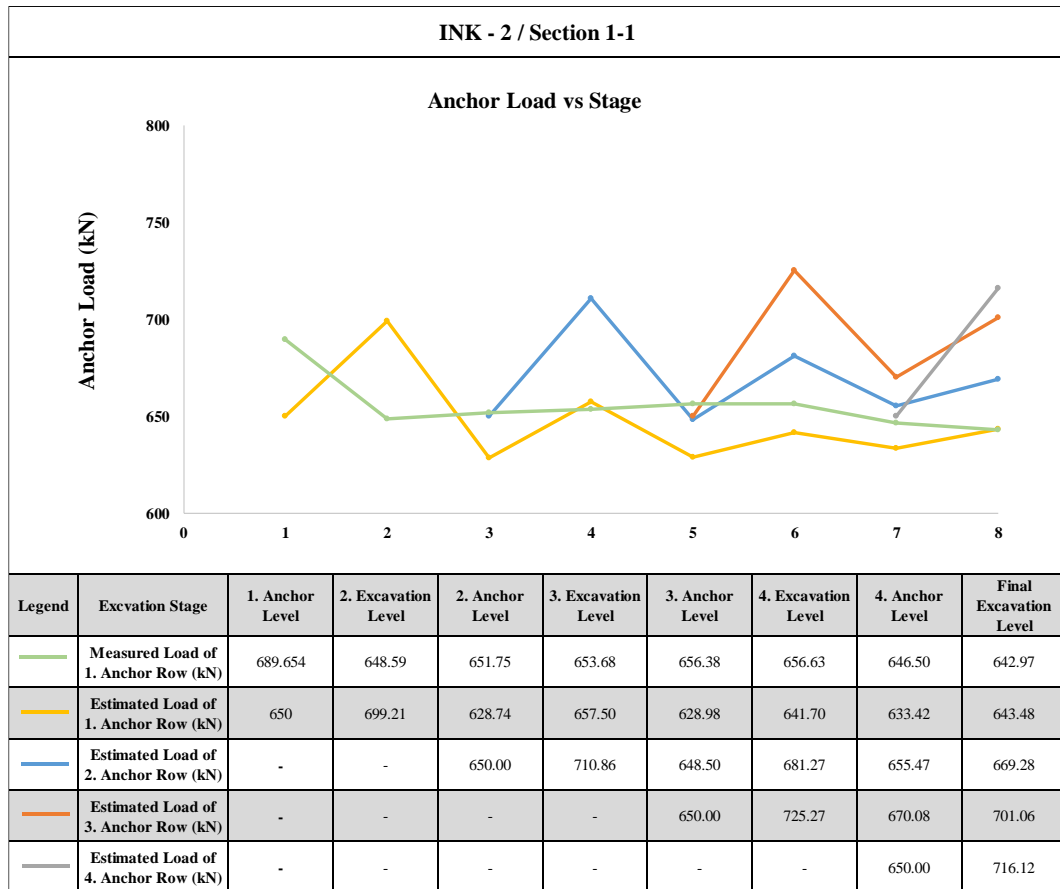
Figure A. 20. Measured and Estimated Anchor Loads

INK-1 – Calibrated, Estimated and Measured Displacements
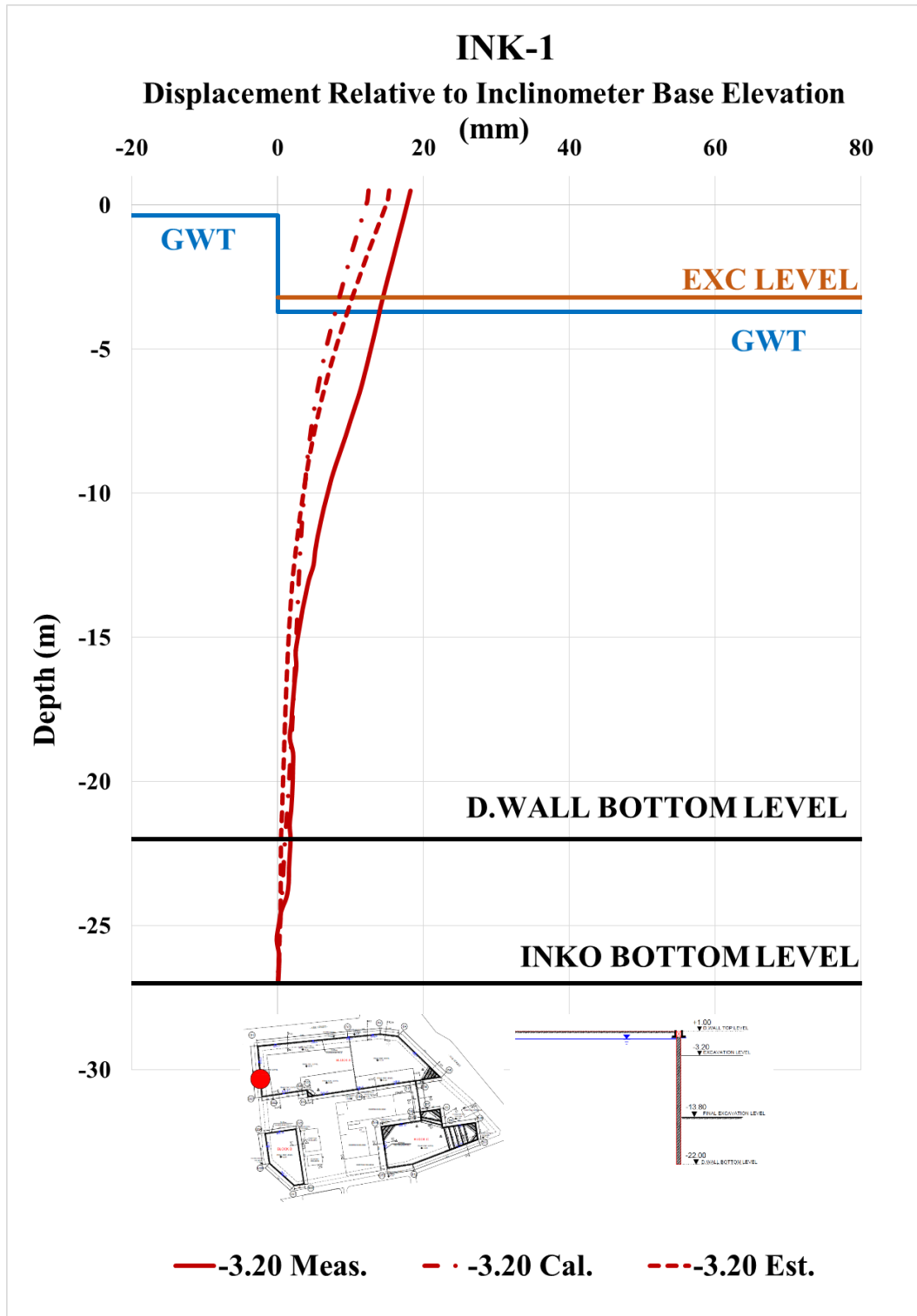
Figure A. 21. Calibrated and Measured Displ. Rel. to Inc. Base Elev. at -3.20 m
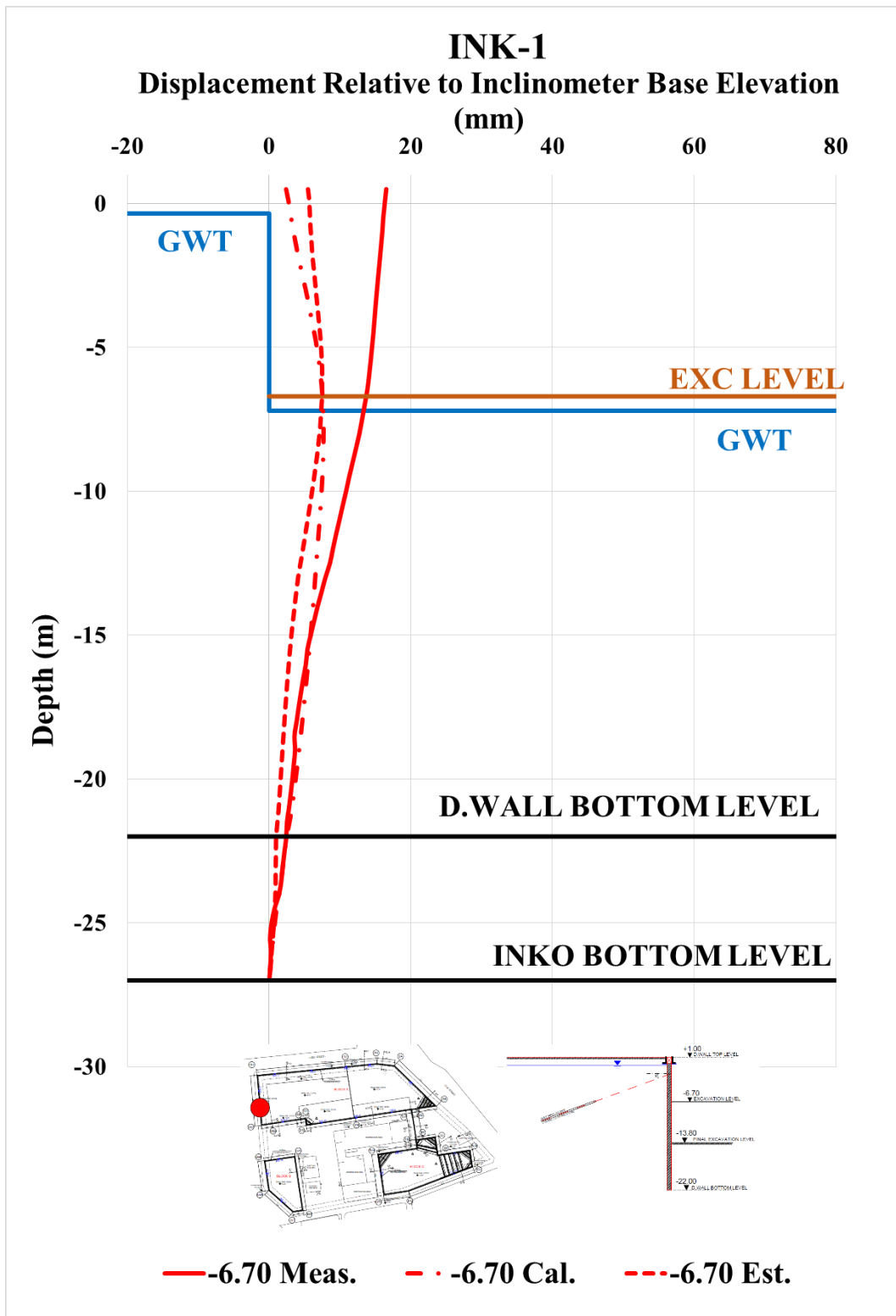
Figure A. 22. Calibrated and Measured Displ. Rel. to Inc. Base Elev. at -6.70 m
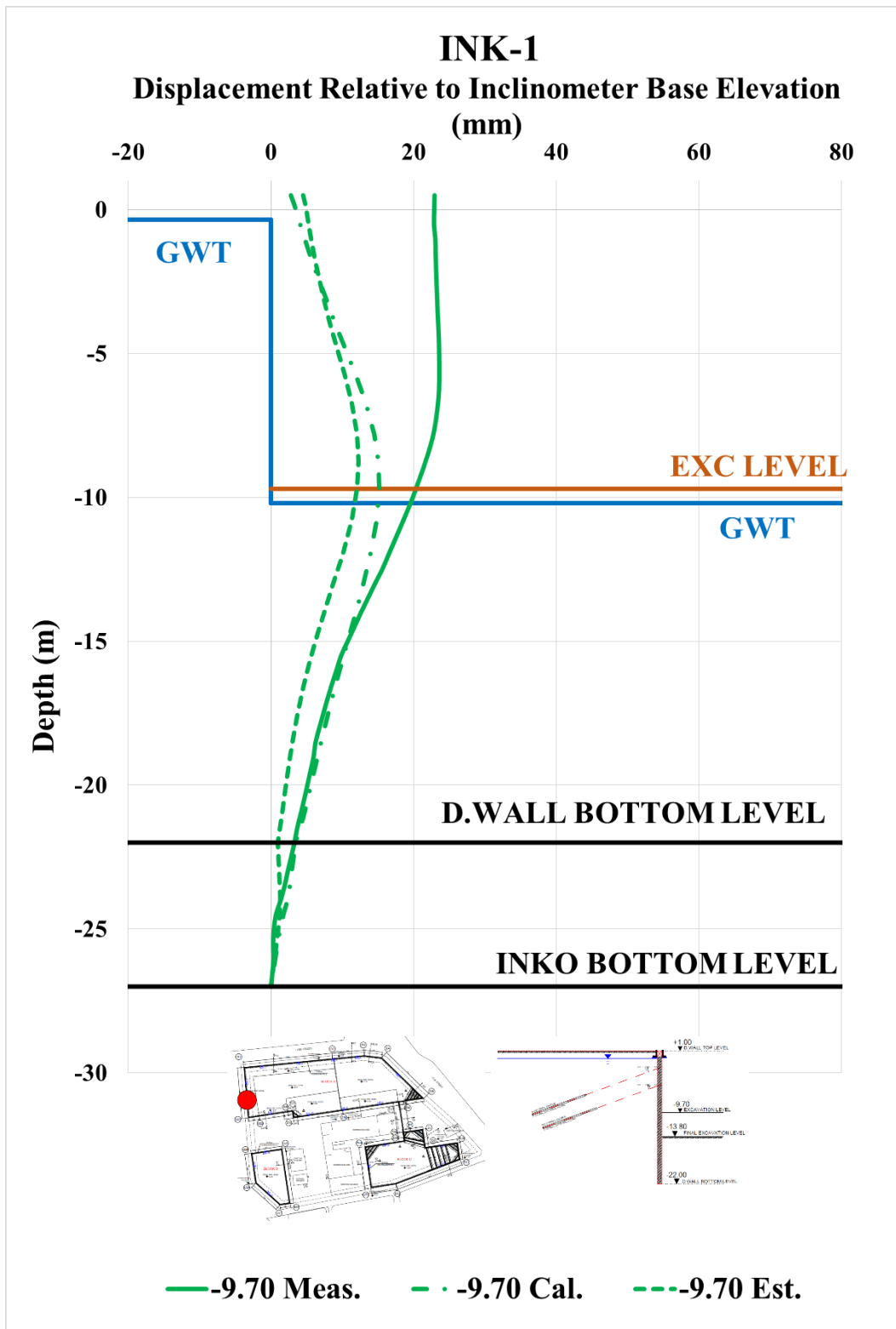
Figure A. 23. Calibrated and Measured Displ. Rel. to Inc. Base Elev. at -9.70 m
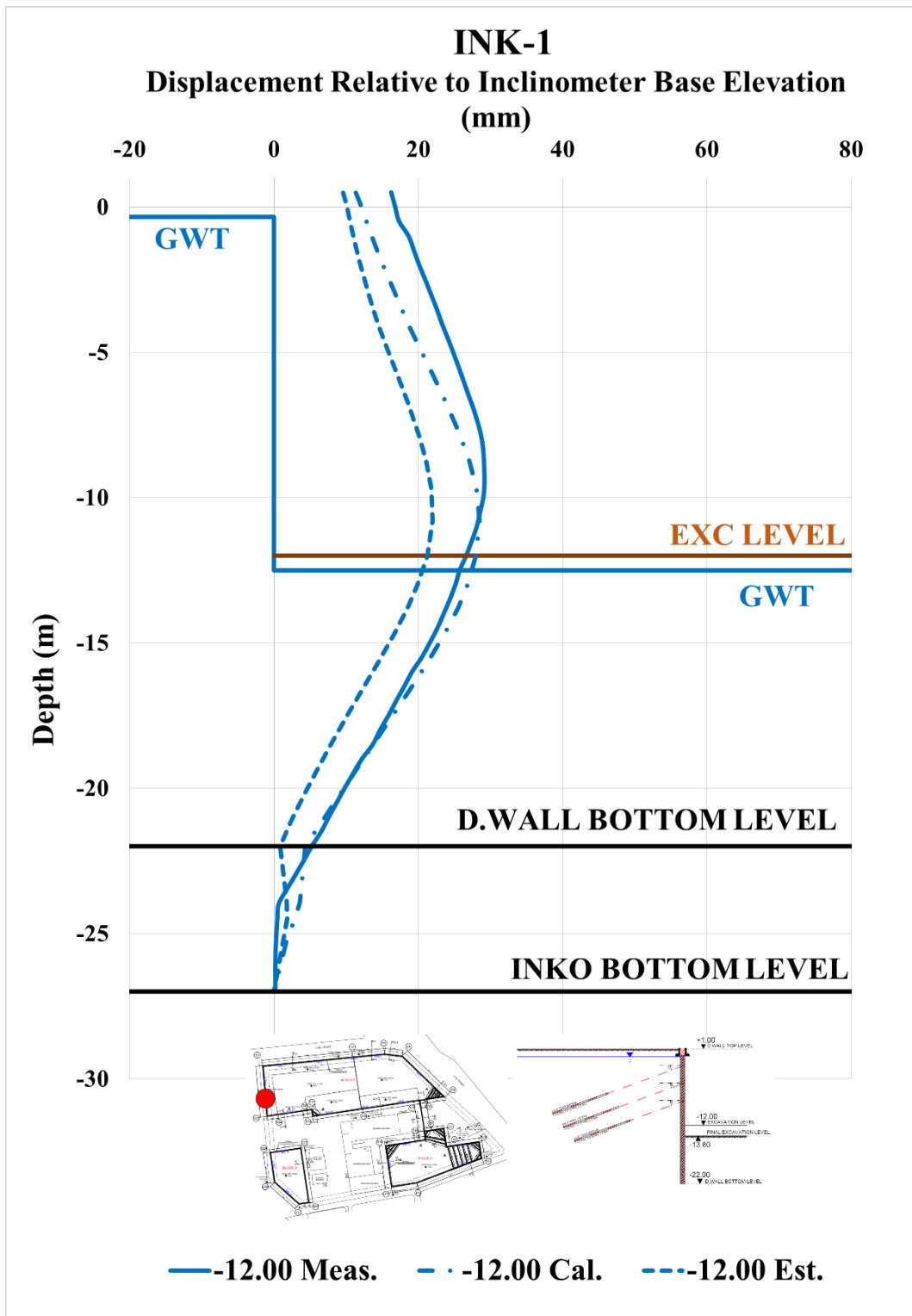
Figure A. 24. Calibrated and Measured Displ. Rel. to Inc. Base Elev. at -12.00 m
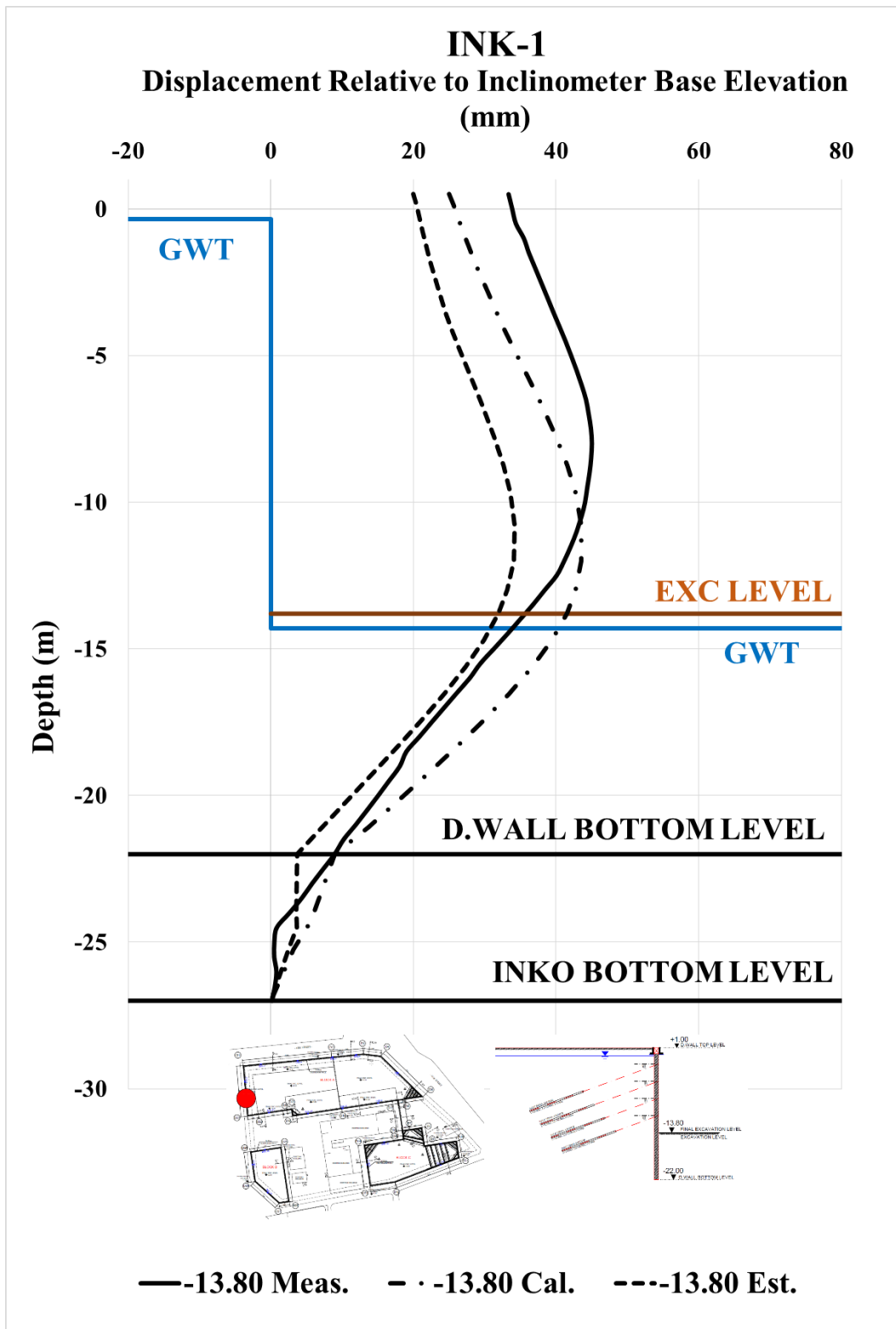
Figure A. 25. Calibrated and Measured Displ. Rel. to Inc. Base Elev. at -13.80 m

Table A. 5. Internal Forces of Diaphragm Wall

INK - 1 / Section 1-1					
Excvation Stage	1	2	3	4	5
Excavation Level (m)	-3,20	-6,70	-9,70	-12,00	-13,80
N_{max} (kN/m)	86,48	249,30	439,60	610,90	728,10
V_{max} (kN/m)	61,19	220,30	308,30	357,10	357,10
M_{max} (kN.m/m)	158,10	339,40	672,30	961,70	1142,00

Legend	Excvation Stage	1. Anchor Level	2. Excavation Level	2. Anchor Level	3. Excavation Level	3. Anchor Level	4. Excavation Level	4. Anchor Level	Final Excavation Level
	Measured Load of 1. Anchor Row (kN)	709.36	643.40	635.94	631.86	634.18	627.22	621.16	600.65
	Estimated Load of 1. Anchor Row (kN)	650.00	697.51	628.14	657.06	630.58	644.02	637.46	648.81
	Estimated Load of 2. Anchor Row (kN)	-	-	650.00	710.62	651.98	685.04	660.77	675.20
	Estimated Load of 3. Anchor Row (kN)	-	-	-	-	650.00	726.62	672.11	703.00
	Estimated Load of 4. Anchor Row (kN)	-	-	-	-	-	-	650.00	718.82
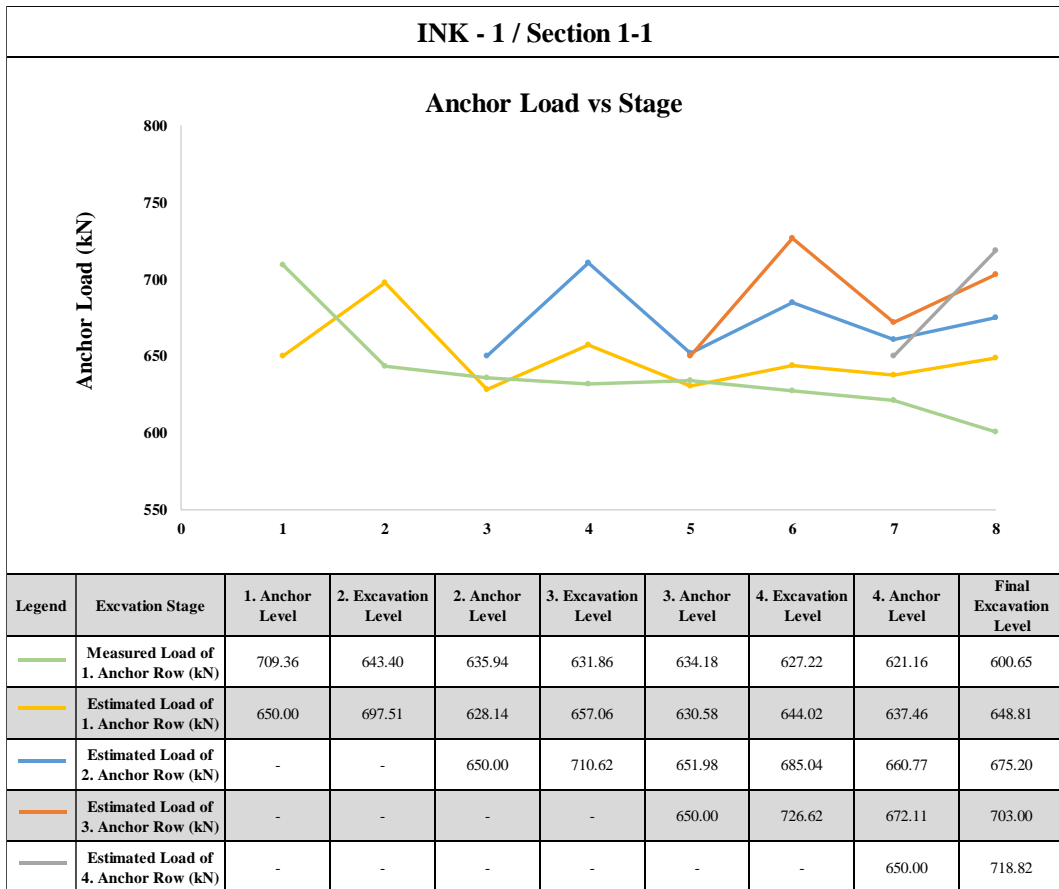
Figure A. 26. Measured and Estimated Anchor Loads

Table A. 6. Summary of Displacement Results of INK-1

INK - 1 / SECTION 1 - 1

Excvation Level (m)	Excvation Depth (m)	u_{meas} (mm) Inclinometer Measurements	u_{est} (mm) Estimation with Plaxis 2D Analysis	u_{cal} (mm) Calibration with Plaxis 2D Analysis	$u_{literature}$ (mm) FHWA-IF-99-015 (1999) - Maksimum	$u_{literature}$ (mm) FHWA-IF-99-015 (1999) - Average	$u_{literature}$ (mm) Goldberg et al. (1976)	$u_{literature}$ (mm) Clough et al. (1990) - Maksimum	$u_{literature}$ (mm) Clough et al. (1990) - Average	$u_{literature}$ (mm) Long (2001)	$u_{literature}$ (mm) Long (2001) (Extraordinary cases eliminated)	$u_{literature}$ (mm) Long (2001) Cantilever System
-3.20	4.20	18.20	15.30	12.41	21.00	8.40	21.00	21.00	8.40	7.98	5.88	15.12
-6.70	7.70	16.54	7.53	7.68	38.50	15.40	38.50	38.50	15.40	14.63	10.78	-
-9.70	10.70	23.61	12.32	15.19	53.50	21.40	53.50	53.50	21.40	20.33	14.98	-
-12.00	13.00	29.18	22.02	28.53	65.00	26.00	65.00	65.00	26.00	24.70	18.20	-
-13.80	14.80	45.01	34.19	43.53	74.00	29.60	74.00	74.00	29.60	28.12	20.72	-

Figure A. 27. Estimated and Measured Displacements of INK - 1
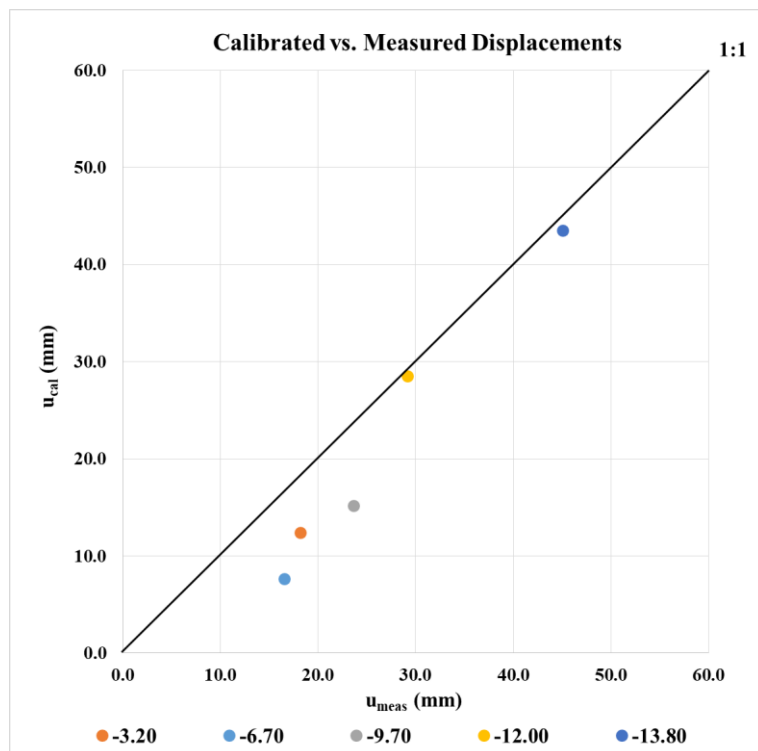
Figure A. 28. Calibrated and Measured Displacements of INK - 1

INK-2 - Calibrated, Estimated and Measured Displacements
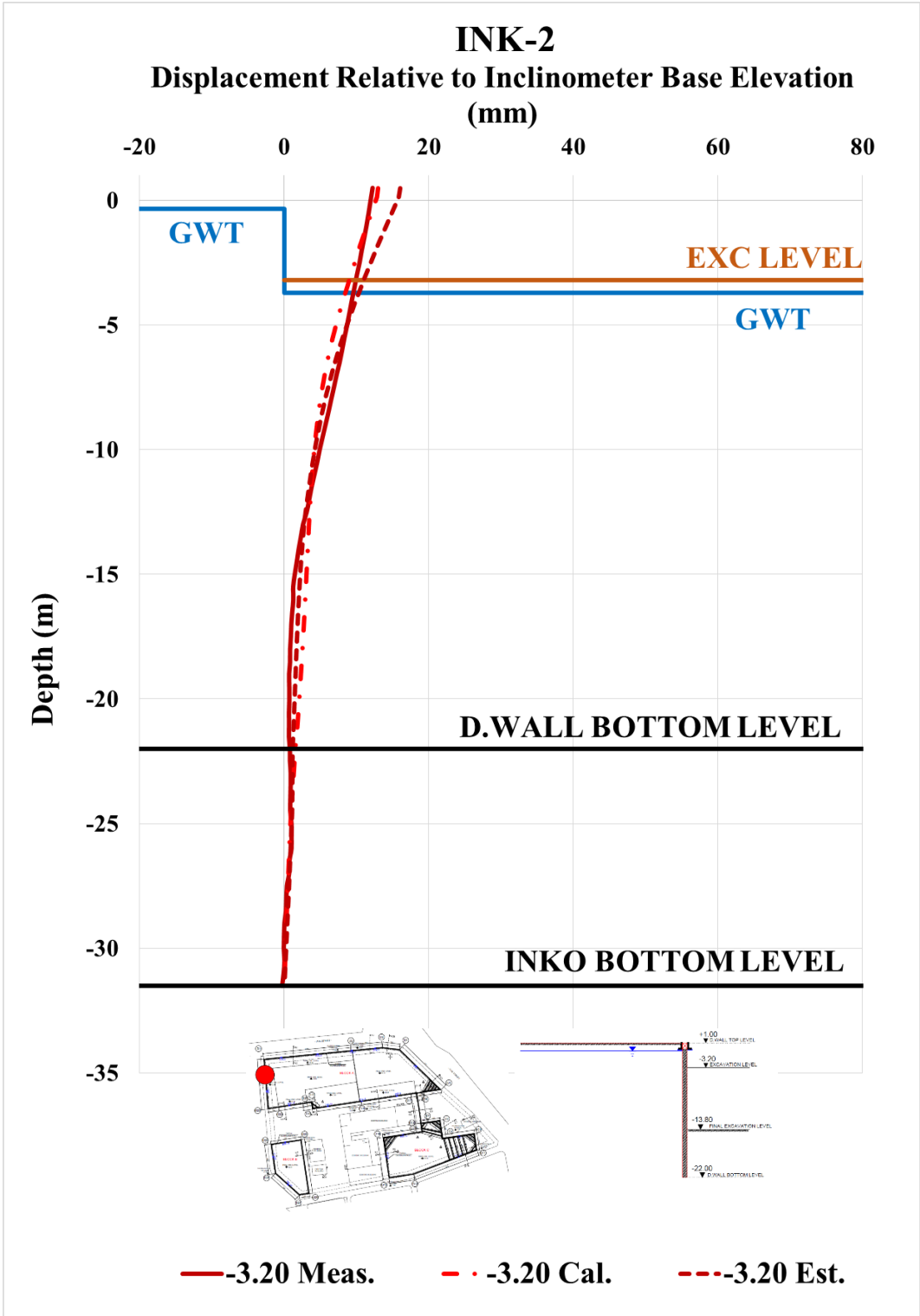
Figure A. 29. Calibrated and Measured Displ. Rel. to Inc. Base Elev. at -3.20 m
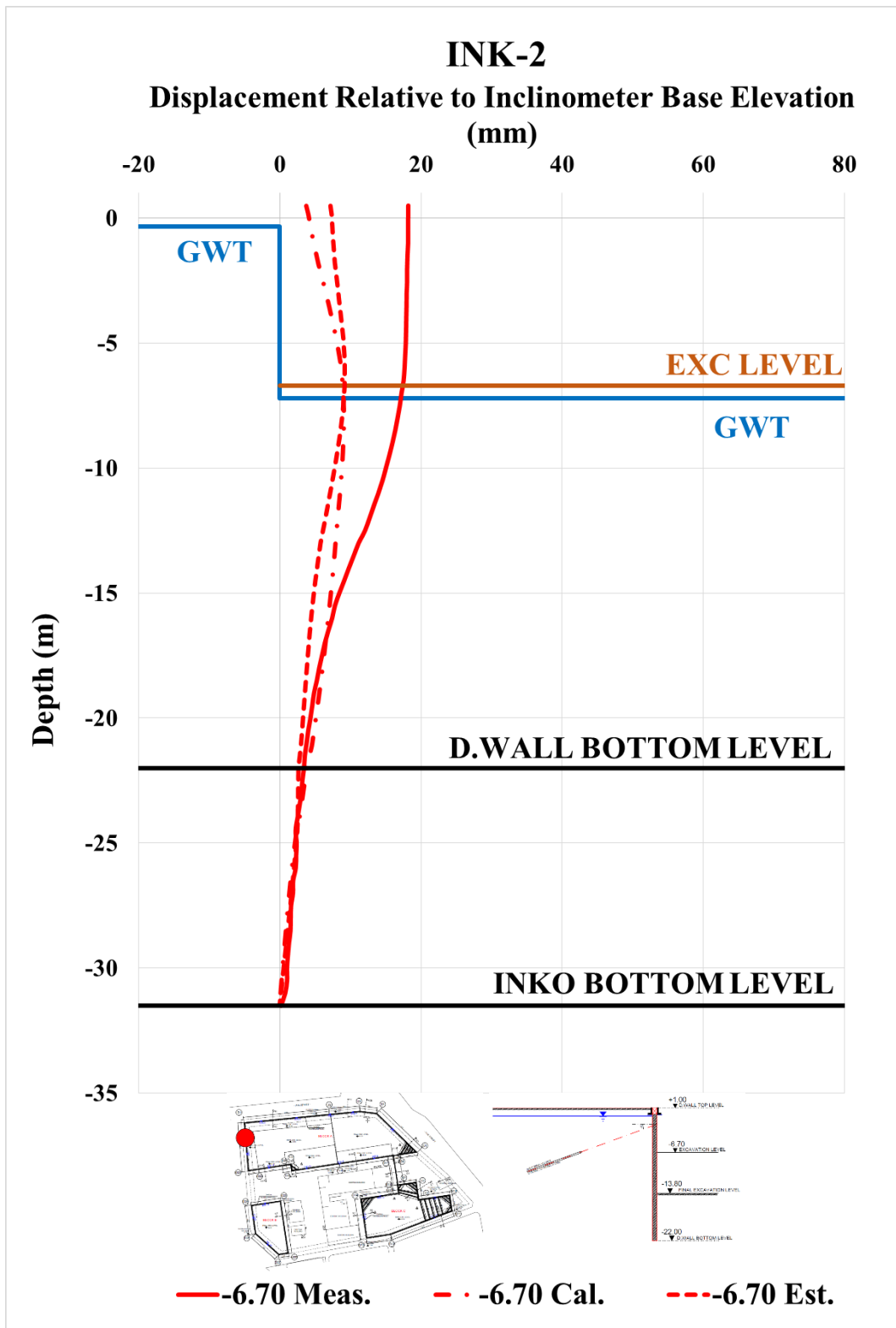
Figure A. 30. Calibrated and Measured Displ. Rel. to Inc. Base Elev. at -6.70 m
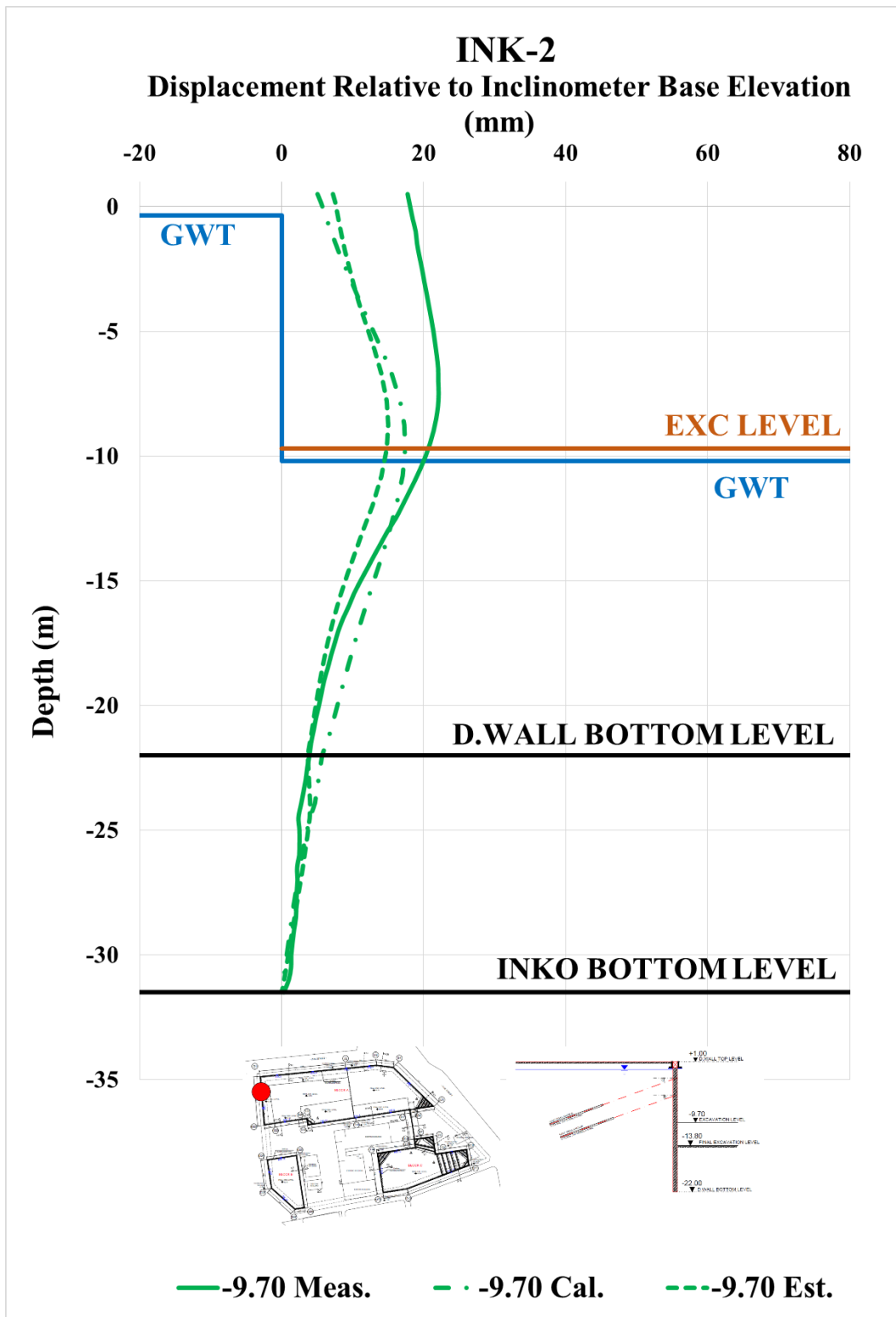
Figure A. 31. Calibrated and Measured Displ. Rel. to Inc. Base Elev. at -9.70 m
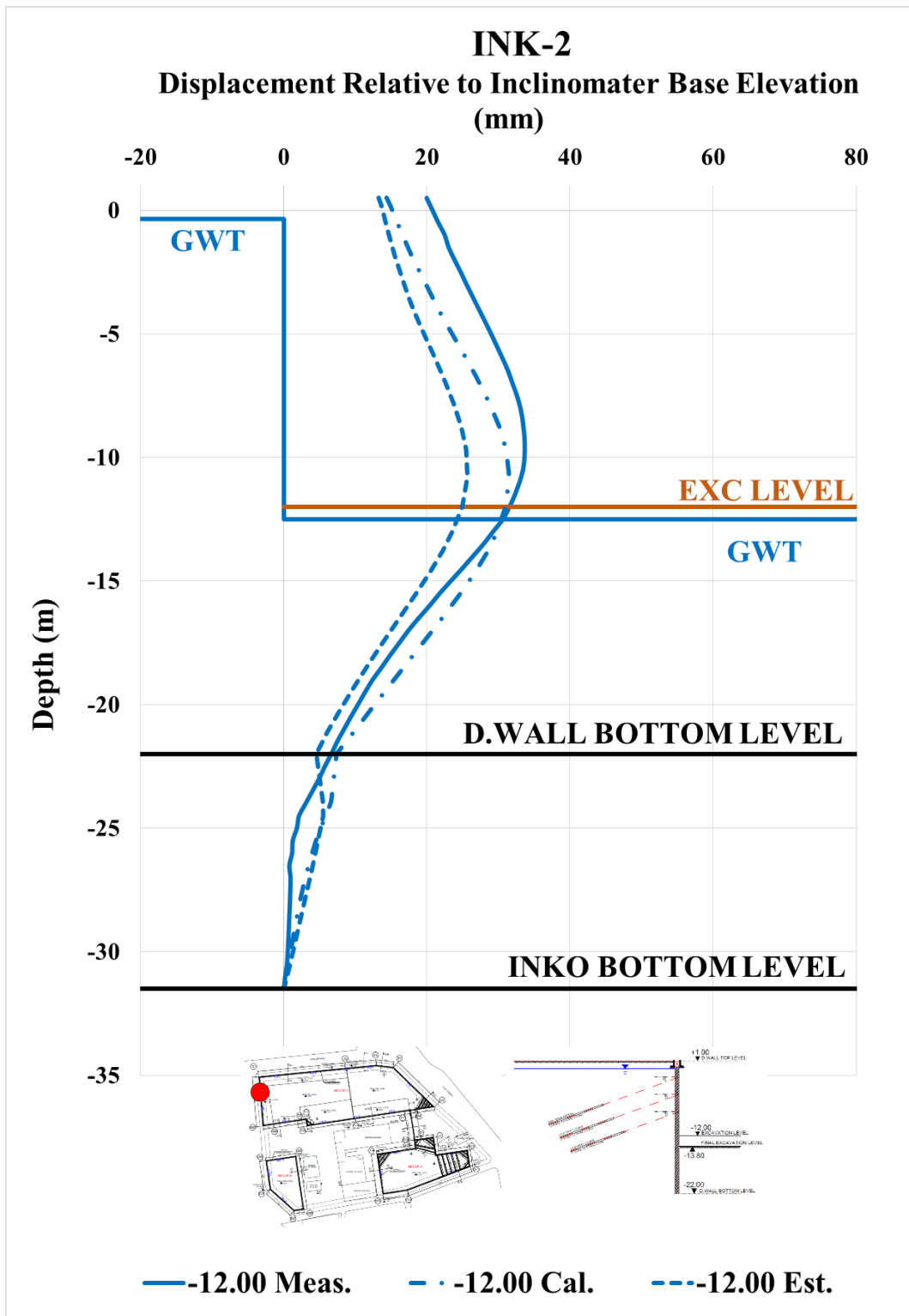
Figure A. 32. Calibrated and Measured Displ. Rel. to Inc. Base Elev. at -12.00 m
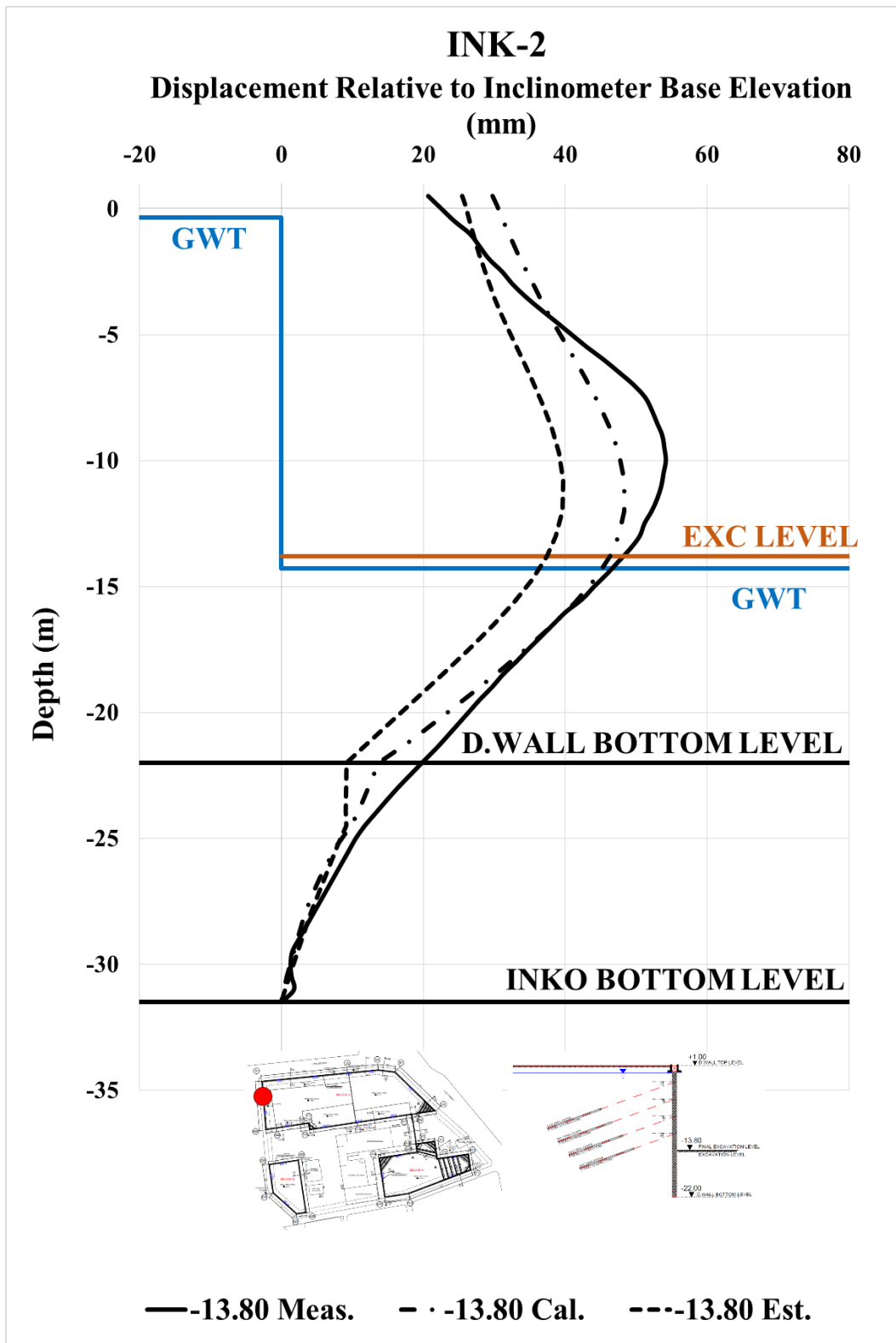
Figure A. 33. Calibrated and Measured Displ. Rel. to Inc. Base Elev. at -13.80 m

170

Table A. 7. Internal Forces of Diaphragm Wall

INK - 2 / Section 1-1					
Excvation Stage	1	2	3	4	5
Excavation Level (m)	-3,20	-6,70	-9,70	-12,00	-13,80
N_{max} (kN/m)	86,48	249,30	439,60	610,90	728,10
V_{max} (kN/m)	61,19	220,30	308,30	357,10	357,10
M_{max} (kN.m/m)	158,10	339,40	672,30	961,70	1142,00

Legend	Excvation Stage	1. Anchor Level	2. Excavation Level	2. Anchor Level	3. Excavation Level	3. Anchor Level	4. Excavation Level	4. Anchor Level	Final Excavation Level
	Measured Load of 1. Anchor Row (kN)	689.654	648.59	651.75	653.68	656.38	656.63	646.50	642.97
	Estimated Load of 1. Anchor Row (kN)	650	697.51	628.14	657.06	630.58	644.02	637.46	648.81
	Estimated Load of 2. Anchor Row (kN)	-	-	650.00	710.62	651.98	685.04	660.77	675.20
	Estimated Load of 3. Anchor Row (kN)	-	-	-	-	650.00	726.62	672.11	703.00
	Estimated Load of 4. Anchor Row (kN)	-	-	-	-	-	-	650.00	718.82
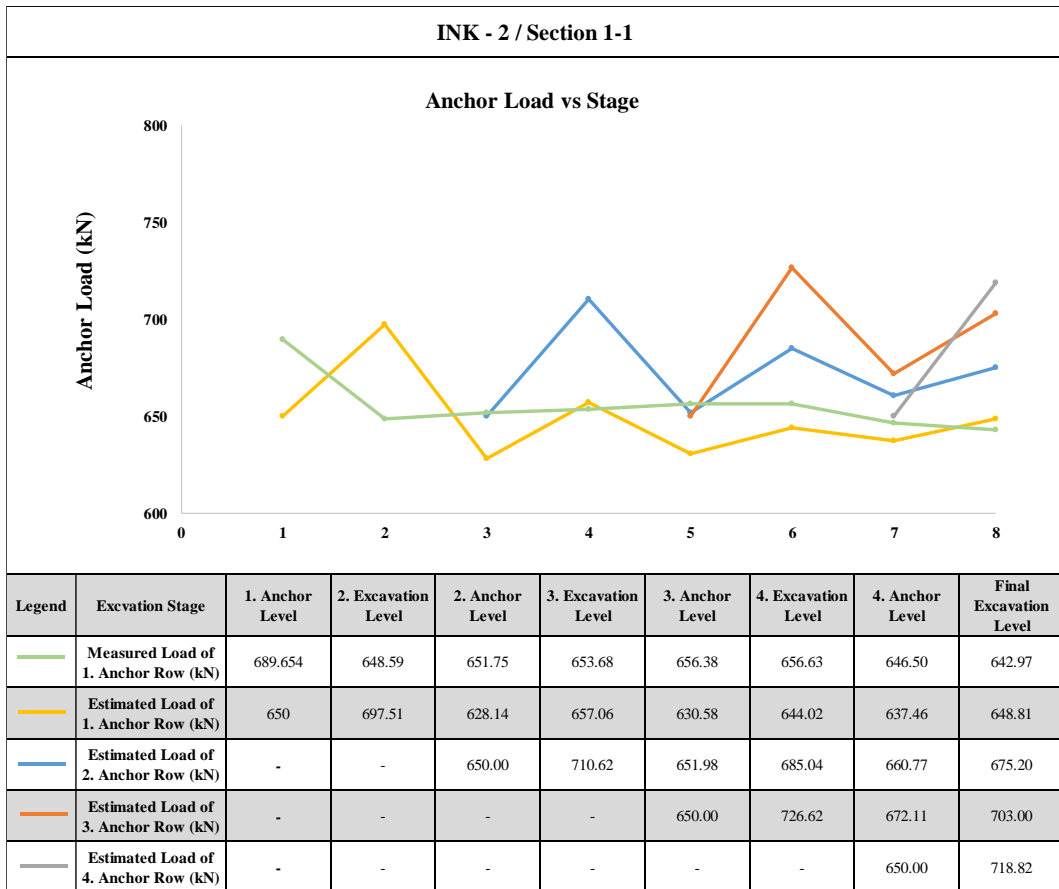
Figure A. 34. Measured and Estimated Anchor Loads

Table A. 8. Summary of Displacement Results of INK-2

INK - 2 / SECTION 1 - 1

Excvation Level (m)	Excvation Depth (m)	u_{meas} (mm) Inclinometer Measurements	u_{est} (mm) Estimation with Plaxis 2D Analysis	u_{cal} (mm) Calibration with Plaxis 2D Analysis	$u_{literature}$ (mm) FHWA-IF-99-015 (1999) - Maksimum	$u_{literature}$ (mm) FHWA-IF-99-015 (1999) - Average	$u_{literature}$ (mm) Goldberg et al. (1976)	$u_{literature}$ (mm) Clough et al. (1990) - Maksimum	$u_{literature}$ (mm) Clough et al. (1990) - Average	$u_{literature}$ (mm) Long (2001)	$u_{literature}$ (mm) Long (2001) (Extraordinary cases eliminated)	$u_{literature}$ (mm) Long (2001) Cantilever System
-3.20	4.20	12.22	16.01	12.94	21.00	8.40	21.00	21.00	8.40	7.98	5.88	15.12
-6.70	7.70	18.15	9.22	9.04	38.50	15.40	38.50	38.50	15.40	14.63	10.78	-
-9.70	10.70	22.11	14.98	17.42	53.50	21.40	53.50	53.50	21.40	20.33	14.98	-
-12.00	13.00	33.67	25.68	31.53	65.00	26.00	65.00	65.00	26.00	24.70	18.20	-
-13.80	14.80	54.18	39.72	48.28	74.00	29.60	74.00	74.00	29.60	28.12	20.72	-

172
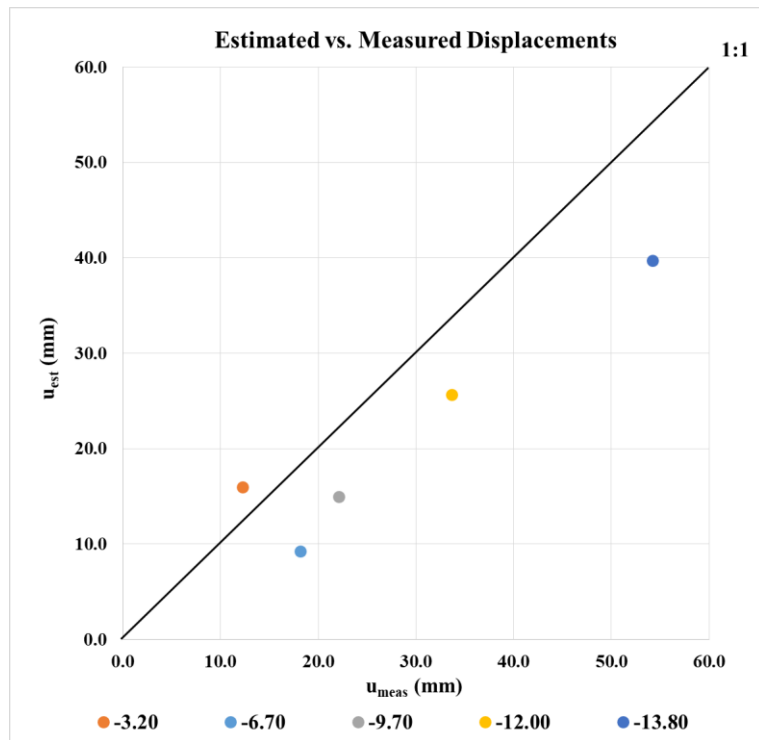
Figure A. 35. Estimated and Measured Displacements of INK - 2
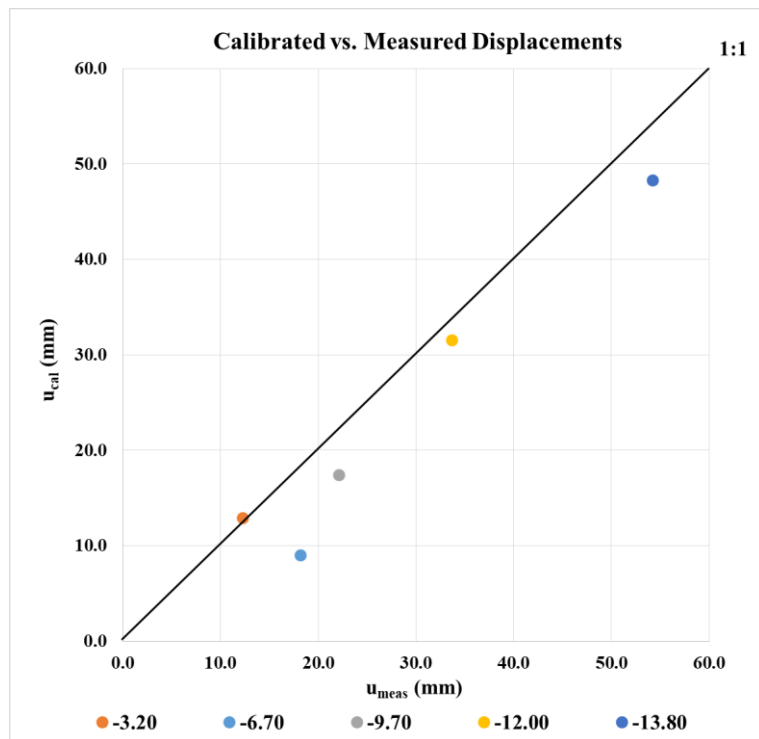
Figure A. 36. Calibrated and Measured Displacements of INK - 2

Area A2
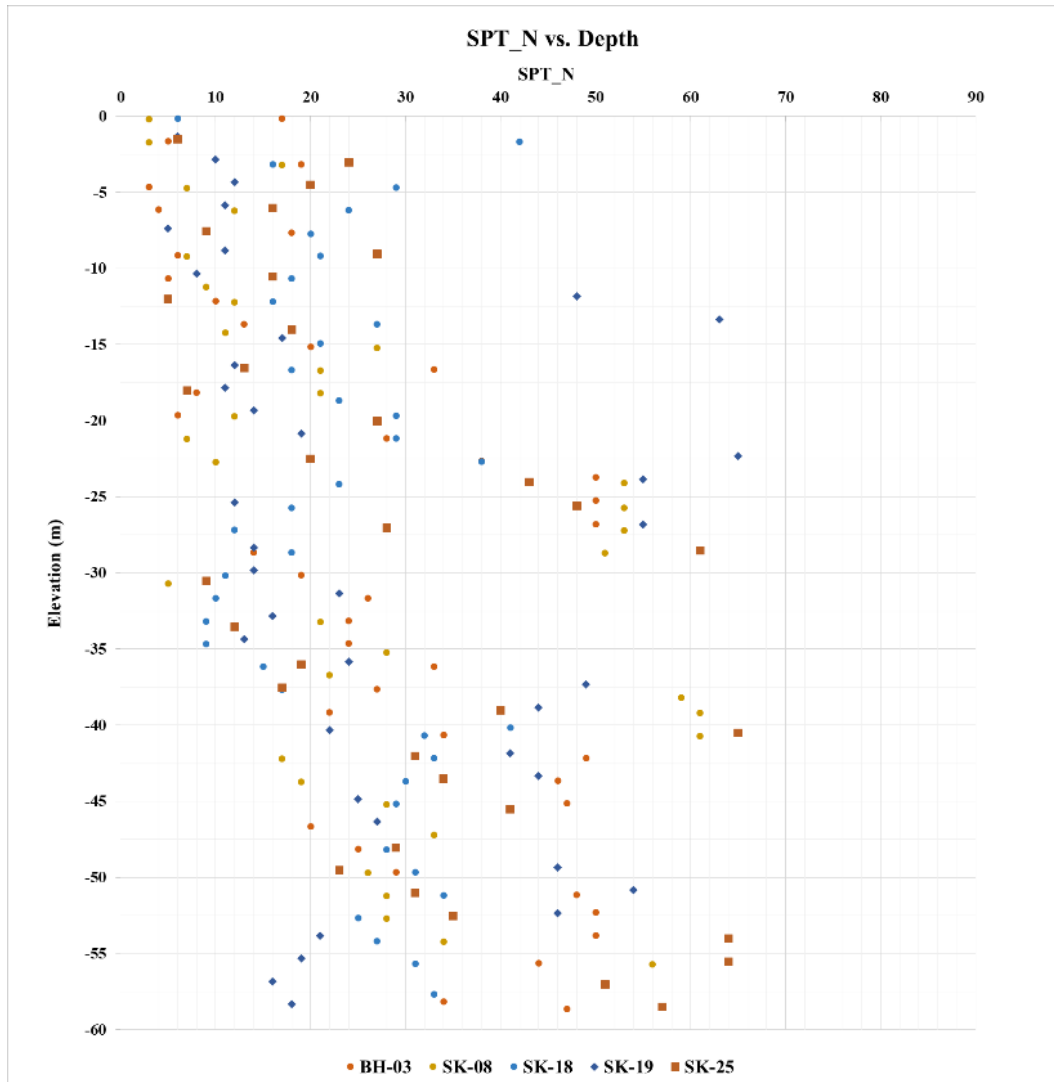
Figure A. 37. SPT-N vs. Depth for Area A2

174
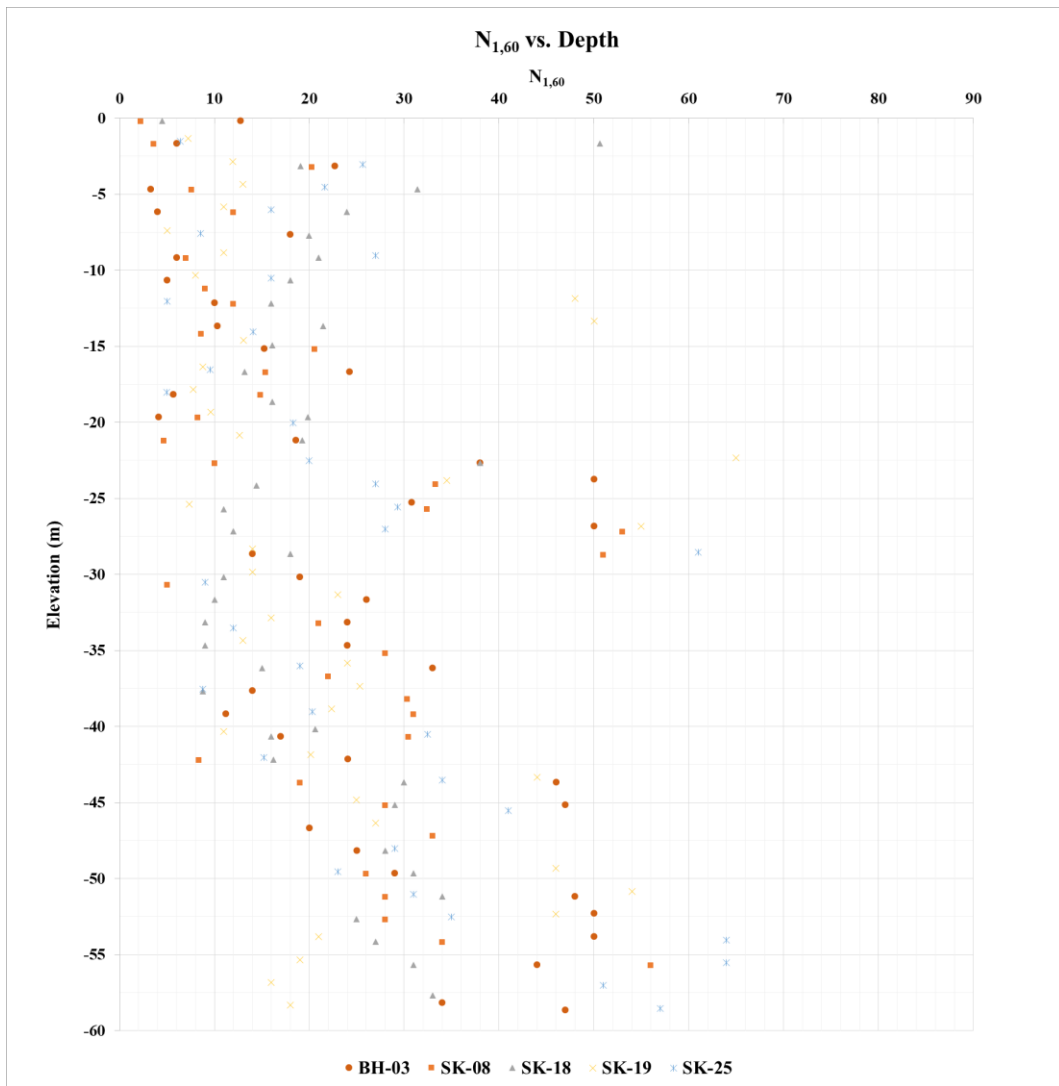
Figure A. 38. SPT-$N_{1,60}$ vs. Depth for Area A2
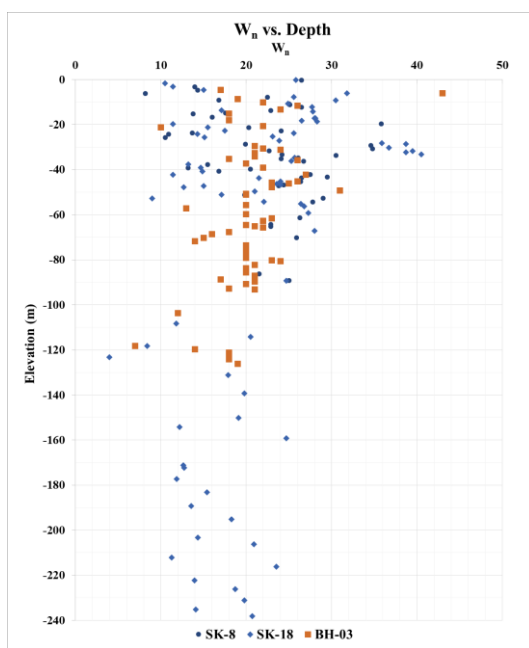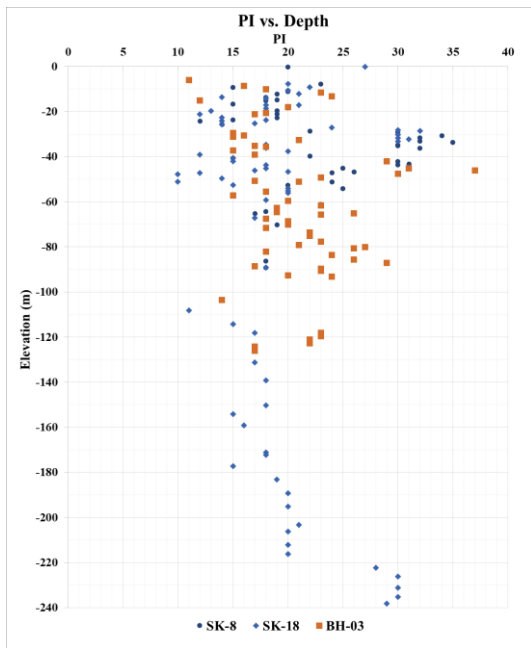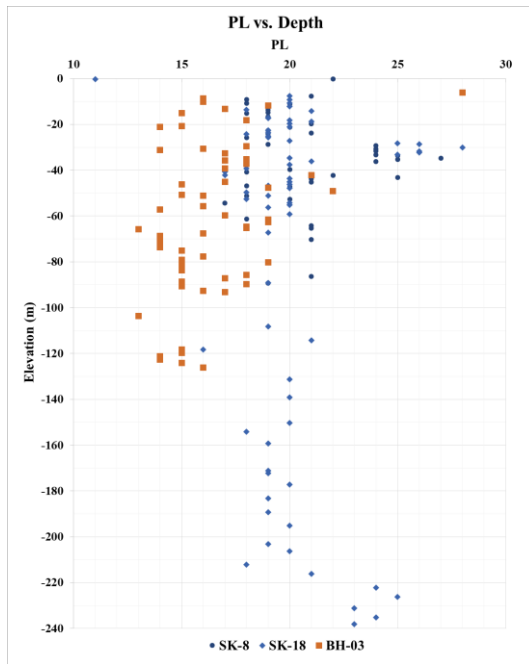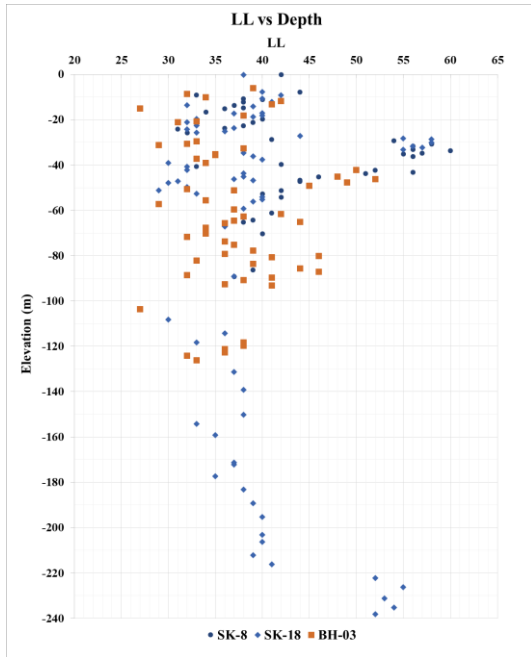
Figure A. 39. Variation of LL, PL, PI, and w_n for Area A2
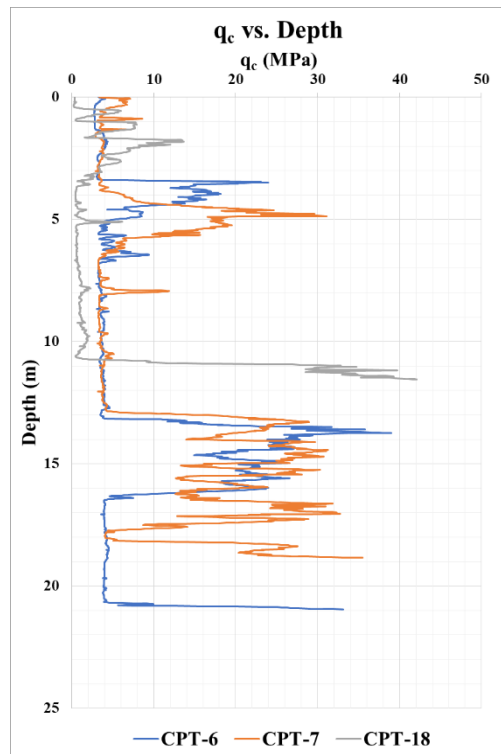
Figure A. 40. Variation of q_c along with the Depth for Area A2
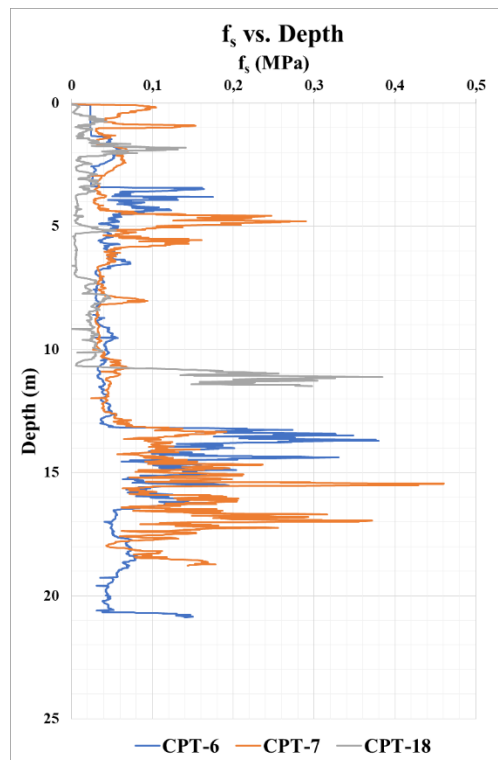
Figure A. 41. Variation of f_s along with the Depth for Area A2

177
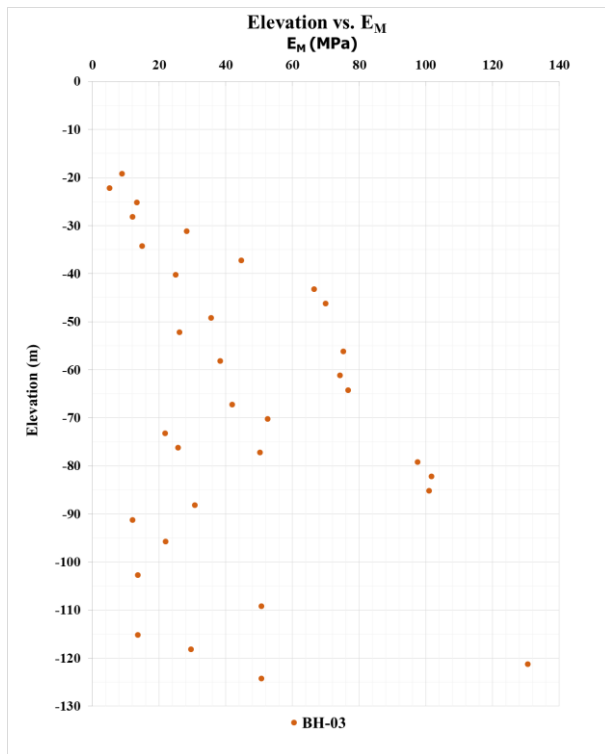
Figure A. 42. Variation of E_m along with the Depth for Area A2
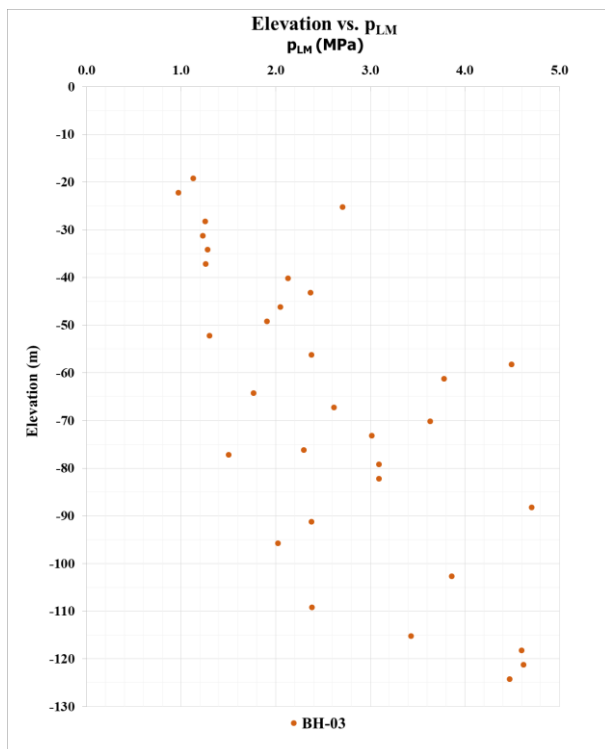
Figure A. 43. Variation of p_{Lm} along with the Depth for Area A2

3 boreholes (SK-8, SK-18, and BH-3) and 3 CPT (CPT-6, CPT-7, and CPT-18) were considered. The depths of boreholes are changing between 100 m to 240 m. Depths of CPT are changing between 11.55 m to 20.95 m. The total depth of boreholes and CPTs is 470 m and 51.35 m respectively. Atterberg limit tests were performed on the samples taken from SK-8, SK-18, and BH-3. LL, PL, PI, and w_n vary in 27 – 60 % (avg. 39.6 %), 11 – 28 % (avg. 19 %), 10 – 37 % (avg. 20.6 %), and 4 – 43 % (avg. 21.1 %) respectively. E_m, and p_{LM} values are 5 MPa – 130.5 MPa (avg. 44.2 MPa) and 0.971 MPa – 5.781 MPa (avg. 2.711 MPa) respectively. Unified soil classification (USCS) was performed for each sample. By considering USCS, SPT $N_{1,60}$ values, and CPT results, the thickness of soil layers was determined. Detailed soil parameters are given in below table;

- Boreholes: SK-8, SK-18, and BH-3 (Change in between 100 m to 240 m. 470 m in total)
- CPTs: CPT-6, CPT-7, and CPT-18 (Change in between 11.55 m to 20.95 m. 51.35 m in total)
- LL: 27 – 60 % (avg. 39.6 %)
- PL: 11 – 28 % (avg. 19 %)
- PI: 10 – 37 % (avg. 20.6 %)
- w_n: 4 – 43 % (avg. 21.1 %)

Table A. 9. Soil Profile of Area 2 (A2)

Layer No	Elevation (m)		USCS	Type	Thickness (m)	N	$N_{1,60}$	N_{60}	PI	y_{wet} (kN/m³)	y_{sat} (kN/m³)	c_u (kPa)	c (kPa)	φ (°)	ψ (°)	E_{50}^{ref} (MPa)	E_{oed}^{ref} (MPa)	E_{ur}^{ref} (MPa)	m	v_{ur}	P_{ref} (kPa)	R_f
1	1.8	- -0.2	CL	Cohesive	2.0	9.0	6.0	6.0	23.5	17.6	19.2	35.0	3.5	29.6	0.0	6.6	3.3	19.8	1.0	0.2	30.8	0.9
2	-0.2	- -6.2	GP-GM	Cohesionless	6.0	15.0	17.0	13.0	0.0	19.2	20.0	-	2.0	32.0	2.0	37.0	37.0	111.0	0.5	0.2	100.0	0.9
3	-6.2	- -15.2	CL	Cohesive	9.0	17.0	17.0	17.0	19.0	18.4	20.0	100.0	10.0	30.0	0.0	19.8	9.9	59.4	1.0	0.2	138.5	0.9
4	-15.2	- -25.5	SC-GC	Cohesionless	10.3	25.0	20.0	25.0	15.0	19.2	20.0	-	4.0	35.0	5.0	40.0	40.0	120.0	0.5	0.2	100.0	0.9
5	-25.5	- -39.5	CL	Cohesive	14.0	23.0	23.0	23.0	23.0	18.4	20.0	130.0	13.0	30.0	0.0	25.0	12.5	75.0	1.0	0.2	379.2	0.9
6	-39.5	- -44.5	SC-GC	Cohesionless	5.0	40.0	20.0	40.0	11.8	20.0	21.6	-	3.0	36.0	6.0	40.0	40.0	120.0	0.5	0.2	100.0	0.9
7	-44.5	- -60.5	CL	Cohesive	16.0	36.0	36.0	36.0	23.2	18.4	20.0	200.0	20.0	29.7	0.0	39.6	19.8	118.8	1.0	0.2	574.7	0.9
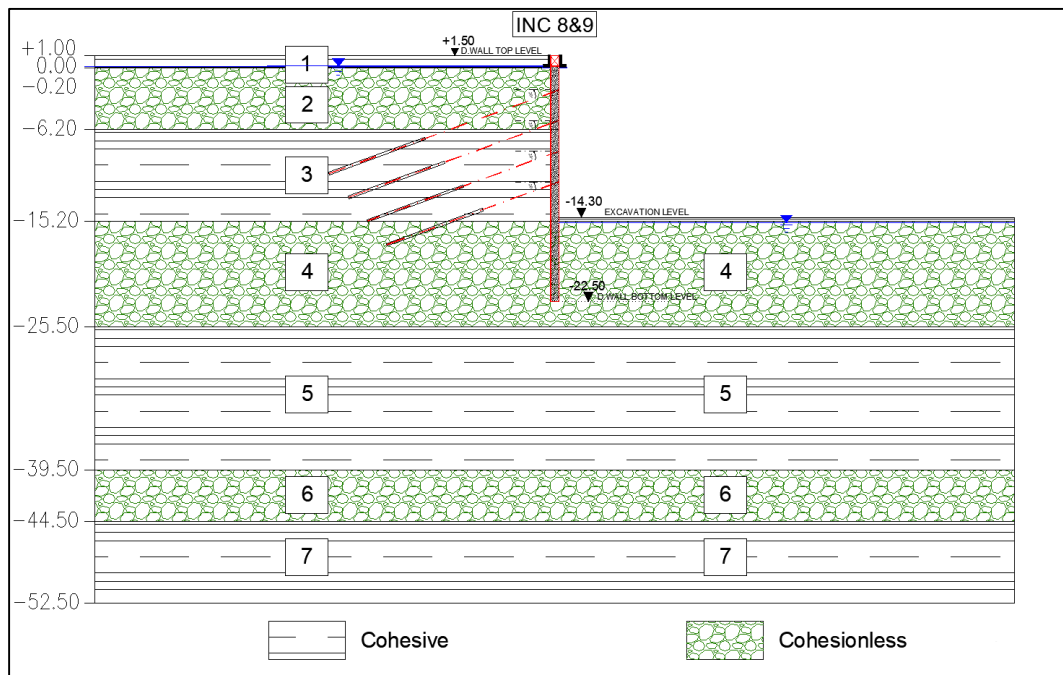
Figure A. 44. Section 2A – 2A

Table A. 10. Section Properties of 2A – 2A

SECTION 2A - 2A									
Diaphragm Wall			SBMA Type Anchor				Excavation Properties		
Top Level (m)	Bottom Level (m)	Length (m)	Anchor No	Anchor Level (m)	Anchor Length (m)	Horizontal Spacing (m)	Top Level (m)	Bottom Level (m)	Depth (m)
1.50	-22.50	24.00	1	-1.80	24.00	1.40	1.50	-14.30	15.80
			2	-4.80	22.00	1.40			
			3	-7.80	20.00	1.40			
			4	-10.80	18.00	1.40			

INK-8 – Estimated and Measured Displacements
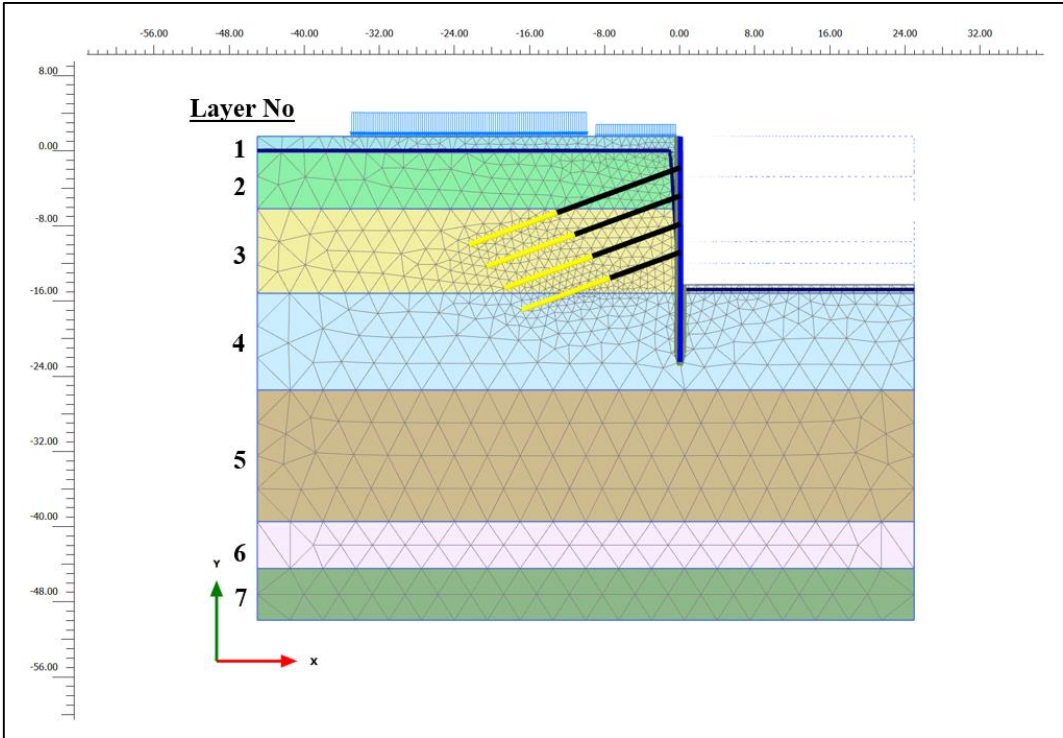
Figure A. 45. Meshed Model for INK-8
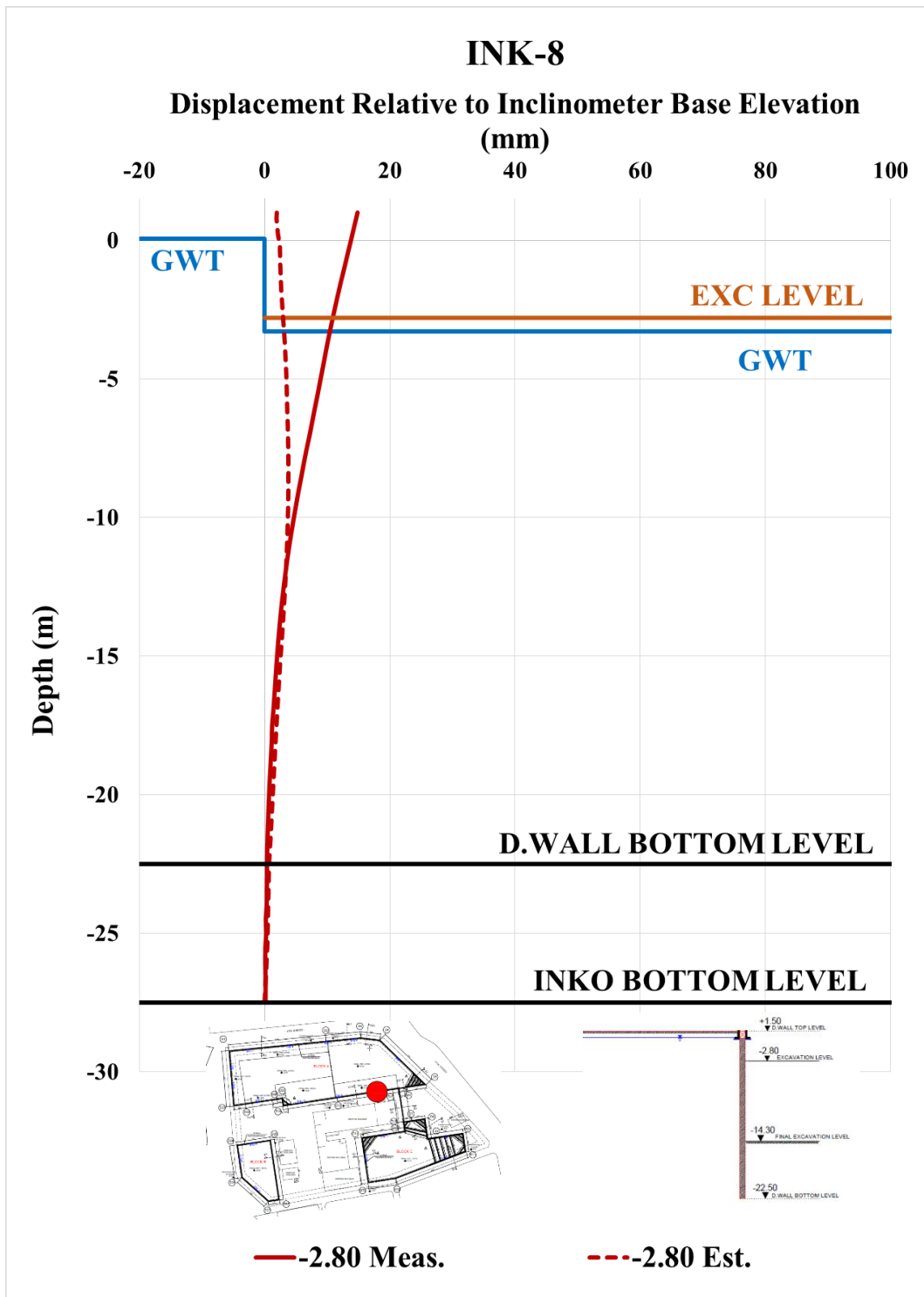
Figure A. 46. Estimated and Measured Displ. Rel. to Inc. Base Elev. at -2.80 m
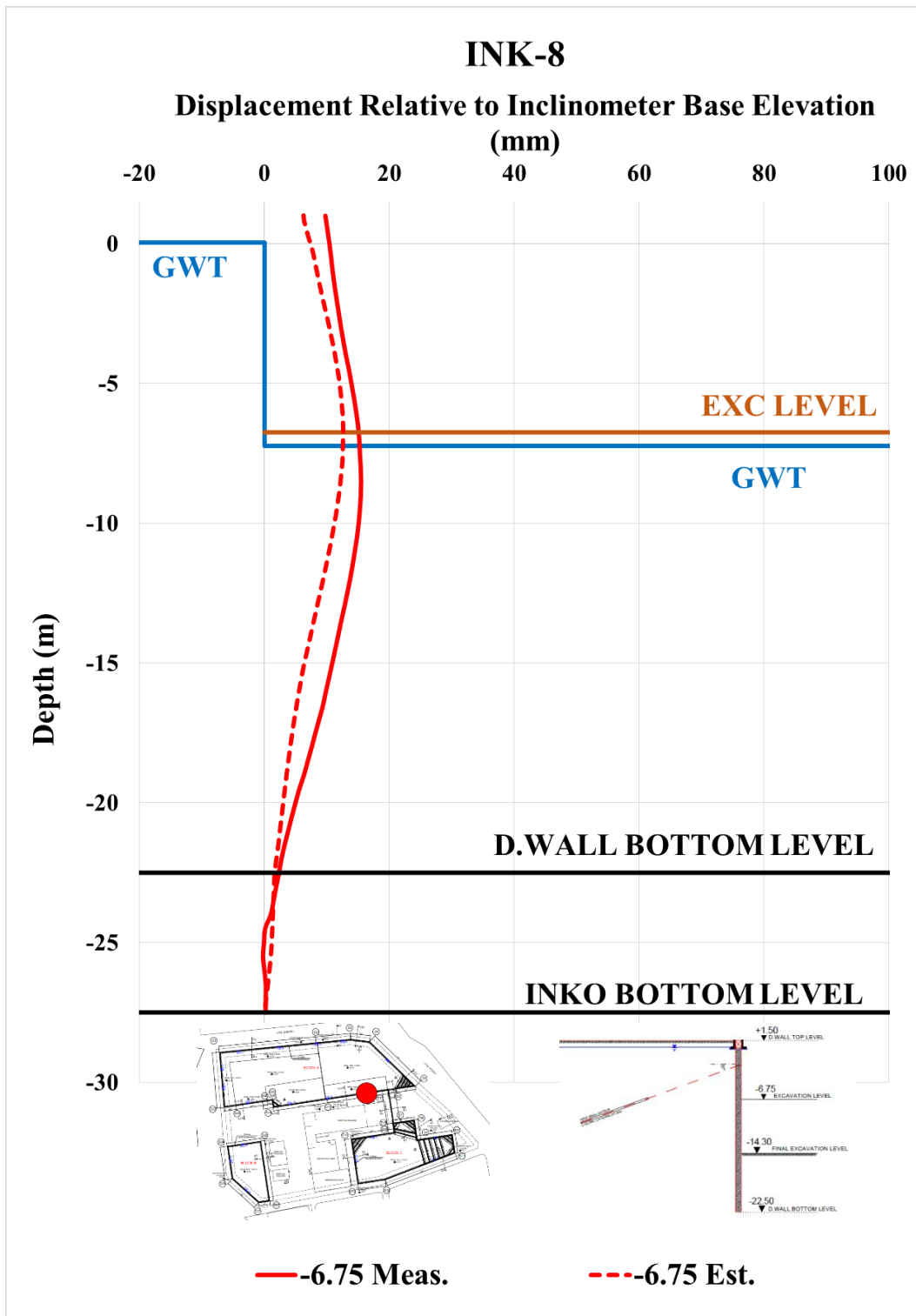
Figure A. 47. Estimated and Measured Displ. Rel. to Inc. Base Elev. at -6.75 m
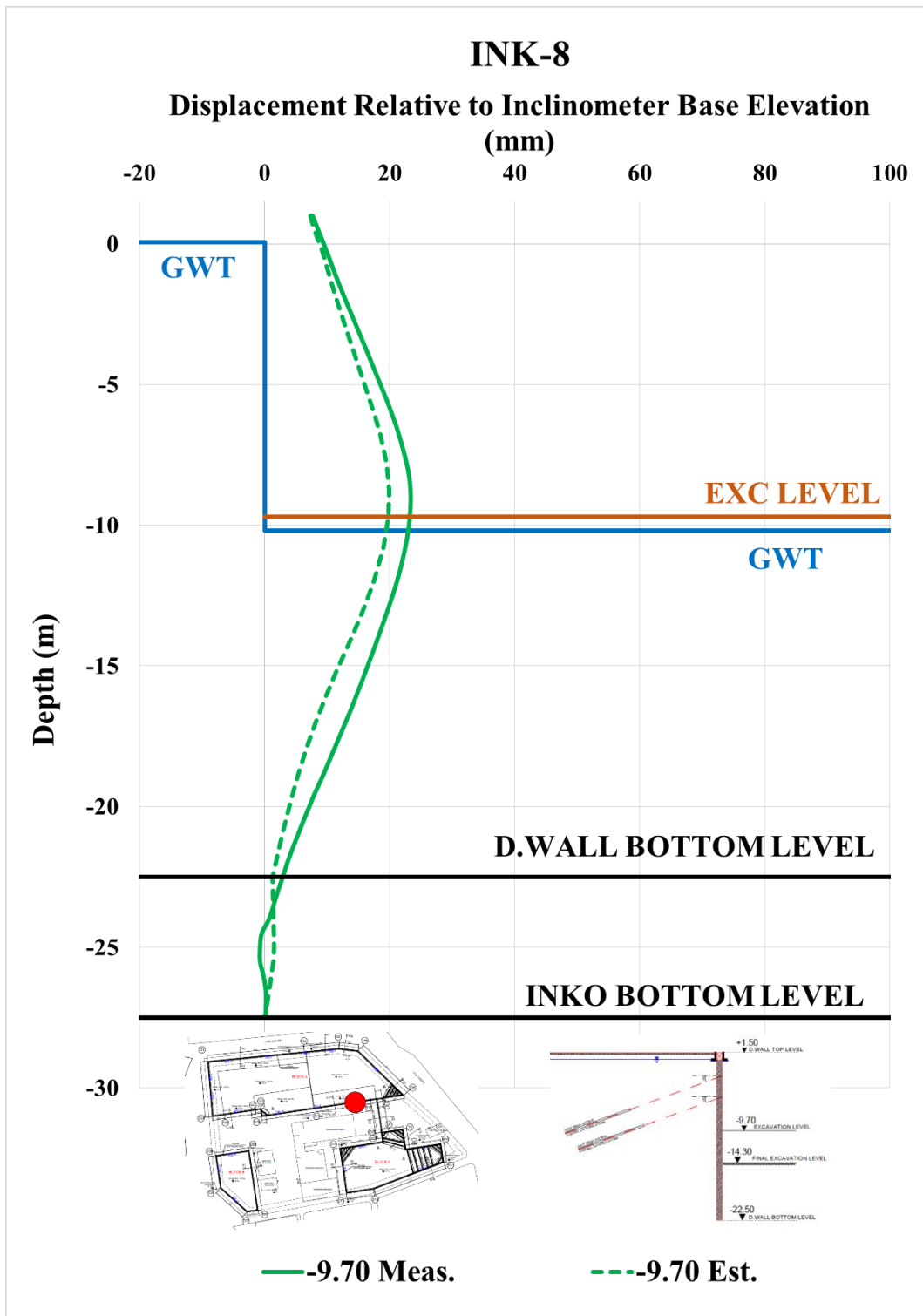
Figure A. 48. Estimated and Measured Displ. Rel. to Inc. Base Elev. at -9.70 m
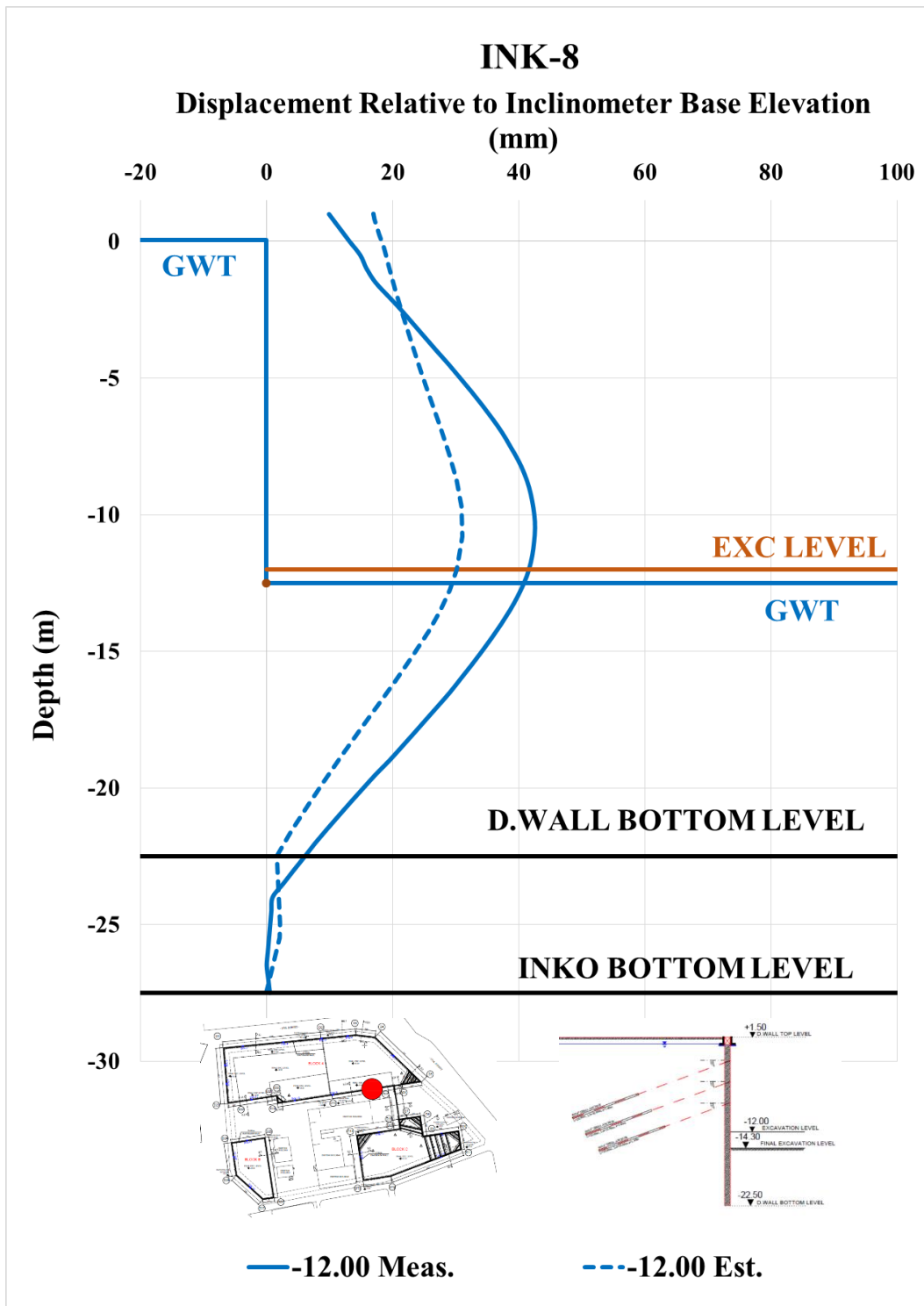
Figure A. 49. Estimated and Measured Displ. Rel. to Inc. Base Elev. at -12.00 m
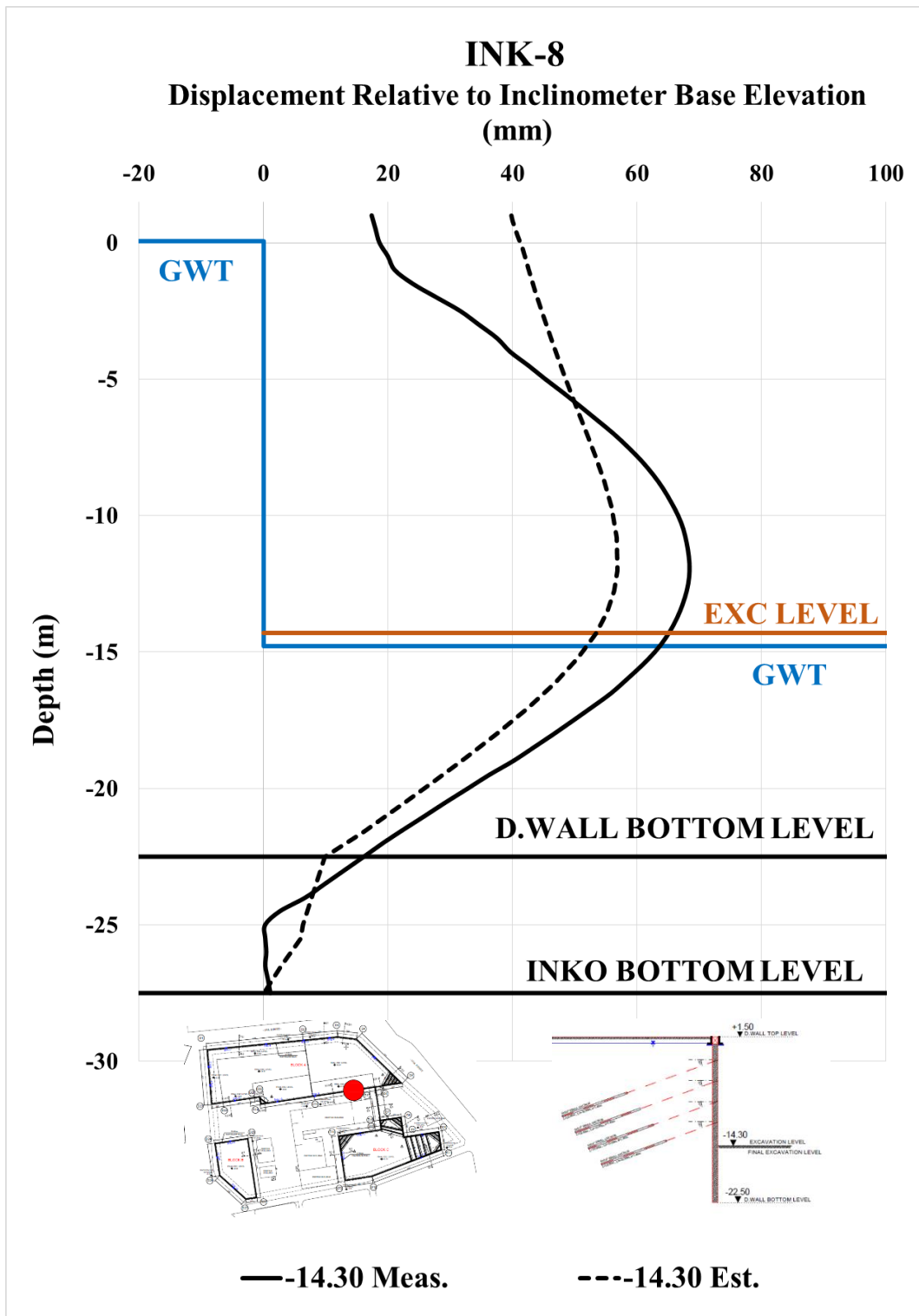
Figure A. 50. Estimated and Measured Displ. Rel. to Inc. Base Elev. at -14.30 m

Table A. 11. Internal Forces of Diaphragm Wall

INK - 8 / Section 2A-2A					
Excvation Stage	1	2	3	4	5
Excavation Level (m)	-2,80	-6,75	-9,70	-12,00	-14,30
N_{max} (kN/m)	120,20	310,70	502,40	689,00	867,30
V_{max} (kN/m)	69,80	309,50	383,30	447,60	470,20
M_{max} (kN.m/m)	196,20	486,10	822,60	1051,00	1415,00

Legend	Excvation Stage	1. Anchor Level	2. Excavation Level	2. Anchor Level	3. Excavation Level	3. Anchor Level	4. Excavation Level	4. Anchor Level	Final Excavation Level
	Measured Load of 1. Anchor Row (kN)	651.28	599.00	596.92	598.63	606.23	601.64	597.53	590.10
	Estimated Load of 1. Anchor Row (kN)	650.00	695.63	614.12	633.90	606.34	613.83	608.21	616.12
	Estimated Load of 2. Anchor Row (kN)	-	-	650.00	699.96	623.57	643.49	613.17	622.22
	Estimated Load of 3. Anchor Row (kN)	-	-	-	-	650.00	702.93	628.22	657.60
	Estimated Load of 4. Anchor Row (kN)	-	-	-	-	-	-	650.00	741.01

Figure A. 51. Measured and Estimated Anchor Loads

INK-9 – Estimated and Measured Displacements
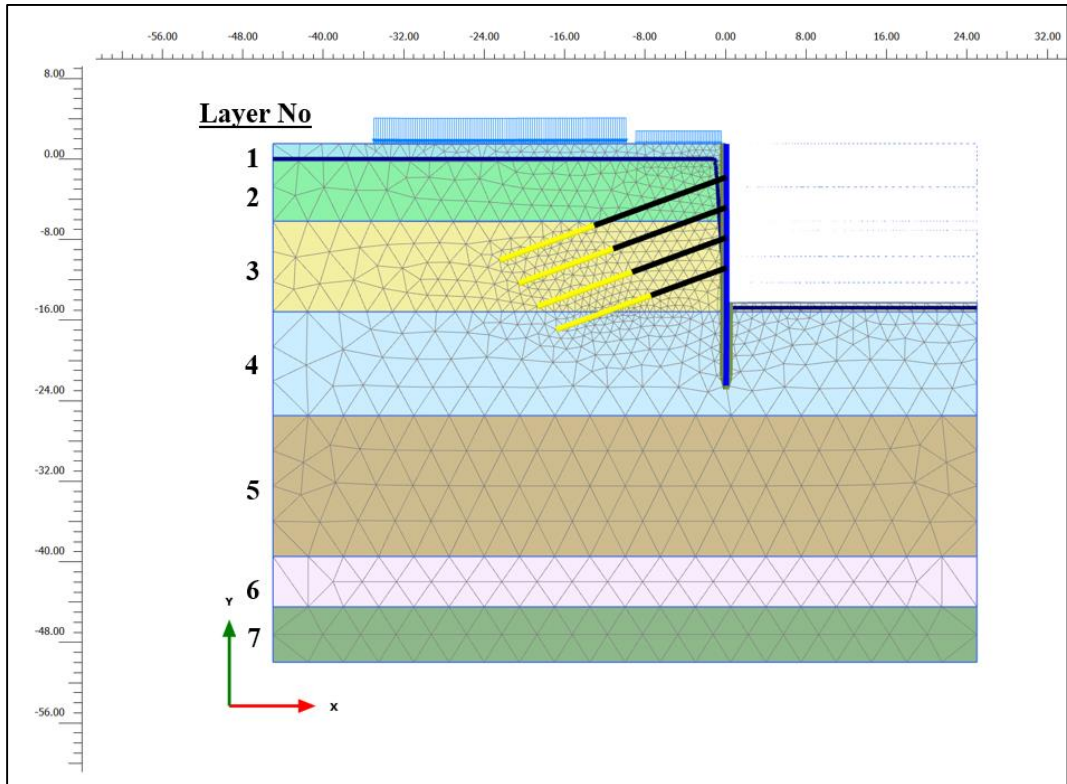
Figure A. 52. Meshed Model for INK-9
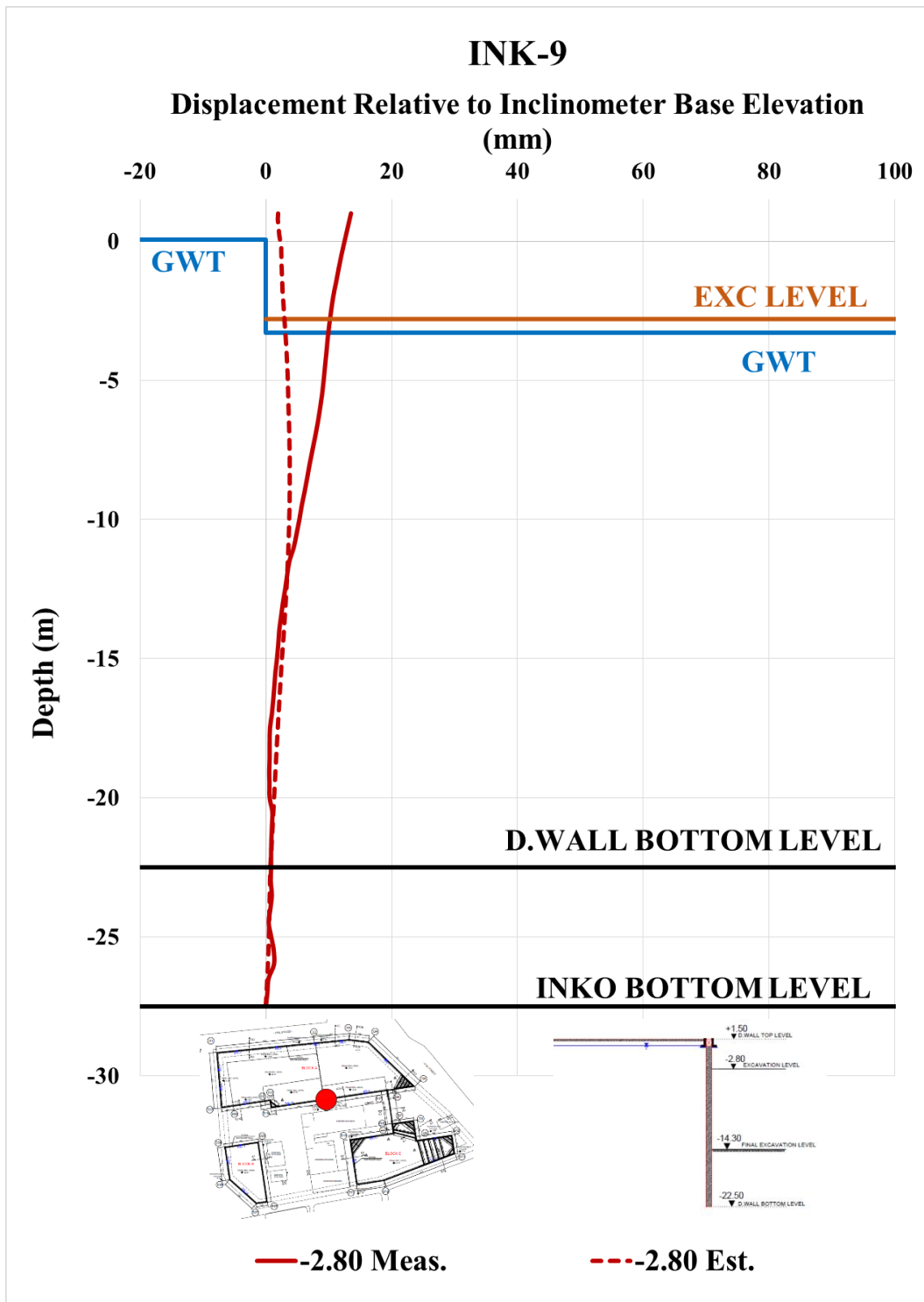
Figure A. 53. Estimated and Measured Displ. Rel. to Inc. Base Elev. at -2.80 m
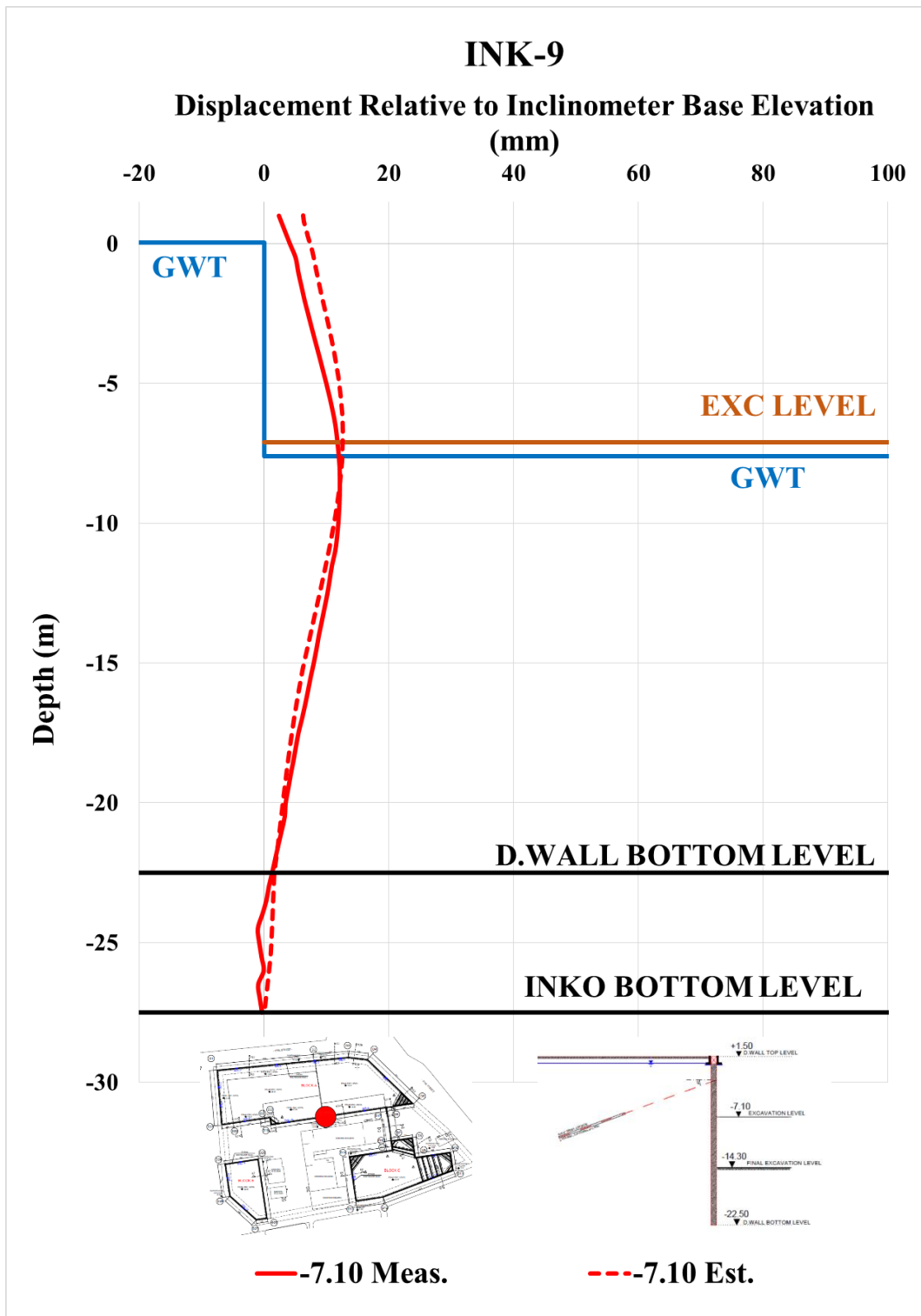
Figure A. 54. Estimated and Measured Displ. Rel. to Inc. Base Elev. at -7.10 m
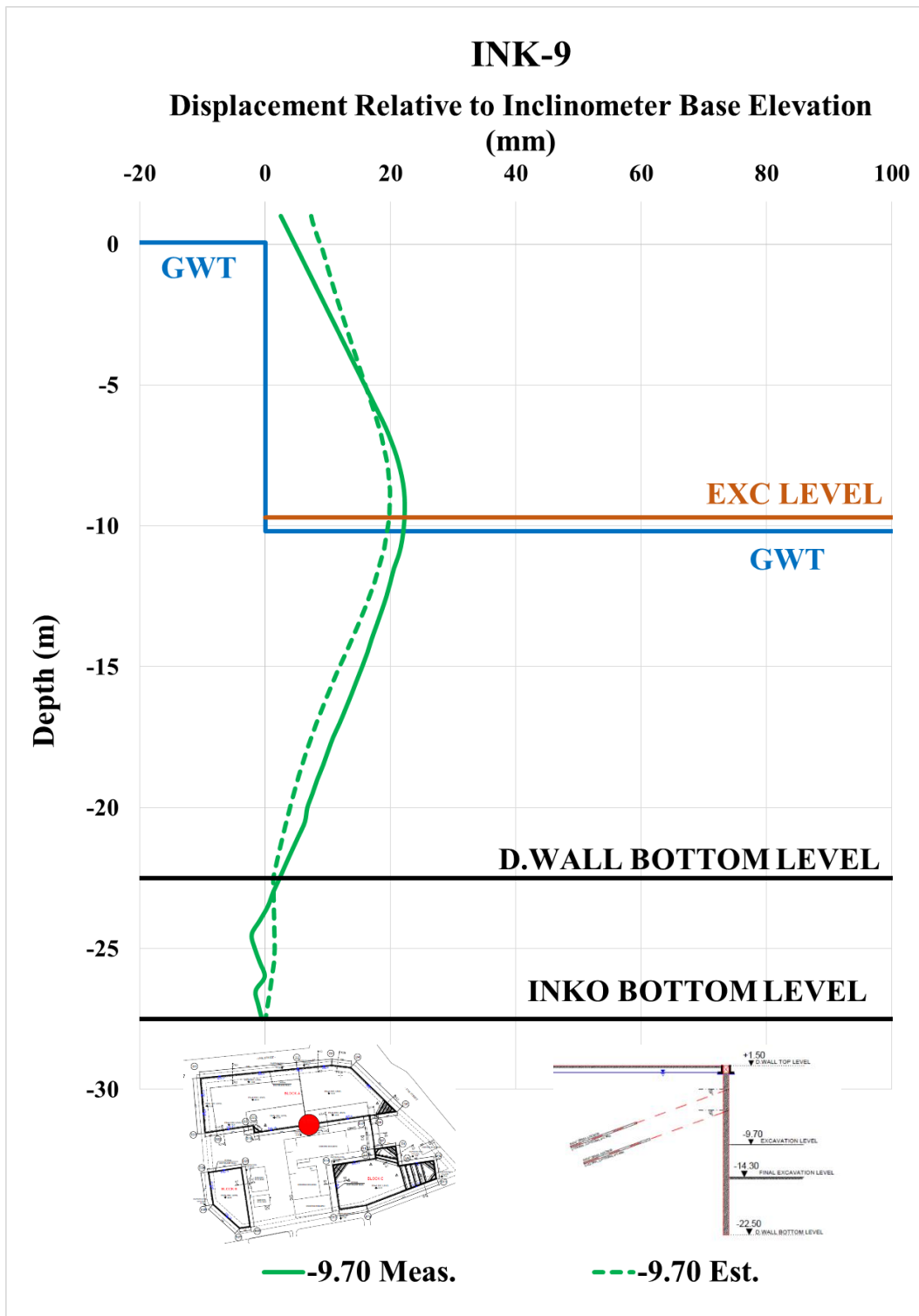
Figure A. 55. Estimated and Measured Displ. Rel. to Inc. Base Elev. at -9.70 m
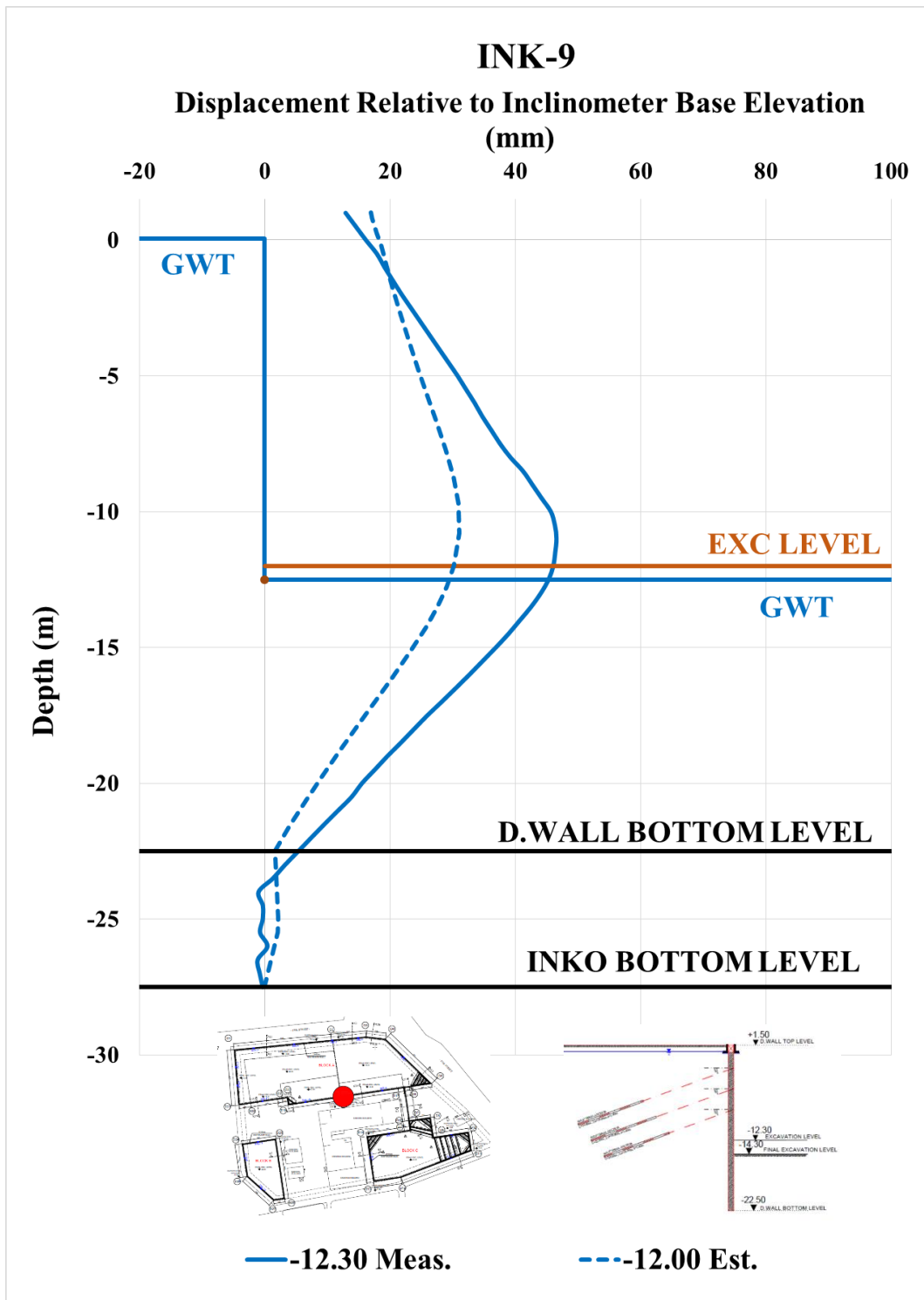
Figure A. 56. Estimated and Measured Displ. Rel. to Inc. Base Elev. at -12.30 m
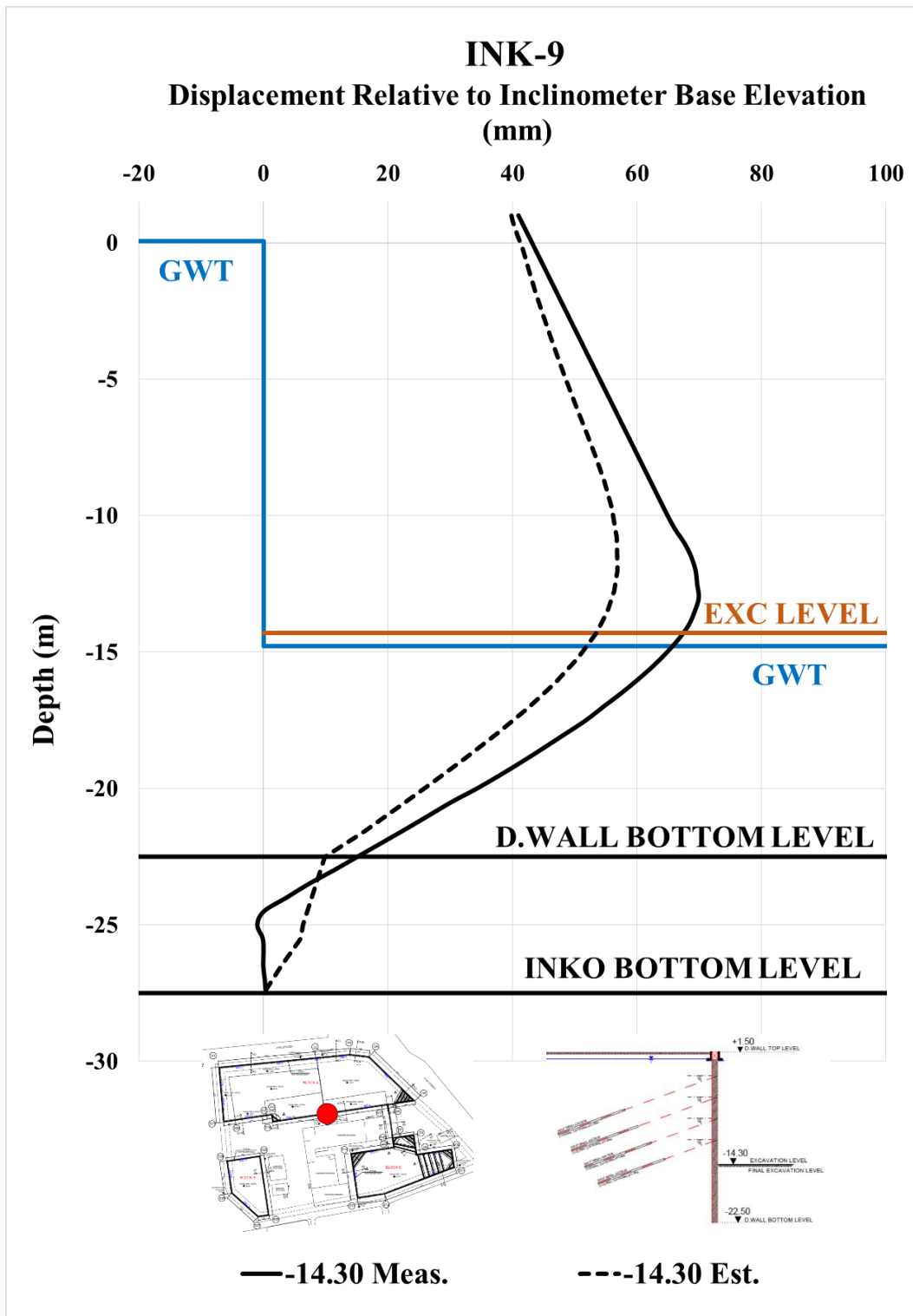
Figure A. 57. Estimated and Measured Displ. Rel. to Inc. Base Elev. at -14.30 m

Table A. 12. Internal Forces of Diaphragm Wall

INK - 9 / Section 2A-2A					
Excvation Stage	1	2	3	4	5
Excavation Level (m)	-2,80	-7,10	-9,70	-12,30	-14,30
N_{max} (kN/m)	120,20	329,30	505,10	717,80	873,50
V_{max} (kN/m)	69,53	317,60	385,50	464,70	467,40
M_{max} (kN.m/m)	194,50	194,50	835,80	1173,00	1442,00

INK - 9 / Section 2A-2A

Anchor Load vs Stage

Legend	Excvation Stage	1. Anchor Level	2. Excavation Level	2. Anchor Level	3. Excavation Level	3. Anchor Level	4. Excavation Level	4. Anchor Level	Final Excavation Level
	Estimated Load of 1. Anchor Row (kN)	650.00	702.04	621.62	637.76	609.53	617.77	612.17	618.98
	Estimated Load of 2. Anchor Row (kN)	-	-	650.00	692.30	615.06	640.07	609.34	616.45
	Estimated Load of 3. Anchor Row (kN)	-	-	-	-	650.00	719.48	643.66	666.50
	Estimated Load of 4. Anchor Row (kN)	-	-	-	-	-	-	650.00	722.98

Figure A. 58. Measured and Estimated Anchor Loads

195
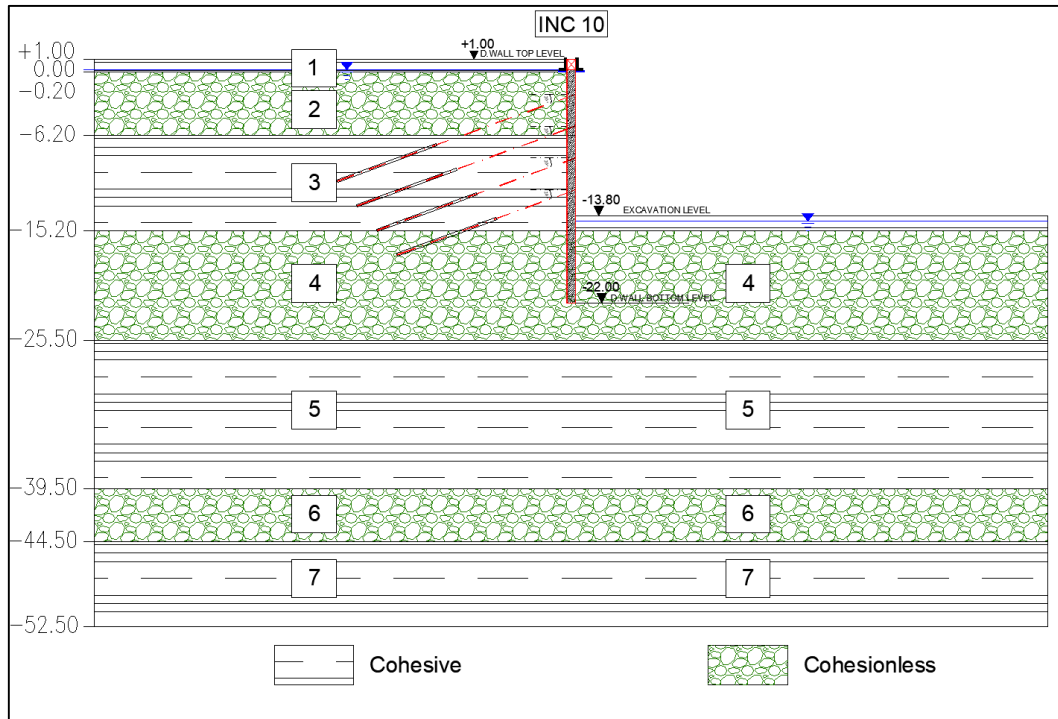
Figure A. 59. Section 1 – 1

Table A. 13. Section Properties of 1 – 1

SECTION 1 - 1									
Diaphragm Wall			SBMA Type Anchor				Excavation Properties		
Top Level (m)	Bottom Level (m)	Length (m)	Anchor No	Anchor Level (m)	Anchor Length (m)	Horizontal Spacing (m)	Top Level (m)	Bottom Level (m)	Depth (m)
1.00	-22.00	23.00	1	-1.80	24.00	2.00	1.00	-13.80	14.80
			2	-4.80	22.00	2.00			
			3	-7.80	20.00	2.00			
			4	-10.80	18.00	2.00			

INK-10 – Estimated and Measured Displacements
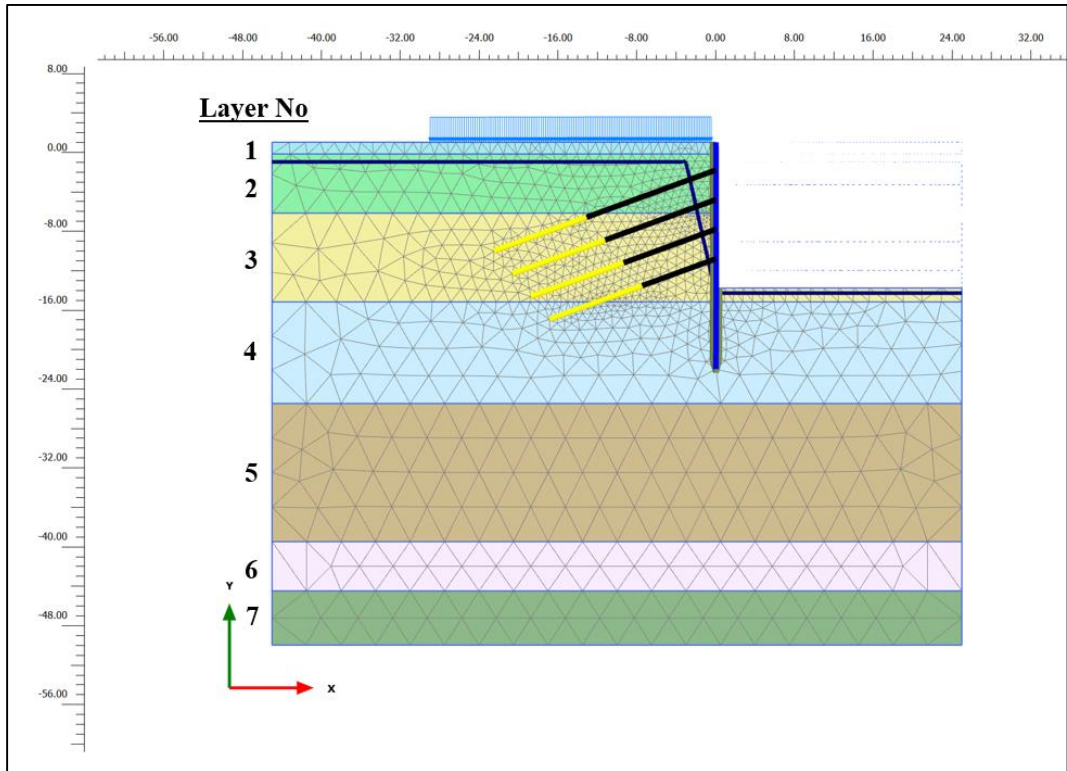
Figure A. 60. Meshed Model for INK-10
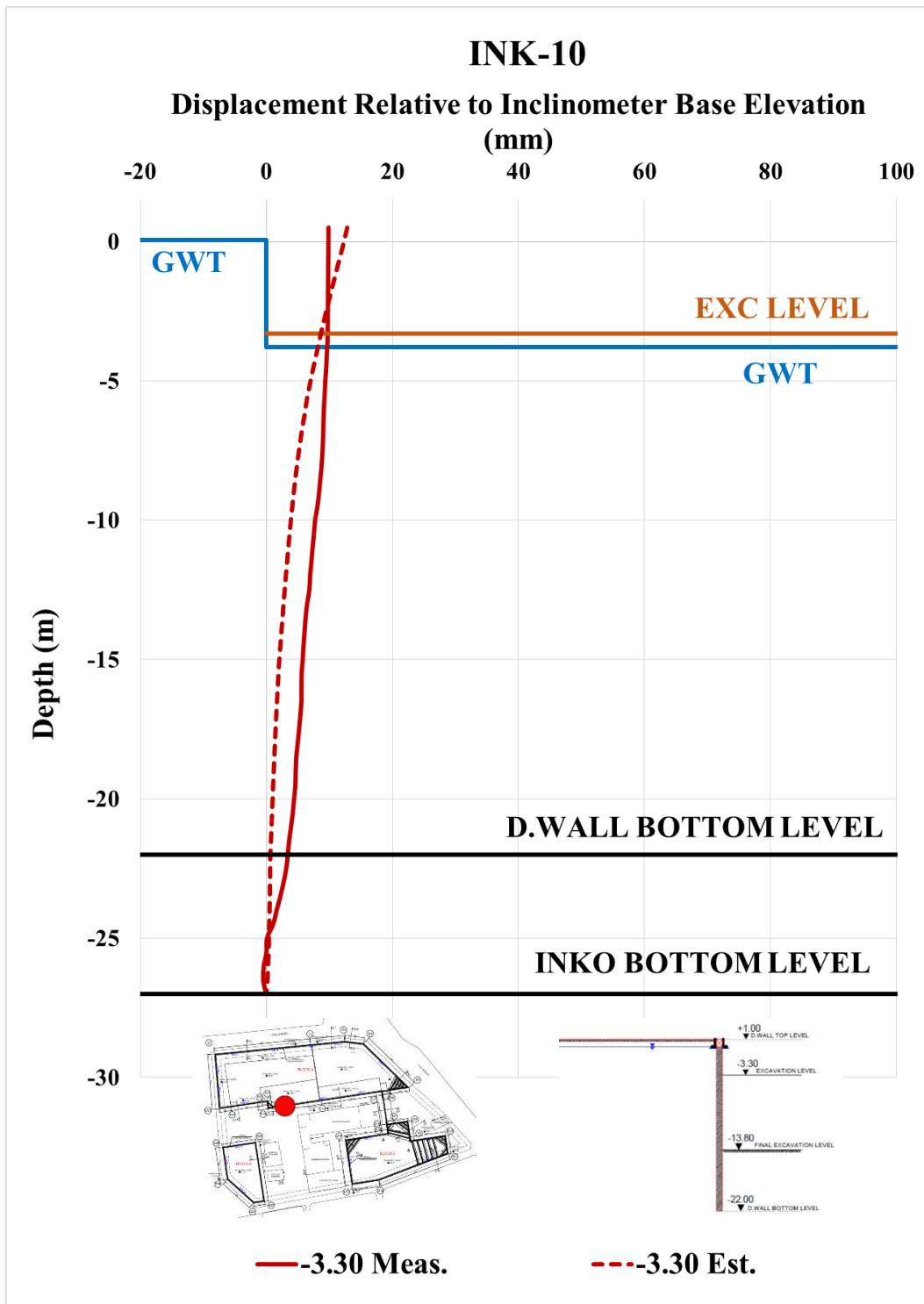
Figure A. 61. Estimated and Measured Displ. Rel. to Inc. Base Elev. at -3.30 m
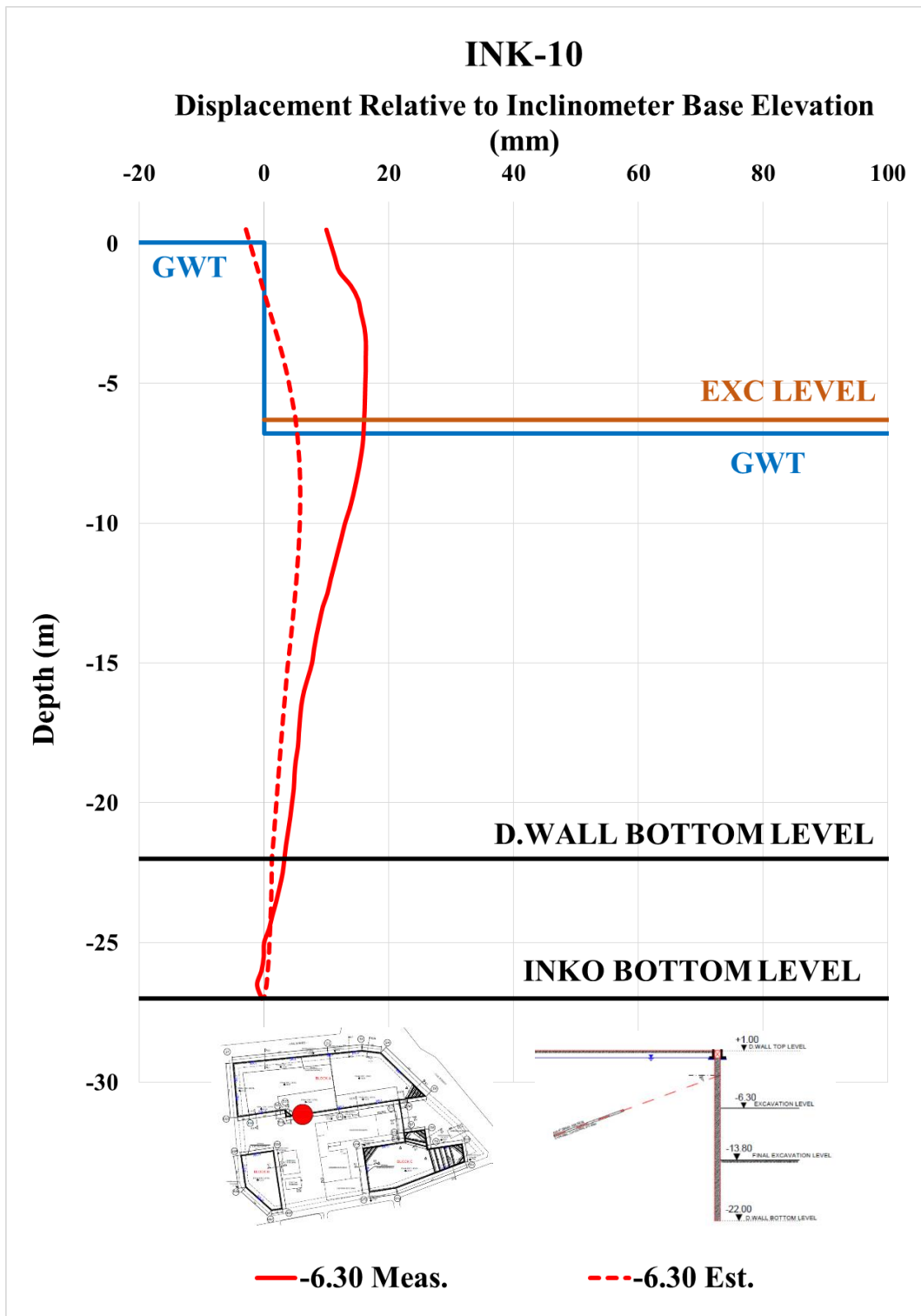
Figure A. 62. Estimated and Measured Displ. Rel. to Inc. Base Elev. at -6.30 m
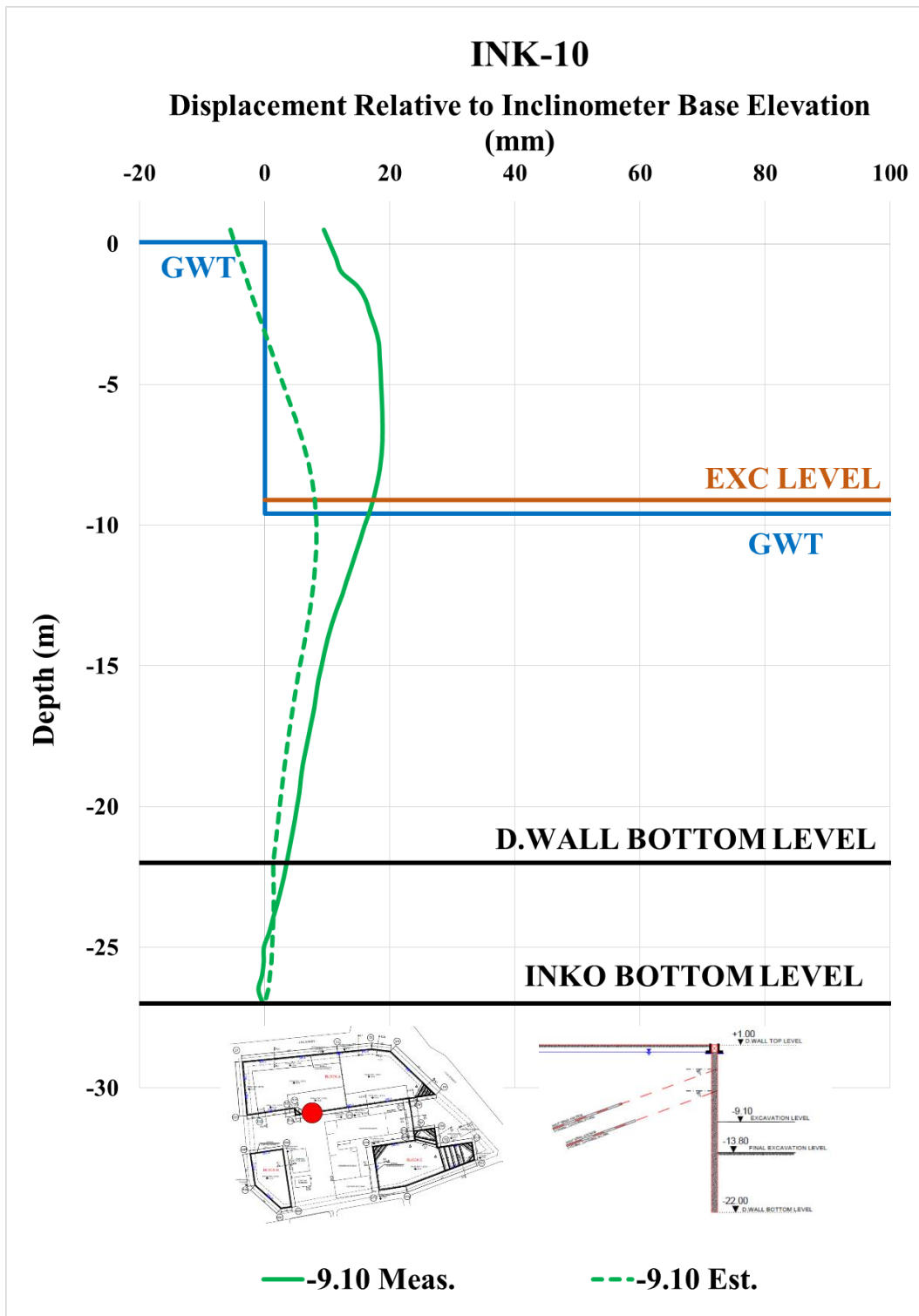
Figure A. 63. Estimated and Measured Displ. Rel. to Inc. Base Elev. at -9.10 m
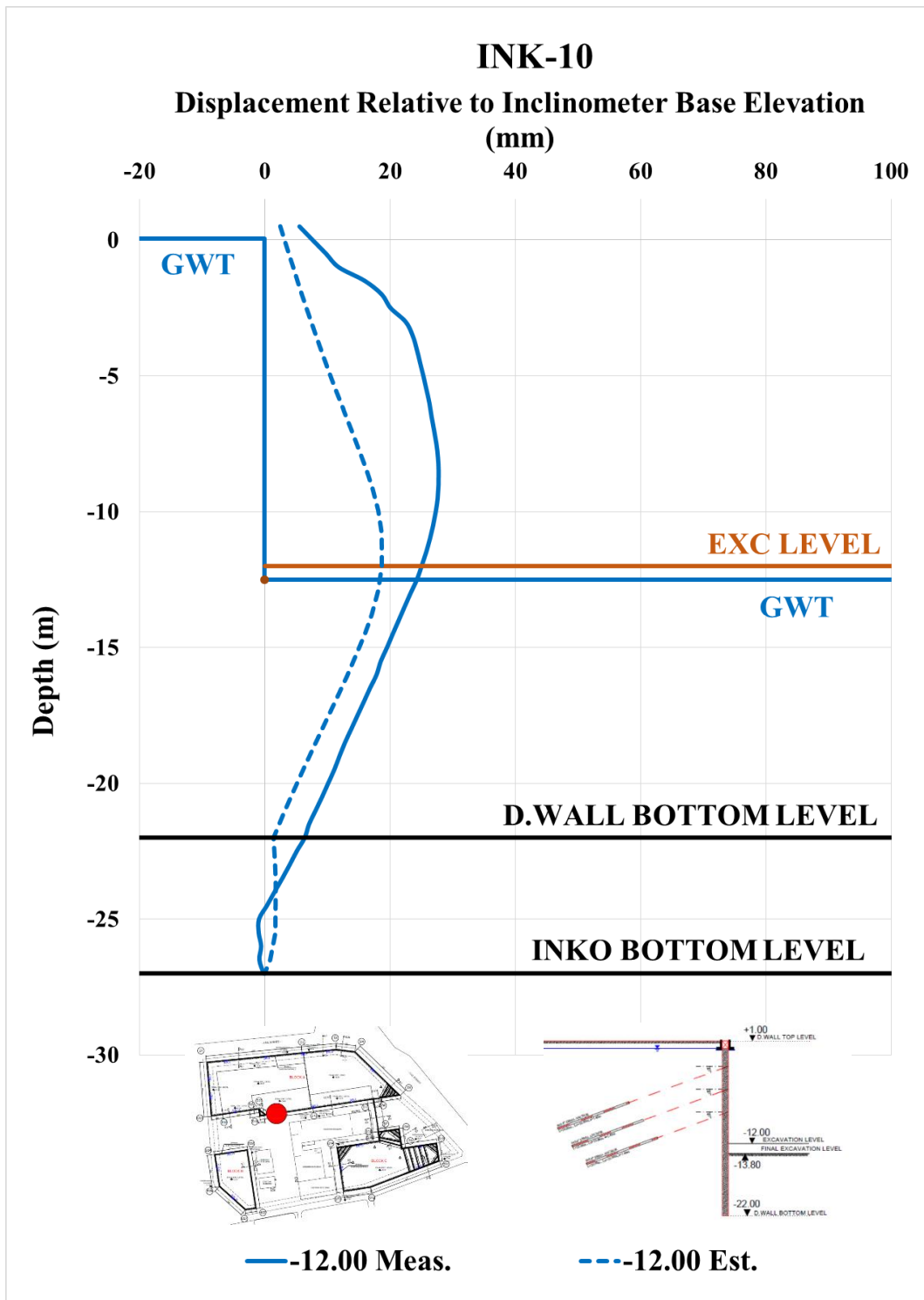
Figure A. 64. Estimated and Measured Displ. Rel. to Inc. Base Elev. at -12.00 m
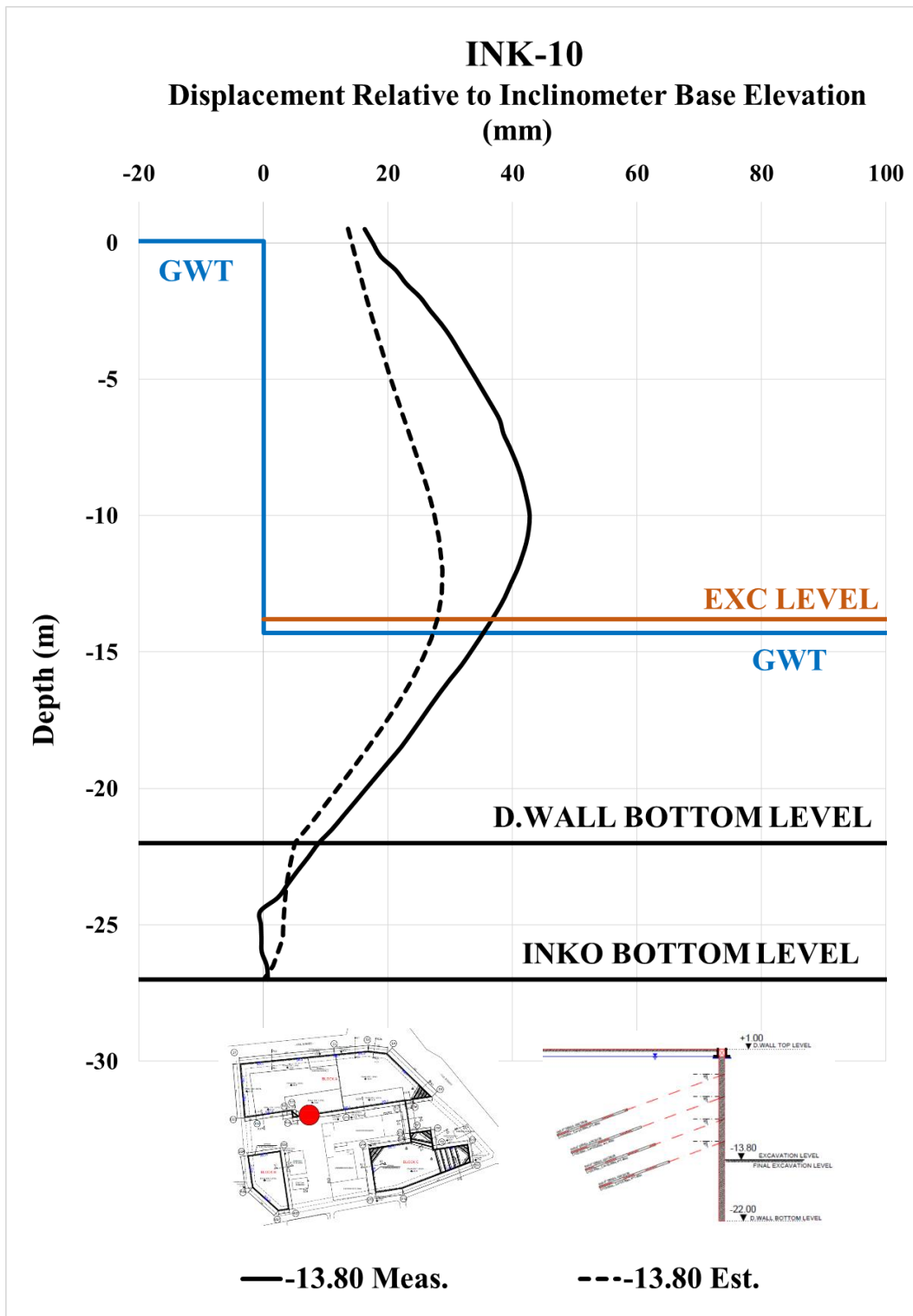
Figure A. 65. Estimated and Measured Displ. Rel. to Inc. Base Elev. at -13.80 m

Table A. 14. Internal Forces of Diaphragm Wall

INK - 10 / Section 1-1					
Excvation Stage	1	2	3	4	5
Excavation Level (m)	-3,30	-6,30	-9,10	-12,00	-13,80
N_{max} (kN/m)	100,90	259,40	440,50	635,00	767,10
V_{max} (kN/m)	53,43	285,70	337,60	412,90	412,90
M_{max} (kN.m/m)	138,70	398,40	587,30	866,40	963,80

Legend	Excvation Stage	1. Anchor Level	2. Excavation Level	2. Anchor Level	3. Excavation Level	3. Anchor Level	4. Excavation Level	4. Anchor Level	Final Excavation Level
	Estimated Load of 1. Anchor Row (kN)	650.00	650.00	565.80	581.38	553.59	562.85	557.22	562.35
	Estimated Load of 2. Anchor Row (kN)	-	-	650.00	681.45	605.15	626.83	597.44	602.69
	Estimated Load of 3. Anchor Row (kN)	-	-	-	-	650.00	703.15	630.45	644.19
	Estimated Load of 4. Anchor Row (kN)	-	-	-	-	-	-	650.00	690.94

Figure A. 66. Measured and Estimated Anchor Loads

INK-8 – Calibrated, Estimated and Measured Displacements
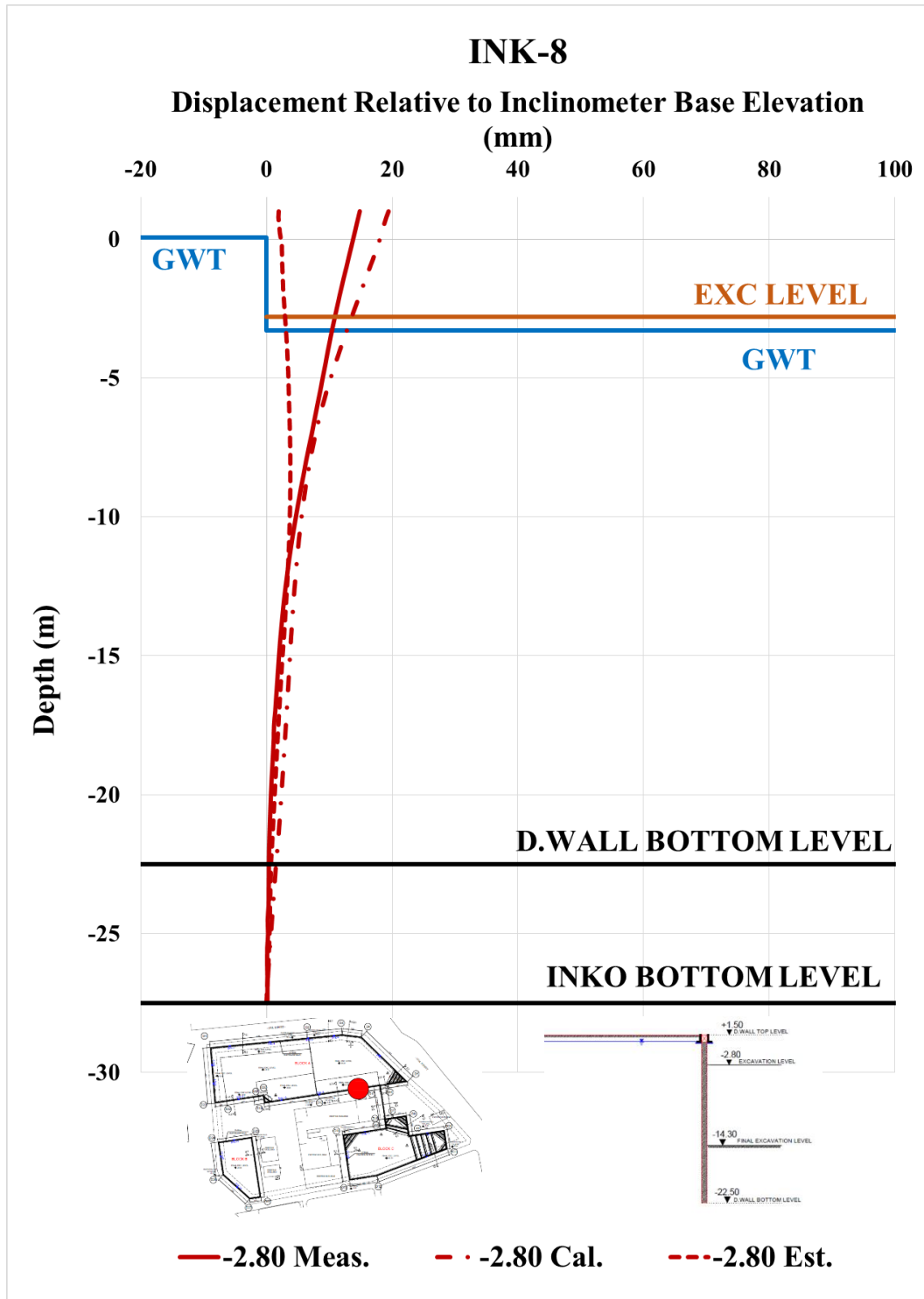
Figure A. 67. Calibrated and Measured Displ. Rel. to Inc. Base Elev. at -2.80 m
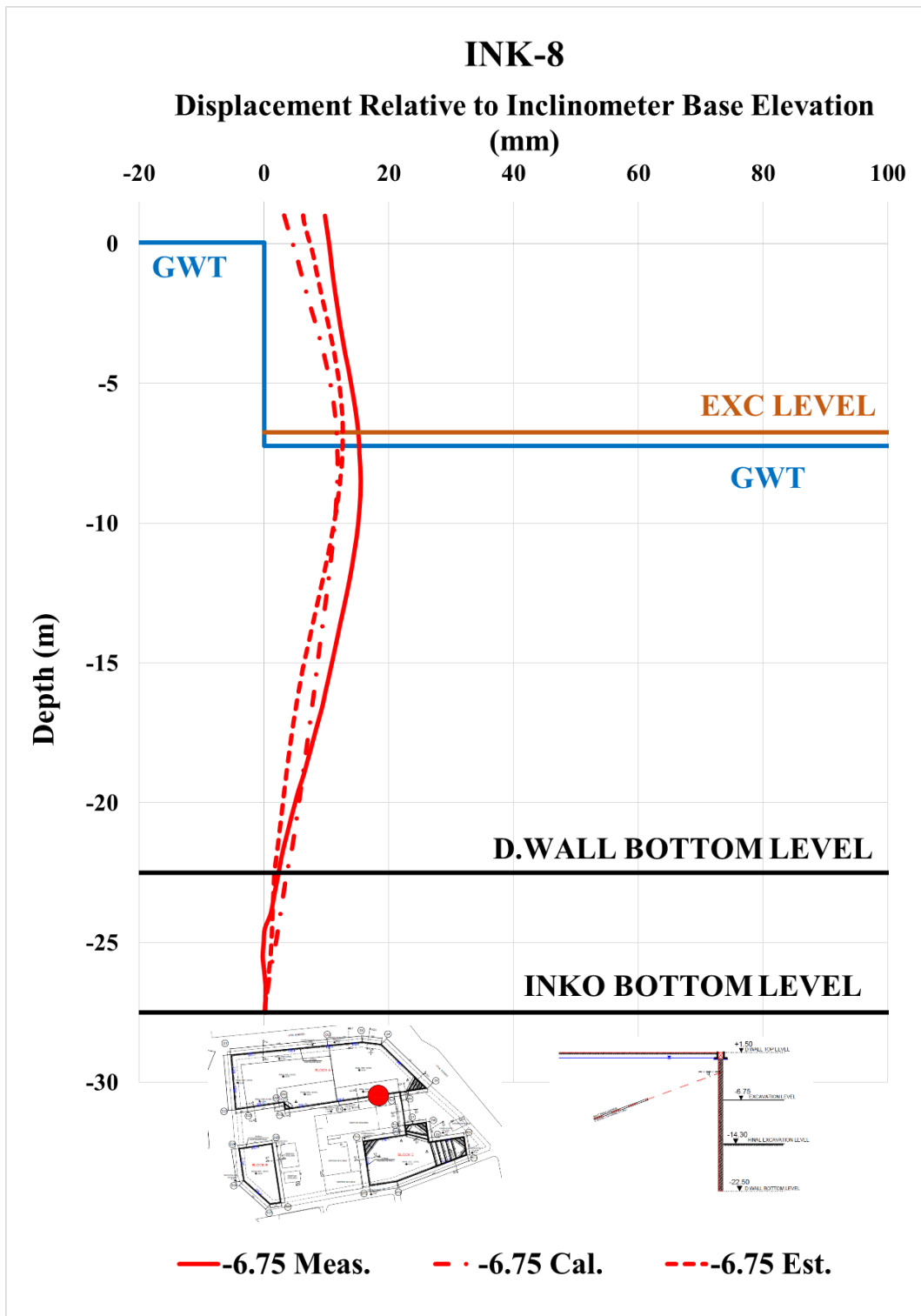
Figure A. 68. Calibrated and Measured Displ. Rel. to Inc. Base Elev. at -6.75 m
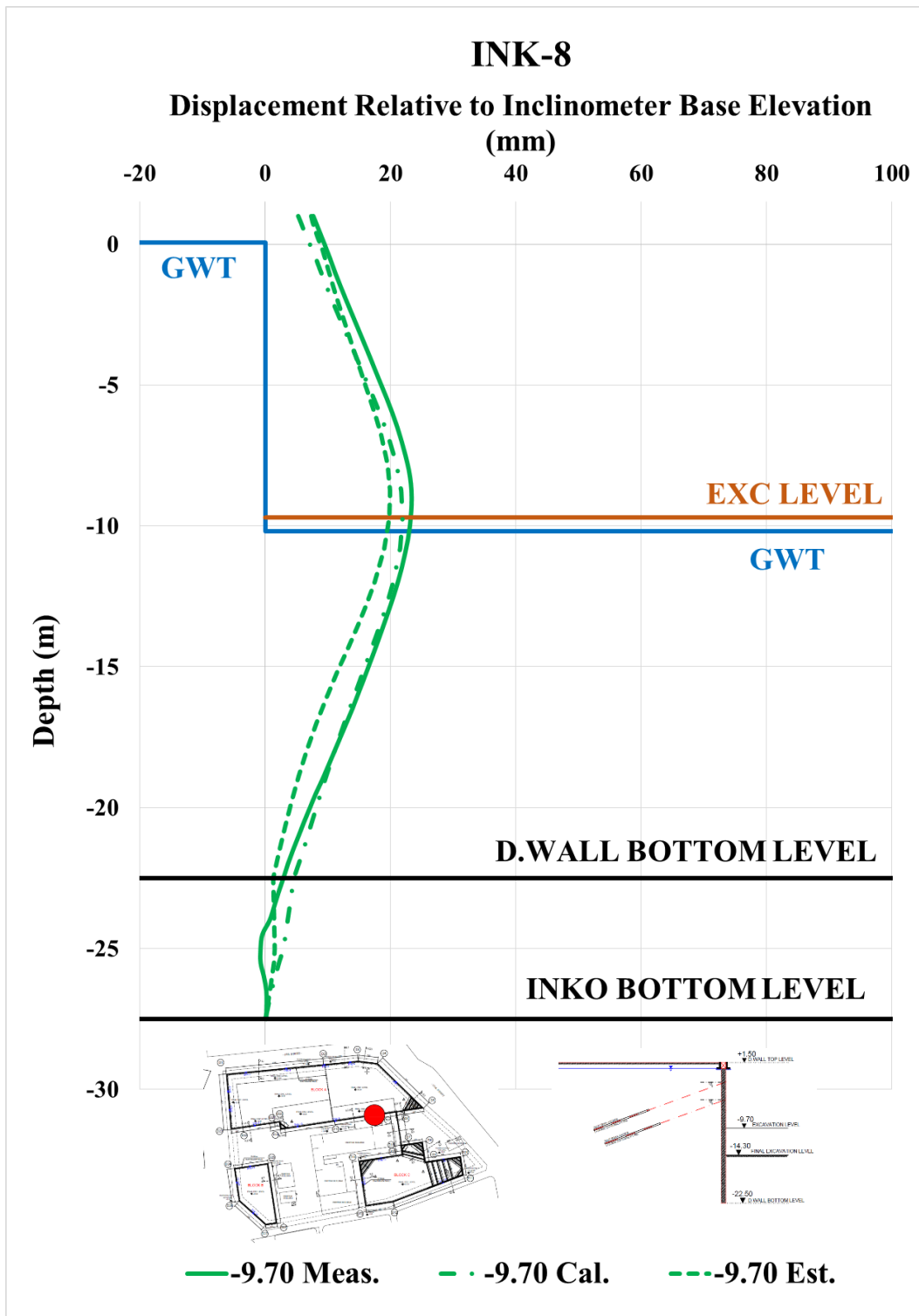
Figure A. 69. Calibrated and Measured Displ. Rel. to Inc. Base Elev. at -9.70 m
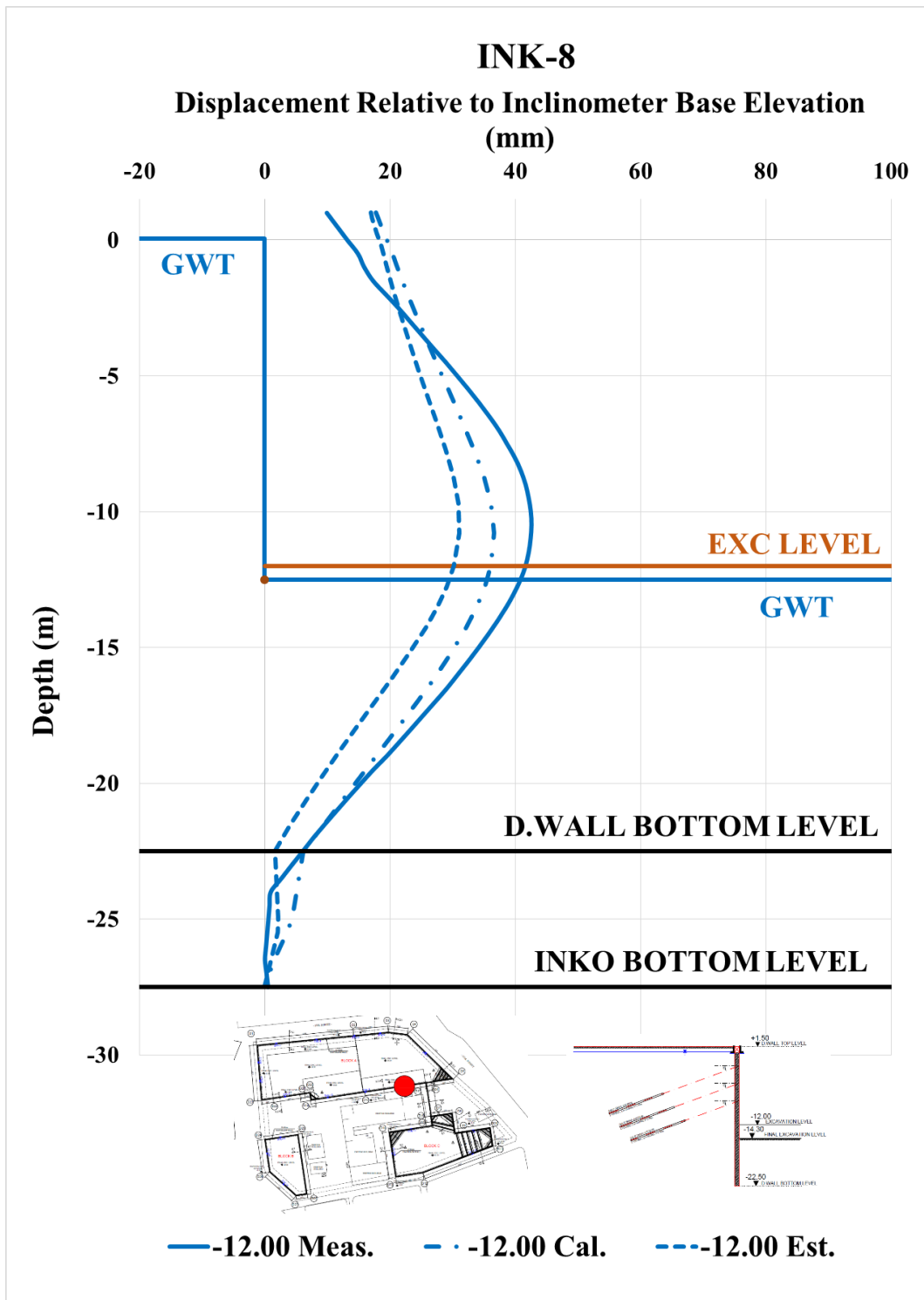
Figure A. 70. Calibrated and Measured Displ. Rel. to Inc. Base Elev. at -12.00 m
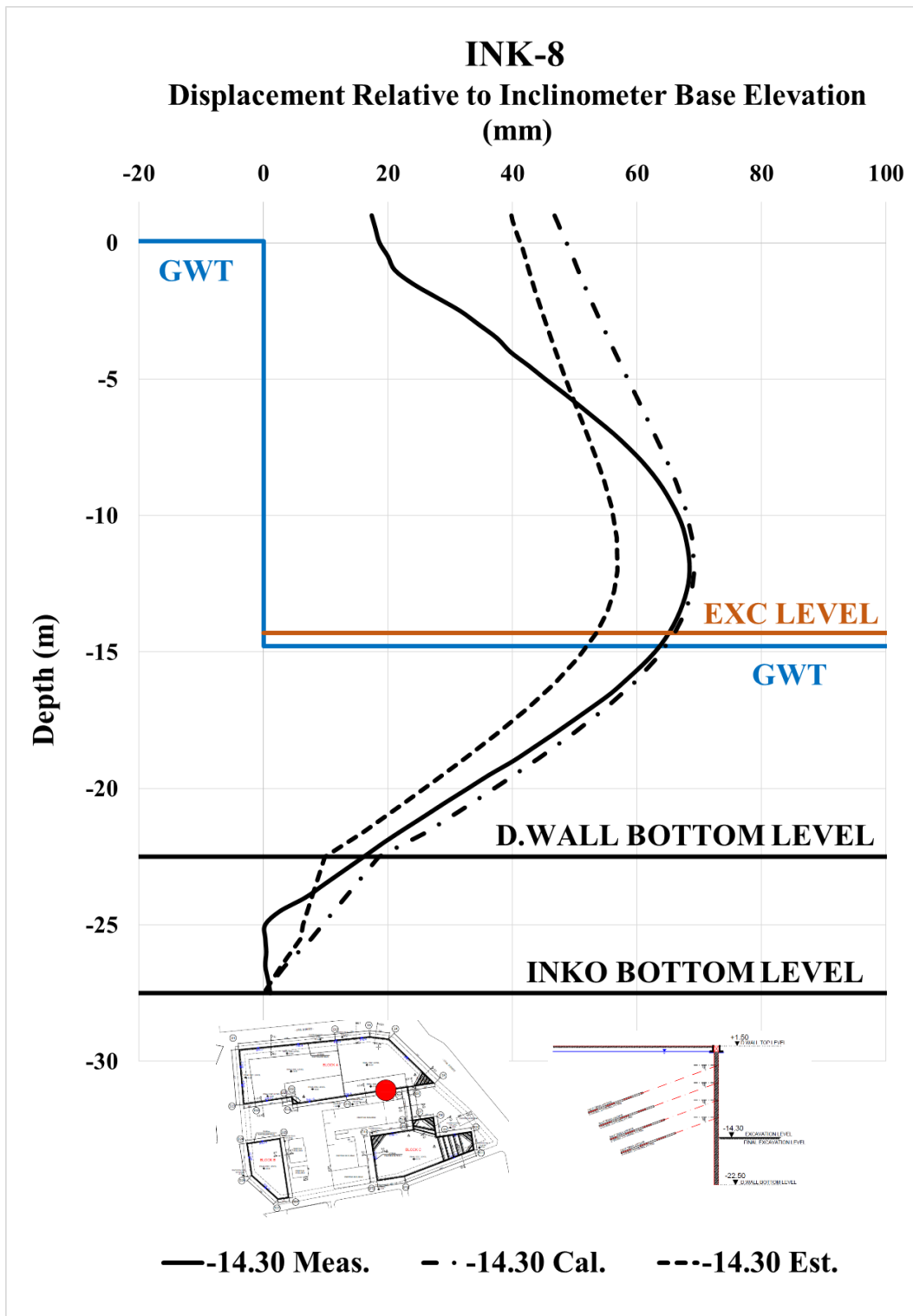
Figure A. 71. Calibrated and Measured Displ. Rel. to Inc. Base Elev. at -14.30 m

Table A. 15. Internal Forces of Diaphragm Wall

INK - 8 / Section 2A-2A					
Excvation Stage	1	2	3	4	5
Excavation Level (m)	-3,25	-6,70	-9,70	-12,00	-14,30
N_{max} (kN/m)	109,30	301,40	504,40	685,60	853,20
V_{max} (kN/m)	70,68	311,70	385,40	447,80	475,60
M_{max} (kN.m/m)	219,60	459,20	822,00	1083,00	1520,00

INK - 8 / Section 2A-2A

Anchor Load vs Stage

Legend	Excvation Stage	1. Anchor Level	2. Excavation Level	2. Anchor Level	3. Excavation Level	3. Anchor Level	4. Excavation Level	4. Anchor Level	Final Excavation Level
	Measured Load of 1. Anchor Row (kN)	651.28	599.00	596.92	598.63	606.23	601.64	597.53	590.10
	Estimated Load of 1. Anchor Row (kN)	650.00	693.10	605.22	627.20	599.30	607.20	603.00	612.57
	Estimated Load of 2. Anchor Row (kN)	-	-	650.00	703.03	630.09	650.55	622.65	631.46
	Estimated Load of 3. Anchor Row (kN)	-	-	-	-	650.00	703.25	633.38	661.01
	Estimated Load of 4. Anchor Row (kN)	-	-	-	-	-	-	650.00	735.26

Figure A. 72. Measured and Estimated Anchor Loads

Table A. 16. Summary of Displacement Results of INK-8

INK - 8 / SECTION 2A - 2A

Excvation Level (m)	Excvation Depth (m)	u_{meas} (mm) Inclinometer Measurements	u_{est} (mm) Estimation with Plaxis 2D Analysis	u_{cal} (mm) Calibration with Plaxis 2D Analysis	$u_{literature}$ (mm) FHWA-IF-99-015 (1999) - Maksimum	$u_{literature}$ (mm) FHWA-IF-99-015 (1999) - Average	$u_{literature}$ (mm) Goldberg et al. (1976)	$u_{literature}$ (mm) Clough et al. (1990) - Maksimum	$u_{literature}$ (mm) Clough et al. (1990) - Average	$u_{literature}$ (mm) Long (2001)	$u_{literature}$ (mm) Long (2001) (Extraordinary cases eliminated)	$u_{literature}$ (mm) Long (2001) Cantilever System
-3.30	4.80	14.84	3.84	19.43	24.00	9.60	24.00	24.00	9.60	9.12	6.72	17.28
-6.30	7.80	15.47	12.58	11.79	39.00	15.60	39.00	39.00	15.60	14.82	10.92	-
-9.10	10.60	23.35	19.86	21.95	53.00	21.20	53.00	53.00	21.20	20.14	14.84	-
-12.00	13.50	42.57	31.11	36.63	67.50	27.00	67.50	67.50	27.00	25.65	18.90	-
-13.80	15.30	68.42	56.86	69.22	76.50	30.60	76.50	76.50	30.60	29.07	21.42	-
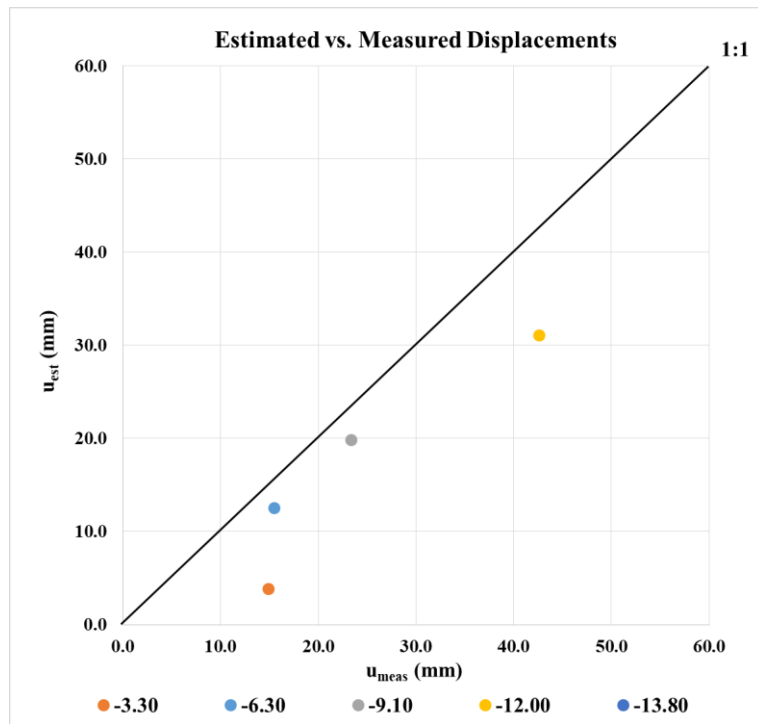
Figure A. 73. Estimated and Measured Displacements of INK - 8
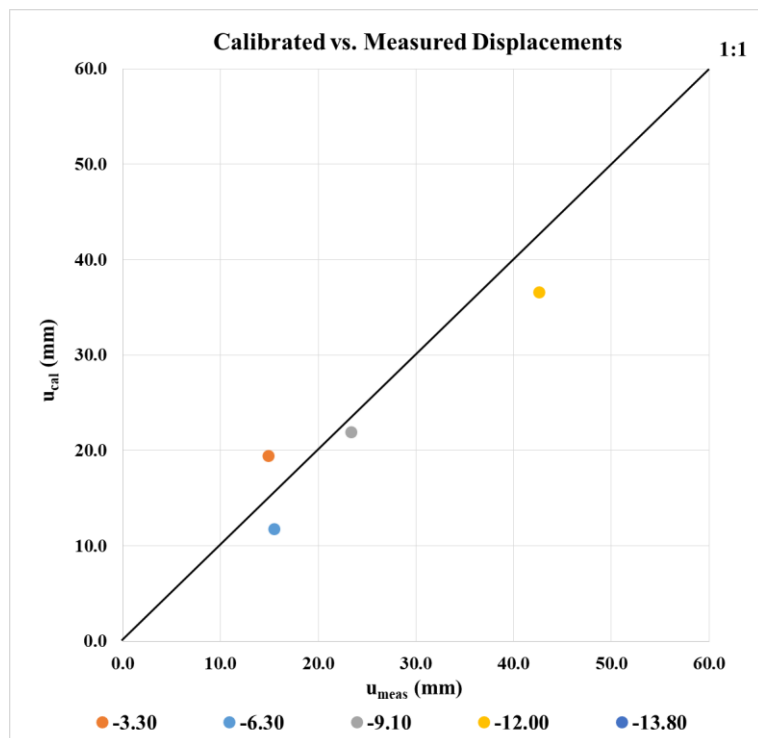
Figure A. 74. Calibrated and Measured Displacements of INK - 8

INK-9 – Calibrated, Estimated and Measured Displacements
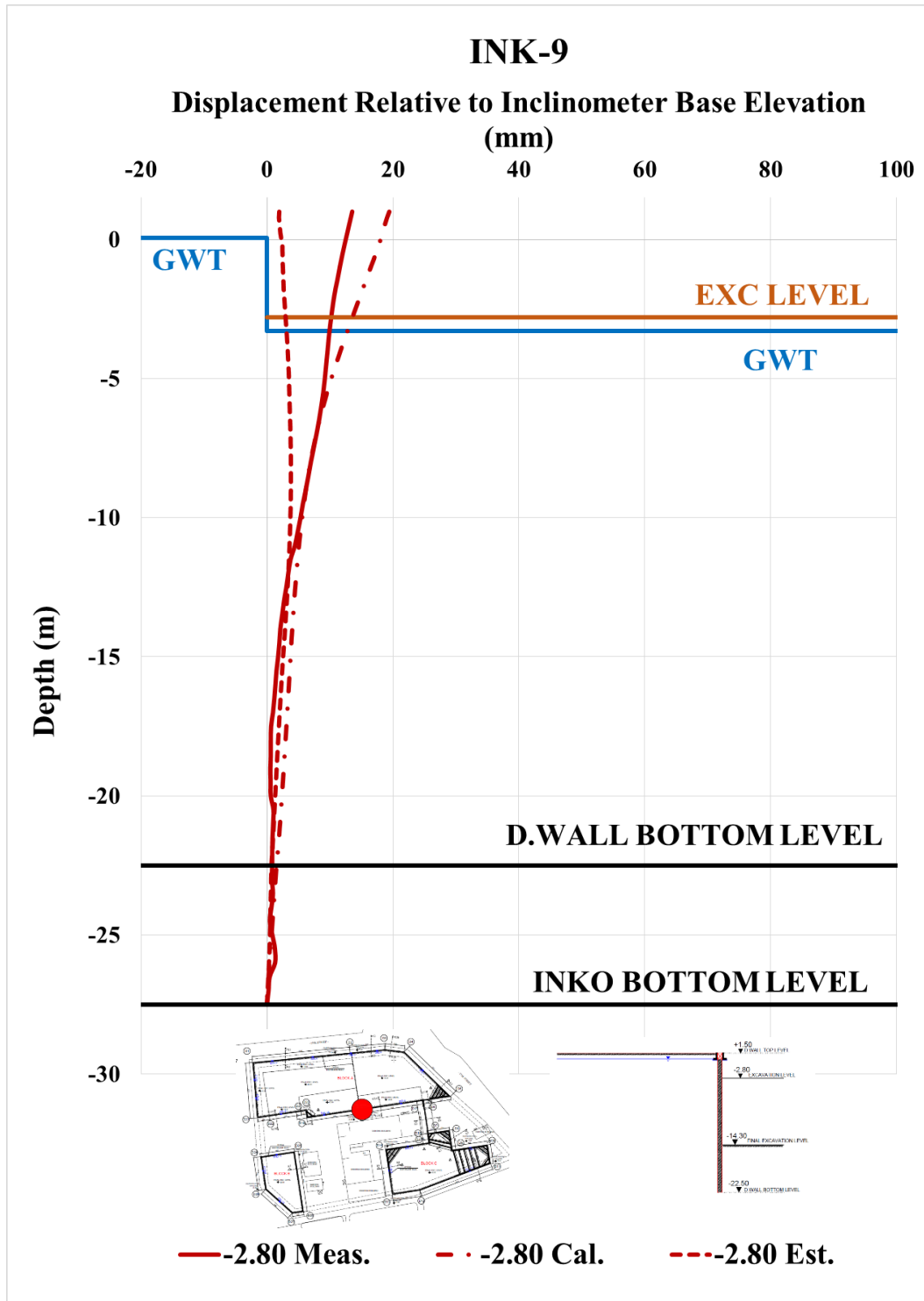
Figure A. 75. Calibrated and Measured Displ. Rel. to Inc. Base Elev. at -2.80 m
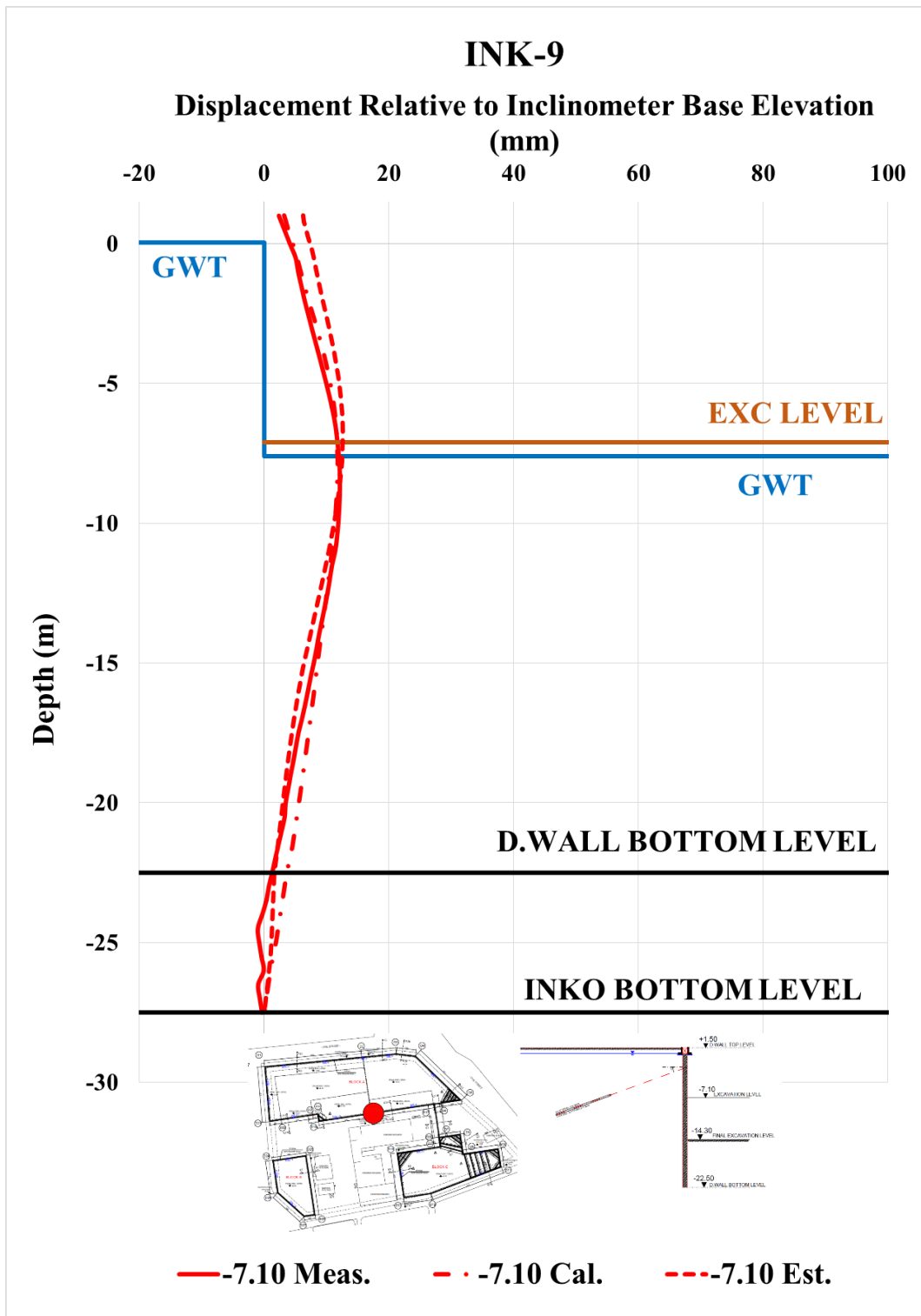
Figure A. 76. Calibrated and Measured Displ. Rel. to Inc. Base Elev. at -7.10 m
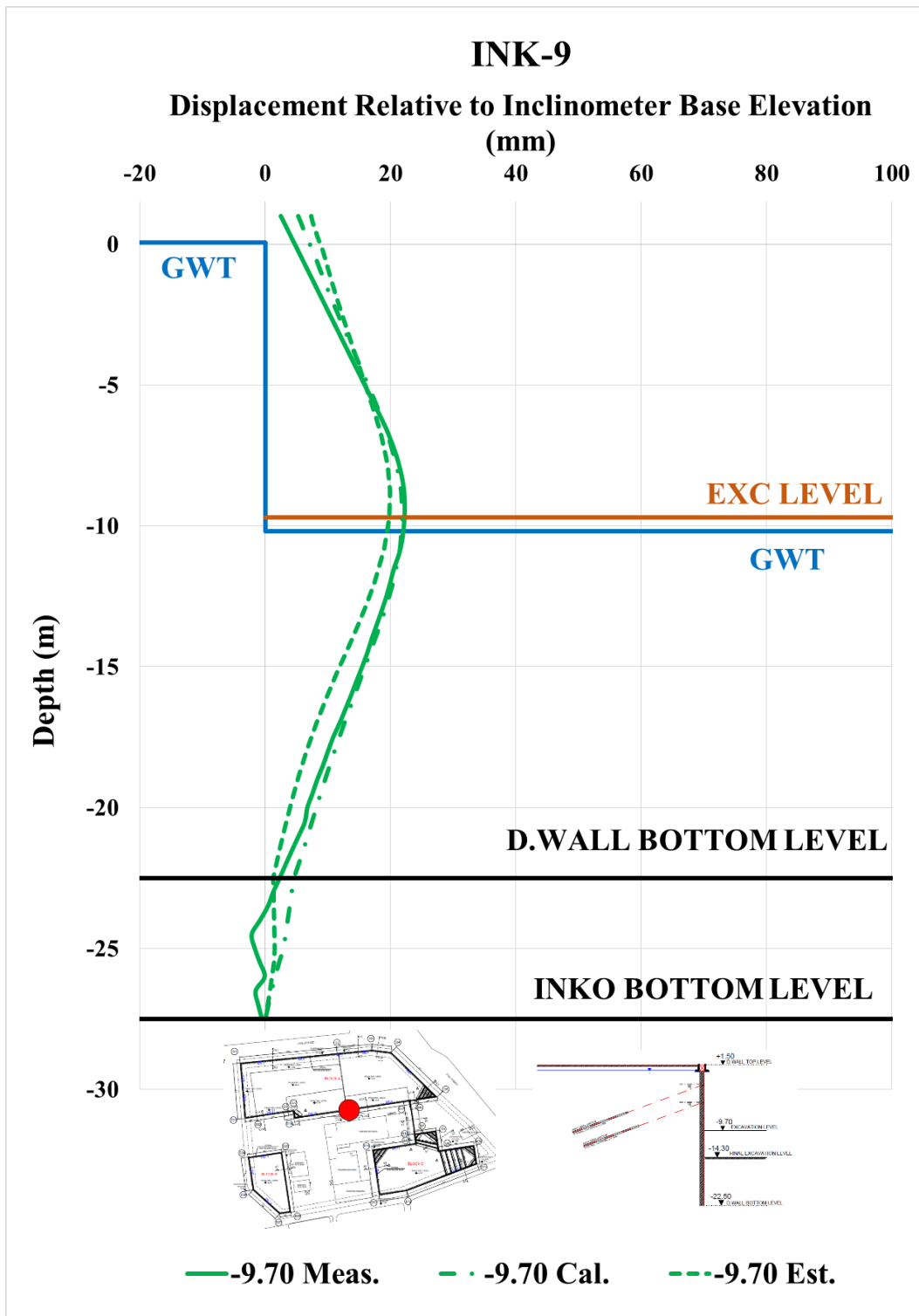
Figure A. 77. Calibrated and Measured Displ. Rel. to Inc. Base Elev. at -9.70 m
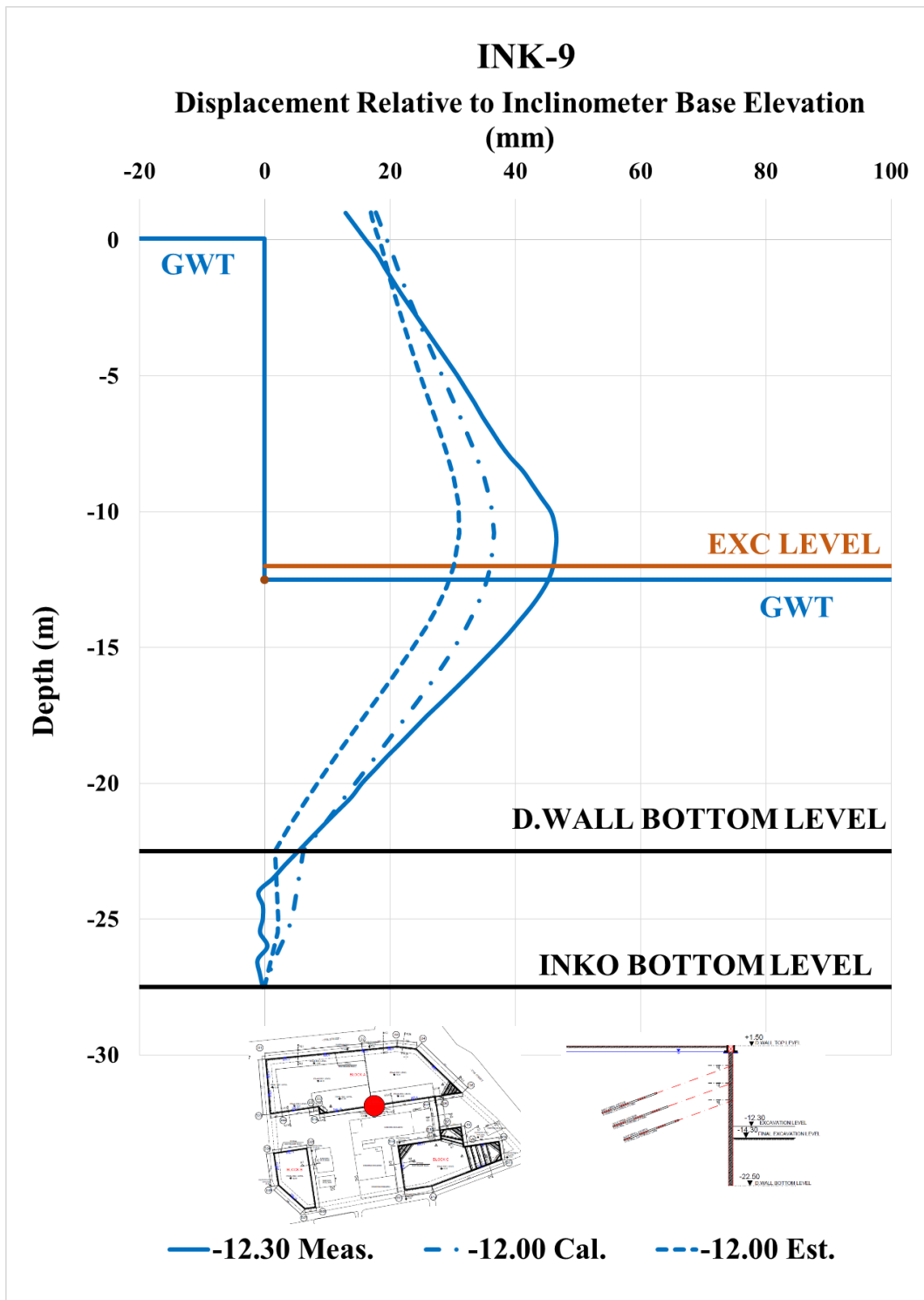
Figure A. 78. Calibrated and Measured Displ. Rel. to Inc. Base Elev. at -12.00 m
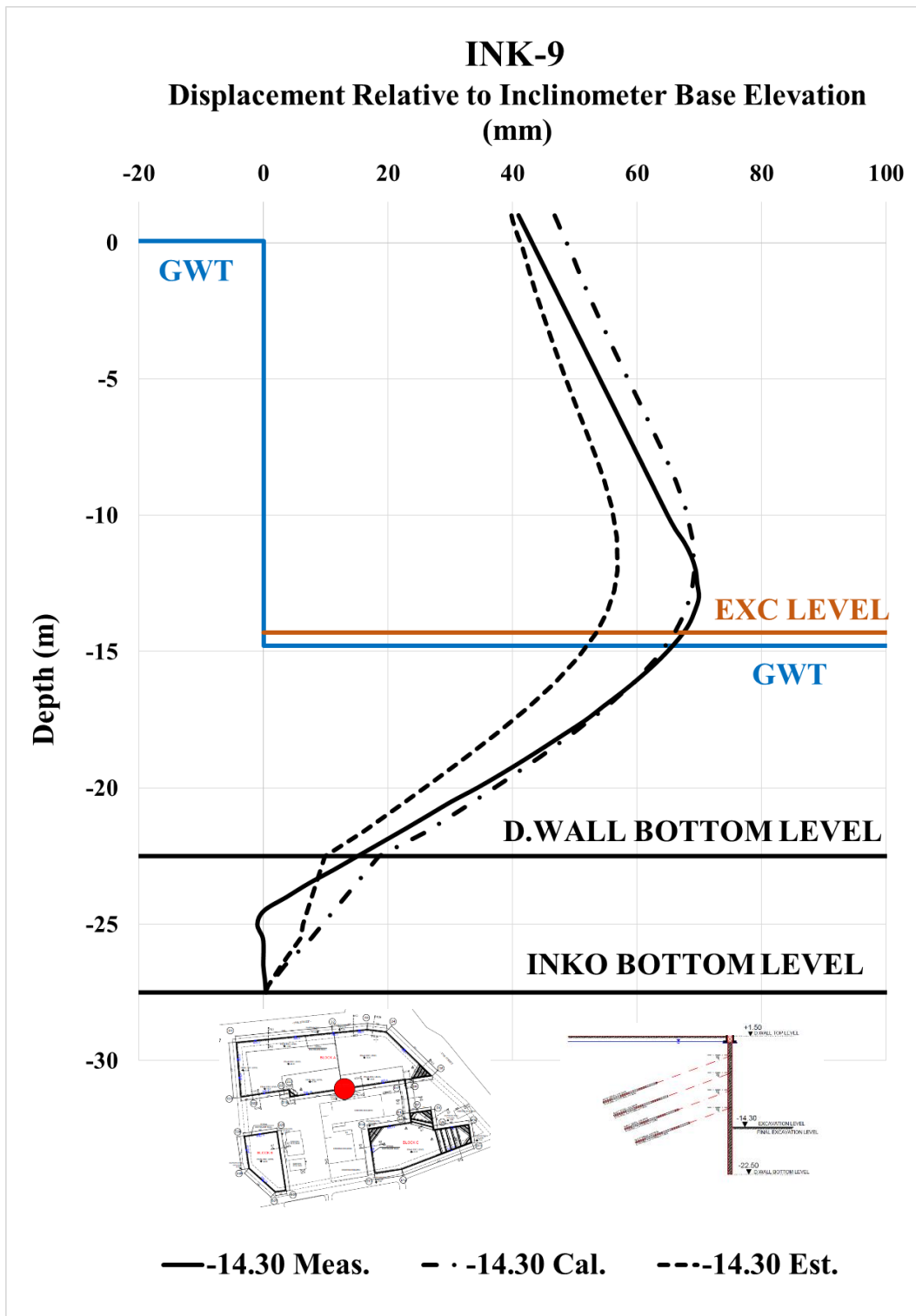
Figure A. 79. Calibrated and Measured Displ. Rel. to Inc. Base Elev. at -14.30 m

Table A. 17. Internal Forces of Diaphragm Wall

INK - 9 / Section 2A-2A					
Excvation Stage	**1**	**2**	**3**	**4**	**5**
Excavation Level (m)	-2,80	-7,10	-9,70	-12,30	-14,30
N_{max} **(kN/m)**	109,30	323,00	508,70	715,20	861,00
V_{max} **(kN/m)**	71,20	319,40	387,50	466,20	475,80
M_{max} **(kN.m/m)**	222,40	527,00	832,10	1214,00	1554,00

Legend	Excvation Stage	1. Anchor Level	2. Excavation Level	2. Anchor Level	3. Excavation Level	3. Anchor Level	4. Excavation Level	4. Anchor Level	Final Excavation Level
	Estimated Load of 1. Anchor Row (kN)	650.00	701.00	613.85	631.84	603.31	611.66	607.52	615.85
	Estimated Load of 2. Anchor Row (kN)	-	-	650.00	695.51	621.72	647.27	618.80	625.58
	Estimated Load of 3. Anchor Row (kN)	-	-	-	-	650.00	720.22	648.78	670.32
	Estimated Load of 4. Anchor Row (kN)	-	-	-	-	-	-	650.00	719.03

Figure A. 80. Measured and Estimated Anchor Loads

Table A. 18. Summary of Displacement Results of INK-9

INK - 9 / SECTION 2A - 2A

Excvation Level (m)	Excvation Depth (m)	u_{meas} (mm) Inclinometer Measurements	u_{est} (mm) Estimation with Plaxis 2D Analysis	u_{cal} (mm) Calibration with Plaxis 2D Analysis	$u_{literature}$ (mm) FHWA-IF-99-015 (1999) - Maksimum	$u_{literature}$ (mm) FHWA-IF-99-015 (1999) - Average	$u_{literature}$ (mm) Goldberg et al. (1976)	$u_{literature}$ (mm) Clough et al. (1990) - Maksimum	$u_{literature}$ (mm) Clough et al. (1990) - Average	$u_{literature}$ (mm) Long (2001)	$u_{literature}$ (mm) Long (2001) (Extraordinary cases eliminated)	$u_{literature}$ (mm) Long (2001) Cantilever System
-3.25	4.75	13.53	18.98	19.70	23.75	9.50	23.75	23.75	9.50	9.03	6.65	17.1
-6.70	8.20	12.15	14.10	13.78	41.00	16.40	41.00	41.00	16.40	15.58	11.48	-
-9.70	11.20	22.25	20.44	22.76	56.00	22.40	56.00	56.00	22.40	21.28	15.68	-
-12.00	13.50	46.56	36.86	43.58	67.50	27.00	67.50	67.50	27.00	25.65	18.90	-
-14.30	15.80	69.90	58.66	71.74	79.00	31.60	79.00	79.00	31.60	30.02	22.12	-

218
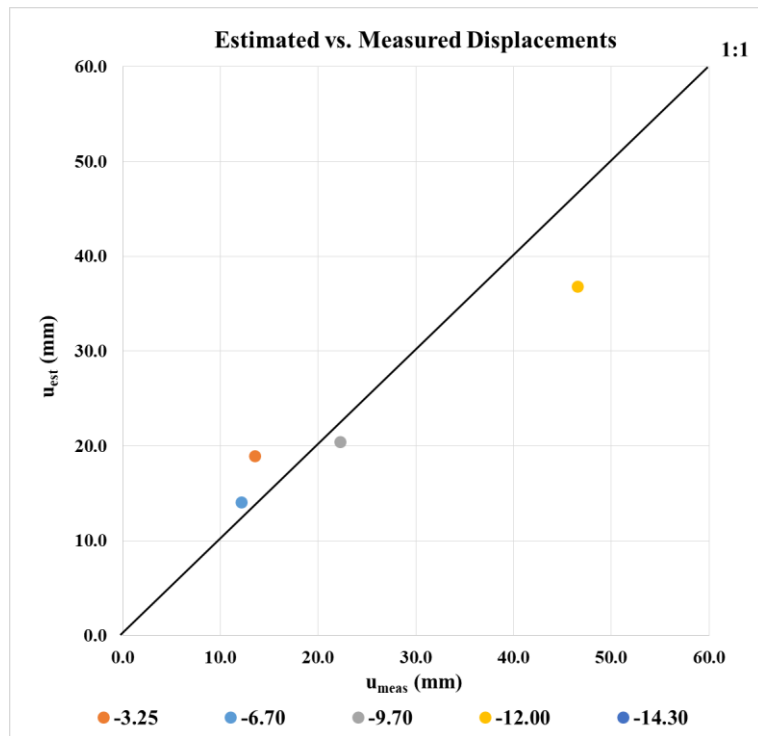
Figure A. 81. Estimated and Measured Displacements of INK - 9
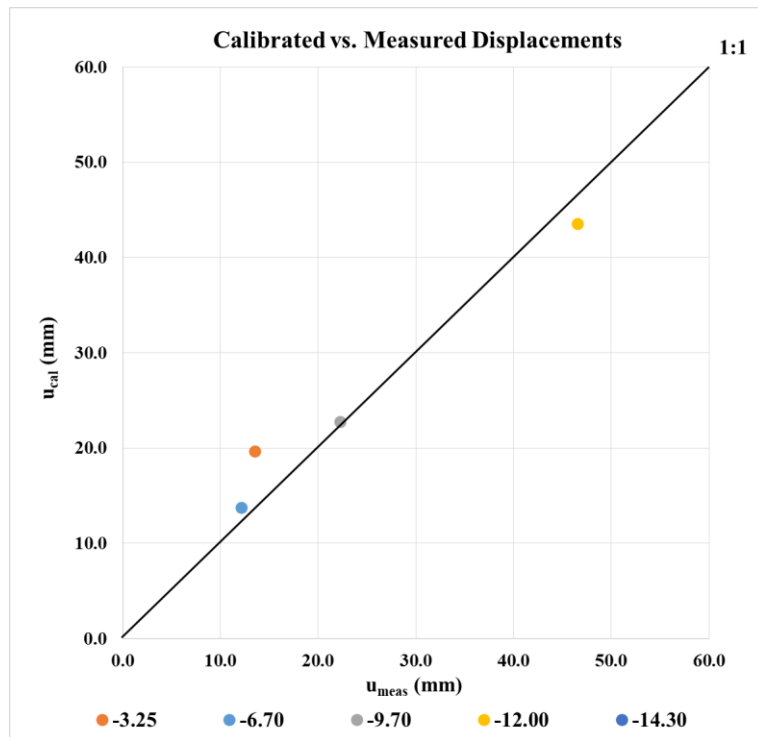
Figure A. 82. Calibrated and Measured Displacements of INK - 9

INK-10 – Calibrated, Estimated and Measured Displacements
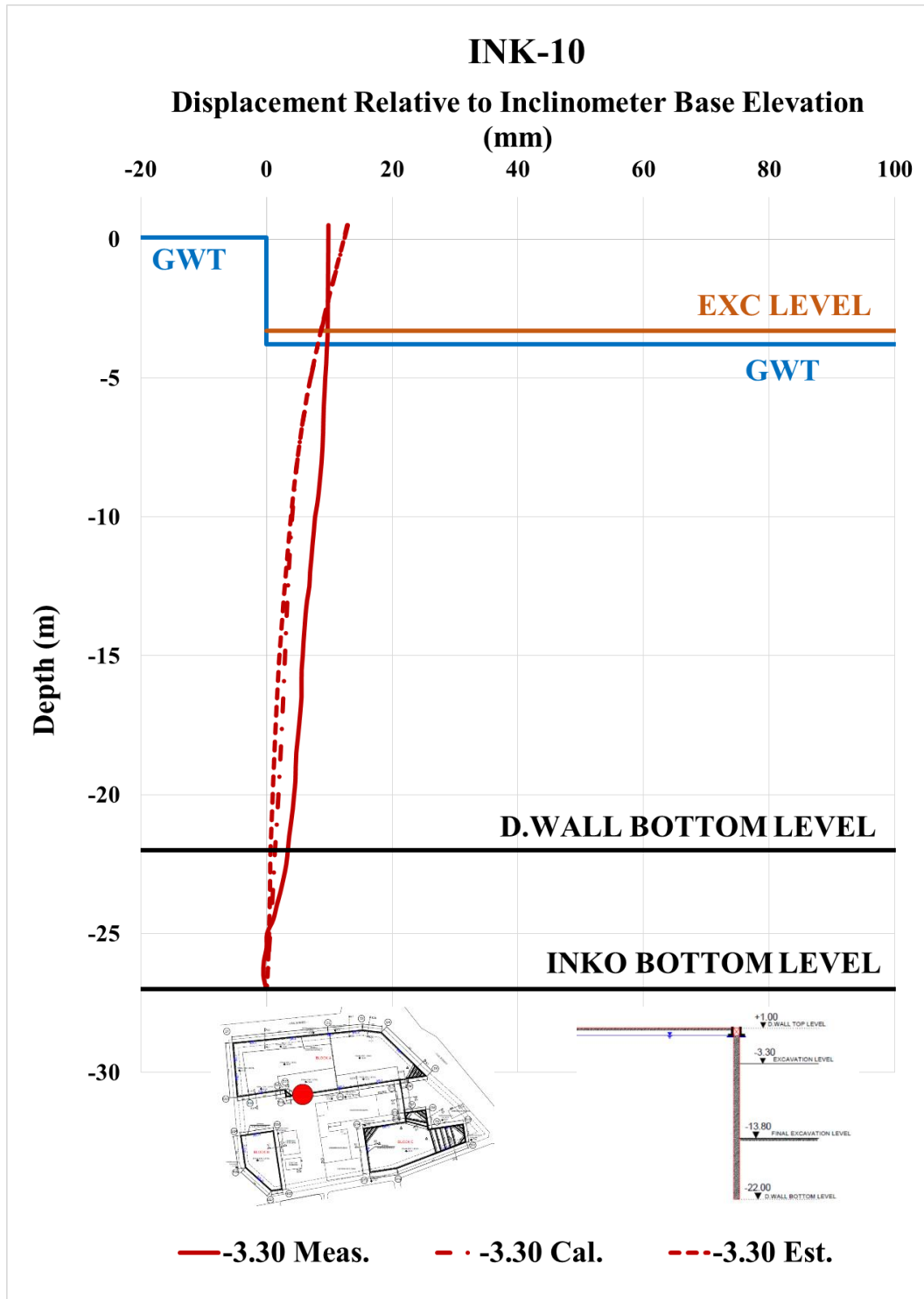
Figure A. 83. Calibrated and Measured Displ. Rel. to Inc. Base Elev. at -3.30 m
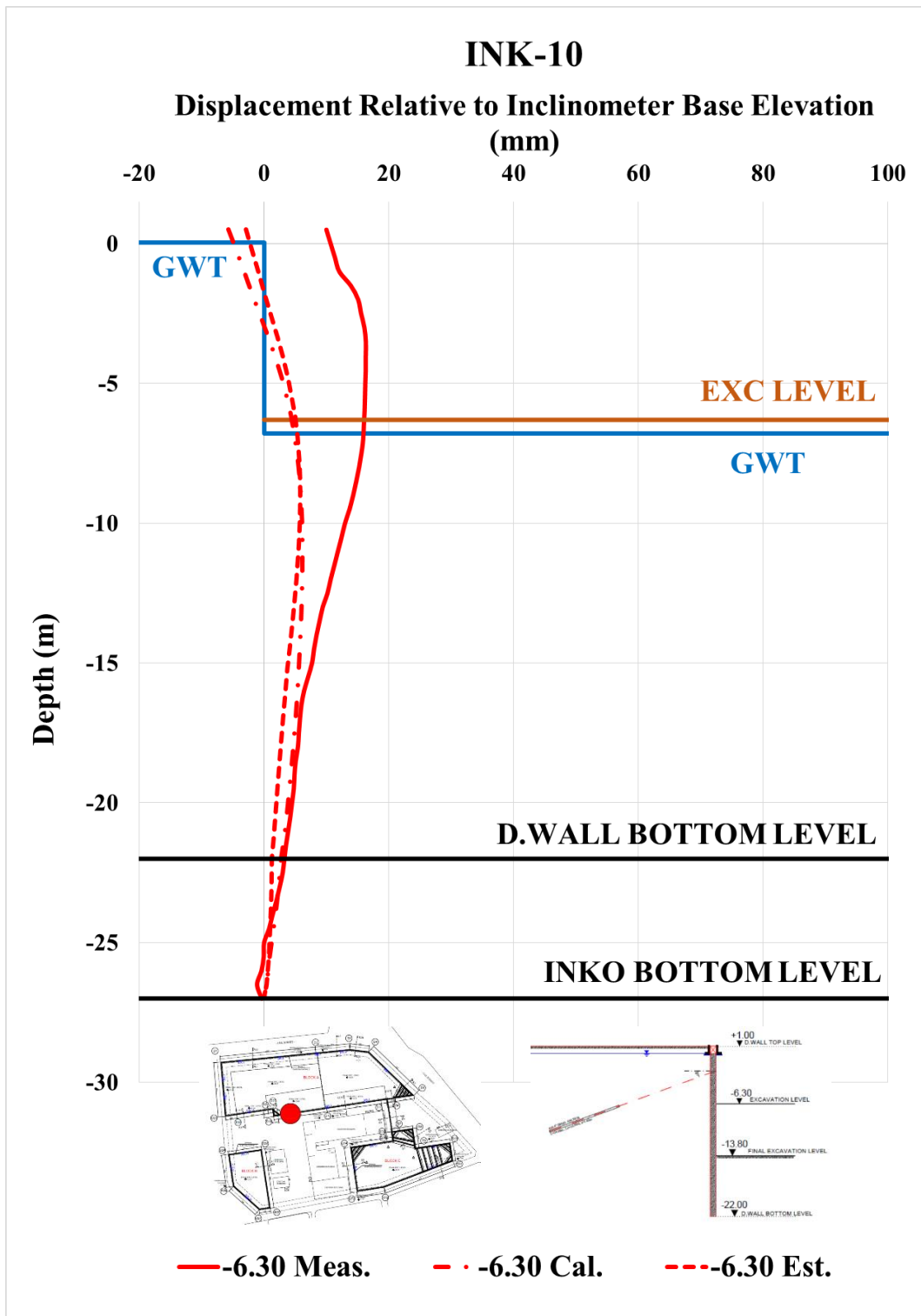
Figure A. 84. Calibrated and Measured Displ. Rel. to Inc. Base Elev. at -6.30

m
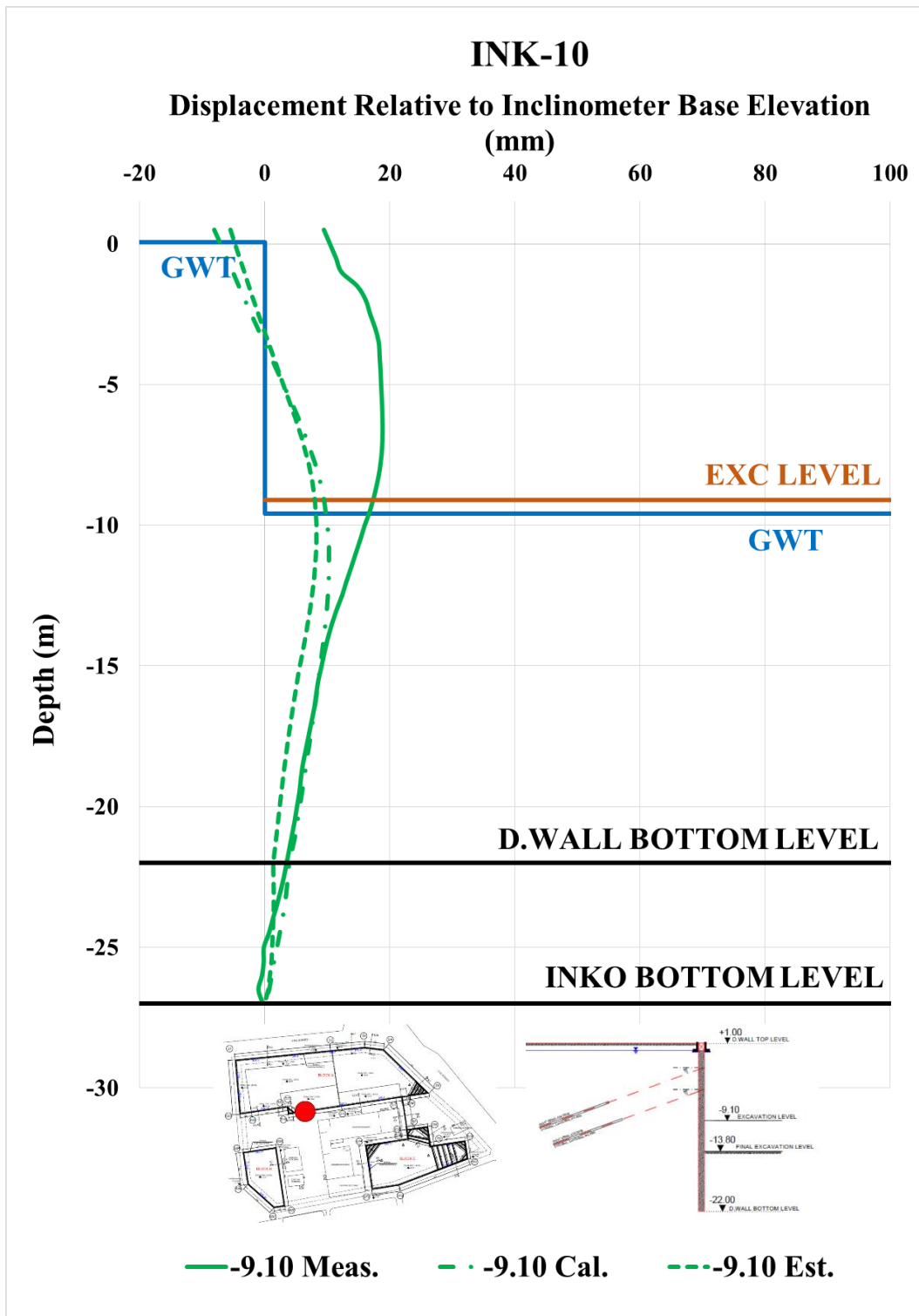
Figure A. 85. Calibrated and Measured Displ. Rel. to Inc. Base Elev. at -9.10 m
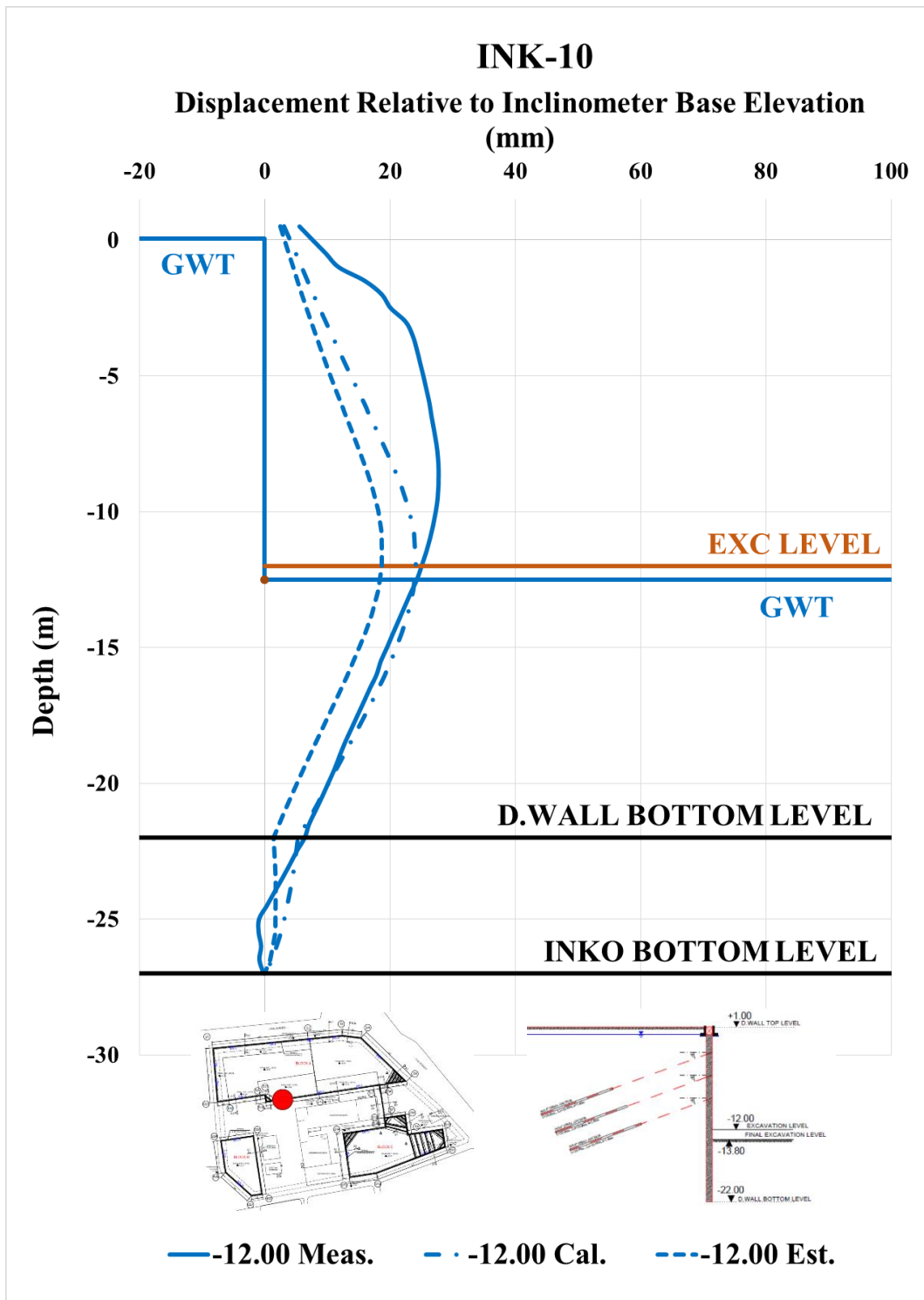
Figure A. 86. Calibrated and Measured Displ. Rel. to Inc. Base Elev. at -12.00 m
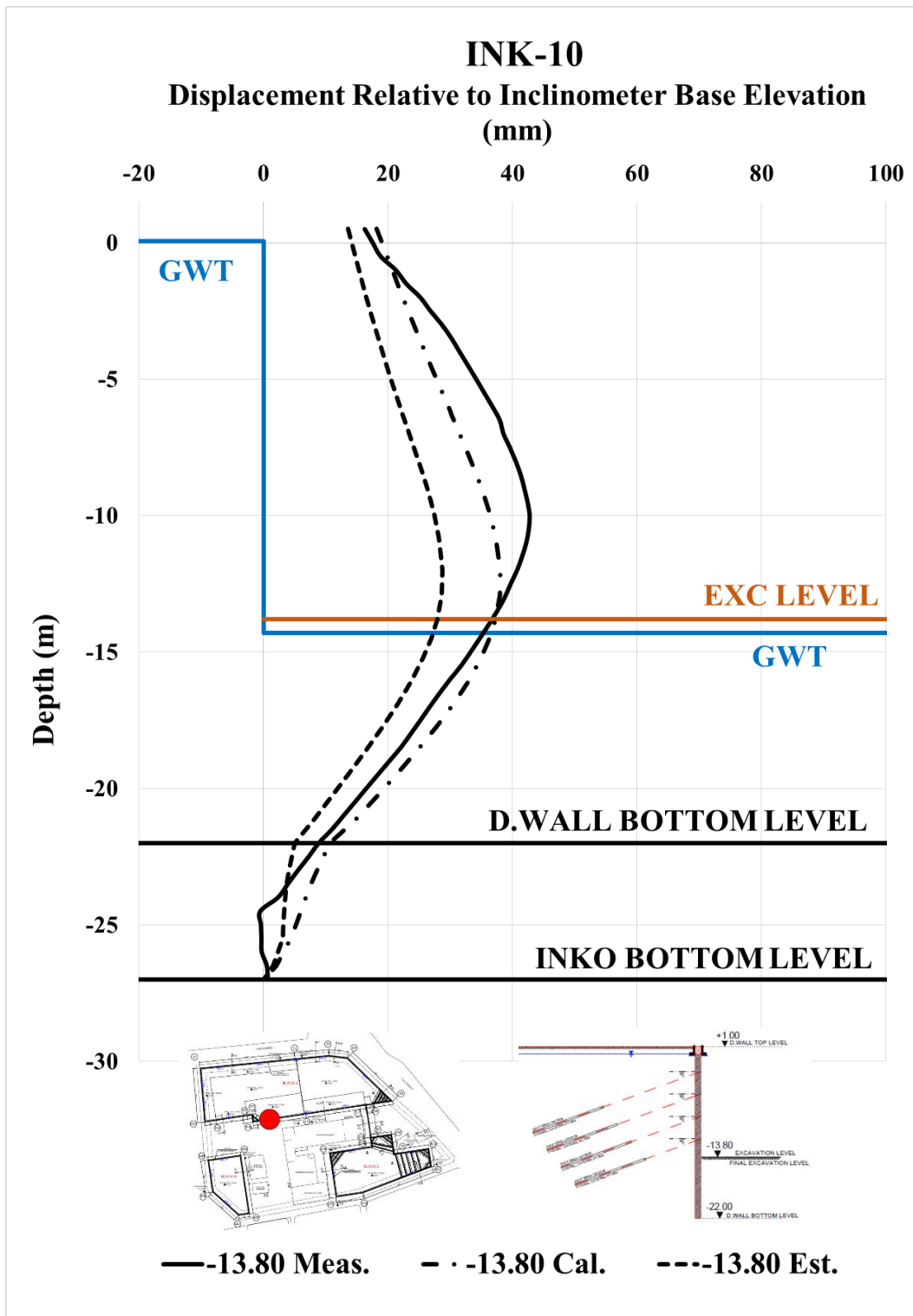
Figure A. 87. Calibrated and Measured Displ. Rel. to Inc. Base Elev. at -13.80 m

Table A. 19. Internal Forces of Diaphragm Wall

INK - 10 / Section 1-1					
Excvation Stage	1	2	3	4	5
Excavation Level (m)	-3,30	-6,30	-9,10	-12,00	-13,80
N_{max} (kN/m)	-91,50	255,90	438,40	628,30	755,80
V_{max} (kN/m)	56,81	291,50	345,00	411,20	411,20
M_{max} (kN.m/m)	162,40	413,00	603,90	912,60	1068,00

Legend	Excvation Stage	1. Anchor Level	2. Excavation Level	2. Anchor Level	3. Excavation Level	3. Anchor Level	4. Excavation Level	4. Anchor Level	Final Excavation Level
	Estimated Load of 1. Anchor Row (kN)	650.00	650.00	559.43	576.00	548.09	557.78	553.71	559.85
	Estimated Load of 2. Anchor Row (kN)	-	-	650.00	681.76	609.22	631.77	604.93	610.92
	Estimated Load of 3. Anchor Row (kN)	-	-	-	-	650.00	704.36	636.41	650.99
	Estimated Load of 4. Anchor Row (kN)	-	-	-	-	-	-	650.00	691.60

Figure A. 88. Measured and Estimated Anchor Loads

225

Table A. 20. Summary of Displacement Results of INK-10

INK - 10 / SECTION 1 - 1

Excvation Level (m)	Excvation Depth (m)	u_{meas} (mm) Inclinometer Measurements	u_{est} (mm) Estimation with Plaxis 2D Analysis	u_{cal} (mm) Calibration with Plaxis 2D Analysis	$u_{literature}$ (mm) FHWA-IF-99-015 (1999) - Maksimum	$u_{literature}$ (mm) FHWA-IF-99-015 (1999) - Average	$u_{literature}$ (mm) Goldberg et al. (1976)	$u_{literature}$ (mm) Clough et al. (1990) - Maksimum	$u_{literature}$ (mm) Clough et al. (1990) - Average	$u_{literature}$ (mm) Long (2001)	$u_{literature}$ (mm) Long (2001) (Extraordinary cases eliminated)	$u_{literature}$ (mm) Long (2001) Cantilever System
-3.25	**4.25**	9.86	12.78	12.97	21.25	8.50	21.25	21.25	8.50	8.08	5.95	15.3
-6.70	**7.70**	16.30	5.79	6.20	38.50	15.40	38.50	38.50	15.40	14.63	10.78	-
-9.70	**10.70**	18.82	8.31	10.28	53.50	21.40	53.50	53.50	21.40	20.33	14.98	-
-12.00	**13.00**	27.74	18.62	24.10	65.00	26.00	65.00	65.00	26.00	24.70	18.20	-
-14.30	**15.30**	42.74	28.79	38.03	76.50	30.60	76.50	76.50	30.60	29.07	21.42	-
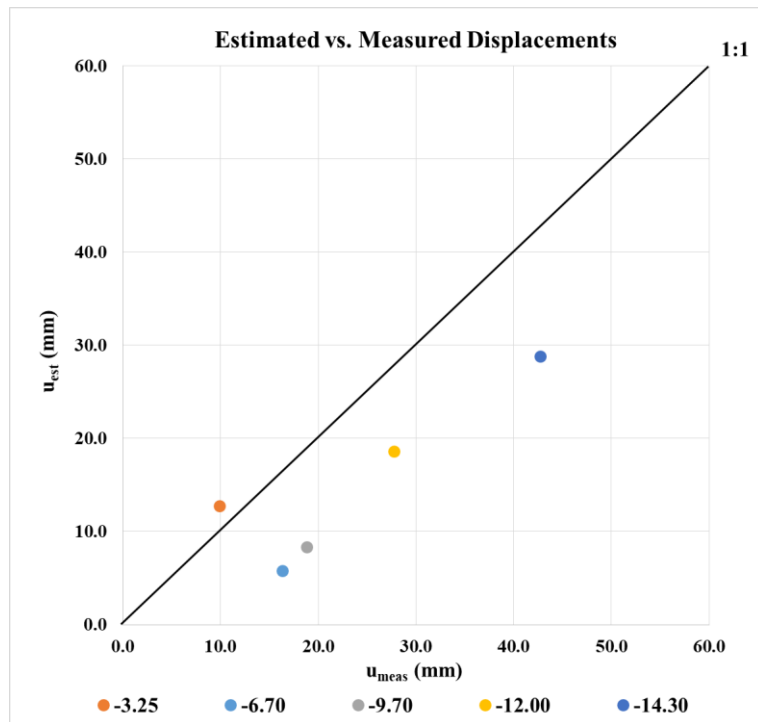
Figure A. 89. Estimated and Measured Displacements of INK - 10
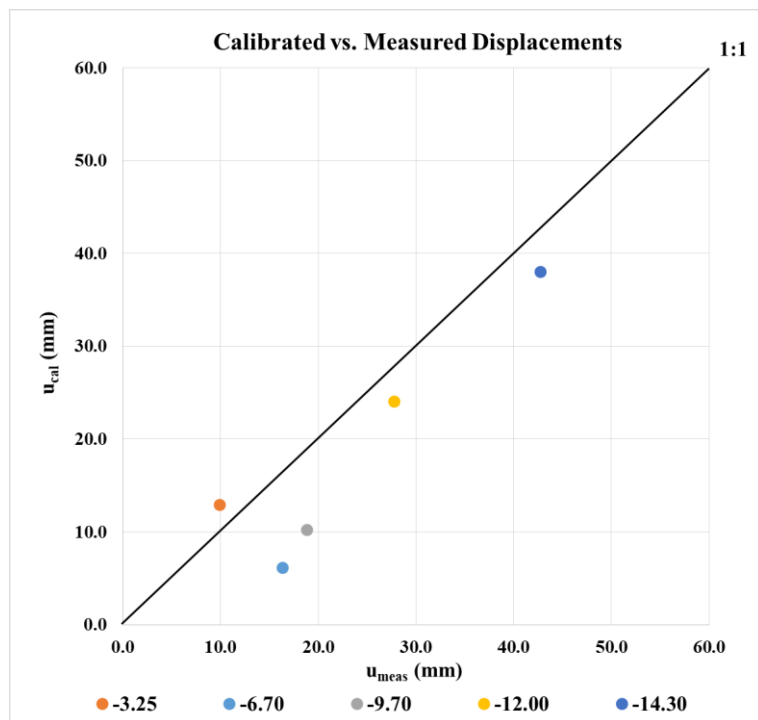
Figure A. 90. Calibrated and Measured Displacements of INK - 10

Area A3
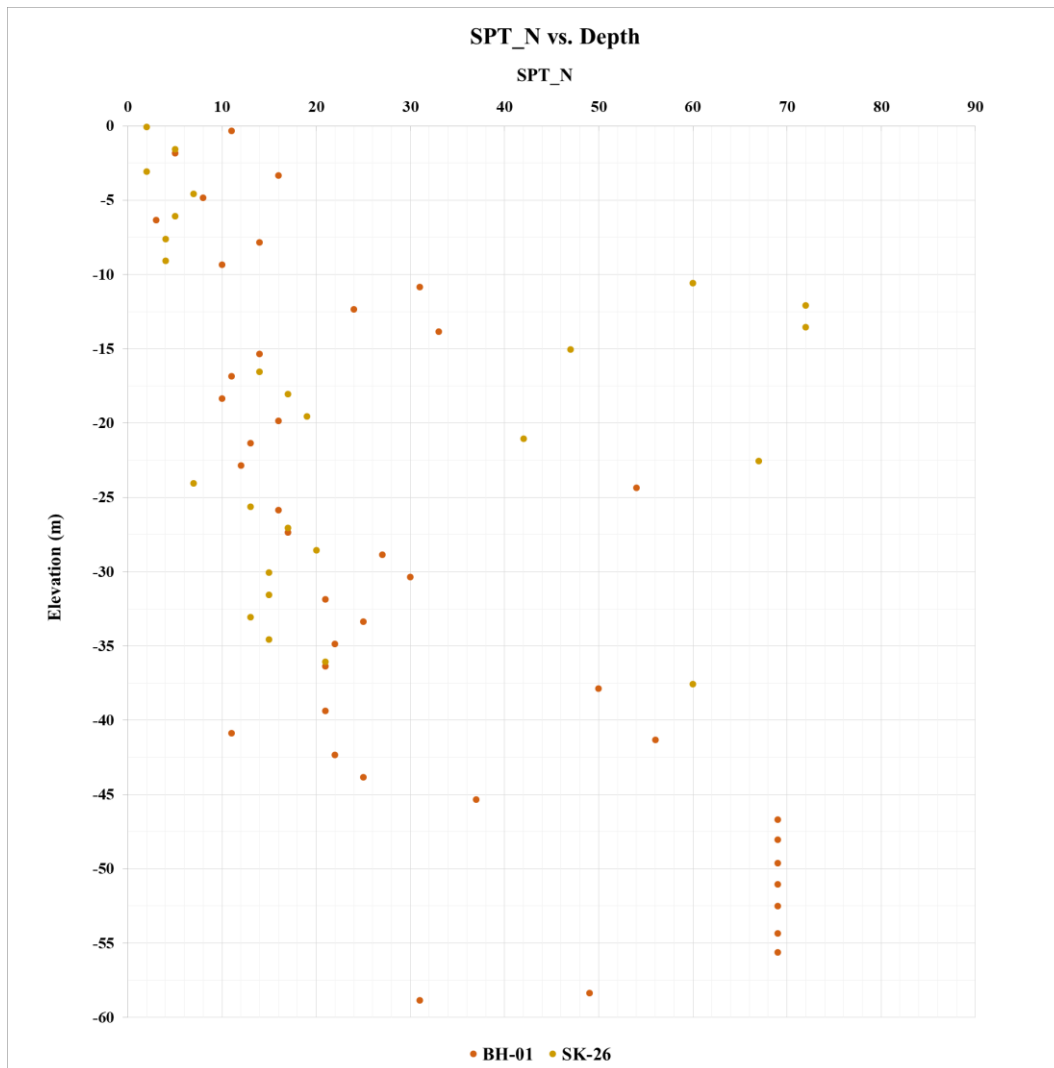
Figure A. 91. SPT-N vs. Depth for Area A3
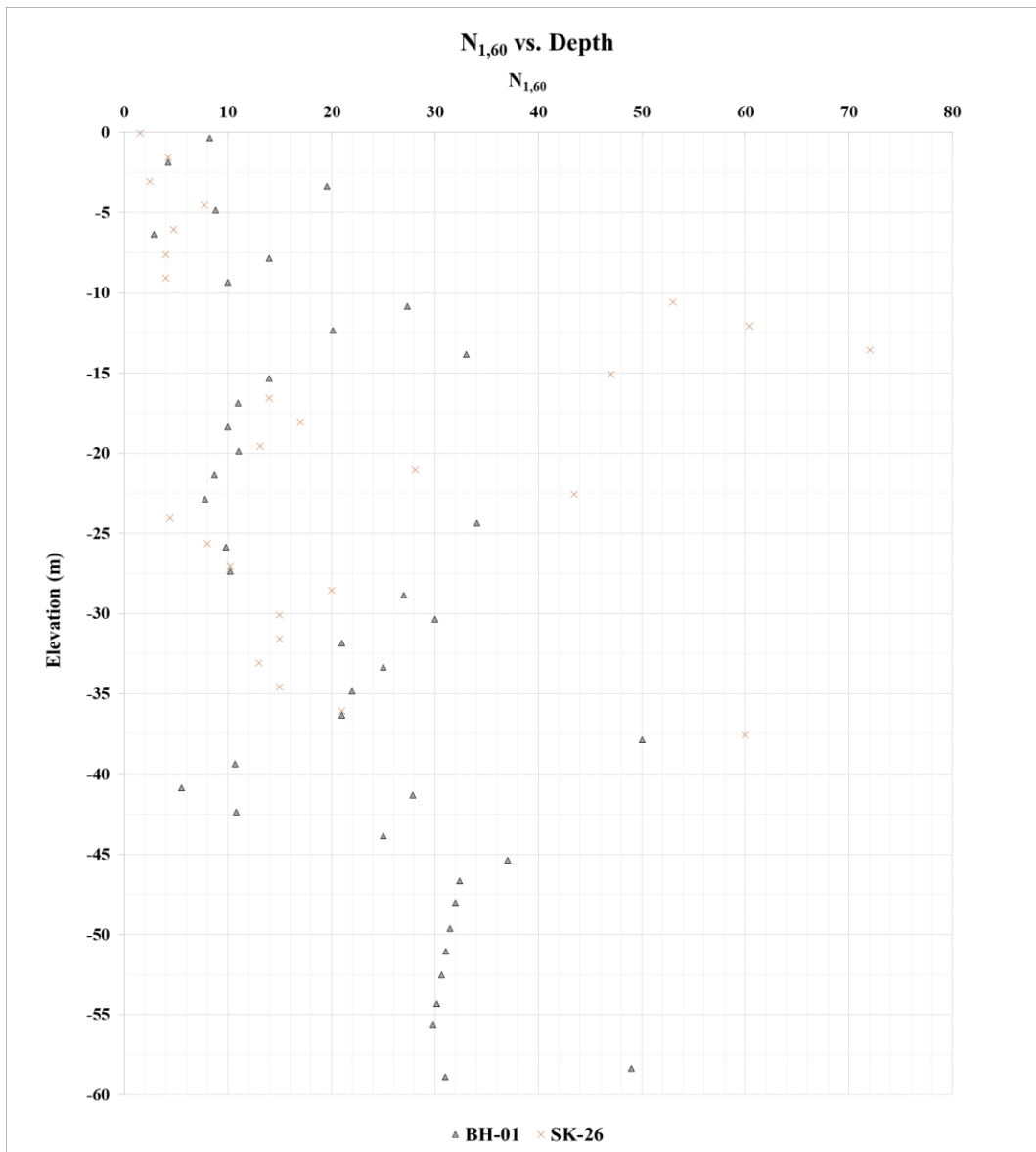
Figure A. 92. SPT-$N_{1,60}$ vs. Depth for Area A3
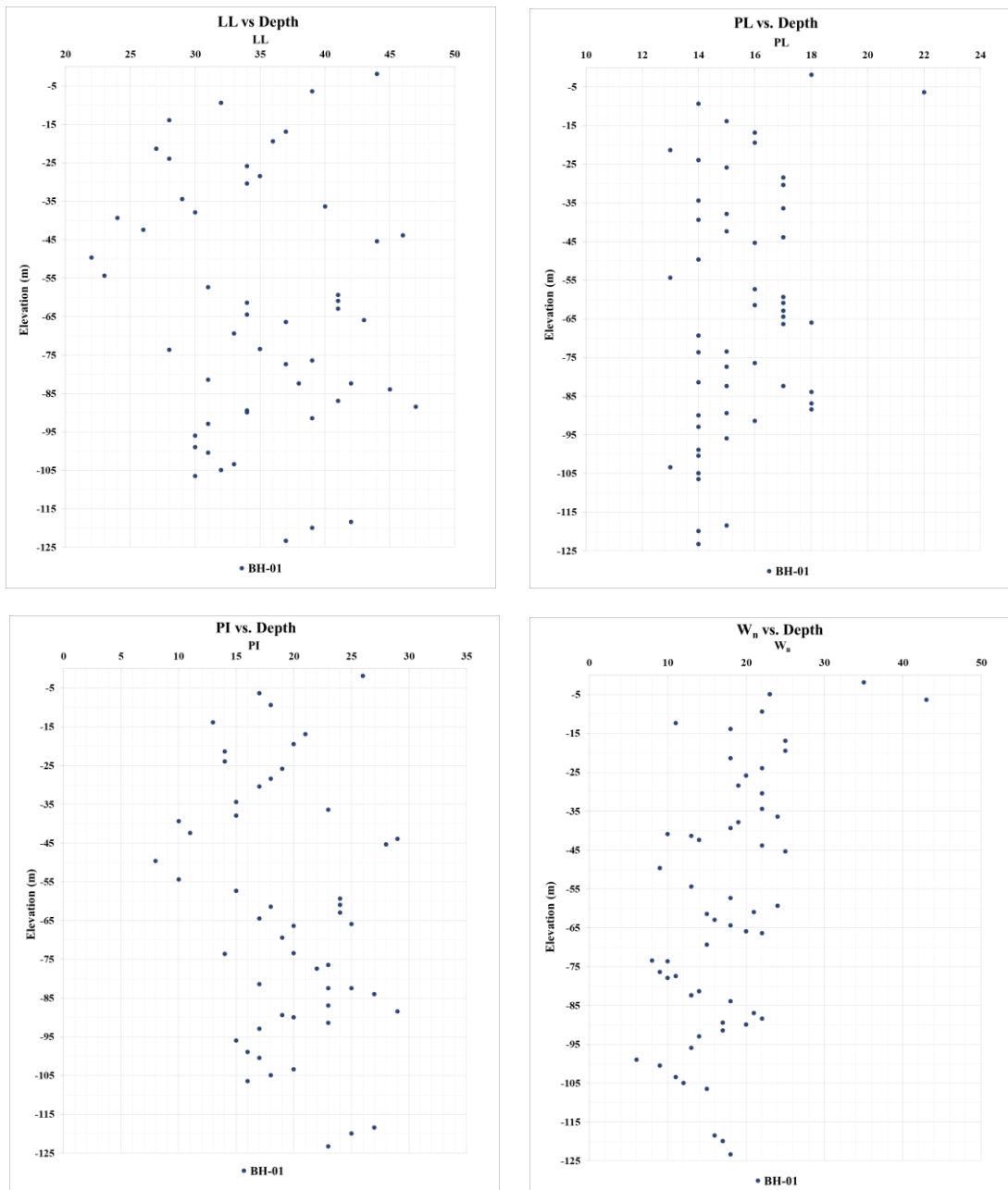
Figure A. 93. Variation of LL, PL, PI, and w_n for Area A3
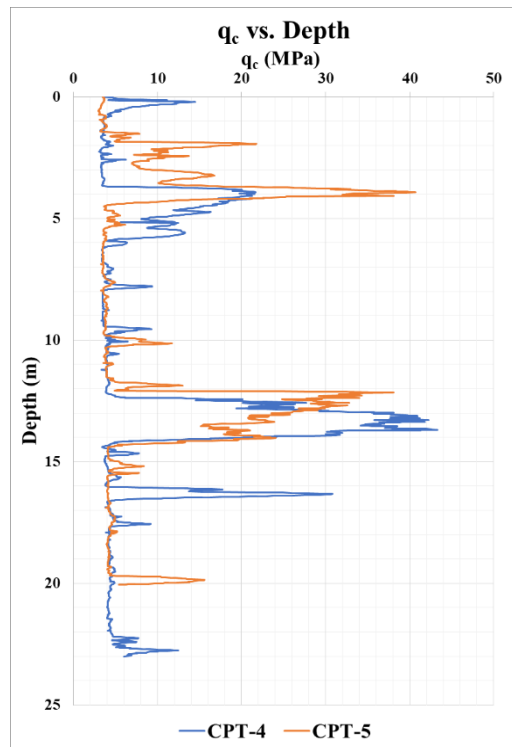
Figure A. 94. Variation of q_c along with the Depth for Area A3
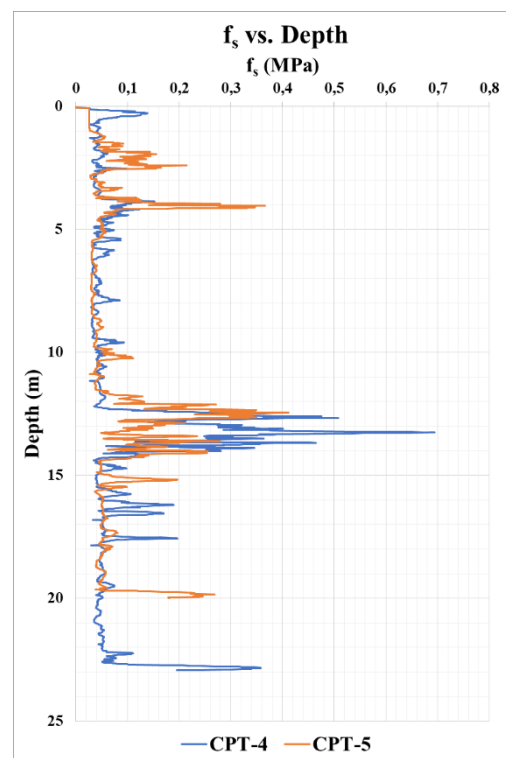
Figure A. 95. Variation of f_s along with the Depth for Area A3

2 boreholes (SK-26, and BH-1) and 2 CPT (CPT-4, and CPT-5) were considered. The depths of boreholes are changing between 40 m to 130 m. Depths of CPT are changing between 20 m to 23 m. The total depth of boreholes and CPTs is 170 m and 43 m respectively. Atterberg limit tests were performed on the samples taken from BH-1. LL, PL, PI, and w_n vary in 22 – 47 % (avg. 35 %), 13 – 22 % (avg. 15.5 %), 8 – 29 % (avg. 19.5 %), and 6 – 43 % (avg. 17.5 %) respectively. Unified soil classification (USCS) was performed for each sample. By considering USCS, SPT $N_{1,60}$ values, and CPT results, the thickness of soil layers was determined. Detailed soil parameters are given in below table;

- Boreholes: SK-26, and BH-1 (Change in between 40 m to 130 m. 170 m in total)
- CPTs: CPT-4, and CPT-5 (Change in between 20 m to 23 m. 43 m in total)
- LL: 22 – 47 % (avg. 35 %)
- PL: 13 – 22 % (avg. 15.5 %)
- PI: 8 – 29 % (avg. 19.5 %)
- w_n: 6 – 43 % (avg. 17.5 %)

Table A. 21. Soil Profile of Area 3 (A3)

Layer No	Elevation (m)		USCS	Type	Thickness (m)	N	$N_{1,60}$	N_{60}	PI	y_{wet} (kN/m³)	y_{sat} (kN/m³)	c_u (kPa)	c (kPa)	φ (°)	ψ (°)	E_{50}^{ref} (MPa)	E_{oed}^{ref} (MPa)	E_{ur}^{ref} (MPa)	m	v_{ur}	p_{ref} (kPa)	R_f
1.0	1.8	-1.7	CL	Cohesive	3.5	6.0	5.0	5.0	26.0	17.6	19.2	30.0	3.0	29.3	0.0	5.0	2.5	15.0	1.0	0.2	30.8	0.9
2.0	-1.7	-4.7	SM	Cohesionless	3.0	12.0	9.0	7.0	0.0	19.2	20.0	-	2.0	30.0	0.0	27.0	27.0	81.0	0.5	0.2	100.0	0.9
3.0	-4.7	-10.2	CL	Cohesive	5.5	8.0	7.0	7.0	17.5	17.6	19.2	45.0	4.5	30.4	0.4	8.4	4.2	25.2	1.0	0.2	102.6	0.9
4.0	-10.2	-13.2	GP-GM	Cohesionless	3.0	47.0	40.0	47.0	0.0	20.0	21.6	-	1.0	40.0	10.0	57.0	57.0	171.0	0.5	0.2	100.0	0.9
5.0	-13.2	-19.2	CL	Cohesive	6.0	28.0	28.0	28.0	18.0	18.4	20.0	170.0	17.0	30.3	0.3	33.6	16.8	100.8	1.0	0.2	192.7	0.9
6.0	-19.2	-28.2	SC-GC	Cohesionless	9.0	25.0	16.0	25.0	16.0	19.2	20.0	160.0	4.0	36.0	6.0	36.0	36.0	108.0	0.5	0.2	100.0	0.9
7.0	-28.2	-37.7	CL	Cohesive	9.5	26.0	26.0	26.0	17.5	18.4	20.0	155.0	15.5	30.4	0.4	31.2	15.6	93.6	1.0	0.2	360.2	0.9
8.0	-37.7	-42.2	SC-GC	Cohesionless	4.5	30.0	18.0	30.0	5.3	19.2	20.0	-	2.0	33.0	3.0	38.0	38.0	114.0	0.5	0.2	100.0	0.9
9.0	-42.2	-45.2	CL	Cohesive	3.0	18.0	18.0	18.0	28.5	18.4	20.0	100.0	10.0	28.8	0.0	16.2	8.1	48.6	1.0	0.2	467.7	0.9
10.0	-45.2	-55.2	SC-GC	Cohesionless	10.0	65.0	30.0	65.0	9.0	20.0	21.6	-	3.0	39.0	9.0	50.0	50.0	150.0	0.5	0.2	100.0	0.9
11.0	-55.2	-58.2	CL	Cohesive	3.0	37.0	37.0	37.0	19.5	18.4	20.0	220.0	22.0	30.0	0.0	42.9	21.5	128.8	1.0	0.2	613.7	0.9

233
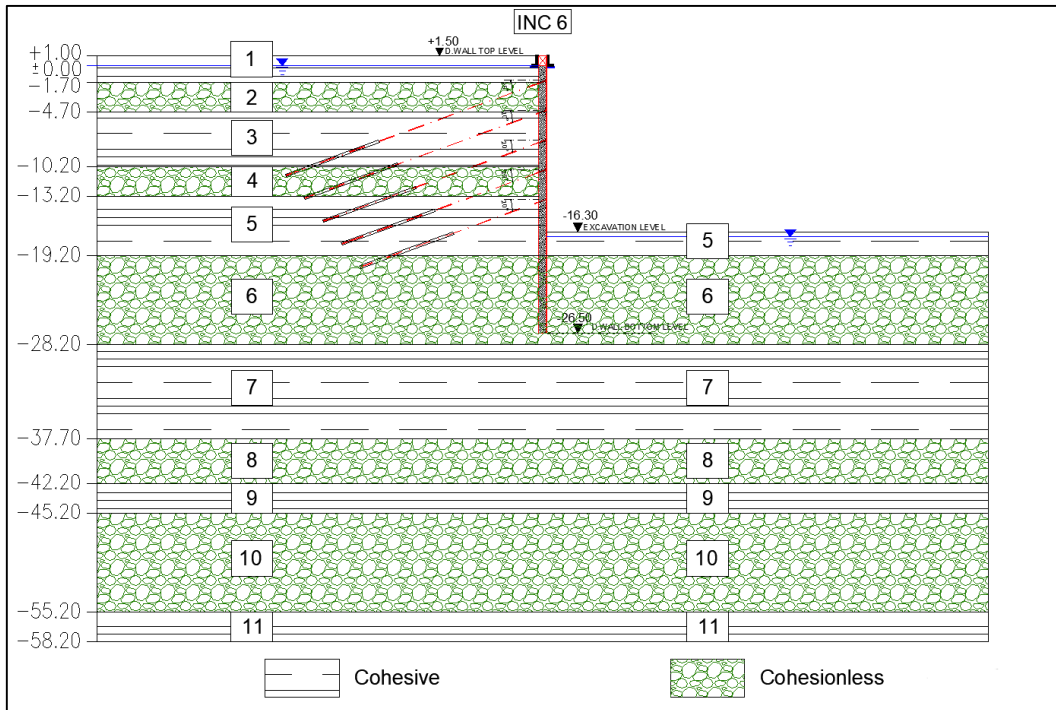
Figure A. 96. Section 2 – 2

Table A. 22. Section Properties of 2 – 2

SECTION 2 - 2									
Diaphragm Wall			SBMA Type Anchor				Excavation Properties		
Top Level (m)	Bottom Level (m)	Length (m)	Anchor No	Anchor Level (m)	Anchor Length (m)	Horizontal Spacing (m)	Top Level (m)	Bottom Level (m)	Depth (m)
1.50	-26.50	28.00	1	-1.00	28.00	1.40	1.50	-16.30	17.80
			2	-4.00	26.00	1.40			
			3	-7.00	24.00	1.40			
			4	-10.00	22.00	1.40			
			5	-13.00	20.00	1.40			

234

INK-6 – Estimated and Measured Displacements

Figure A. 97. Meshed Model for INK-6
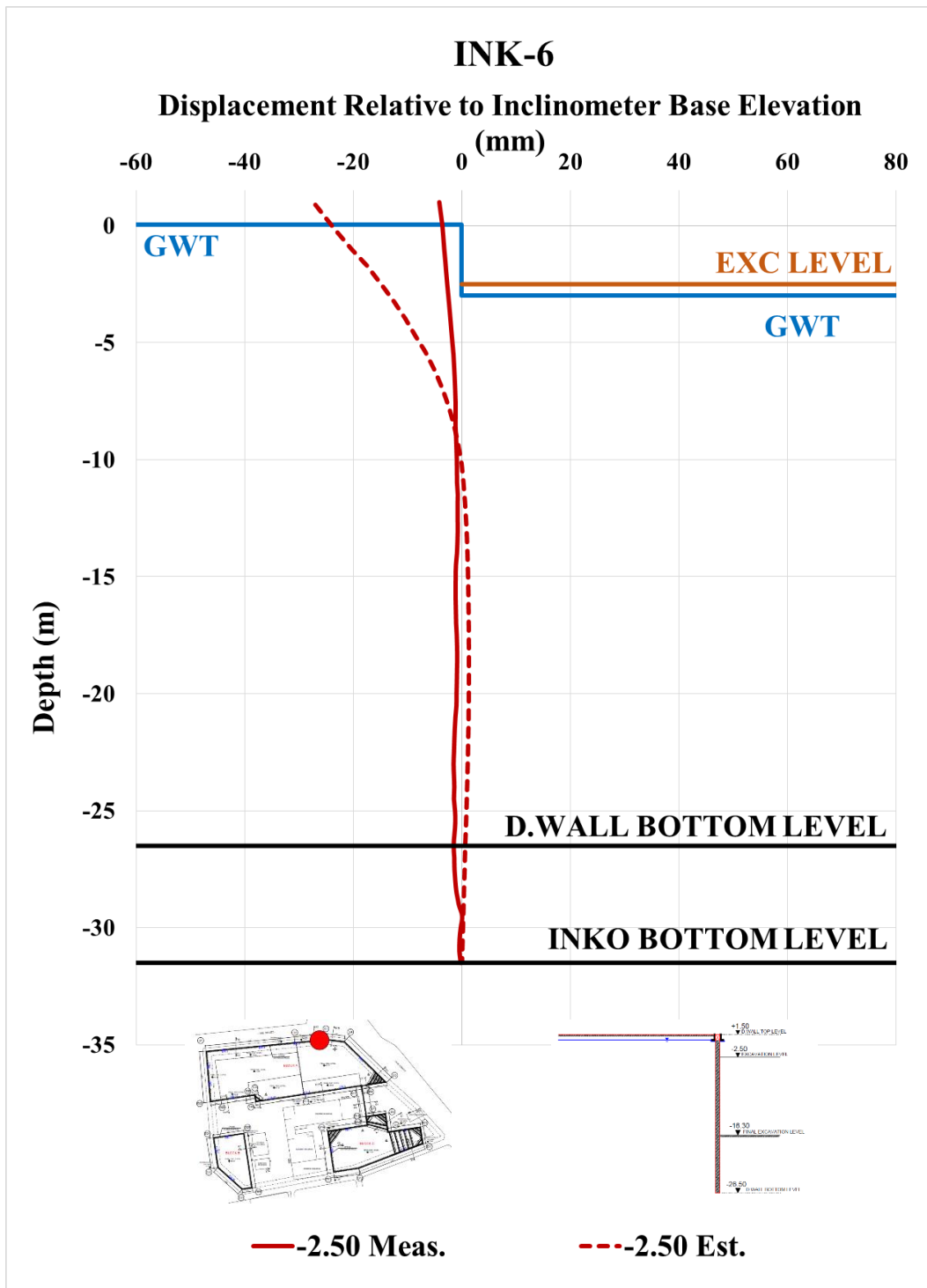
Figure A. 98. Estimated and Measured Displ. Rel. to Inc. Base Elev. at -2.50 m
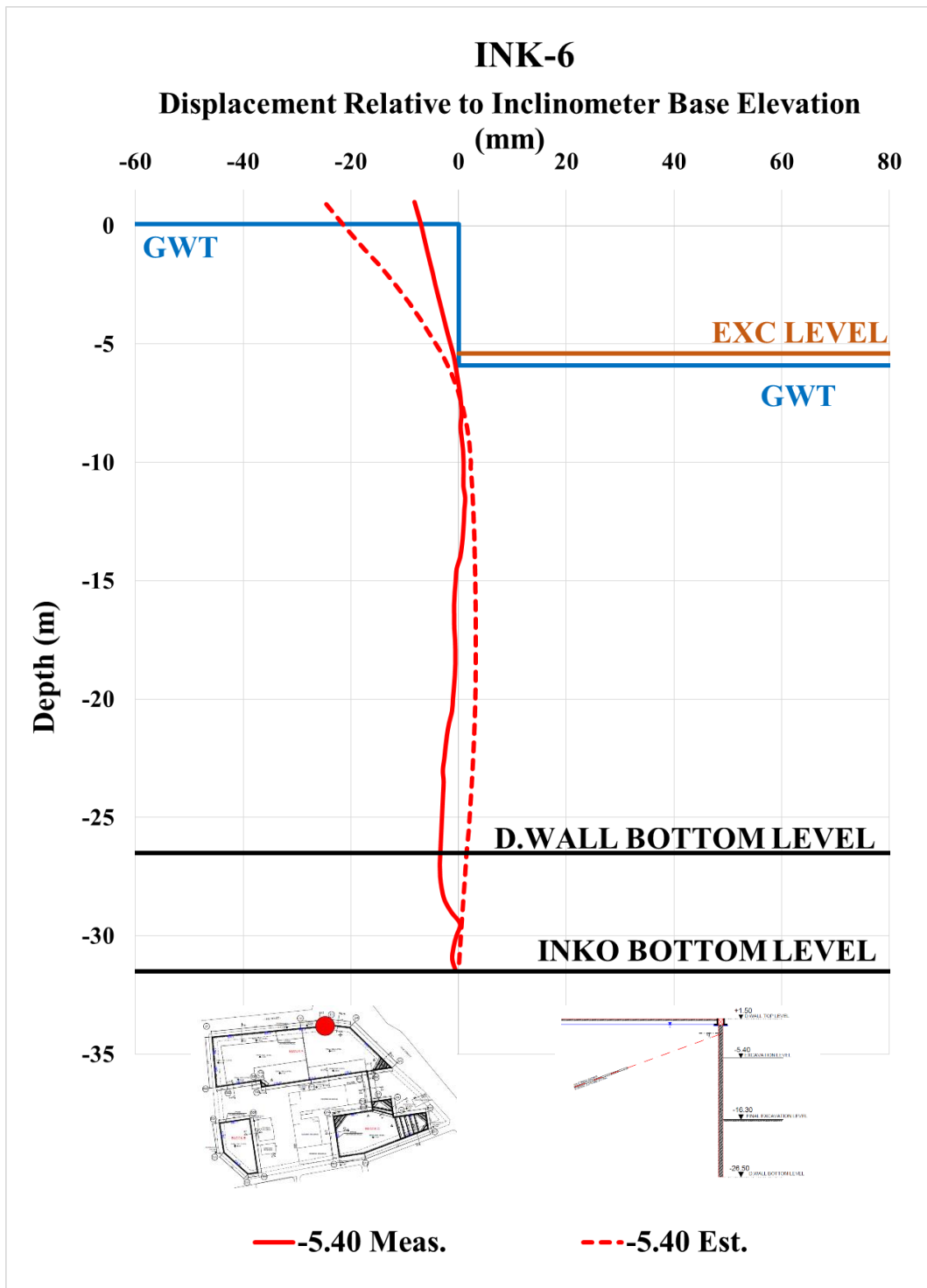
Figure A. 99. Estimated and Measured Displ. Rel. to Inc. Base Elev. at -5.40 m
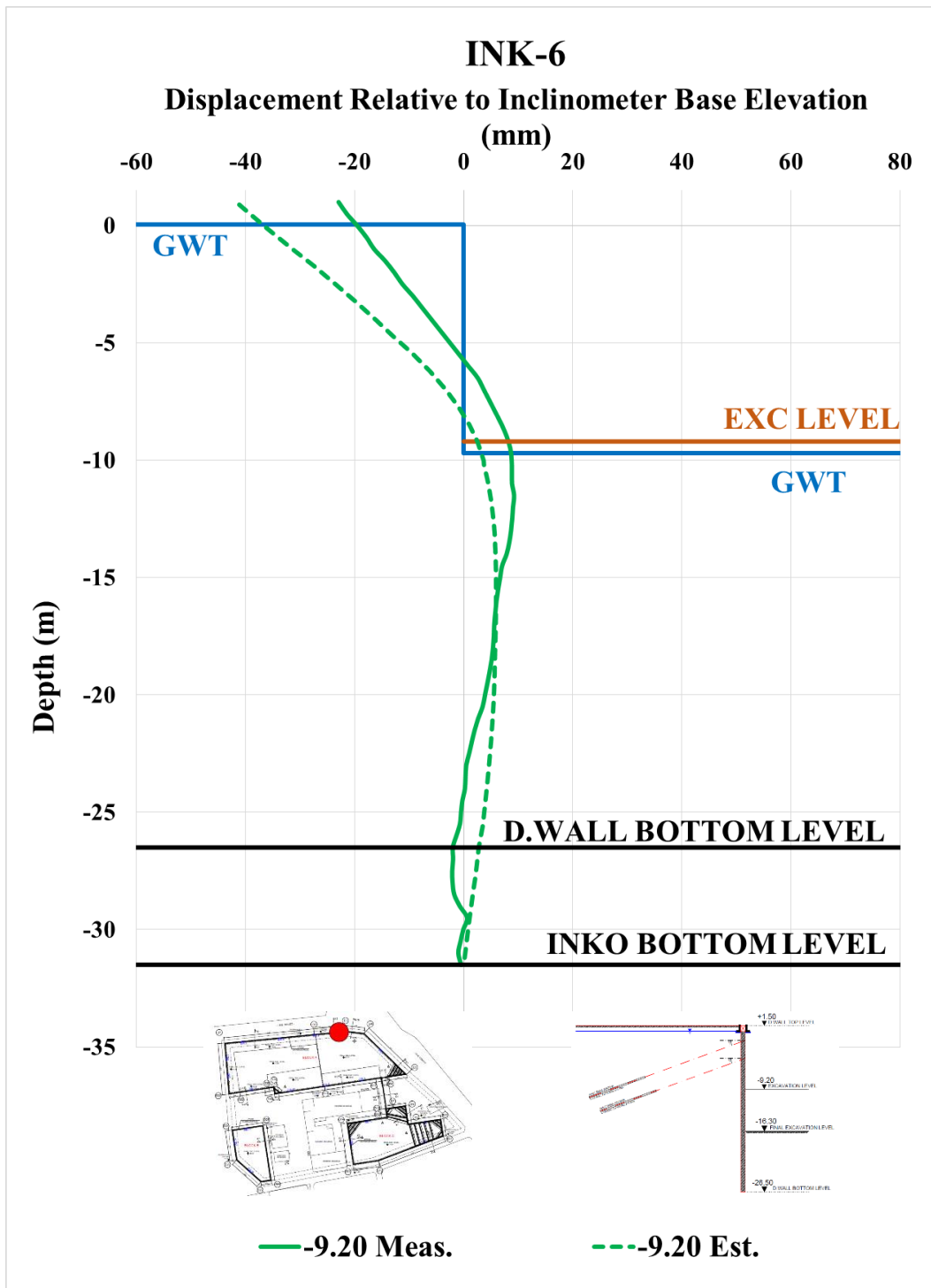
Figure A. 100. Estimated and Measured Displ. Rel. to Inc. Base Elev. at -9.20 m
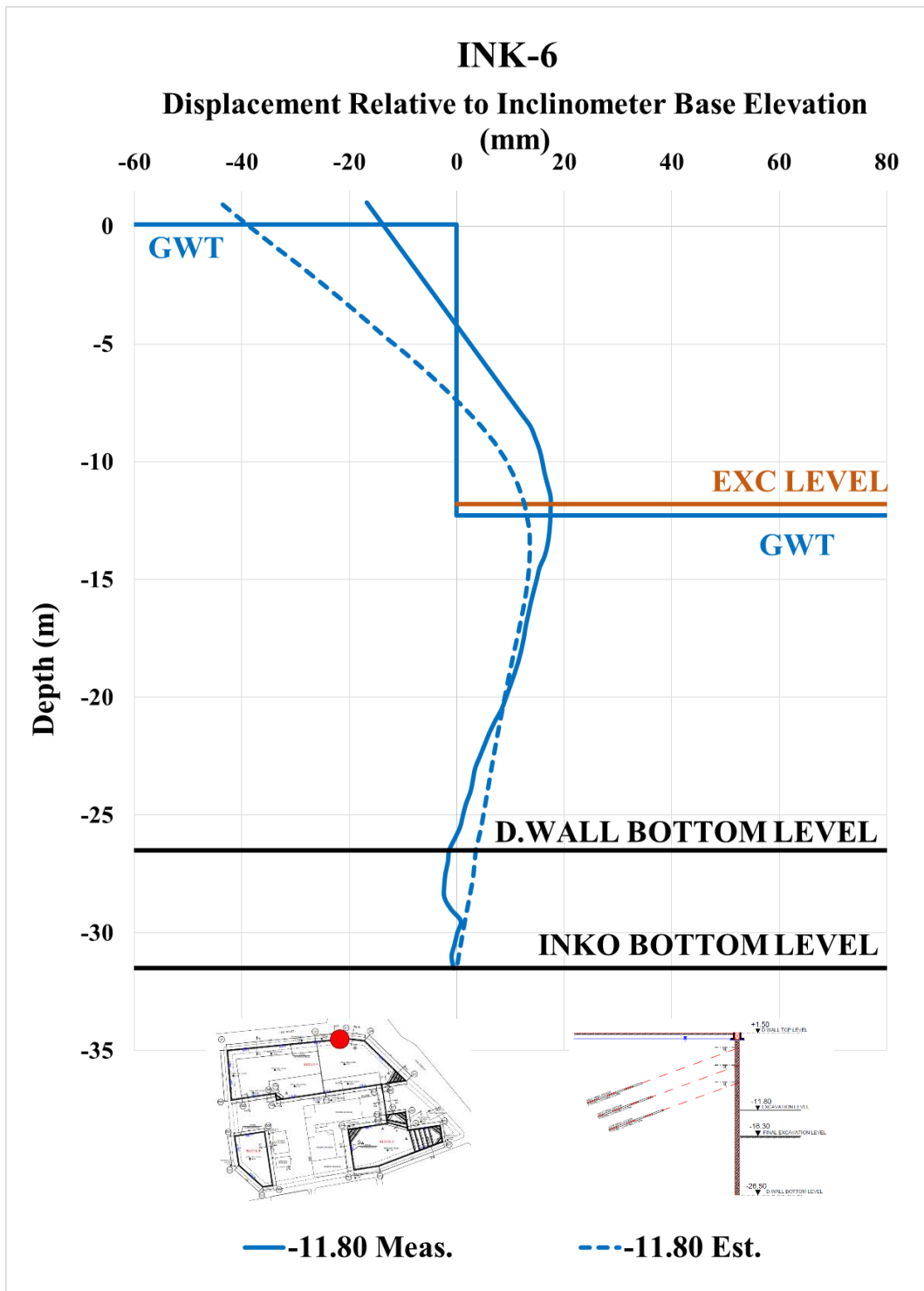
Figure A. 101. Estimated and Measured Displ. Rel. to Inc. Base Elev. at -11.80 m
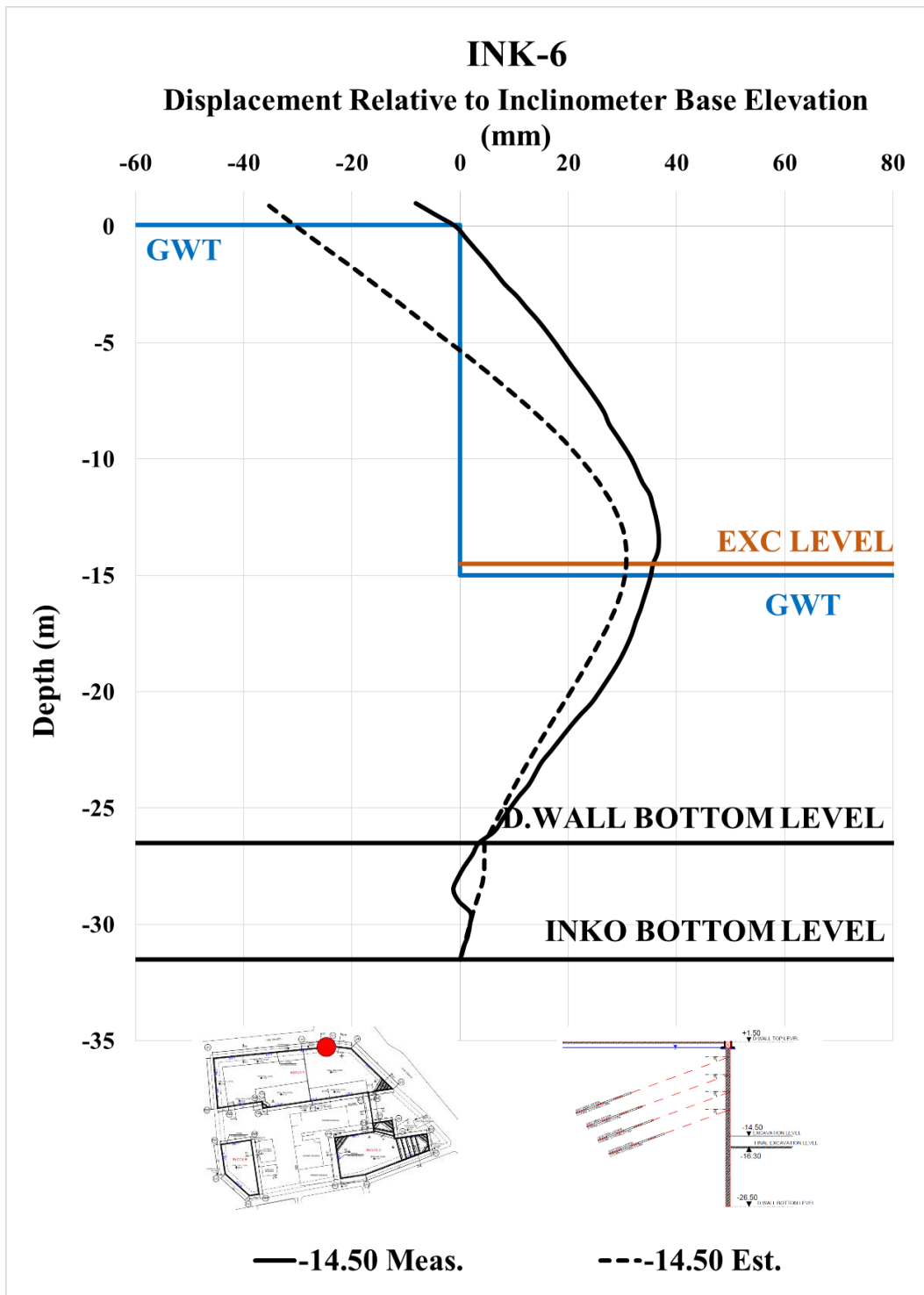
Figure A. 102. Estimated and Measured Displ. Rel. to Inc. Base Elev. at -14.50 m
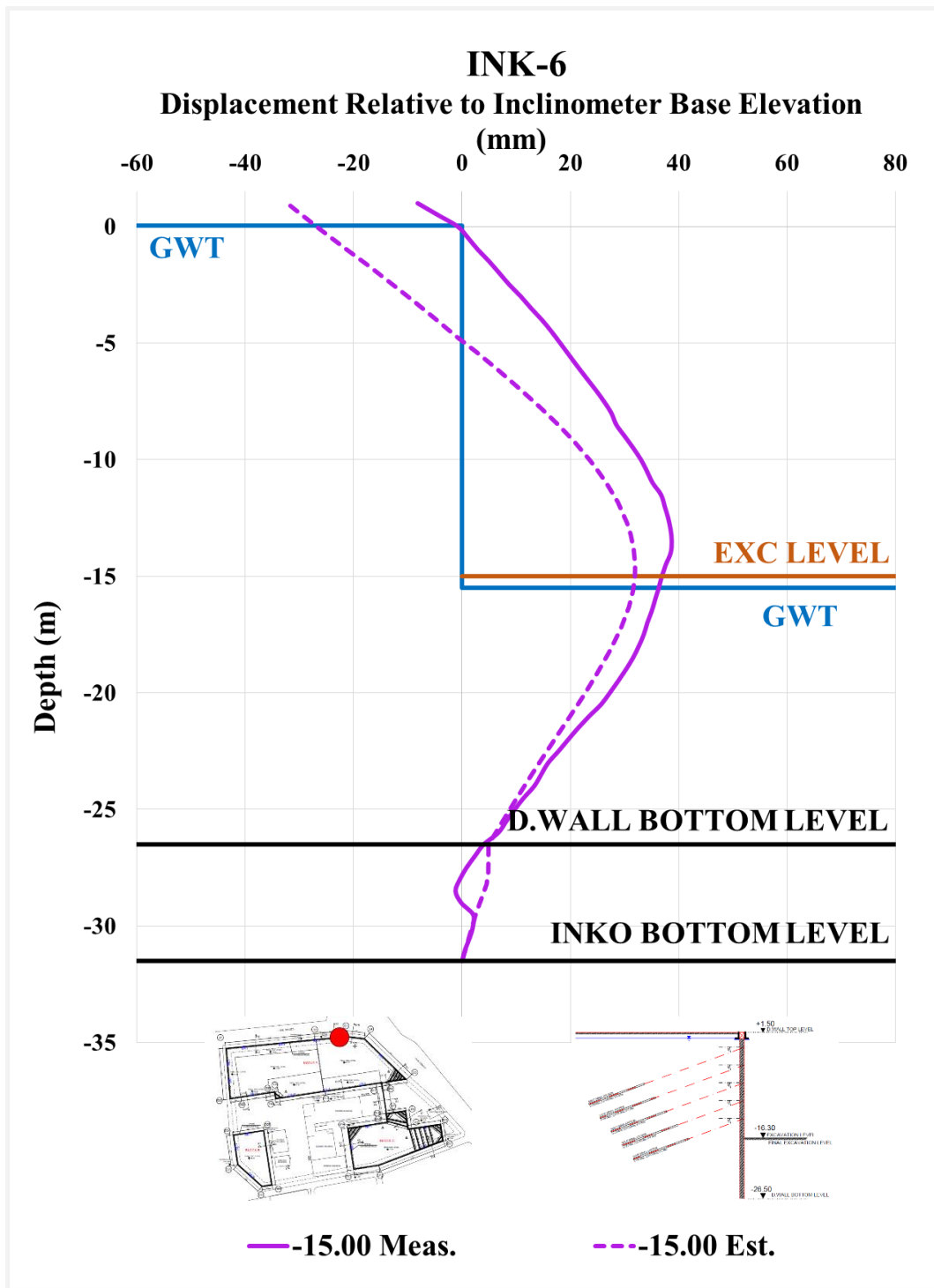
Figure A. 103. Estimated and Measured Displ. Rel. to Inc. Base Elev. at -15.00 m
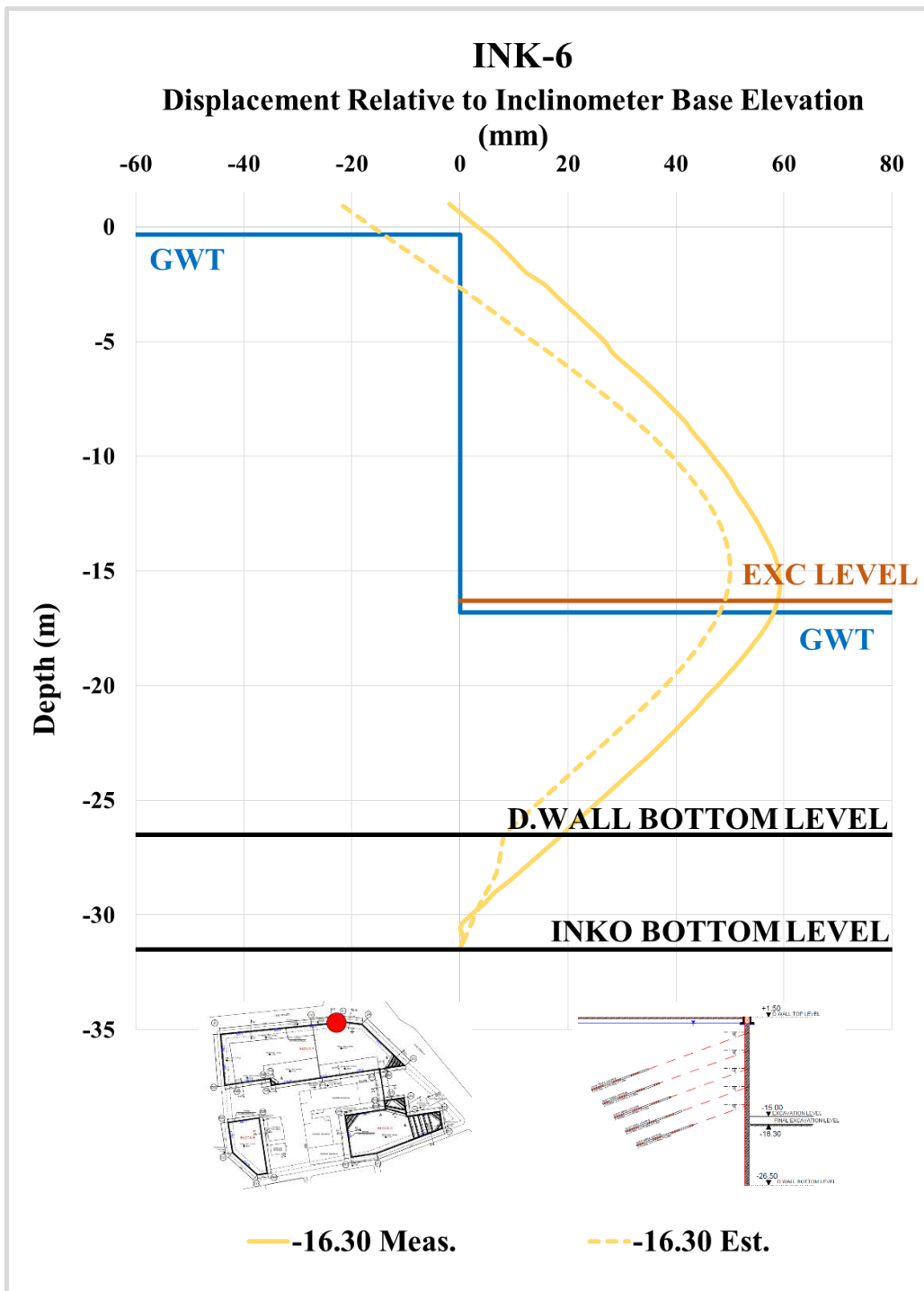
Figure A. 104. Estimated and Measured Displ. Rel. to Inc. Base Elev. at -16.30 m

Table A. 23. Internal Forces of Diaphragm Wall

INK - 6 / Section 2-2							
Excvation Stage	1	2	3	4	5	6	7
Excavation Level (m)	-2,50	-5,40	-9,20	-11,80	-14,50	-15,00	-16,30
N_{max} (kN/m)	95,36	204,90	362,90	562,20	816,80	922,00	988,50
V_{max} (kN/m)	60,12	395,00	395,00	395,00	438,50	438,50	438,50
M_{max} (kN.m/m)	275,70	733,80	974,00	1108,00	1369,00	1369,00	1465,00

Legend	Excvation Stage	1. Anchor Level	2. Excavation Level	2. Anchor Level	3. Excavation Level	3. Anchor Level	4. Excavation Level	4. Anchor Level	5. Excavation Level	5. Anchor Level	6. Excavation Level	Final Excavation Level
	Measured Load of 1. Anchor Row (kN)	656.64	523.96	524.98	526.63	523.73	522.10	504.36	510.85	509.40	508.85	509.84
	Estimated Load of 1. Anchor Row (kN)	650.00	675.08	537.76	557.05	511.64	515.84	506.76	504.24	506.22	507.13	507.73
	Estimated Load of 2. Anchor Row (kN)	-	-	650.00	681.73	601.29	616.83	587.49	588.43	582.25	583.19	580.48
	Estimated Load of 3. Anchor Row (kN)	-	-	-	-	650.00	683.39	625.83	643.71	624.18	625.59	624.78
	Estimated Load of 4. Anchor Row (kN)	-	-	-	-	-	-	650.00	701.35	656.33	660.63	675.61
	Estimated Load of 5. Anchor Row (kN)	-	-	-	-	-	-	-	-	650.00	656.74	699.73

Figure A. 105. Measured and Estimated Anchor Loads
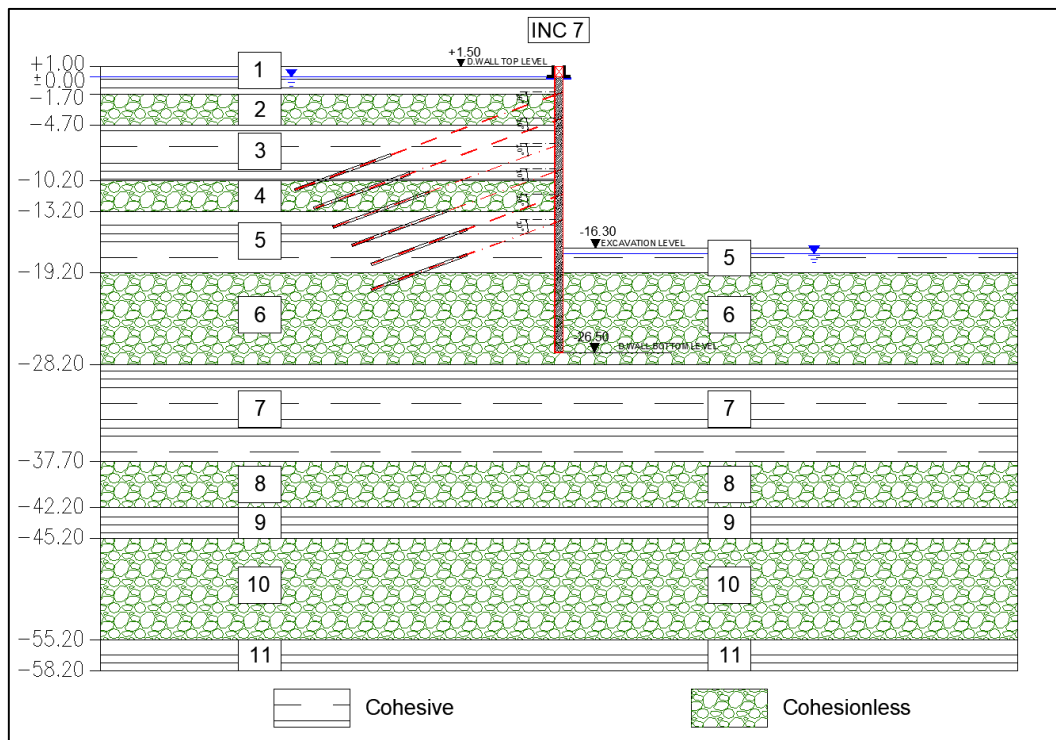
Figure A. 106. Section 2B – 2B

Table A. 24. Section Properties of 2B – 2B

SECTION 2B - 2B									
Diaphragm Wall			SBMA Type Anchor				Excavation Properties		
Top Level (m)	Bottom Level (m)	Length (m)	Anchor No	Anchor Level (m)	Anchor Length (m)	Horizontal Spacing (m)	Top Level (m)	Bottom Level (m)	Depth (m)
1.50	-26.50	28.00	1	-1.00	28.00	1.40	1.50	-16.30	17.80
			2	-3.50	26.00	1.40			
			3	-6.00	24.00	1.40			
			4	-8.50	22.00	1.40			
			5	-11.00	20.00	1.40			
			6	-13.50	20.00	1.40			

244

INK-7 – Estimated and Measured Displacements
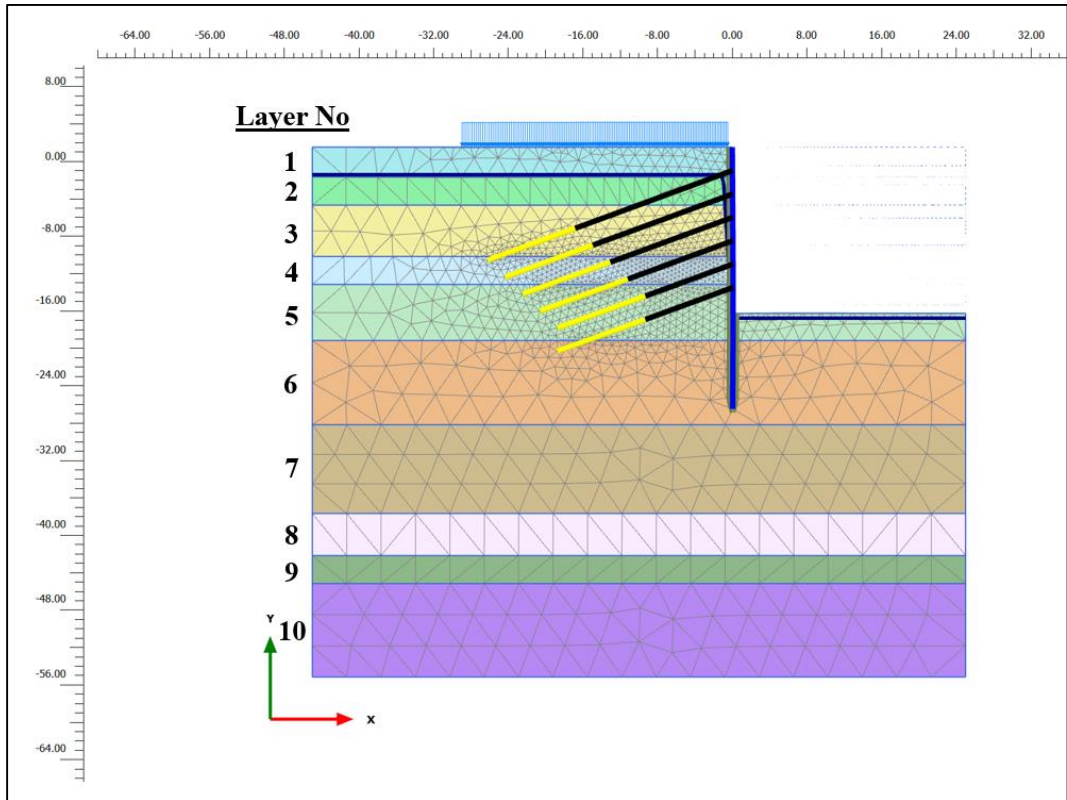
Figure A. 107 Meshed Model for INK-7
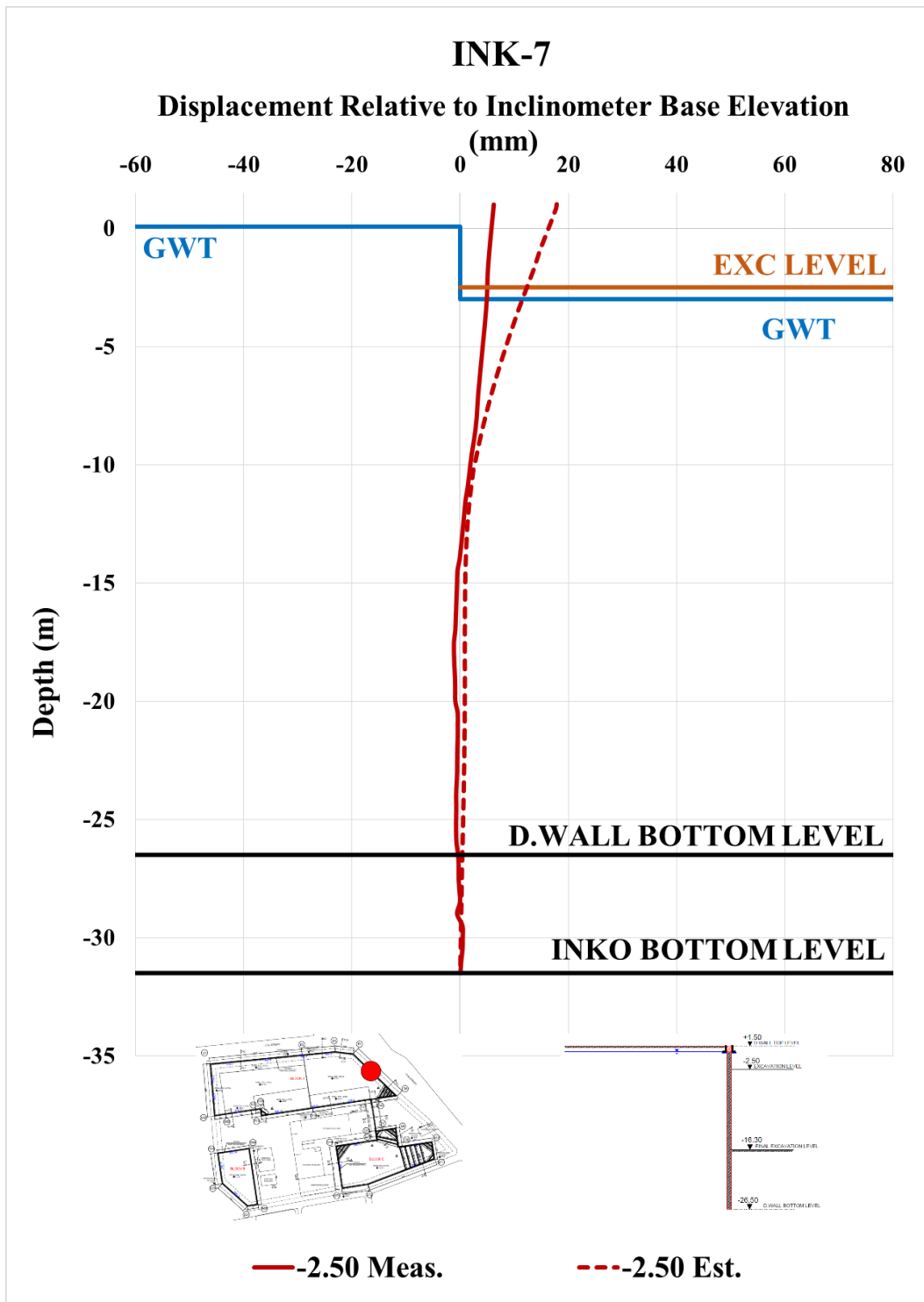
Figure A. 108. Estimated and Measured Displ. Rel. to Inc. Base Elev. at -2.50 m
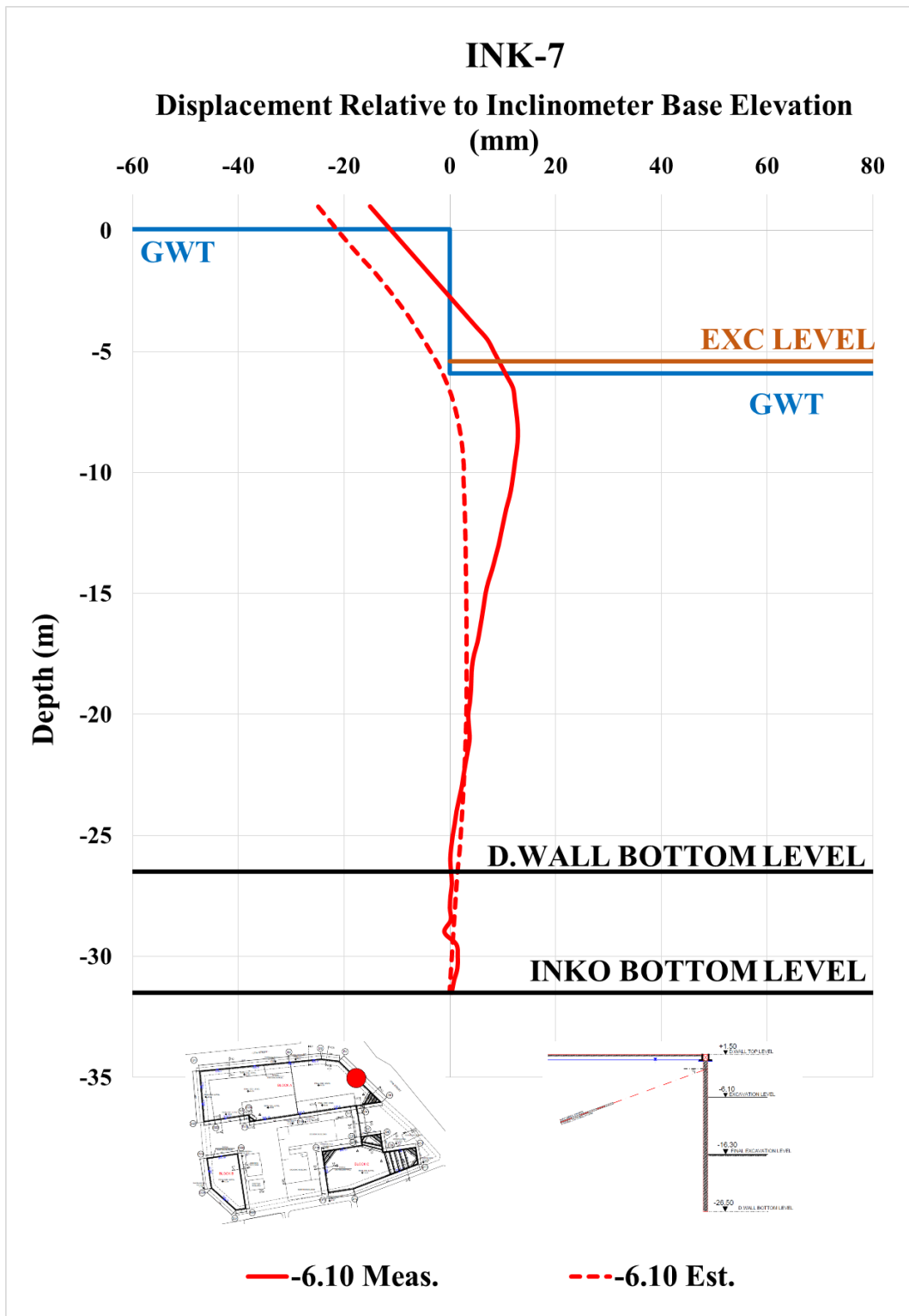
Figure A. 109. Estimated and Measured Displ. Rel. to Inc. Base Elev. at -6.10 m
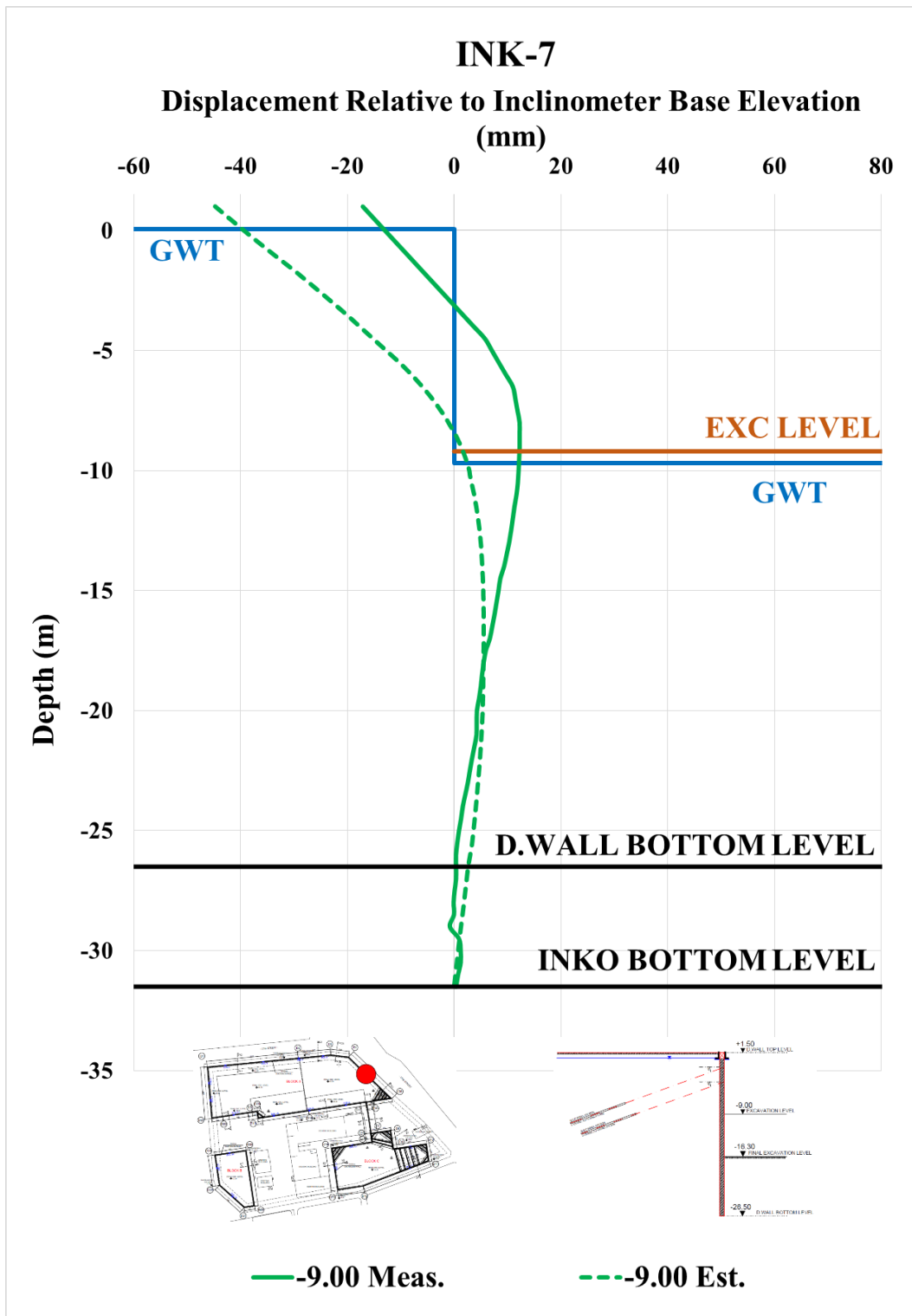
Figure A. 110. Estimated and Measured Displ. Rel. to Inc. Base Elev. at -9.00 m
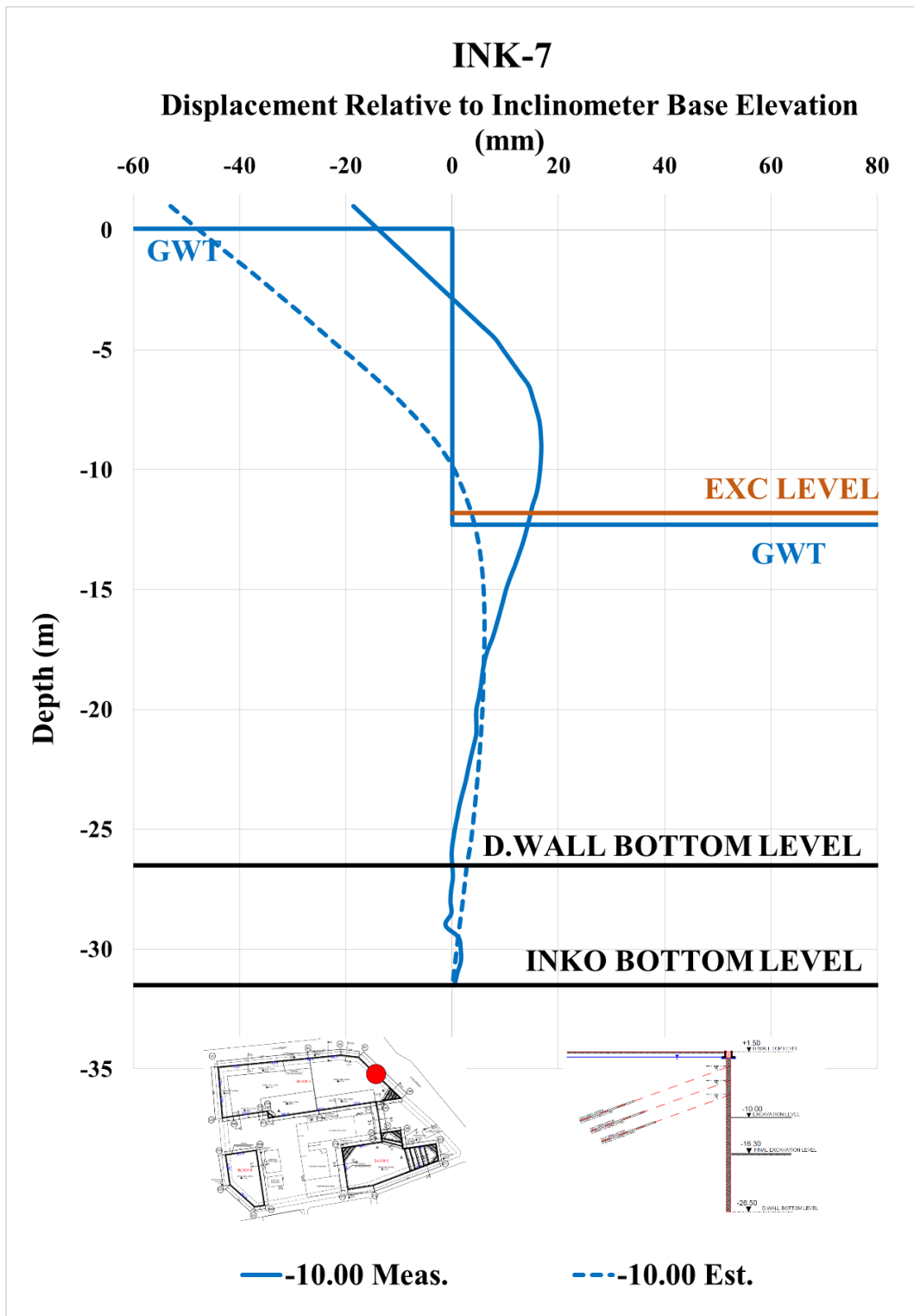
Figure A. 111. Estimated and Measured Displ. Rel. to Inc. Base Elev. at -10.00 m
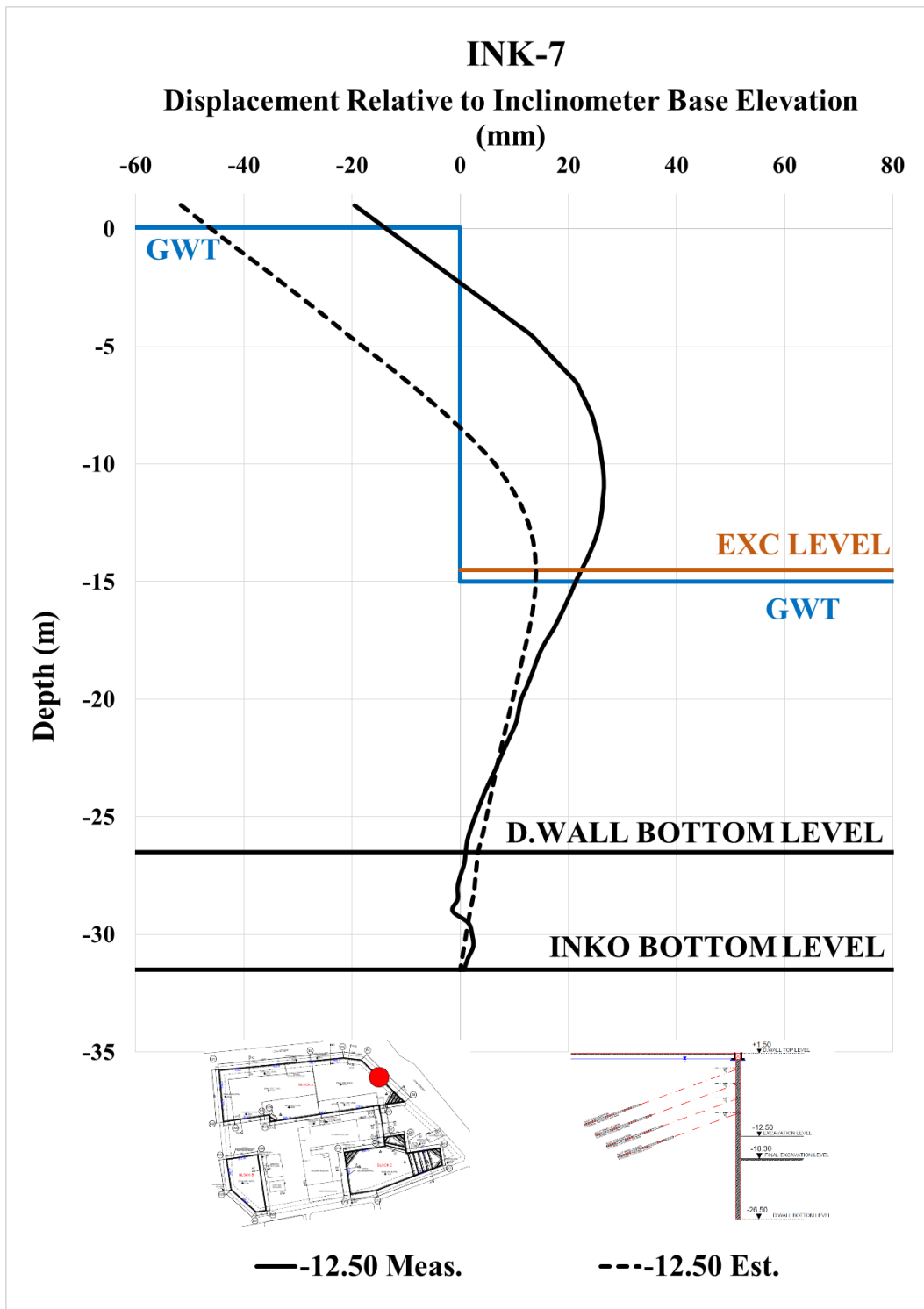
Figure A. 112. Estimated and Measured Displ. Rel. to Inc. Base Elev. at -12.50 m
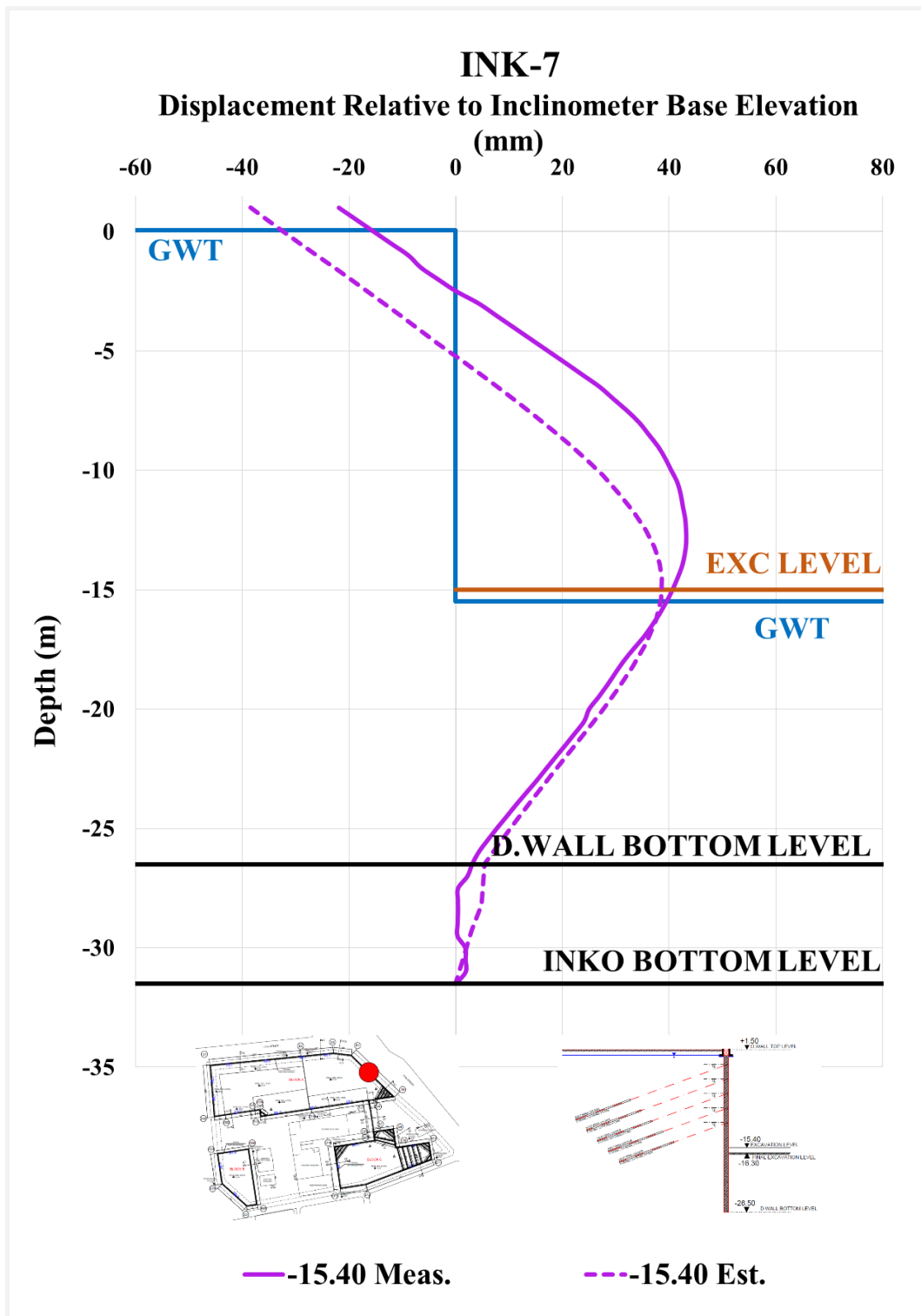
Figure A. 113. Estimated and Measured Displ. Rel. to Inc. Base Elev. at -15.40 m
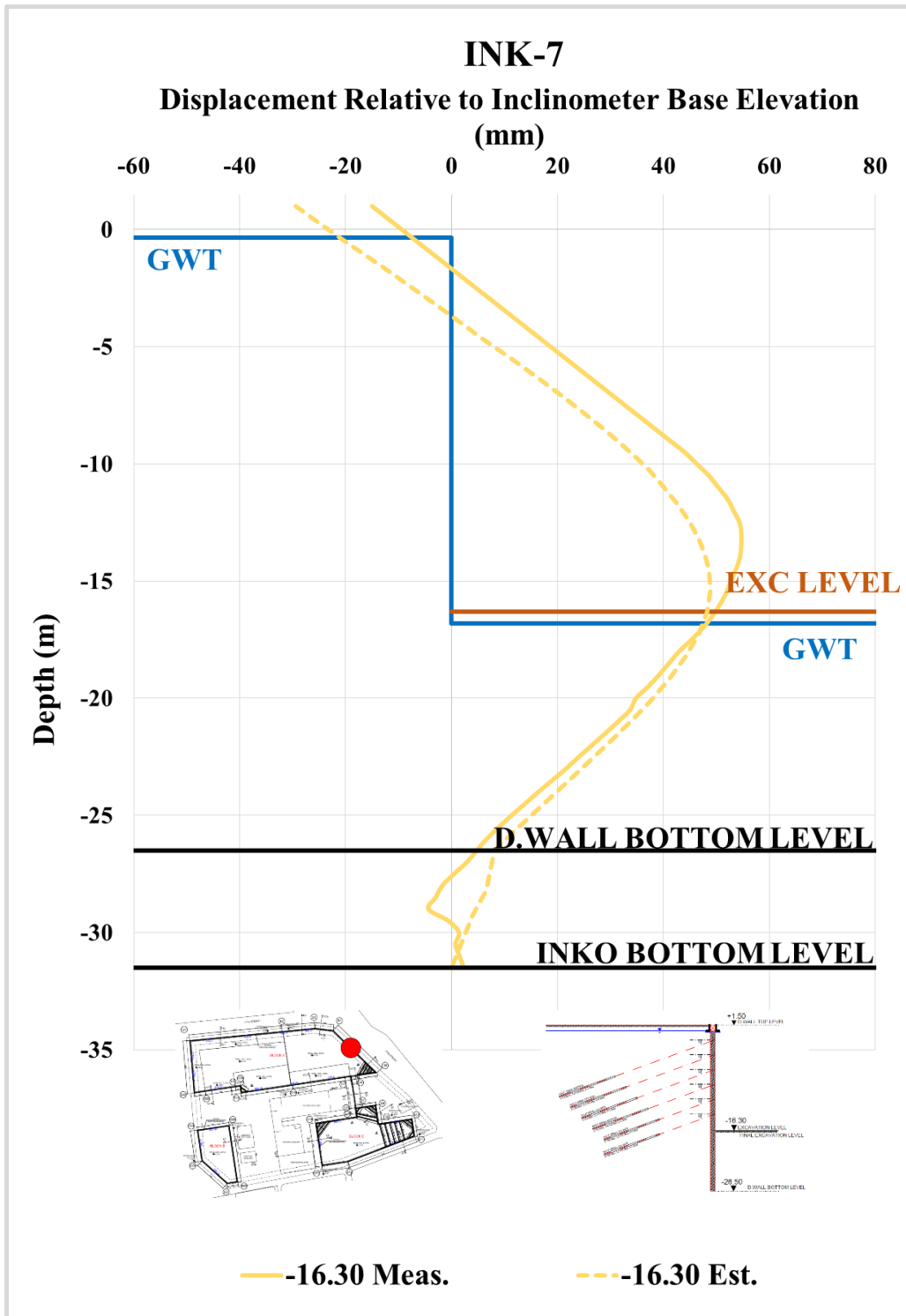
Figure A. 114. Estimated and Measured Displ. Rel. to Inc. Base Elev. at -16.30 m

Table A. 25. Internal Forces of Diaphragm Wall

INK - 7 / Section 2B-2B							
Excvation Stage	1	2	3	4	5	6	7
Excavation Level (m)	-2,50	-6,10	-9,00	-10,00	-12,50	-15,40	-16,30
N_{max} (kN/m)	94,94	222,80	353,10	460,40	645,70	902,00	1006,00
V_{max} (kN/m)	60,05	401,40	401,40	401,40	444,90	446,00	446,00
M_{max} (kN.m/m)	277,30	795,30	1024,00	1024,00	1208,00	1561,00	1561,00

Legend	Excvation Stage	1. Anchor Level	2. Excavation Level	2. Anchor Level	3. Excavation Level	3. Anchor Level	4. Excavation Level	4. Anchor Level	5. Excavation Level	5. Anchor Level	6. Excavation Level	6. Anchor Level	Final Excavation Level
	Measured Load of 1. Anchor Row (kN)	623.53	562.41	558.52	499.64	498.87	505.90	498.62	498.15	488.09	476.53	475.02	474.46
	Estimated Load of 1. Anchor Row (kN)	650.00	683.23	529.46	540.96	476.26	478.01	456.91	459.89	457.94	455.30	458.30	460.20
	Estimated Load of 2. Anchor Row (kN)	-	-	650.00	668.06	572.60	576.50	533.61	540.94	527.67	525.14	523.46	524.02
	Estimated Load of 3. Anchor Row (kN)	-	-	-	-	650.00	654.29	580.17	595.53	565.94	566.60	557.42	554.68
	Estimated Load of 4. Anchor Row (kN)	-	-	-	-	-	-	650.00	681.65	627.63	651.86	627.85	628.75
	Estimated Load of 5. Anchor Row (kN)	-	-	-	-	-	-	-	-	650.00	711.80	658.99	668.75
	Estimated Load of 6. Anchor Row (kN)	-	-	-	-	-	-	-	-	-	-	650.00	671.44

Figure A. 115. Measured and Estimated Anchor Loads

INK-6 – Calibrated, Estimated and Measured Displacements
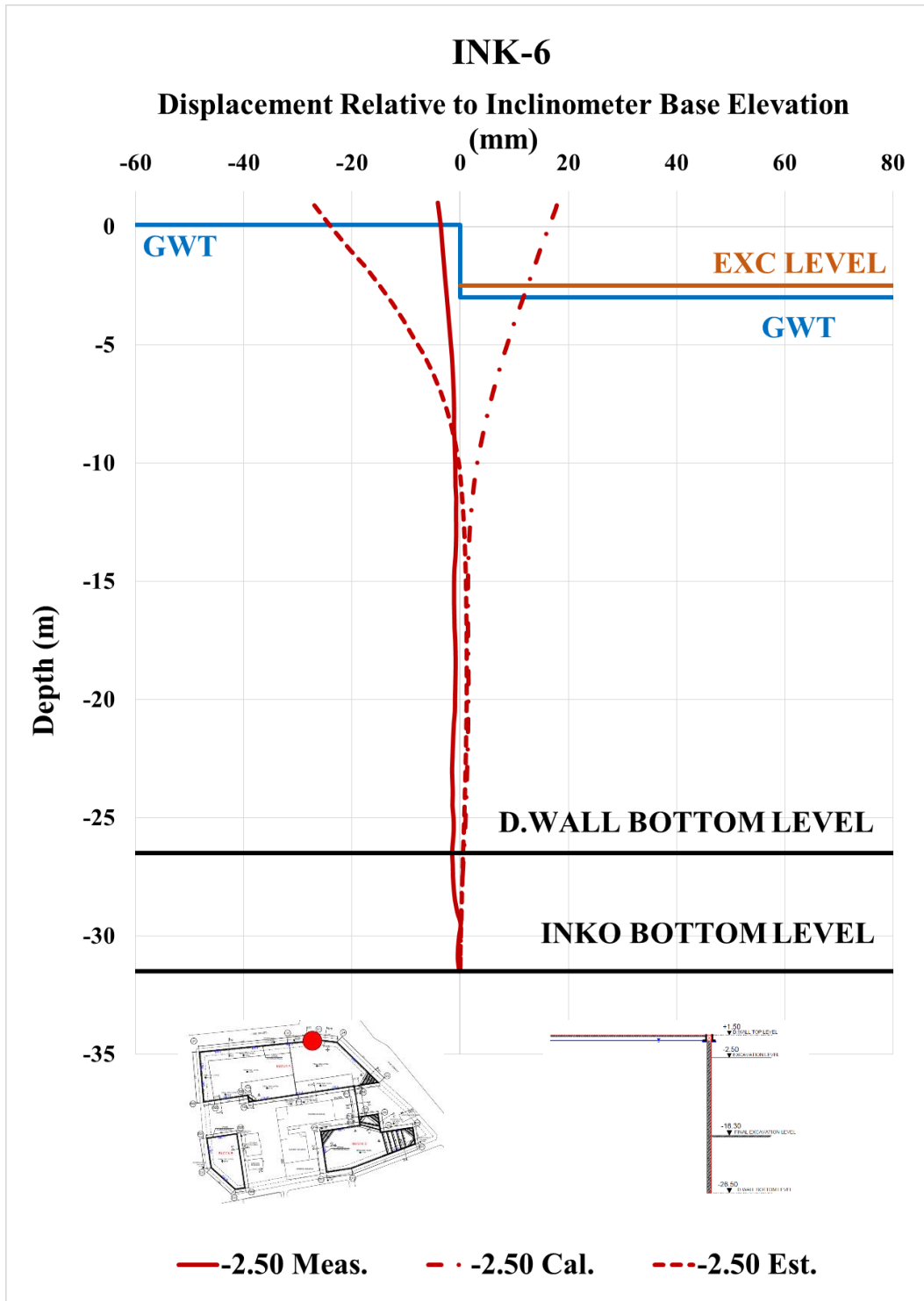
Figure A. 116. Calibrated and Measured Displ. Rel. to Inc. Base Elev. at -2.50 m
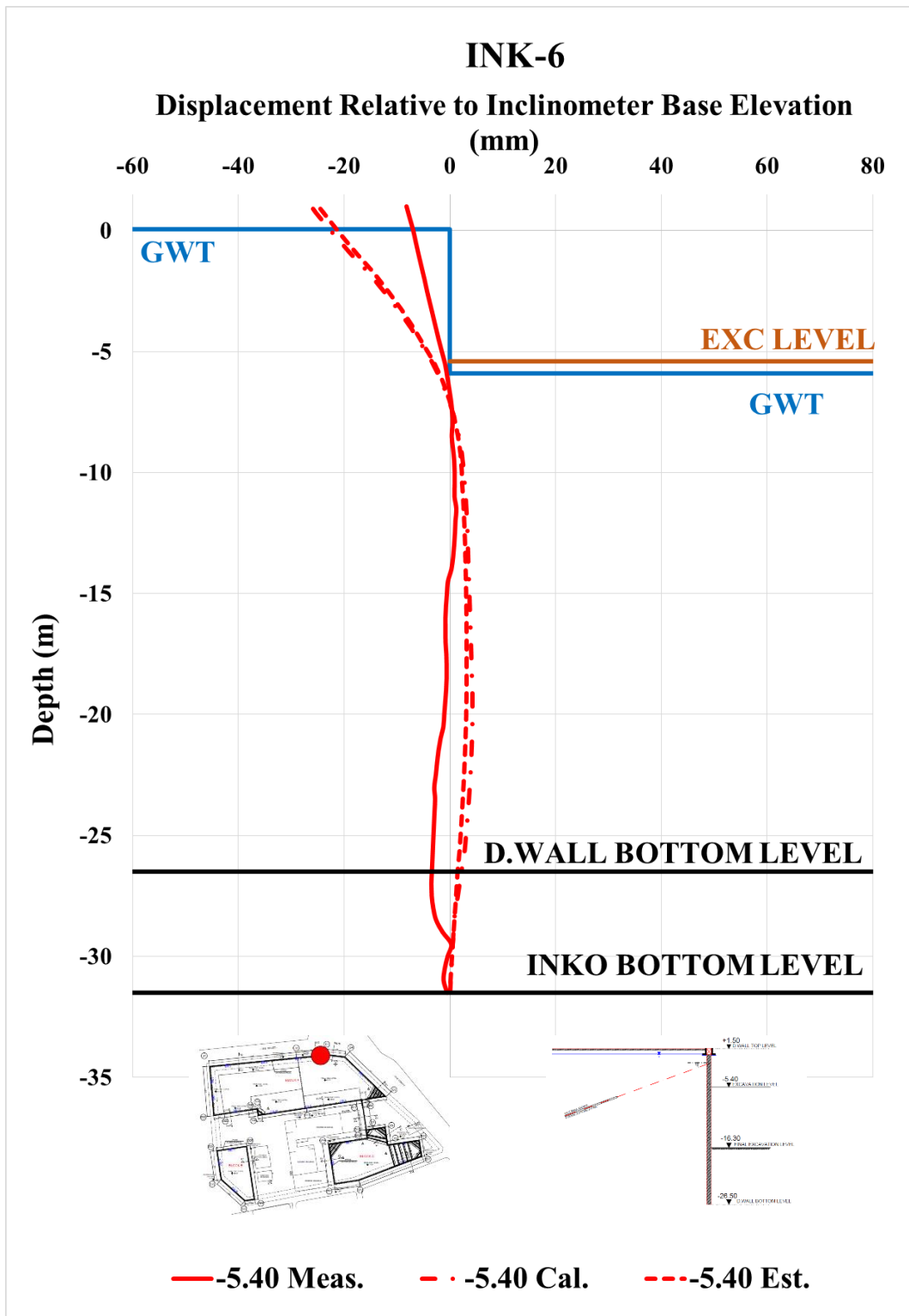
Figure A. 117. Calibrated and Measured Displ. Rel. to Inc. Base Elev. at -5.40 m
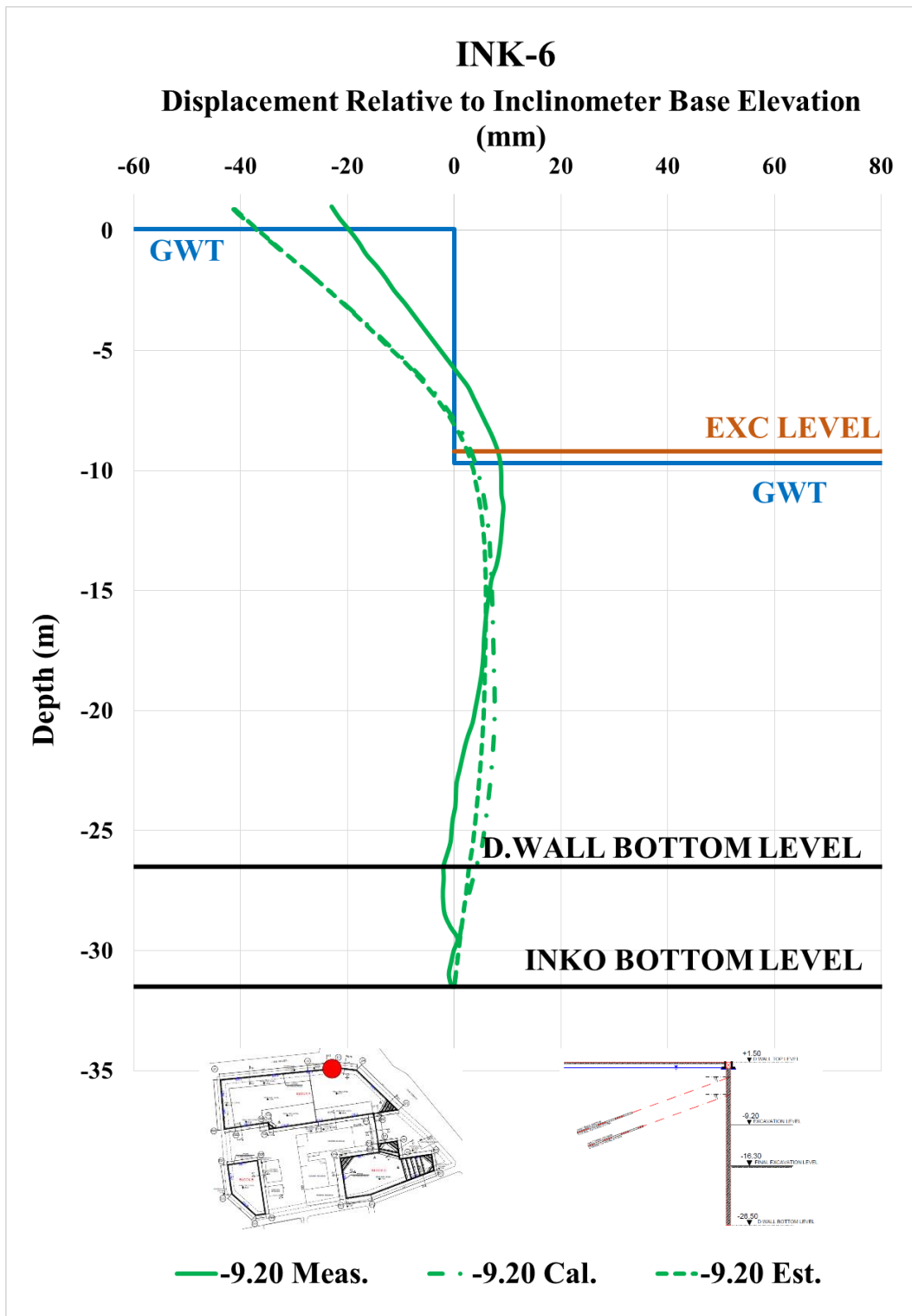
Figure A. 118. Calibrated and Measured Displ. Rel. to Inc. Base Elev. at -9.20 m

256
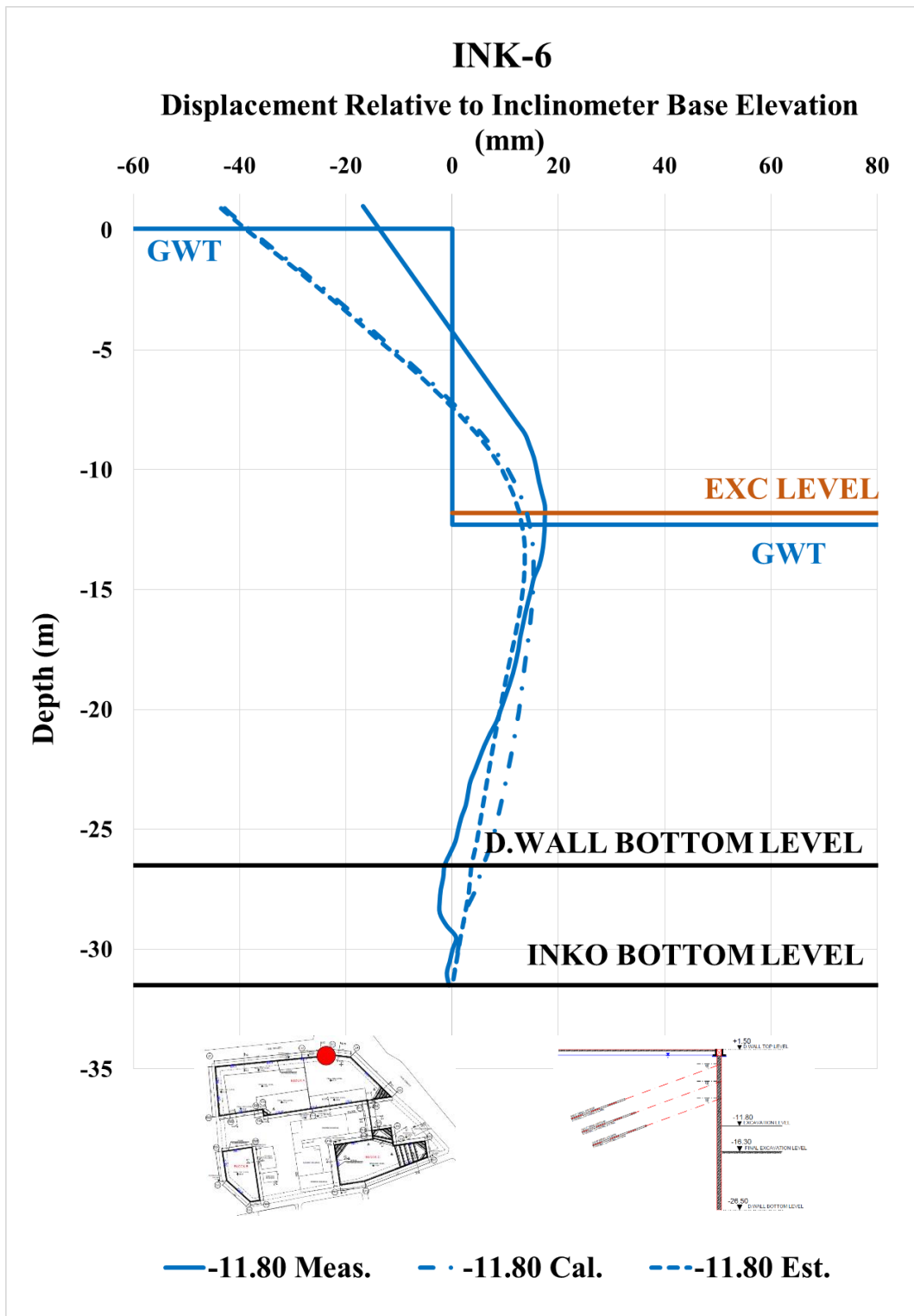
Figure A. 119. Calibrated and Measured Displ. Rel. to Inc. Base Elev. at -11.80 m
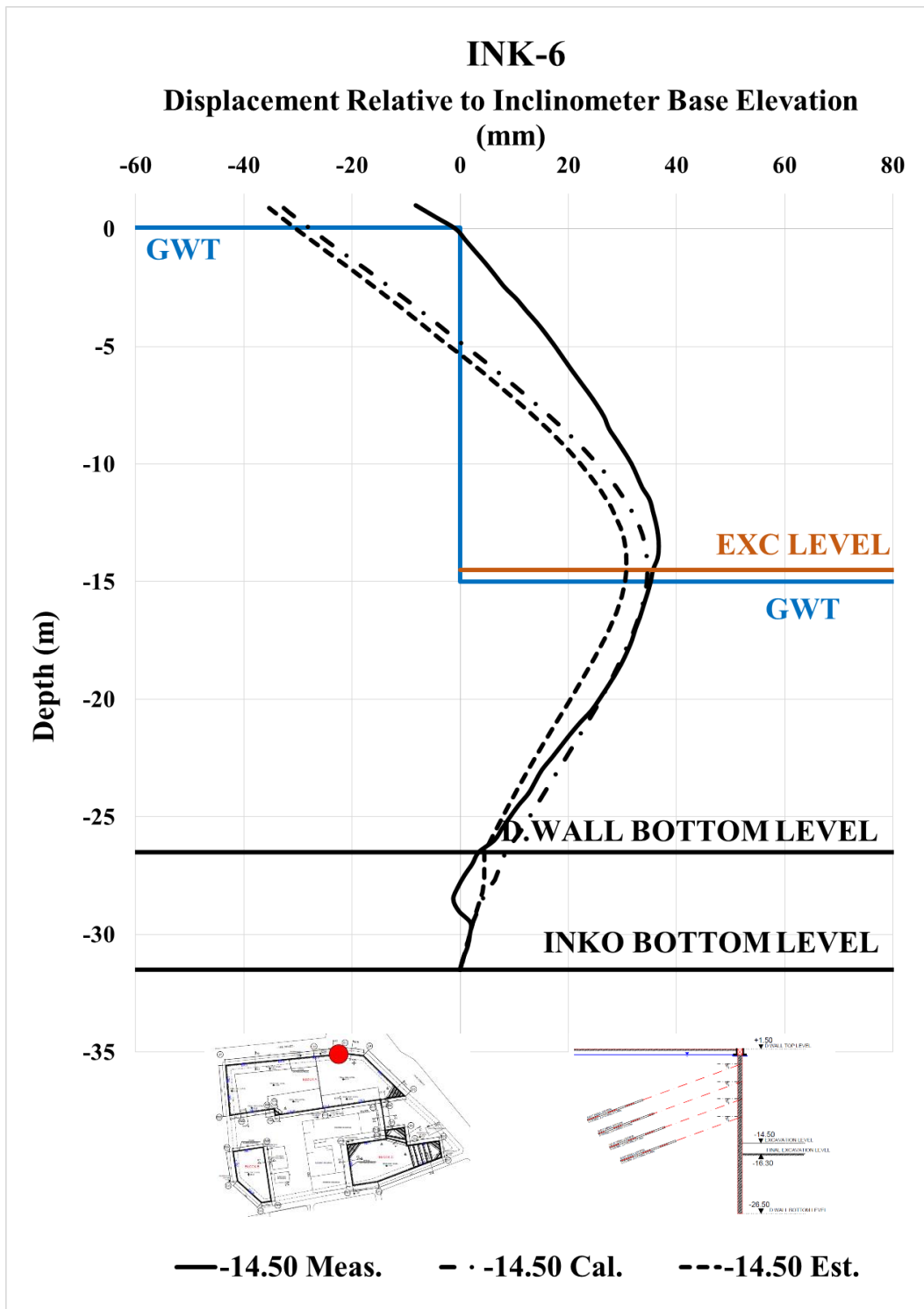
Figure A. 120. Calibrated and Measured Displ. Rel. to Inc. Base Elev. at -14.50 m
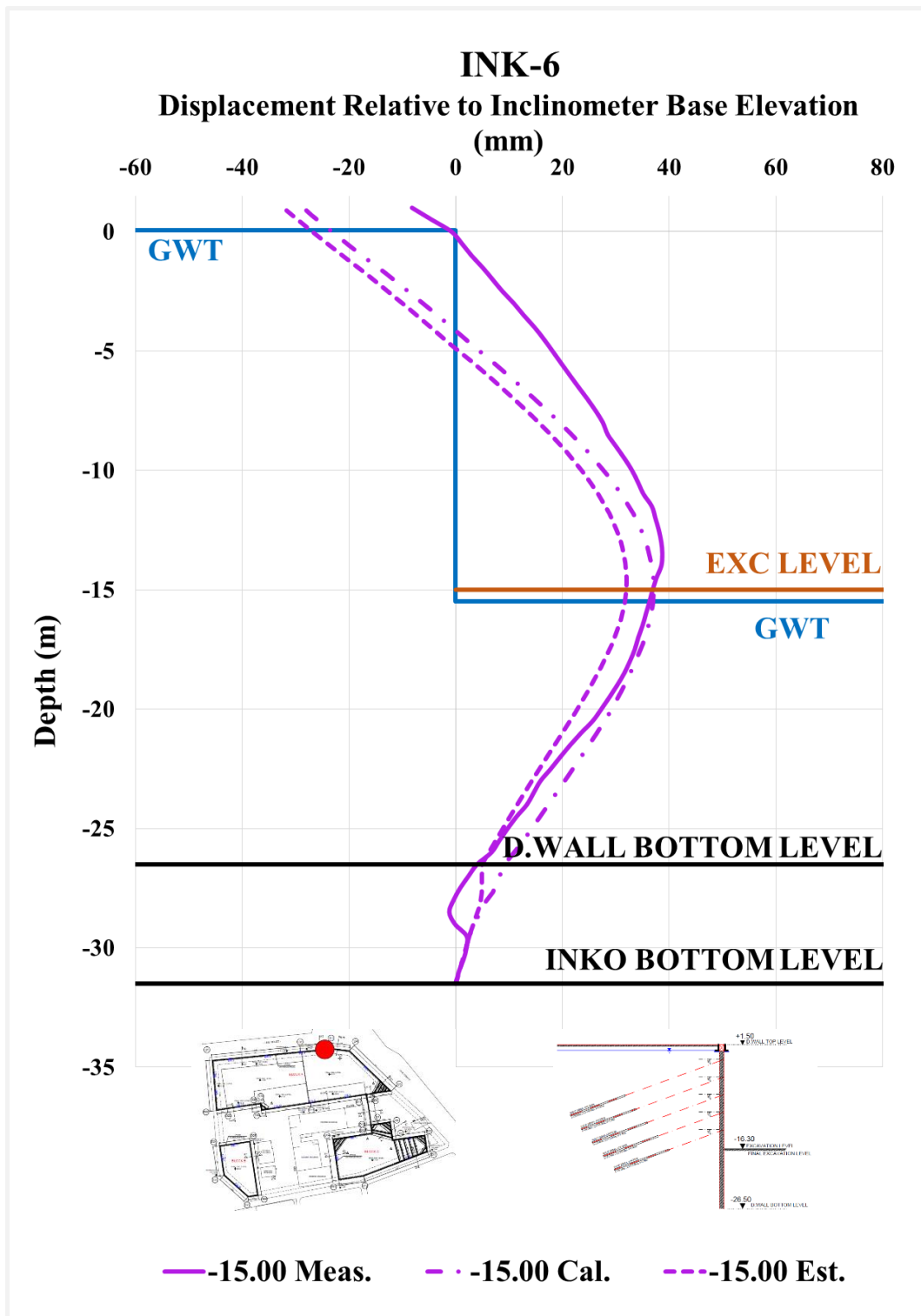
Figure A. 121. Calibrated and Measured Displ. Rel. to Inc. Base Elev. at -15.00 m
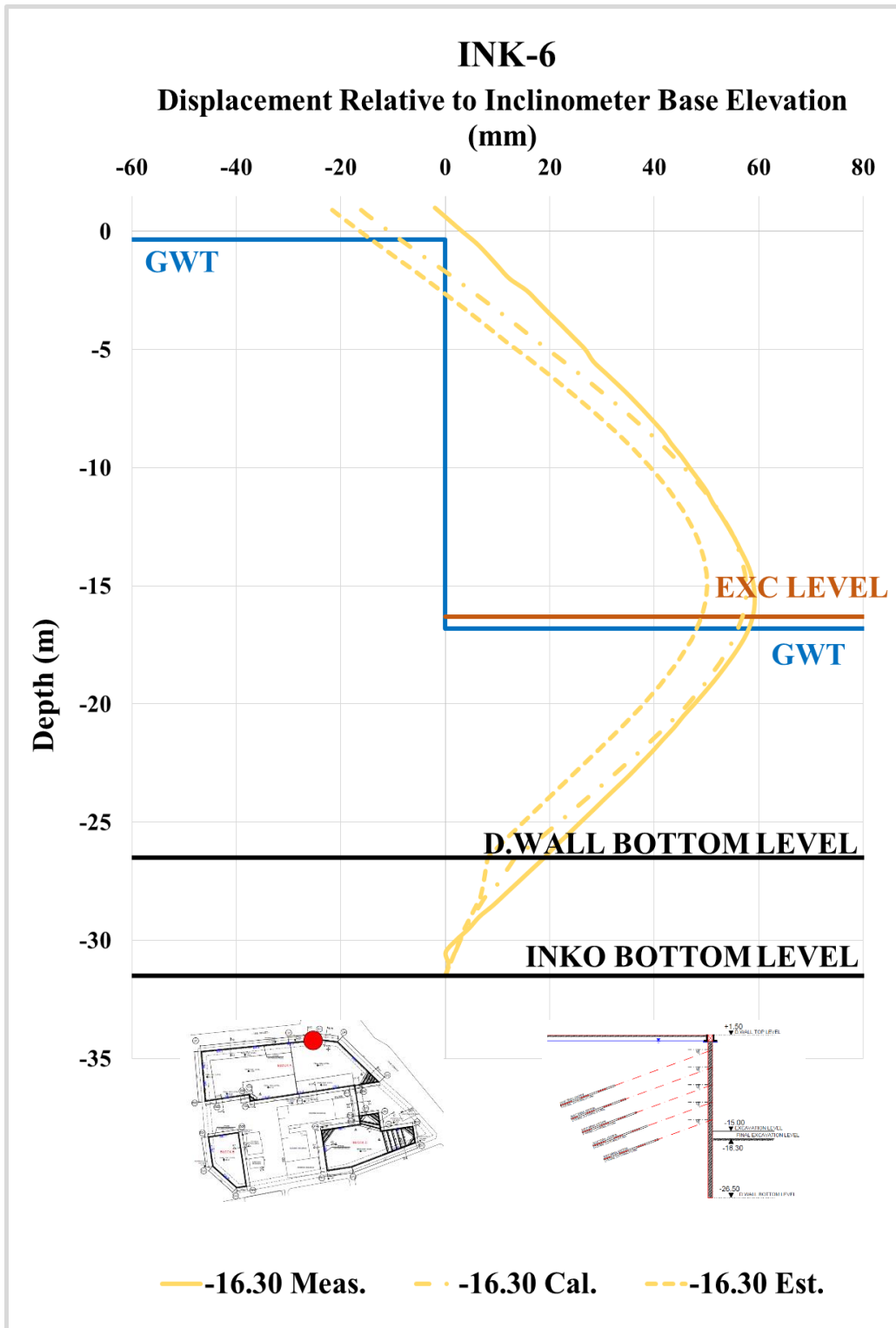
Figure A. 122. Calibrated and Measured Displ. Rel. to Inc. Base Elev. at -16.30 m

Table A. 26. Internal Forces of Diaphragm Wall

INK - 6 / Section 2-2							
Excvation Stage	1	2	3	4	5	6	7
Excavation Level (m)	-2,50	-5,40	-9,20	-11,80	-14,50	-15,00	-16,30
N_{max} (kN/m)	182,40	205,70	363,50	558,40	806,70	908,50	963,10
V_{max} (kN/m)	364,80	386,40	386,40	390,20	423,40	423,40	423,40
M_{max} (kN.m/m)	606,80	741,20	990,60	1078,00	1312,00	1312,00	1471,00

Legend	Excvation Stage	1. Anchor Level	2. Excavation Level	2. Anchor Level	3. Excavation Level	3. Anchor Level	4. Excavation Level	4. Anchor Level	5. Excavation Level	5. Anchor Level	6. Excavation Level	Final Excavation Level
	Measured Load of 1. Anchor Row (kN)	656.64	523.96	524.98	526.63	523.73	522.10	504.36	510.85	509.40	508.85	509.84
	Estimated Load of 1. Anchor Row (kN)	650.00	675.74	535.76	556.06	509.39	514.42	504.86	504.56	506.59	508.30	510.80
	Estimated Load of 2. Anchor Row (kN)	-	-	650.00	682.18	600.68	617.25	586.85	591.37	584.55	586.32	586.36
	Estimated Load of 3. Anchor Row (kN)	-	-	-	-	650.00	684.47	627.78	647.30	626.44	628.60	630.06
	Estimated Load of 4. Anchor Row (kN)	-	-	-	-	-	-	650.00	703.48	657.67	662.41	678.14
	Estimated Load of 5. Anchor Row (kN)	-	-	-	-	-	-	-	-	650.00	656.92	669.09

Figure A. 123. Measured and Estimated Anchor Loads

Table A. 27. Summary of Displacement Results of INK-6

INK - 6 / SECTION 2 - 2

Excvation Level (m)	Excvation Depth (m)	u_{meas} (mm) Inclinometer Measurements	u_{est} (mm) Estimation with Plaxis 2D Analysis	u_{cal} (mm) Calibration with Plaxis 2D Analysis	$u_{literature}$ (mm) FHWA-IF-99-015 (1999) - Maksimum	$u_{literature}$ (mm) FHWA-IF-99-015 (1999) - Average	$u_{literature}$ (mm) Goldberg et al. (1976)	$u_{literature}$ (mm) Clough et al. (1990) - Maksimum	$u_{literature}$ (mm) Clough et al. (1990) - Average	$u_{literature}$ (mm) Long (2001)	$u_{literature}$ (mm) Long (2001) (Extraordinary cases eliminated)	$u_{literature}$ (mm) Long (2001) Cantilever System
-2.50	4.00	0.07	1.28	17.80	20.00	8.00	20.00	20.00	8.00	7.60	5.60	14.4
-5.40	6.90	1.22	3.21	4.24	34.50	13.80	34.50	34.50	13.80	13.11	9.66	-
-9.20	10.70	9.23	5.93	7.56	53.50	21.40	53.50	53.50	21.40	20.33	14.98	-
-11.80	13.30	17.44	13.61	15.27	66.50	26.60	66.50	66.50	26.60	25.27	18.62	-
-14.50	16.00	36.72	30.71	34.71	80.00	32.00	80.00	80.00	32.00	30.40	22.40	-
-15.00	16.50	38.71	31.98	37.17	82.50	33.00	82.50	82.50	33.00	31.35	23.10	-
-16.30	17.80	59.24	50.11	57.60	89.00	35.60	89.00	89.00	35.60	33.82	24.92	-

262
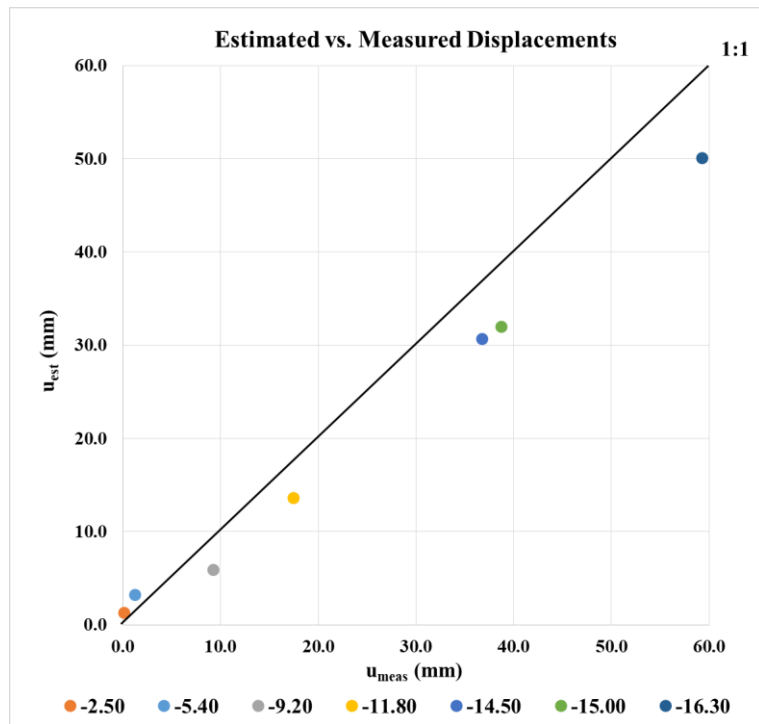
Figure A. 124. Estimated and Measured Displacements of INK - 6
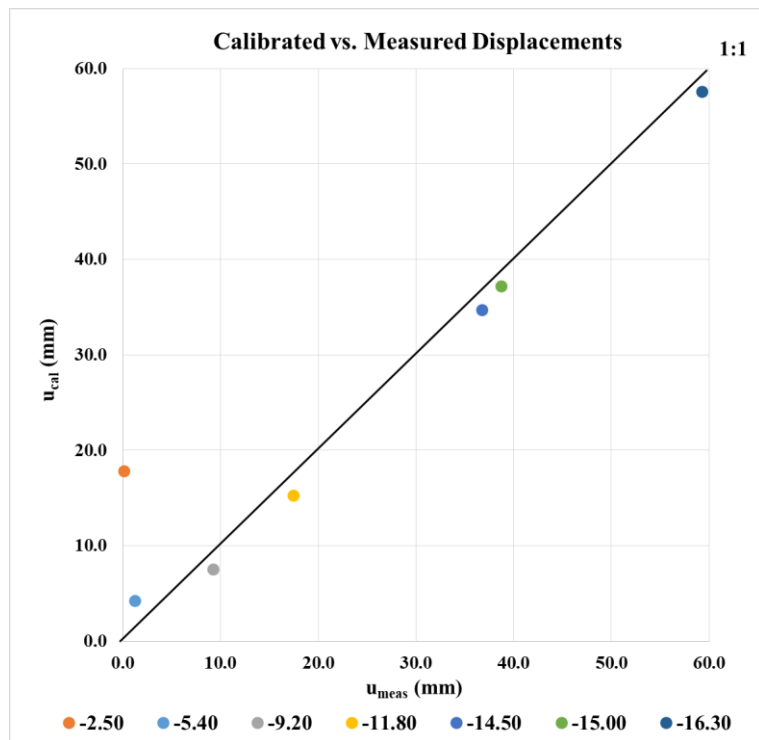
Figure A. 125. Calibrated and Measured Displacements of INK - 6
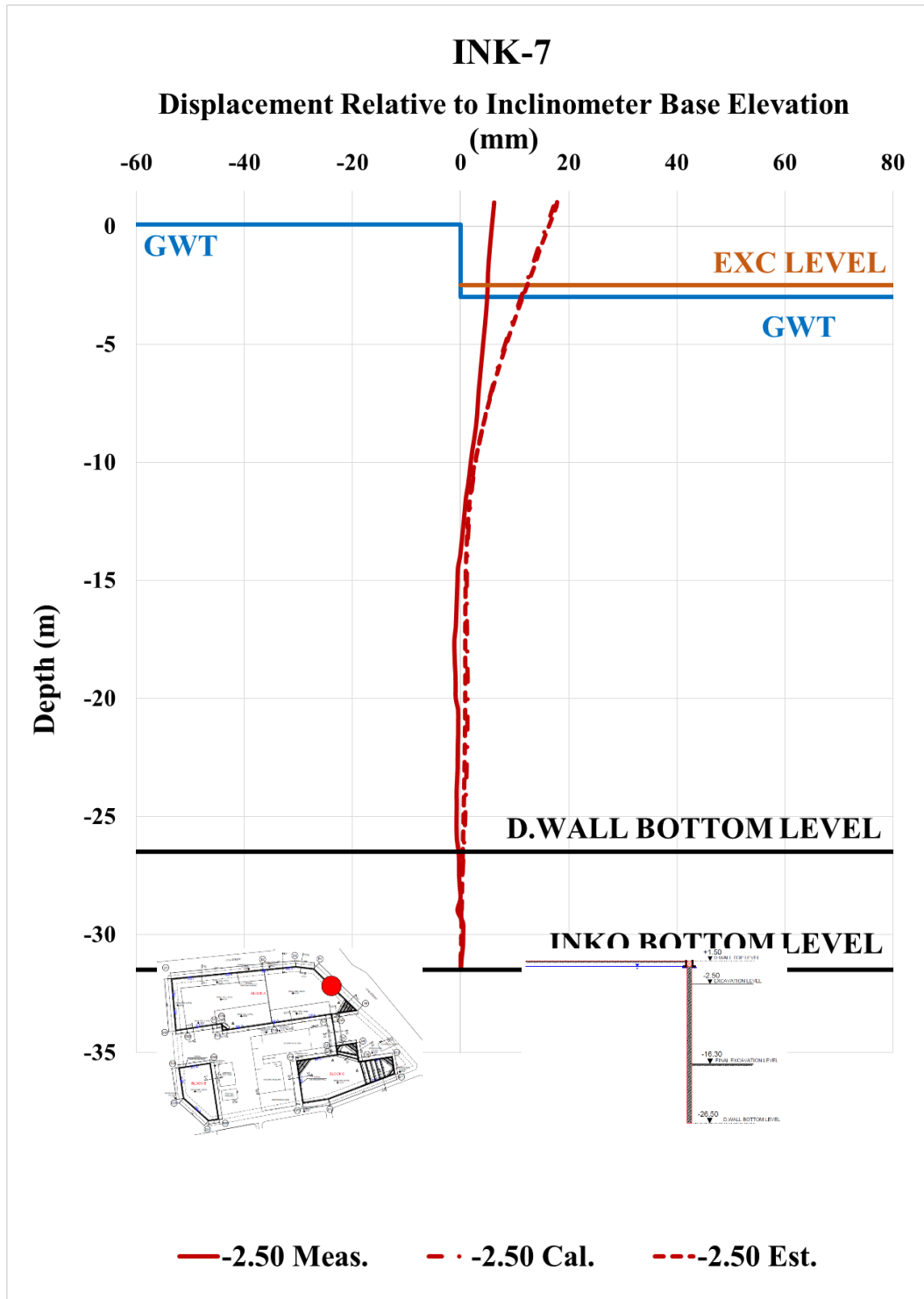
Figure A. 126. Calibrated and Measured Displ. Rel. to Inc. Base Elev. at -2.50 m
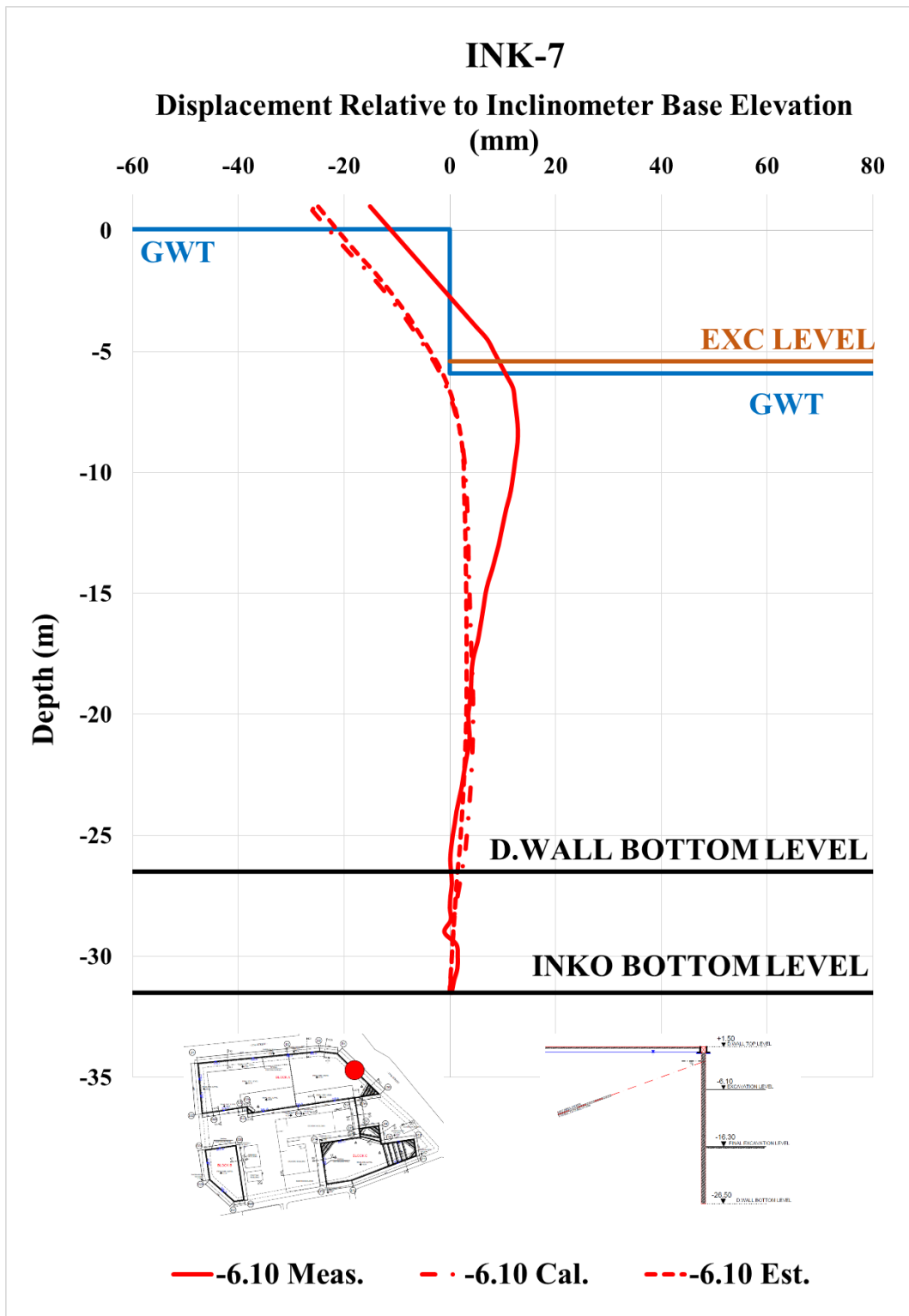
Figure A. 127. Calibrated and Measured Displ. Rel. to Inc. Base Elev. at -6.10 m
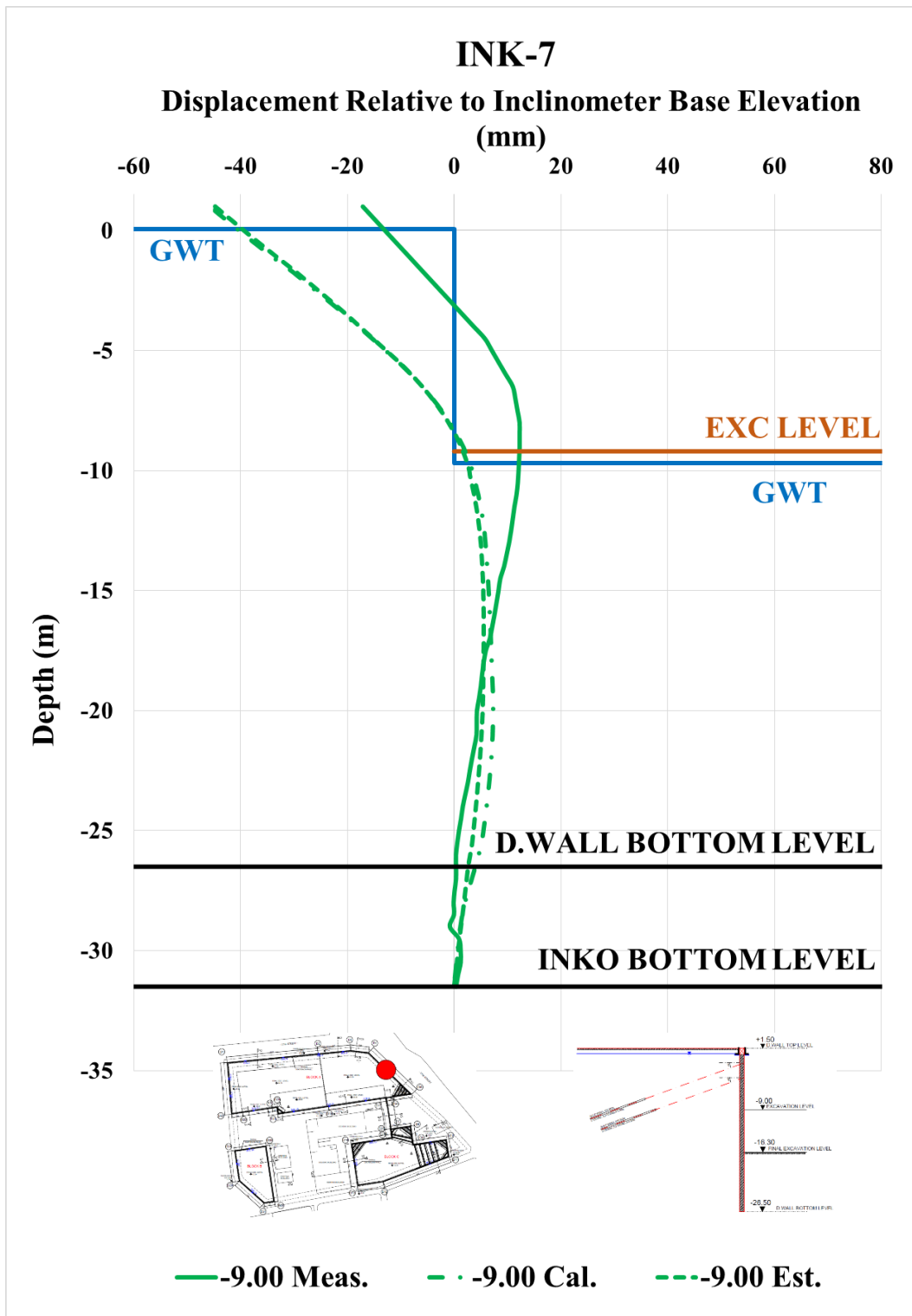
Figure A. 128. Calibrated and Measured Displ. Rel. to Inc. Base Elev. at -9.00 m
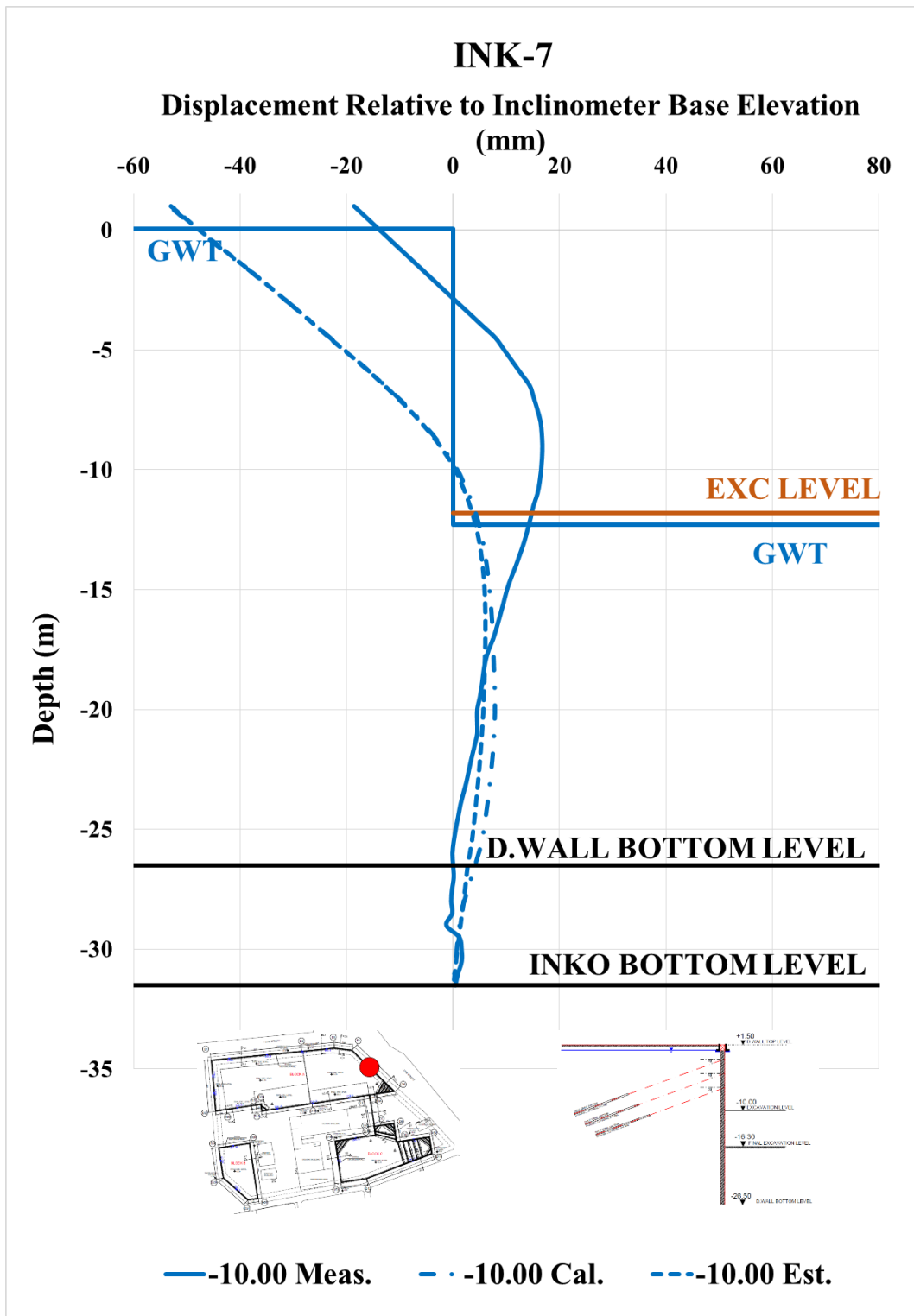
Figure A. 129. Calibrated and Measured Displ. Rel. to Inc. Base Elev. at -10.00 m
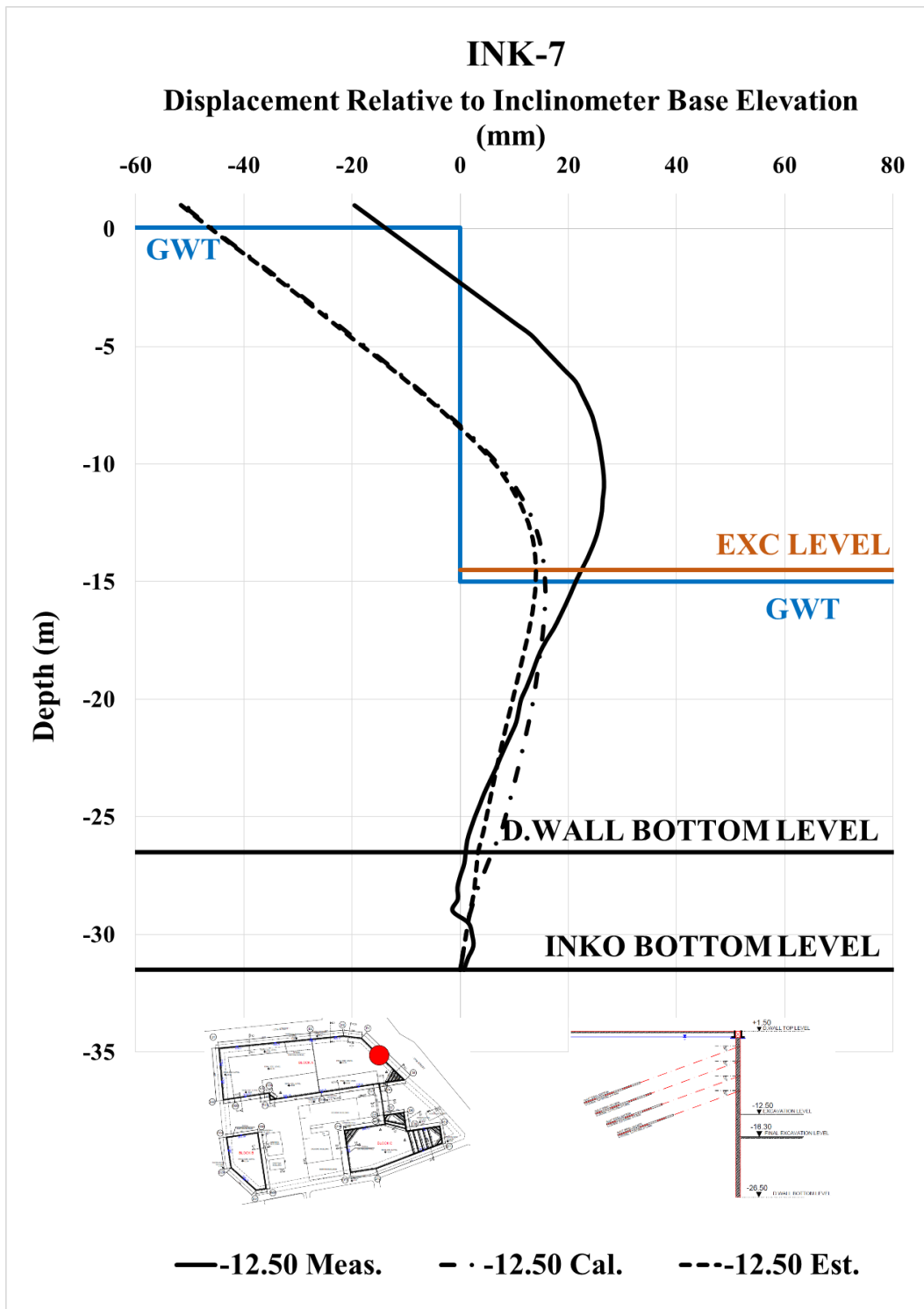
Figure A. 130. Calibrated and Measured Displ. Rel. to Inc. Base Elev. at -12.50 m
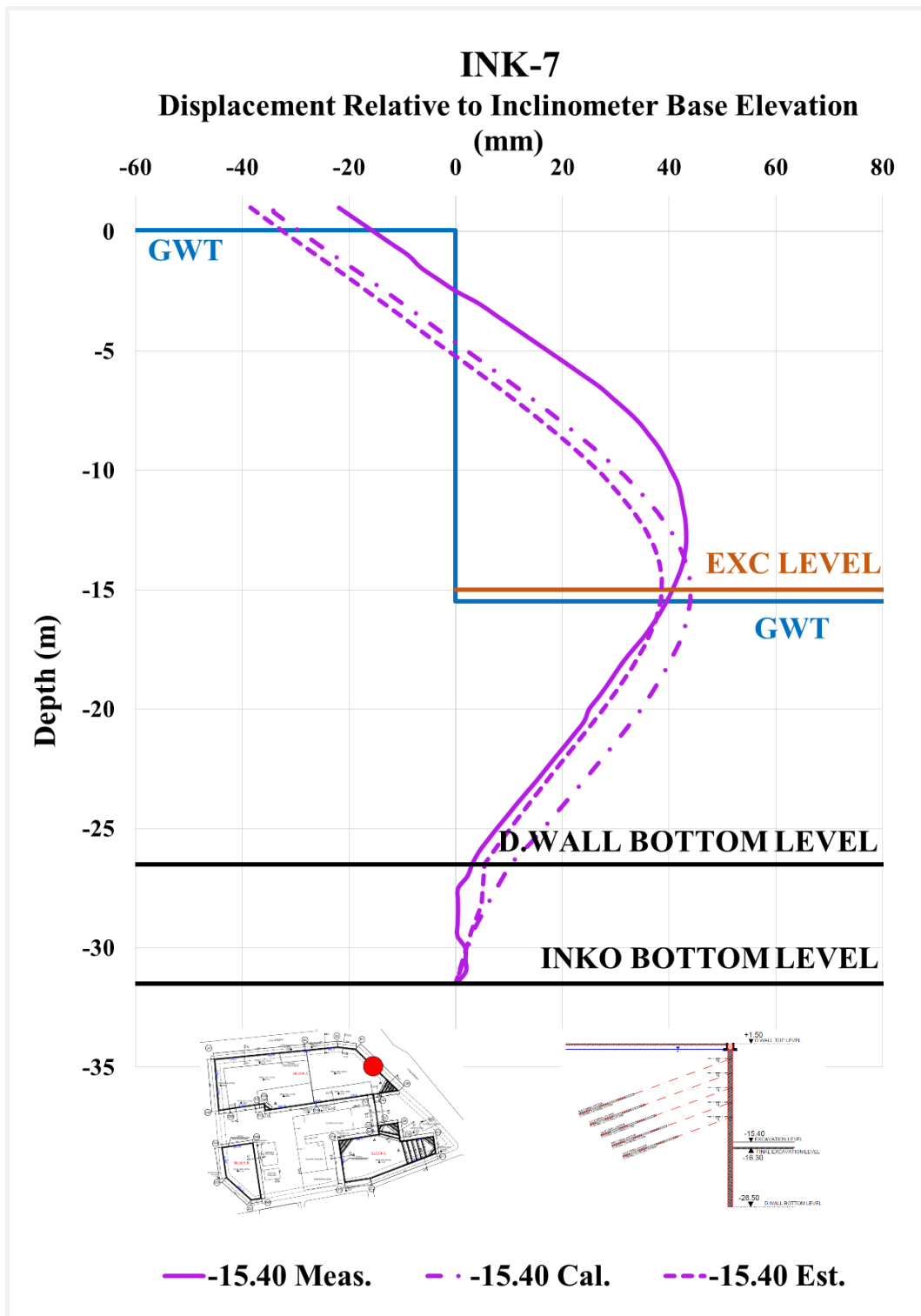
Figure A. 131. Calibrated and Measured Displ. Rel. to Inc. Base Elev. at -15.40 m
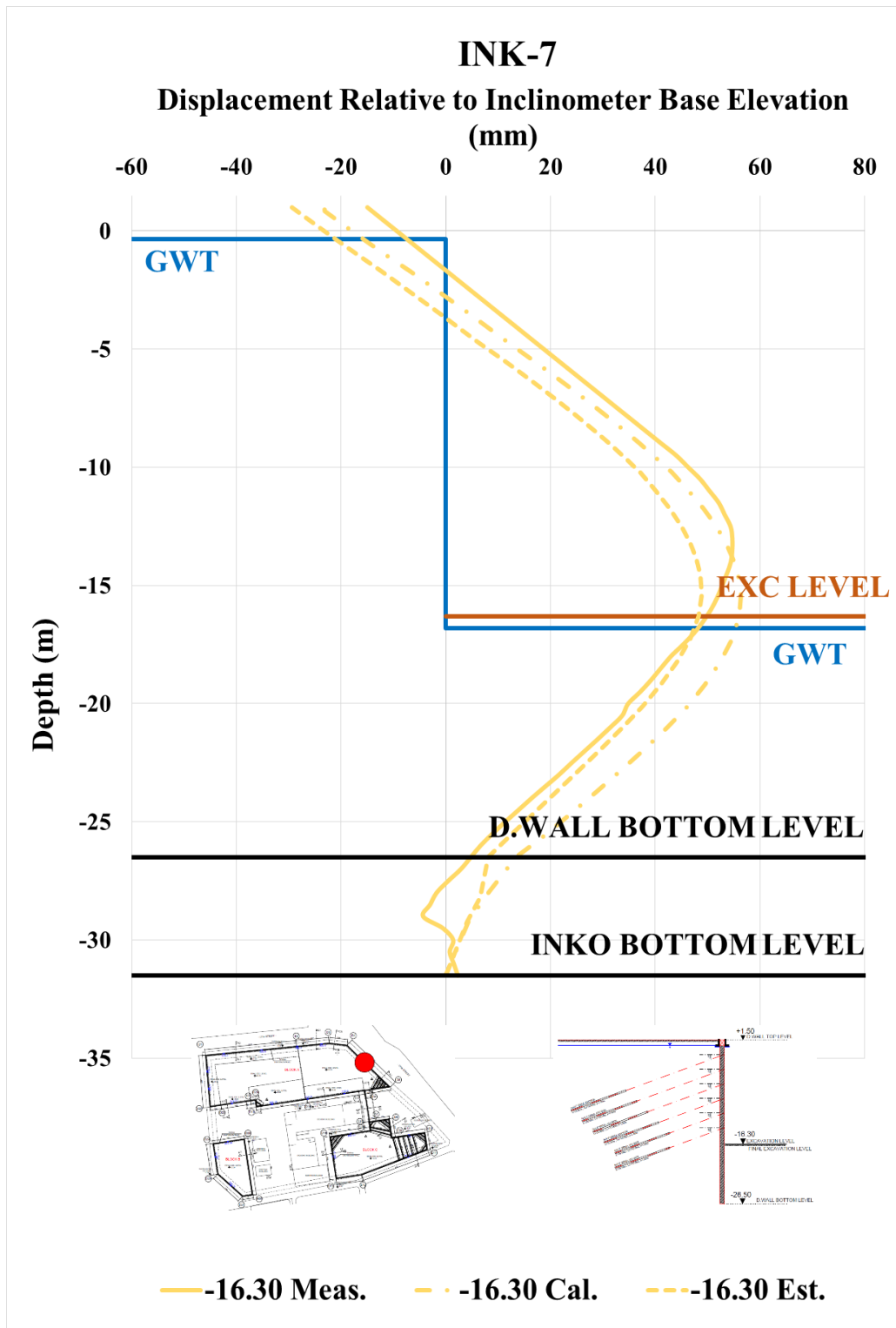
Figure A. 132. Calibrated and Measured Displ. Rel. to Inc. Base Elev. at -16.30 m

Table A. 28. Internal Forces of Diaphragm Wall

INK - 7 / Section 2B-2B							
Excvation Stage	1	2	3	4	5	6	7
Excavation Level (m)	-2,50	-6,10	-9,00	-10,00	-12,50	-15,40	-16,30
N_{max} (kN/m)	182,50	222,00	350,70	455,00	631,60	879,30	974,30
V_{max} (kN/m)	365,20	393,20	405,40	405,40	428,90	447,00	447,00
M_{max} (kN.m/m)	609,60	799,90	1038,00	1038,00	1137,00	1521,00	1529,00

Legend	Excvation Stage	1. Anchor Level	2. Excavation Level	2. Anchor Level	3. Excavation Level	3. Anchor Level	4. Excavation Level	4. Anchor Level	5. Excavation Level	5. Anchor Level	6. Excavation Level	6. Anchor Level	Final Excavation Level
	Measured Load of 1. Anchor Row (kN)	623.53	562.41	558.52	499.64	498.87	505.90	498.62	498.15	488.09	476.53	475.02	474.46
	Estimated Load of 1. Anchor Row (kN)	650.00	683.62	526.22	539.42	473.83	476.43	454.68	458.56	456.52	456.80	459.97	463.46
	Estimated Load of 2. Anchor Row (kN)	-	-	650.00	669.53	572.73	577.51	533.57	541.75	527.88	529.52	537.38	528.97
	Estimated Load of 3. Anchor Row (kN)	-	-	-	-	650.00	656.09	580.72	597.76	566.56	572.72	562.40	560.38
	Estimated Load of 4. Anchor Row (kN)	-	-	-	-	-	-	650.00	682.55	625.65	654.34	629.13	630.81
	Estimated Load of 5. Anchor Row (kN)	-	-	-	-	-	-	-	-	650.00	714.33	662.04	672.30
	Estimated Load of 6. Anchor Row (kN)	-	-	-	-	-	-	-	-	-	-	650.00	671.62

Figure A. 133. Measured and Estimated Anchor Loads

271

Table A. 29. Summary of Displacement Results of INK-7

INK - 7 / SECTION 2B - 2B

Excavation Level (m)	Excavation Depth (m)	u_{meas} (mm) Inclinometer Measurements	u_{est} (mm) Estimation with Plaxis 2D Analysis	u_{cal} (mm) Calibration with Plaxis 2D Analysis	$u_{literature}$ (mm) FHWA-IF-99-015 (1999) - Maksimum	$u_{literature}$ (mm) FHWA-IF-99-015 (1999) - Average	$u_{literature}$ (mm) Goldberg et al. (1976)	$u_{literature}$ (mm) Clough et al. (1990) - Maksimum	$u_{literature}$ (mm) Clough et al. (1990) - Average	$u_{literature}$ (mm) Long (2001)	$u_{literature}$ (mm) Long (2001) (Extraordinary cases eliminated)	$u_{literature}$ (mm) Long (2001) Cantilever System
-2.50	4.00	6.20	17.85	17.76	20.00	8.00	20.00	20.00	8.00	7.60	5.60	14.4
-6.10	7.60	12.87	3.24	4.38	38.00	15.20	38.00	38.00	15.20	14.44	10.64	-
-9.00	10.50	12.27	5.57	7.37	52.50	21.00	52.50	52.50	21.00	19.95	14.70	-
-10.00	11.50	16.78	6.03	7.88	57.50	23.00	57.50	57.50	23.00	21.85	16.10	-
-12.50	14.00	26.58	14.03	15.74	70.00	28.00	70.00	70.00	28.00	26.60	19.60	-
-15.40	16.90	43.19	38.67	43.95	84.50	33.80	84.50	84.50	33.80	32.11	23.66	-
-16.30	17.80	49.73	48.91	56.33	89.00	35.60	89.00	89.00	35.60	33.82	24.92	-

272
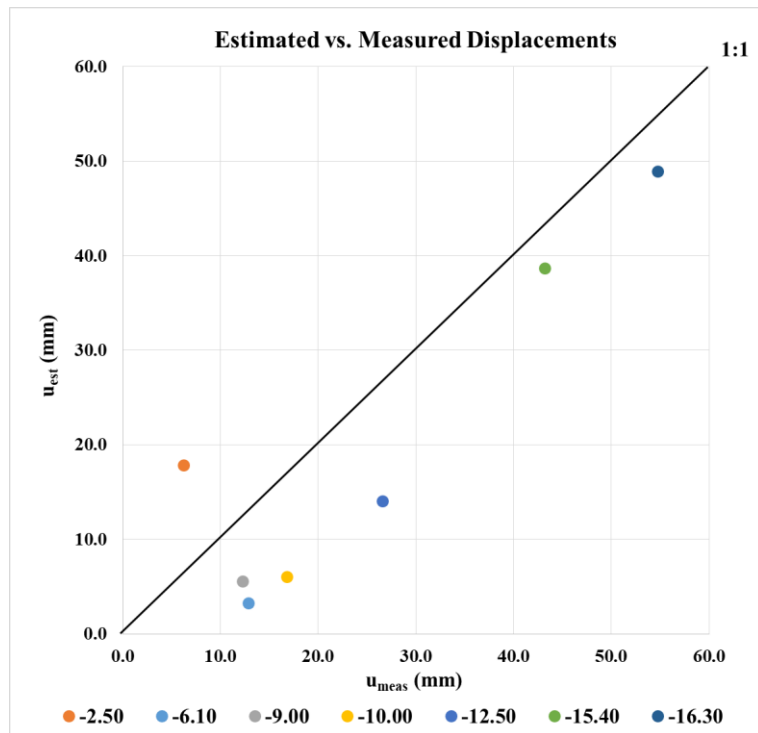
Figure A. 134. Estimated and Measured Displacements of INK - 7
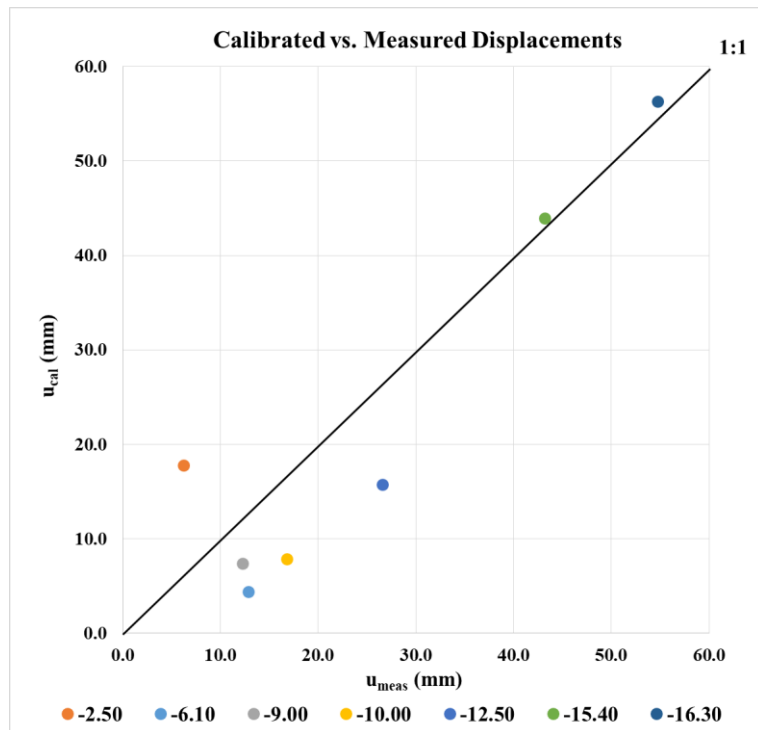
Figure A. 135. Calibrated and Measured Displacements of INK - 7

Area A4

Figure A. 136. SPT-N vs. Depth for Area A4
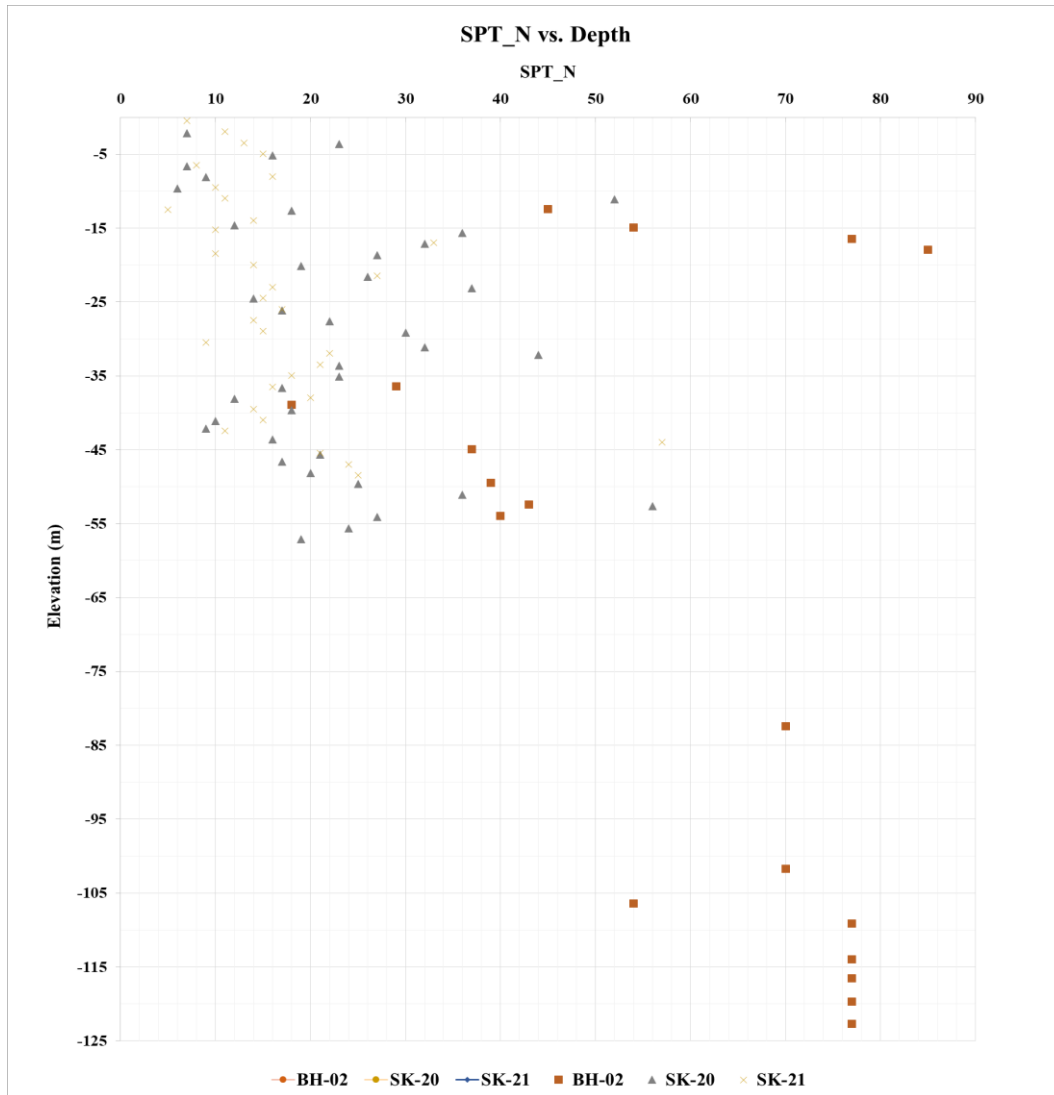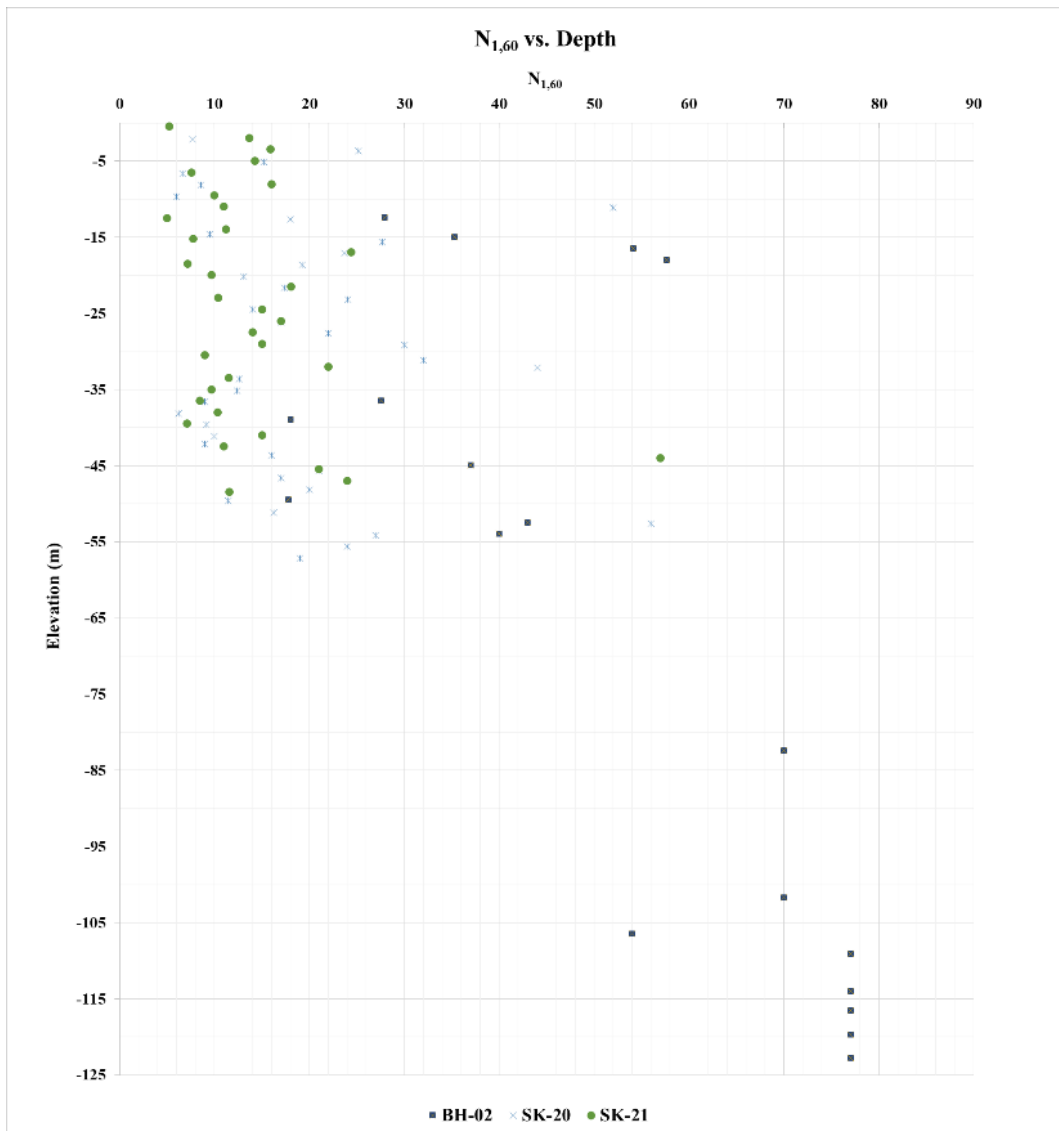
Figure A. 137. SPT-$N_{1,60}$ vs. Depth for Area A4
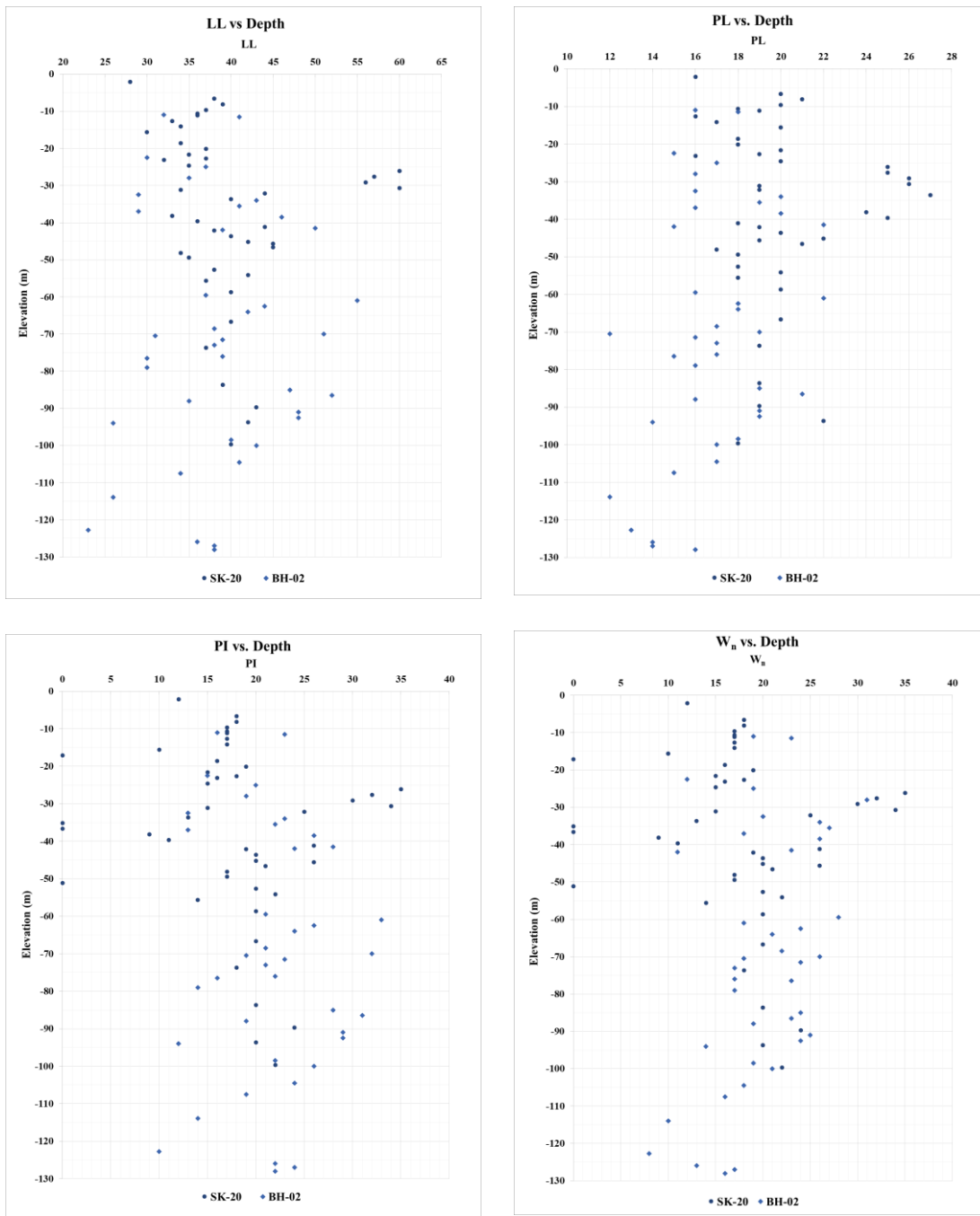
Figure A. 138. Variation of LL, PL, PI, and w_n for Area A4
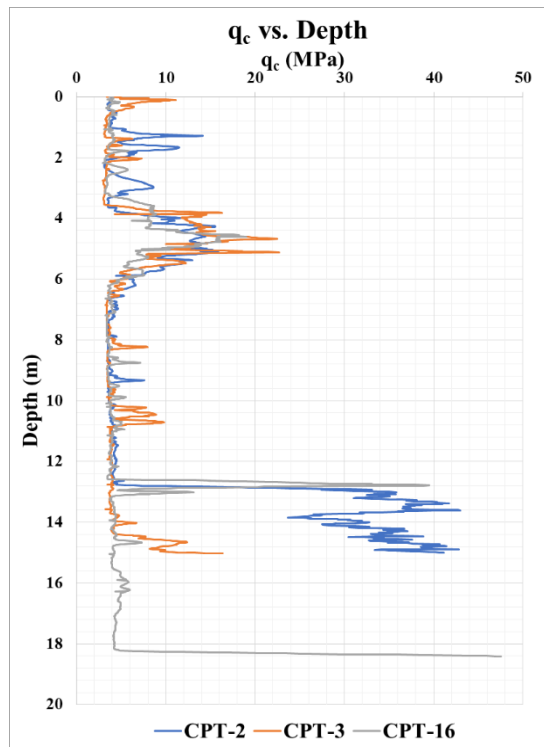
Figure A. 139. Variation of q$_c$ along with the Depth for Area A4
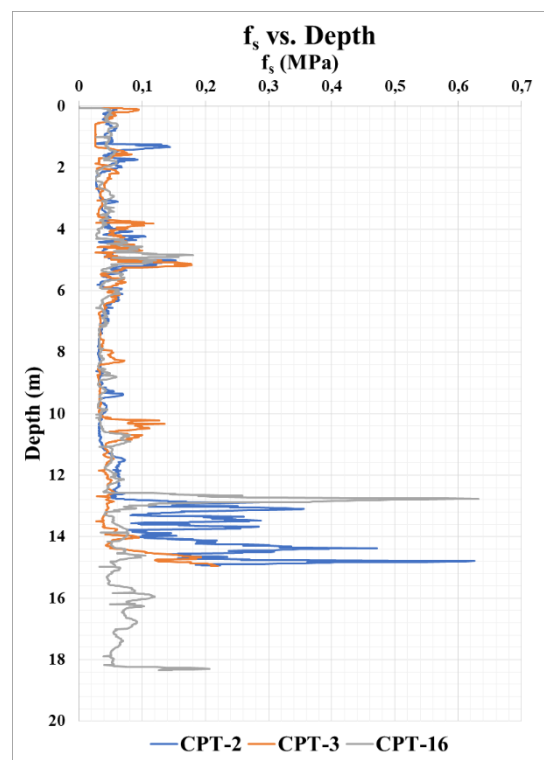
Figure A. 140. Variation of f$_s$ along with the Depth for Area A4

3 boreholes (SK-20, SK-21, and BH-2) and 3 CPT (CPT-2, CPT-3, and CPT-16) were considered. The depths of boreholes are changing between 50 m to 130 m. Depths of CPT are changing between 15 m to 18.4 m. The total depth of boreholes and CPTs is 280 m and 48.4 m respectively. Atterberg limit tests were performed on the samples taken from SK-20 and BH-2. LL, PL, PI, and w_n vary in 23 – 60 % (avg. 39 %), 12 – 27 % (avg. 18.5 %), 9 – 35 % (avg. 20.5 %), and 6.8 – 38 % (avg. 20 %) respectively. Unified soil classification (USCS) was performed for each sample. By considering USCS, SPT $N_{1,60}$ values, and CPT results, the thickness of soil layers was determined. Detailed soil parameters are given in below table;

- Boreholes: SK-20, SK-21, and BH-2 (Change in between 50 m to 130 m. 280 m in total)
- CPTs: CPT-2, CPT-3, and CPT-16 (Change in between 15 m to 18.4 m. 48.4 m in total)
- LL: 23 – 60 % (avg. 39 %)
- PL: 12 – 27 % (avg. 18.5 %)
- PI: 9 – 35 % (avg. 20.5 %)
- w_n: 6.8 – 38 % (avg. 20 %)

Table A. 30. Soil Profile of Area 4 (A4)

Layer No	Elevation (m)		Layer	Type	Thickness (m)	N	N$_{1,60}$	N$_{60}$	PI	y$_{wet}$ (kN/m³)	y$_{sat}$ (kN/m³)	c$_u$ (kPa)	c (kPa)	φ (°)	ψ (°)	E$_{50}^{ref}$ (MPa)	E$_{oed}^{ref}$ (MPa)	E$_{ur}^{ref}$ (MPa)	m	ν$_{ur}$	p$_{ref}$ (kPa)	R$_f$
1	1.6	-	CL	Cohesive	2.0	8.0	6.0	6.0	17.8	17.6	19.2	35.0	3.5	30.5	0.5	7.2	3.6	21.6	1.0	0.2	30.8	0.9
2	-0.4	-	SC-SM	Cohesionless	3.5	14.0	16.0	12.0	6.0	19.2	20.0	-	2.0	31.5	1.5	36.0	36.0	108.0	0.5	0.2	100.0	0.9
3	-3.9	-	CL	Cohesive	10.0	17.0	16.0	16.0	17.8	18.4	20.0	100.0	10.0	30.5	0.5	19.2	9.6	57.6	1.0	0.2	116.8	0.9
4	-13.9	-	SC-GC	Cohesionless	9.0	32.0	23.0	32.0	13.6	20.0	21.6	-	3.0	37.0	7.0	43.5	43.5	130.5	0.5	0.2	100.0	0.9
5	-22.9	-	CH	Cohesive	9.0	19.0	19.0	19.0	23.8	18.4	20.0	105.0	10.5	29.5	0.0	20.9	10.5	62.7	1.0	0.2	316.2	0.9
6	-31.9	-	SM-SC	Cohesionless	7.5	22.0	11.0	22.0	6.6	19.2	20.0	-	2.0	33.0	3.0	30.0	30.0	90.0	0.5	0.2	100.0	0.9
7	-39.4	-	CL	Cohesive	8.5	20.0	20.0	20.0	22.3	18.4	20.0	115.0	11.5	30.0	0.0	22.4	11.2	67.2	1.0	0.2	478.7	0.9
8	-47.9	-	SC-GC	Cohesionless	3.0	28.0	13.0	28.0	8.5	19.2	20.0	-	3.0	35.0	5.0	32.5	32.5	97.5	0.5	0.2	100.0	0.9
9	-50.9	-	CL	Cohesive	7.5	33.0	33.0	33.0	19.4	18.4	20.0	195.0	19.5	30.0	0.0	38.3	19.1	114.8	1.0	0.2	588.7	0.9
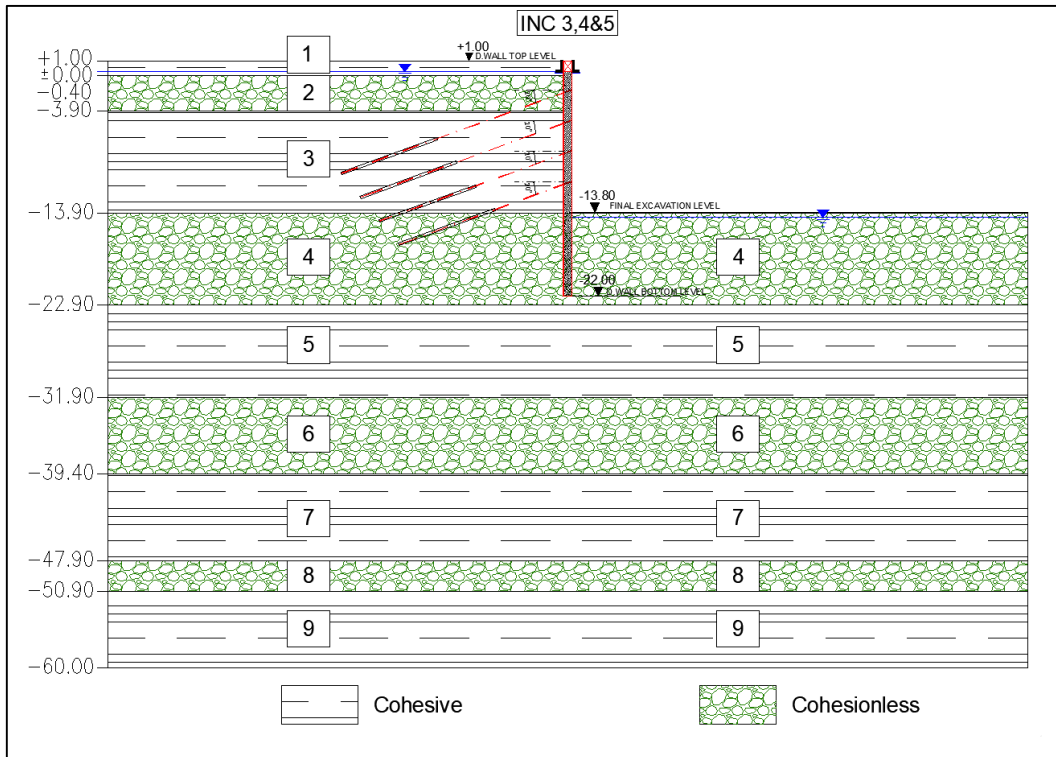
Figure A. 141. Section 1 – 1

Table A. 31. Section Properties of 1 – 1

SECTION 1 - 1									
Diaphragm Wall			**SBMA Type Anchor**				**Excavation Properties**		
Top Level (m)	Bottom Level (m)	Length (m)	Anchor No	Anchor Level (m)	Anchor Length (m)	Horizontal Spacing (m)	Top Level (m)	Bottom Level (m)	Depth (m)
1.00	-22.00	23.00	1	-1.80	24.00	2.00	1.00	-13.80	14.80
			2	-4.80	22.00	2.00			
			3	-7.80	20.00	2.00			
			4	-10.80	18.00	2.00			

INK-3 – Estimated and Measured Displacements
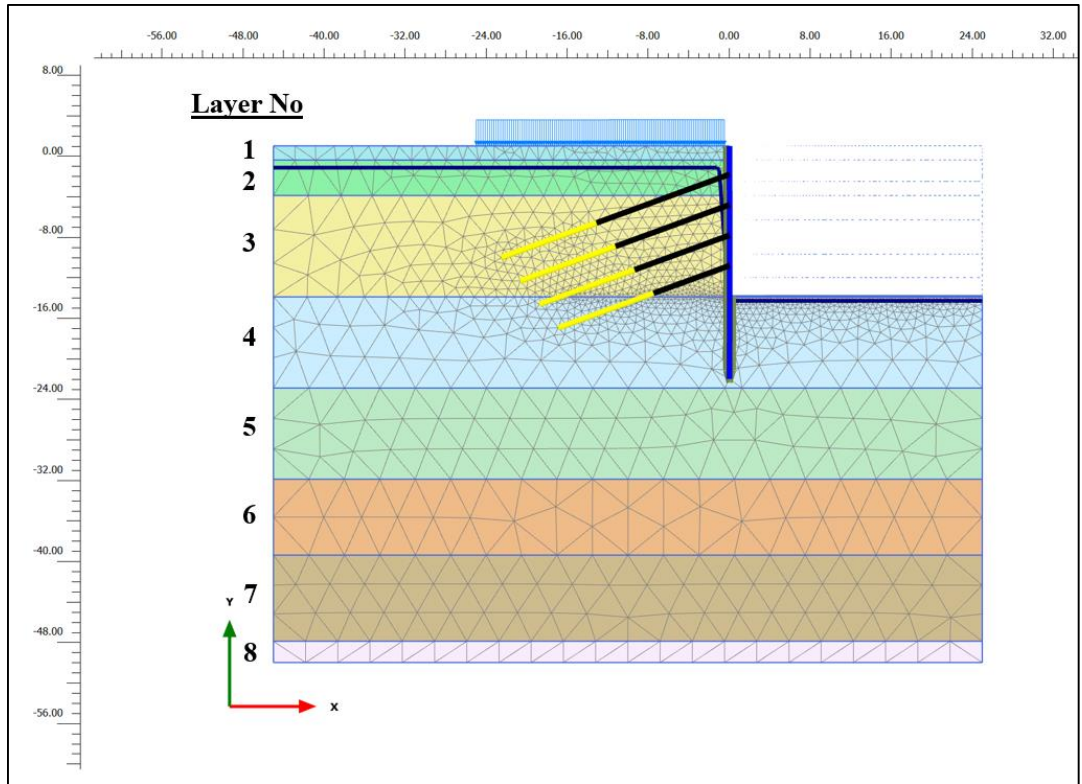
Figure A. 142. Meshed Model for INK-3
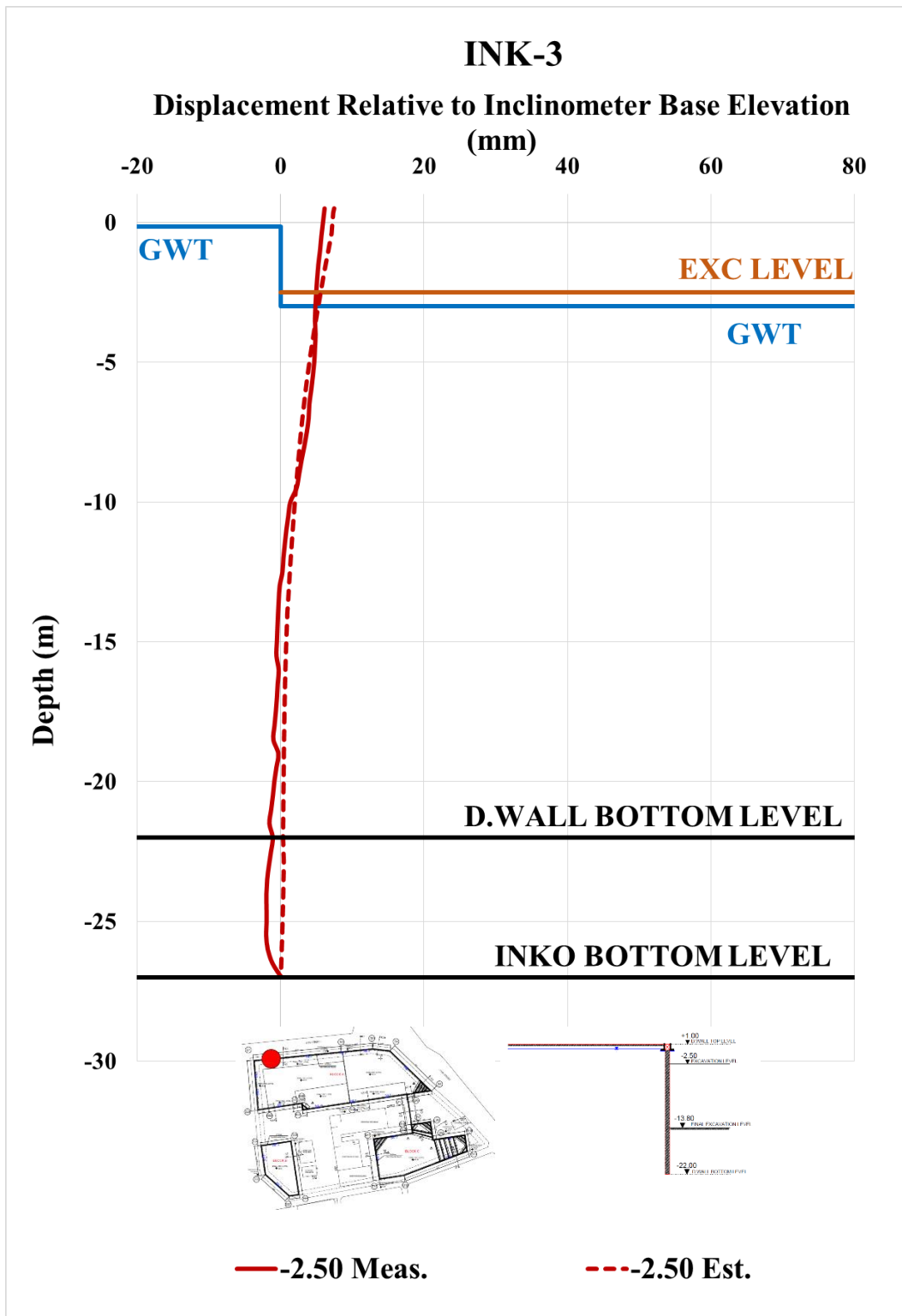
Figure A. 143. Estimated and Measured Displ. Rel. to Inc. Base Elev. at -2.50 m
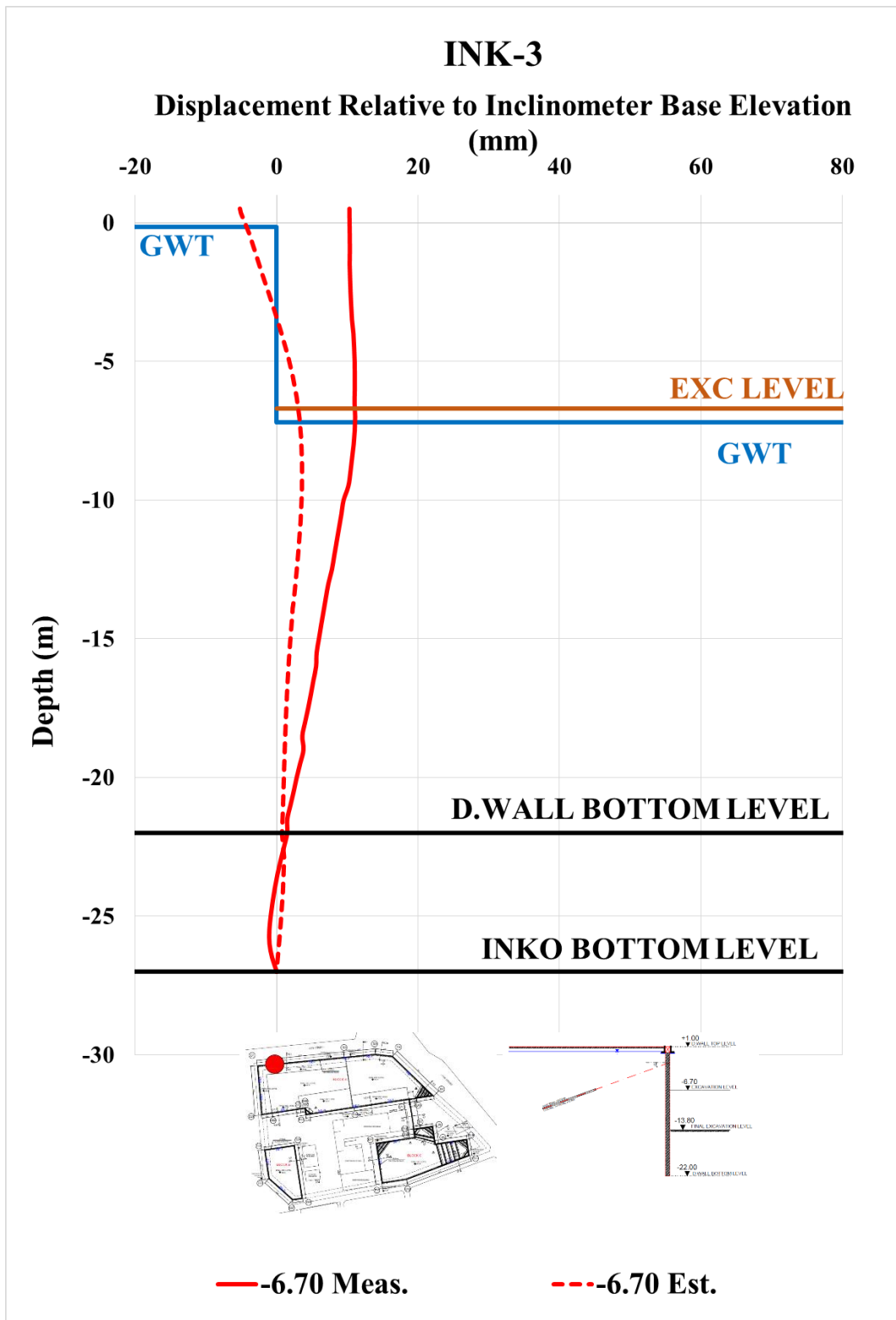
Figure A. 144. Estimated and Measured Displ. Rel. to Inc. Base Elev. at -6.70 m
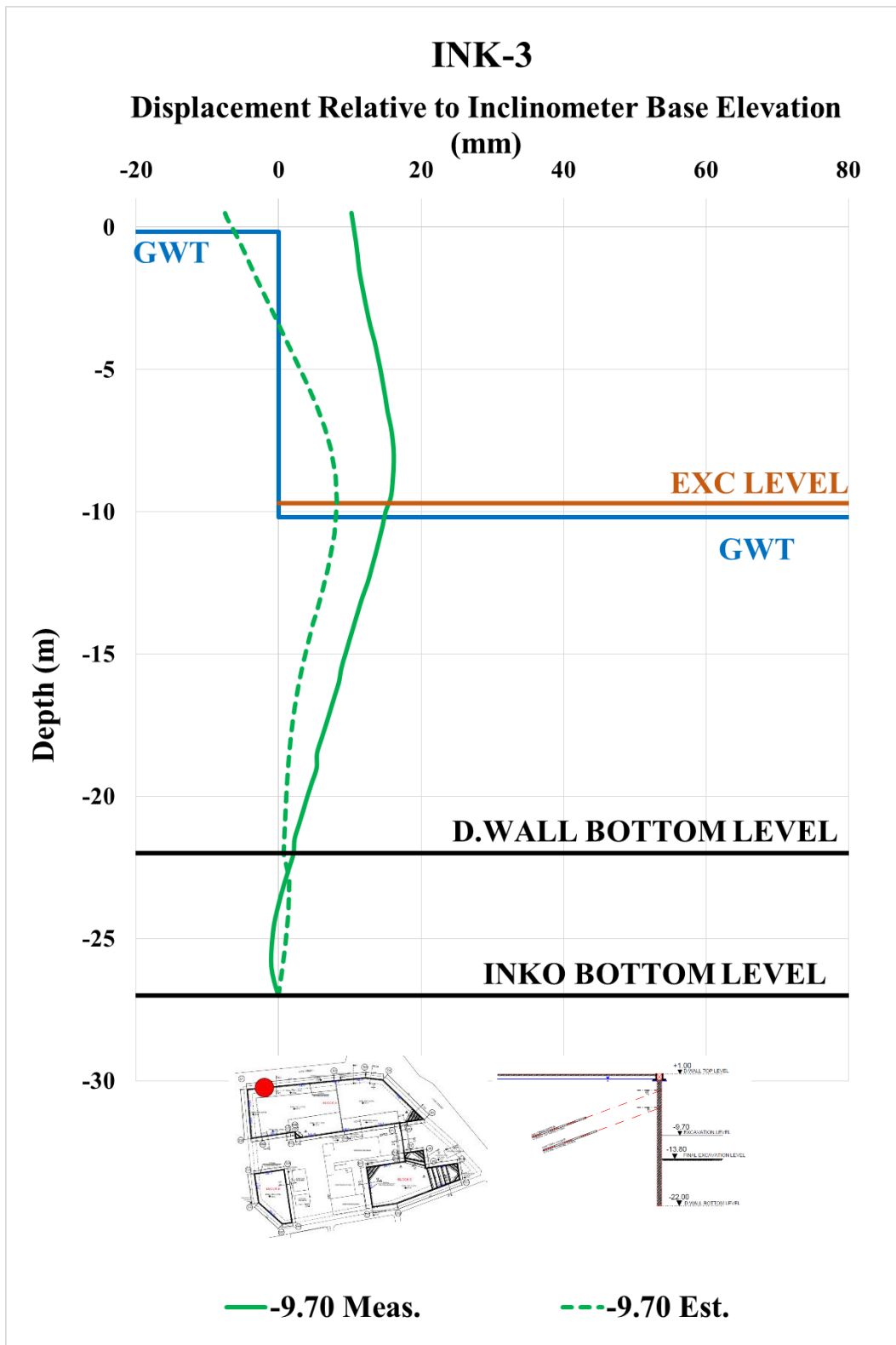
Figure A. 145. Estimated and Measured Displ. Rel. to Inc. Base Elev. at -9.70 m
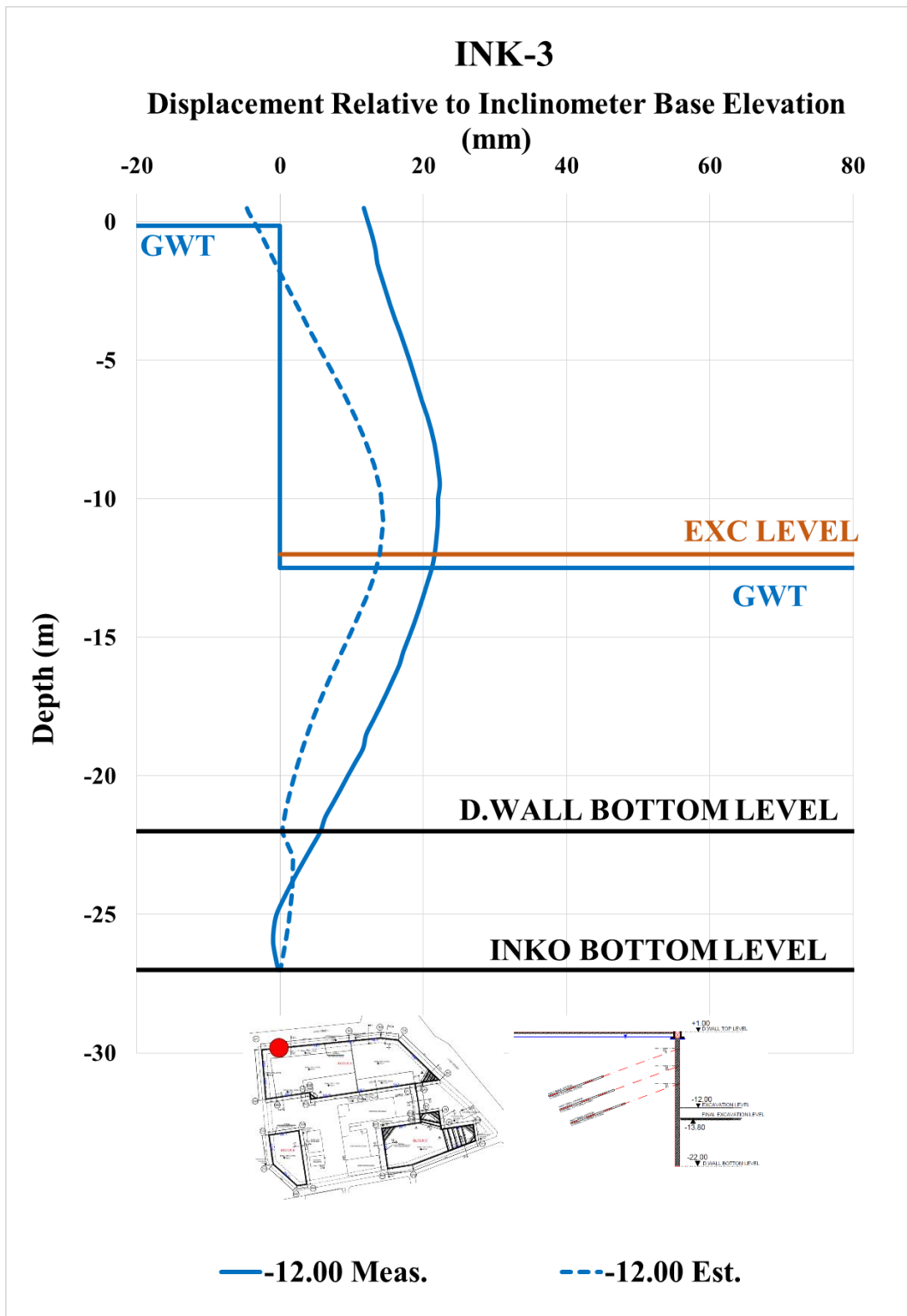
Figure A. 146. Estimated and Measured Displ. Rel. to Inc. Base Elev. at -12.00 m
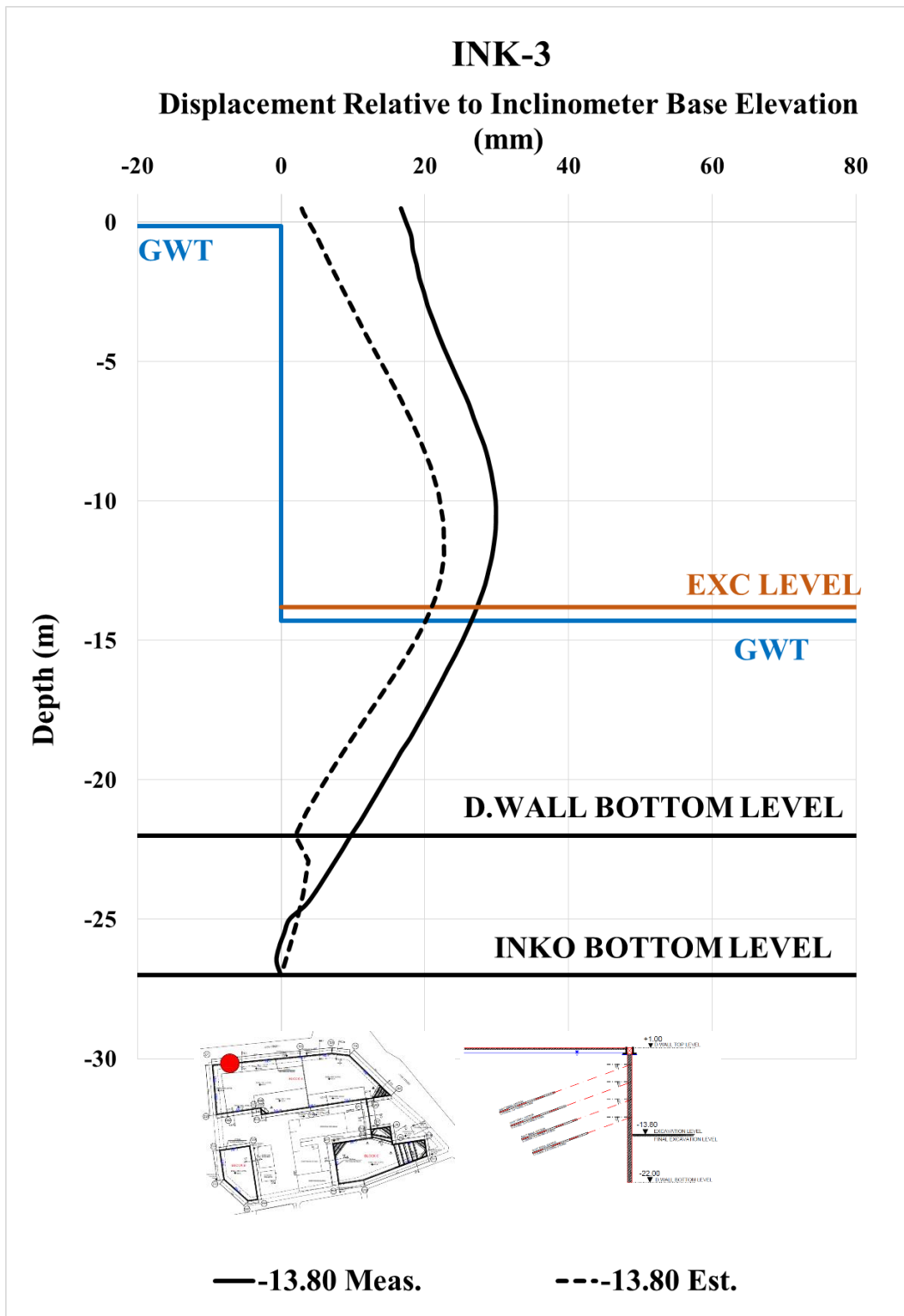
Figure A. 147. Estimated and Measured Displ. Rel. to Inc. Base Elev. at -13.80 m

Table A. 32. Internal Forces of Diaphragm Wall

INK - 3 / Section 1-1					
Excvation Stage	1	2	3	4	5
Excavation Level (m)	-2,50	-6,70	-9,70	-12,00	-13,80
N_{max} (kN/m)	85,29	238,50	418,50	581,50	718,40
V_{max} (kN/m)	36,80	243,30	317,90	346,20	346,20
M_{max} (kN.m/m)	75,10	449,40	810,40	1011,00	1057,00

Legend	Excvation Stage	1. Anchor Level	2. Excavation Level	2. Anchor Level	3. Excavation Level	3. Anchor Level	4. Excavation Level	4. Anchor Level	Final Excavation Level
	Measured Load of 1. Anchor Row (kN)	689.99	631.53	628.43	626.12	623.79	612.10	607.08	595.32
	Estimated Load of 1. Anchor Row (kN)	650.00	705.18	630.99	660.67	632.65	643.84	636.62	644.14
	Estimated Load of 2. Anchor Row (kN)	-	-	650.00	713.36	647.75	677.27	649.70	662.42
	Estimated Load of 3. Anchor Row (kN)	-	-	-	-	650.00	715.02	653.46	682.51
	Estimated Load of 4. Anchor Row (kN)	-	-	-	-	-	-	650.00	716.69
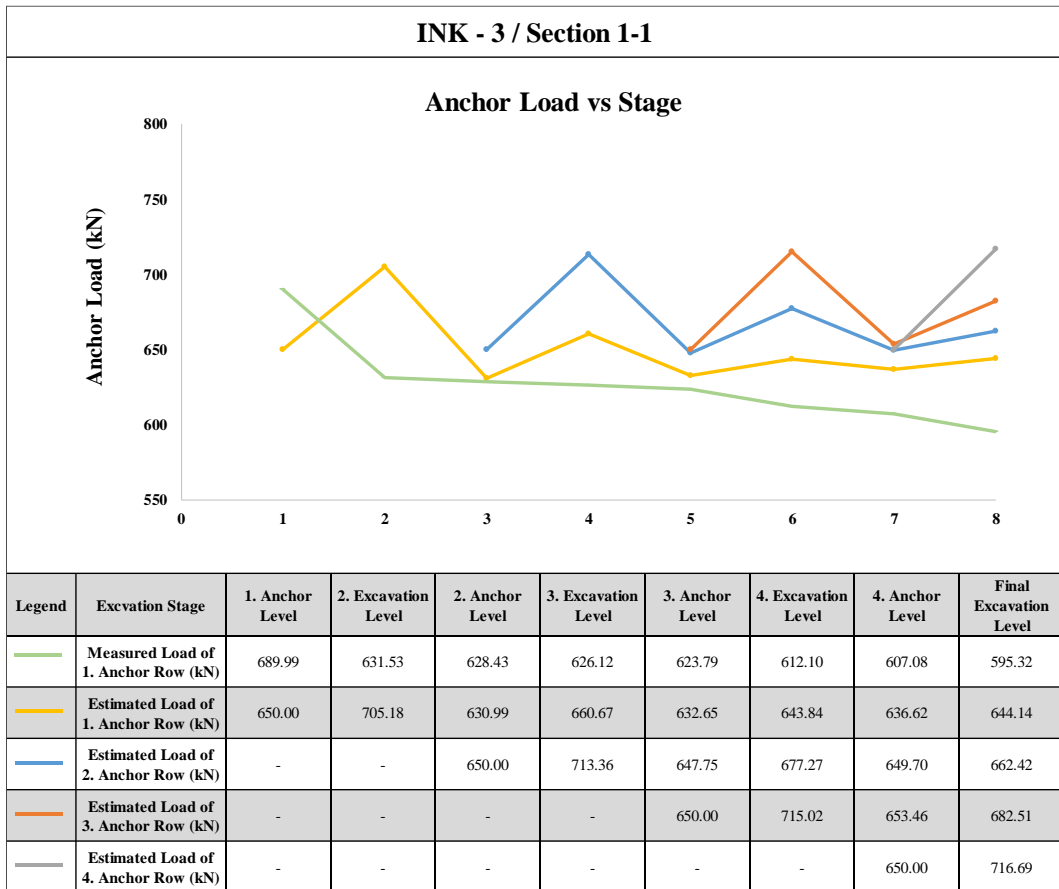
Figure A. 148. Measured and Estimated Anchor Loads

INK-4 – Estimated and Measured Displacements
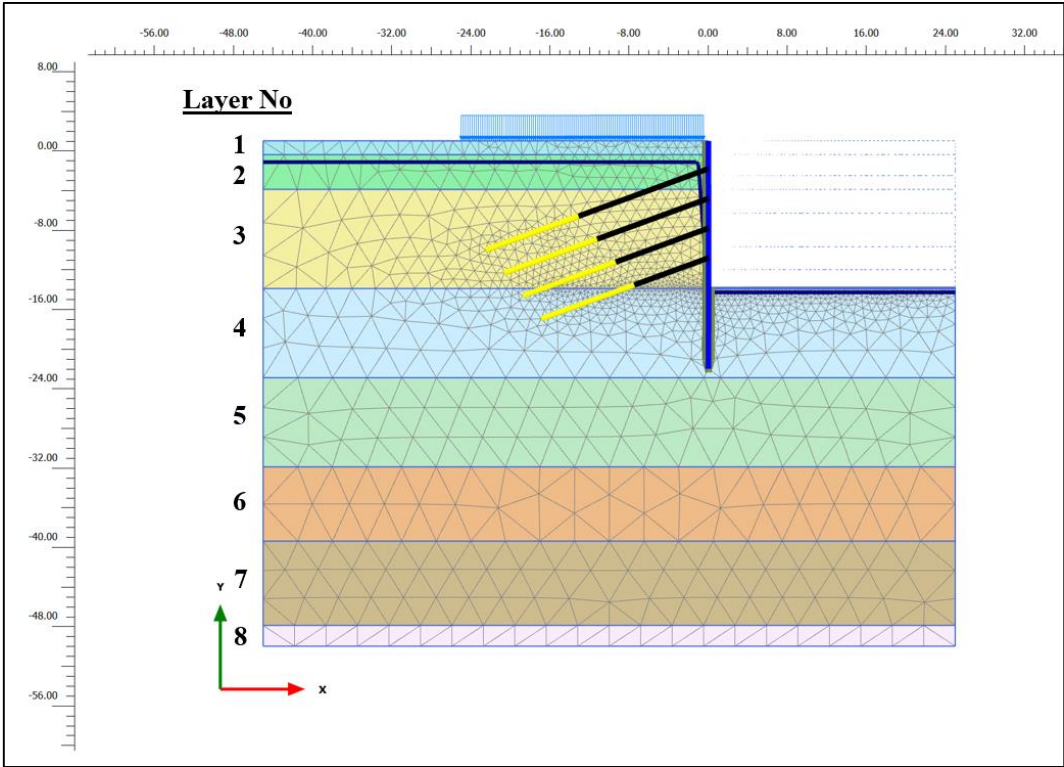
Figure A. 149. Meshed Model for INK-4
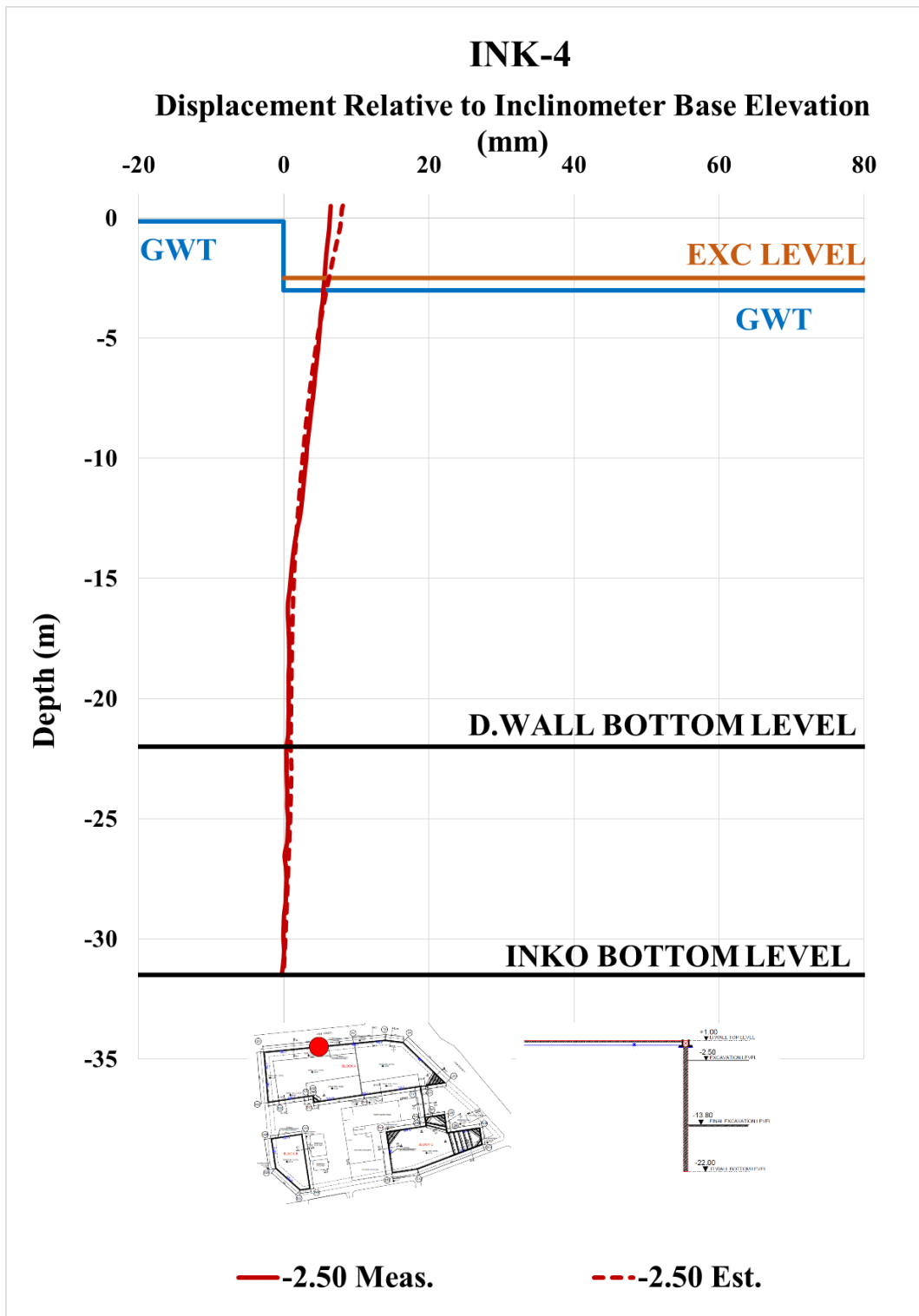
Figure A. 150. Estimated and Measured Displ. Rel. to Inc. Base Elev. at -2.50 m
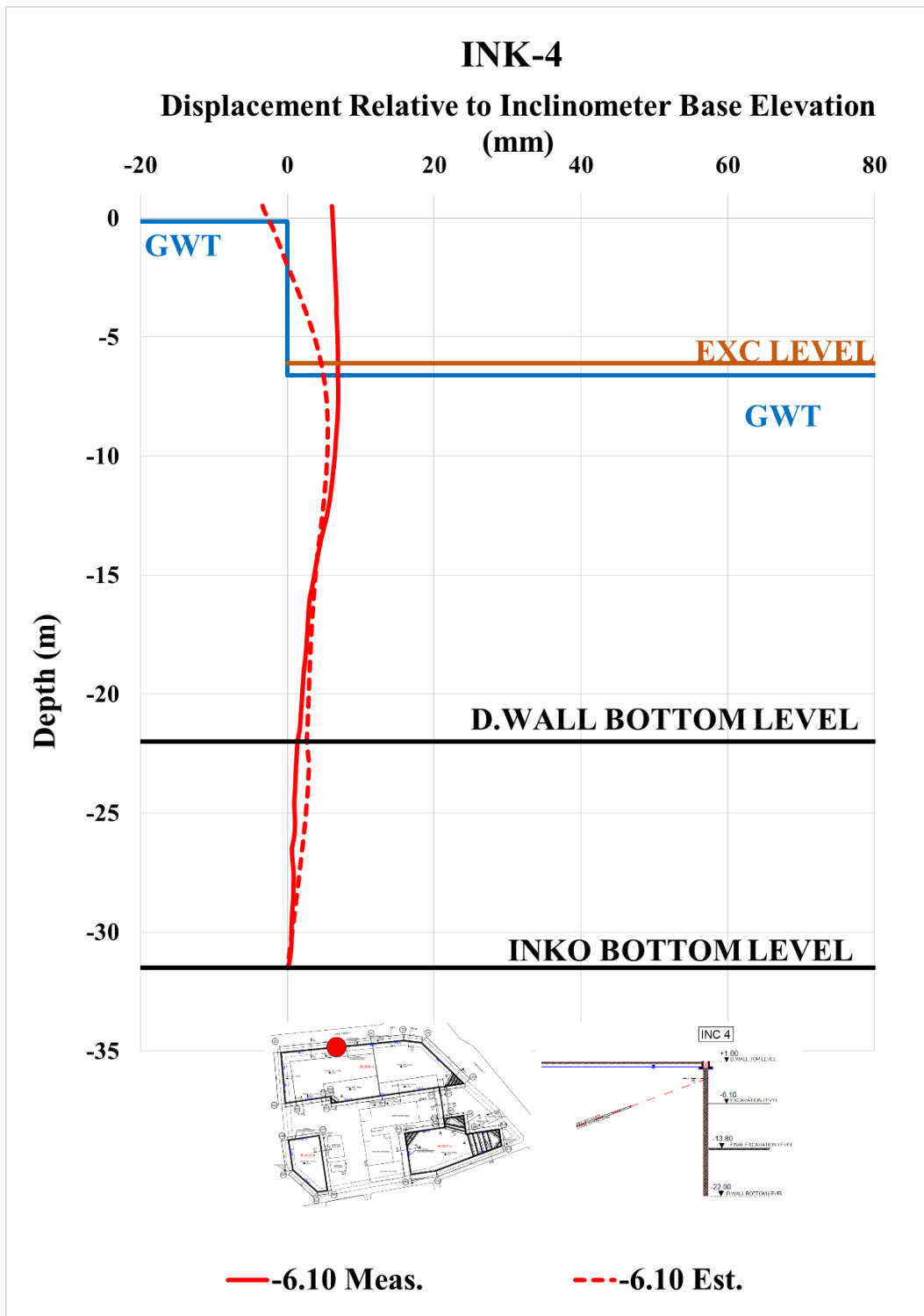
Figure A. 151. Estimated and Measured Displ. Rel. to Inc. Base Elev. at -6.10 m
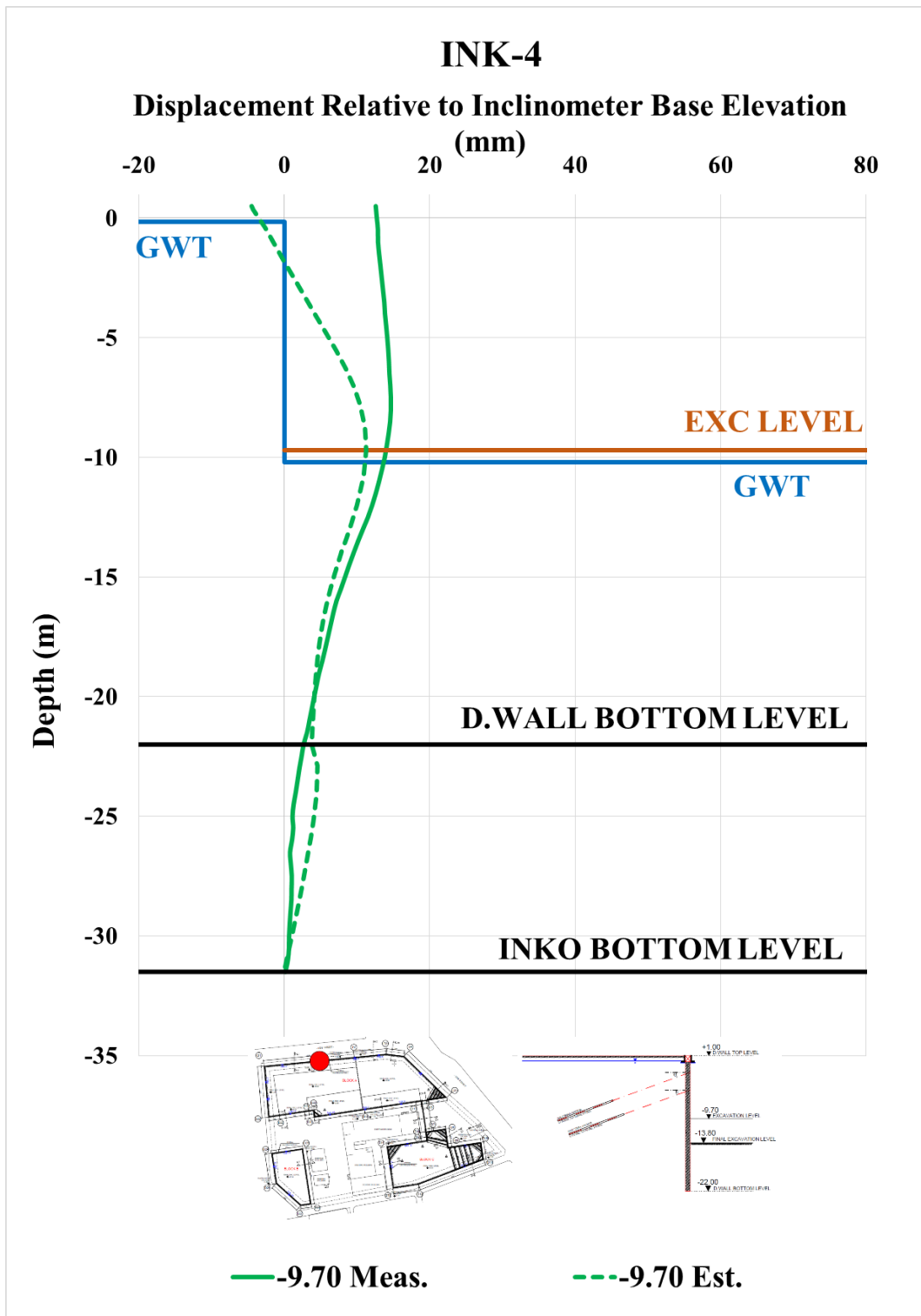
Figure A. 152. Estimated and Measured Displ. Rel. to Inc. Base Elev. at -9.70 m
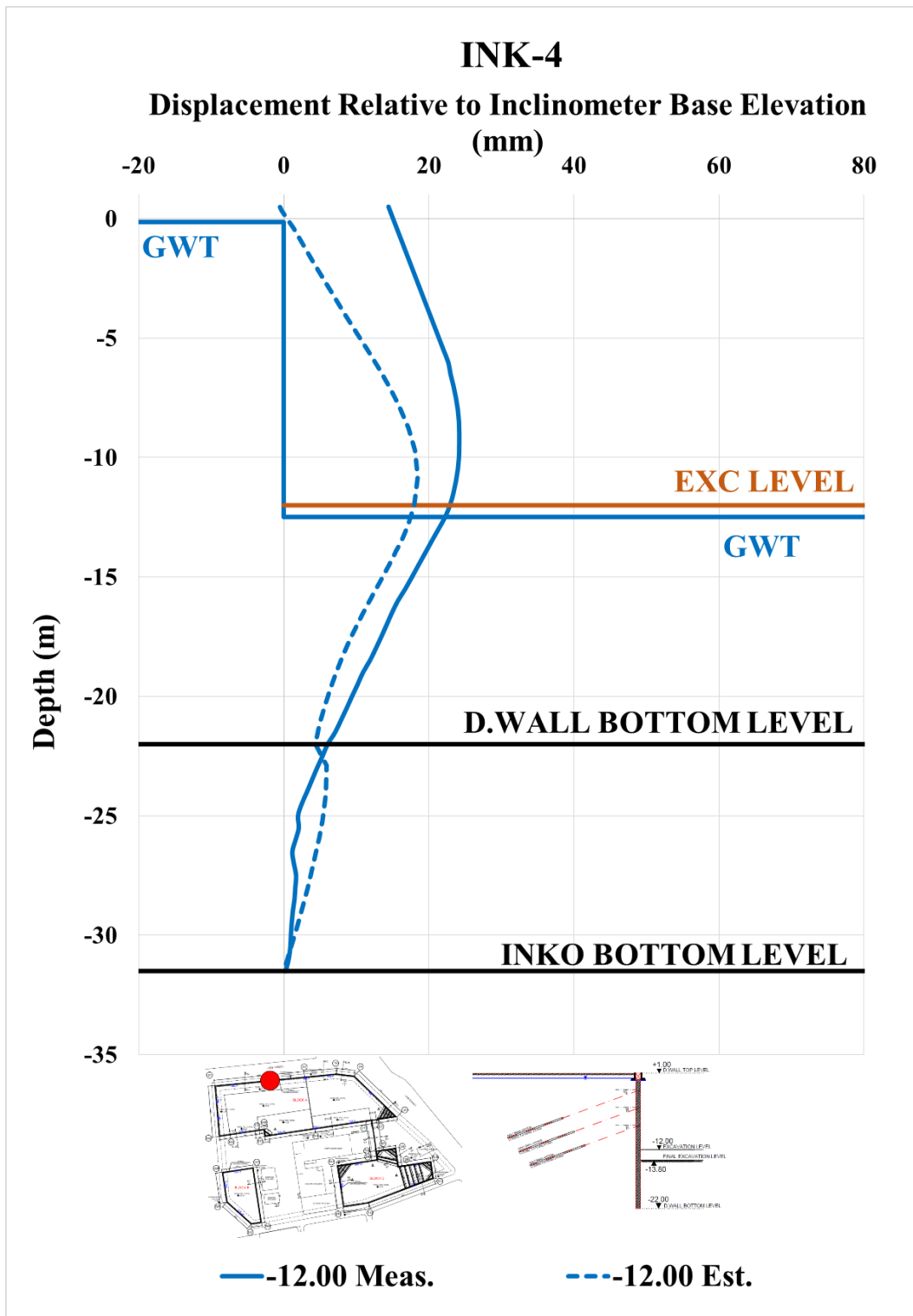
Figure A. 153. Estimated and Measured Displ. Rel. to Inc. Base Elev. at -12.00 m
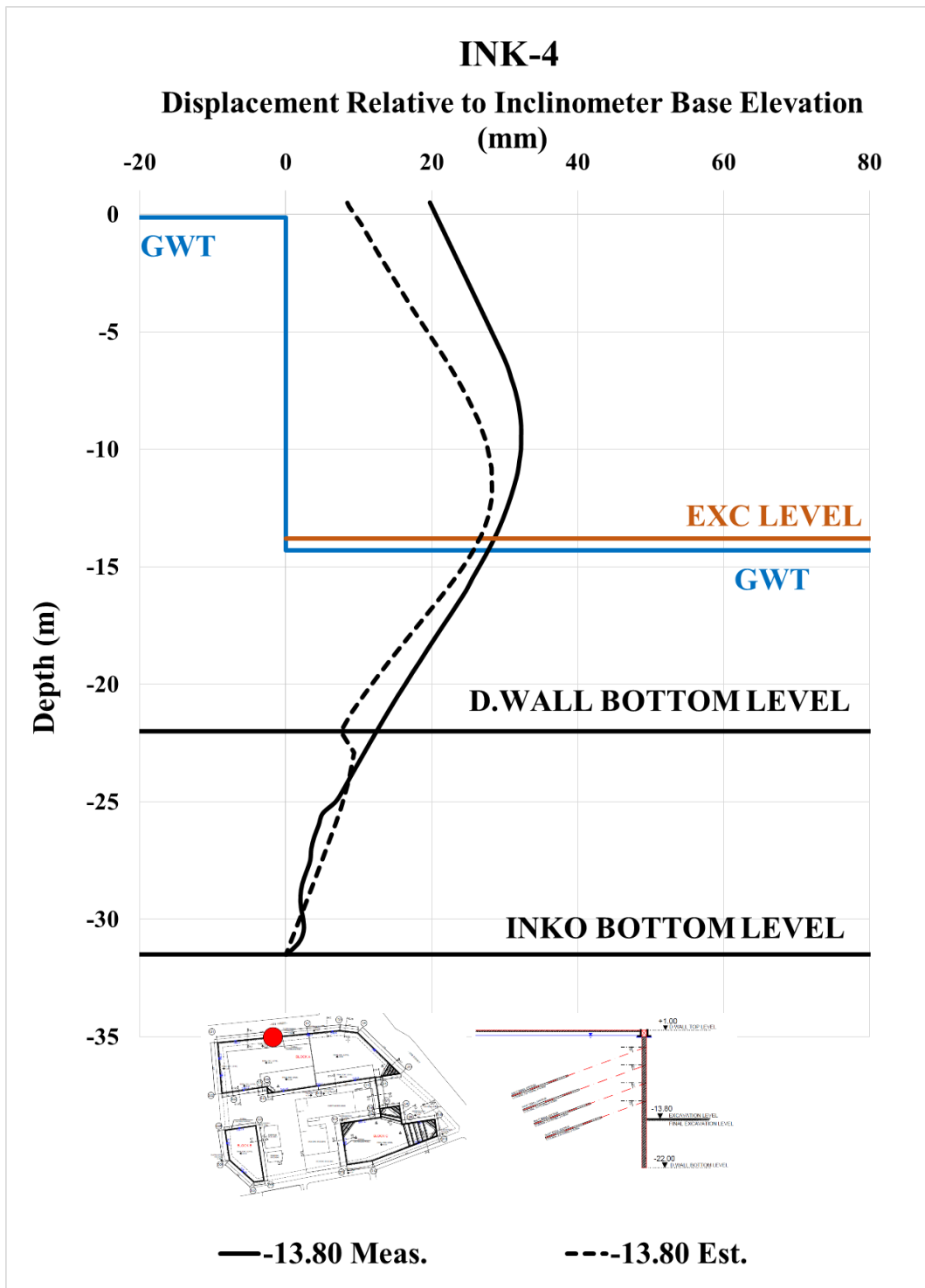
Figure A. 154. Estimated and Measured Displ. Rel. to Inc. Base Elev. at -13.80 m

Table A. 33. Internal Forces of Diaphragm Wall

INK - 4 / Section 1-1					
Excvation Stage	1	2	3	4	5
Excavation Level (m)	-2,50	-6,10	-9,70	-12,00	-13,80
N_{max} (kN/m)	82,61	213,90	416,60	579,90	709,50
V_{max} (kN/m)	37,44	232,40	312,90	322,10	332,10
M_{max} (kN.m/m)	77,50	366,60	760,30	908,20	938,00

Legend	Excvation Stage	1. Anchor Level	2. Excavation Level	2. Anchor Level	3. Excavation Level	3. Anchor Level	4. Excavation Level	4. Anchor Level	Final Excavation Level
	Measured Load of 1. Anchor Row (kN)	689.38	628.79	642.49	638.04	643.08	632.32	623.70	620.28
	Estimated Load of 1. Anchor Row (kN)	650.00	694.50	620.46	655.19	627.42	638.17	630.94	639.06
	Estimated Load of 2. Anchor Row (kN)	-	-	650.00	719.87	656.60	683.64	657.44	670.12
	Estimated Load of 3. Anchor Row (kN)	-	-	-	-	650.00	709.12	651.83	680.64
	Estimated Load of 4. Anchor Row (kN)	-	-	-	-	-	-	650.00	709.58

Figure A. 155. Measured and Estimated Anchor Loads

INK-5 – Estimated and Measured Displacements
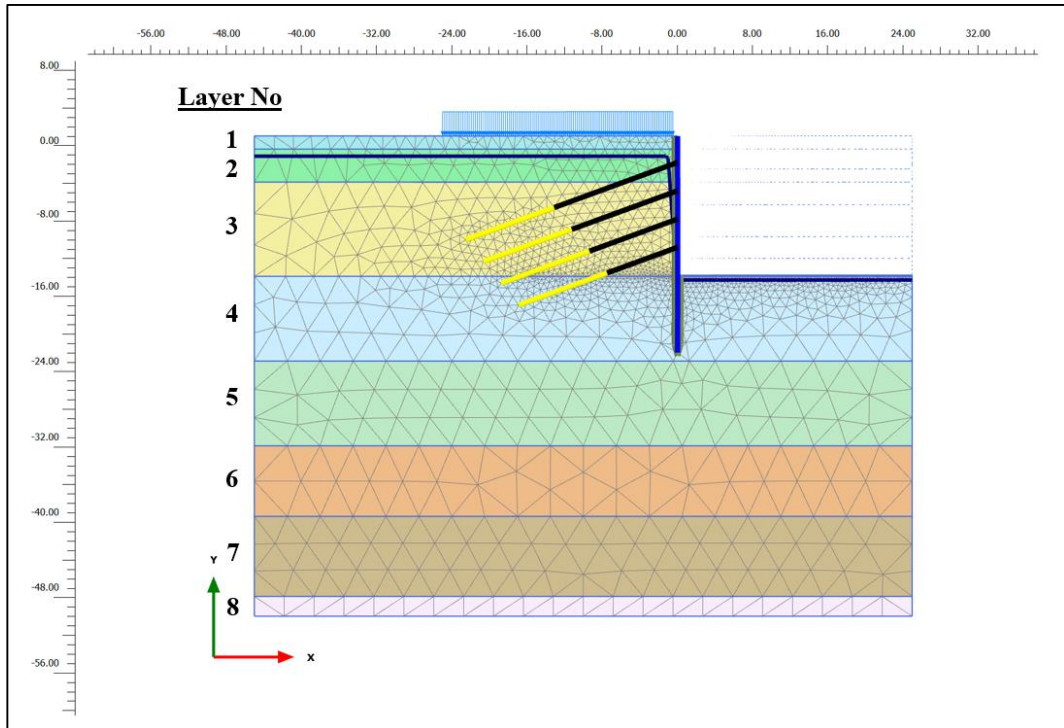
Figure A. 156. Meshed Model for INK-5
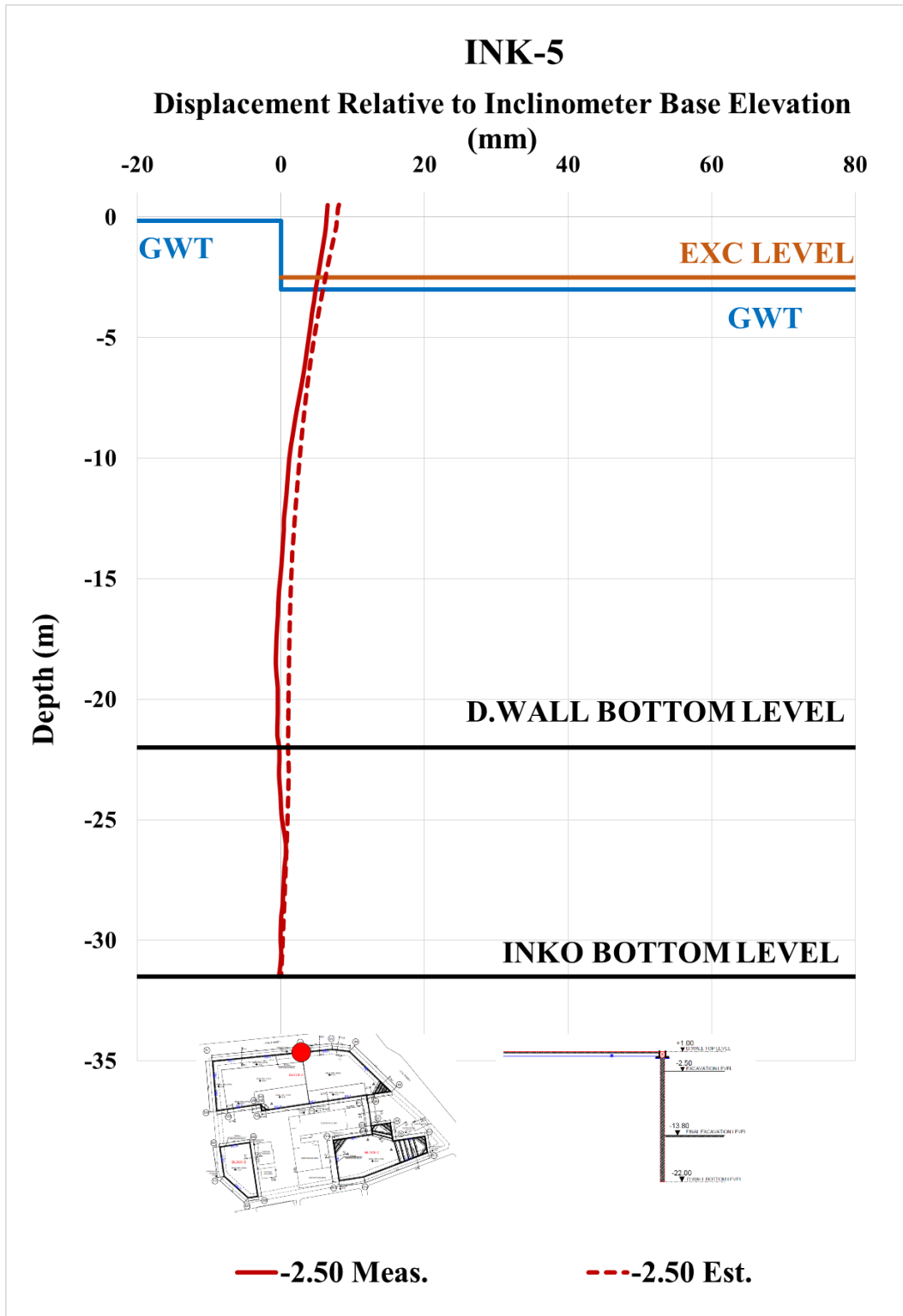
Figure A. 157. Estimated and Measured Displ. Rel. to Inc. Base Elev. at -2.50 m
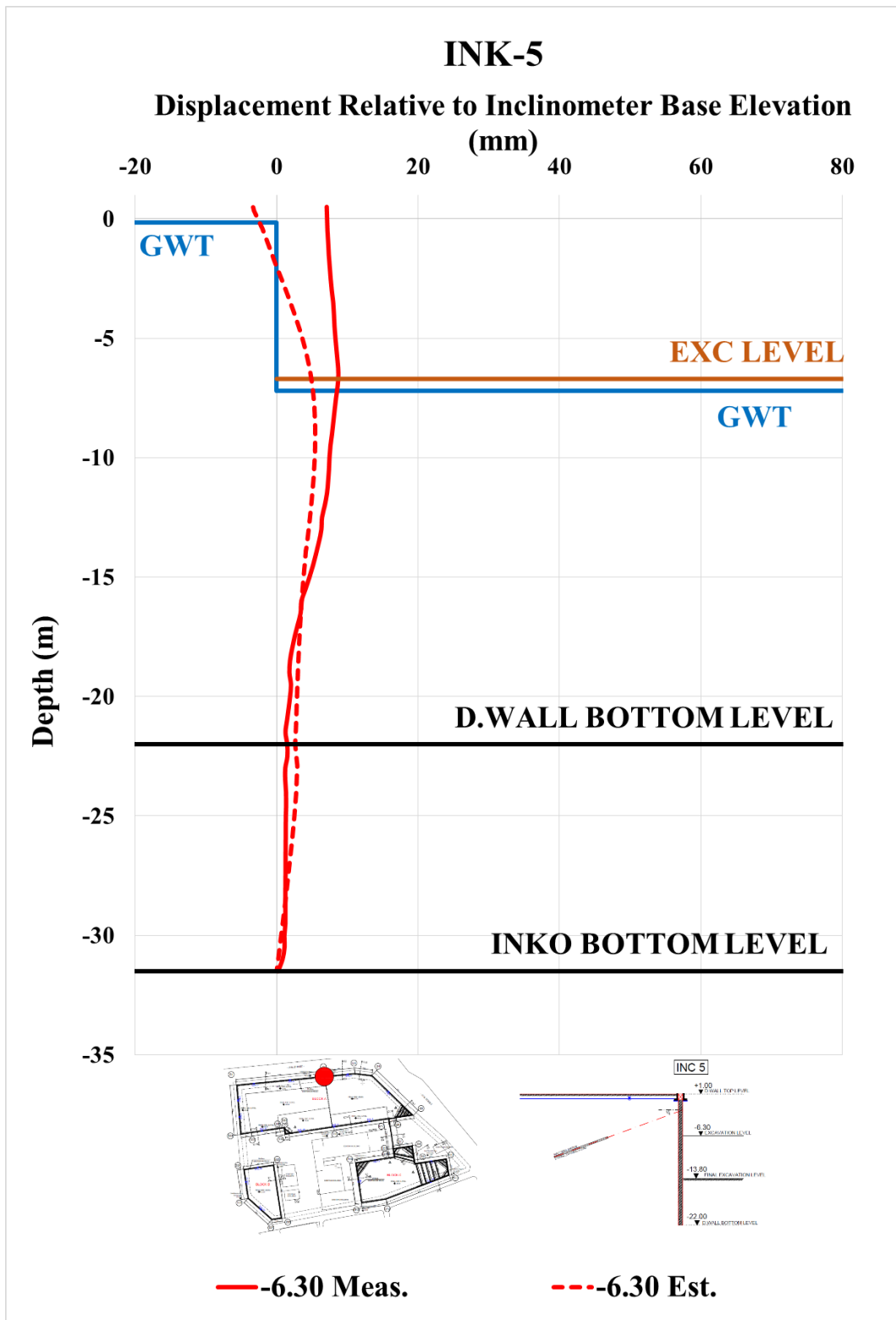
Figure A. 158. Estimated and Measured Displ. Rel. to Inc. Base Elev. at -6.30 m
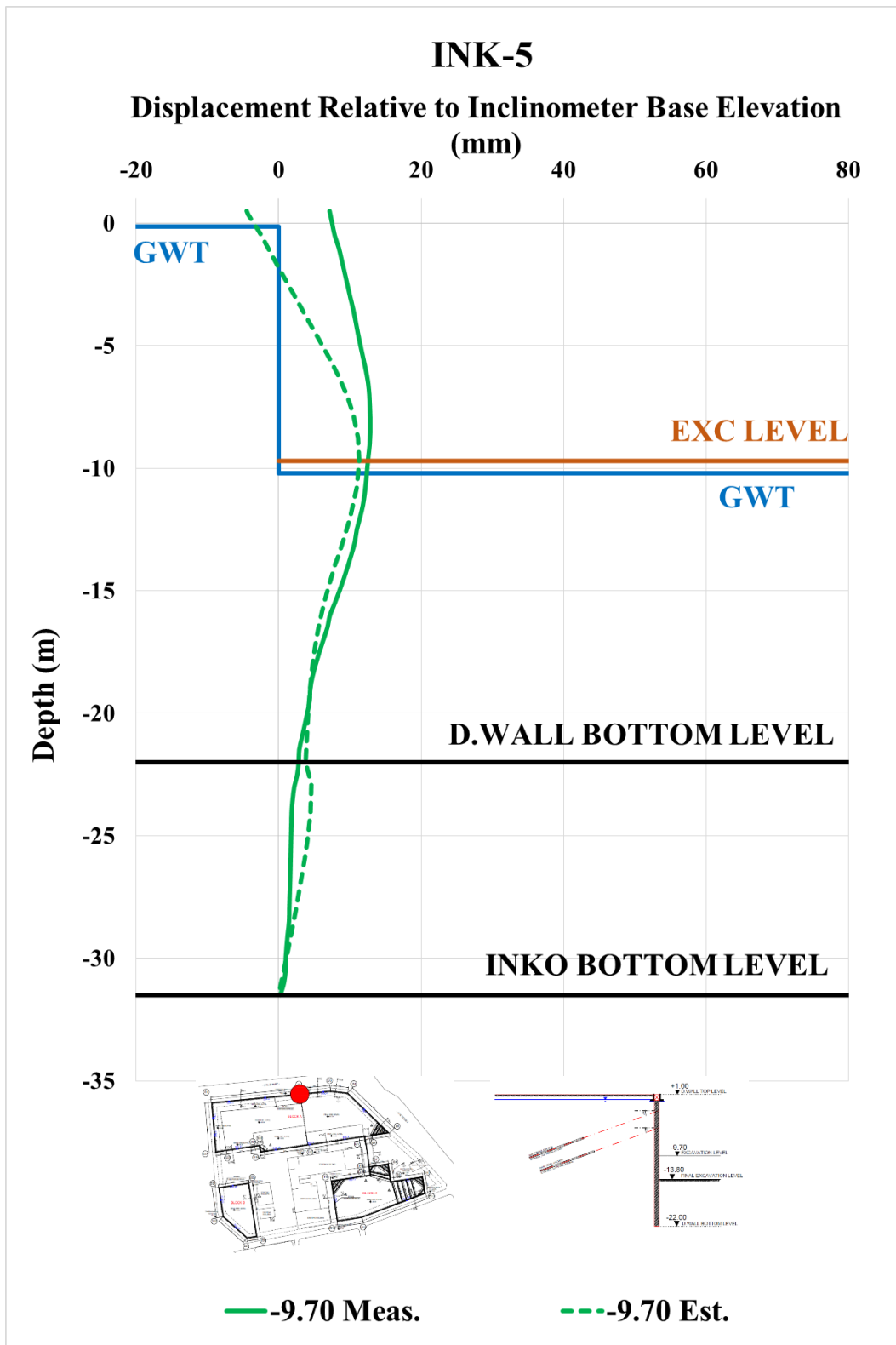
Figure A. 159. Estimated and Measured Displ. Rel. to Inc. Base Elev. at -9.70 m
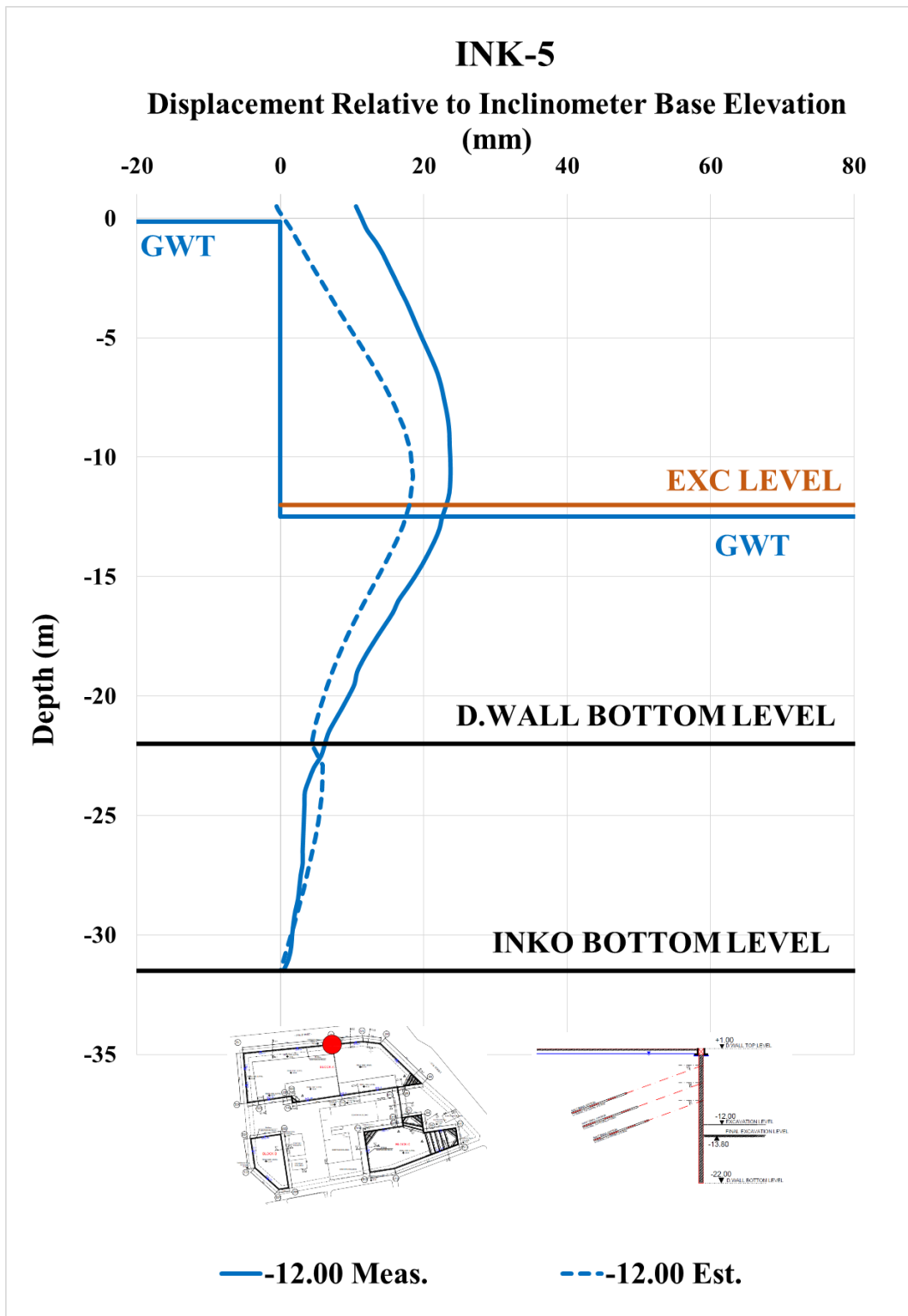
Figure A. 160. Estimated and Measured Displ. Rel. to Inc. Base Elev. at -12.00 m
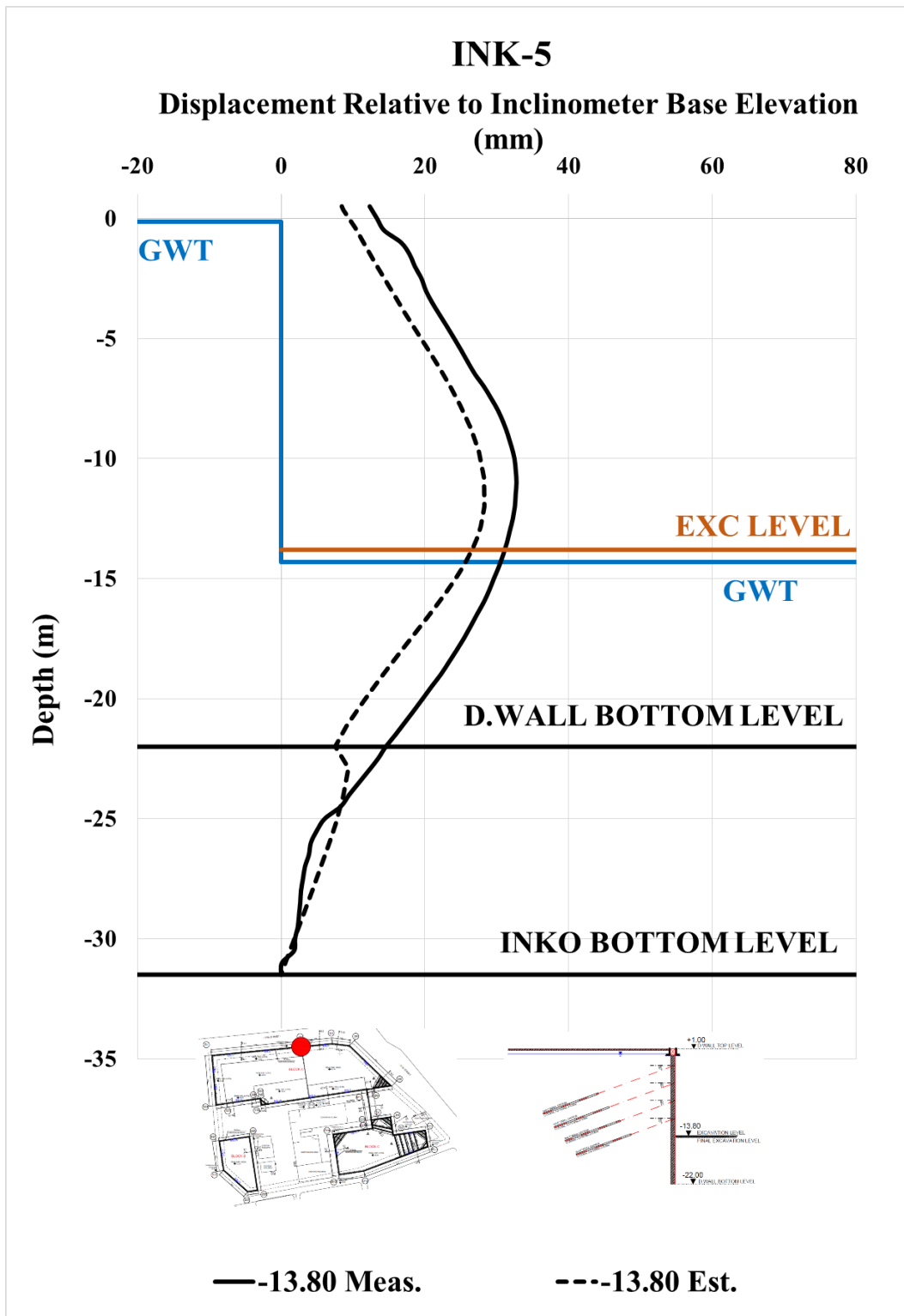
Figure A. 161. Estimated and Measured Displ. Rel. to Inc. Base Elev. at -13.80 m

Table A. 34. Internal Forces of Diaphragm Wall

INK - 5 / Section 1-1					
Excvation Stage	1	2	3	4	5
Excavation Level (m)	-2,50	-6,30	-9,70	-12,00	-13,80
N_{max} (kN/m)	82,83	219,40	410,20	573,80	703,10
V_{max} (kN/m)	36,72	233,30	308,20	330,80	330,80
M_{max} (kN.m/m)	75,84	383,30	739,00	896,60	925,50

INK - 5 / Section 1-1

Anchor Load vs Stage

Legend	Excvation Stage	1. Anchor Level	2. Excavation Level	2. Anchor Level	3. Excavation Level	3. Anchor Level	4. Excavation Level	4. Anchor Level	Final Excavation Level
	Measured Load of 1. Anchor Row (kN)	681.46	628.91	637.70	642.85	634.94	630.10	627.03	615.77
	Estimated Load of 1. Anchor Row (kN)	650.00	696.96	624.50	655.52	627.79	638.77	631.54	639.40
	Estimated Load of 2. Anchor Row (kN)	-	-	650.00	712.33	649.34	676.97	650.79	663.45
	Estimated Load of 3. Anchor Row (kN)	-	-	-	-	650.00	709.69	652.35	680.49
	Estimated Load of 4. Anchor Row (kN)	-	-	-	-	-	-	650.00	708.21

Figure A. 162. Measured and Estimated Anchor Loads

INK-3 – Calibrated, Estimated and Measured Displacements
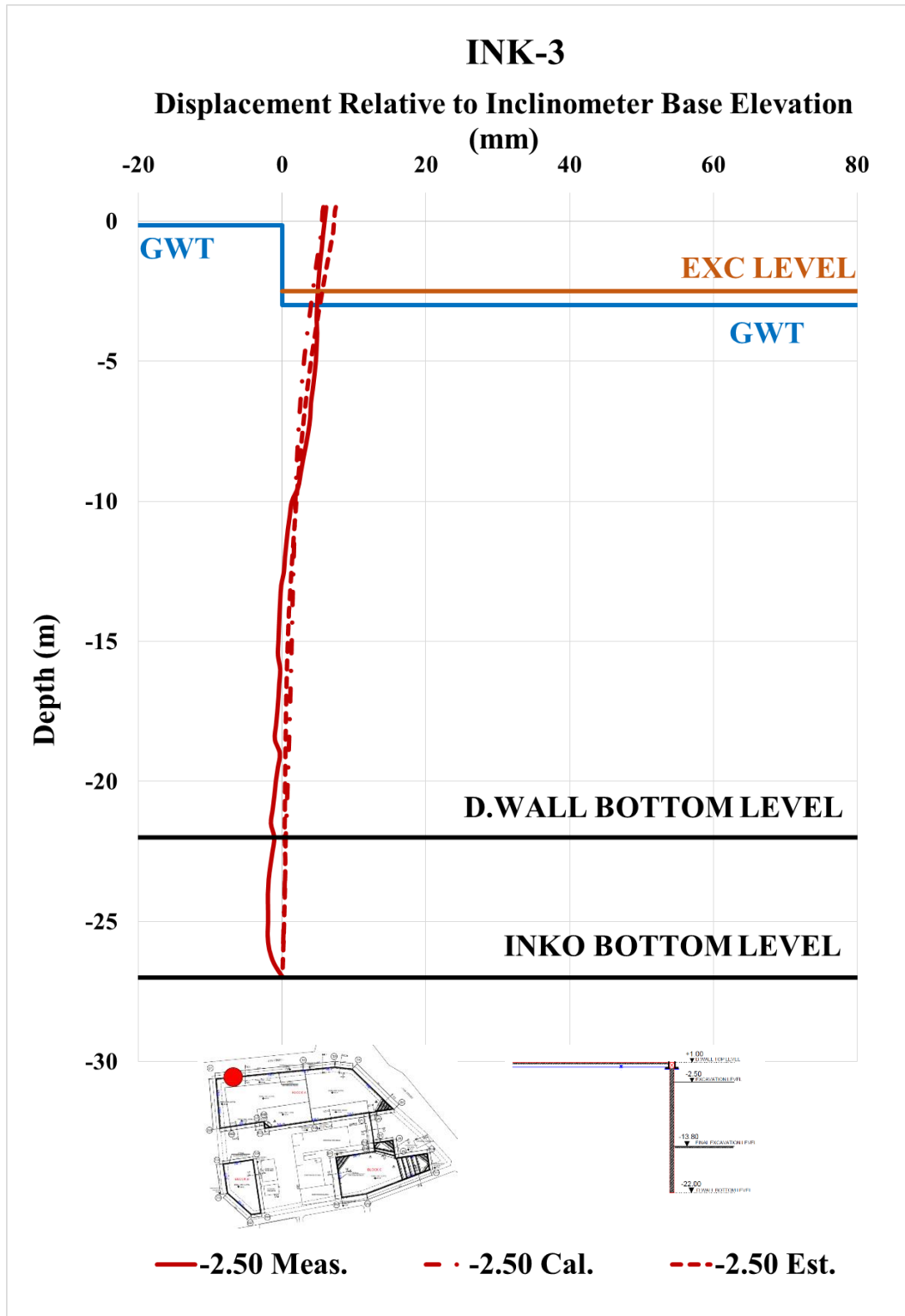
Figure A. 163. Calibrated and Measured Displ. Rel. to Inc. Base Elev. at -2.50 m
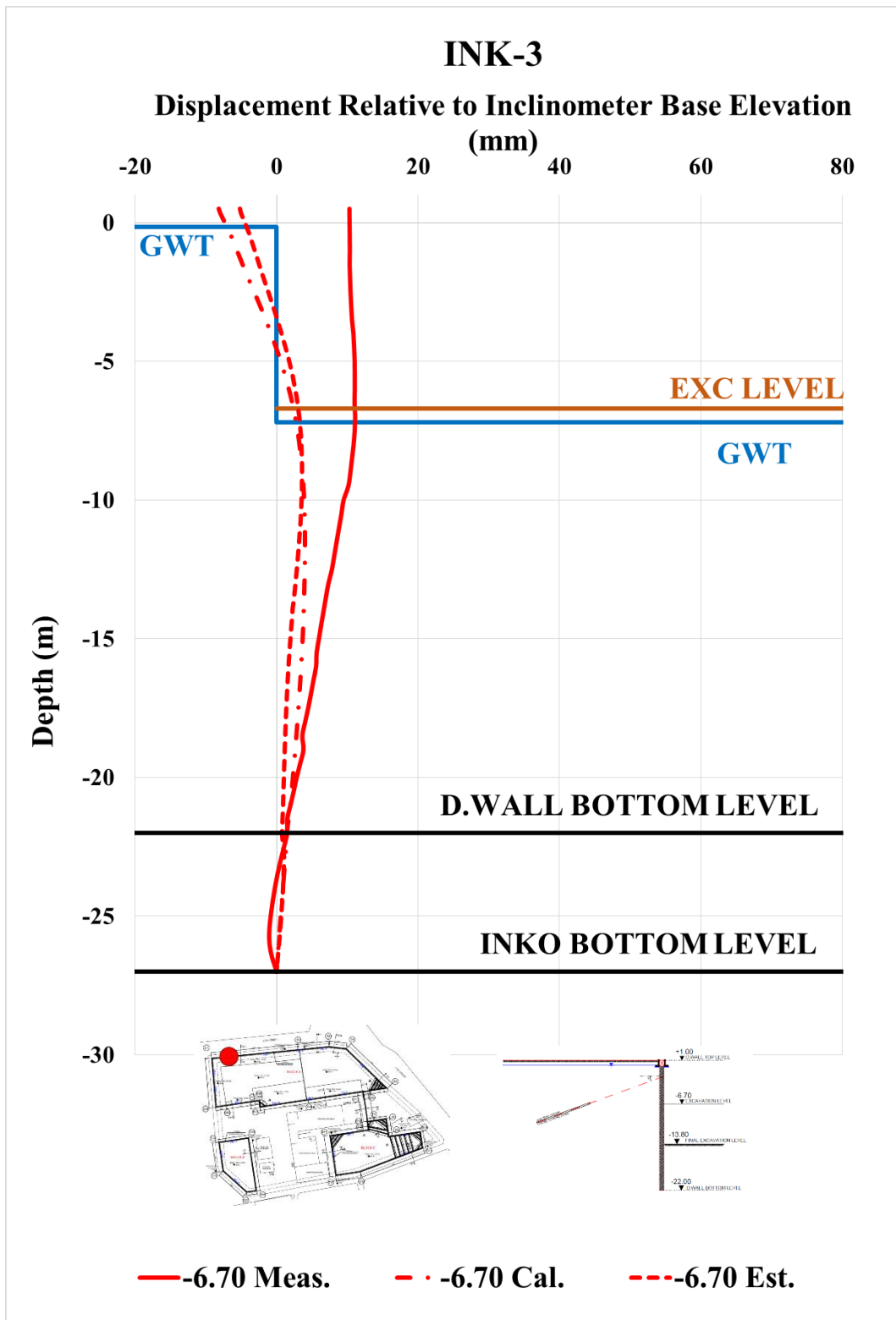
Figure A. 164. Calibrated and Measured Displ. Rel. to Inc. Base Elev. at -6.70 m
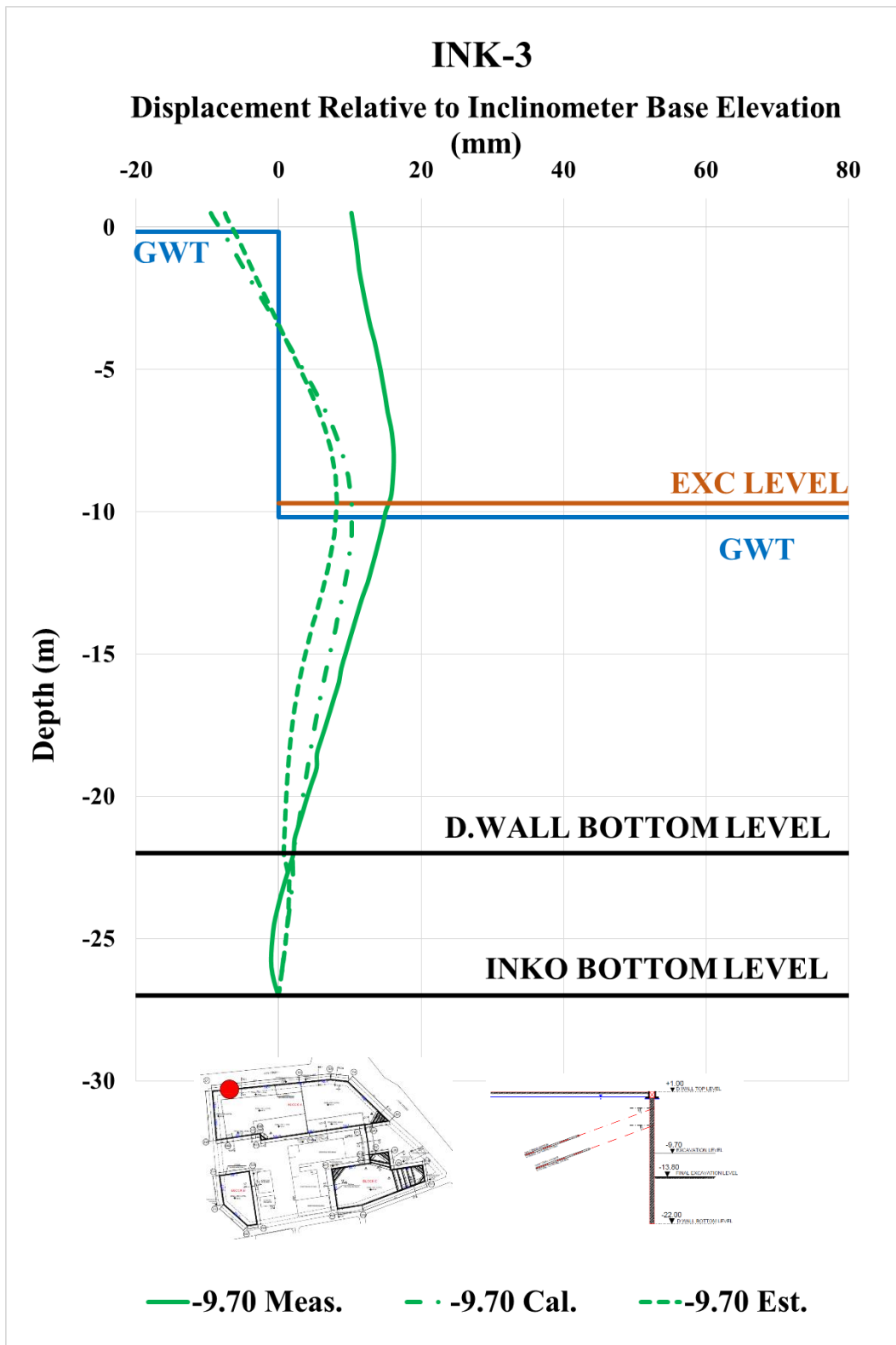
Figure A. 165. Calibrated and Measured Displ. Rel. to Inc. Base Elev. at -9.70 m
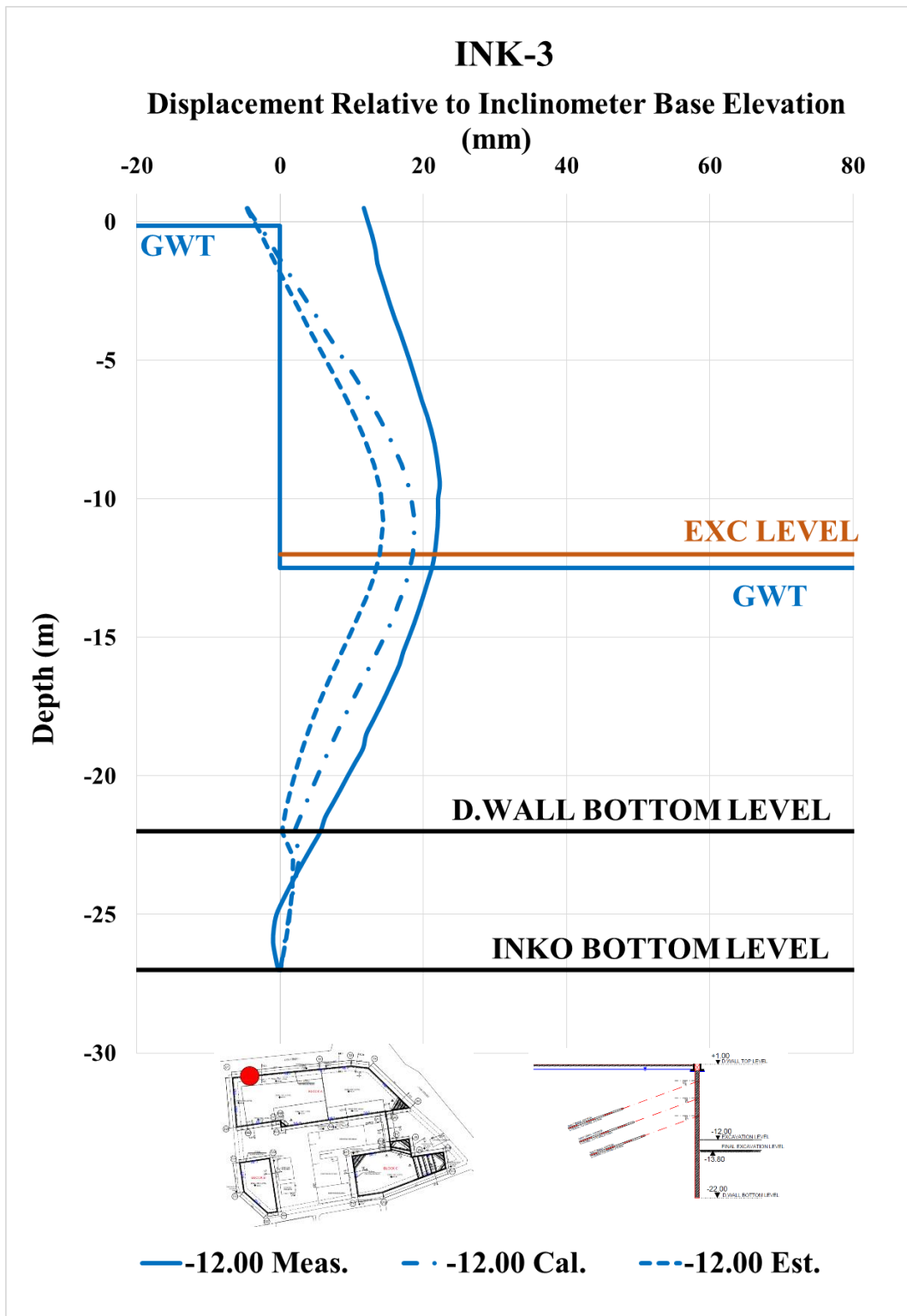
Figure A. 166. Calibrated and Measured Displ. Rel. to Inc. Base Elev. at -12.00 m
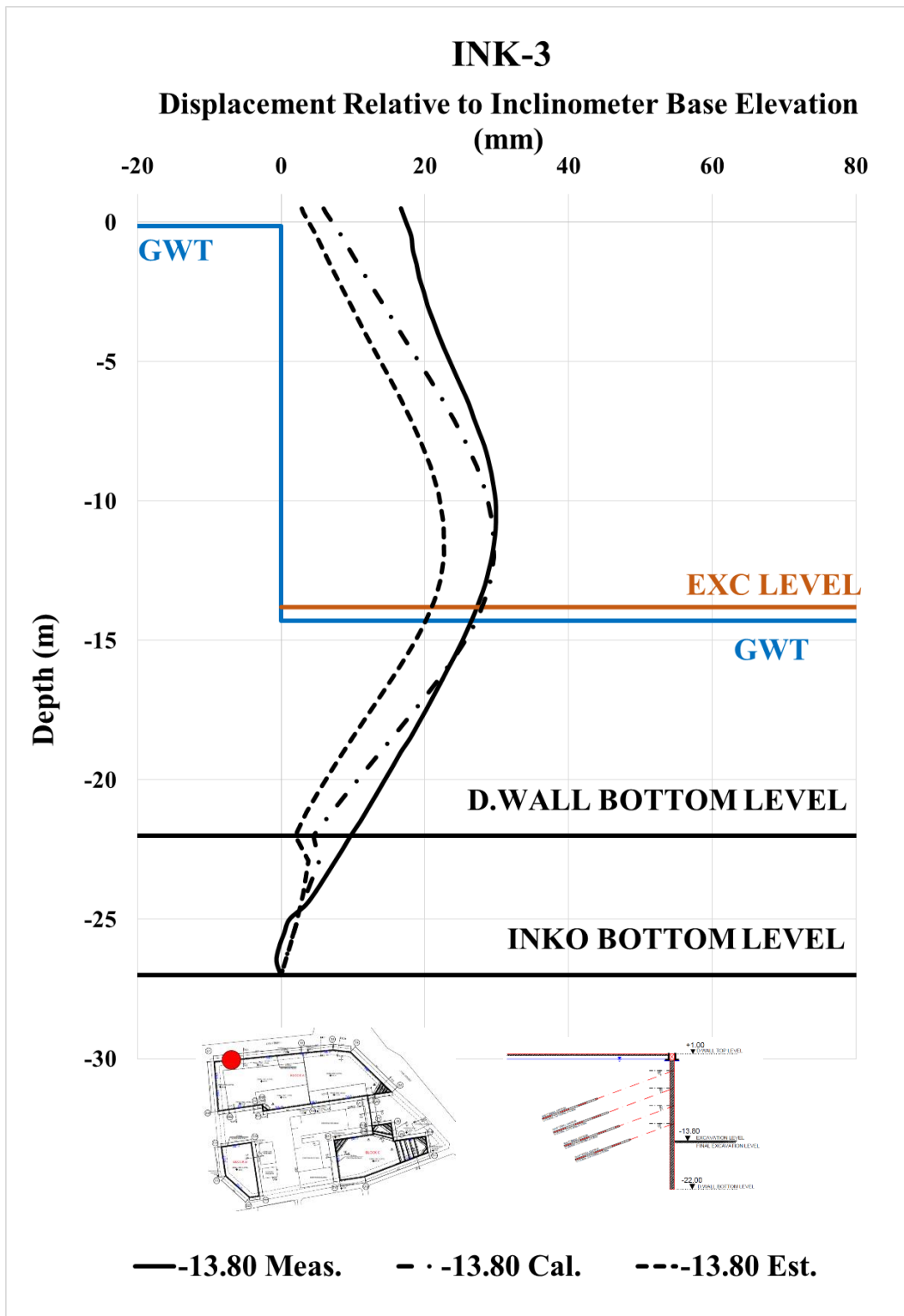
Figure A. 167. Calibrated and Measured Displ. Rel. to Inc. Base Elev. at -13.80 m

Table A. 35. Internal Forces of Diaphragm Wall

INK - 3 / Section 1-1					
Excvation Stage	1	2	3	4	5
Excavation Level (m)	-2,50	-6,70	-9,70	-12,00	-13,80
N_{max} (kN/m)	85,29	238,50	418,50	581,50	718,40
V_{max} (kN/m)	36,80	243,30	317,90	346,20	346,20
M_{max} (kN.m/m)	75,10	449,40	810,40	1011,00	1057,00

Legend	Excvation Stage	1. Anchor Level	2. Excavation Level	2. Anchor Level	3. Excavation Level	3. Anchor Level	4. Excavation Level	4. Anchor Level	Final Excavation Level
	Measured Load of 1. Anchor Row (kN)	689.99	631.53	628.43	626.12	623.79	612.10	607.08	595.32
	Estimated Load of 1. Anchor Row (kN)	650.00	694.23	622.20	653.95	628.17	639.61	634.29	643.07
	Estimated Load of 2. Anchor Row (kN)	-	-	650.00	713.24	654.96	682.29	658.55	671.11
	Estimated Load of 3. Anchor Row (kN)	-	-	-	-	650.00	709.47	654.97	682.76
	Estimated Load of 4. Anchor Row (kN)	-	-	-	-	-	-	650.00	710.94

Figure A. 168. Measured and Estimated Anchor Loads

Table A. 36. Summary of Displacement Results of INK-3

INK - 3 / SECTION 1 - 1

Excavation Level (m)	Excavation Depth (m)	u_{meas} (mm) Inclinometer Measurements	u_{est} (mm) Estimation with Plaxis 2D Analysis	u_{cal} (mm) Calibration with Plaxis 2D Analysis	$u_{literature}$ (mm) FHWA-IF-99-015 (1999) - Maksimum	$u_{literature}$ (mm) FHWA-IF-99-015 (1999) - Average	$u_{literature}$ (mm) Goldberg et al. (1976)	$u_{literature}$ (mm) Clough et al. (1990) - Maksimum	$u_{literature}$ (mm) Clough et al. (1990) - Average	$u_{literature}$ (mm) Long (2001)	$u_{literature}$ (mm) Long (2001) (Extraordinary cases eliminated)	$u_{literature}$ (mm) Long (2001) Cantilever System
-2.50	3.50	6.12	7.47	5.71	17.50	7.00	17.50	17.50	7.00	6.65	4.90	12.6
-6.70	7.70	11.08	3.64	4.03	38.50	15.40	38.50	38.50	15.40	14.63	10.78	-
-9.70	10.70	16.15	8.22	10.25	53.50	21.40	53.50	53.50	21.40	20.33	14.98	-
-12.00	13.00	22.27	14.38	18.76	65.00	26.00	65.00	65.00	26.00	24.70	18.20	-
-13.80	14.80	29.89	22.72	29.66	74.00	29.60	74.00	74.00	29.60	28.12	20.72	-
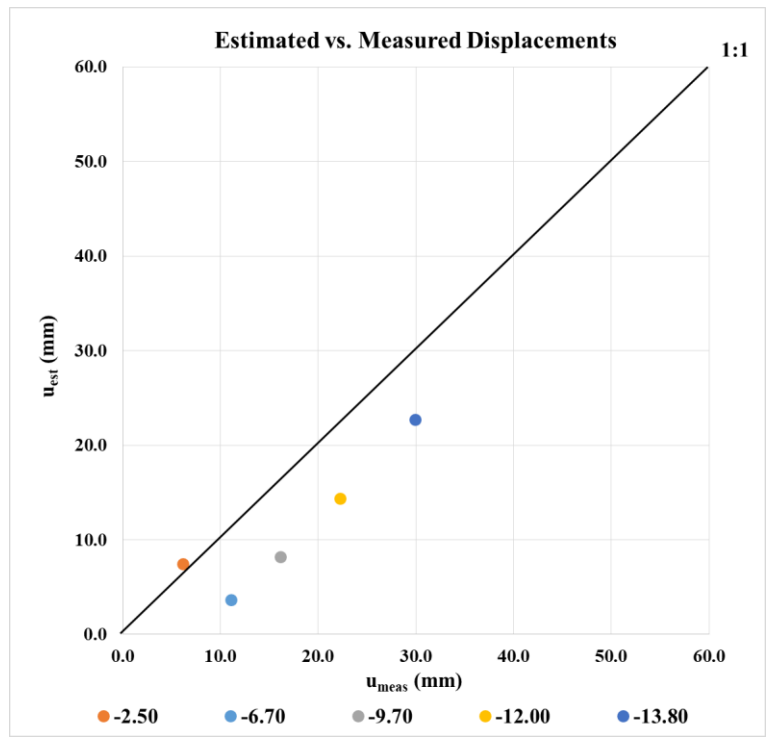
Figure A. 169. Estimated and Measured Displacements of INK - 3
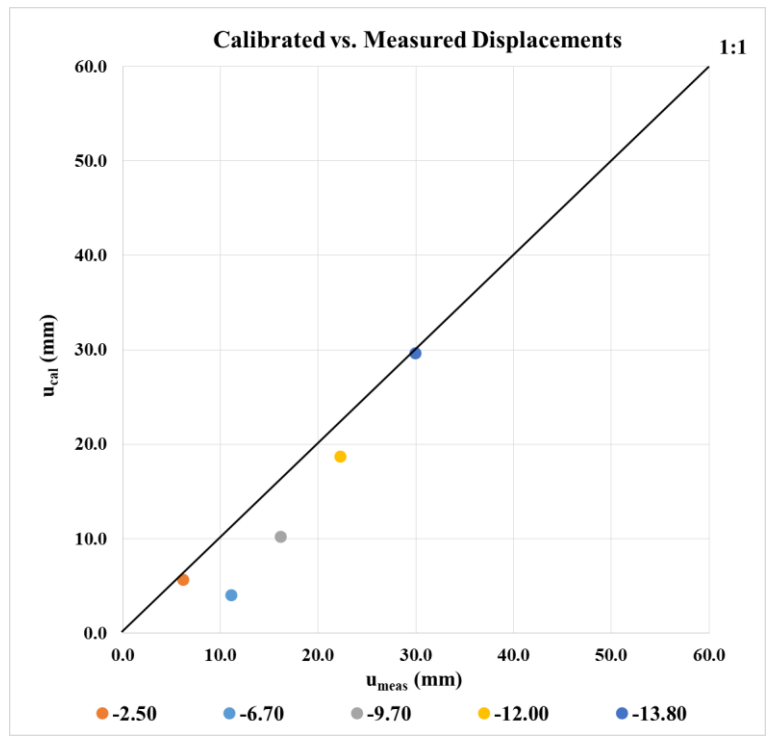
Figure A. 170. Calibrated and Measured Displacements of INK - 3

INK-4 – Calibrated, Estimated and Measured Displacements
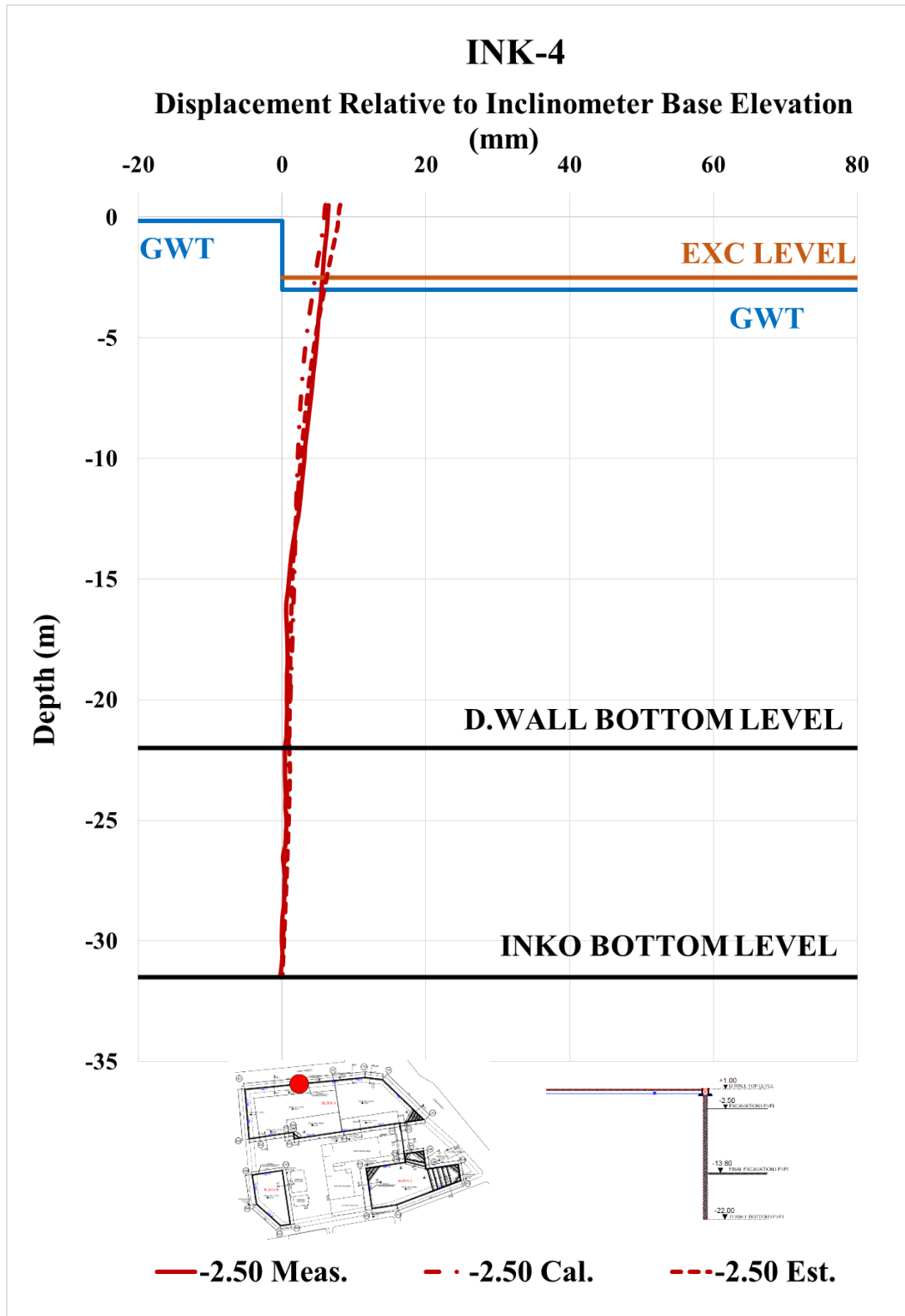
Figure A. 171. Calibrated and Measured Displ. Rel. to Inc. Base Elev. at -2.50 m
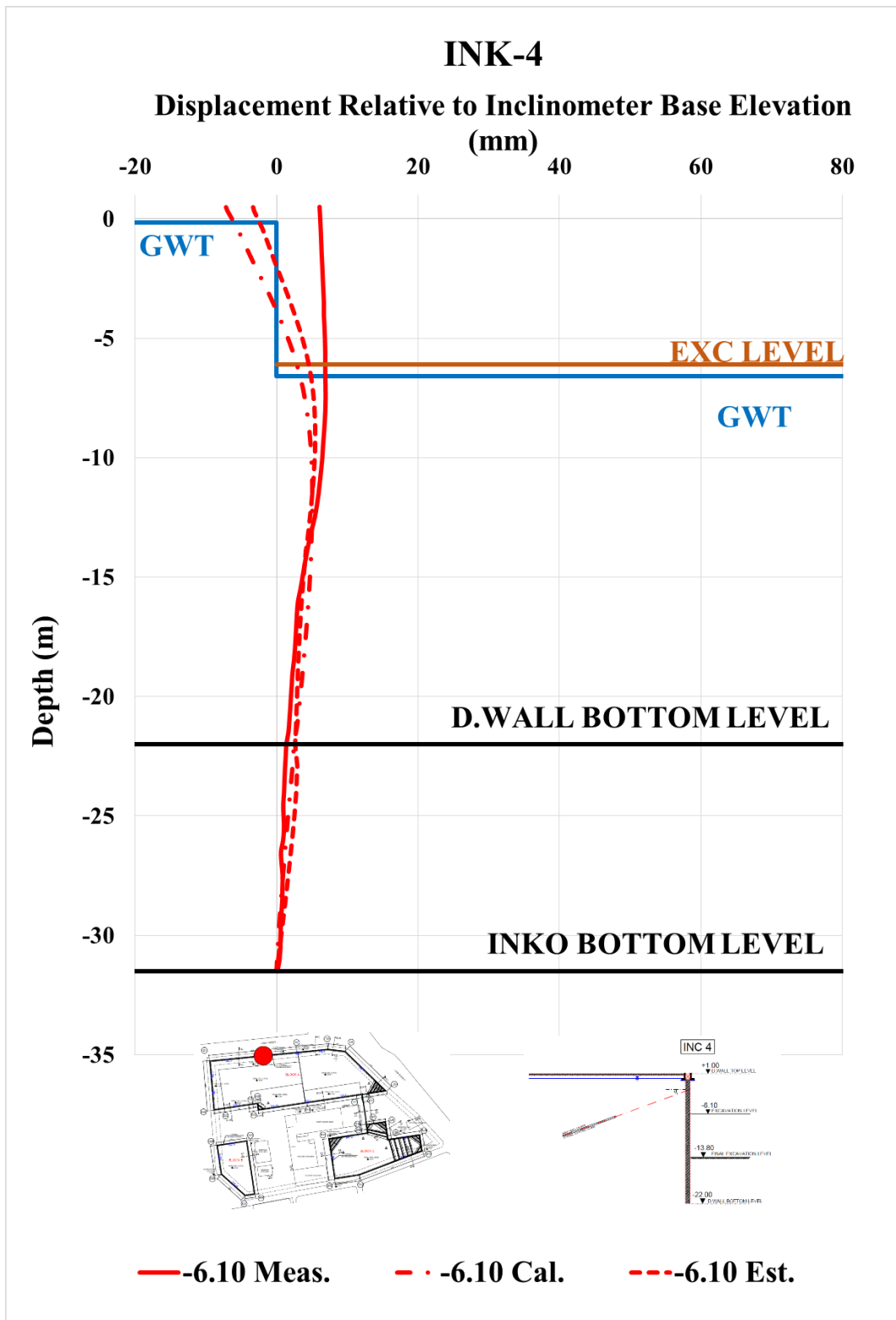
Figure A. 172. Calibrated and Measured Displ. Rel. to Inc. Base Elev. at -6.10 m
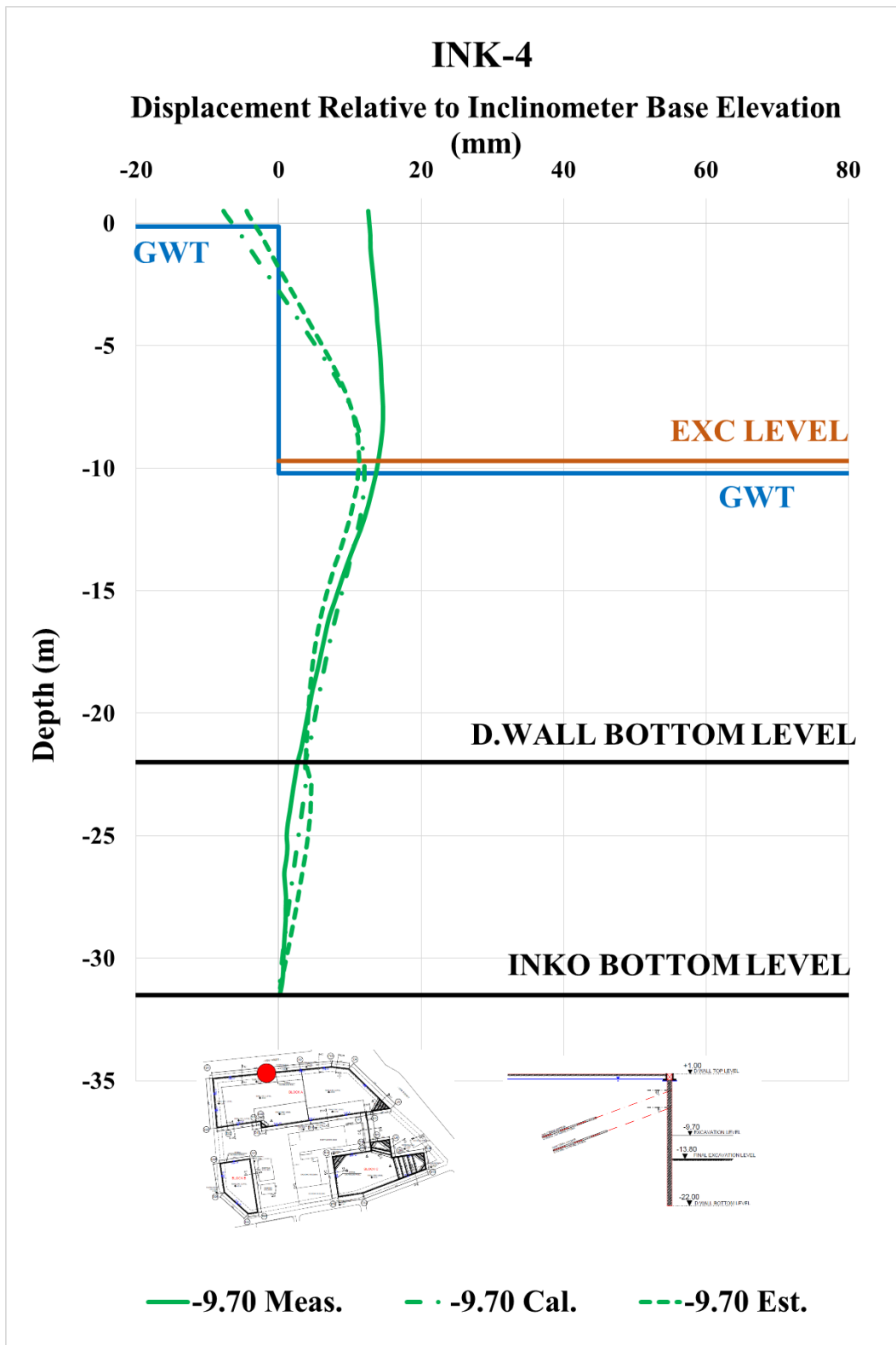
Figure A. 173. Calibrated and Measured Displ. Rel. to Inc. Base Elev. at -9.70 m
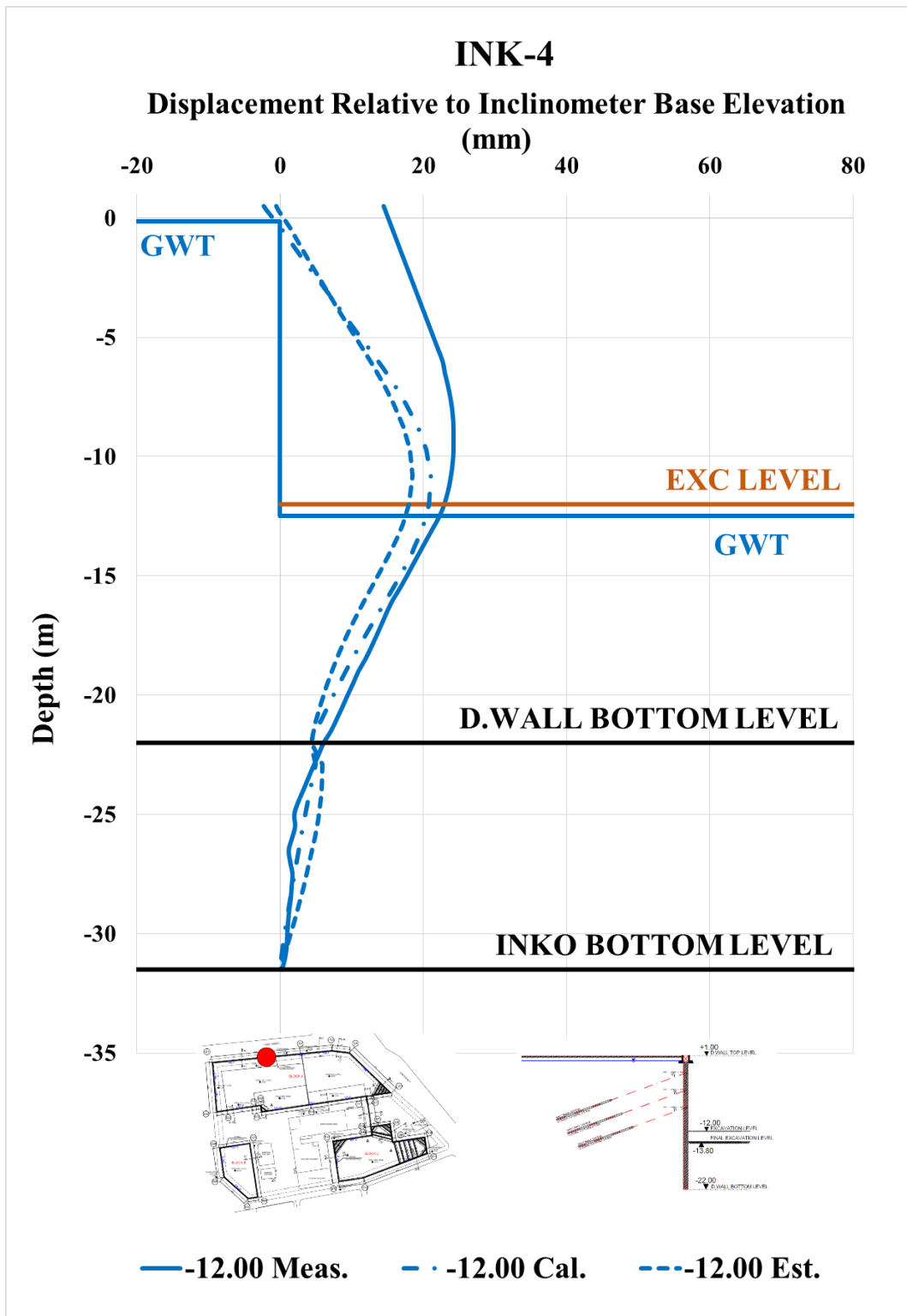
Figure A. 174. Calibrated and Measured Displ. Rel. to Inc. Base Elev. at -12.00 m
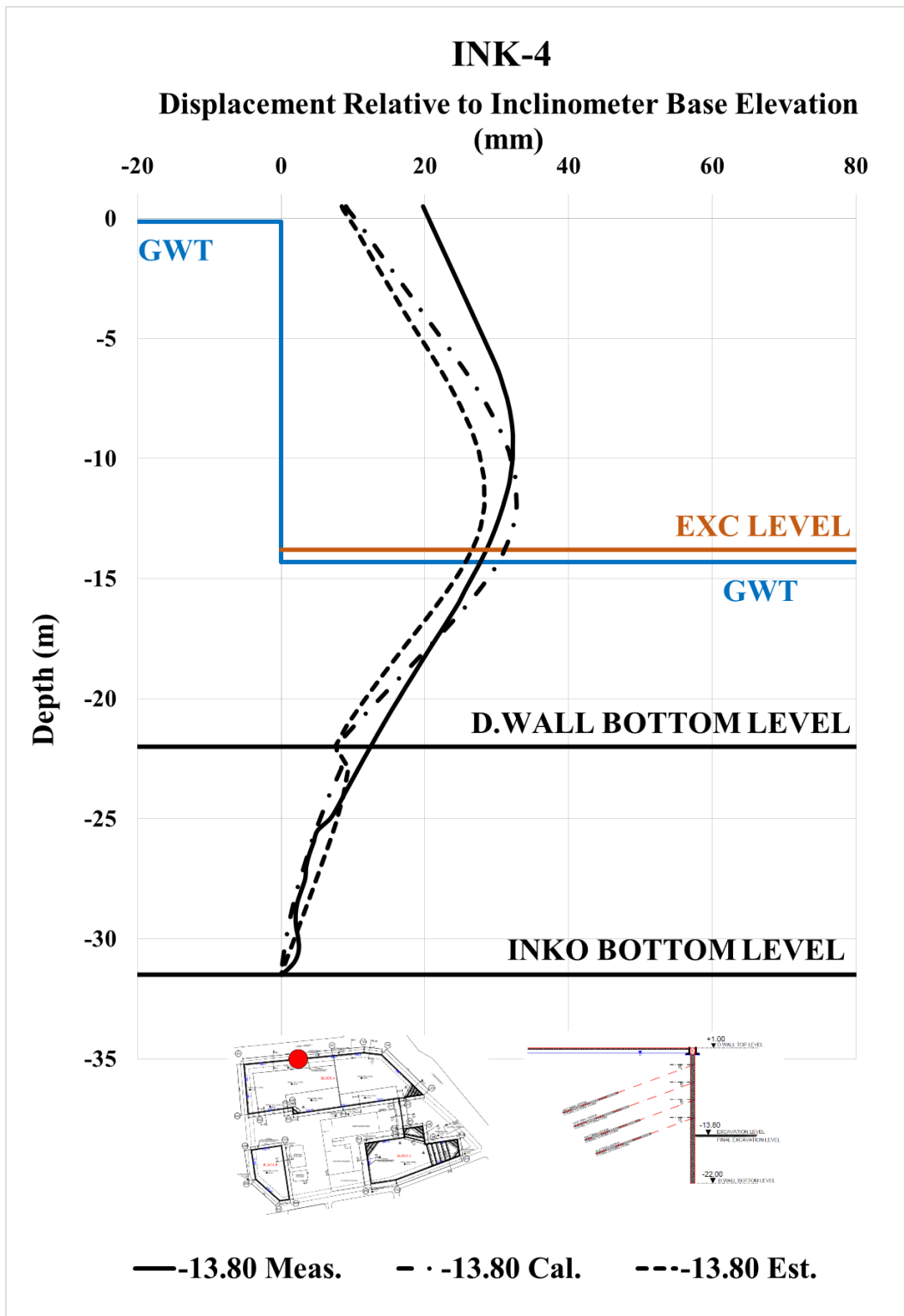
Figure A. 175. Calibrated and Measured Displ. Rel. to Inc. Base Elev. at -13.80 m

Table A. 37. Internal Forces of Diaphragm Wall

INK - 4 / Section 1-1					
Excvation Stage	1	2	3	4	5
Excavation Level (m)	-2,50	-6,10	-9,70	-12,00	-13,80
N_{max} (kN/m)	82,61	213,90	416,60	579,90	709,50
V_{max} (kN/m)	37,44	232,40	312,90	332,10	332,10
M_{max} (kN.m/m)	77,50	366,60	760,30	908,20	938,00

Legend	Excvation Stage	1. Anchor Level	2. Excavation Level	2. Anchor Level	3. Excavation Level	3. Anchor Level	4. Excavation Level	4. Anchor Level	Final Excavation Level
	Measured Load of 1. Anchor Row (kN)	689.38	628.79	642.49	638.04	643.08	632.32	623.70	620.28
	Estimated Load of 1. Anchor Row (kN)	650.00	694.23	622.20	653.95	628.17	639.61	634.29	643.07
	Estimated Load of 2. Anchor Row (kN)	-	-	650.00	713.24	654.96	682.29	658.55	671.11
	Estimated Load of 3. Anchor Row (kN)	-	-	-	-	650.00	709.47	654.97	682.76
	Estimated Load of 4. Anchor Row (kN)	-	-	-	-	-	-	650.00	710.94

Figure A. 176. Measured and Estimated Anchor Loads

Table A. 38. Summary of Displacement Results of INK-4

INK - 4 / SECTION 1 - 1

Excvation Level (m)	Excvation Depth (m)	u_{meas} (mm) Inclinometer Measurements	u_{est} (mm) Estimation with Plaxis 2D Analysis	u_{cal} (mm) Calibration with Plaxis 2D Analysis	$u_{literature}$ (mm) FHWA-IF-99-015 (1999) - Maksimum	$u_{literature}$ (mm) FHWA-IF-99-015 (1999) - Average	$u_{literature}$ (mm) Goldberg et al. (1976)	$u_{literature}$ (mm) Clough et al. (1990) - Maksimum	$u_{literature}$ (mm) Clough et al. (1990) - Average	$u_{literature}$ (mm) Long (2001)	$u_{literature}$ (mm) Long (2001) (Extraordinary cases eliminated)	$u_{literature}$ (mm) Long (2001) Cantilever System
-2.50	3.50	6.45	8.12	6.07	17.50	7.00	17.50	17.50	7.00	6.65	4.90	12.6
-6.70	7.70	6.91	5.48	5.07	38.50	15.40	38.50	38.50	15.40	14.63	10.78	-
-9.70	10.70	14.65	11.27	12.04	53.50	21.40	53.50	53.50	21.40	20.33	14.98	-
-12.00	13.00	24.18	18.50	21.03	65.00	26.00	65.00	65.00	26.00	24.70	18.20	-
-13.80	14.80	32.24	28.26	32.76	74.00	29.60	74.00	74.00	29.60	28.12	20.72	-
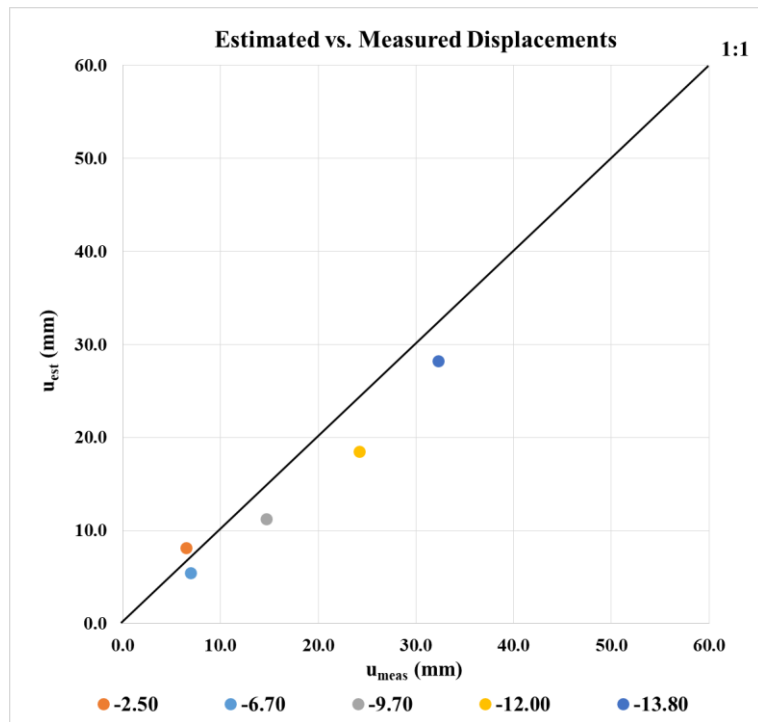
Figure A. 177. Estimated and Measured Displacements of INK - 4
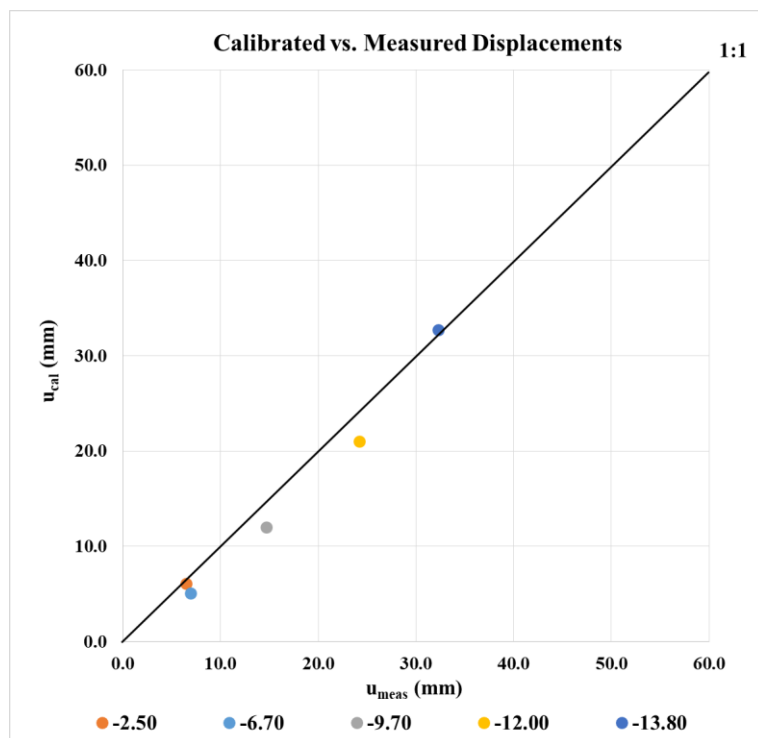
Figure A. 178. Calibrated and Measured Displacements of INK - 4

INK-5 - Calibrated, Estimated and Measured Displacements
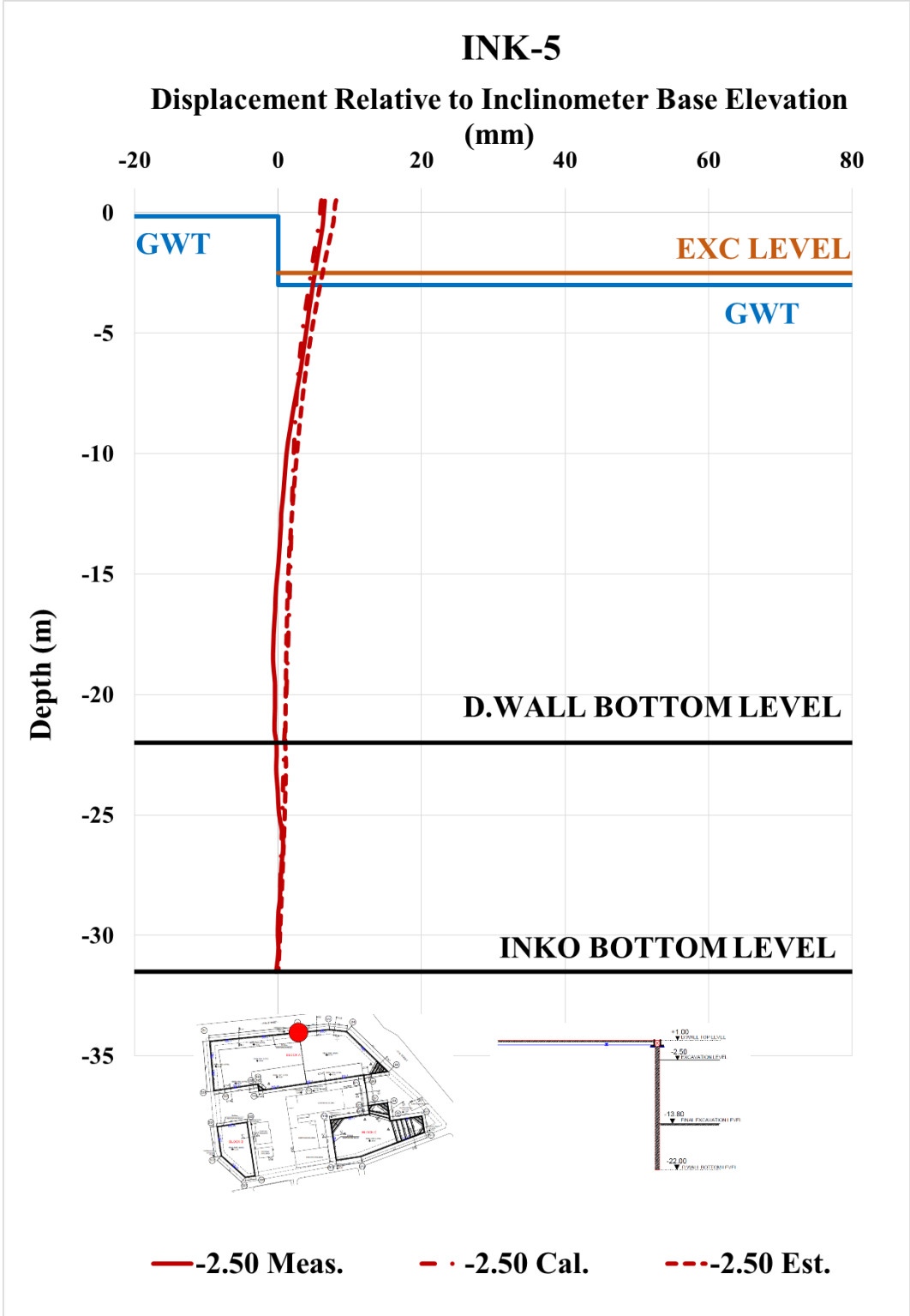
Figure A. 179. Calibrated and Measured Displ. Rel. to Inc. Base Elev. at -2.50 m
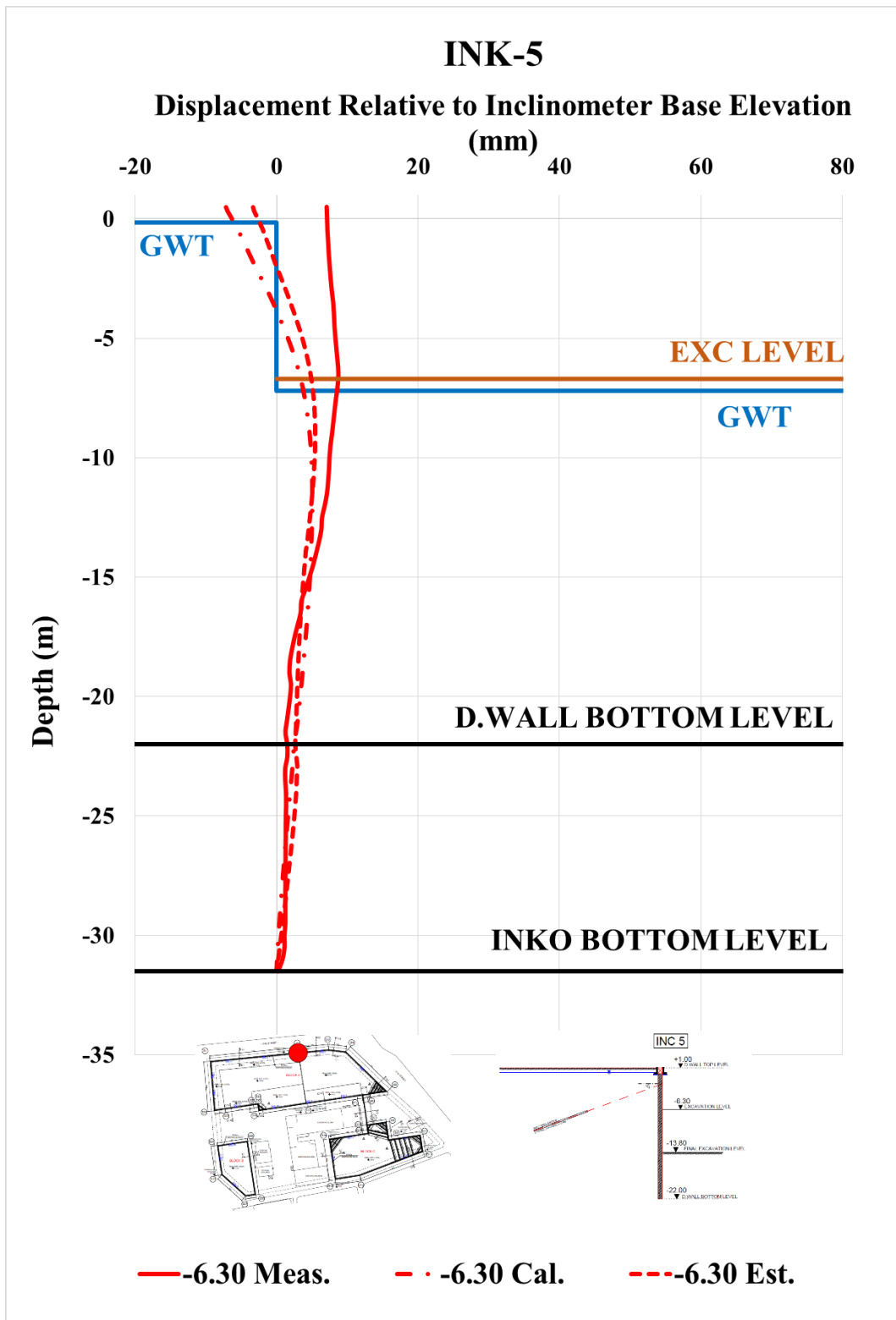
Figure A. 180. Calibrated and Measured Displ. Rel. to Inc. Base Elev. at -6.30 m
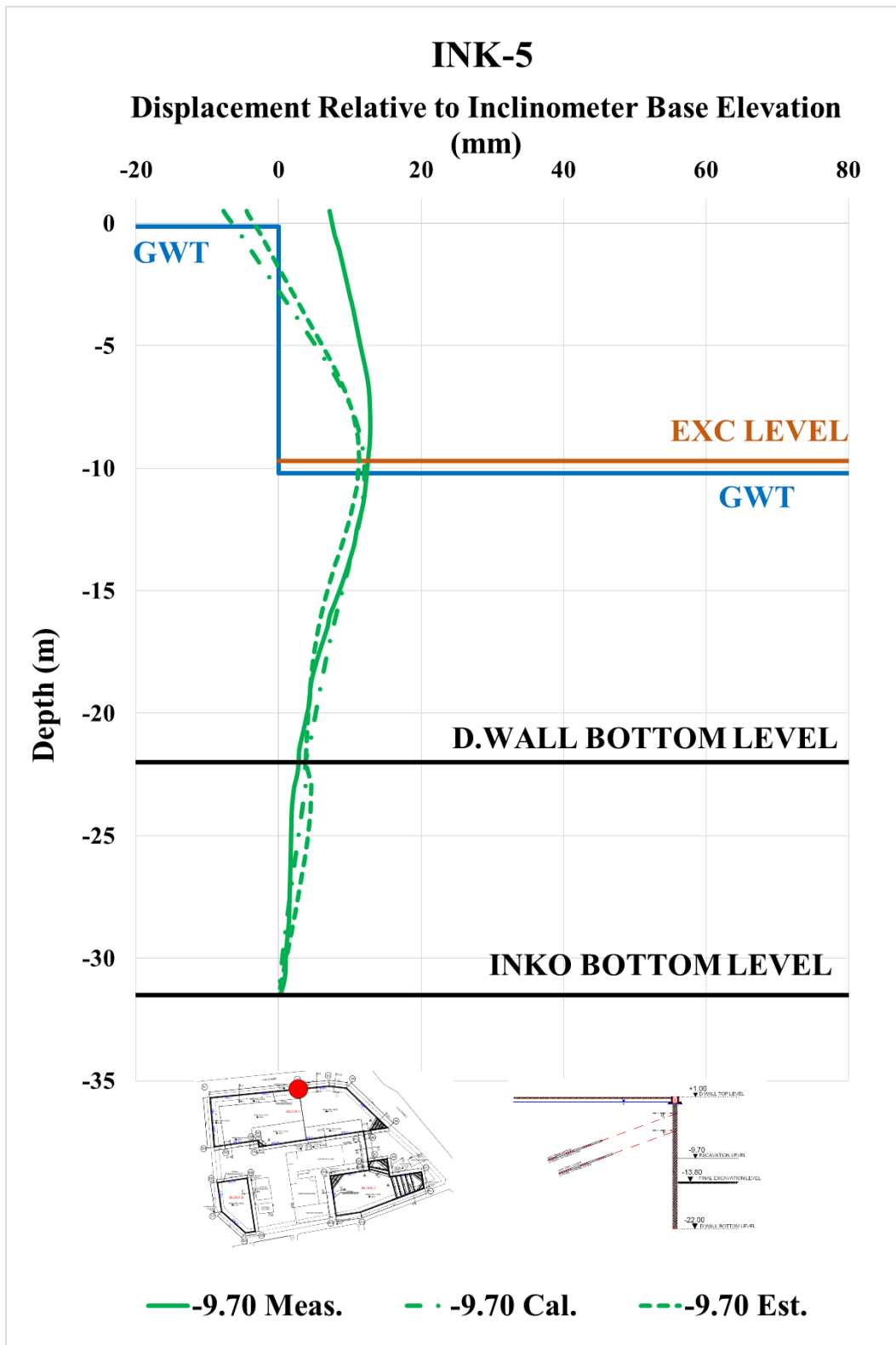
Figure A. 181. Calibrated and Measured Displ. Rel. to Inc. Base Elev. at -9.70 m
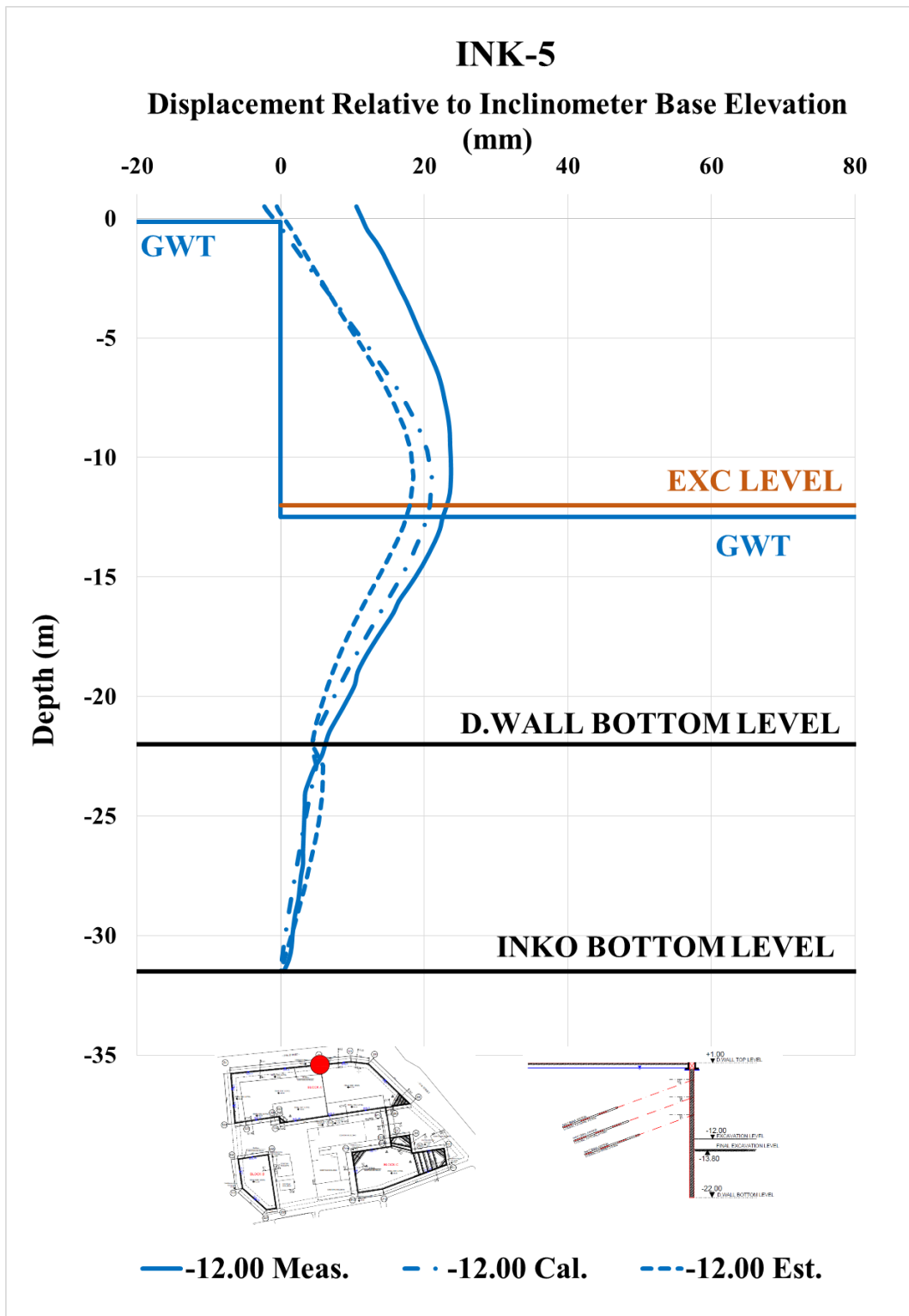
Figure A. 182. Calibrated and Measured Displ. Rel. to Inc. Base Elev. at -12.00 m
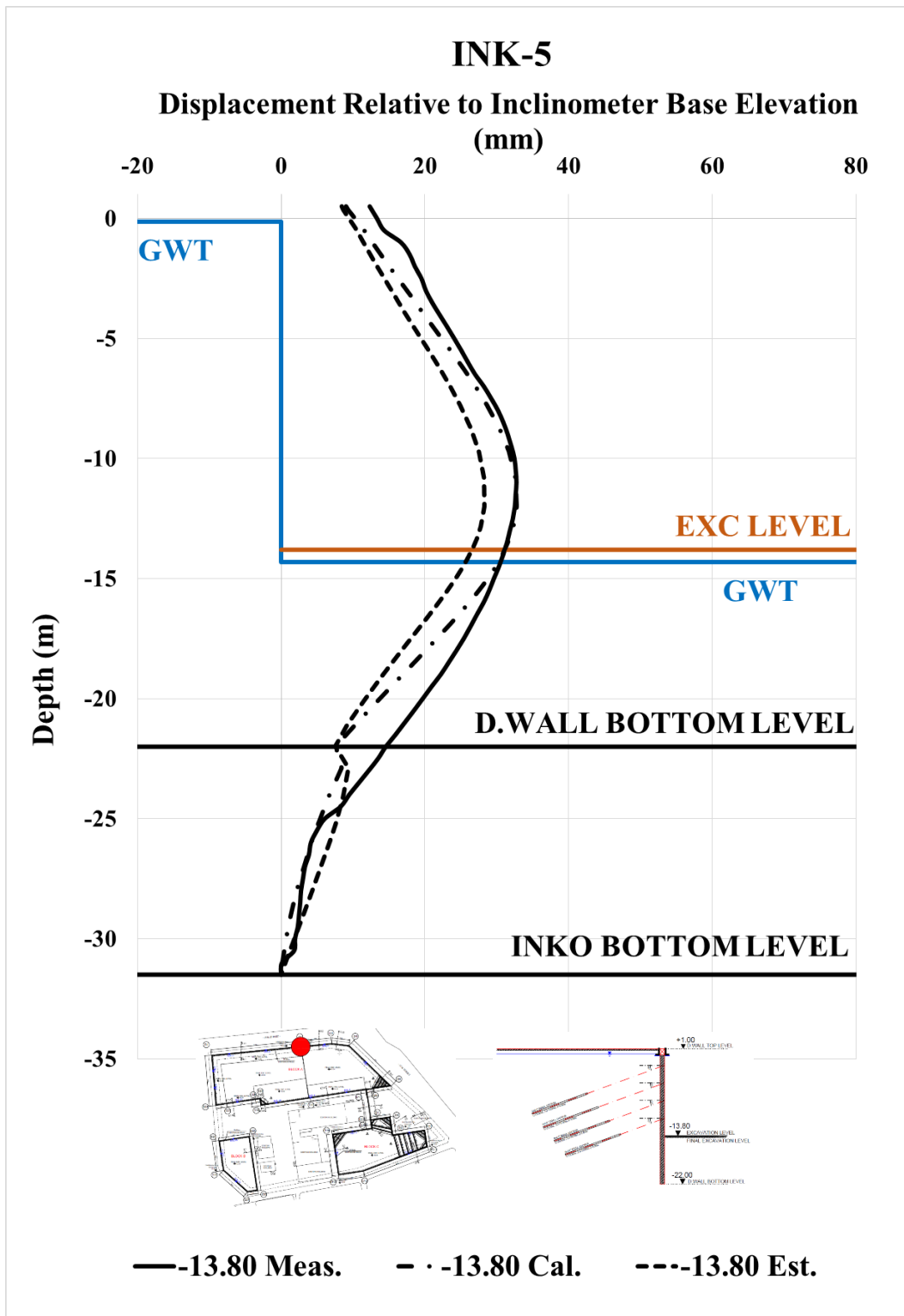
Figure A. 183. Calibrated and Measured Displ. Rel. to Inc. Base Elev. at -13.80 m

Table A. 39. Internal Forces of Diaphragm Wall

INK - 5 / Section 1-1					
Excvation Stage	1	2	3	4	5
Excavation Level (m)	-2,50	-6,30	-9,70	-12,00	-13,80
N_{max} (kN/m)	76,59	221,20	421,30	583,60	708,50
V_{max} (kN/m)	38,93	237,00	308,60	333,00	333,00
M_{max} (kN.m/m)	88,54	386,50	759,30	953,70	1031,00

Legend	Excvation Stage	1. Anchor Level	2. Excavation Level	2. Anchor Level	3. Excavation Level	3. Anchor Level	4. Excavation Level	4. Anchor Level	Final Excavation Level
	Measured Load of 1. Anchor Row (kN)	681.46	628.91	637.70	642.85	634.94	630.10	627.03	615.77
	Estimated Load of 1. Anchor Row (kN)	650.00	694.23	622.20	653.95	628.17	639.61	634.29	643.07
	Estimated Load of 2. Anchor Row (kN)	-	-	650.00	713.24	654.96	682.29	658.55	671.11
	Estimated Load of 3. Anchor Row (kN)	-	-	-	-	650.00	709.47	654.97	682.76
	Estimated Load of 4. Anchor Row (kN)	-	-	-	-	-	-	650.00	710.94

Figure A. 184. Measured and Estimated Anchor Loads

Table A. 40. Summary of Displacement Results of INK-5

INK - 5 / SECTION 1 - 1

Excvation Level (m)	Excvation Depth (m)	u_{meas} (mm) Inclinometer Measurements	u_{est} (mm) Estimation with Plaxis 2D Analysis	u_{cal} (mm) Calibration with Plaxis 2D Analysis	$u_{literature}$ (mm) FHWA-IF-99-015 (1999) - Maksimum	$u_{literature}$ (mm) FHWA-IF-99-015 (1999) - Average	$u_{literature}$ (mm) Goldberg et al. (1976)	$u_{literature}$ (mm) Clough et al. (1990) - Maksimum	$u_{literature}$ (mm) Clough et al. (1990) - Average	$u_{literature}$ (mm) Long (2001)	$u_{literature}$ (mm) Long (2001) (Extraordinary cases eliminated)	$u_{literature}$ (mm) Long (2001) Cantilever System
-2.50	3.50	6.49	8.12	6.07	17.50	7.00	17.50	17.50	7.00	6.65	4.90	12.6
-6.70	7.70	8.72	5.48	5.07	38.50	15.40	38.50	38.50	15.40	14.63	10.78	-
-9.70	10.70	12.86	11.27	12.04	53.50	21.40	53.50	53.50	21.40	20.33	14.98	-
-12.00	13.00	23.70	18.50	21.03	65.00	26.00	65.00	65.00	26.00	24.70	18.20	-
-13.80	14.80	32.74	28.26	32.76	74.00	29.60	74.00	74.00	29.60	28.12	20.72	-

324
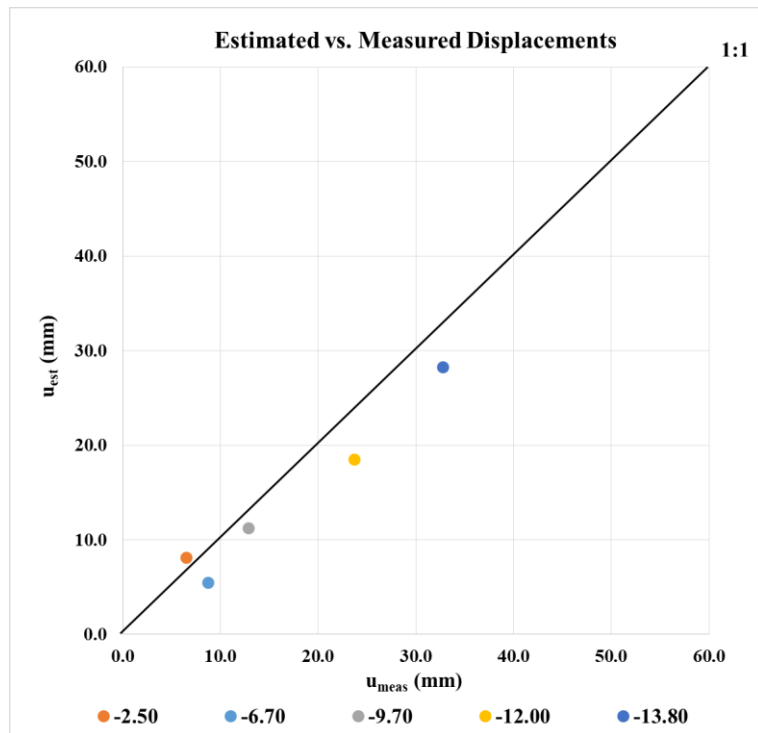
Figure A. 185. Estimated and Measured Displacements of INK – 5
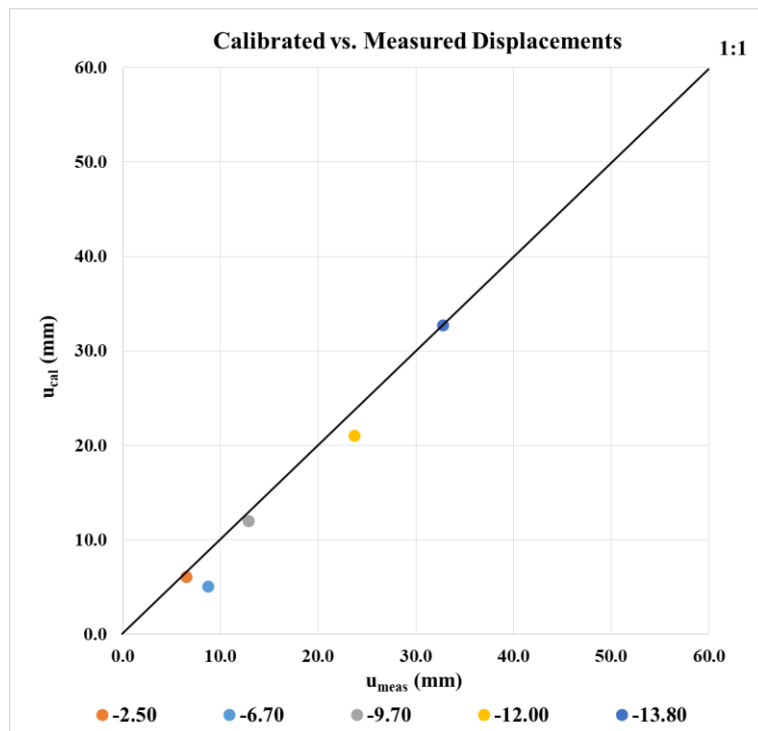
Figure A. 186. Calibrated and Measured Displacements of INK - 5

Area B1
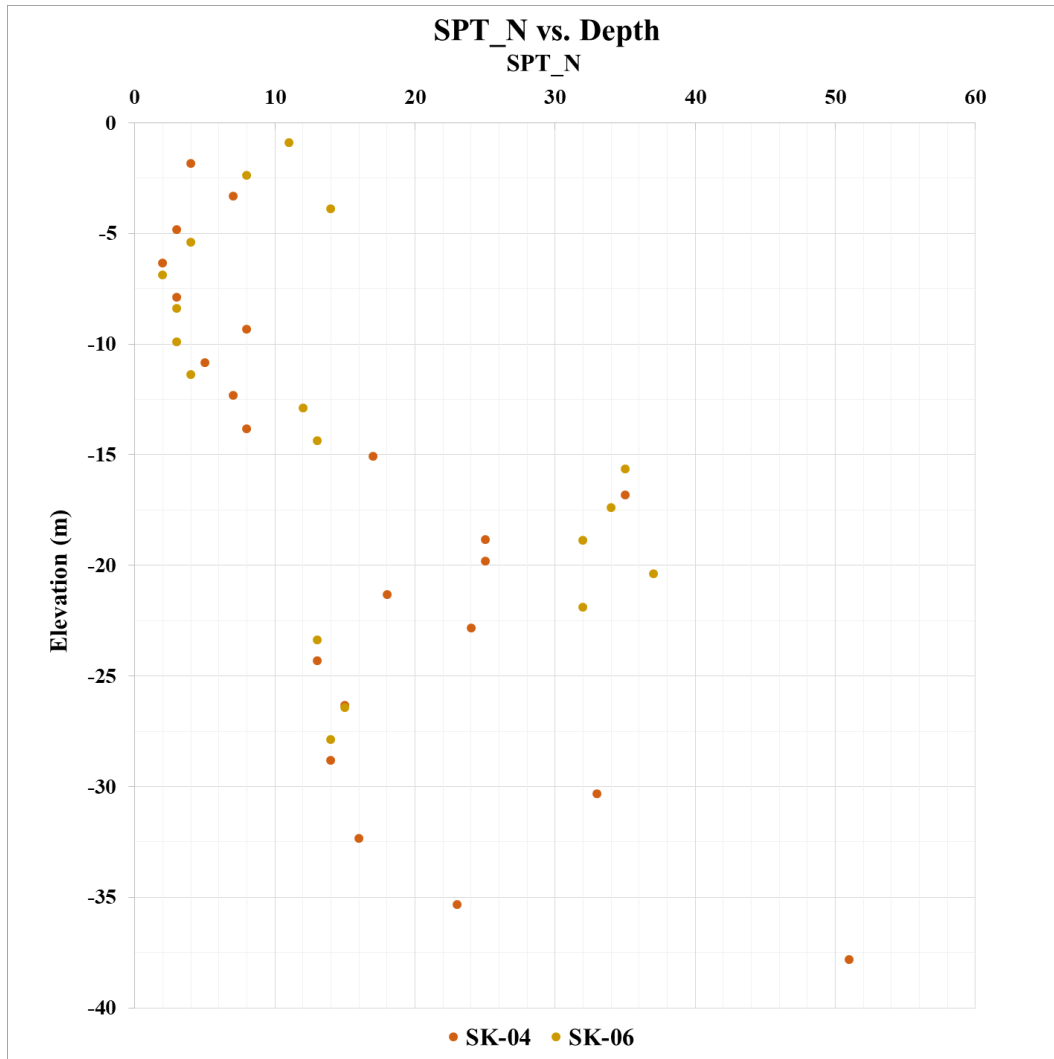
Figure A. 187. SPT-N vs. Depth for Area B1
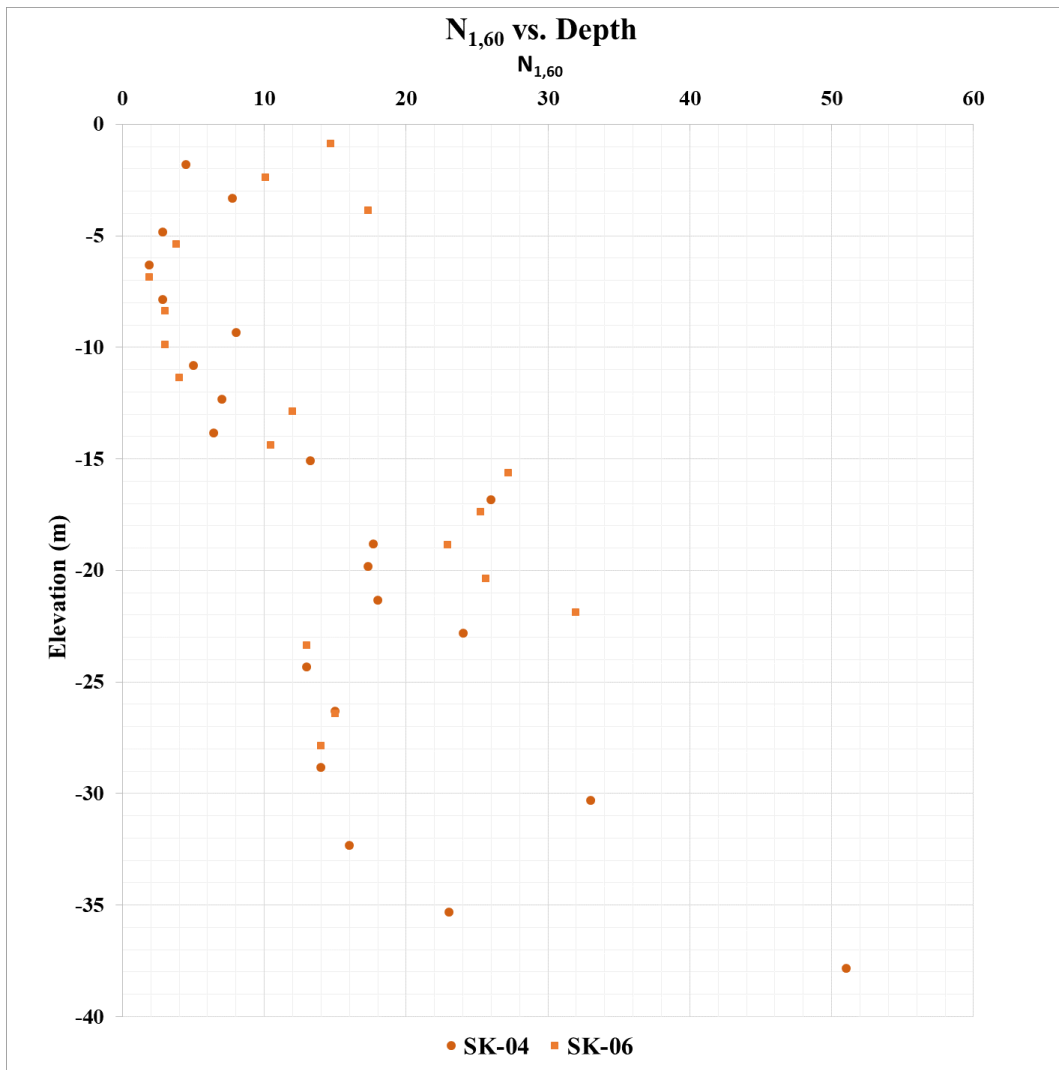
Figure A. 188. SPT-$N_{1,60}$ vs. Depth for Area B1
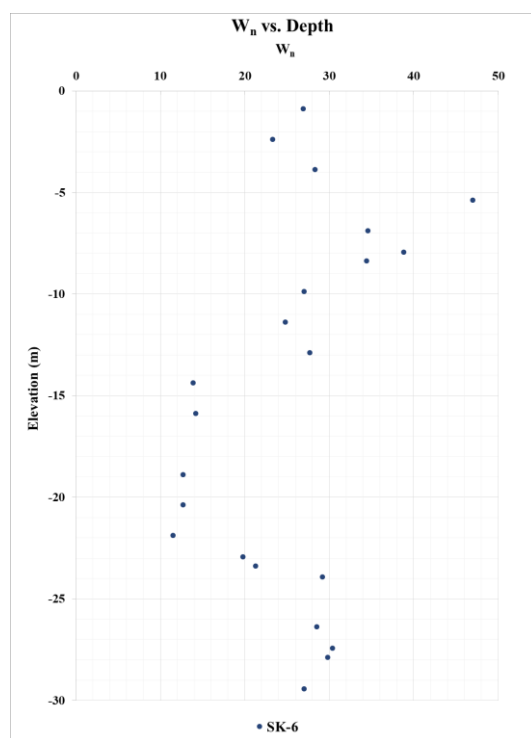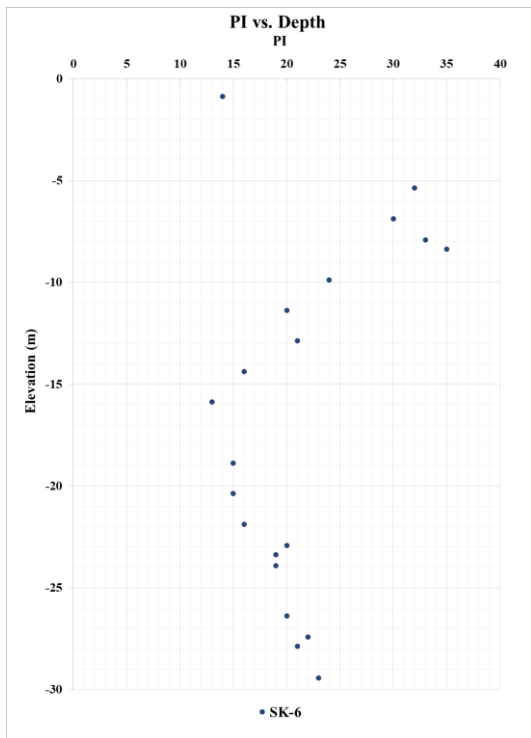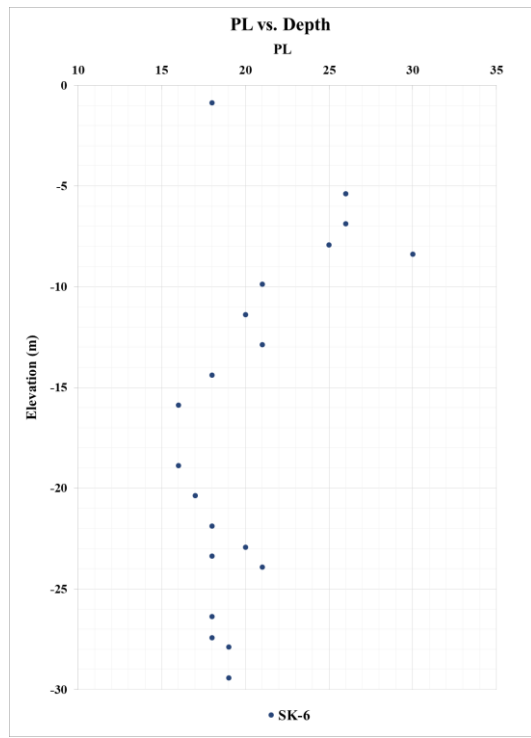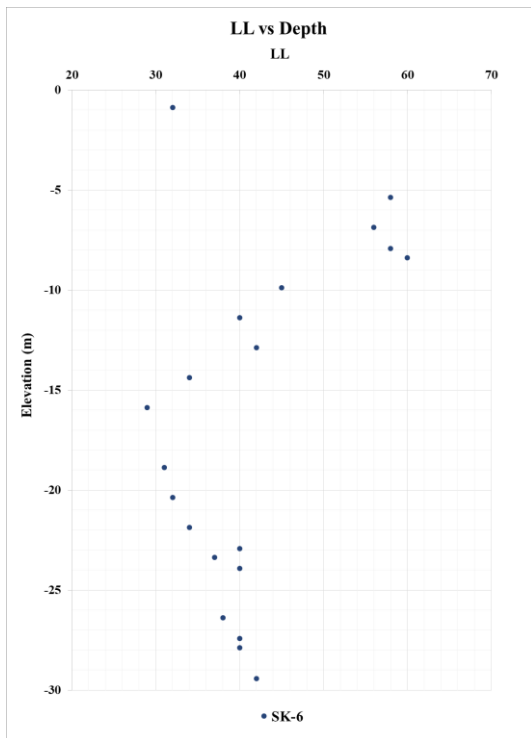
Figure A. 189. Variation of LL, PL, PI, and w_n for B1
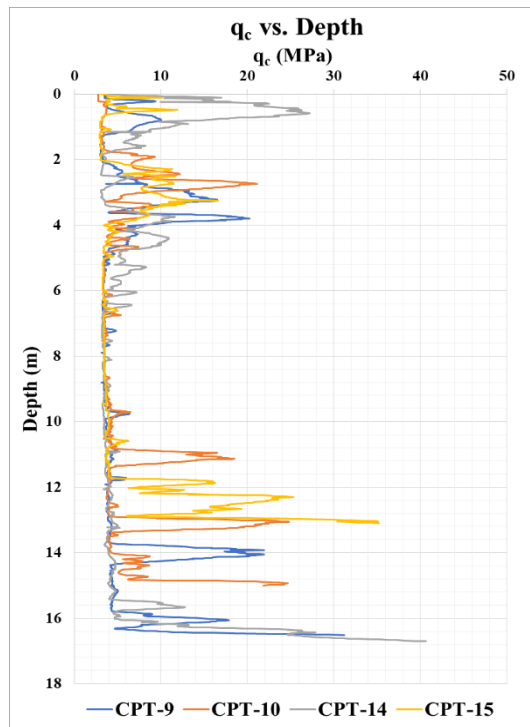
Figure A. 190. Variation of q_c along with the Depth for Area B1
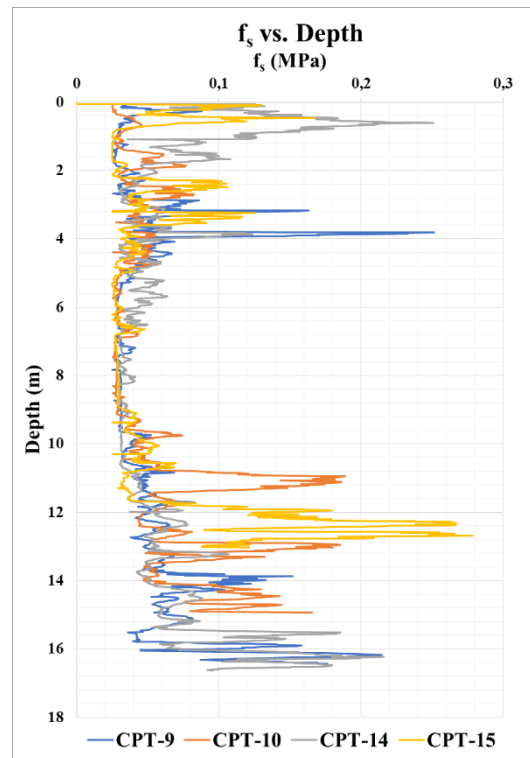
Figure A. 191. Variation of f_s along with the Depth for Area B1

2 boreholes (SK-4, and SK-6) and 4 CPT (CPT-9, CPT-10, CPT-14, and CPT-15) were considered. The depths of boreholes are changing from 30 m to 40 m. Depths of CPT are changing between 13 m to 16.6 m. The total depth of boreholes and CPTs is 70 m and 61.1 m respectively. Atterberg limit tests were performed on the samples taken from SK-6. LL, PL, PI, and w_n vary in 29 – 60 % (avg. 41.4 %), 16 – 30 % (avg. 21 %), 13 – 35 % (avg. 21 %), and 11.5 – 47 % (avg. 25.6 %) respectively. Unified soil classification (USCS) was performed for each sample. By considering USCS, SPT $N_{1,60}$ values, and CPT results, the thickness of soil layers was determined. Detailed soil parameters are given in below table;

- Boreholes: SK-4, and SK-6 (Change in between 30 m to 40 m. 70 m in total)
- CPTs: CPT-9, CPT-10, CPT-14, and CPT-15 (Change in between 13 m to 16.6 m. 61.1 m in total)
- LL: 29 – 60 % (avg. 41.4 %)
- PL: 29 – 60 % (avg. 41.4 %)
- PI: 13 – 35 % (avg. 21 %)
- w_n: 11.5 – 47 % (avg. 25.6 %)

Table A. 41. Soil Profile of Area 5 (B1)

Layer No	Elevation (m)		USCS	Type	Thickness (m)	N	$N_{1,60}$	N_{60}	PI	y_{wet} (kN/m³)	y_{sat} (kN/m³)	c_u (kPa)	c (kPa)	φ (°)	ψ (°)	E_{50}^{ref} (MPa)	E_{oed}^{ref} (MPa)	E_{ur}^{ref} (MPa)	m	v_{ur}	p_{ref} (kPa)	R_f
1	1.4	-3.7	SC-SM	Cohesionless	5.0	8.0	9.0	6.0	4.7	17.6	19.2	-	2.0	29.0	0.0	27.0	27.0	81.0	0.5	0.2	100.0	0.9
2	-3.7	-13.0	CH	Cohesive	9.0	6.0	6.0	6.0	27.9	17.6	6.0	35.0	3.5	29.0	0.0	5.5	2.8	16.6	1.0	0.2	27.6	0.9
3	-13.0	-21.0	SC-GC	Cohesionless	8.0	26.0	19.0	26.0	15.0	19.2	20.0	-	4.0	35.0	5.0	40.0	40.0	120.0	0.5	0.2	100.0	0.9
4	-21.0	-31.0	CL	Cohesive	10.0	14.0	14.0	14.0	20.6	18.4	20.0	80.0	8.0	30.0	0.0	16.1	8.1	48.3	1.0	0.2	139.6	0.9
5	-31.0	-41.0	CL	Cohesive	10.0	31.0	31.0	31.0	20.6	18.4	20.0	180.0	18.0	30.0	0.0	35.7	17.8	107.0	1.0	0.2	239.6	0.9
6	-41.0	-51.0	CL	Cohesive	10.0	35.0	35.0	35.0	20.6	18.4	20.0	200.0	20.0	30.0	0.0	40.3	20.1	120.8	1.0	0.2	339.6	0.9
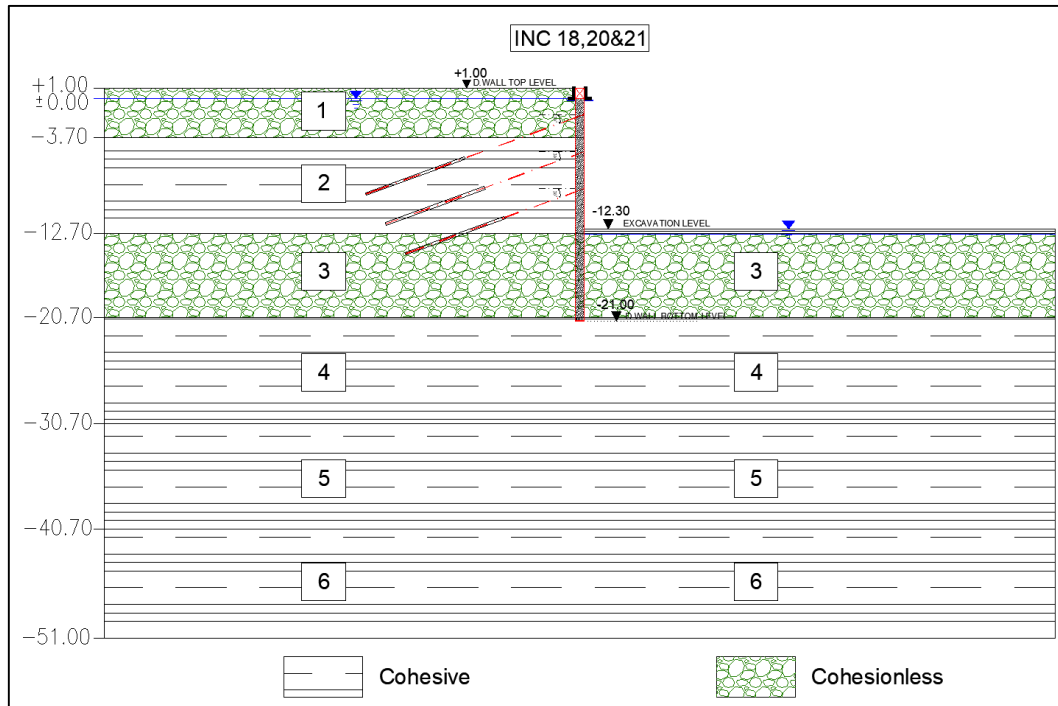
Figure A. 192. Section 7 – 7

Table A. 42. Section Properties of 7 – 7

SECTION 7 - 7									
Diaphragm Wall			**SBMA Type Anchor**				**Excavation Properties**		
Top Level (m)	Bottom Level (m)	Length (m)	Anchor No	Anchor Level (m)	Anchor Length (m)	Horizontal Spacing (m)	Top Level (m)	Bottom Level (m)	Depth (m)
1.00	-21.00	22.00	1	-1.50	22.00	2.00	1.00	-12.30	13.30
			2	-5.00	20.00	2.00			
			3	-8.50	18.00	2.00			

INK-18 – Estimated and Measured Displacements
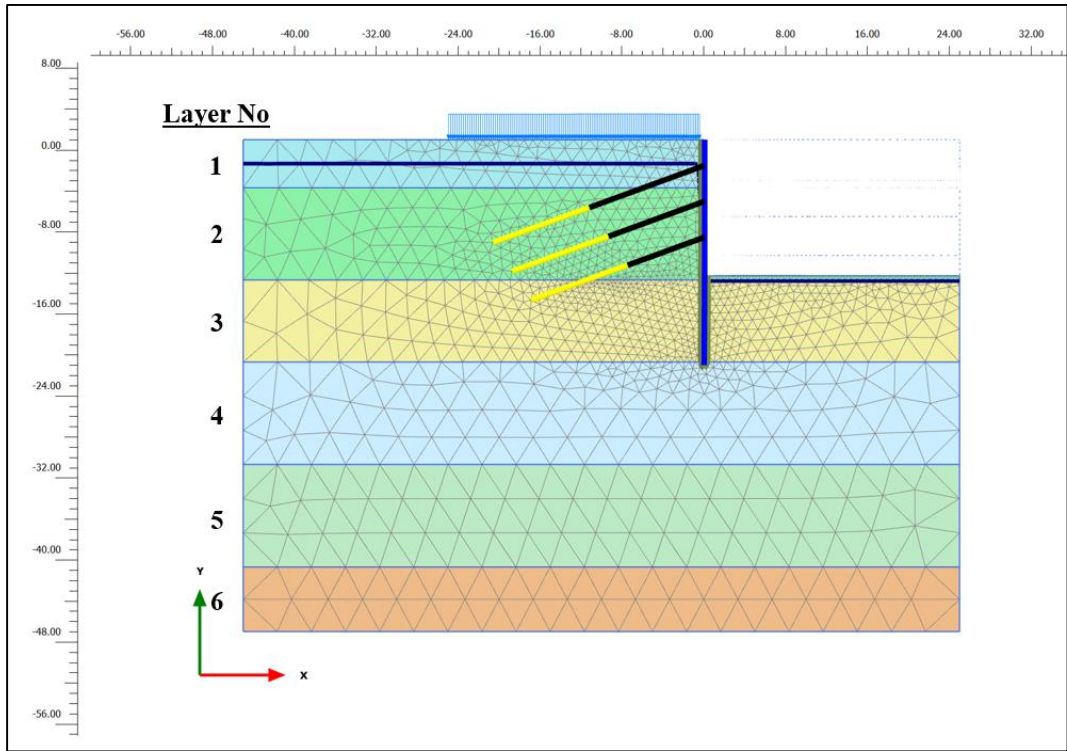
Figure A. 193. Meshed Model for INK-18
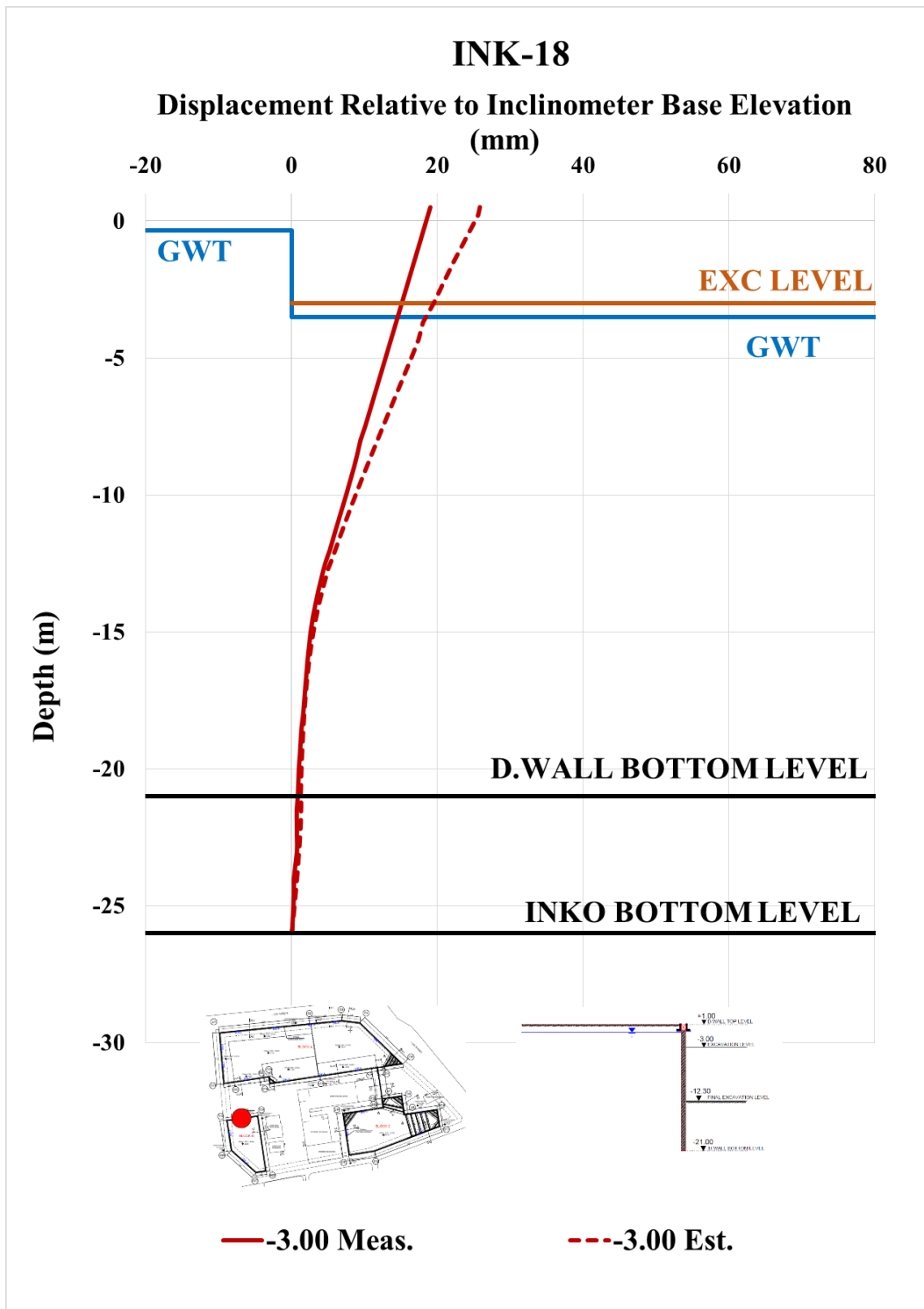
Figure A. 194. Estimated and Measured Displ. Rel. to Inc. Base Elev. at -3.00 m
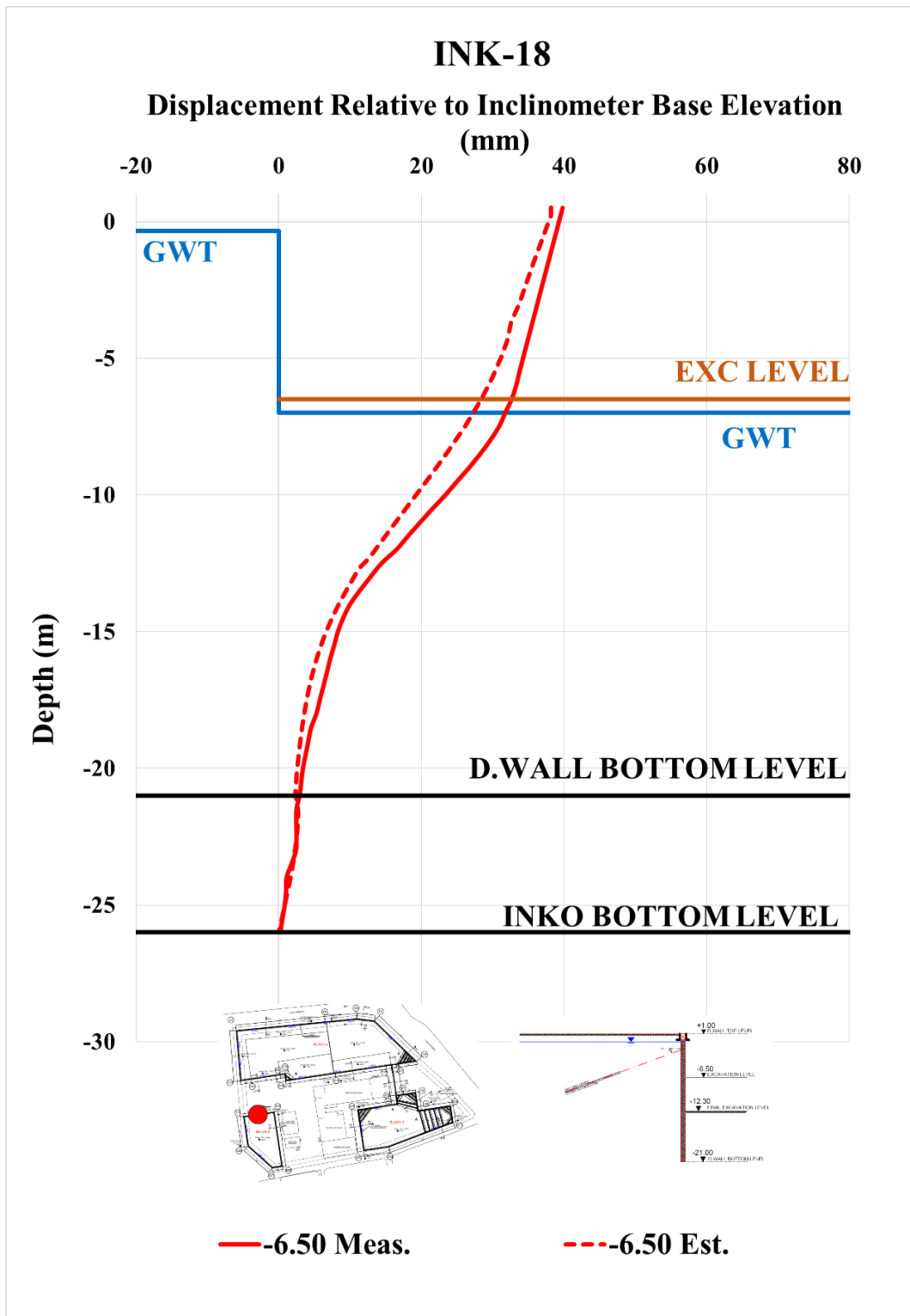
Figure A. 195. Estimated and Measured Displ. Rel. to Inc. Base Elev. at -6.50 m
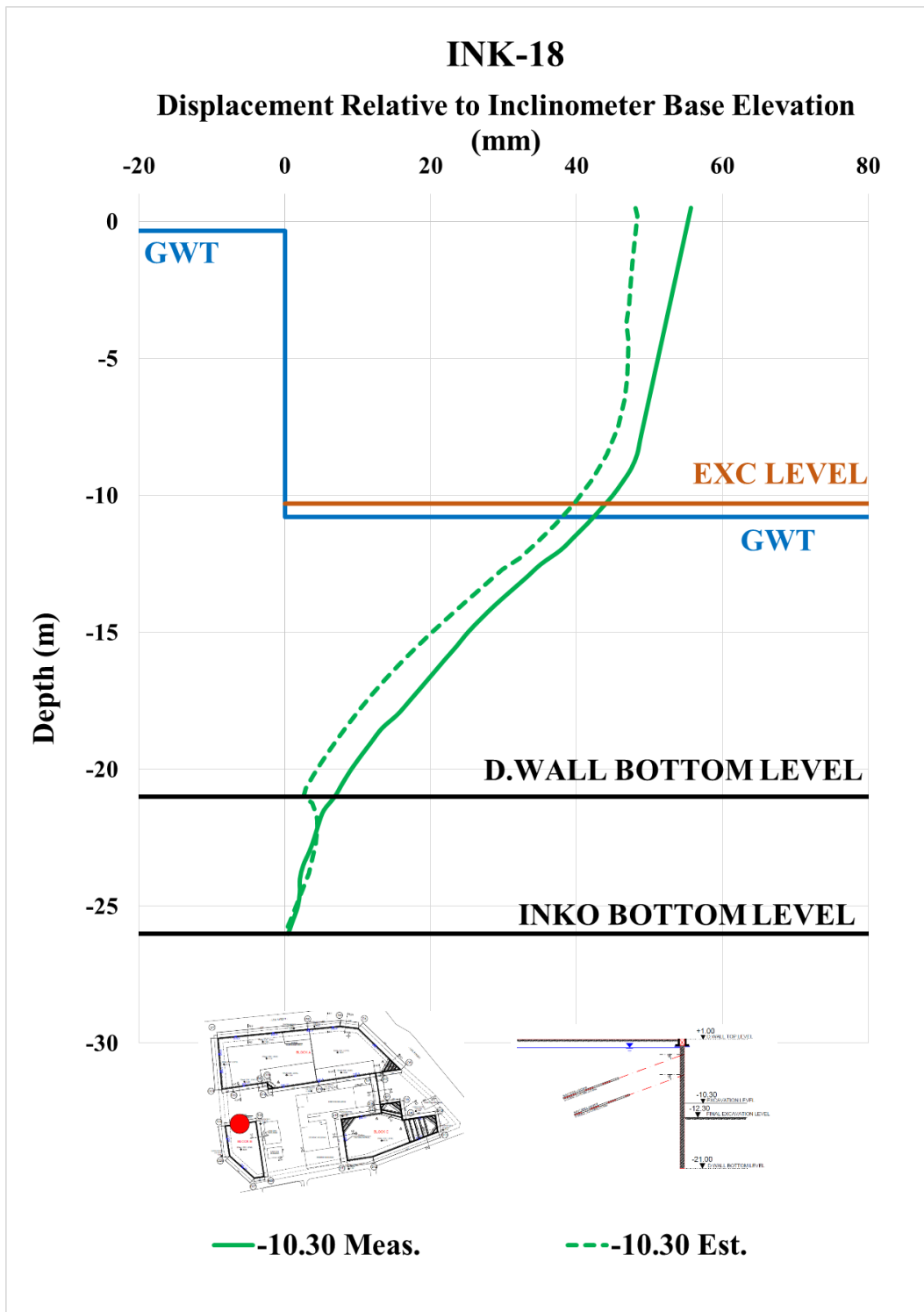
Figure A. 196. Estimated and Measured Displ. Rel. to Inc. Base Elev. at -10.30 m
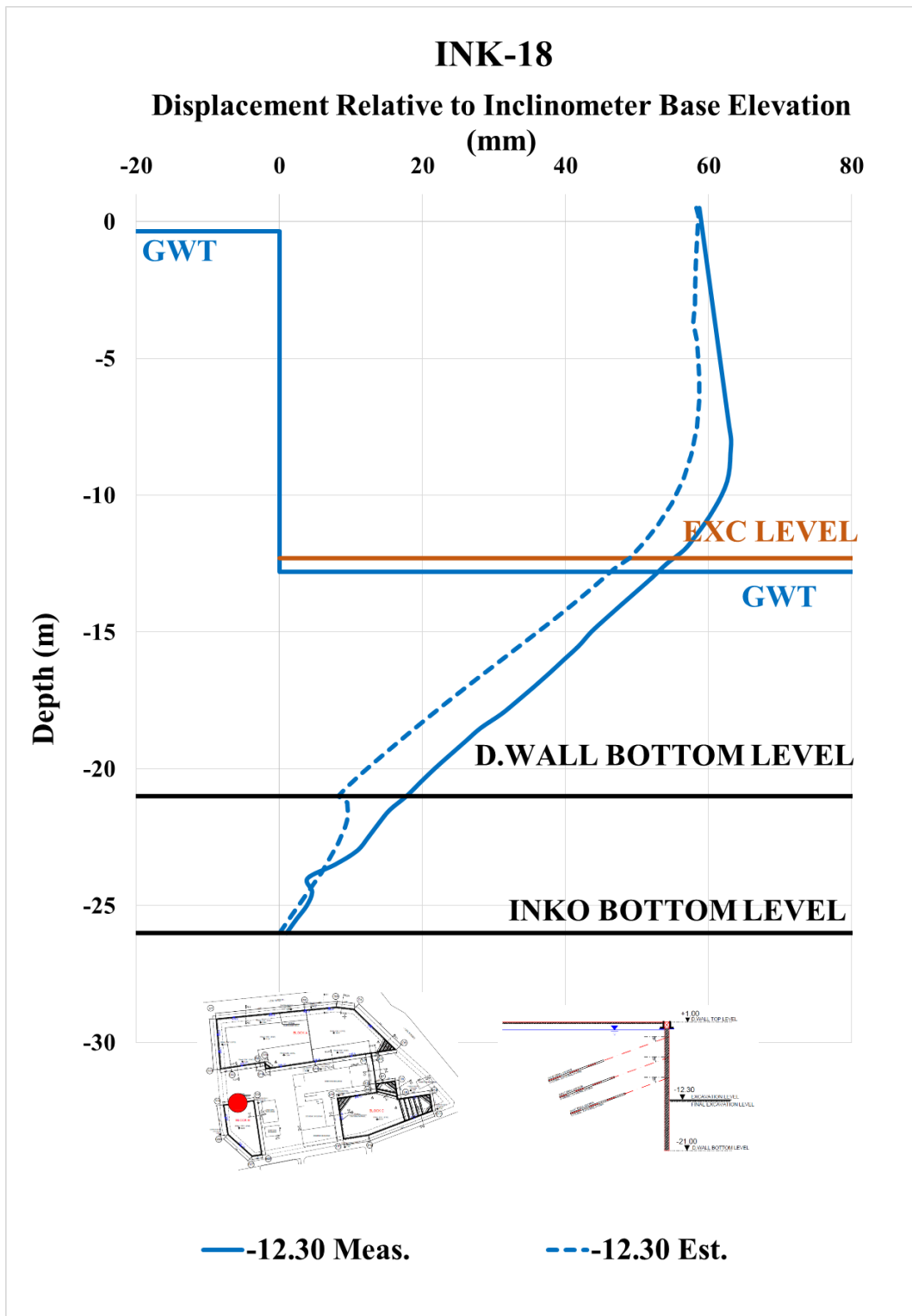
Figure A. 197. Estimated and Measured Displ. Rel. to Inc. Base Elev. at -12.30 m

Table A. 43. Internal Forces of Diaphragm Wall

INK - 18 / Section 7-7				
Excvation Stage	1	2	3	4
Excavation Level (m)	-3,00	-6,50	-10,30	-12,00
N_{max} (kN/m)	100,20	214,80	440,30	587,40
V_{max} (kN/m)	96,58	240,60	365,00	365,00
M_{max} (kN.m/m)	524,70	582,20	982,70	1069,00

INK - 18 / Section 7-7

Anchor Load vs Stage

Legend	Excvation Stage	1. Anchor Level	2. Excavation Level	2. Anchor Level	3. Excavation Level	3. Anchor Level	4. Excavation Level
	Estimated Load of 1. Anchor Row (kN)	650.00	728.72	616.21	664.69	630.61	643.04
	Estimated Load of 2. Anchor Row (kN)	-	-	650.00	774.71	683.43	711.46
	Estimated Load of 3. Anchor Row (kN)	-	-	-	-	650.00	727.51
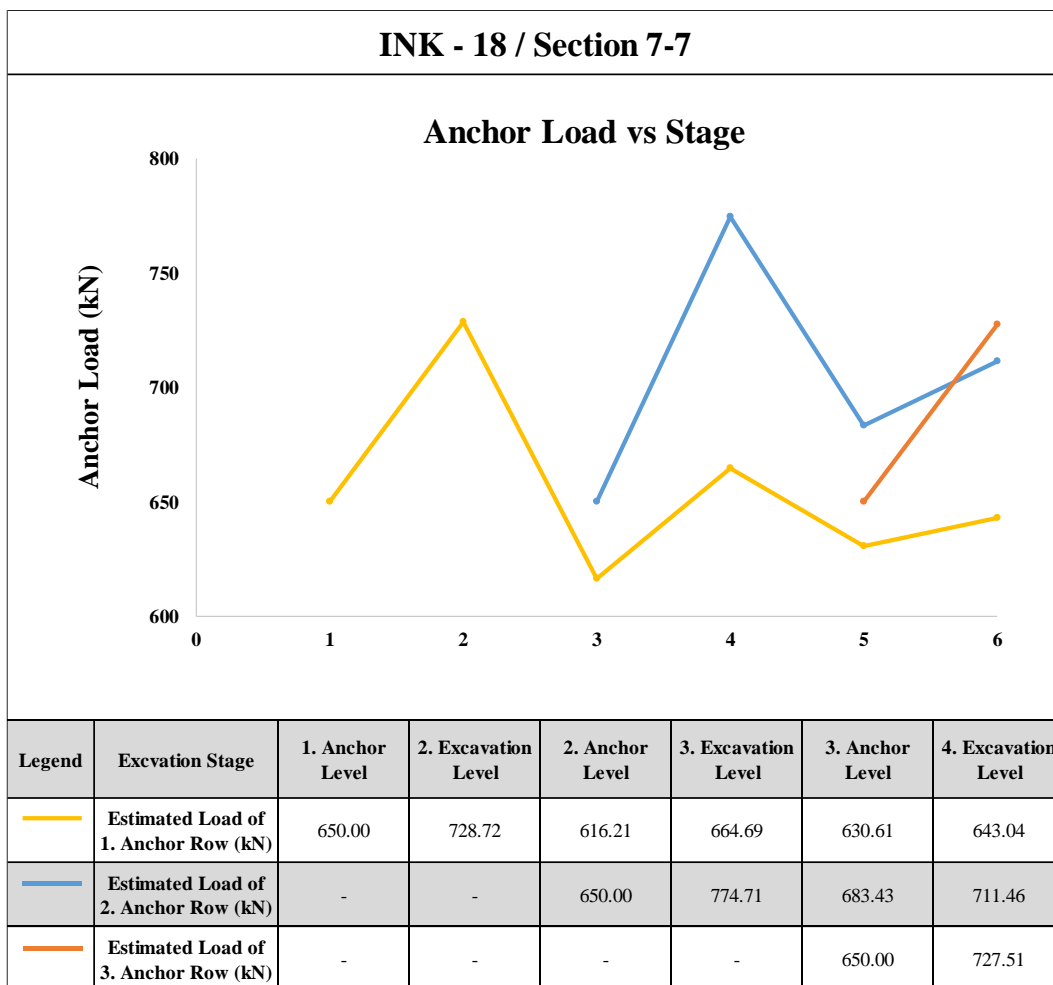
Figure A. 198. Estimated Anchor Loads

INK-20 – Estimated and Measured Displacements
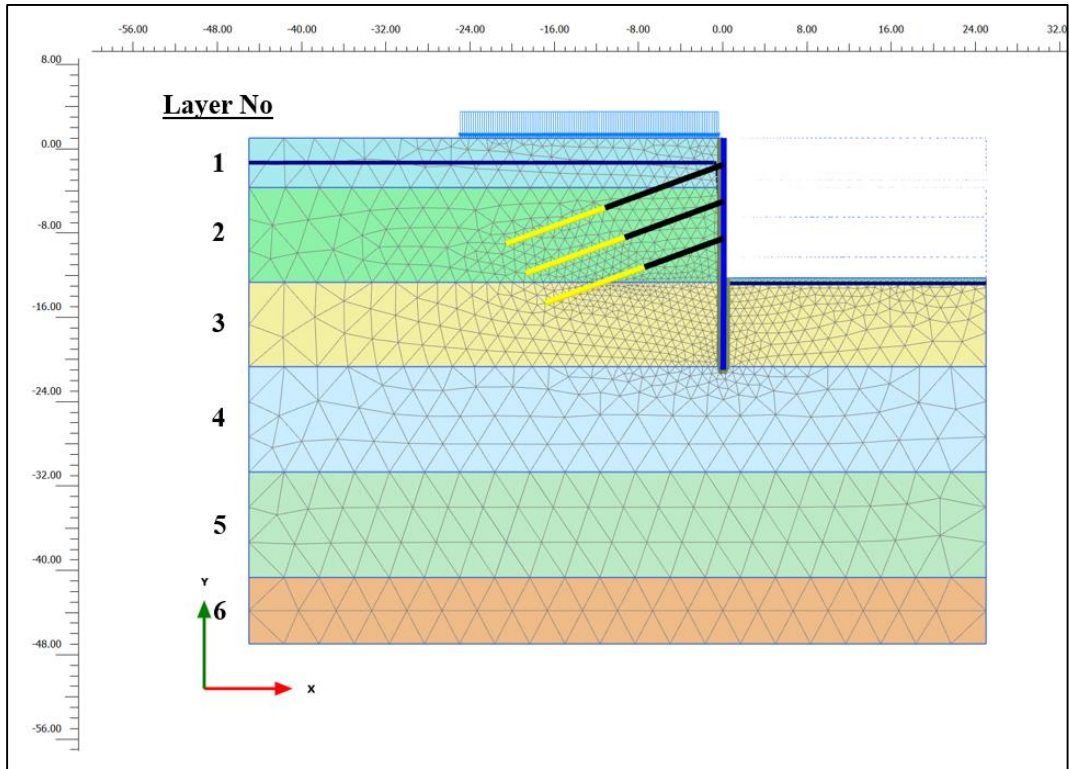
Figure A. 199. Meshed Model for INK-20
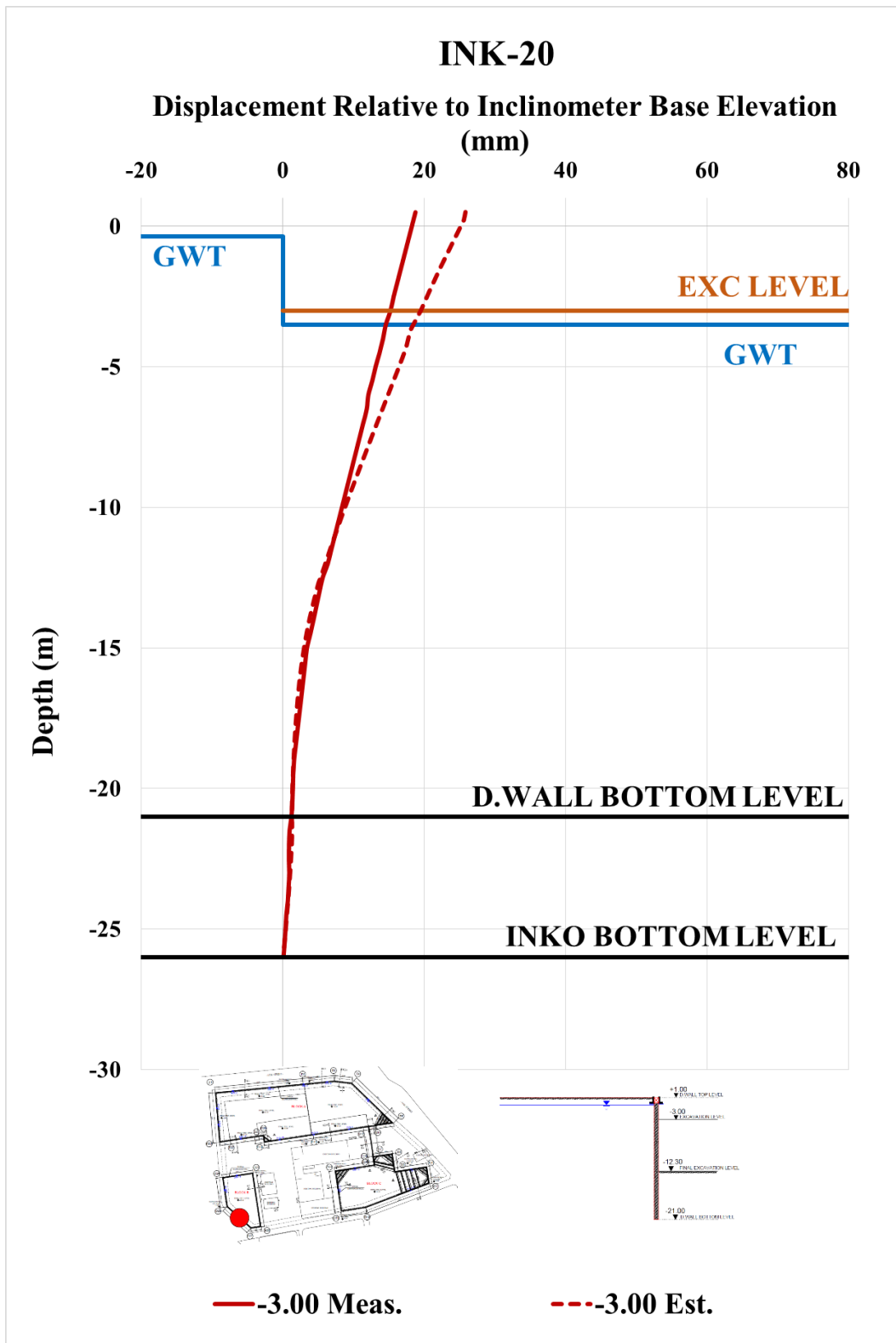
Figure A. 200. Estimated and Measured Displ. Rel. to Inc. Base Elev. at -3.00 m
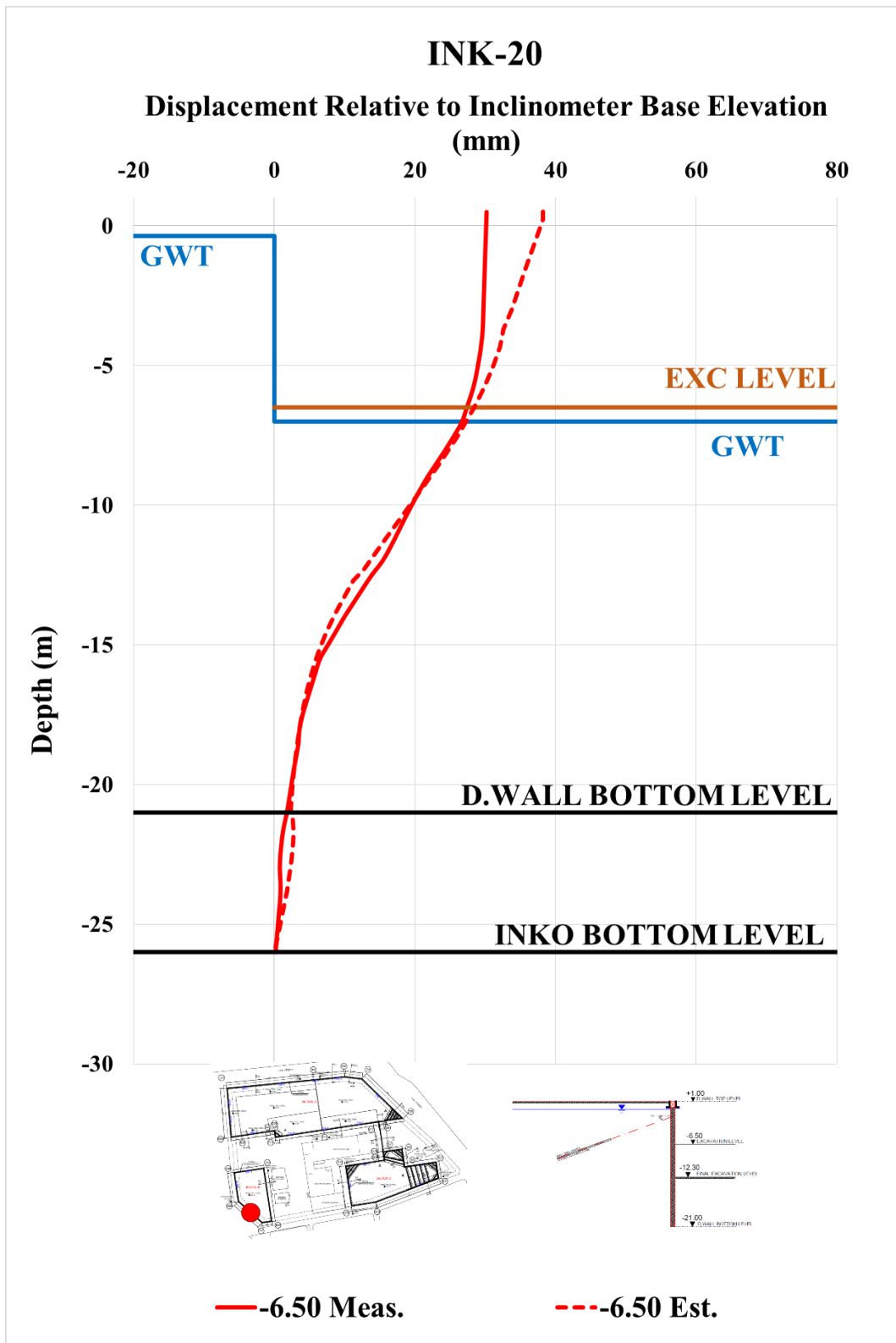
Figure A. 201. Estimated and Measured Displ. Rel. to Inc. Base Elev. at -6.50 m
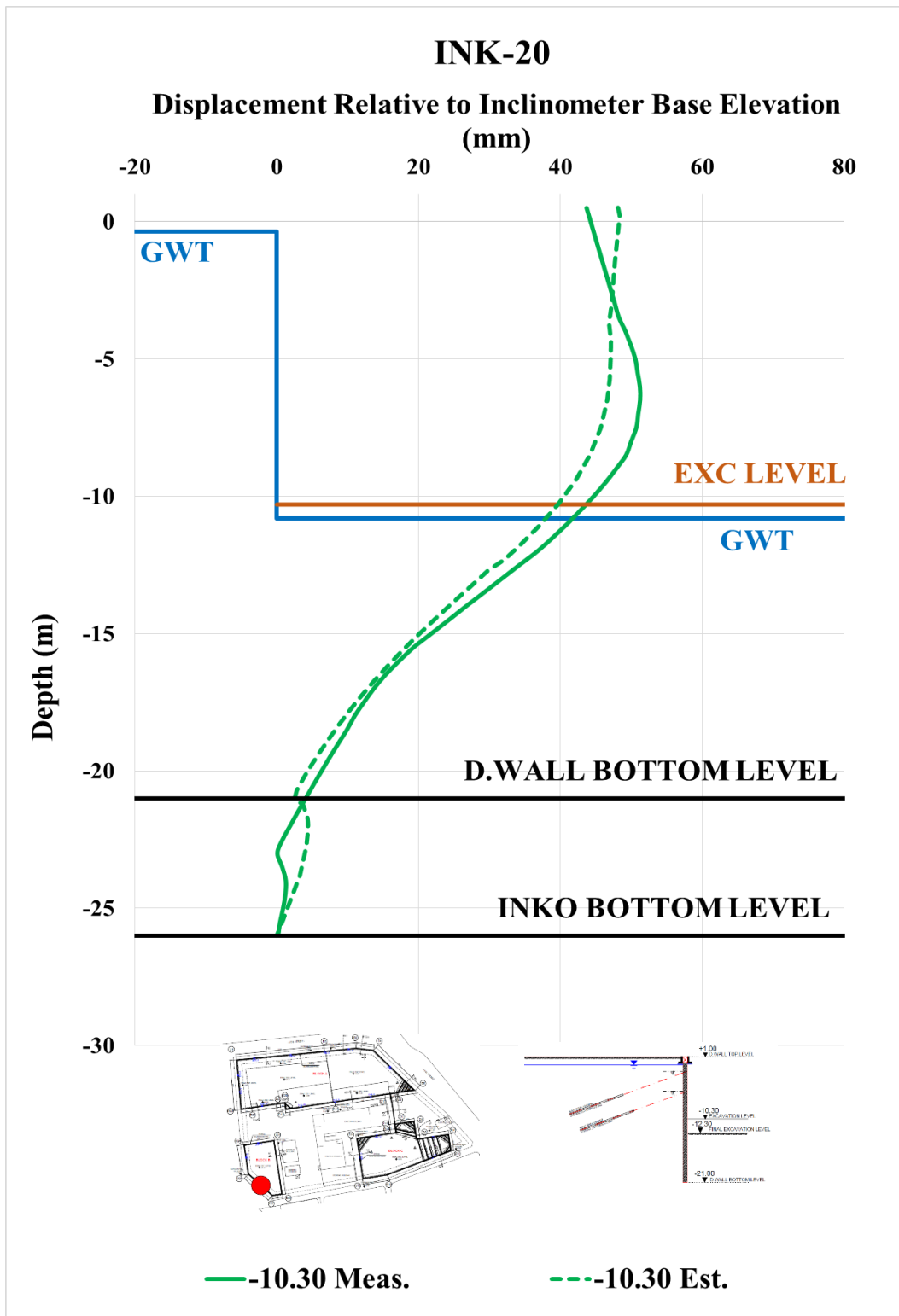
Figure A. 202. Estimated and Measured Displ. Rel. to Inc. Base Elev. at -10.30 m
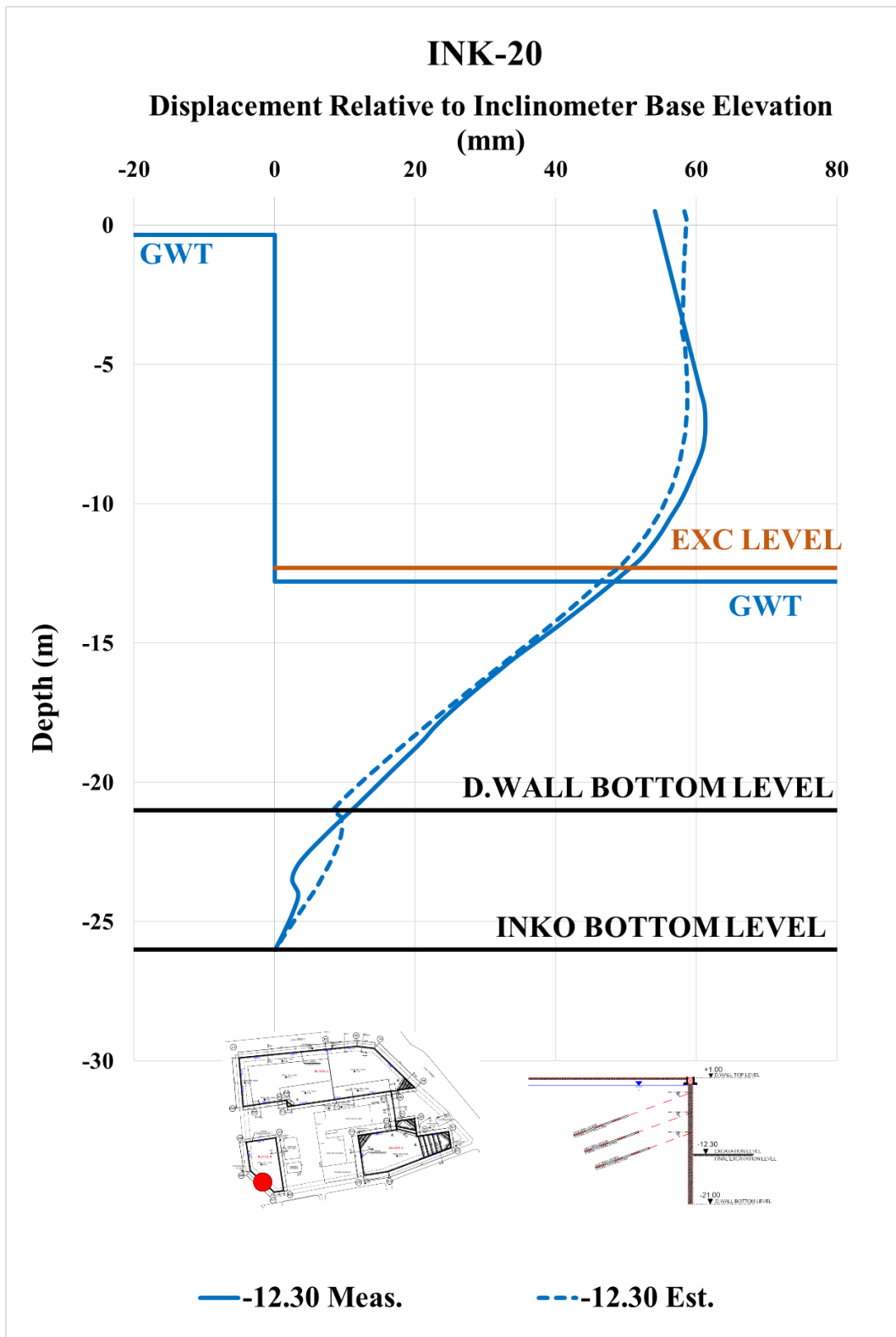
Figure A. 203. Estimated and Measured Displ. Rel. to Inc. Base Elev. at -12.30 m

Table A. 44. Internal Forces of Diaphragm Wall

INK - 20 / Section 7-7				
Excvation Stage	1	2	3	4
Excavation Level (m)	-3,00	-6,50	-10,30	-12,30
N_{max} (kN/m)	100,20	214,80	440,30	587,40
V_{max} (kN/m)	96,58	240,60	365,00	365,00
M_{max} (kN.m/m)	524,70	582,20	982,70	1069,00

Legend	Excvation Stage	1. Anchor Level	2. Excavation Level	2. Anchor Level	3. Excavation Level	3. Anchor Level	4. Excavation Level
	Estimated Load of 1. Anchor Row (kN)	650.00	728.72	616.21	664.69	630.61	643.04
	Estimated Load of 2. Anchor Row (kN)	-	-	650.00	774.71	683.43	711.46
	Estimated Load of 3. Anchor Row (kN)	-	-	-	-	650.00	727.51
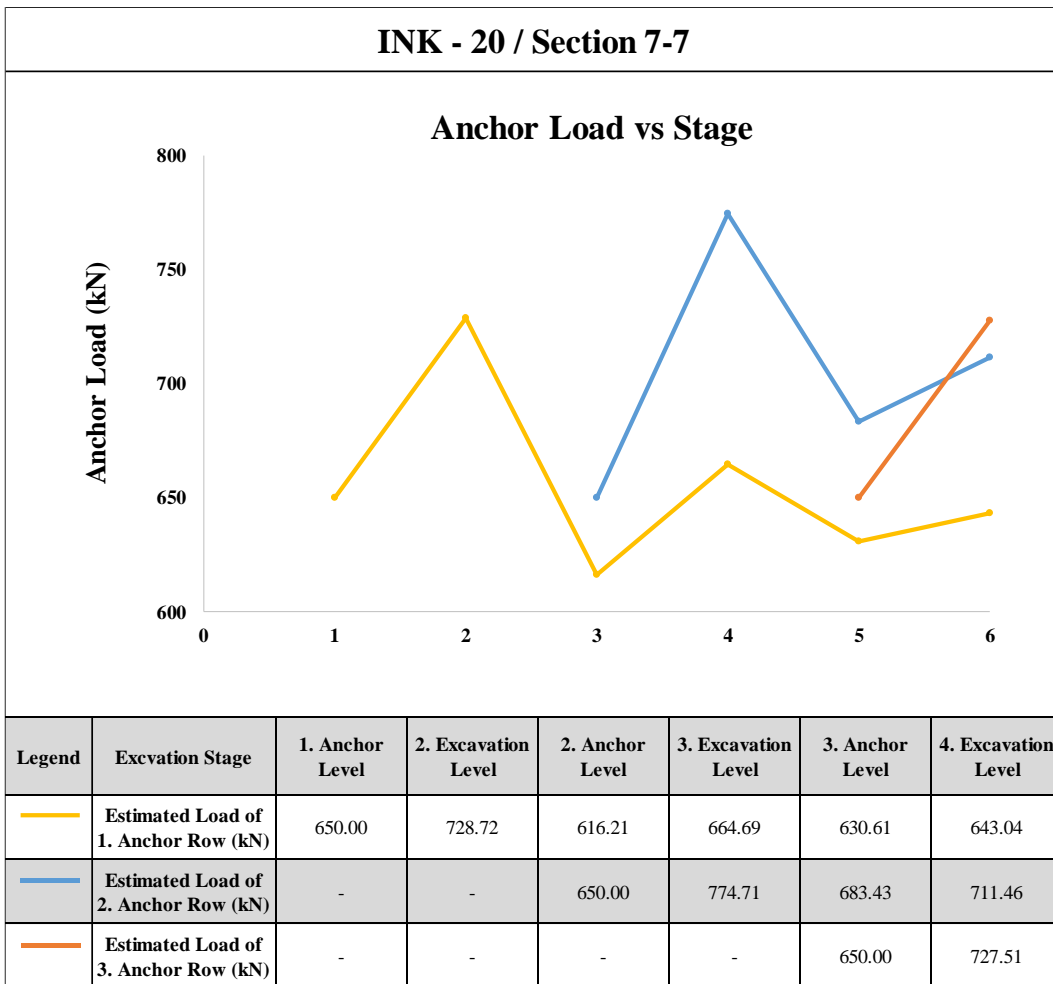
Figure A. 204. Estimated Anchor Loads

INK-21 – Estimated and Measured Displacements
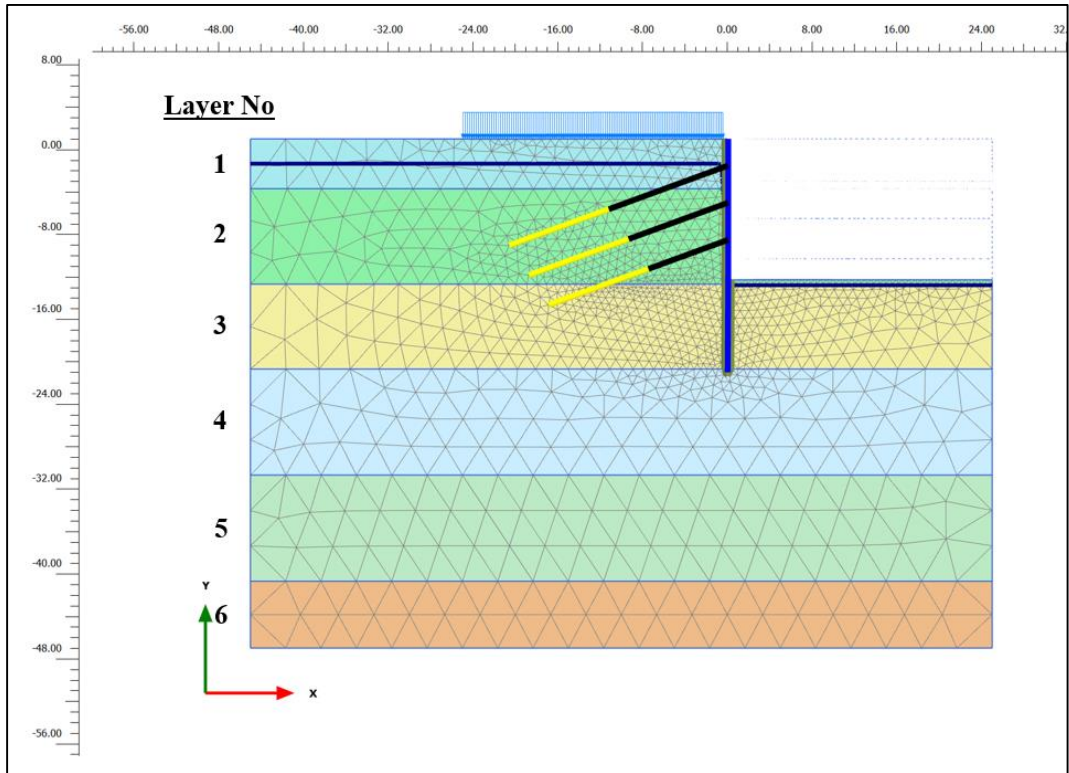
Figure A. 205. Meshed Model for INK-21

INK-21

Displacement Relative to Inclinometer Base Elevation (mm)
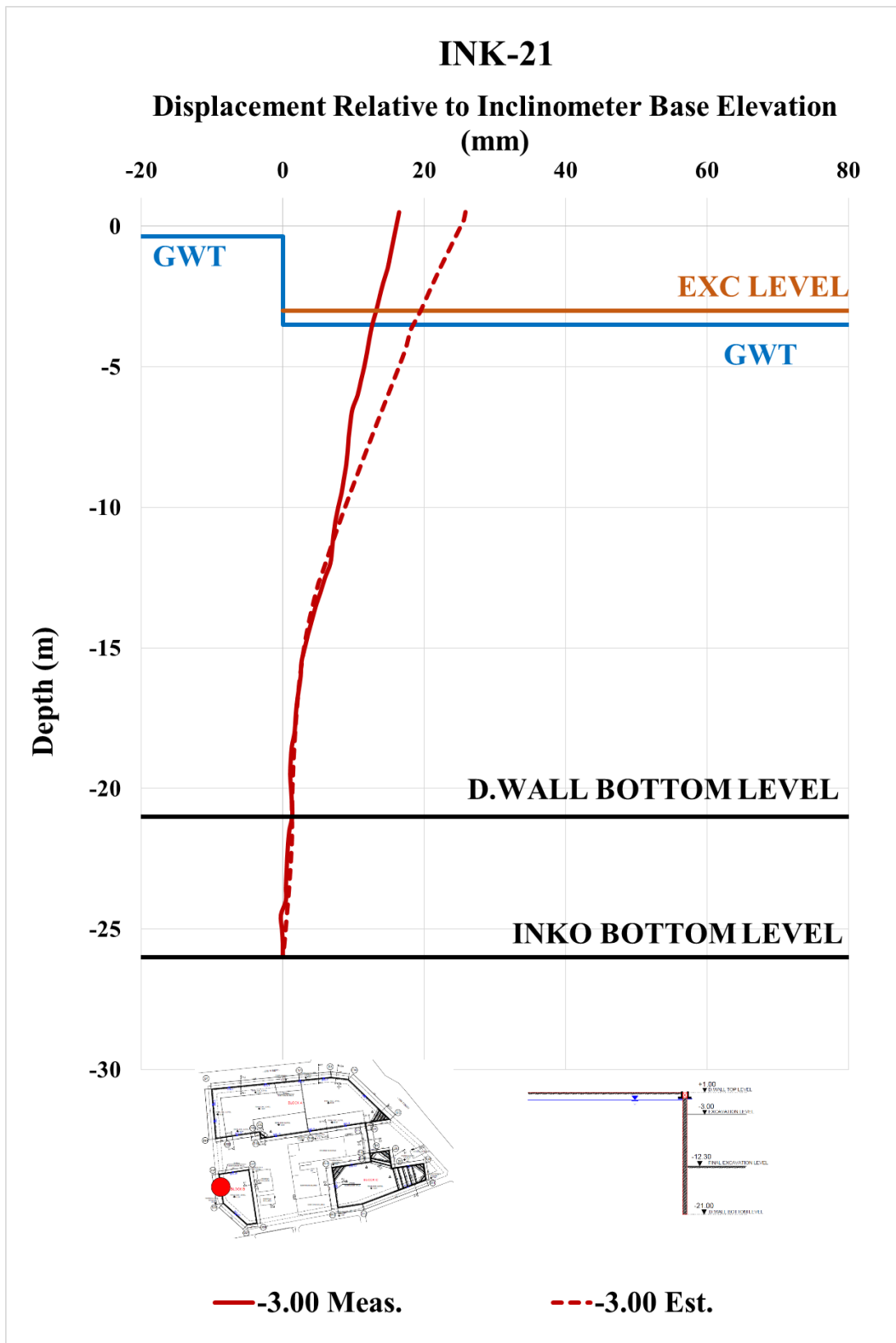
Figure A. 206. Estimated and Measured Displ. Rel. to Inc. Base Elev. at -3.00 m
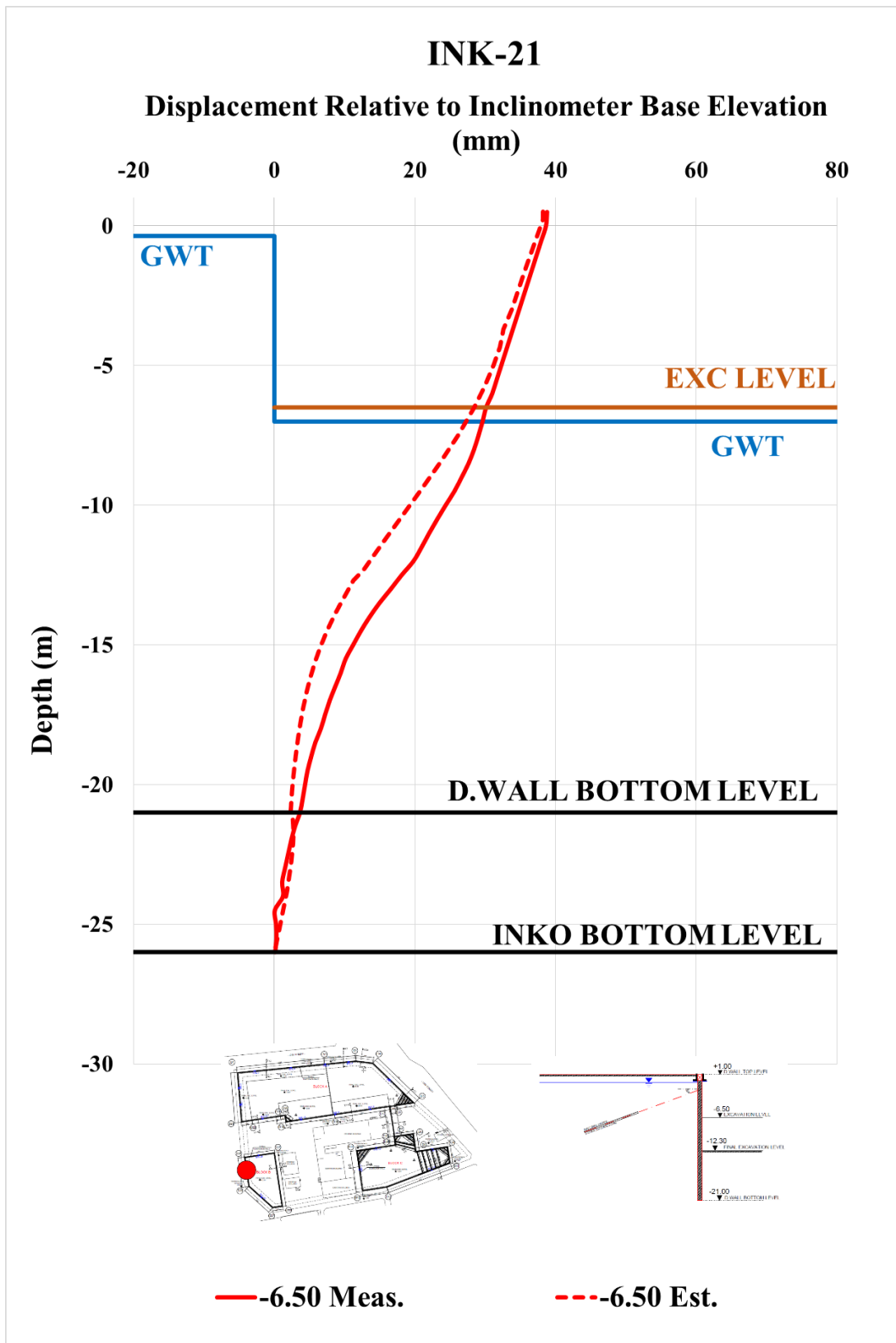
Figure A. 207. Estimated and Measured Displ. Rel. to Inc. Base Elev. at -6.50 m

INK-21

Displacement Relative to Inclinometer Base Elevation (mm)
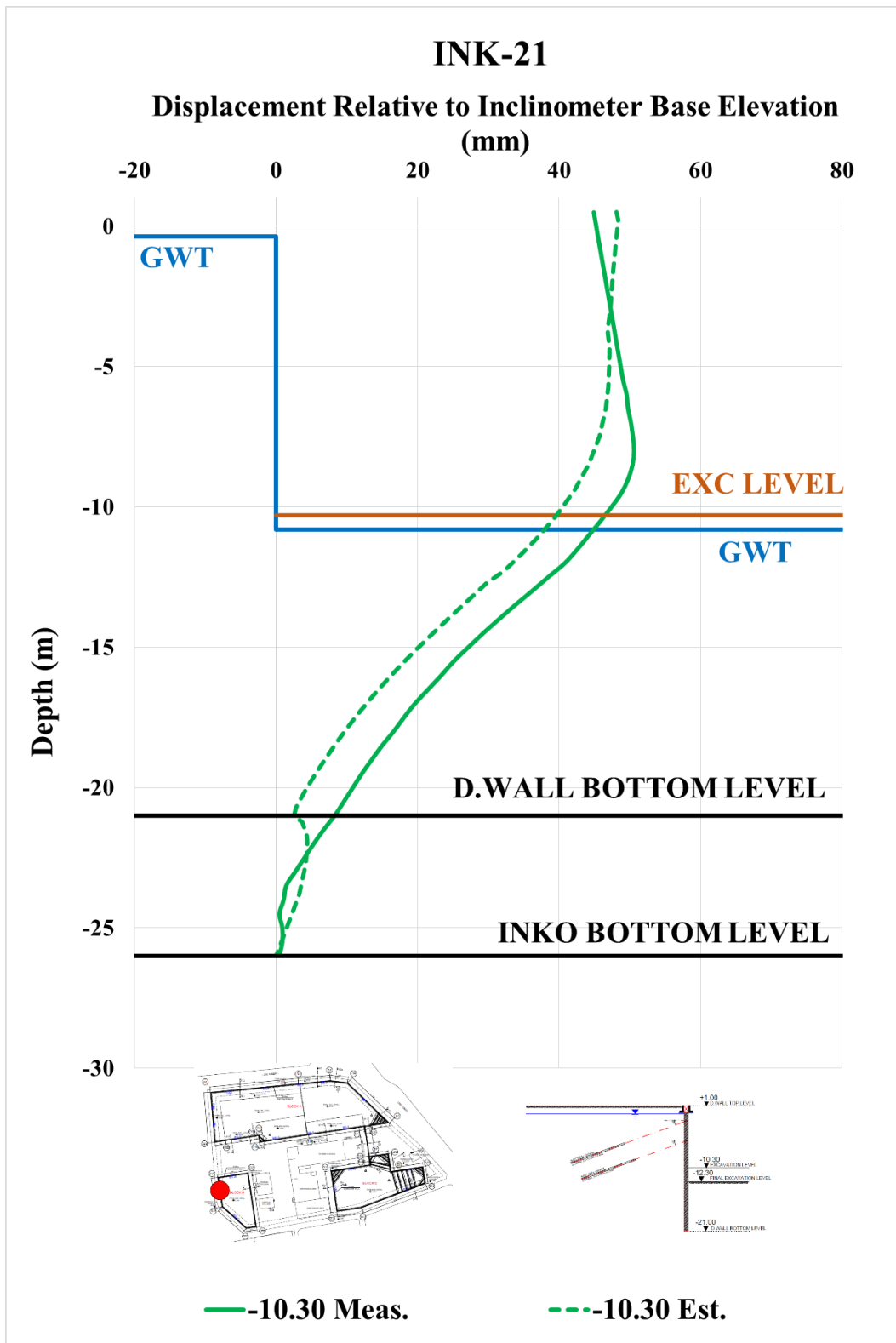
Figure A. 208. Estimated and Measured Displ. Rel. to Inc. Base Elev. at -10.30 m
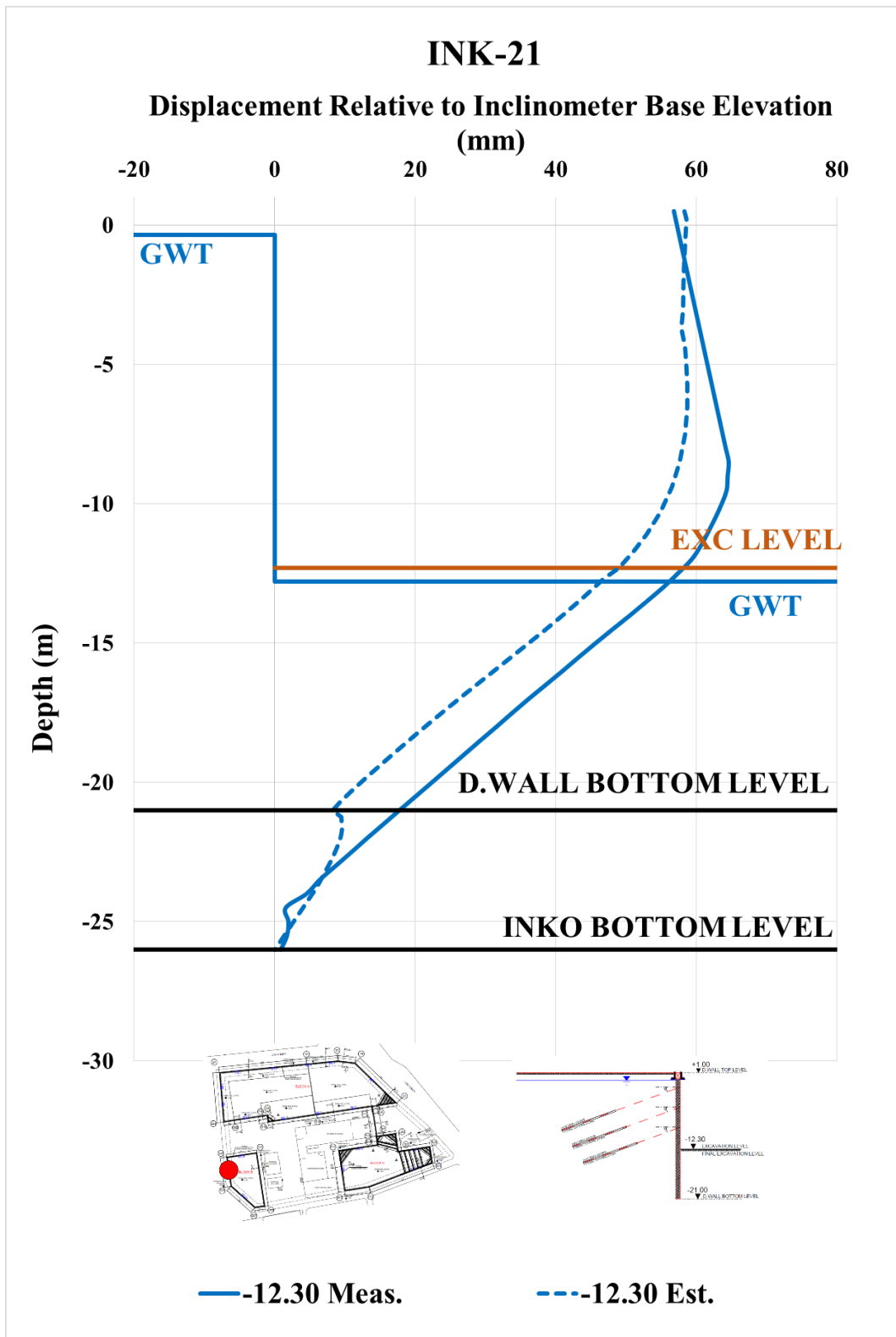
Figure A. 209. Estimated and Measured Displ. Rel. to Inc. Base Elev. at -12.30 m

Table A. 45. Internal Forces of Diaphragm Wall

INK - 21 / Section 7-7				
Excvation Stage	1	2	3	4
Excavation Level (m)	-3,00	-6,50	-10,30	-12,30
N_{max} (kN/m)	100,20	214,80	440,30	587,40
V_{max} (kN/m)	96,58	240,60	365,00	365,00
M_{max} (kN.m/m)	524,70	582,20	982,70	1069,00

INK - 21 / Section 7-7

Anchor Load vs Stage

Legend	Excvation Stage	1. Anchor Level	2. Excavation Level	2. Anchor Level	3. Excavation Level	3. Anchor Level	4. Excavation Level
	Estimated Load of 1. Anchor Row (kN)	650.00	728.72	616.21	664.69	630.61	643.04
	Estimated Load of 2. Anchor Row (kN)	-	-	650.00	774.71	683.43	711.46
	Estimated Load of 3. Anchor Row (kN)	-	-	-	-	650.00	727.51
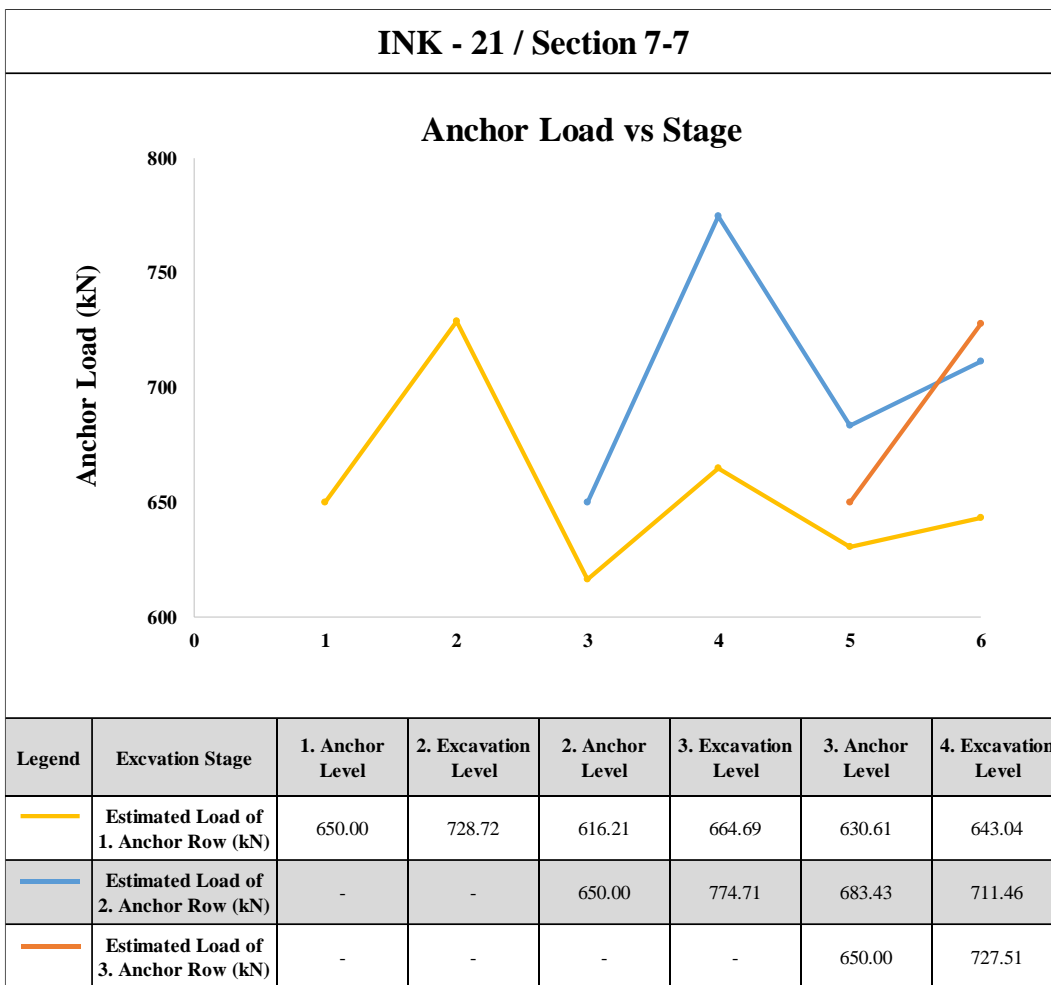
Figure A. 210. Estimated Anchor Loads

INK-18 – Calibrated, Estimated and Measured Displacements
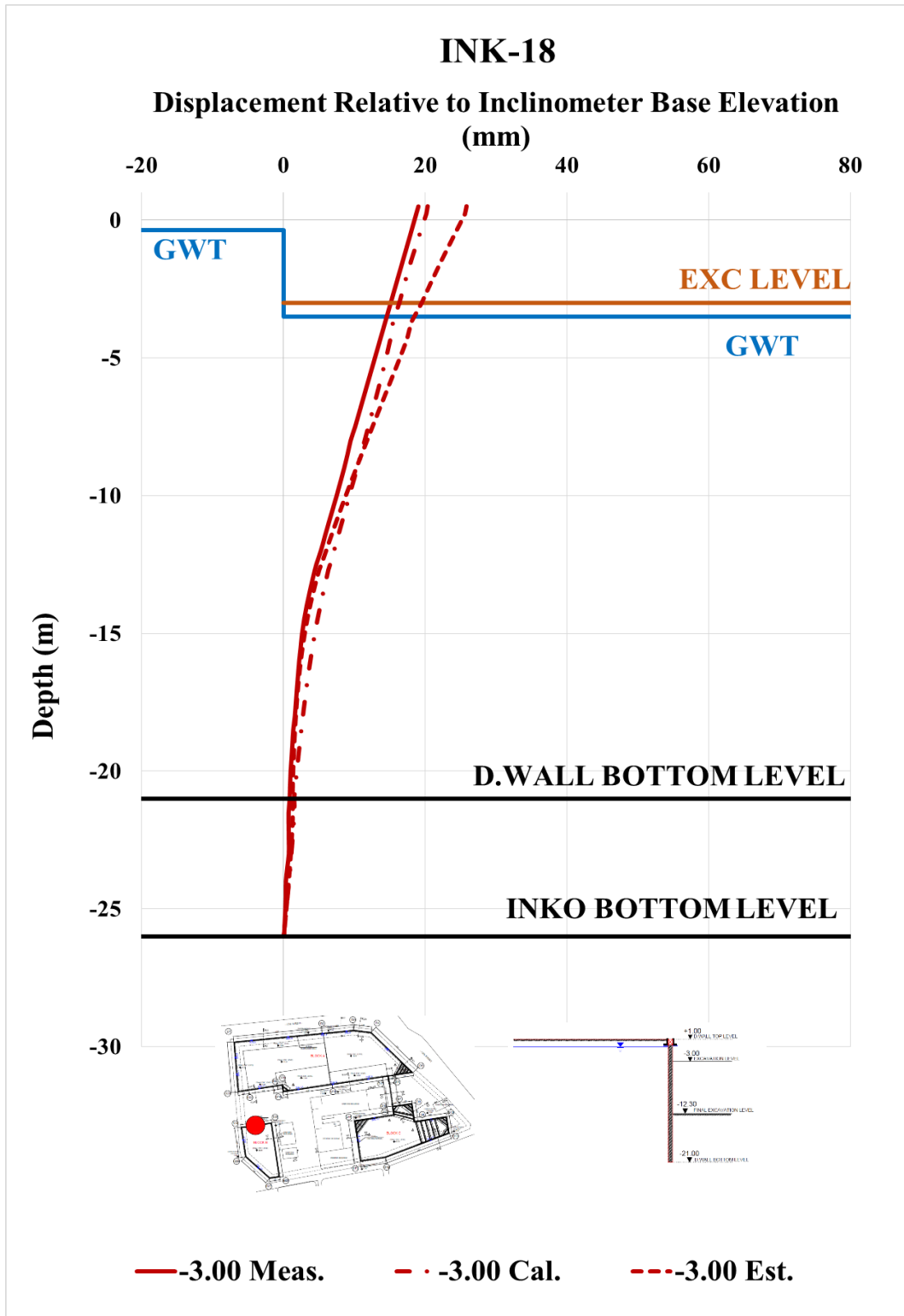
Figure A. 211. Calibrated and Measured Displ. Rel. to Inc. Base Elev. at -3.00 m

INK-18

Displacement Relative to Inclinometer Base Elevation (mm)
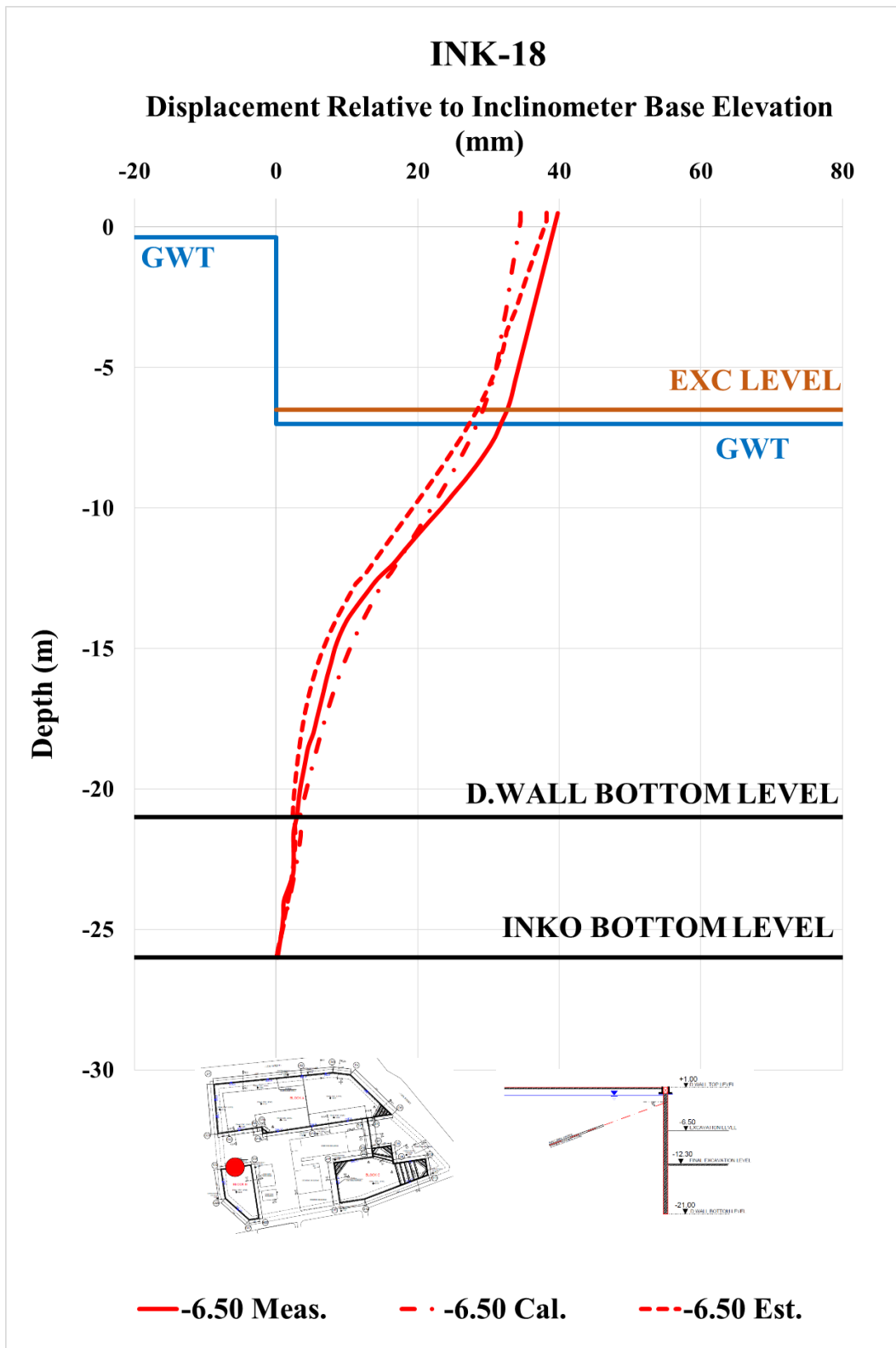
Figure A. 212. Calibrated and Measured Displ. Rel. to Inc. Base Elev. at -6.50 m
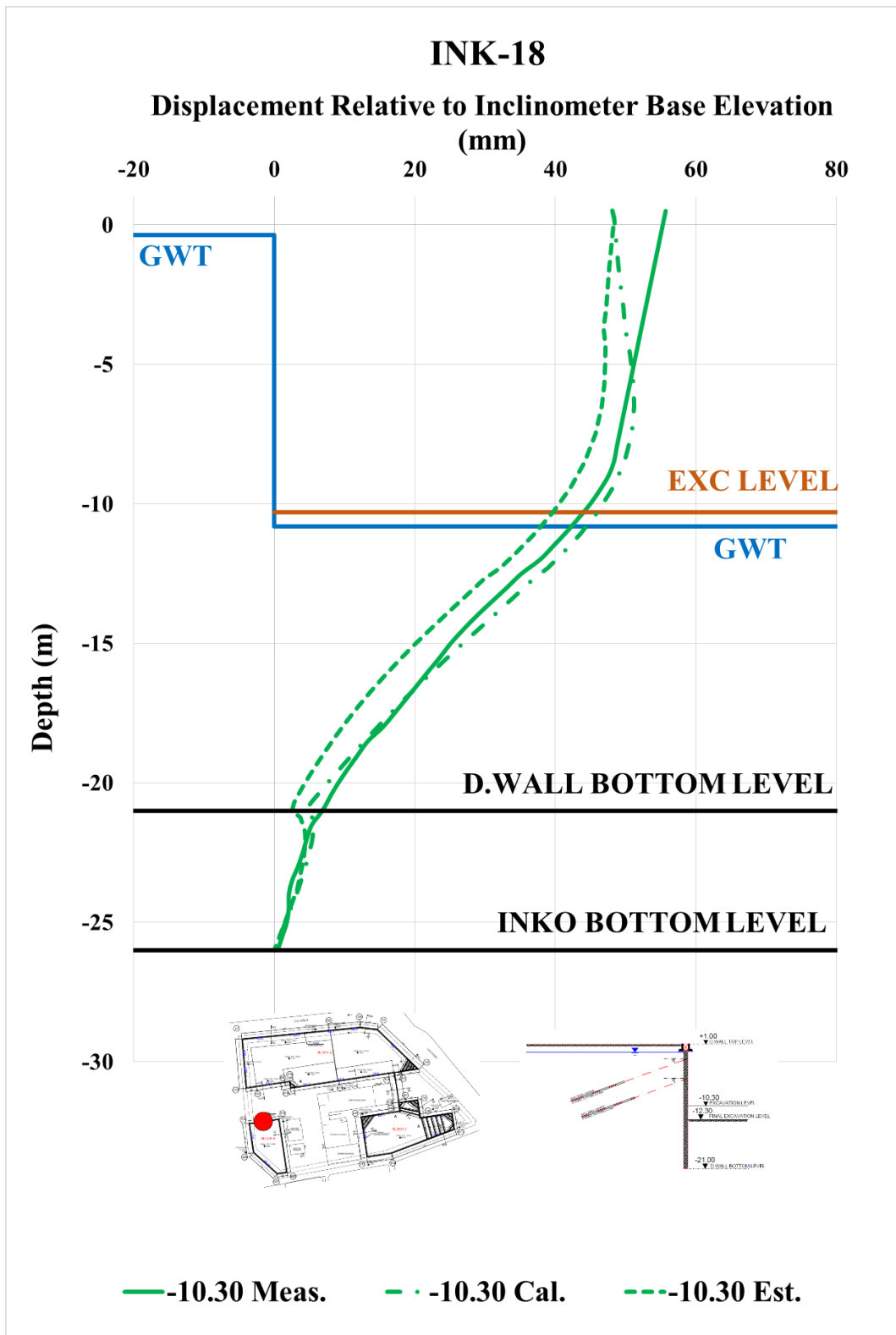
Figure A. 213. Calibrated and Measured Displ. Rel. to Inc. Base Elev. at -10.30 m
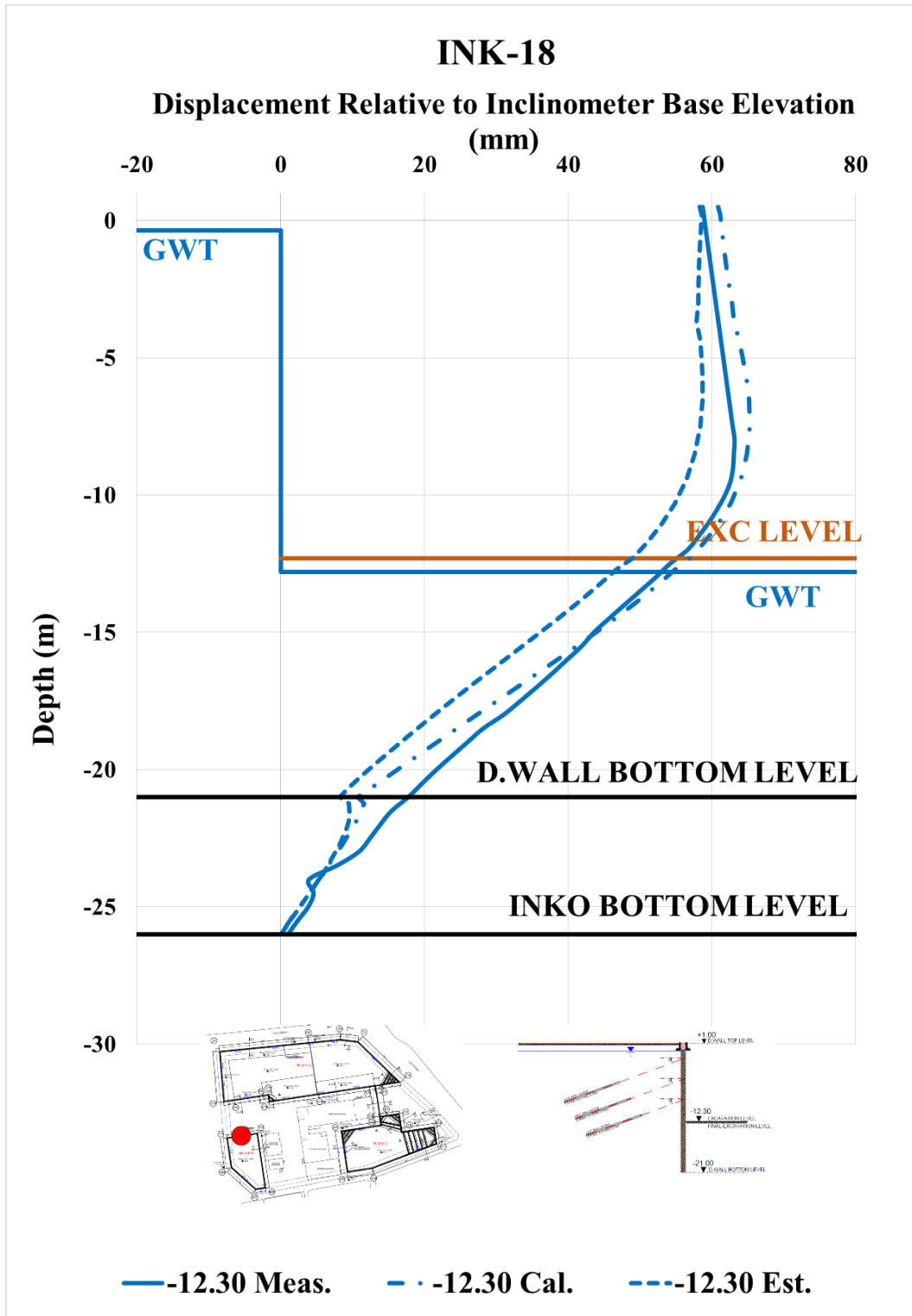
Figure A. 214. Calibrated and Measured Displ. Rel. to Inc. Base Elev. at -12.30 m

Table A. 46. Internal Forces of Diaphragm Wall

INK - 18 / Section 7-7				
Excvation Stage	1	2	3	4
Excavation Level (m)	-3,00	-6,50	-10,30	-12,30
N_{max} (kN/m)	94,15	224,80	457,90	603,90
V_{max} (kN/m)	69,28	251,90	377,20	377,20
M_{max} (kN.m/m)	383,70	518,20	1091,00	1206,00

INK - 18 / Section 7-7

Anchor Load vs Stage

Legend	Excvation Stage	1. Anchor Level	2. Excavation Level	2. Anchor Level	3. Excavation Level	3. Anchor Level	4. Excavation Level
	Estimated Load of 1. Anchor Row (kN)	650.00	736.19	622.89	678.60	643.22	657.61
	Estimated Load of 2. Anchor Row (kN)	-	-	650.00	785.42	691.77	722.66
	Estimated Load of 3. Anchor Row (kN)	-	-	-	-	650.00	731.85
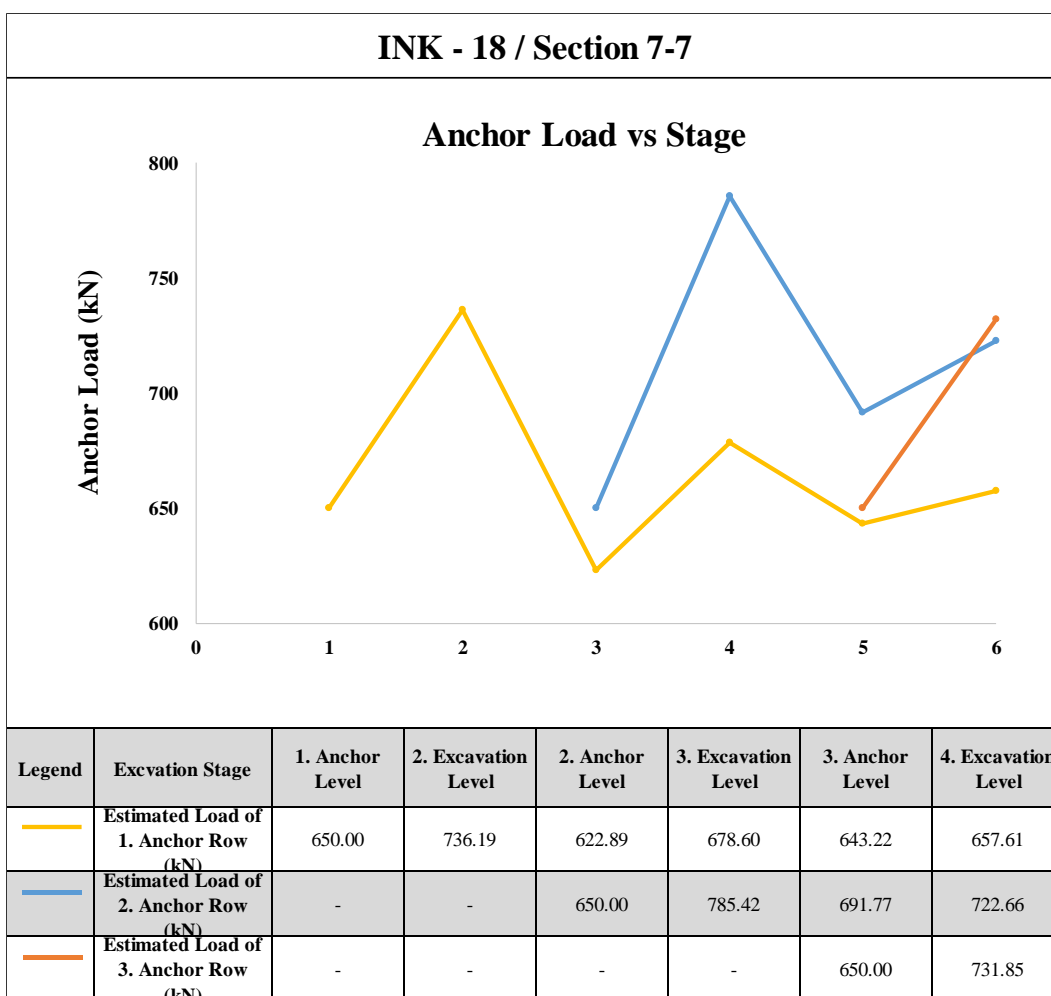
Figure A. 215. Estimated Anchor Loads

Table A. 47. Summary of Displacement Results of INK-18

INK - 18 / SECTION 7 - 7

Excvation Level (m)	Excvation Depth (m)	u_{meas} (mm) Inclinometer Measurements	u_{est} (mm) Estimation with Plaxis 2D Analysis	u_{cal} (mm) Calibration with Plaxis 2D Analysis	$u_{literature}$ (mm) FHWA-IF-99-015 (1999) - Maksimum	$u_{literature}$ (mm) FHWA-IF-99-015 (1999) - Average	$u_{literature}$ (mm) Goldberg et al. (1976)	$u_{literature}$ (mm) Clough et al. (1990) - Maksimum	$u_{literature}$ (mm) Clough et al. (1990) - Average	$u_{literature}$ (mm) Long (2001)	$u_{literature}$ (mm) Long (2001) (Extraordinary cases eliminated)	$u_{literature}$ (mm) Long (2001) Cantilever System
-3.00	4.00	19.04	25.86	20.39	20.00	8.00	20.00	20.00	8.00	7.60	5.60	14.4
-6.50	7.50	39.78	38.19	34.52	37.50	15.00	37.50	37.50	15.00	14.25	10.50	-
-10.30	11.30	55.68	48.31	51.20	56.50	22.60	56.50	56.50	22.60	21.47	15.82	-
-12.30	13.30	63.12	58.72	65.20	66.50	26.60	66.50	66.50	26.60	25.27	18.62	-
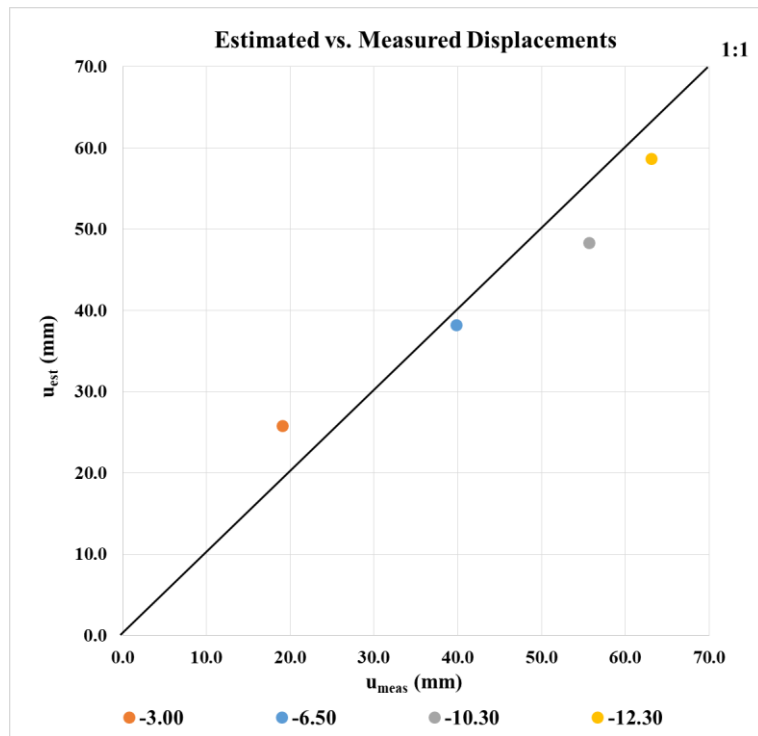
Figure A. 216. Estimated and Measured Displacements of INK – 18
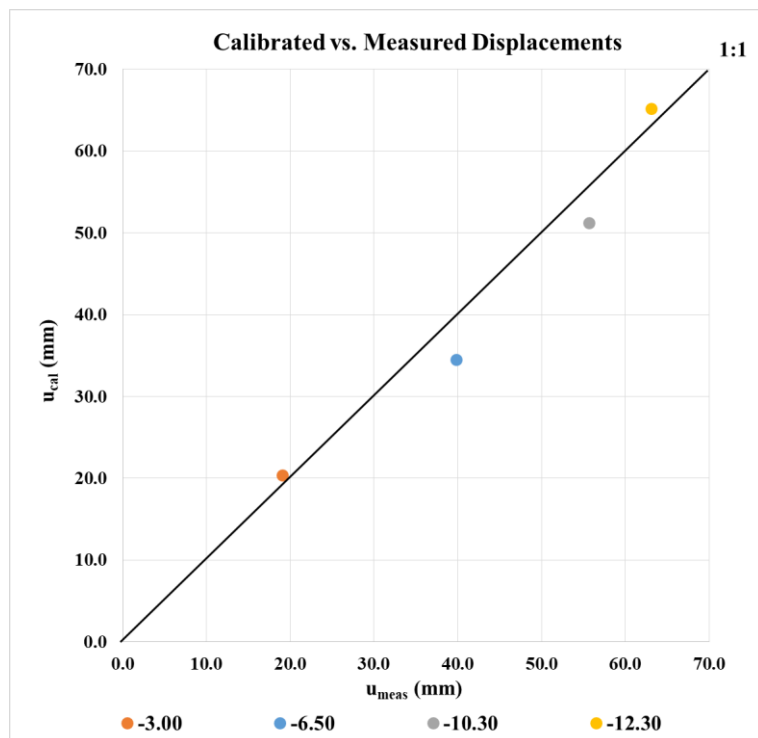
Figure A. 217. Calibrated and Measured Displacements of INK - 18

357

INK-20 – Calibrated, Estimated and Measured Displacements
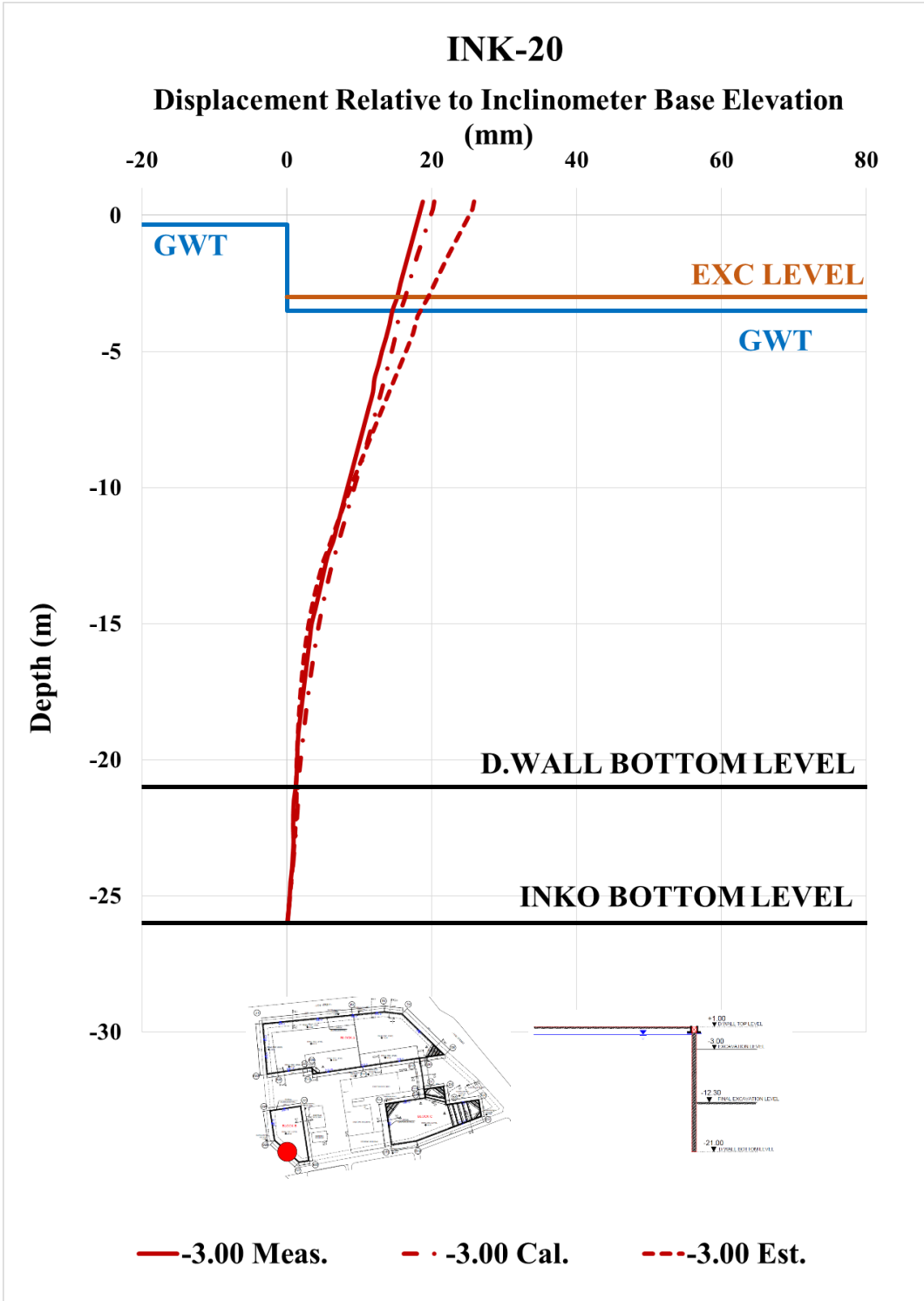
Figure A. 218. Calibrated and Measured Displ. Rel. to Inc. Base Elev. at -3.00 m
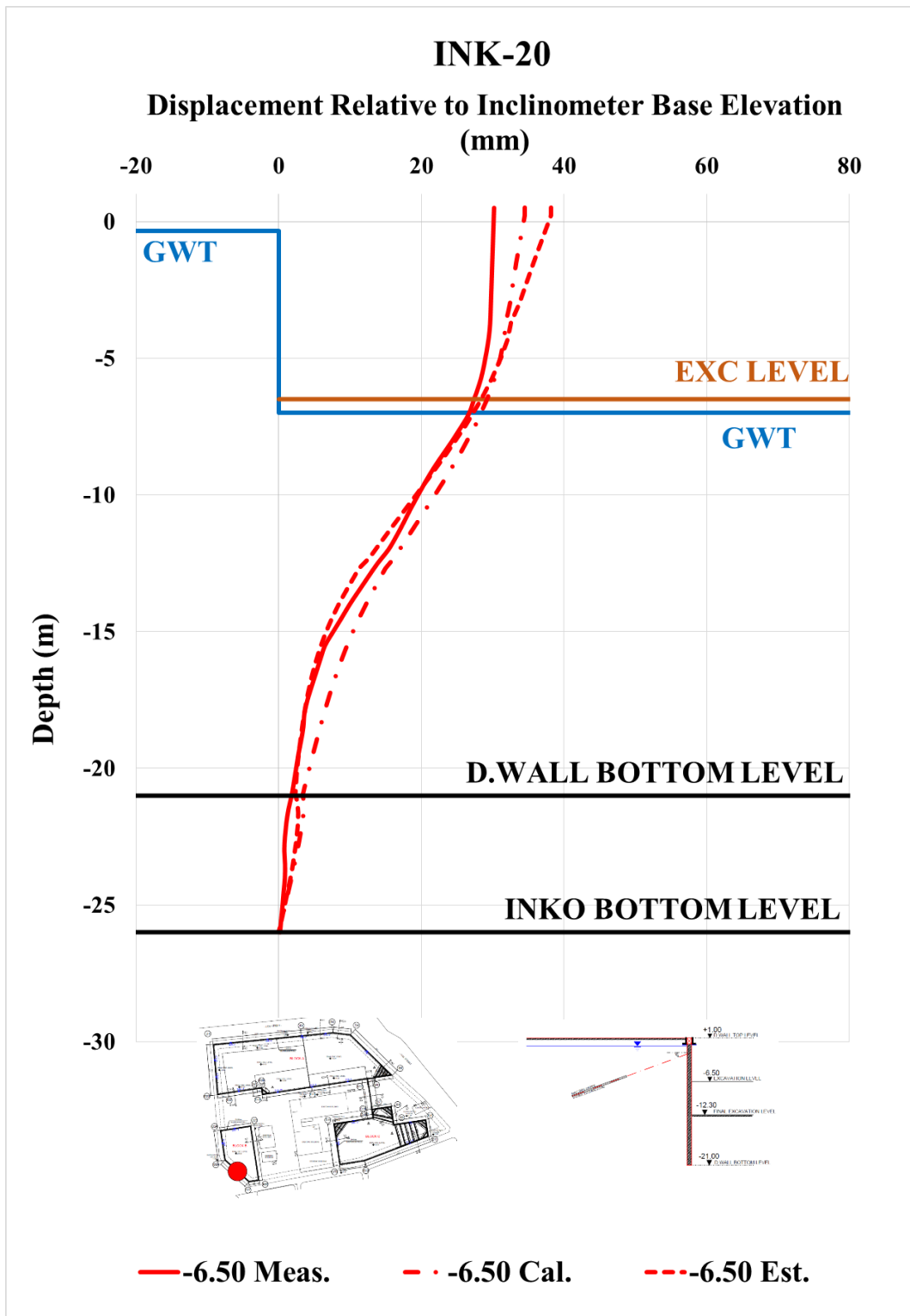
Figure A. 219. Calibrated and Measured Displ. Rel. to Inc. Base Elev. at -6.50 m
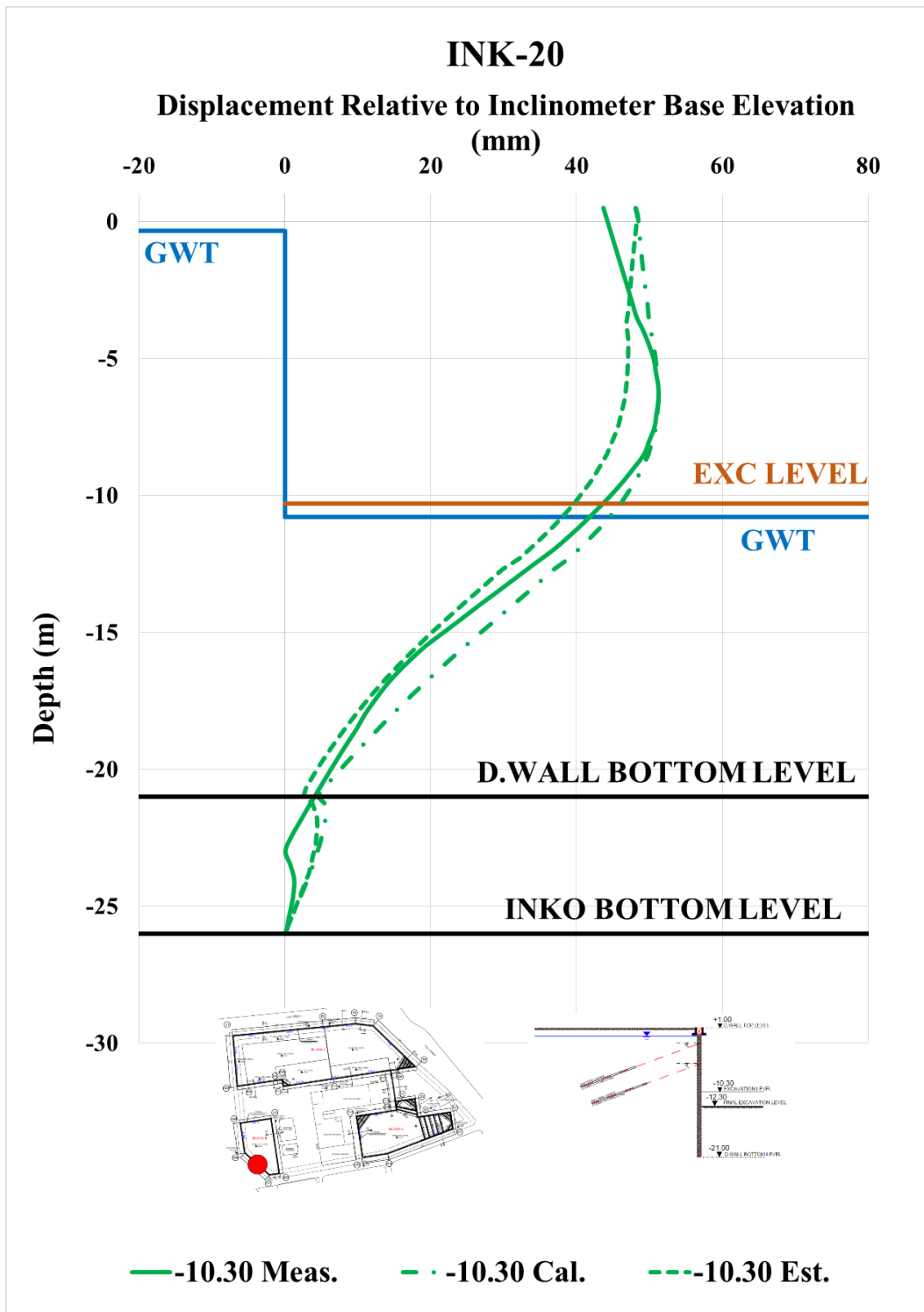
Figure A. 220. Calibrated and Measured Displ. Rel. to Inc. Base Elev. at -10.30 m
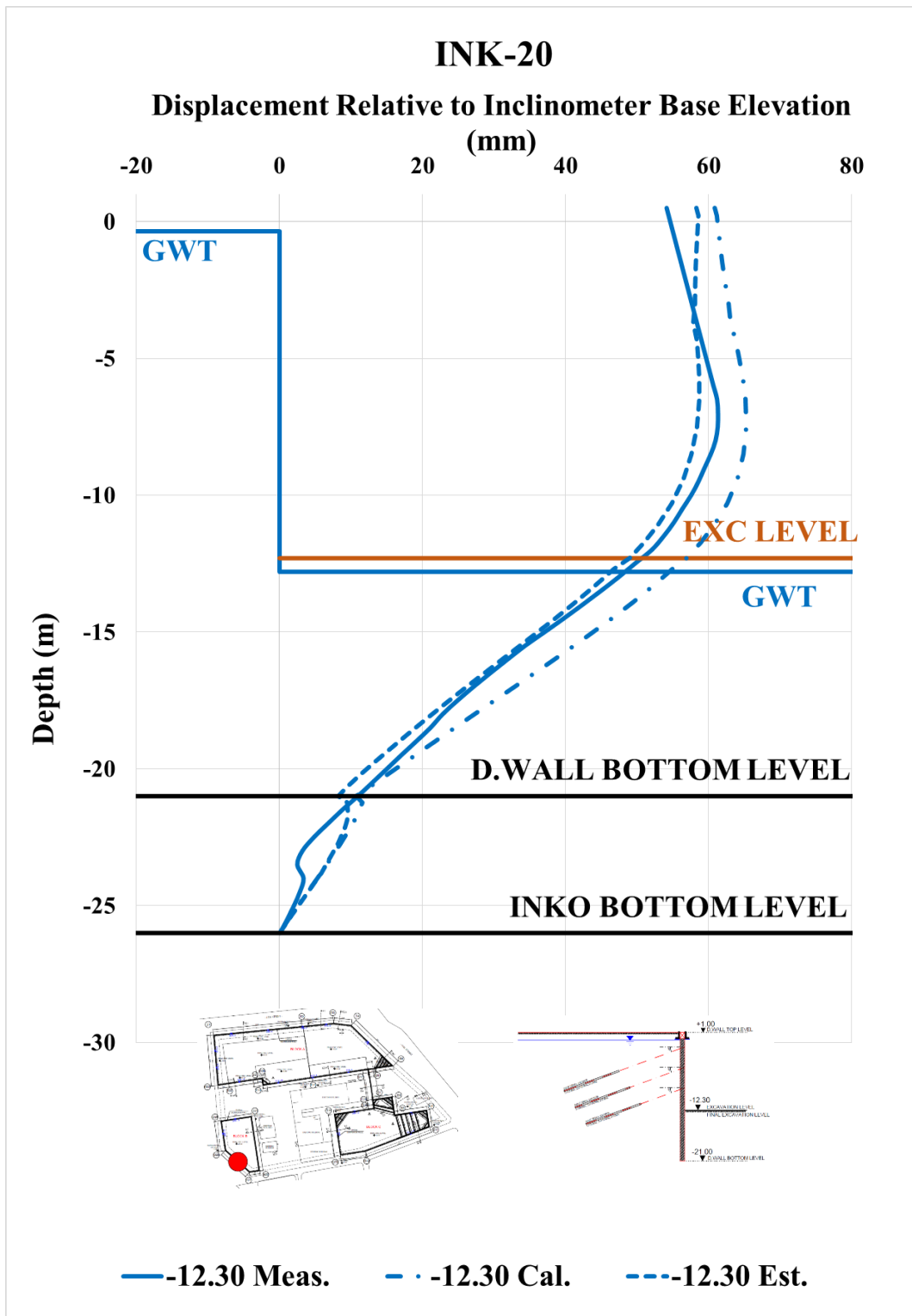
Figure A. 221. Calibrated and Measured Displ. Rel. to Inc. Base Elev. at -12.30 m

Table A. 48. Internal Forces of Diaphragm Wall

INK - 20 / Section 7-7				
Excvation Stage	**1**	**2**	**3**	**4**
Excavation Level (m)	-3,00	-6,50	-10,30	-12,30
N$_{max}$ (kN/m)	94,15	224,80	457,90	603,90
V$_{max}$ (kN/m)	69,28	251,90	377,20	377,20
M$_{max}$ (kN.m/m)	383,70	518,20	1091,00	1206,00

INK - 20 / Section 7-7

Anchor Load vs Stage

Legend	Excvation Stage	1. Anchor Level	2. Excavation Level	2. Anchor Level	3. Excavation Level	3. Anchor Level	4. Excavation Level
	Estimated Load of 1. Anchor Row (kN)	650.00	736.19	622.89	678.60	643.22	657.61
	Estimated Load of 2. Anchor Row (kN)	-	-	650.00	785.42	691.77	722.66
	Estimated Load of 3. Anchor Row (kN)	-	-	-	-	650.00	731.85
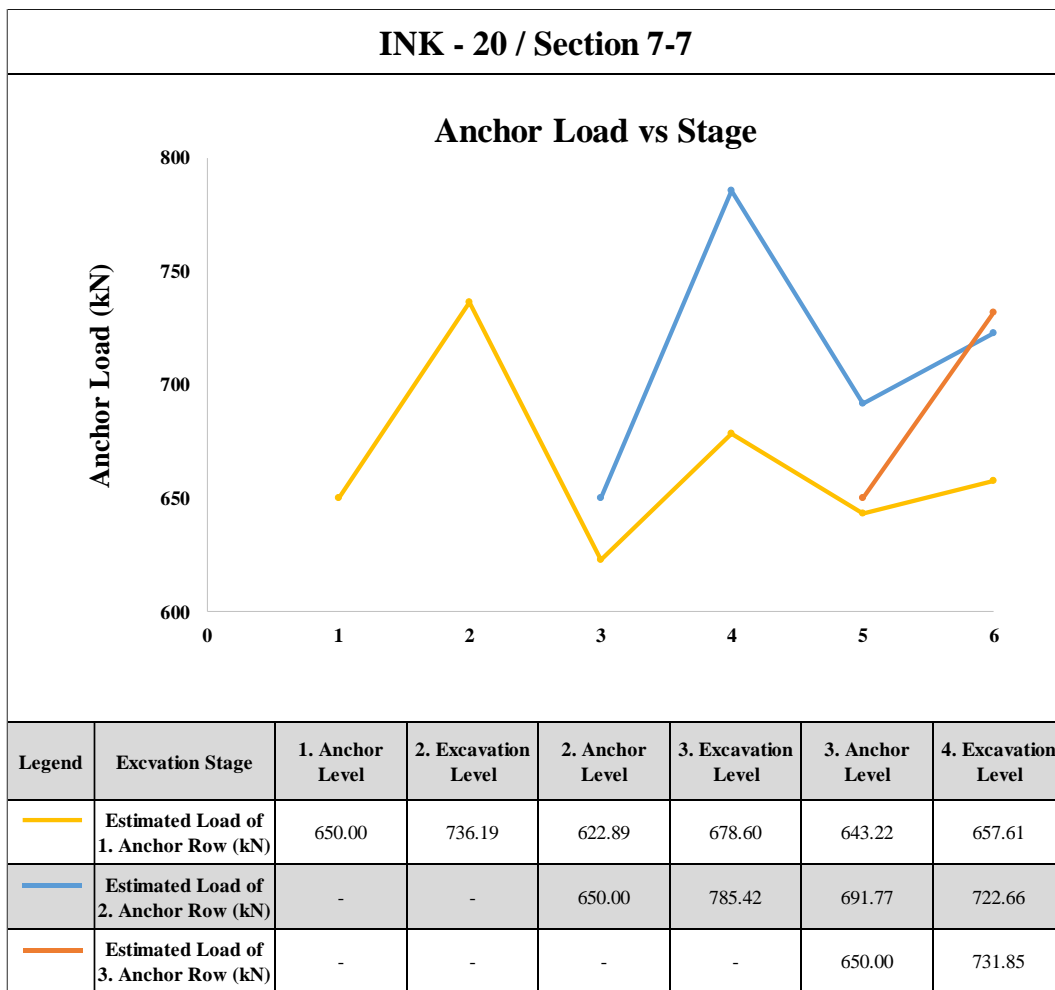
Figure A. 222. Estimated Anchor Loads

Table A. 49. Summary of Displacement Results of INK-20

INK - 20 / SECTION 7 - 7

Excvation Level (m)	Excvation Depth (m)	u_{meas} (mm) Inclinometer Measurements	u_{est} (mm) Estimation with Plaxis 2D Analysis	u_{cal} (mm) Calibration with Plaxis 2D Analysis	$u_{literature}$ (mm) FHWA-IF-99-015 (1999) - Maksimum	$u_{literature}$ (mm) FHWA-IF-99-015 (1999) - Average	$u_{literature}$ (mm) Goldberg et al. (1976)	$u_{literature}$ (mm) Clough et al. (1990) - Maksimum	$u_{literature}$ (mm) Clough et al. (1990) - Average	$u_{literature}$ (mm) Long (2001)	$u_{literature}$ (mm) Long (2001) (Extraordinary cases eliminated)	$u_{literature}$ (mm) Long (2001) Cantilever System
-3.00	4.00	18.76	25.86	20.39	20.00	8.00	20.00	20.00	8.00	7.60	5.60	14.4
-6.50	7.50	30.18	38.19	34.52	37.50	15.00	37.50	37.50	15.00	14.25	10.50	-
-10.30	11.30	51.23	48.31	51.20	56.50	22.60	56.50	56.50	22.60	21.47	15.82	-
-12.30	13.30	61.29	58.72	65.20	66.50	26.60	66.50	66.50	26.60	25.27	18.62	-

363
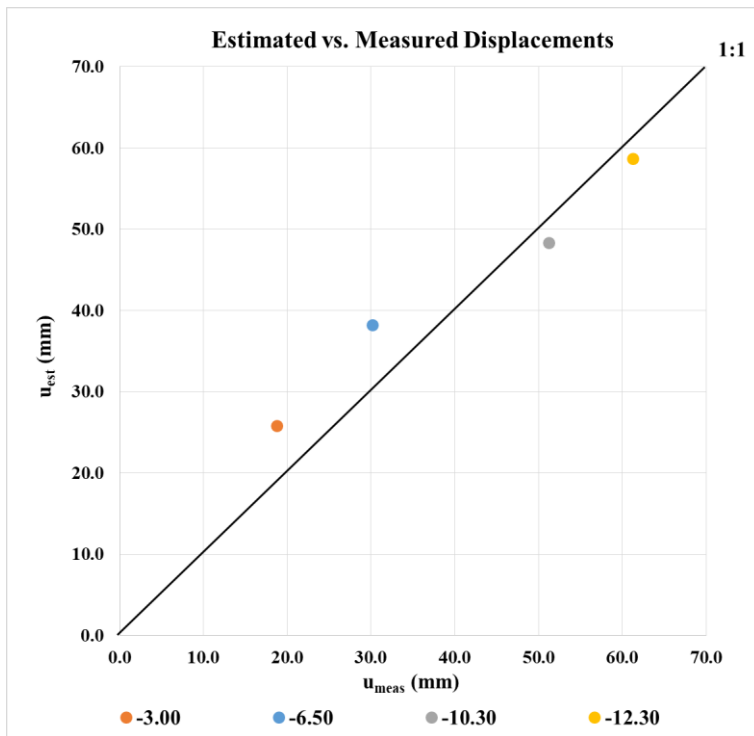
Figure A. 223. Estimated and Measured Displacements of INK - 20
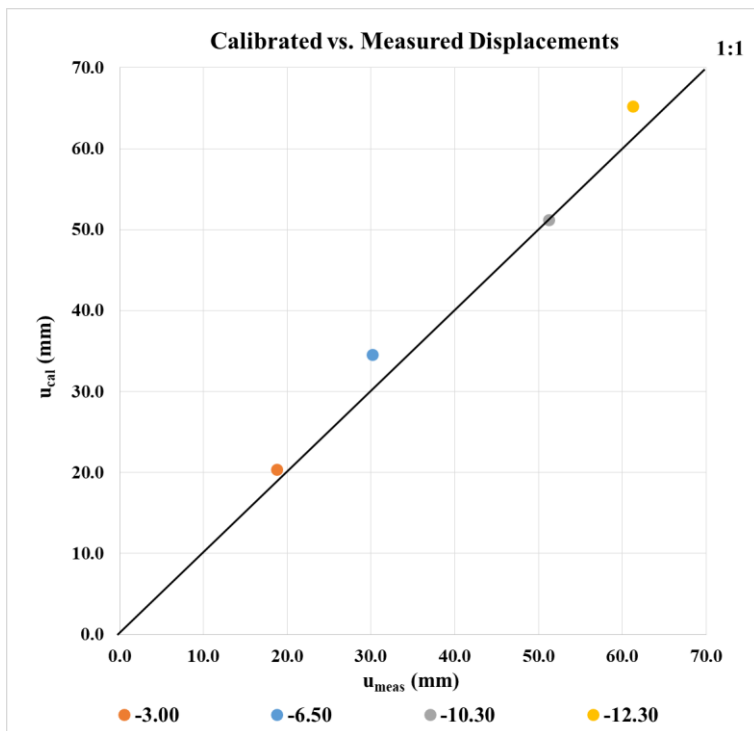
Figure A. 224. Calibrated and Measured Displacements of INK - 20

INK-21 – Calibrated, Estimated and Measured Displacements
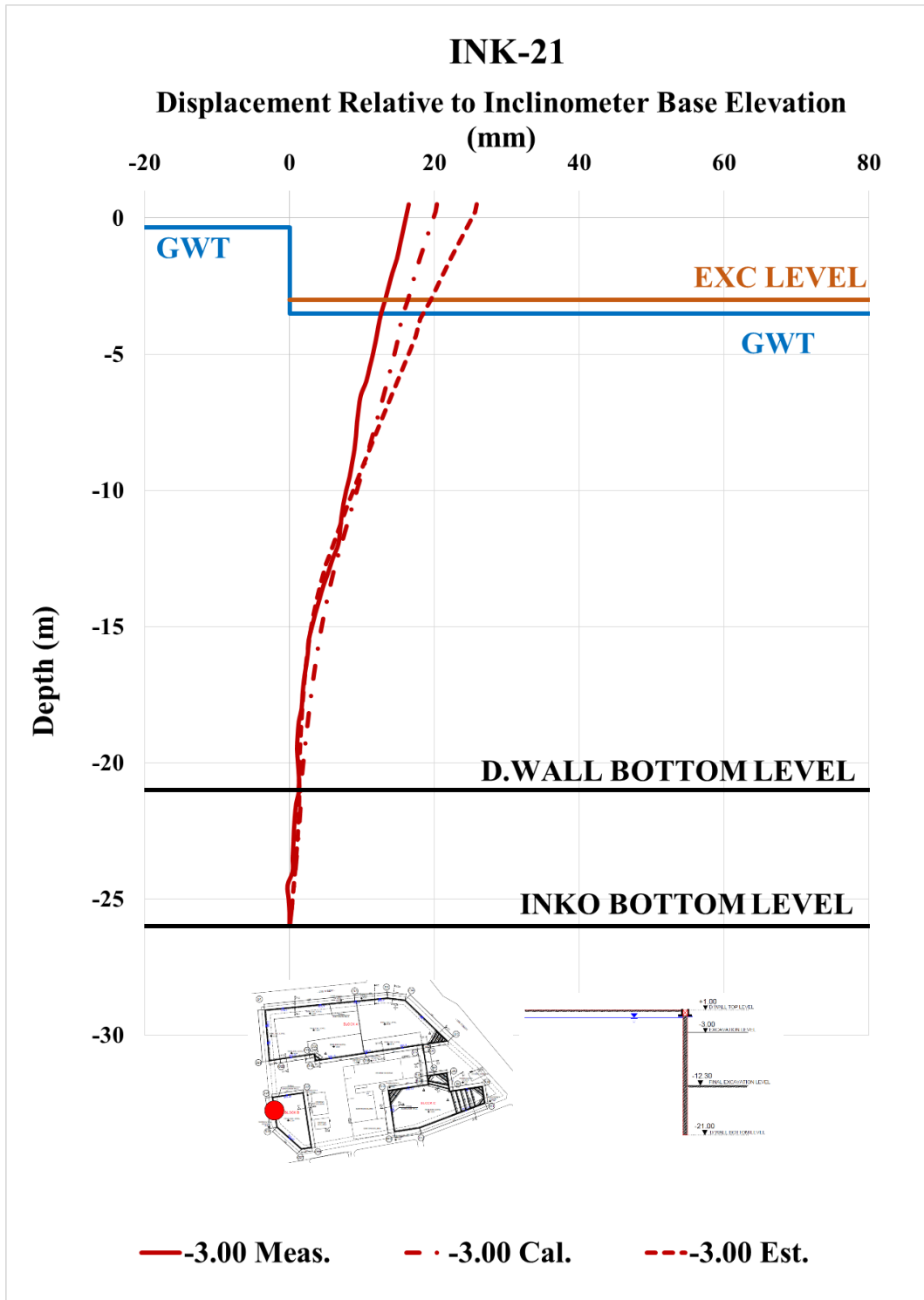
Figure A. 225. Calibrated and Measured Displ. Rel. to Inc. Base Elev. at -3.00 m
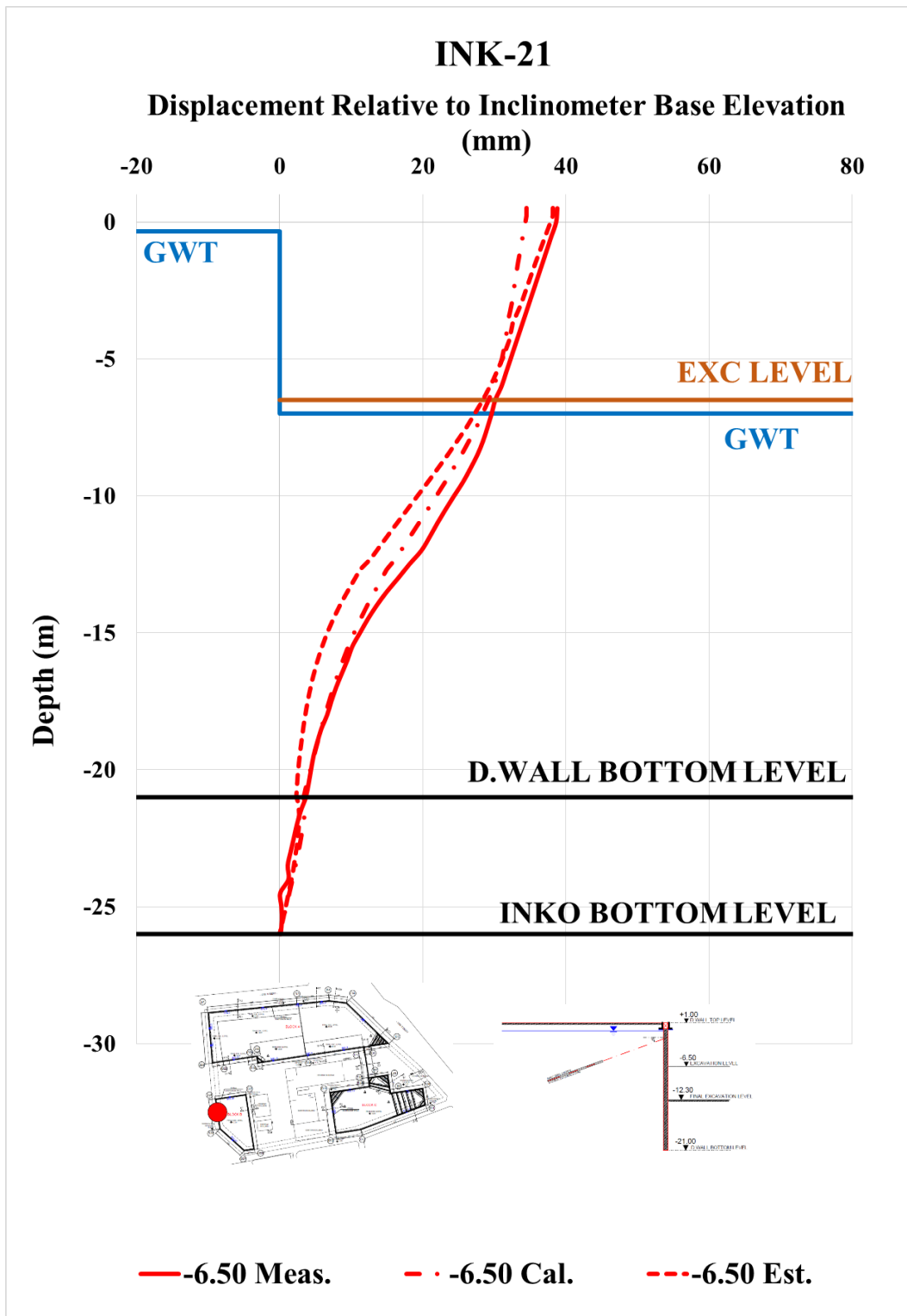
Figure A. 226. Calibrated and Measured Displ. Rel. to Inc. Base Elev. at -6.50 m
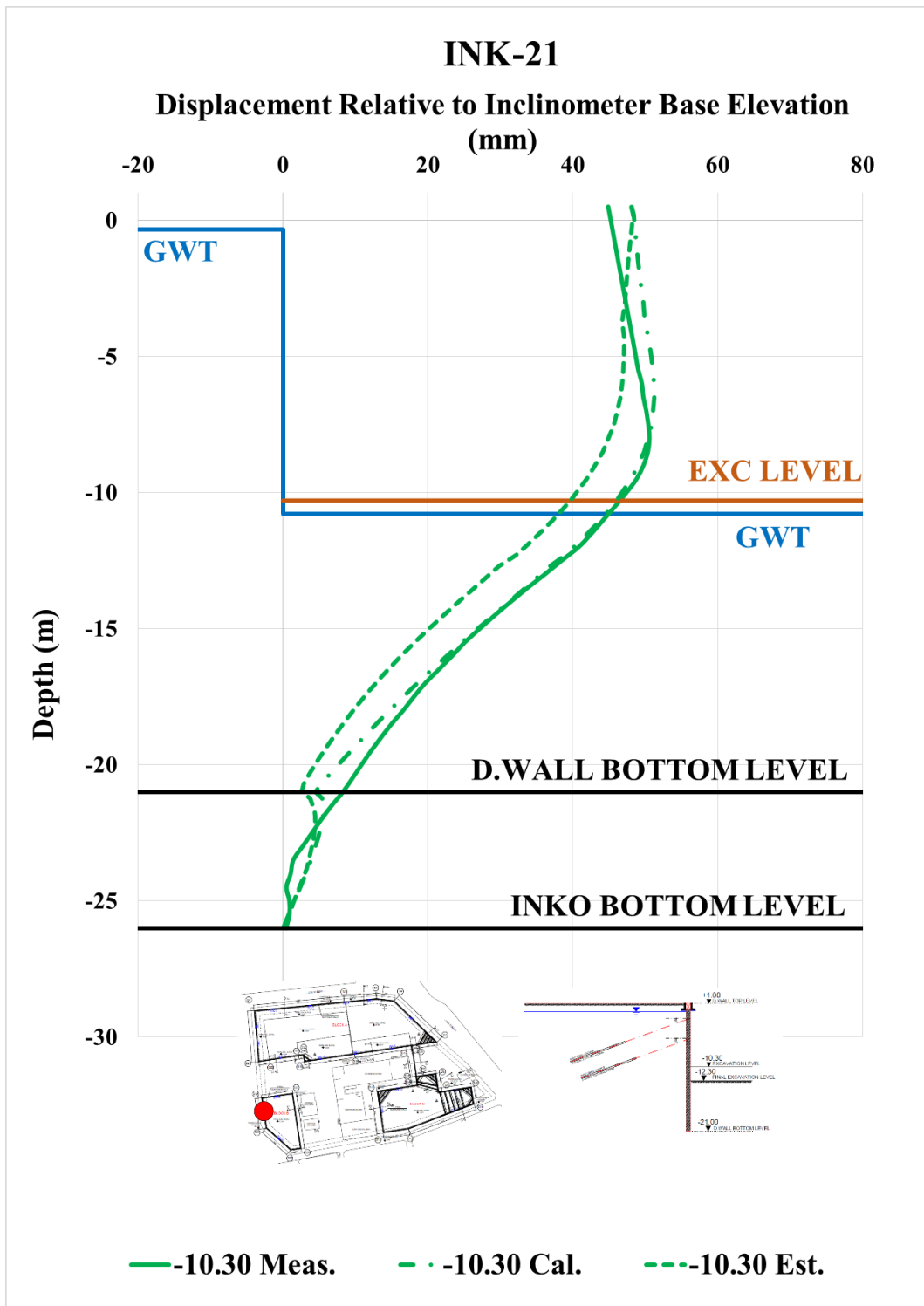
Figure A. 227. Calibrated and Measured Displ. Rel. to Inc. Base Elev. at -10.30 m
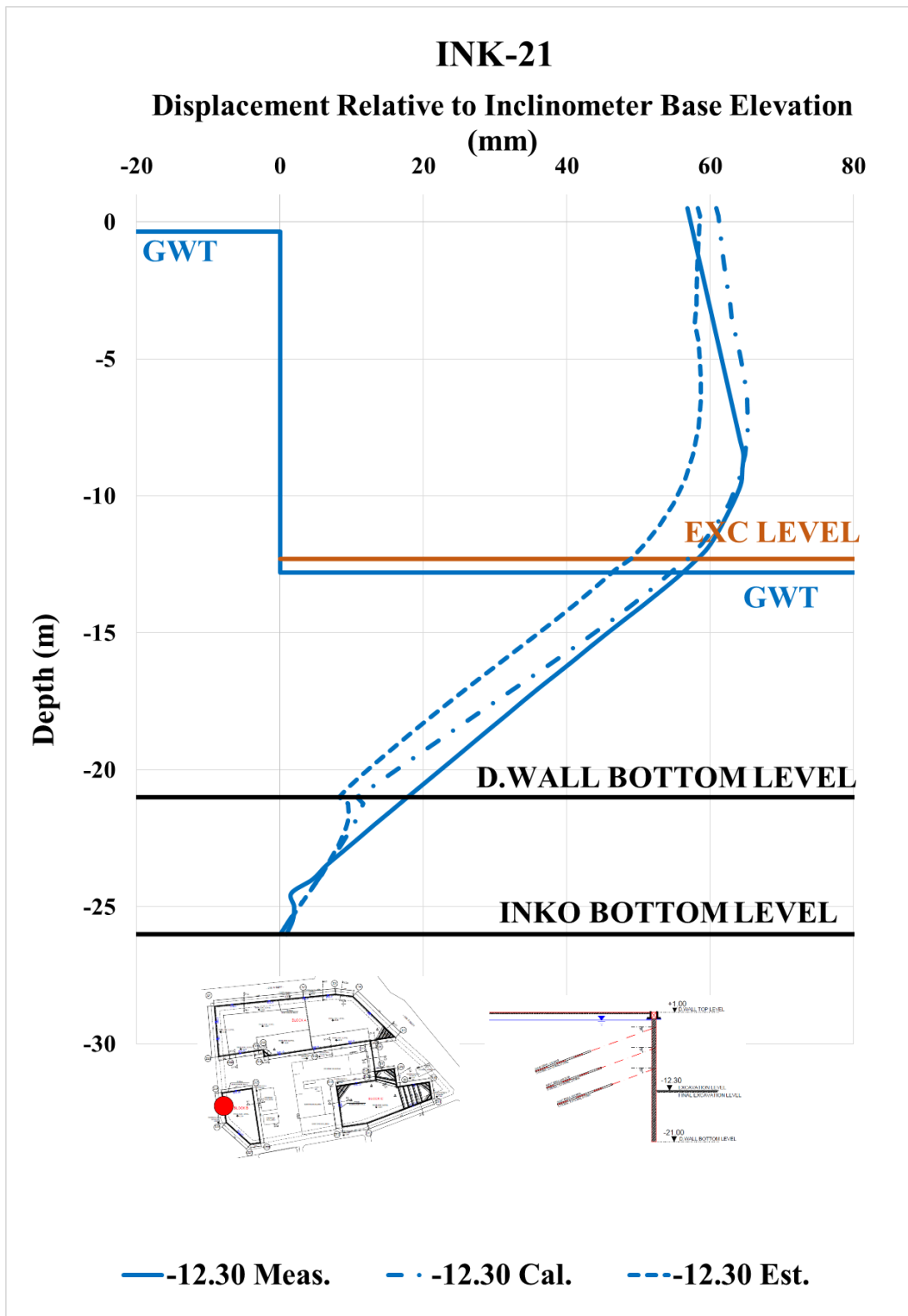
Figure A. 228. Calibrated and Measured Displ. Rel. to Inc. Base Elev. at -12.30 m

Table A. 50. Internal Forces of Diaphragm Wall

INK - 21 / Section 7-7				
Excvation Stage	1	2	3	4
Excavation Level (m)	-3,00	-6,50	-10,30	-12,30
N_{max} (kN/m)	94,15	224,80	457,90	603,90
V_{max} (kN/m)	69,28	251,90	377,20	377,20
M_{max} (kN.m/m)	383,70	518,20	1091,00	1206,00

INK - 21 / Section 7-7

Anchor Load vs Stage

Legend	Excvation Stage	1. Anchor Level	2. Excavation Level	2. Anchor Level	3. Excavation Level	3. Anchor Level	4. Excavation Level
	Estimated Load of 1. Anchor Row (kN)	650.00	736.19	622.89	678.60	643.22	657.61
	Estimated Load of 2. Anchor Row (kN)	-	-	650.00	785.42	691.77	722.66
	Estimated Load of 3. Anchor Row (kN)	-	-	-	-	650.00	731.85

Figure A. 229. Estimated Anchor Loads

Table A. 51. Summary of Displacement Results of INK-21

					INK - 21 / SECTION 7 - 7							
Excavation Level (m)	Excavation Depth (m)	u_{meas} (mm) Inclinometer Measurements	u_{est} (mm) Estimation with Plaxis 2D Analysis	u_{cal} (mm) Calibration with Plaxis 2D Analysis	$u_{literature}$ (mm) FHWA-IF-99-015 (1999) - Maksimum	$u_{literature}$ (mm) FHWA-IF-99-015 (1999) - Average	$u_{literature}$ (mm) Goldberg et al. (1976)	$u_{literature}$ (mm) Clough et al. (1990) - Maksimum	$u_{literature}$ (mm) Clough et al. (1990) - Average	$u_{literature}$ (mm) Long (2001)	$u_{literature}$ (mm) Long (2001) (Extraordinary cases eliminated)	$u_{literature}$ (mm) Long (2001) Cantilever System
-3.00	4.00	16.45	25.86	20.39	20.00	8.00	20.00	20.00	8.00	7.60	5.60	14.4
-6.50	7.50	38.78	38.19	34.52	37.50	15.00	37.50	37.50	15.00	14.25	10.50	-
-10.30	11.30	48.63	48.31	51.20	56.50	22.60	56.50	56.50	22.60	21.47	15.82	-
-12.30	13.30	64.61	58.72	65.20	66.50	26.60	66.50	66.50	26.60	25.27	18.62	-
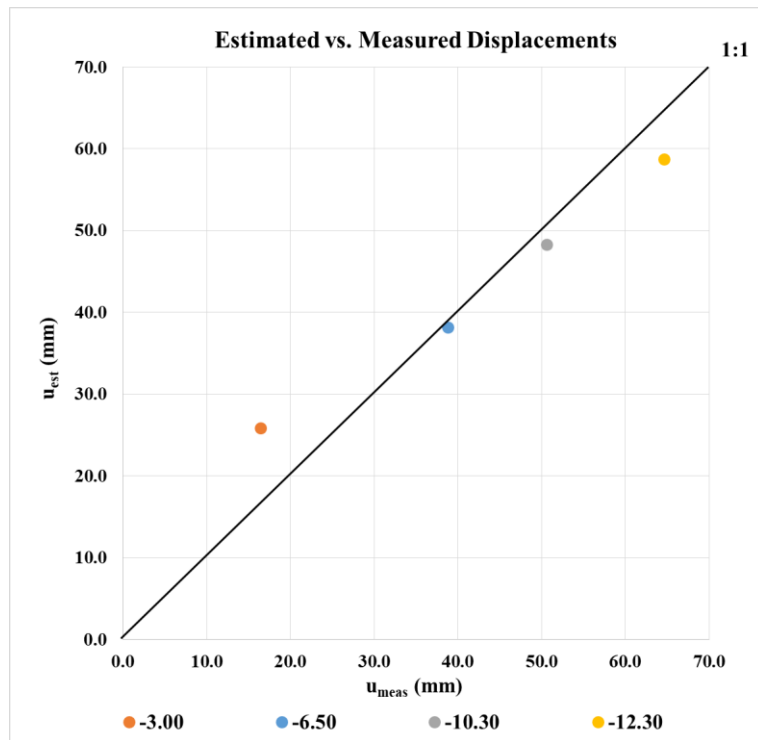
Figure A. 230. Estimated and Measured Displacements of INK - 21
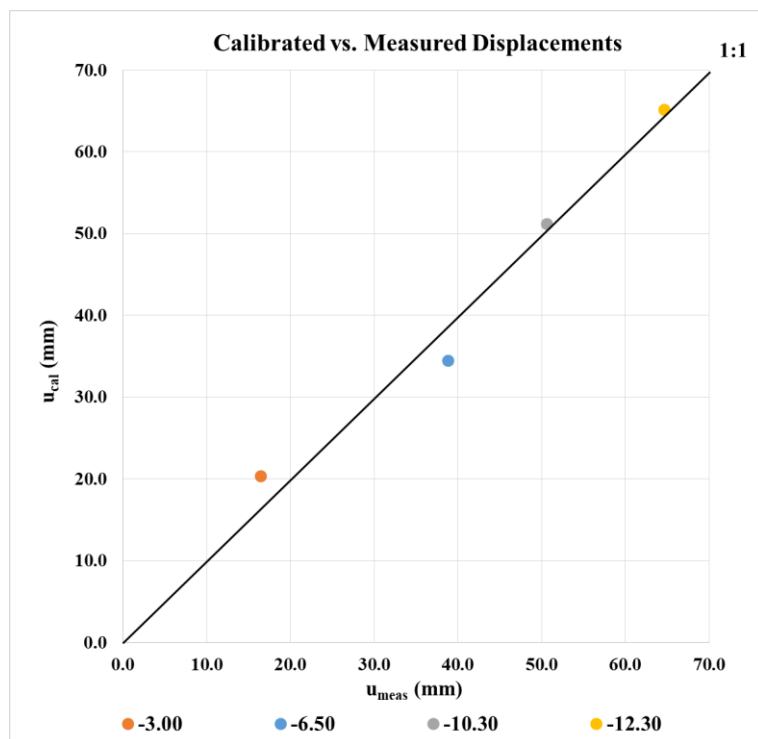
Figure A. 231. Calibrated and Measured Displacements of INK - 21

Area C1
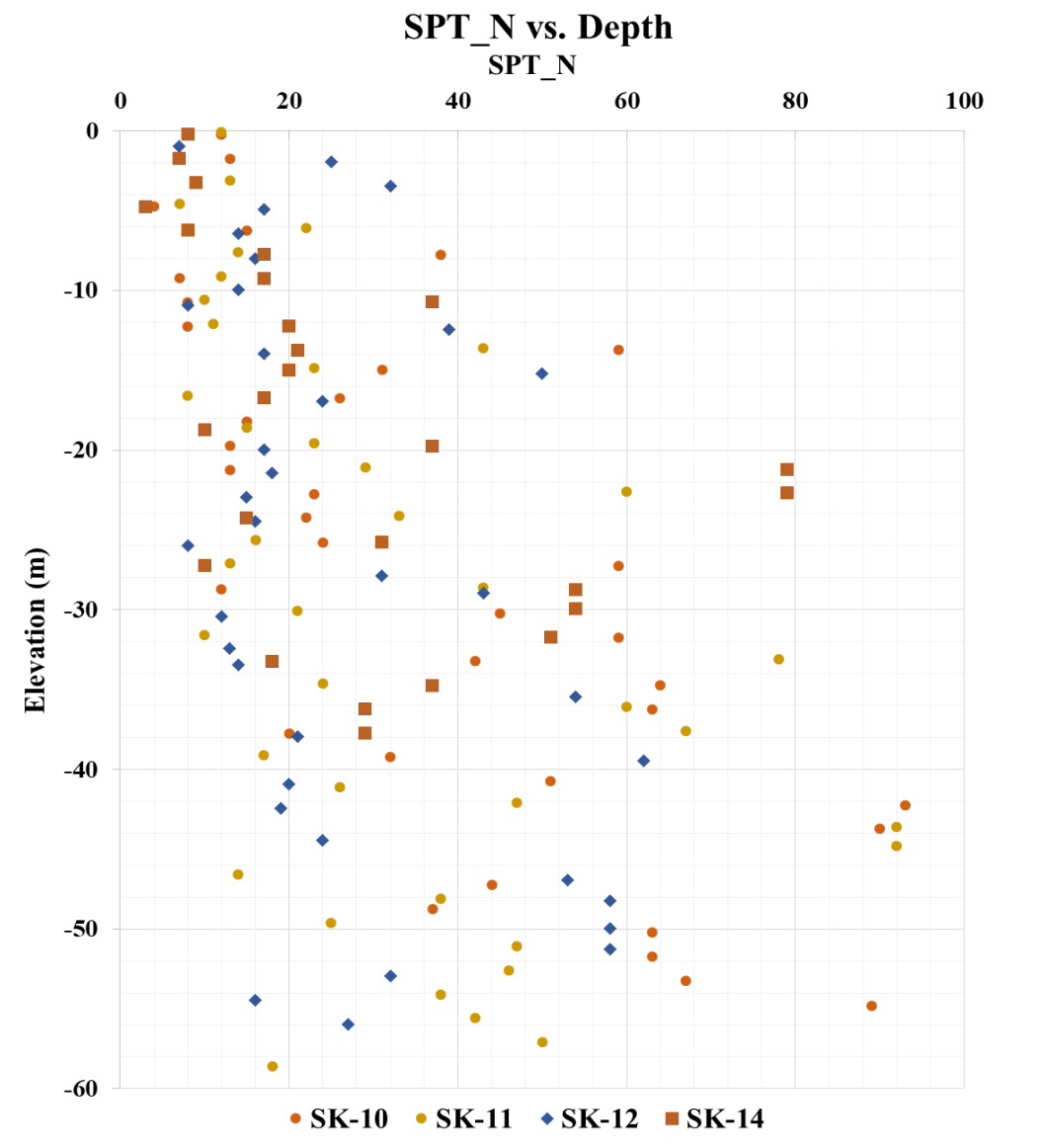
Figure A. 232. SPT-N vs. Depth for Area C1
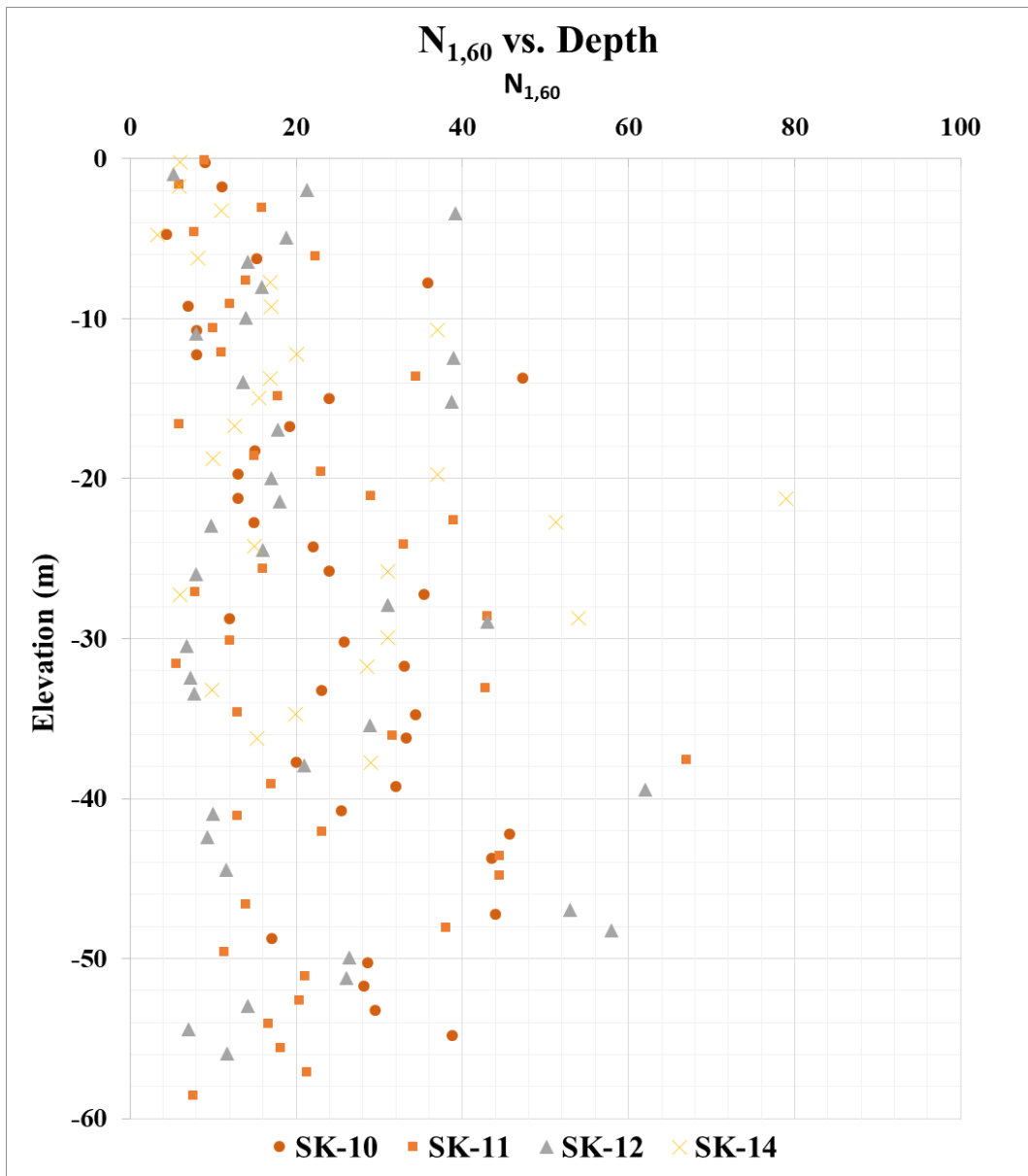
Figure A. 233. SPT-$N_{1,60}$ vs. Depth for Area C1
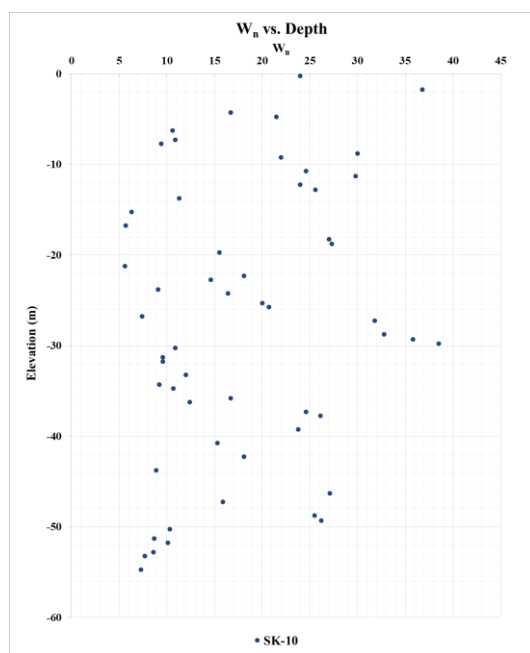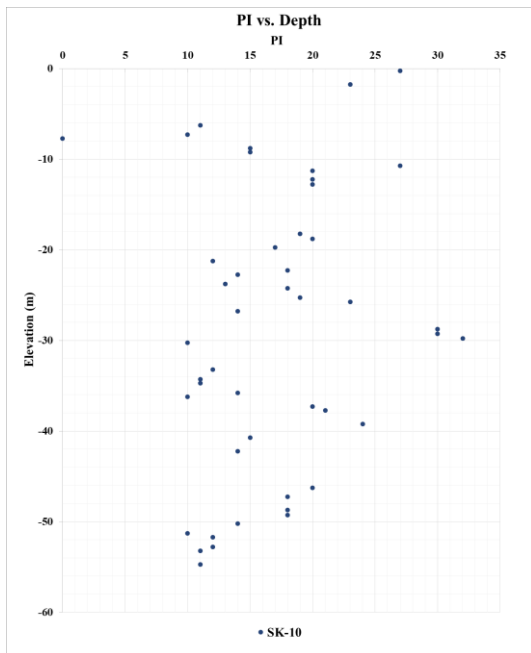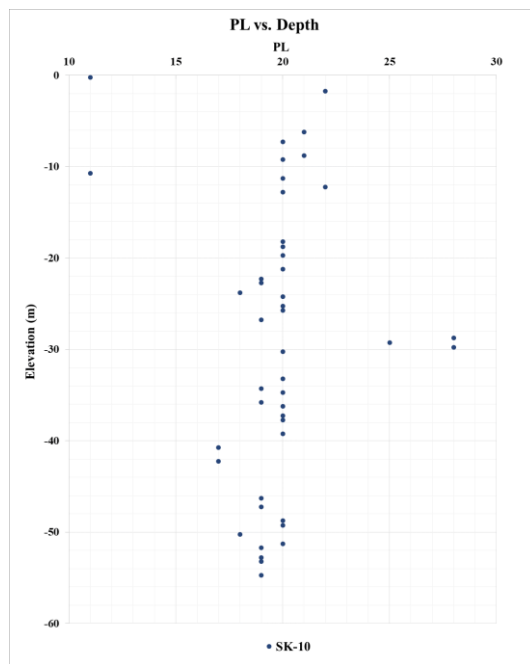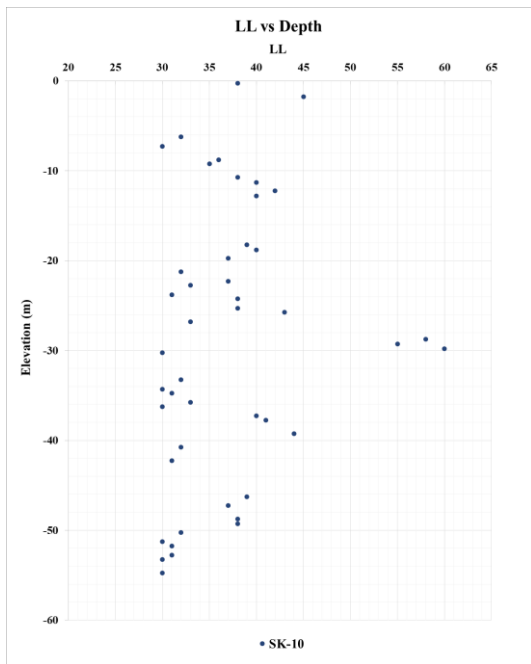
Figure A. 234. Variation of LL, PL, PI, and w_n for Area C1
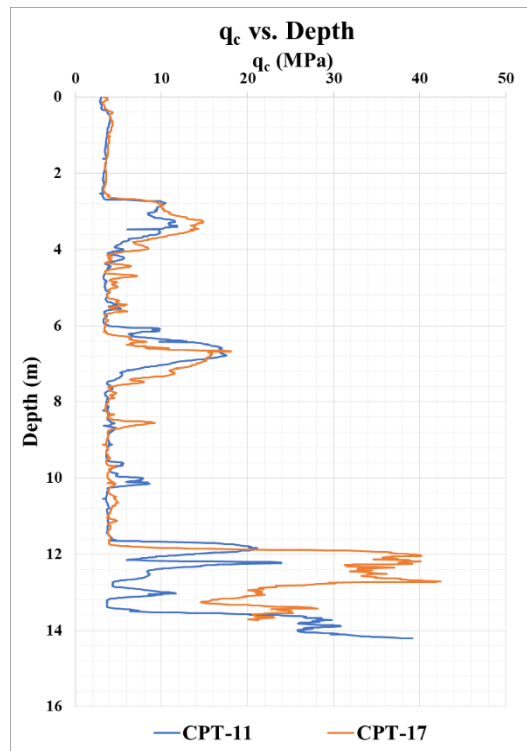
Figure A. 235. Variation of q_c along with the Depth for Area C1
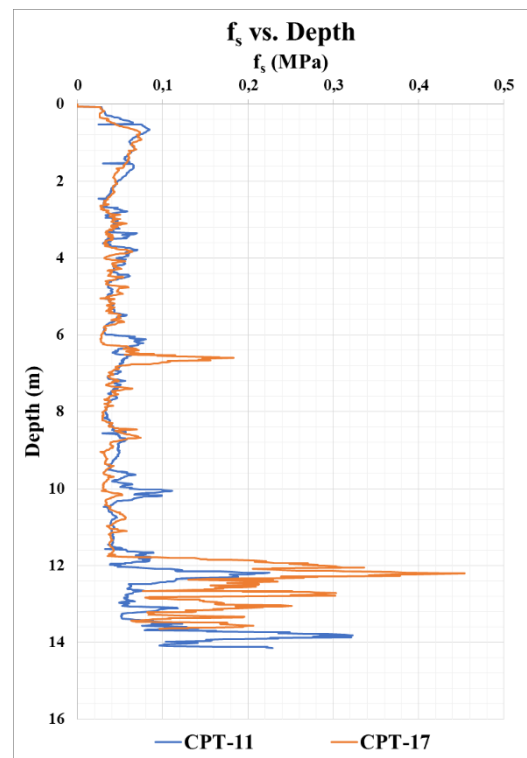
Figure A. 236. Variation of f_s along with the Depth for Area C1

375

4 boreholes (SK-10, SK-11, SK-12, and SK-14) and 2 CPT (CPT-11 and CPT-17 were considered. The depths of boreholes are changing between 40 m to 60 m. Depths of CPT are changing between 13.65 m to 14.15 m. The total depth of boreholes and CPTs is 220 m and 27.8 m respectively. Atterberg limit tests were performed on the samples taken from SK-10. LL, PL, PI, and w_n vary in 30 – 60 % (avg. 36.9 %), 11 – 28 % (avg. 19.7 %), 0 – 32 % (avg. 16.8 %), and 5.6 – 38.5 % (avg. 17.9 %) respectively. Unified soil classification (USCS) was performed for each sample. By considering USCS, SPT $N_{1,60}$ values, and CPT results, the thickness of soil layers was determined. Detailed soil parameters are given in below table;

- Boreholes: SK-10, SK-11, SK-12, and SK-14 (Change in between 40 m to 60 m. 220 m in total)
- CPTs: CPT-11 and CPT-17 (Change in between 13.65 m to 14.15 m. 27.8 m in total)
- LL: 30 – 60 % (avg. 36.9 %)
- PL: 11 – 28 % (avg. 19.7 %)
- PI: 0 – 32 % (avg. 16.8 %)
- w_n: 5.6 – 38.5 % (avg. 17.9 %)

Table A. 52. Soil Profile of Area 6 (C1)

Layer No	Elevation (m)		USCS	Type	Thickness (m)	N	$N_{1,60}$	N_{60}	PI	γ_{wet} (kN/m³)	γ_{sat} (kN/m³)	c_u (kPa)	c (kPa)	φ (°)	ψ (°)	ν	E_{50}^{ref} (MPa)	E_{oed}^{ref} (MPa)	E_{ur}^{ref} (MPa)	m	ν_{ur}	p_{ref} (kPa)	R_f
1	1.8	-1.7	CL	Cohesive	3.5	9.0	7.0	7.0	25.0	18.4	20.0	40.0	4.0	29.5	0.0	0.34	7.0	3.5	21.0	1.0	0.2	32.2	0.9
2	-1.7	-7.7	SM-GC	Cohesionless	6.0	14.0	15.0	14.0	4.2	19.2	20.0	-	2.0	31.4	1.4	0.32	35.0	35.0	105.0	0.5	0.2	100.0	0.9
3	-7.7	-12.7	CL	Cohesive	5.0	14.0	14.0	14.0	19.5	18.4	20.0	80.0	8.0	30.0	0.0	0.33	16.2	8.1	48.7	1.0	0.2	135.1	0.9
4	-12.7	-16.7	GP-GC	Cohesionless	4.0	28.0	22.0	28.0	NP	19.2	20.0	-	1.0	36.0	6.0	0.29	42.0	42.0	126.0	0.5	0.2	100.0	0.9
5	-16.7	-22.2	CL	Cohesive	5.5	26.0	26.0	26.0	18.7	18.4	20.0	155.0	15.5	30.0	0.0	0.33	30.7	15.3	92.0	1.0	0.2	227.6	0.9
6	-22.2	-23.7	SC-GC	Cohesionless	1.5	43.0	32.0	43.0	13.5	20.0	21.6	-	3.0	39.0	9.0	0.27	50.0	50.0	150.0	0.5	0.2	100.0	0.9
7	-23.7	-25.7	CL	Cohesive	2.0	30.0	30.0	30.0	20.0	18.4	20.0	175.0	17.5	30.0	0.0	0.33	34.5	17.3	103.5	1.0	0.2	282.5	0.9
8	-25.7	-27.2	ML-GC	Cohesionless	1.5	29.0	15.0	29.0	7.0	19.2	20.0	-	2.0	34.0	4.0	0.31	35.0	35.0	105.0	0.5	0.2	100.0	0.9
9	-27.2	-29.7	CH	Cohesive	2.5	26.0	26.0	26.0	30.7	18.4	20.0	140.0	14.0	28.5	0.0	0.34	21.8	10.9	65.5	1.0	0.2	320.0	0.9
10	-29.7	-36.2	GP-GC	Cohesionless	6.5	37.0	20.0	37.0	8.5	20.0	21.6	-	3.0	36.0	6.0	0.29	40.0	40.0	120.0	0.5	0.2	100.0	0.9
11	-36.2	-39.2	CL	Cohesive	3.0	30.0	30.0	30.0	21.7	18.4	20.0	170.0	17.0	29.5	0.0	0.34	33.9	17.0	101.7	1.0	0.2	422.9	0.9
12	-39.2	-44.2	GC	Cohesionless	5.0	48.0	25.0	48.0	9.7	20.0	21.6	-	3.0	37.0	7.0	0.28	45.0	45.0	135.0	0.5	0.2	100.0	0.9
13	-44.2	-49.2	CL	Cohesive	5.0	39.0	31.0	39.0	18.5	18.4	20.0	230.0	23.0	30.0	0.0	0.33	46.0	23.0	138.1	1.0	0.2	520.9	0.9
14	-49.2	-60.0	GC	Cohesionless	10.8	46.0	21.0	46.0	11.7	20.0	21.6	-	3.0	36.0	6.0	0.29	41.0	41.0	123.0	0.5	0.2	100.0	0.9
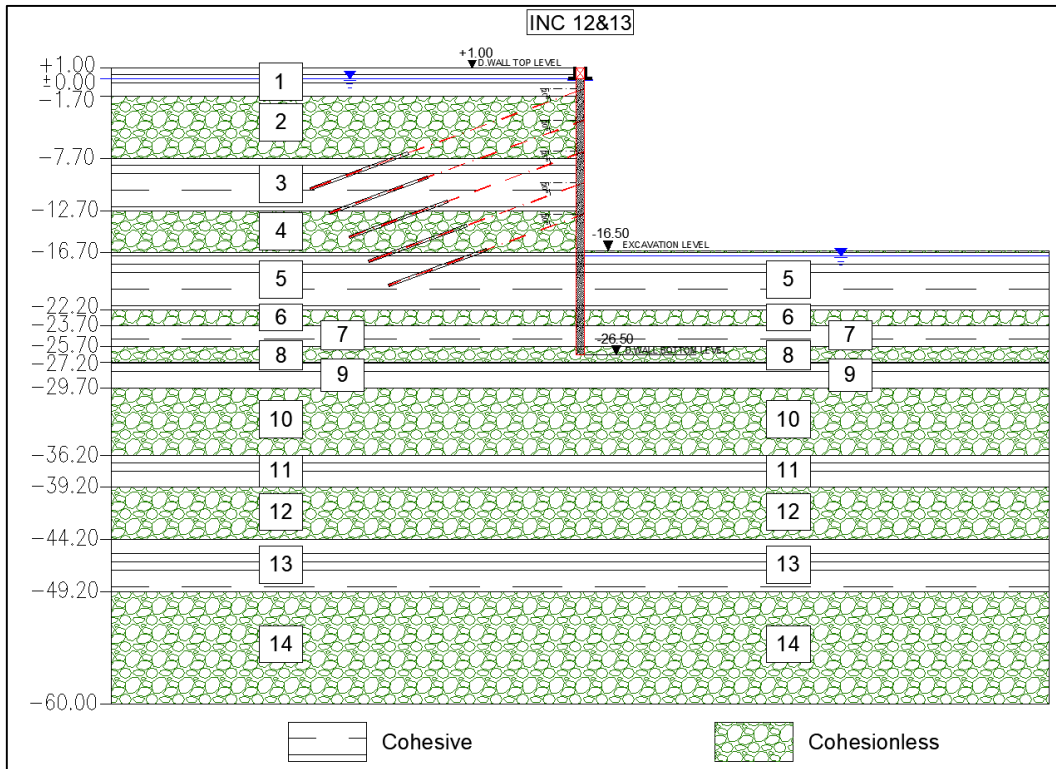
Figure A. 237. Section 6 – 6

Table A. 53. Section Properties of 6 – 6

SECTION 6 - 6									
Diaphragm Wall			SBMA Type Anchor				Excavation Properties		
Top Level (m)	Bottom Level (m)	Length (m)	Anchor No	Anchor Level (m)	Anchor Length (m)	Horizontal Spacing (m)	Top Level (m)	Bottom Level (m)	Depth (m)
1.00	-26.50	27.50	1	-1.00	28.00	1.40	1.00	-16.50	17.50
			2	-4.00	26.00	1.40			
			3	-7.00	24.00	1.40			
			4	-10.00	22.00	1.40			
			5	-13.00	20.00	1.40			

INK-12 – Estimated and Measured Displacements
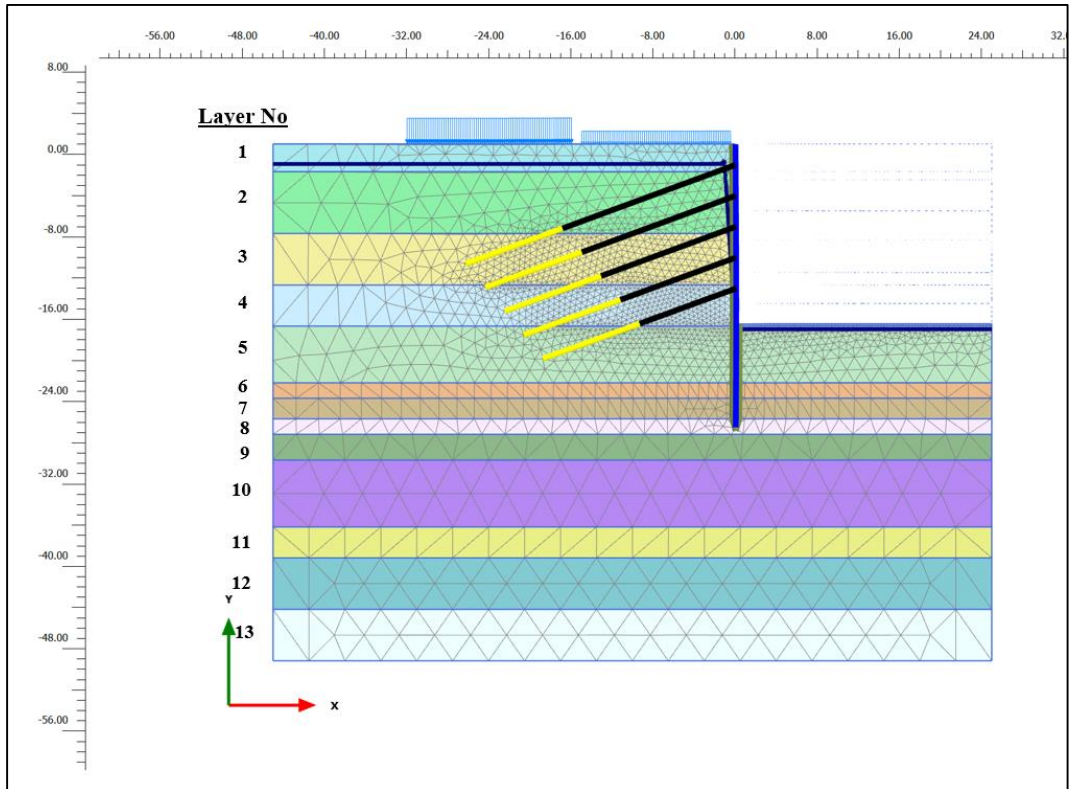
Figure A. 238. Meshed Model for INK-12
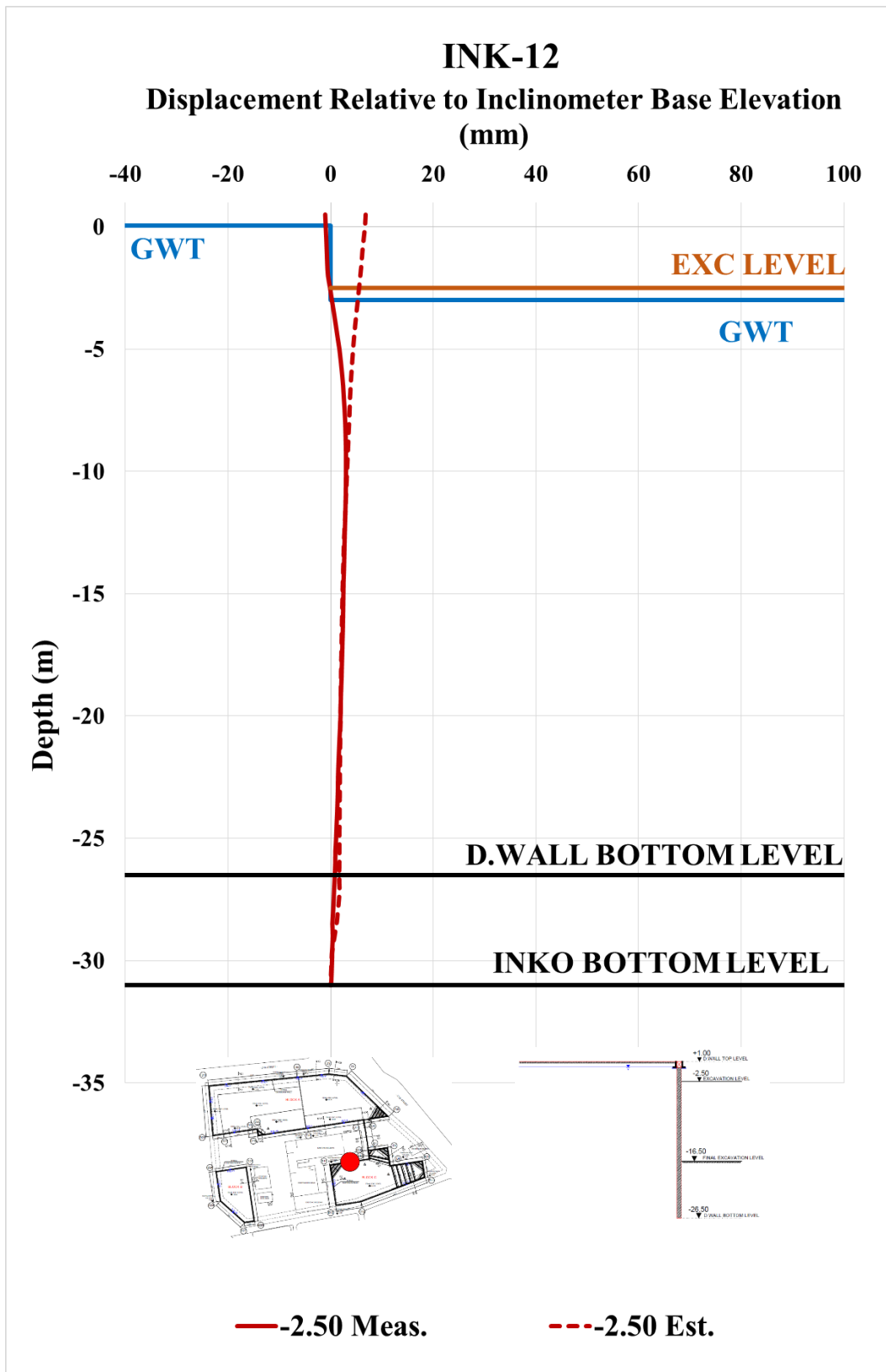
Figure A. 239. Estimated and Measured Displ. Rel. to Inc. Base Elev. at -2.50 m
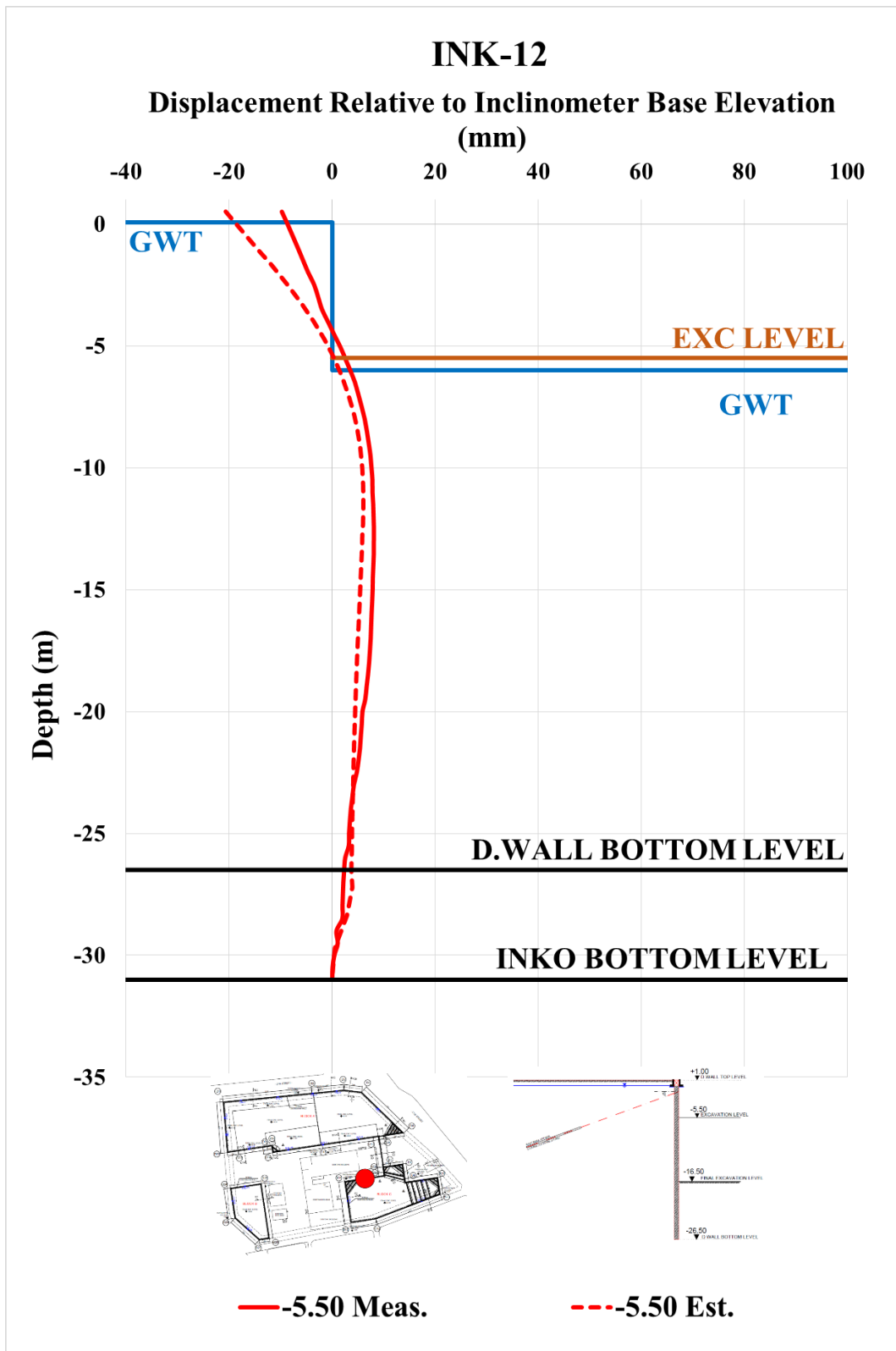
Figure A. 240. Estimated and Measured Displ. Rel. to Inc. Base Elev. at -5.50 m
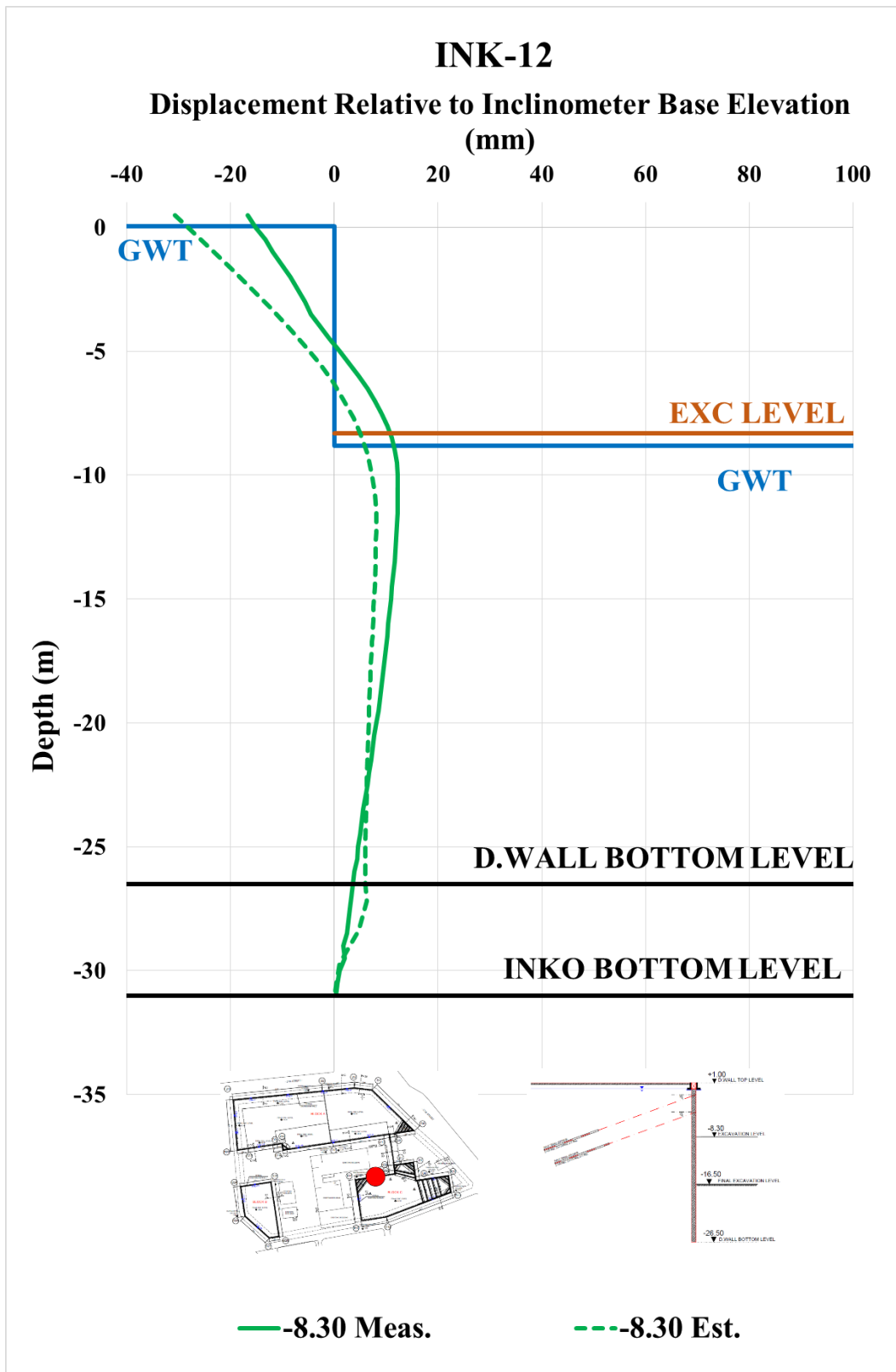
Figure A. 241. Estimated and Measured Displ. Rel. to Inc. Base Elev. at -8.30 m
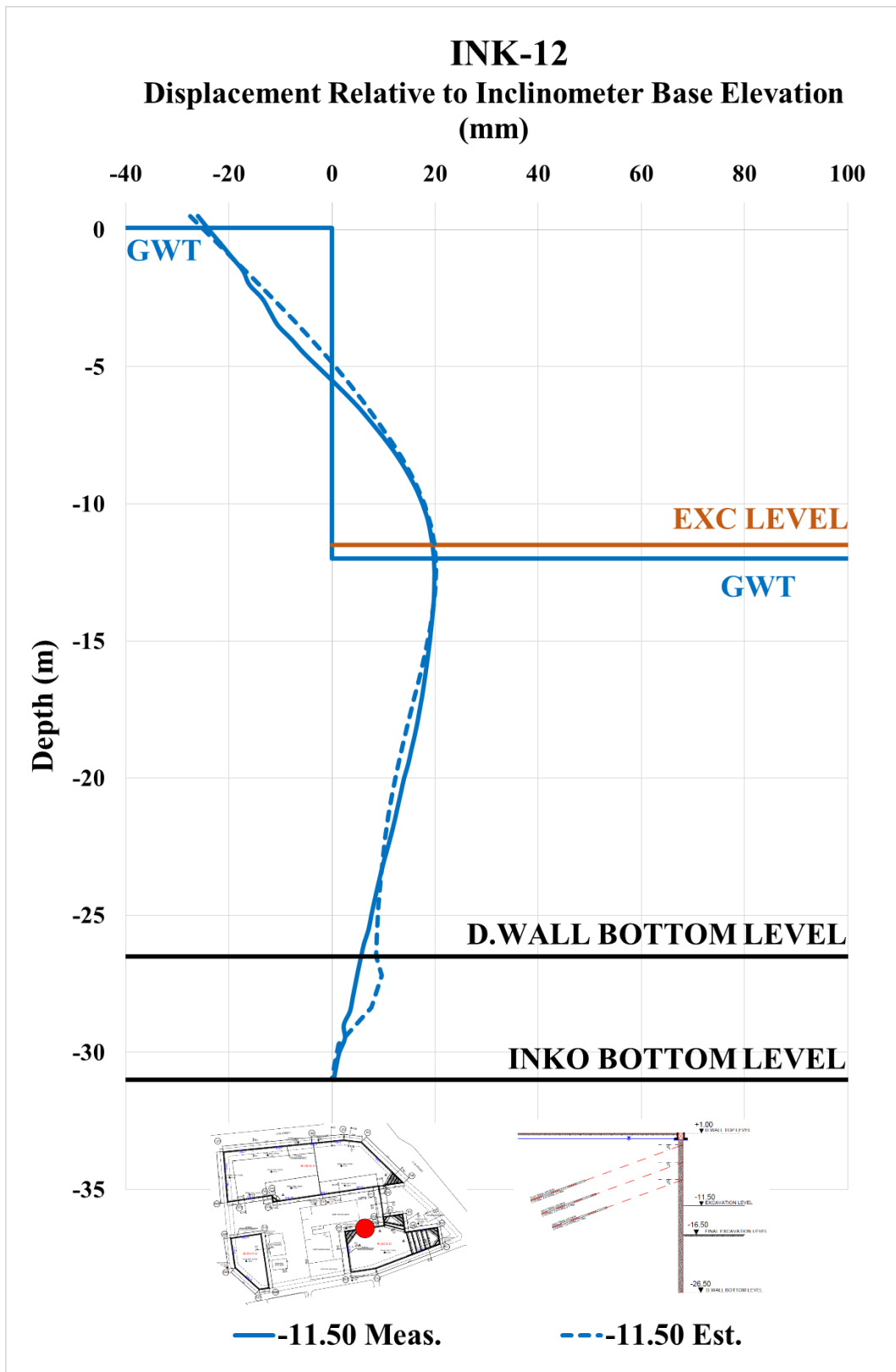
Figure A. 242. Estimated and Measured Displ. Rel. to Inc. Base Elev. at -11.50 m
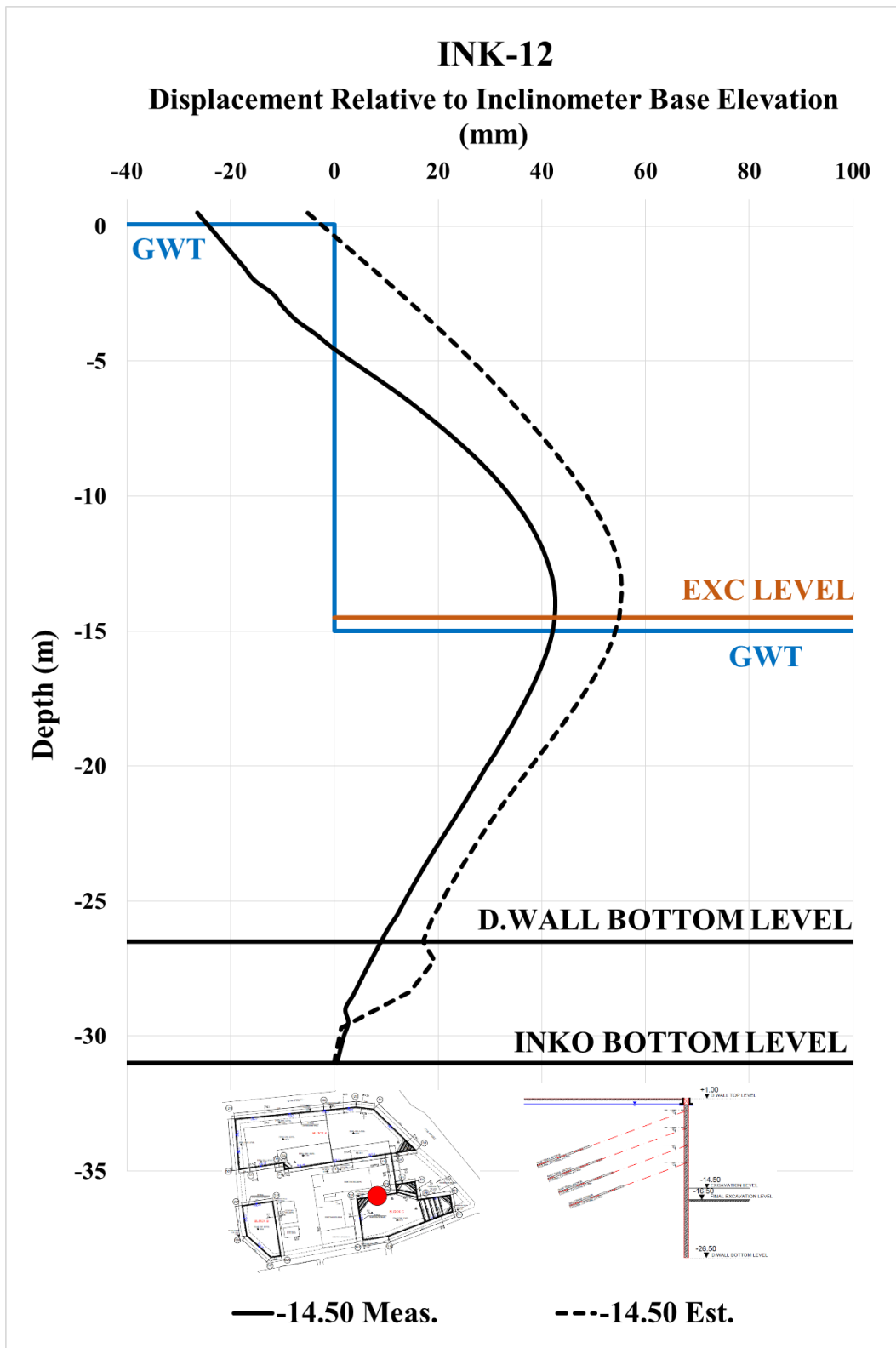
Figure A. 243. Estimated and Measured Displ. Rel. to Inc. Base Elev. at -14.50 m
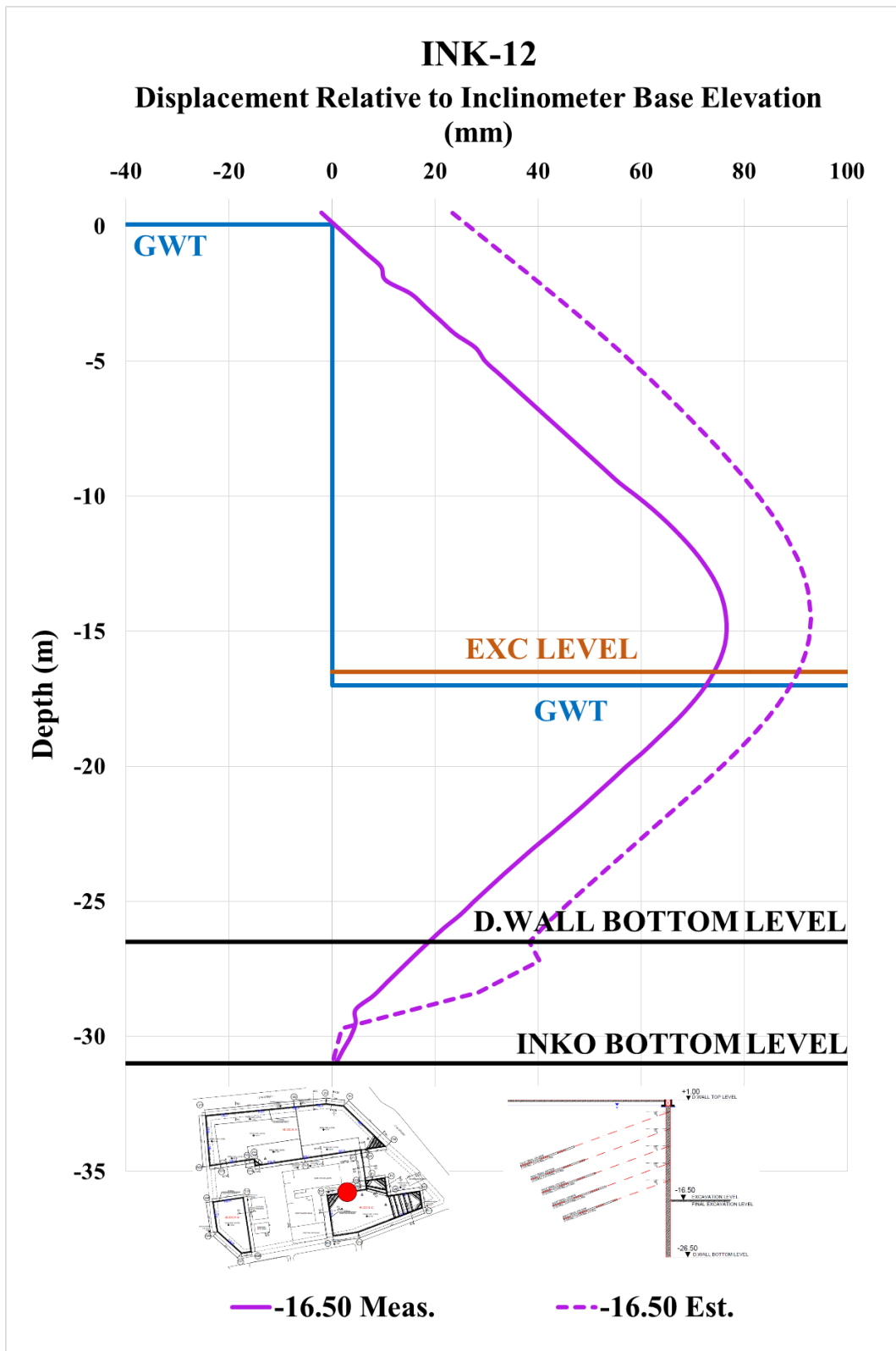
Figure A. 244. Estimated and Measured Displ. Rel. to Inc. Base Elev. at -16.50 m

Table A. 54. Internal Forces of Diaphragm Wall

INK - 12 / Section 6-6						
Excvation Stage	1	2	3	4	5	6
Excavation Level (m)	-2,50	-5,50	-8,30	-11,50	-14,50	-16,50
N_{max} (kN/m)	100,80	206,20	349,30	563,00	810,60	954,40
V_{max} (kN/m)	47,81	398,40	398,40	398,40	462,80	462,80
M_{max} (kN.m/m)	105,50	764,20	957,30	1109,00	1545,00	1704,00

Legend	Excvation Stage	1. Anchor Level	2. Excavation Level	2. Anchor Level	3. Excavation Level	3. Anchor Level	4. Excavation Level	4. Anchor Level	5. Excavation Level	5. Anchor Level	Final Excavation Level
	Estimated Load of 1. Anchor Row (kN)	650.00	664.00	565.31	575.50	544.27	545.97	543.01	535.57	538.95	538.94
	Estimated Load of 2. Anchor Row (kN)	-	-	650.00	670.41	602.69	625.74	599.08	607.32	599.13	600.38
	Estimated Load of 3. Anchor Row (kN)	-	-	-	-	650.00	702.07	639.64	677.82	652.26	653.75
	Estimated Load of 4. Anchor Row (kN)	-	-	-	-	-	-	650.00	741.16	685.57	702.18
	Estimated Load of 5. Anchor Row (kN)	-	-	-	-	-	-	-	-	650.00	697.07

Figure A. 245. Estimated Anchor Loads

INK-13 – Estimated and Measured Displacements
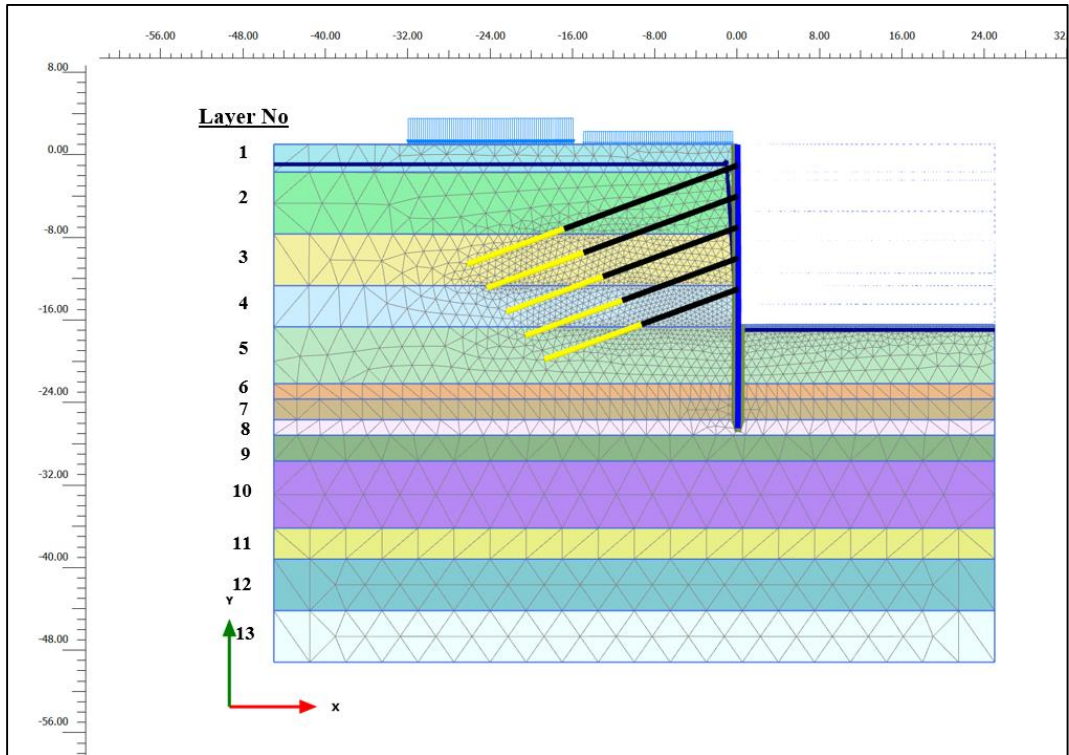
Figure A. 246. Meshed Model for INK-13
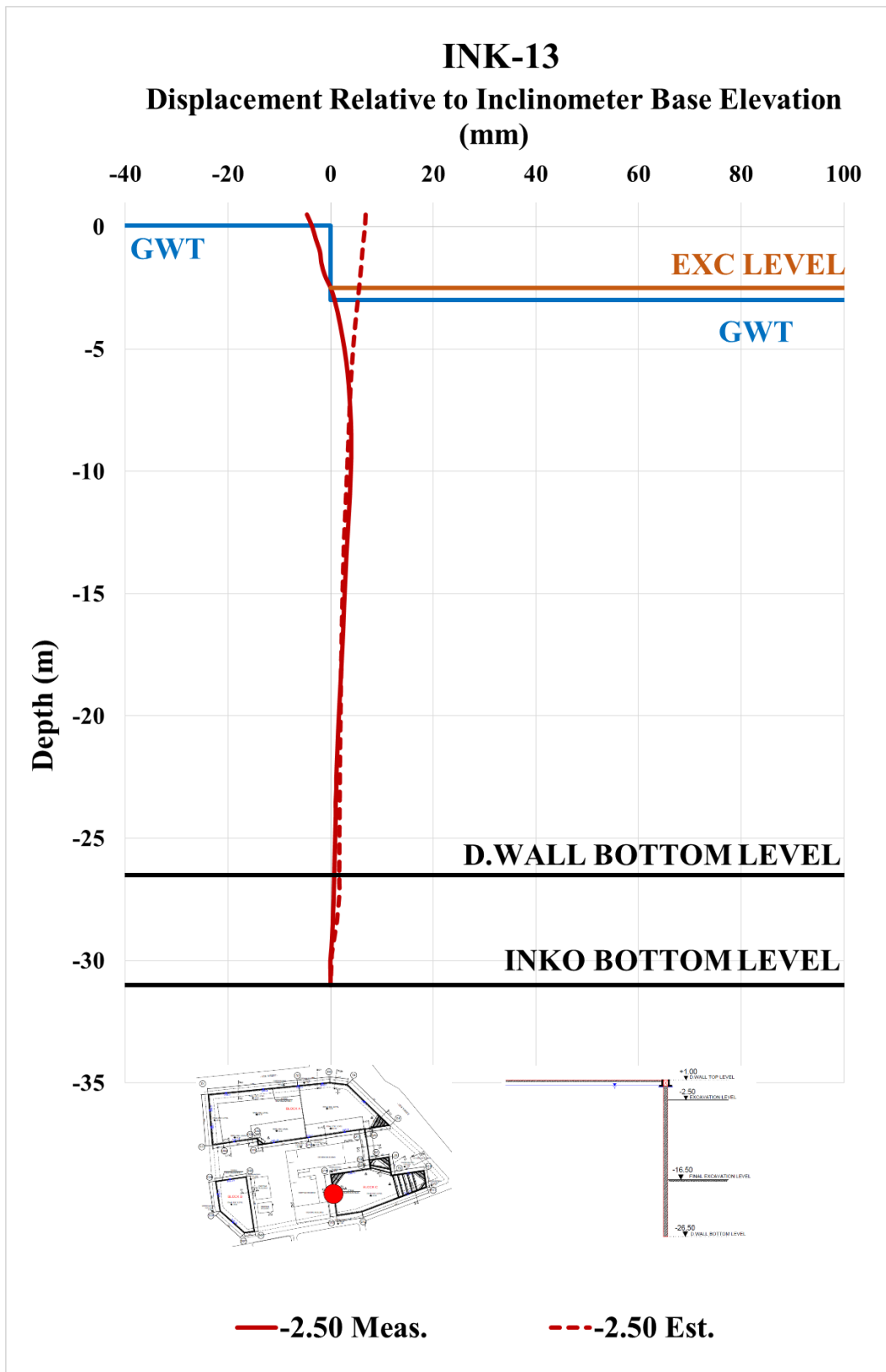
Figure A. 247. Estimated and Measured Displ. Rel. to Inc. Base Elev. at -2.50 m
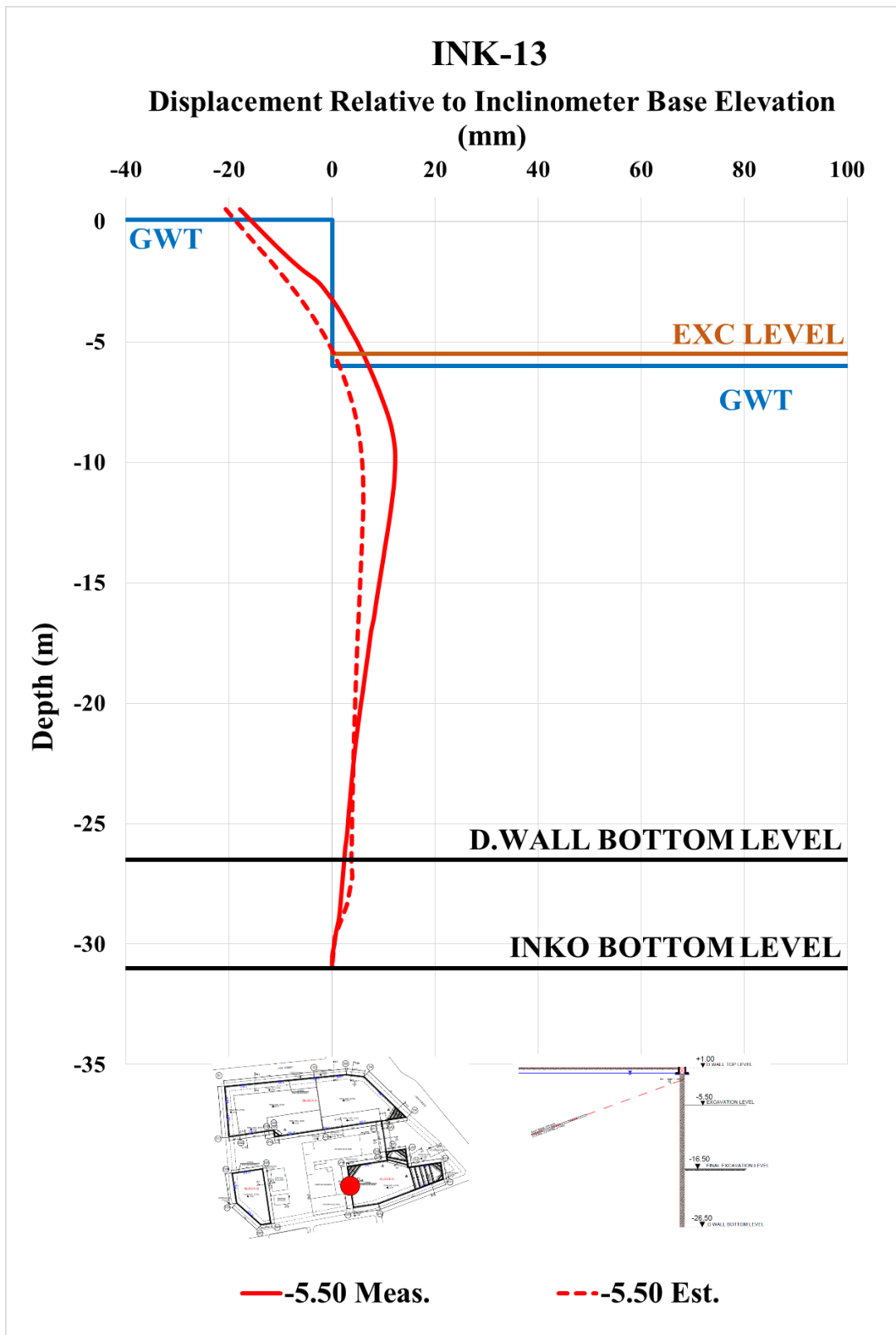
Figure A. 248. Estimated and Measured Displ. Rel. to Inc. Base Elev. at -5.50 m
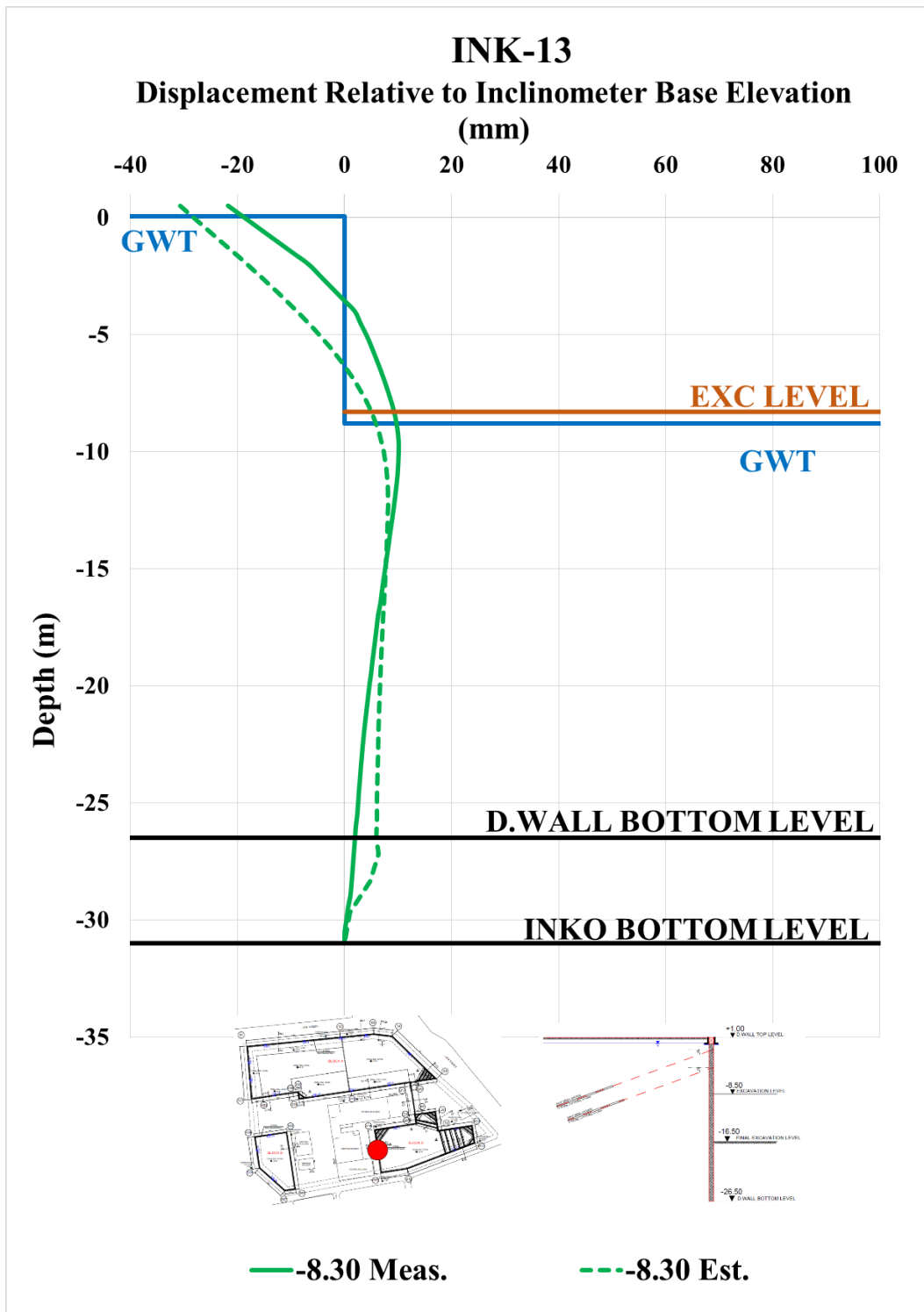
Figure A. 249. Estimated and Measured Displ. Rel. to Inc. Base Elev. at -8.30 m
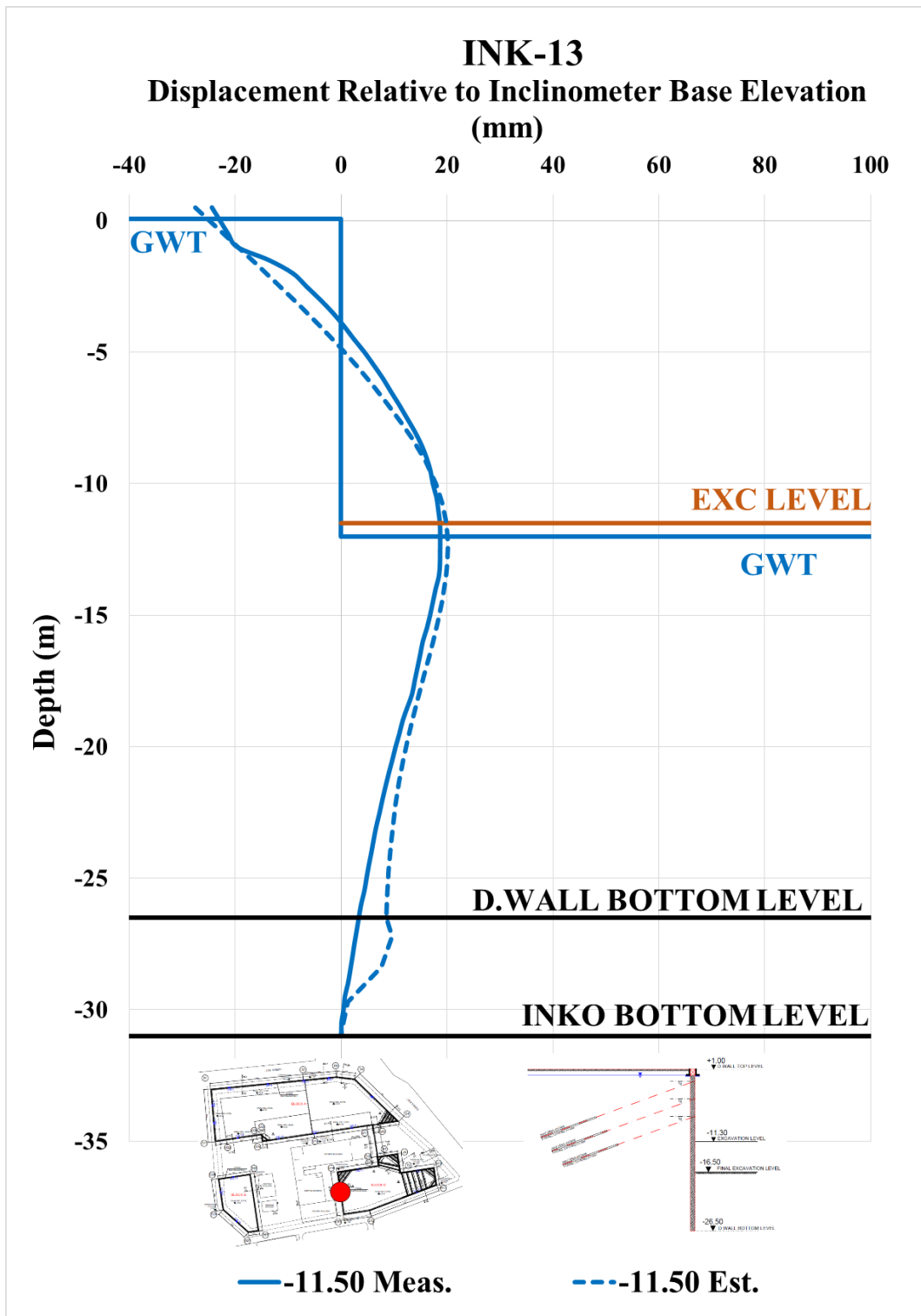
Figure A. 250. Estimated and Measured Displ. Rel. to Inc. Base Elev. at -11.30 m
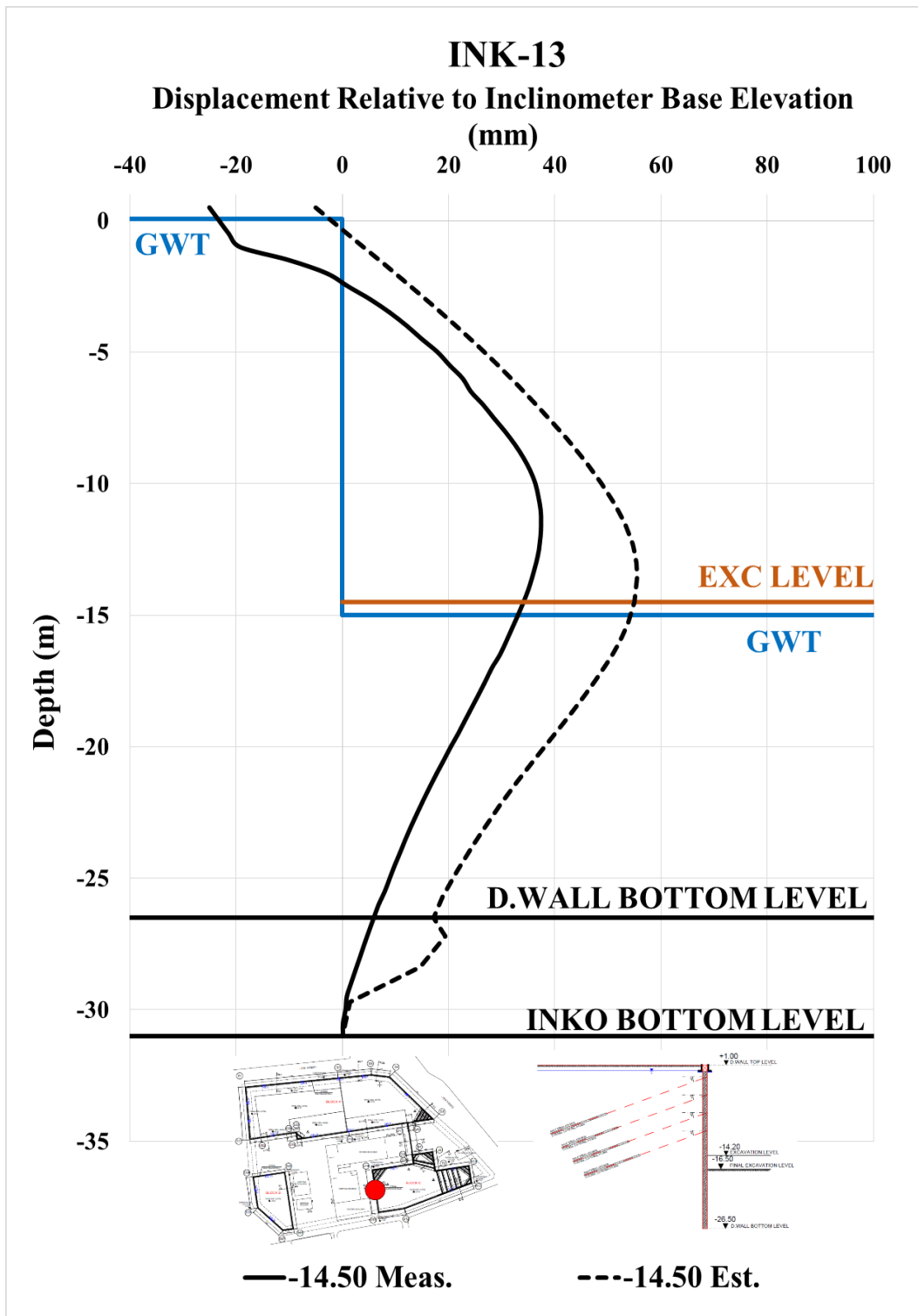
Figure A. 251. Estimated and Measured Displ. Rel. to Inc. Base Elev. at -14.50 m
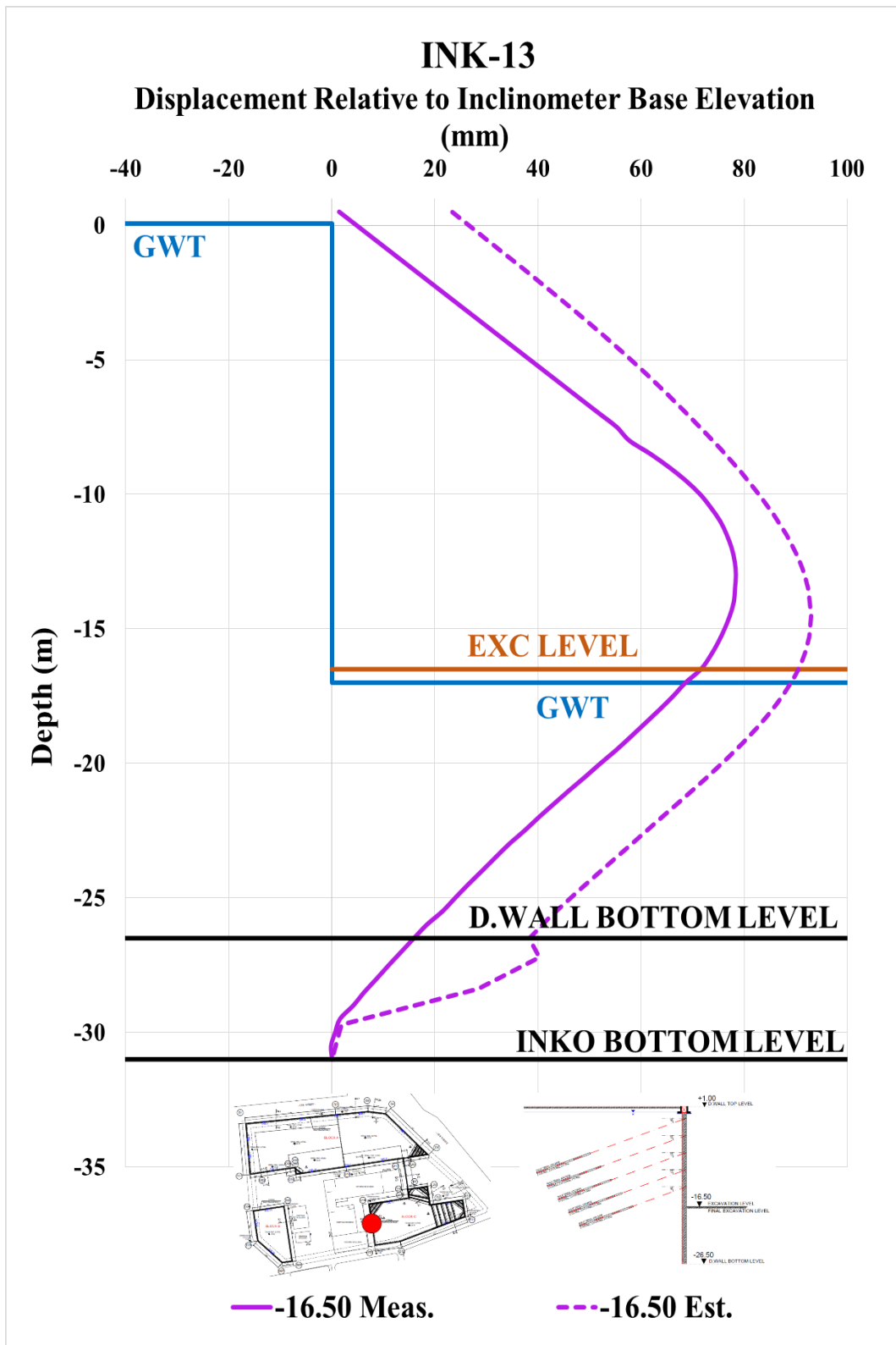
Figure A. 252. Estimated and Measured Displ. Rel. to Inc. Base Elev. at -16.50 m

Table A. 55. Internal Forces of Diaphragm Wall

INK - 13 / Section 6-6						
Excvation Stage	1	2	3	4	5	6
Excavation Level (m)	-2.50	-5.50	-8.50	-11.30	-14.20	-16.50
N_{max} (kN/m)	100.80	206.20	355.80	547.00	783.00	949.30
V_{max} (kN/m)	47.81	398.40	398.40	398.40	438.90	438.90
M_{max} (kN.m/m)	105.50	764.20	980.50	1064.00	1420.00	1663.00

Legend	Excvation Stage	1. Anchor Level	2. Excavation Level	2. Anchor Level	3. Excavation Level	3. Anchor Level	4. Excavation Level	4. Anchor Level	5. Excavation Level	5. Anchor Level	Final Excavation Level
	Estimated Load of 1. Anchor Row (kN)	650.00	664.12	565.40	576.25	545.25	547.49	544.47	539.70	543.05	542.14
	Estimated Load of 2. Anchor Row (kN)	-	-	650.00	672.79	605.14	624.62	598.00	607.58	599.50	600.94
	Estimated Load of 3. Anchor Row (kN)	-	-	-	-	650.00	693.01	630.78	667.20	641.95	645.02
	Estimated Load of 4. Anchor Row (kN)	-	-	-	-	-	-	650.00	732.75	677.80	699.54
	Estimated Load of 5. Anchor Row (kN)	-	-	-	-	-	-	-	-	650.00	709.06

Figure A. 253. Estimated Anchor Loads

394

INK-12 – Calibrated, Estimated and Measured Displacements
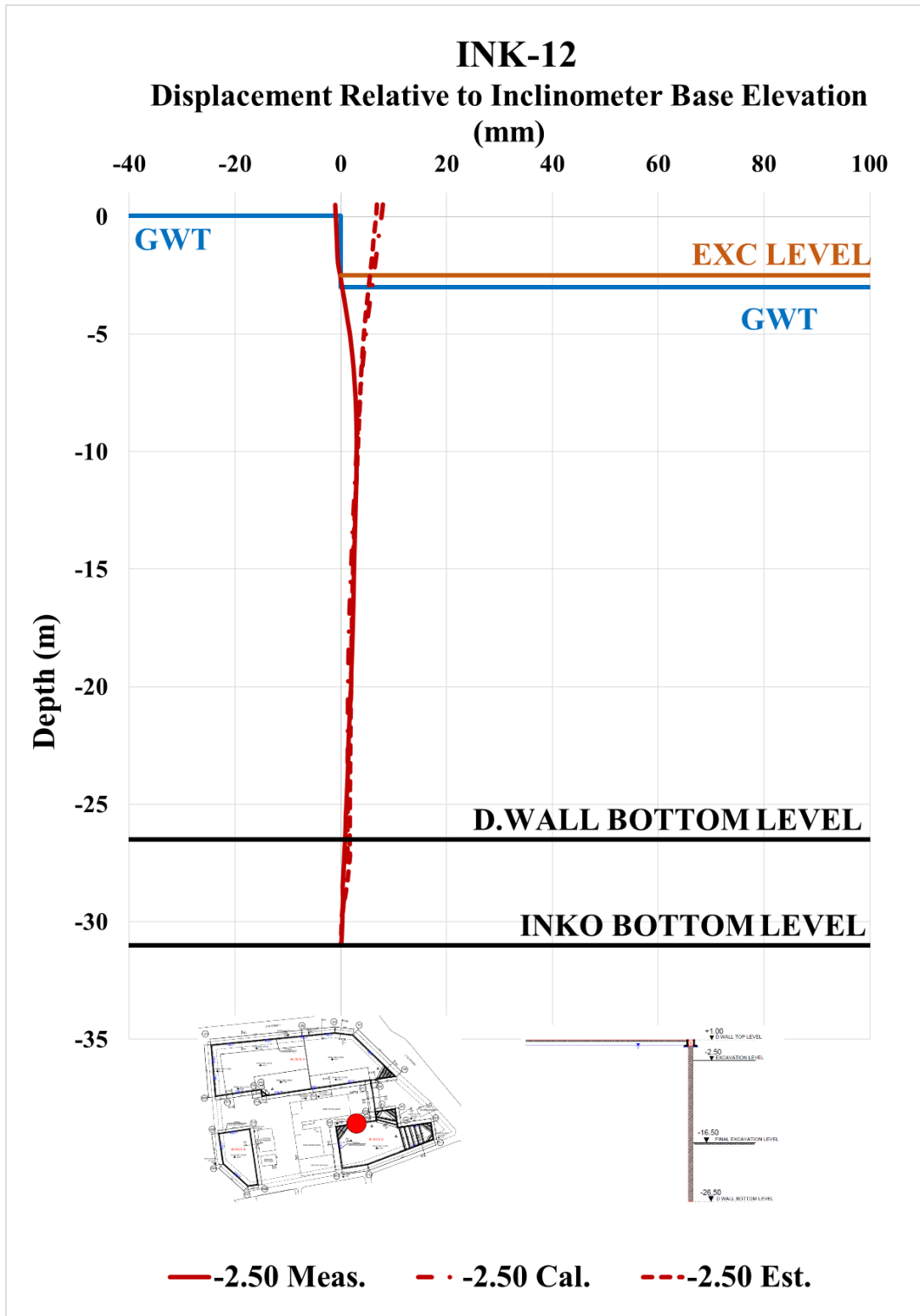
Figure A. 254. Calibrated and Measured Displ. Rel. to Inc. Base Elev. at -2.50 m
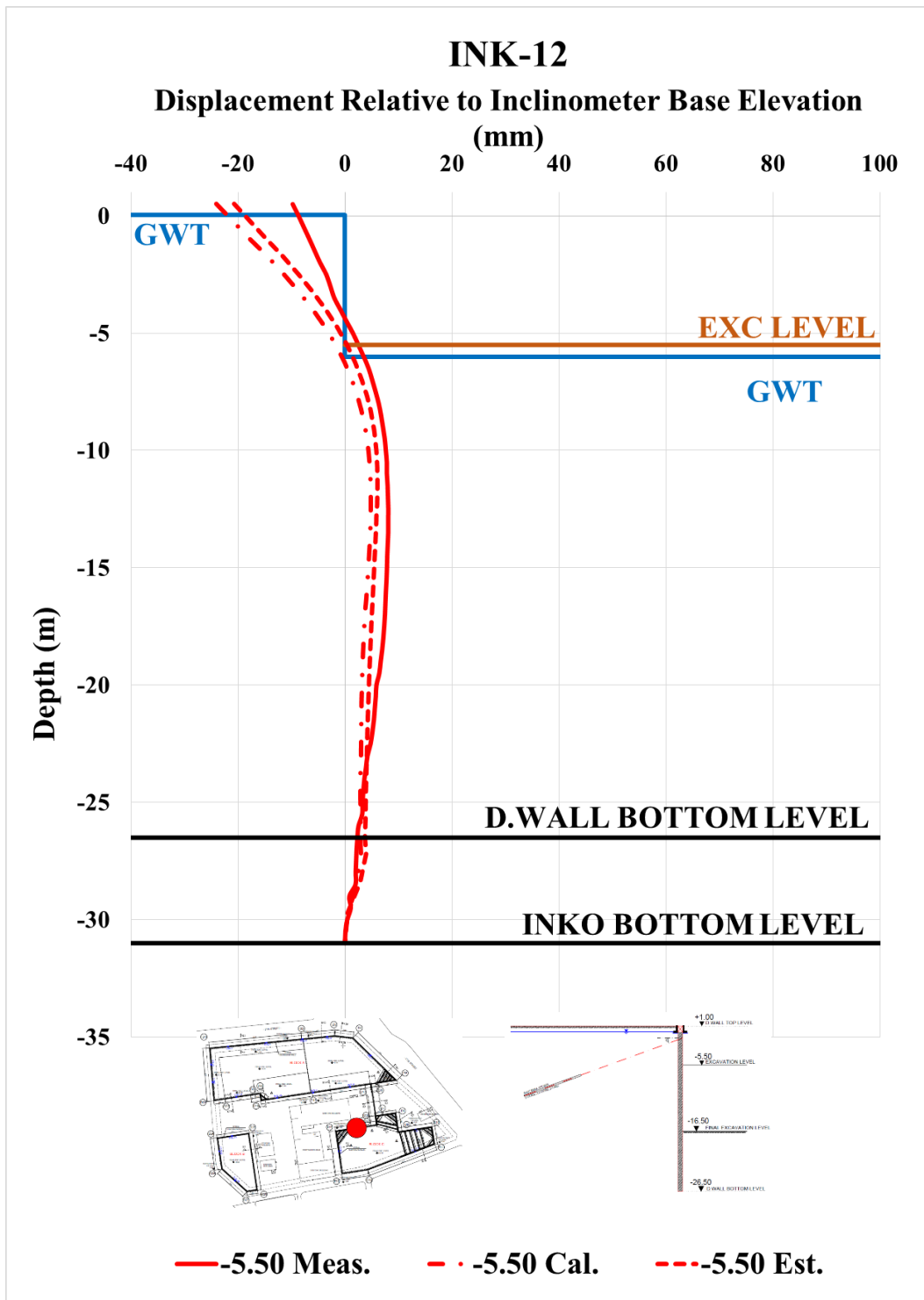
Figure A. 255. Calibrated and Measured Displ. Rel. to Inc. Base Elev. at -5.50 m
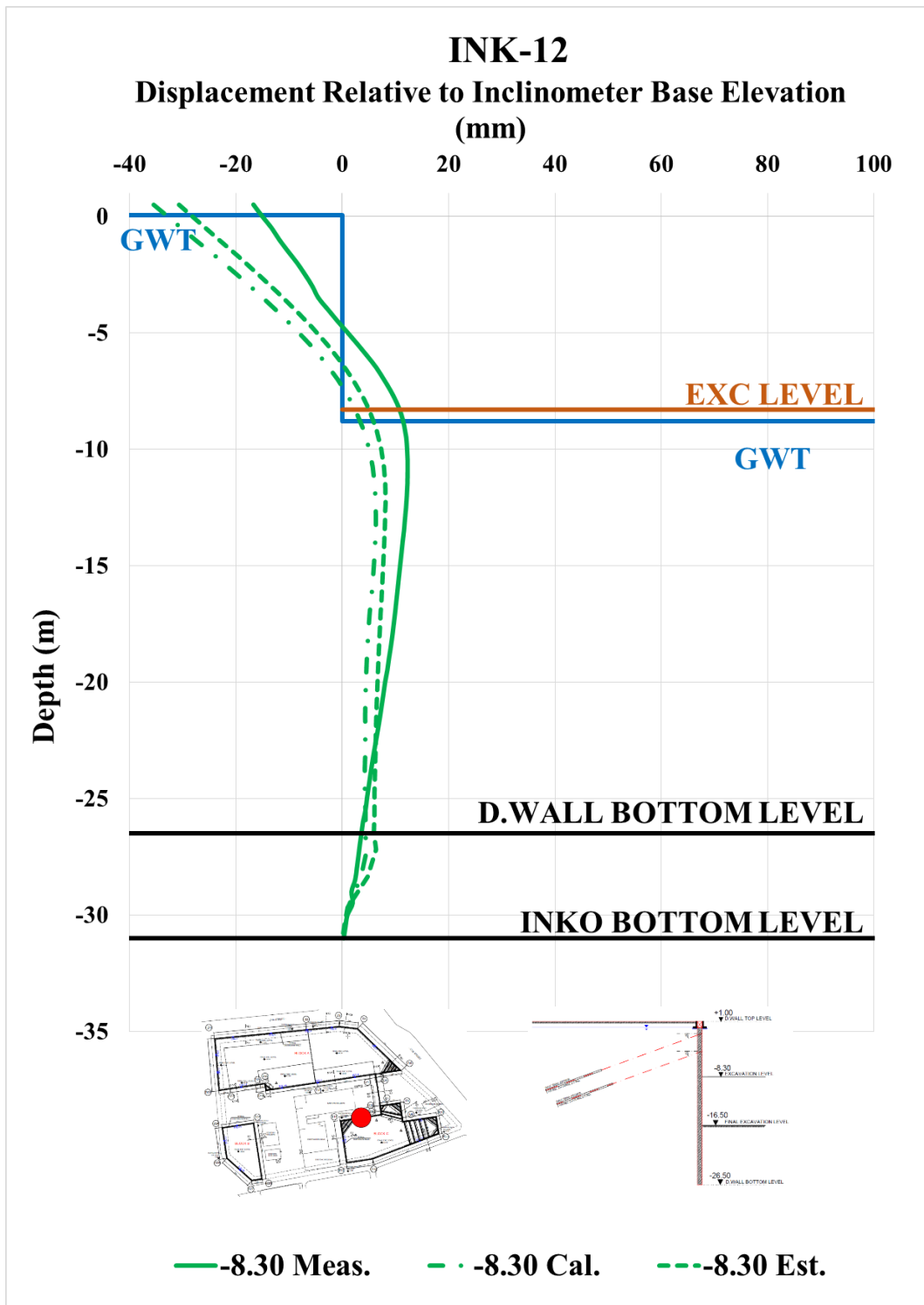
Figure A. 256. Calibrated and Measured Displ. Rel. to Inc. Base Elev. at -8.30 m
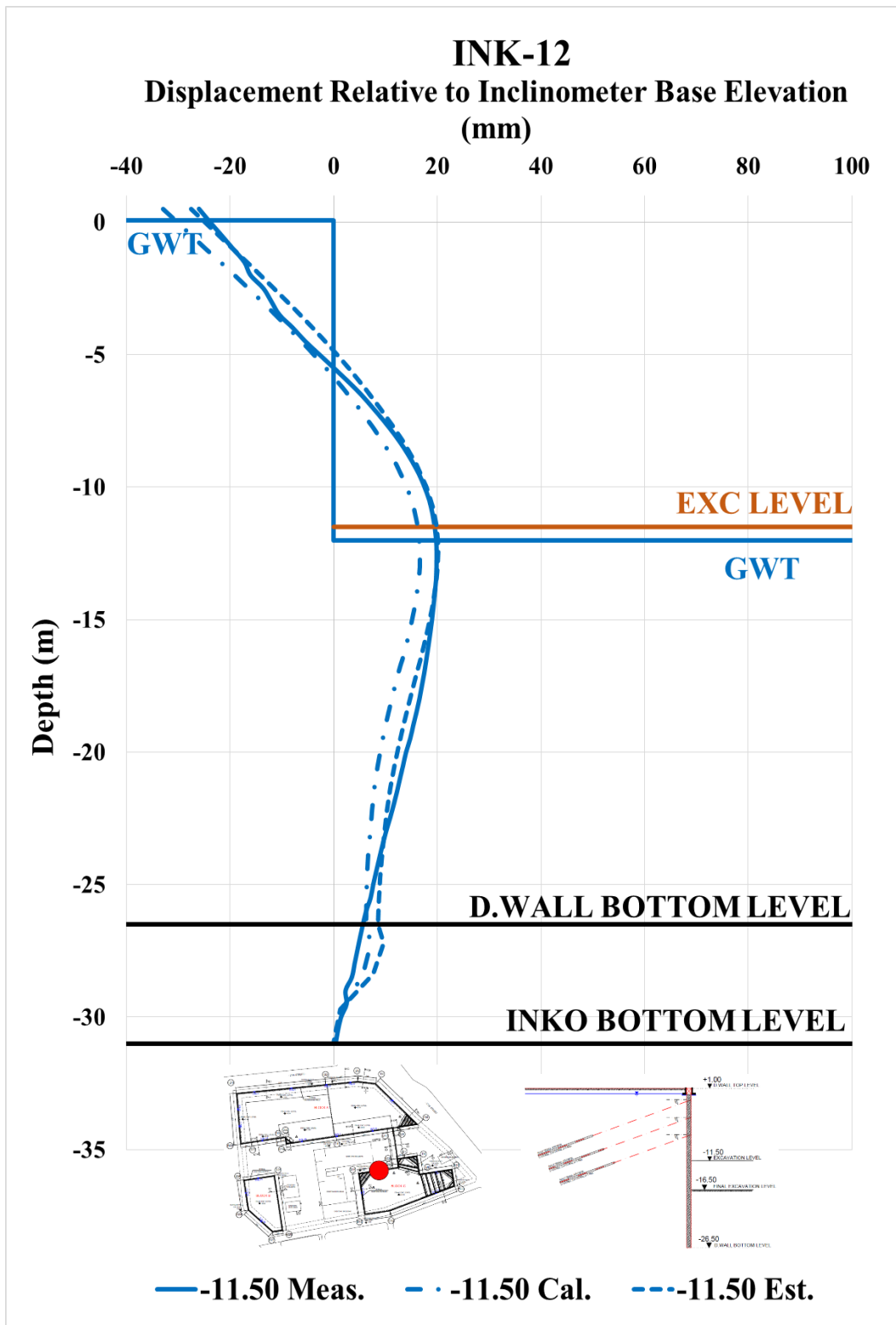
Figure A. 257. Calibrated and Measured Displ. Rel. to Inc. Base Elev. at -11.50 m
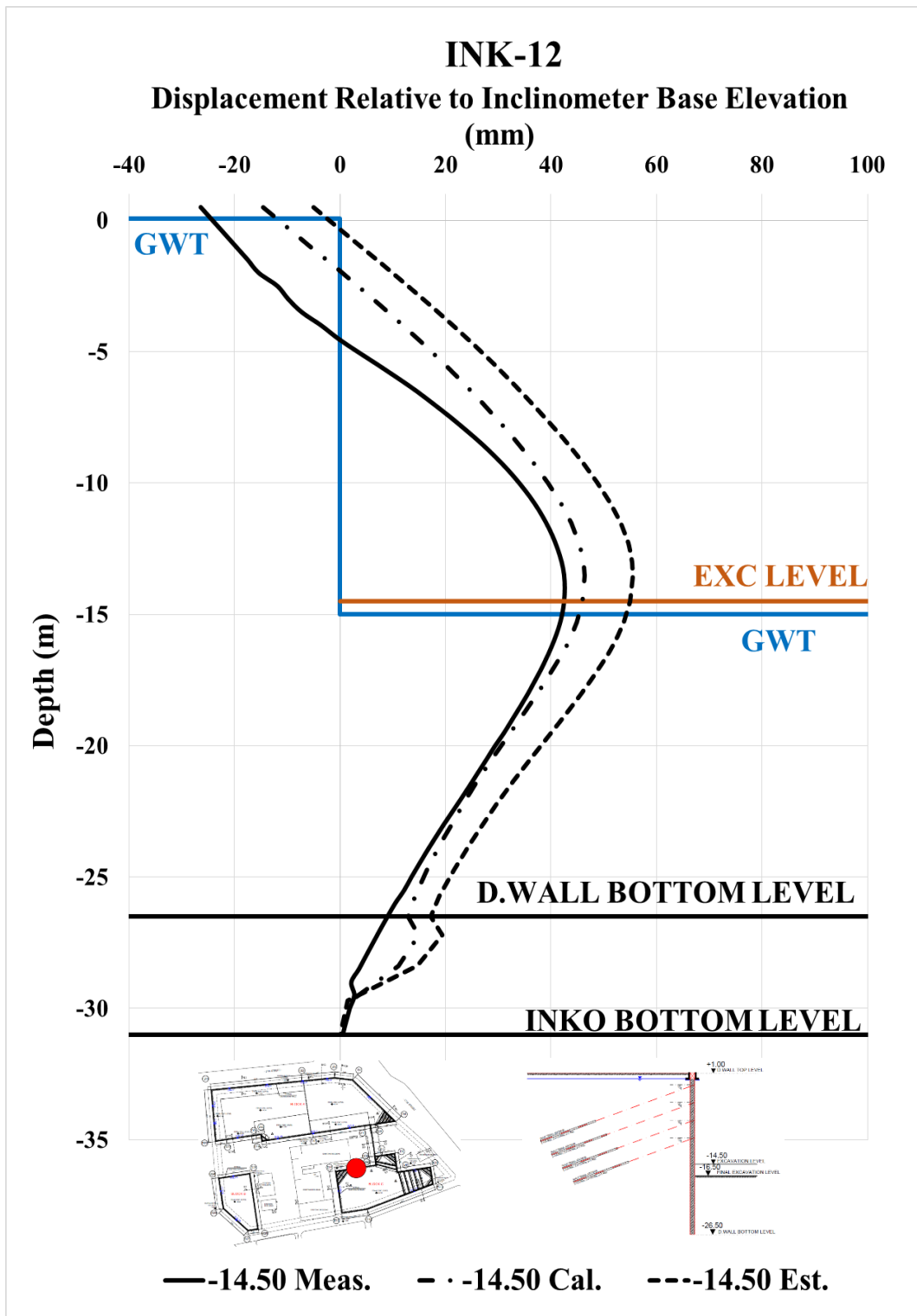
Figure A. 258. Calibrated and Measured Displ. Rel. to Inc. Base Elev. at -14.50 m
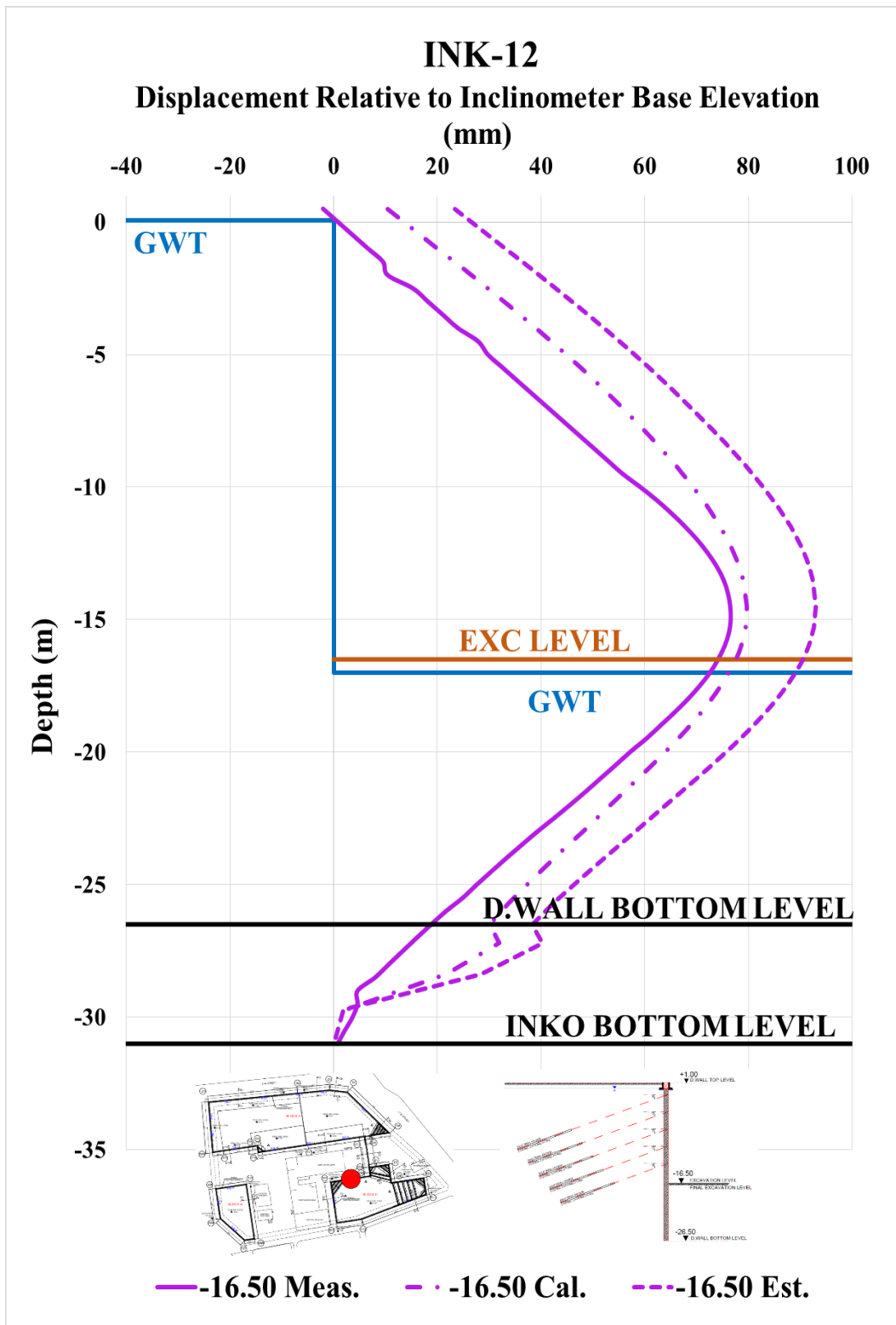
Figure A. 259. Calibrated and Measured Displ. Rel. to Inc. Base Elev. at -16.50 m

Table A. 56. Internal Forces of Diaphragm Wall

INK - 12 / Section 6-6						
Excvation Stage	1	2	3	4	5	6
Excavation Level (m)	-2.50	-5.50	-8.30	-11.50	-14.50	-16.50
N_{max} (kN/m)	99.05	204.10	344.90	561.90	814.80	955.00
V_{max} (kN/m)	45.29	392.20	392.20	392.20	449.40	449.40
M_{max} (kN.m/m)	110.00	774.30	973.10	1142.00	1500.00	1623.00

INK - 12 / Section 6-6

Anchor Load vs Stage

Legend	Excvation Stage	1. Anchor Level	2. Excavation Level	2. Anchor Level	3. Excavation Level	3. Anchor Level	4. Excavation Level	4. Anchor Level	5. Excavation Level	5. Anchor Level	Final Excavation Level
	Estimated Load of 1. Anchor Row (kN)	650.00	665.61	556.59	568.50	533.30	538.32	534.00	530.02	533.43	534.39
	Estimated Load of 2. Anchor Row (kN)	-	-	650.00	671.15	601.53	625.82	598.60	607.91	599.58	601.35
	Estimated Load of 3. Anchor Row (kN)	-	-	-	-	650.00	700.73	638.24	676.08	649.70	654.03
	Estimated Load of 4. Anchor Row (kN)	-	-	-	-	-	-	650.00	738.27	680.34	701.81
	Estimated Load of 5. Anchor Row (kN)	-	-	-	-	-	-	-	-	650.00	702.69

Figure A. 260. Estimated Anchor Loads

Table A. 57. Summary of Displacement Results of INK-12

INK - 12 / SECTION 6 - 6

Excavation Level (m)	Excavation Depth (m)	u_{meas} (mm) Inclinometer Measurements	u_{est} (mm) Estimation with Plaxis 2D Analysis	u_{cal} (mm) Calibration with Plaxis 2D Analysis	$u_{literature}$ (mm) FHWA-IF-99-015 (1999) - Maksimum	$u_{literature}$ (mm) FHWA-IF-99-015 (1999) - Average	$u_{literature}$ (mm) Goldberg et al. (1976)	$u_{literature}$ (mm) Clough et al. (1990) - Maksimum	$u_{literature}$ (mm) Clough et al. (1990) - Average	$u_{literature}$ (mm) Long (2001)	$u_{literature}$ (mm) Long (2001) (Extraordinary cases eliminated)	$u_{literature}$ (mm) Long (2001) Cantilever System
-2.50	3.50	2.93	6.76	7.99	17.50	7.00	17.50	17.50	7.00	6.65	4.90	12.6
-5.50	6.50	8.11	6.11	4.78	32.50	13.00	32.50	32.50	13.00	12.35	9.10	-
-8.30	9.30	12.28	8.12	6.37	46.50	18.60	46.50	46.50	18.60	17.67	13.02	-
-11.50	12.50	19.86	20.25	16.59	62.50	25.00	62.50	62.50	25.00	23.75	17.50	-
-14.50	15.50	42.60	55.44	46.41	77.50	31.00	77.50	77.50	31.00	29.45	21.70	-
-16.50	17.50	76.59	92.97	79.73	87.50	35.00	87.50	87.50	35.00	33.25	24.50	-

402
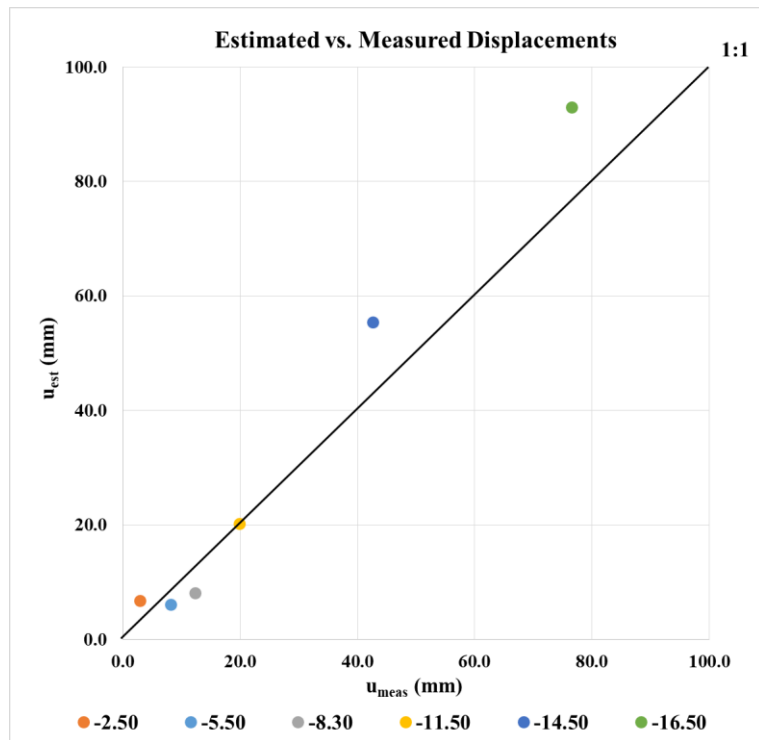
Figure A. 261. Estimated and Measured Displacements of INK – 12
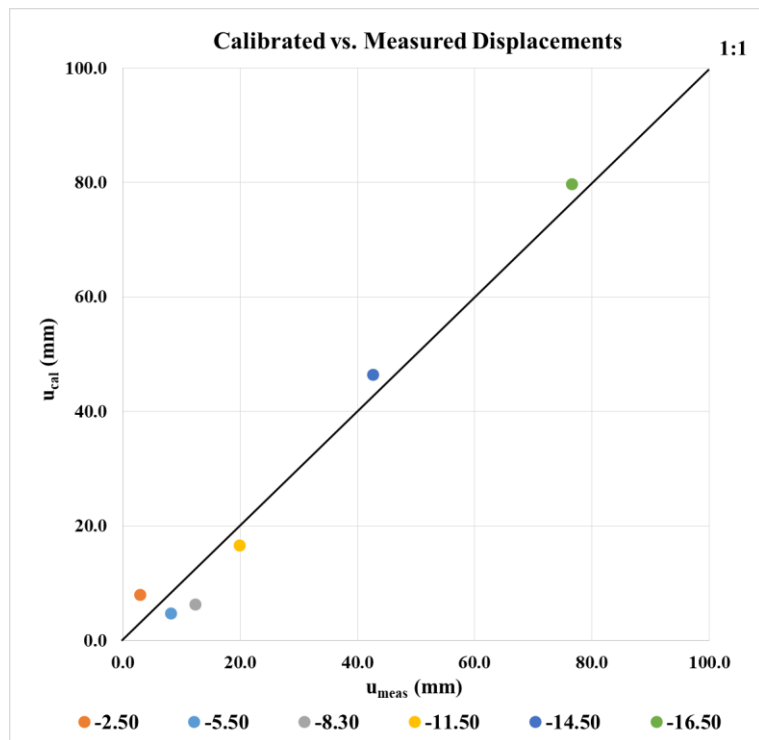
Figure A. 262. Calibrated and Measured Displacements of INK - 12

INK-13 – Calibrated, Estimated and Measured Displacements
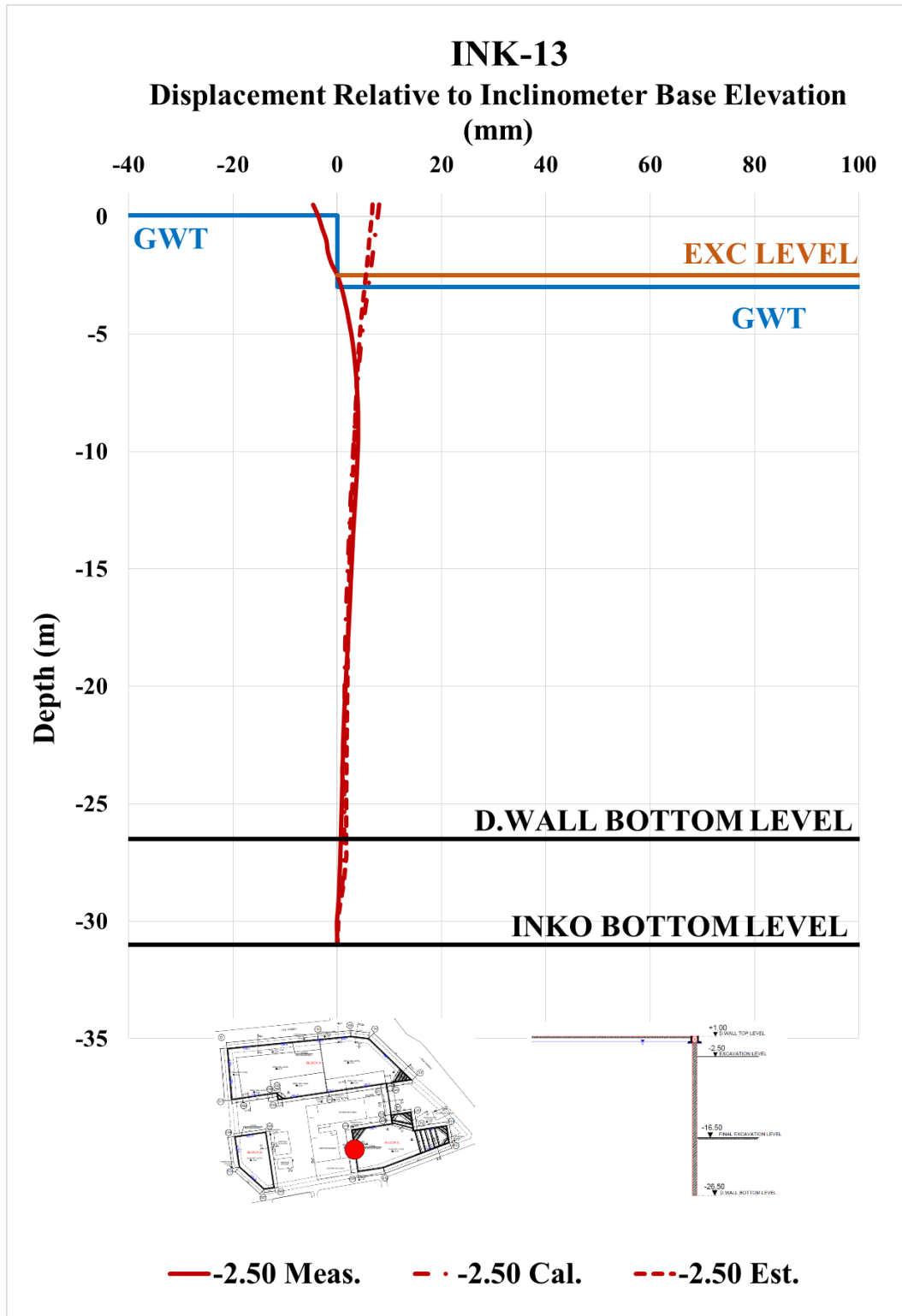
Figure A. 263. Calibrated and Measured Displ. Rel. to Inc. Base Elev. at -2.50 m
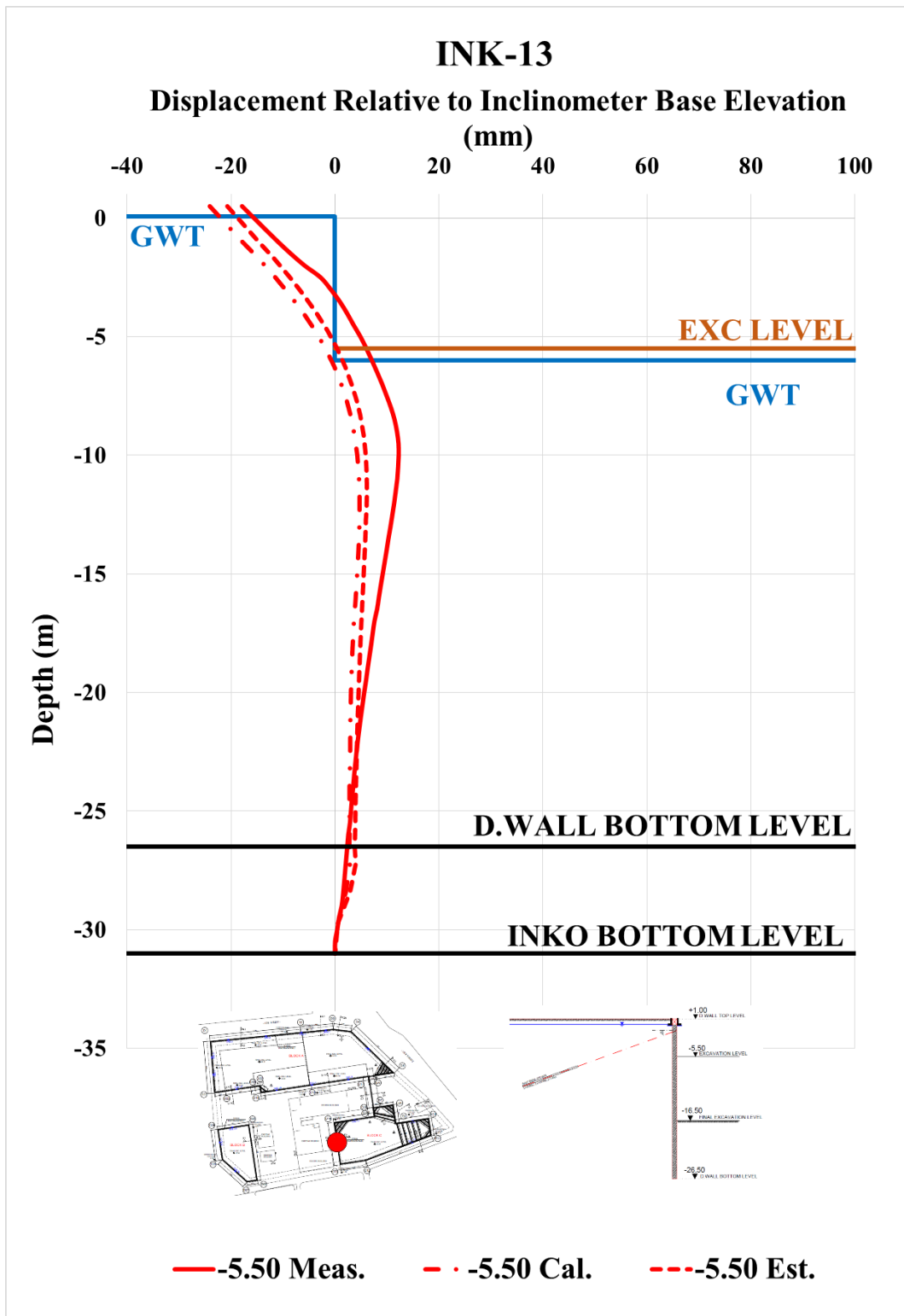
Figure A. 264. Calibrated and Measured Displ. Rel. to Inc. Base Elev. at -5.50 m
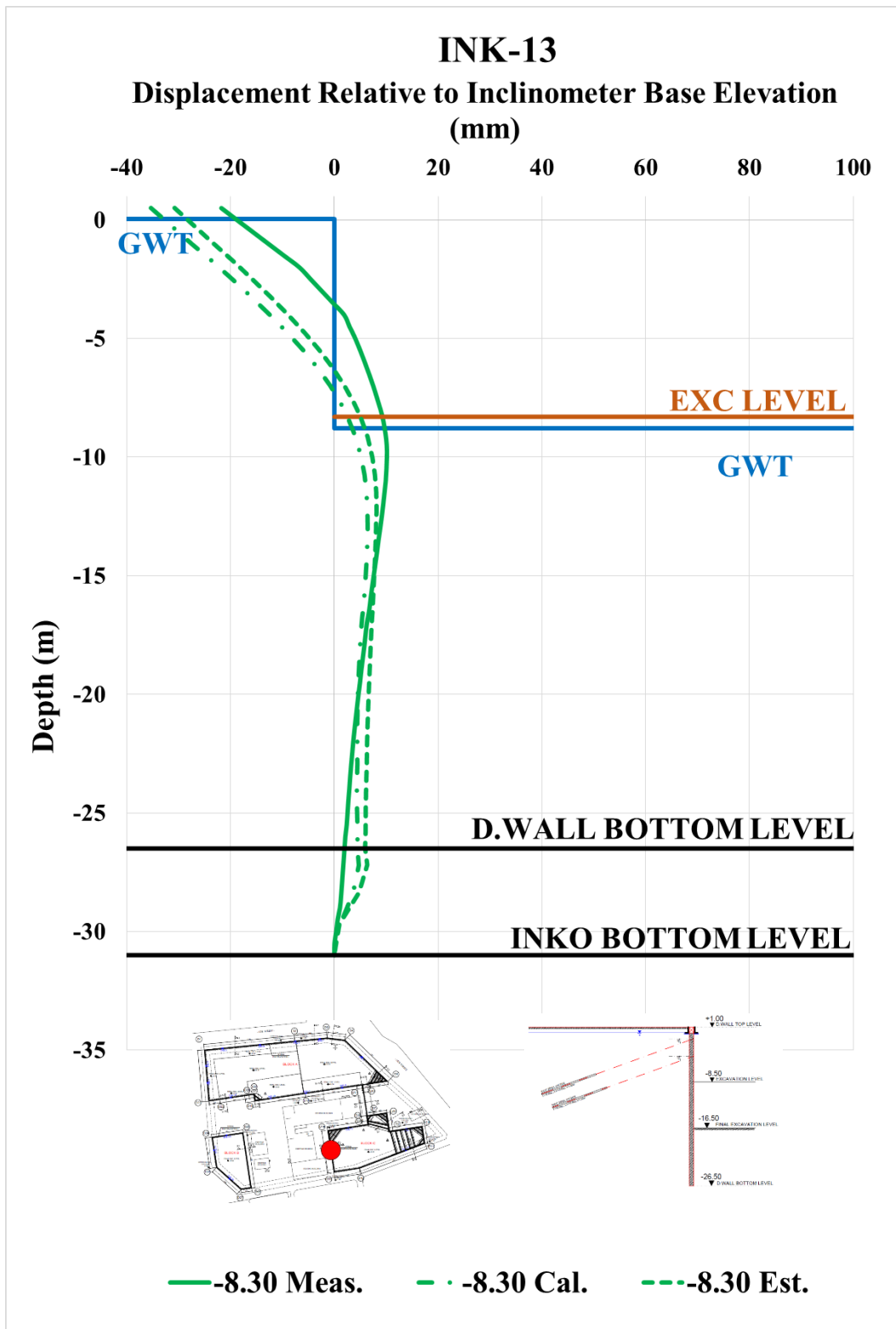
Figure A. 265. Calibrated and Measured Displ. Rel. to Inc. Base Elev. at -8.30 m
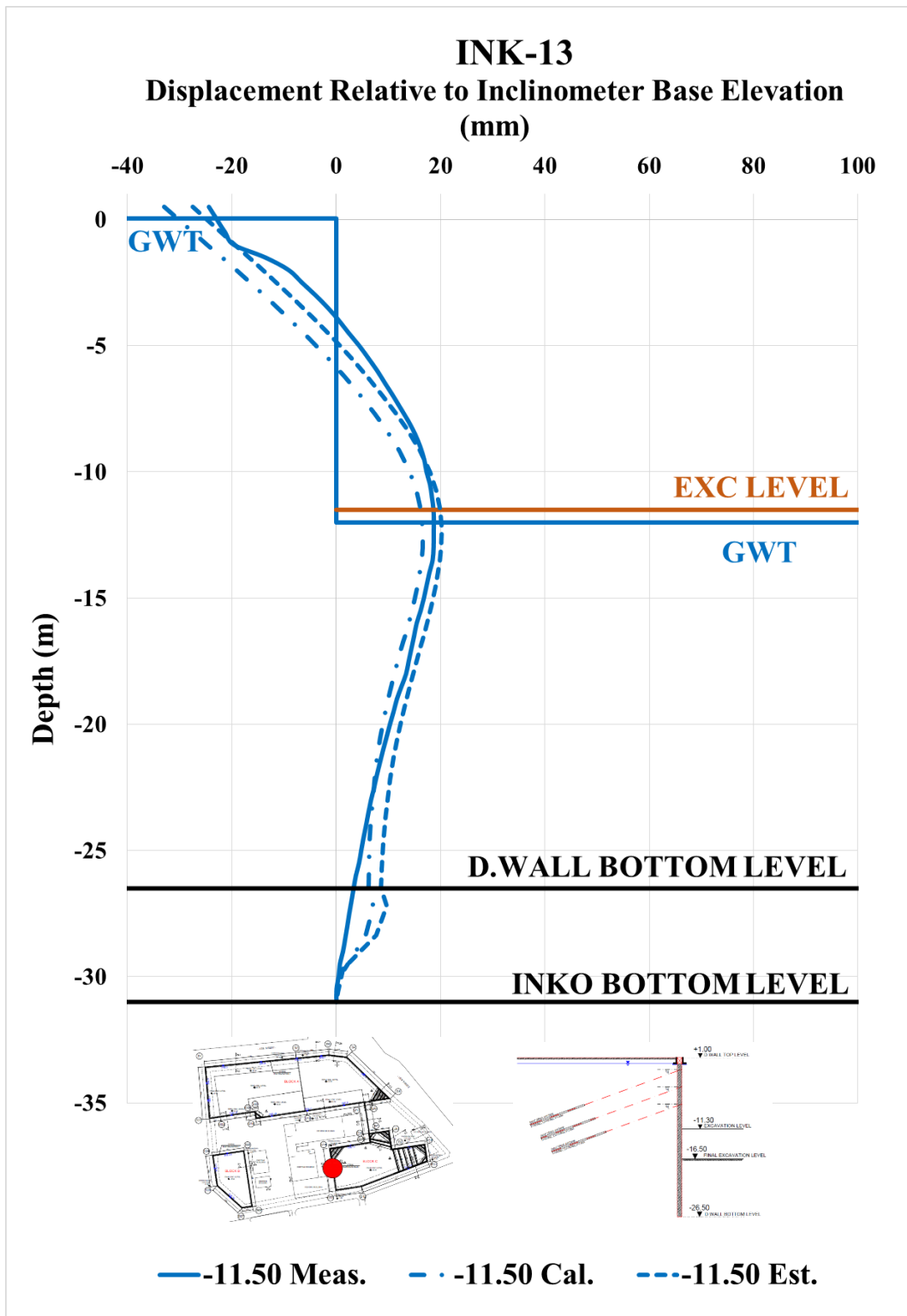
Figure A. 266. Calibrated and Measured Displ. Rel. to Inc. Base Elev. at -11.30 m
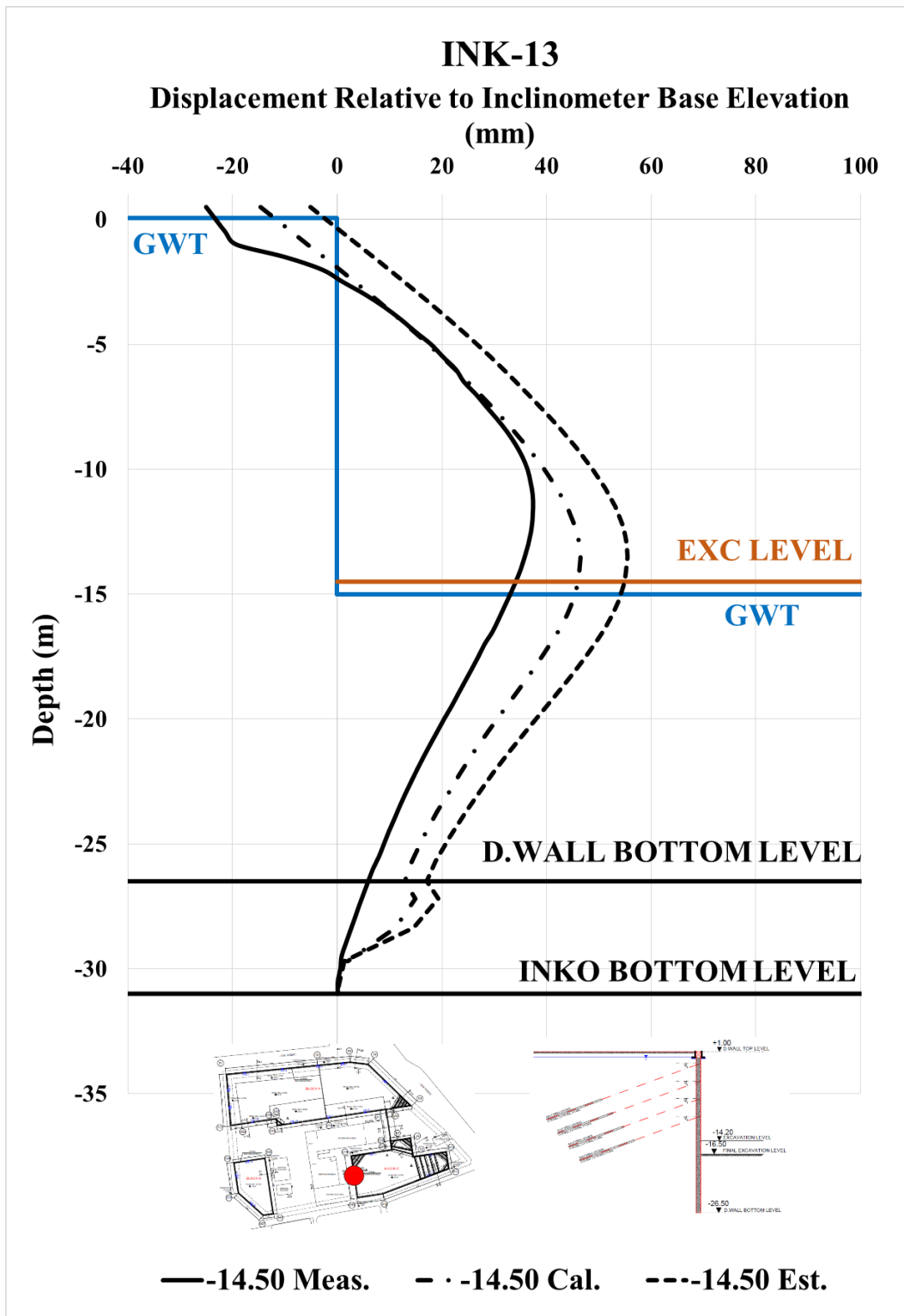
Figure A. 267. Calibrated and Measured Displ. Rel. to Inc. Base Elev. at -14.20 m

INK-13

Displacement Relative to Inclinometer Base Elevation (mm)
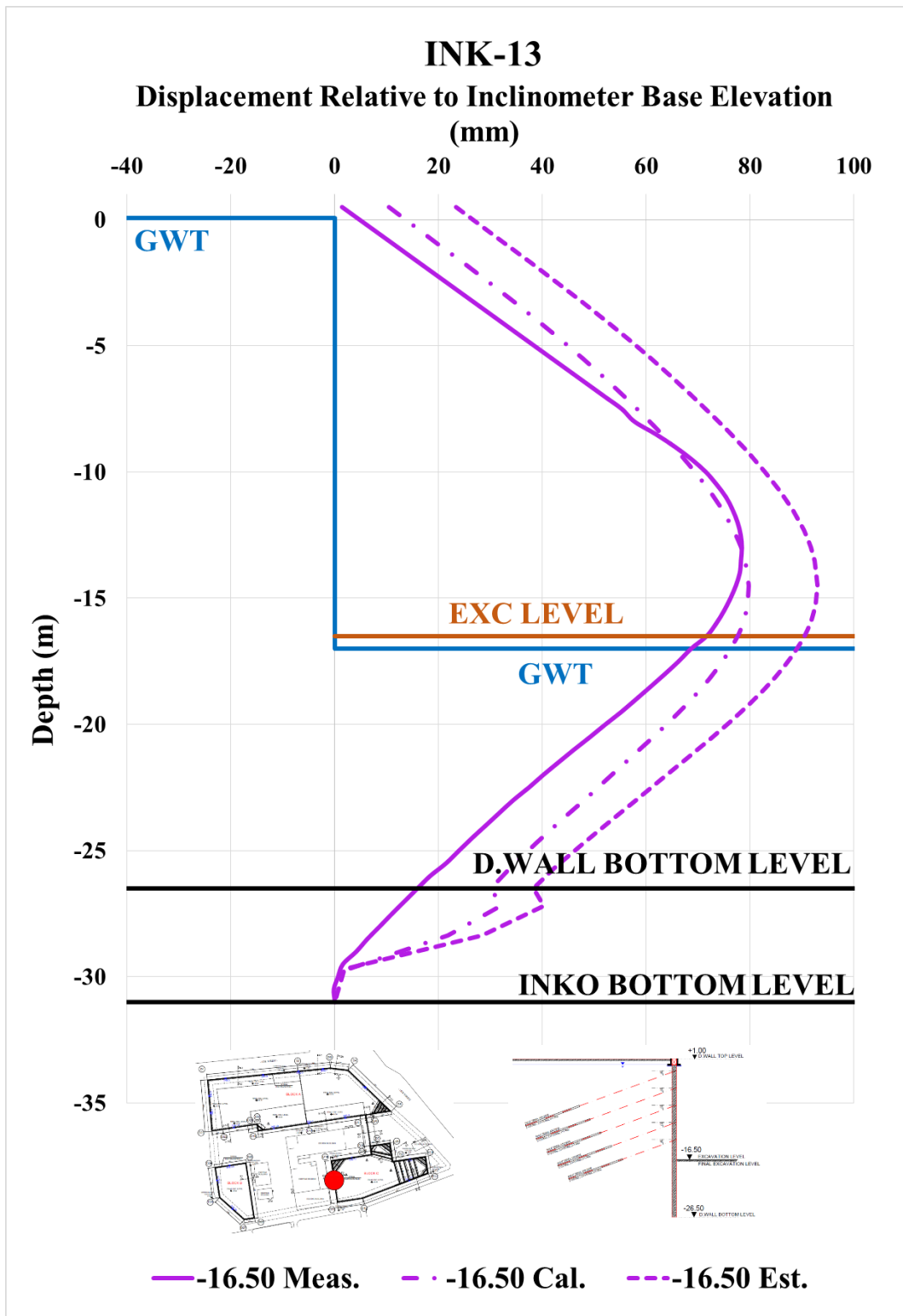
Figure A. 268. Calibrated and Measured Displ. Rel. to Inc. Base Elev. at -16.50 m

Table A. 58. Internal Forces of Diaphragm Wall

INK - 13 / Section 6-6						
Excvation Stage	1	2	3	4	5	6
Excavation Level (m)	-2.50	-5.50	-8.50	-11.30	-14.20	-16.50
N_{max} (kN/m)	99.05	204.20	352.10	545.50	787.20	945.30
V_{max} (kN/m)	45.30	392.20	392.20	392.20	426.10	426.10
M_{max} (kN.m/m)	108.50	775.30	1000.00	1100.00	1389.00	1570.00

Legend	Excvation Stage	1. Anchor Level	2. Excavation Level	2. Anchor Level	3. Excavation Level	3. Anchor Level	4. Excavation Level	4. Anchor Level	5. Excavation Level	5. Anchor Level	Final Excavation Level
	Estimated Load of 1. Anchor Row (kN)	650.00	665.65	556.63	569.53	534.49	539.56	535.07	533.20	536.53	537.54
	Estimated Load of 2. Anchor Row (kN)	-	-	650.00	673.79	604.29	624.72	597.42	607.65	599.53	601.35
	Estimated Load of 3. Anchor Row (kN)	-	-	-	-	650.00	691.39	629.04	664.72	638.93	644.32
	Estimated Load of 4. Anchor Row (kN)	-	-	-	-	-	-	650.00	729.73	672.85	699.18
	Estimated Load of 5. Anchor Row (kN)	-	-	-	-	-	-	-	-	650.00	713.52

Figure A. 269. Estimated Anchor Loads

Table A. 59. Summary of Displacement Results of INK-13

INK - 13 / SECTION 6 - 6

Excavation Level (m)	Excavation Depth (m)	u_{meas} (mm) Inclinometer Measurements	u_{est} (mm) Estimation with Plaxis 2D Analysis	u_{cal} (mm) Calibration with Plaxis 2D Analysis	$u_{literature}$ (mm) FHWA-IF-99-015 (1999) - Maksimum	$u_{literature}$ (mm) FHWA-IF-99-015 (1999) - Average	$u_{literature}$ (mm) Goldberg et al. (1976)	$u_{literature}$ (mm) Clough et al. (1990) - Maksimum	$u_{literature}$ (mm) Clough et al. (1990) - Average	$u_{literature}$ (mm) Long (2001)	$u_{literature}$ (mm) Long (2001) (Extraordinary cases eliminated)	$u_{literature}$ (mm) Long (2001) Cantilever System
-2.50	**3.50**	4.01	6.76	7.91	17.50	7.00	17.50	17.50	7.00	6.65	4.90	12.6
-5.50	**6.50**	12.24	6.11	4.79	32.50	13.00	32.50	32.50	13.00	12.35	9.10	-
-8.30	**9.30**	10.12	8.53	6.73	46.50	18.60	46.50	46.50	18.60	17.67	13.02	-
-11.50	**12.50**	18.71	18.35	14.92	62.50	25.00	62.50	62.50	25.00	23.75	17.50	-
-14.50	**15.50**	37.41	48.57	40.52	77.50	31.00	77.50	77.50	31.00	29.45	21.70	-
-16.50	**17.50**	78.40	91.91	76.93	87.50	35.00	87.50	87.50	35.00	33.25	24.50	-

411
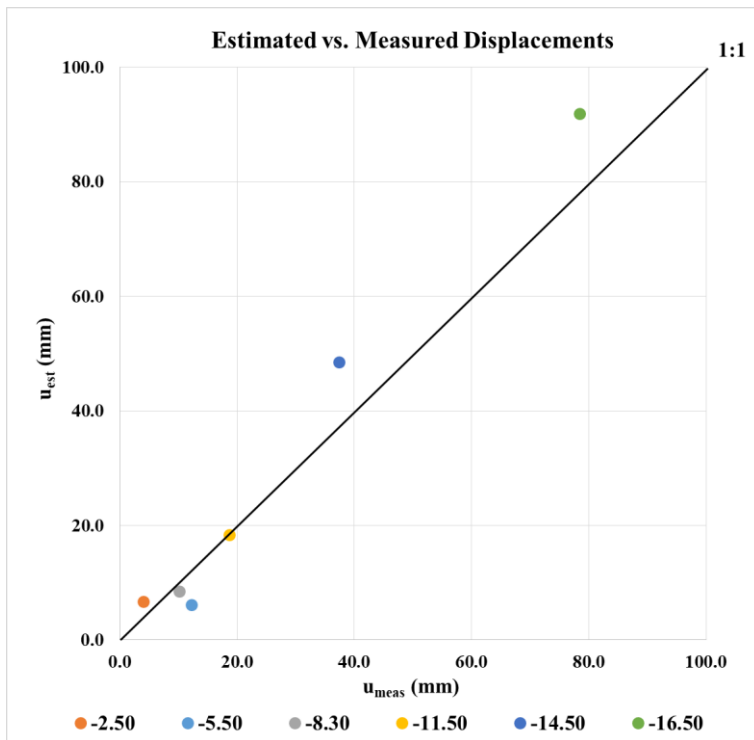
Figure A. 270. Estimated and Measured Displacements of INK - 13
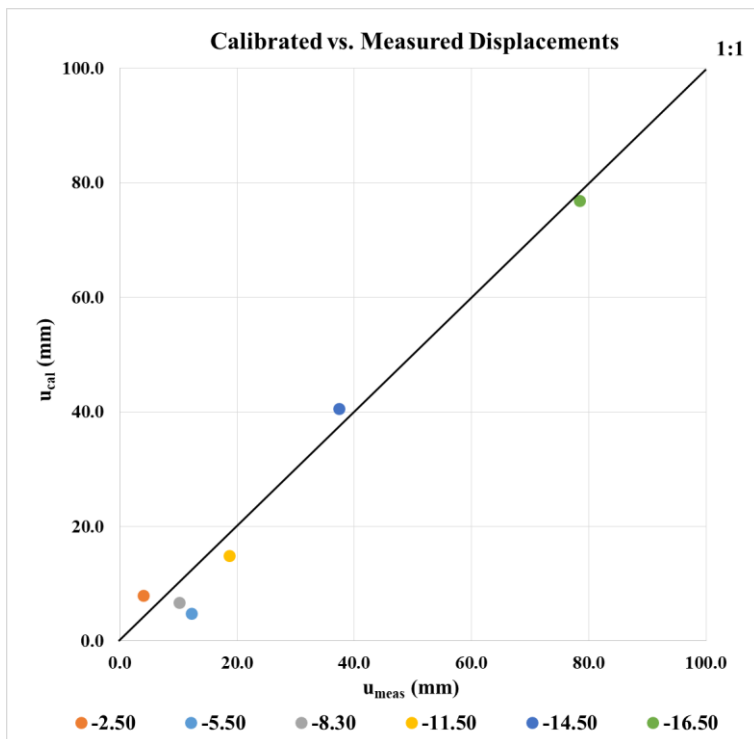
Figure A. 271. Calibrated and Measured Displacements of INK - 13

412
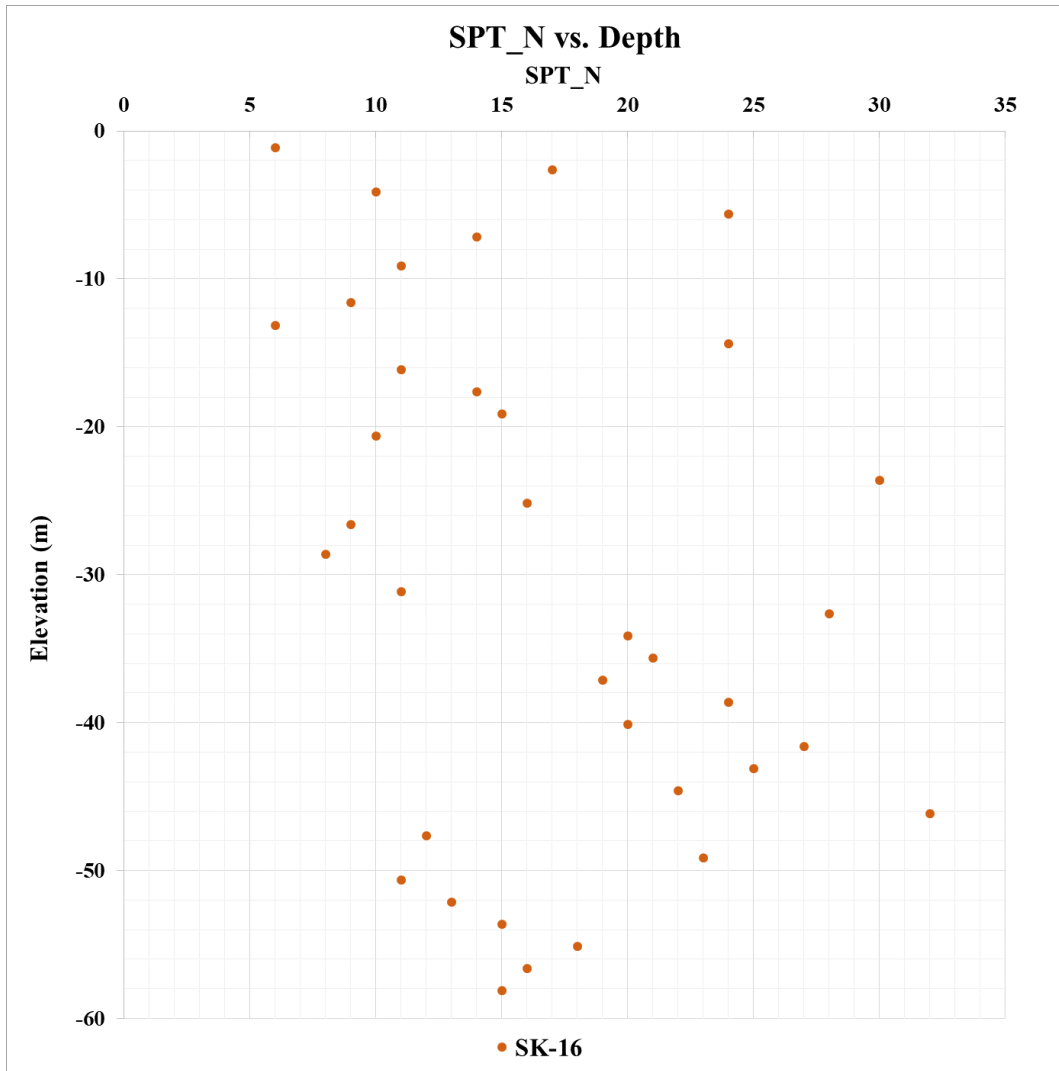
Area C2

Figure A. 272. SPT-N vs. Depth for Area C2
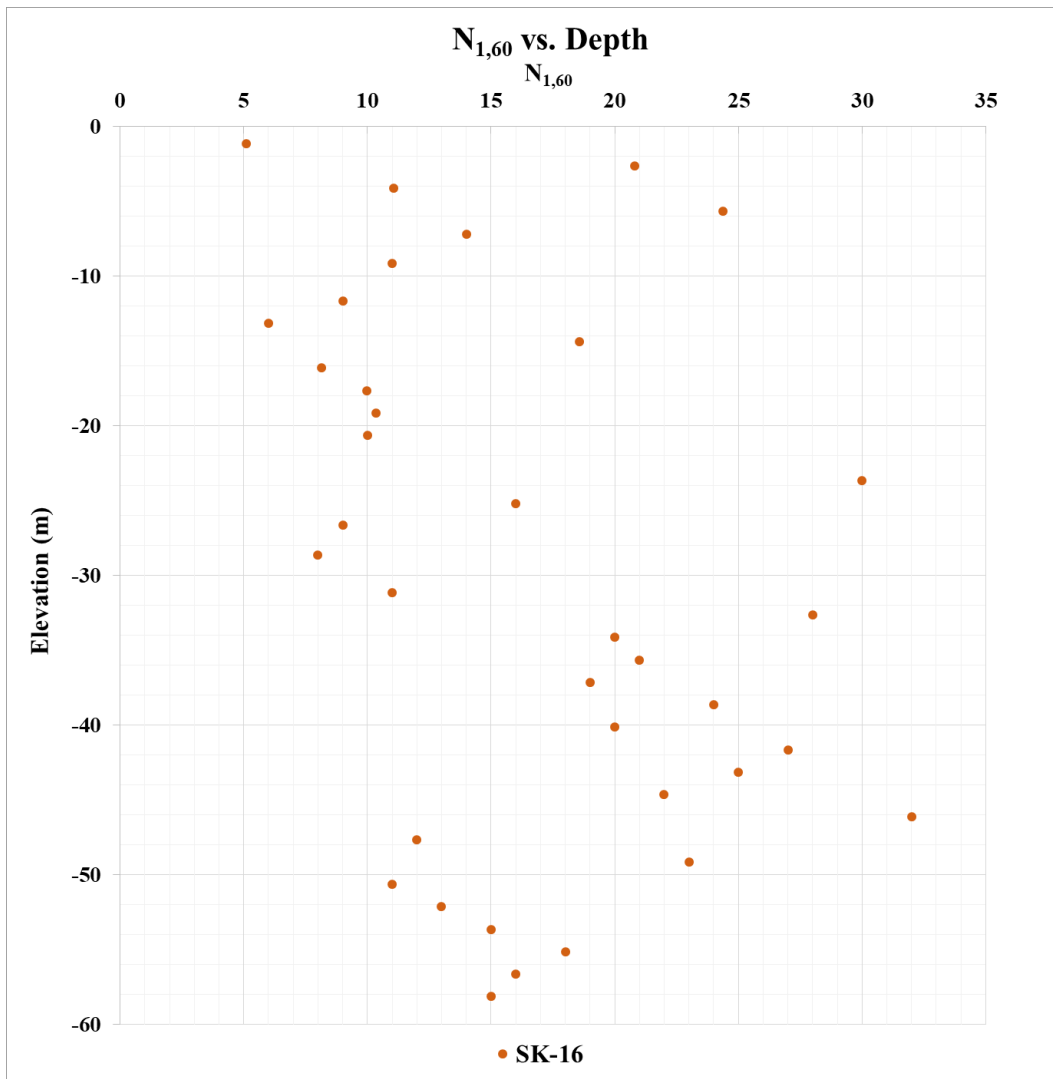
Figure A. 273. SPT-$N_{1,60}$ vs. Depth for Area C2
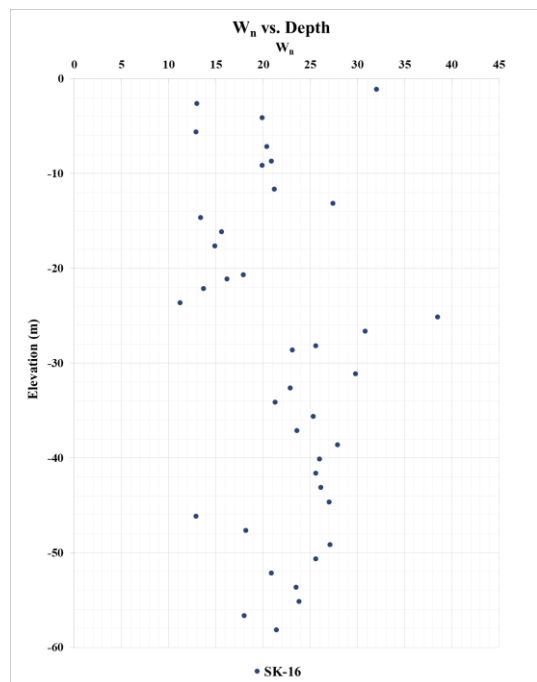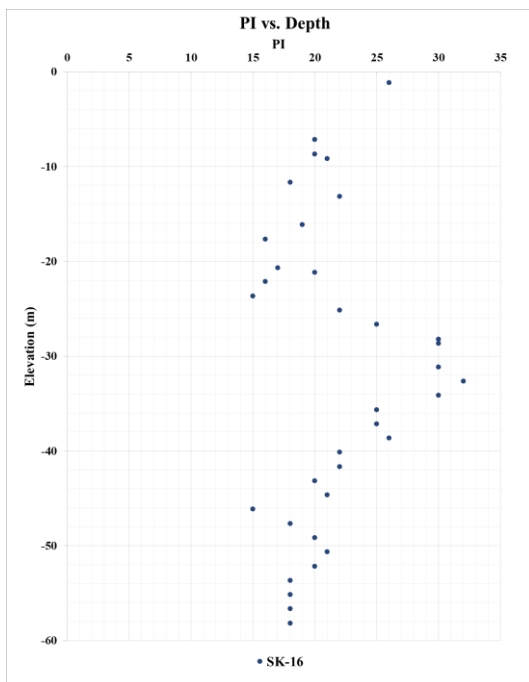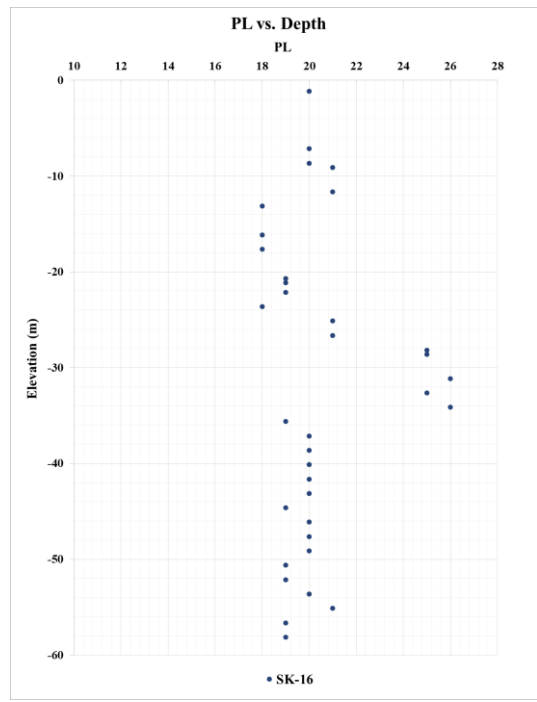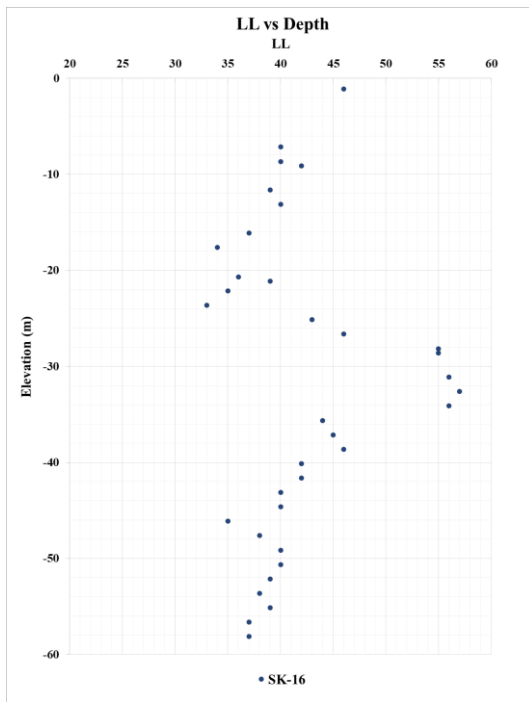
Figure A. 274. Variation of LL, PL, PI, and w_n for Area C2
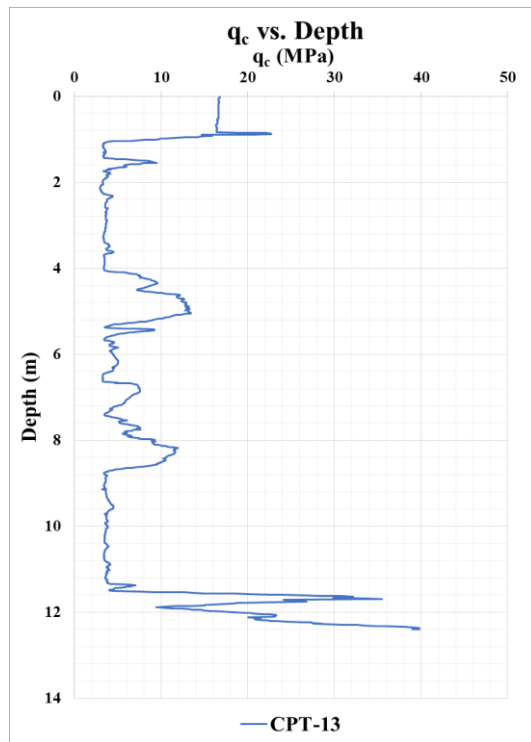
Figure A. 275. Variation of q_c along with the Depth for Area C2
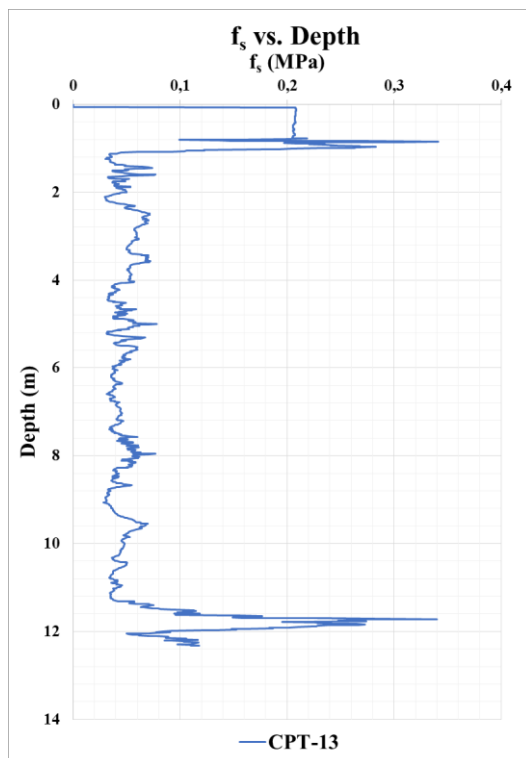
Figure A. 276. Variation of f_s along with the Depth for Area C2

1 borehole (SK-16) and 1 CPT (CPT-13) were considered. The depth of the borehole is 60 m. The depth of CPT is 12.4 m. Atterberg limit tests were performed on the samples taken from SK-16. LL, PL, PI, and w_n vary in 33 – 57 % (avg. 42 %), 18 – 26 % (avg. 20.4 %), 15 – 32 % (avg. 21.7 %), and 11.2 – 38.5 % (avg. 22.1 %) respectively. Unified soil classification (USCS) was performed for each sample. By considering USCS, SPT $N_{1,60}$ values, and CPT results, the thickness of soil layers was determined. Detailed soil parameters are given in below table;

- Boreholes: SK-16 (The depth of the borehole.: 60 m)
- CPTs: CPT-13 (The depth of CPT: 12.4 m)
- LL: 33 – 57 % (avg. 42 %)
- PL: 33 – 57 % (avg. 42 %)
- PI: 15 – 32 % (avg. 21.7 %)
- w_n: 11.2 – 38.5 % (avg. 22.1 %)

Table A. 60. Soil Profile of Area 7 (C2)

Layer No	Elevation (m)		USCS	Type	Thickness (m)	N	$N_{1,60}$	N_{60}	PI	y_{wet} (kN/m³)	y_{sat} (kN/m³)	c_u (kPa)	c (kPa)	φ (°)	ψ (°)	E_{50}^{ref} (MPa)	E_{oed}^{ref} (MPa)	E_{ur}^{ref} (MPa)	m	v_{ur}	p_{ref} (kPa)	R_f
1	2.3	-	CL	Cohesive	3.5	6.0	5.0	5.0	25.5	17.6	19.2	30.0	3.0	29.5	0.0	5.0	2.5	15.0	1.0	0.2	30.8	0.9
2	-1.2	-5.7	SM-GC	Cohesionless	4.5	17.0	19.0	16.0	NP	19.2	20.0	-	1.0	33.0	3.0	39.0	39.0	117.0	0.5	0.2	100.0	0.9
3	-5.7	-13.2	CL	Cohesive	7.5	10.0	10.0	10.0	20.2	18.4	20.0	60.0	6.0	30.0	0.0	11.6	5.8	34.8	1.0	0.2	131.5	0.9
4	-13.2	-19.7	SC-GC	Cohesionless	6.5	12.0	12.0	12.0	12.8	19.2	20.0	-	3.0	30.5	0.5	31.0	31.0	93.0	0.5	0.2	100.0	0.9
5	-19.7	-31.2	CL	Cohesive	11.5	14.0	14.0	14.0	23.6	18.4	20.0	80.0	8.0	29.5	0.0	15.4	7.7	46.2	1.0	0.2	291.5	0.9
6	-31.2	-46.2	CL	Cohesive	15.0	24.0	24.0	24.0	24.8	18.4	20.0	130.0	13.0	29.5	0.0	25.2	12.6	75.6	1.0	0.2	424.0	0.9
7	-46.2	-61.2	CL	Cohesive	15.0	16.0	16.0	16.0	18.4	18.4	20.0	95.0	9.5	30.5	0.5	18.9	9.4	56.6	1.0	0.2	574.0	0.9
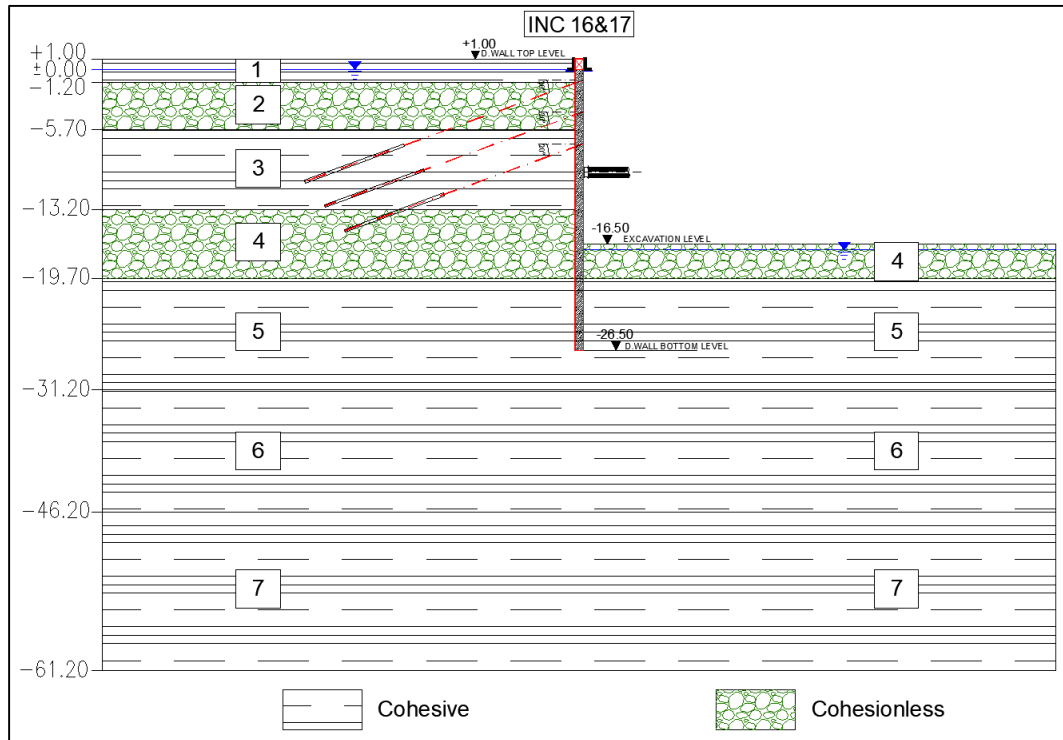
Figure A. 277. Section 6A – 6A

Table A. 61. Section Properties of 6A – 6A

SECTION 6A - 6A											
Diaphragm Wall			SBMA Type Anchor				Excavation Properties			Strut Properties	
Top Level (m)	Bottom Level (m)	Length (m)	Anchor No	Anchor Level (m)	Anchor Length (m)	Horizontal Spacing (m)	Top Level (m)	Bottom Level (m)	Depth (m)	Strut Prop.	Strut Level (m)
1.00	-26.50	27.50	1	-1.00	28.00	1.40	1.00	-16.50	-17.50	Φ=914mm t=13mm	-9.70
			2	-4.00	26.00	1.40					
			3	-7.00	24.00	1.40					

INK-16 – Estimated and Measured Displacements
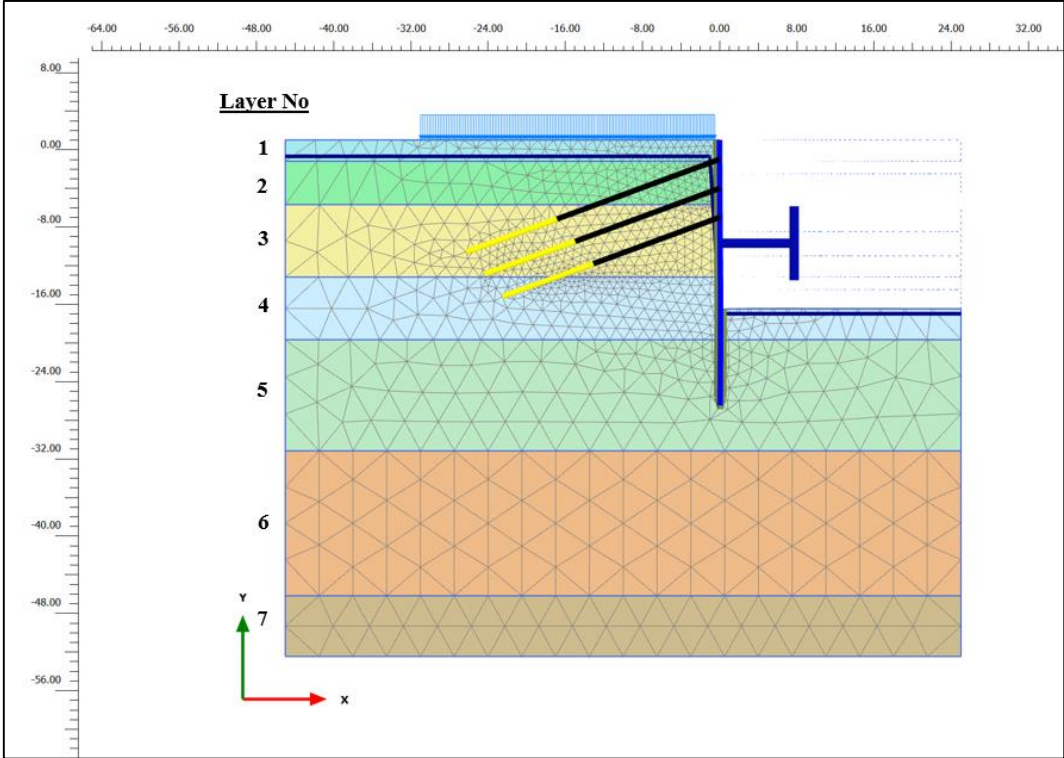
Figure A. 278. Meshed Model for INK-16
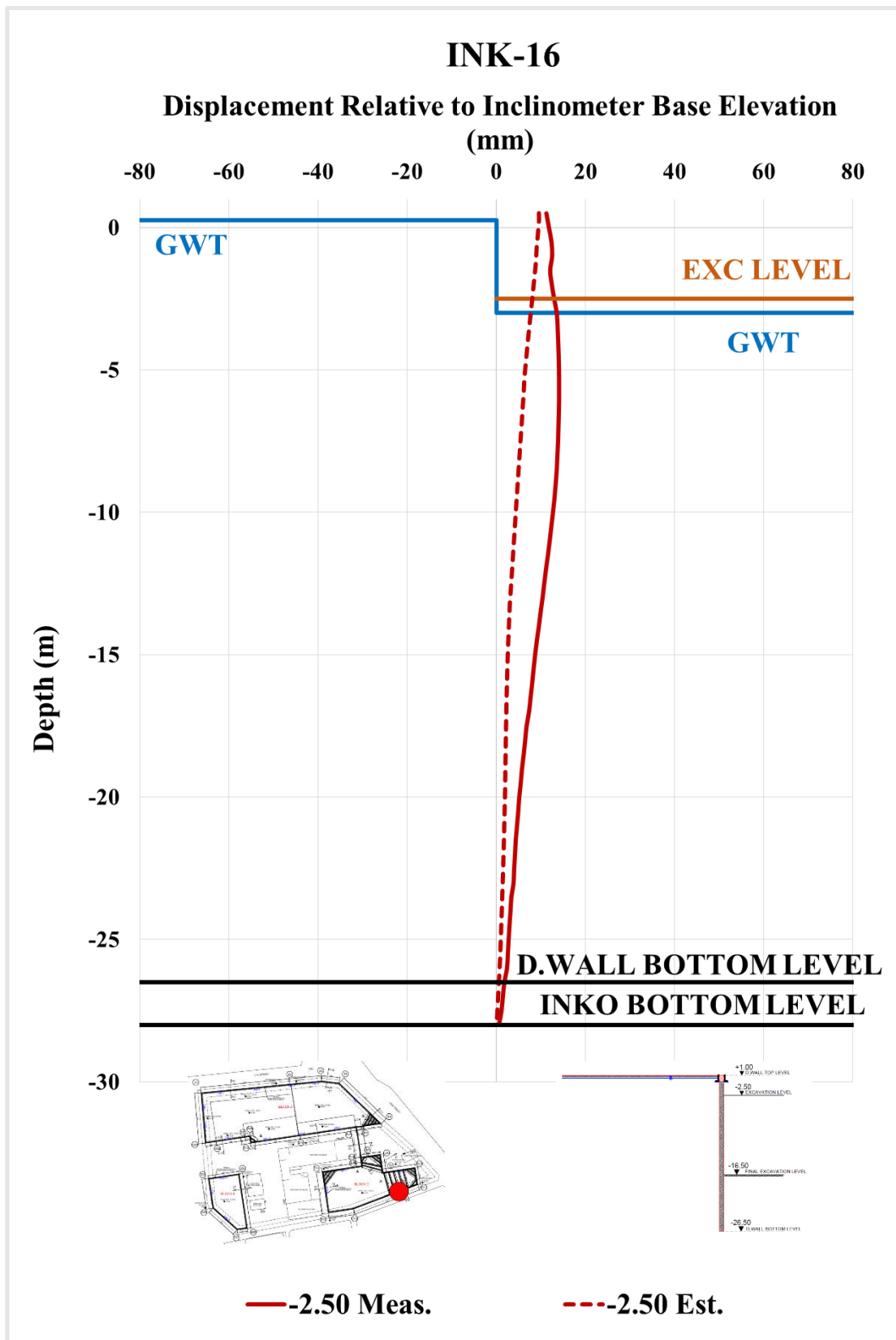
Figure A. 279. Estimated and Measured Displ. Rel. to Inc. Base Elev. at -2.50 m
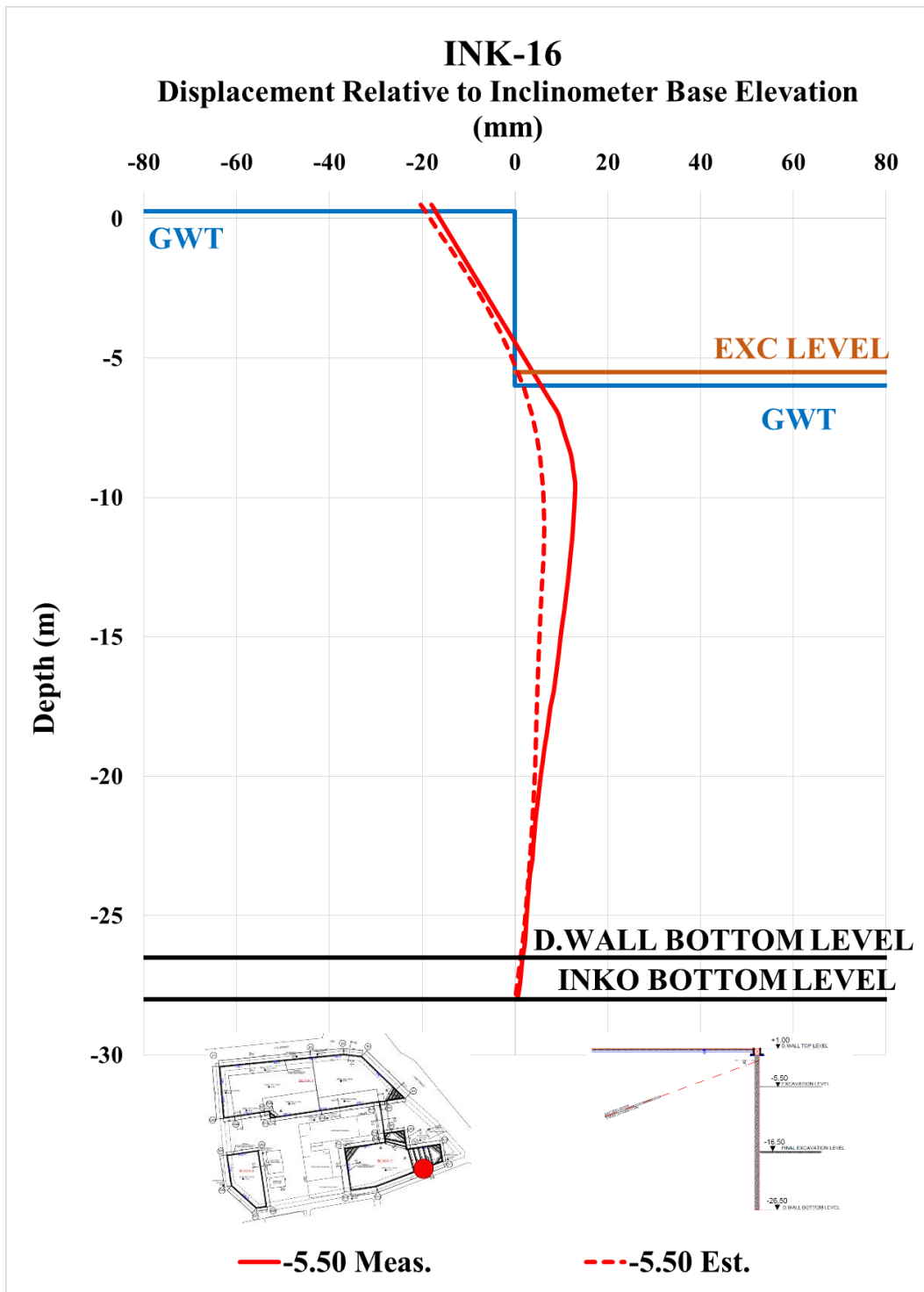
Figure A. 280. Estimated and Measured Displ. Rel. to Inc. Base Elev. at -5.50 m
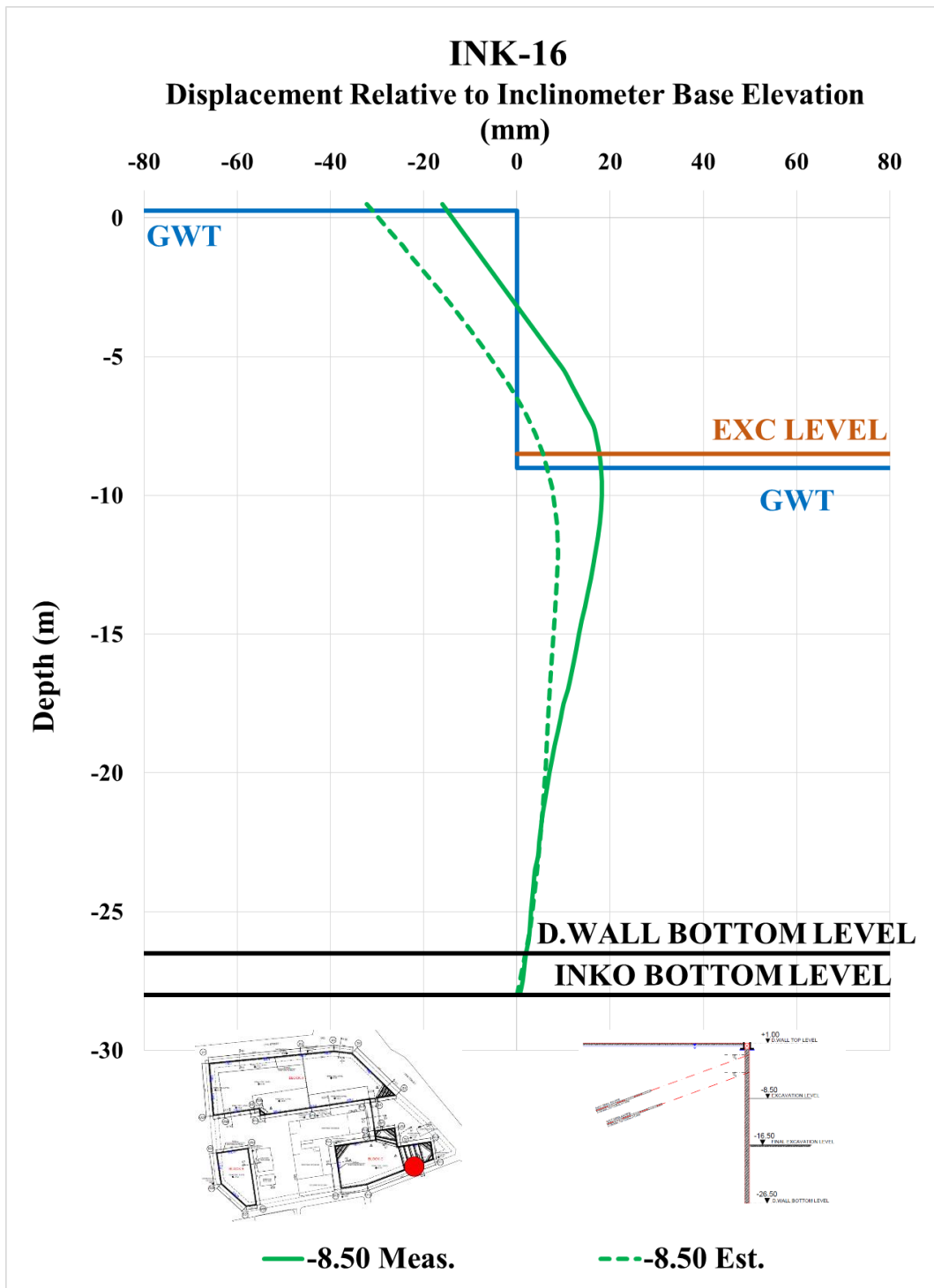
Figure A. 281. Estimated and Measured Displ. Rel. to Inc. Base Elev. at -8.50 m
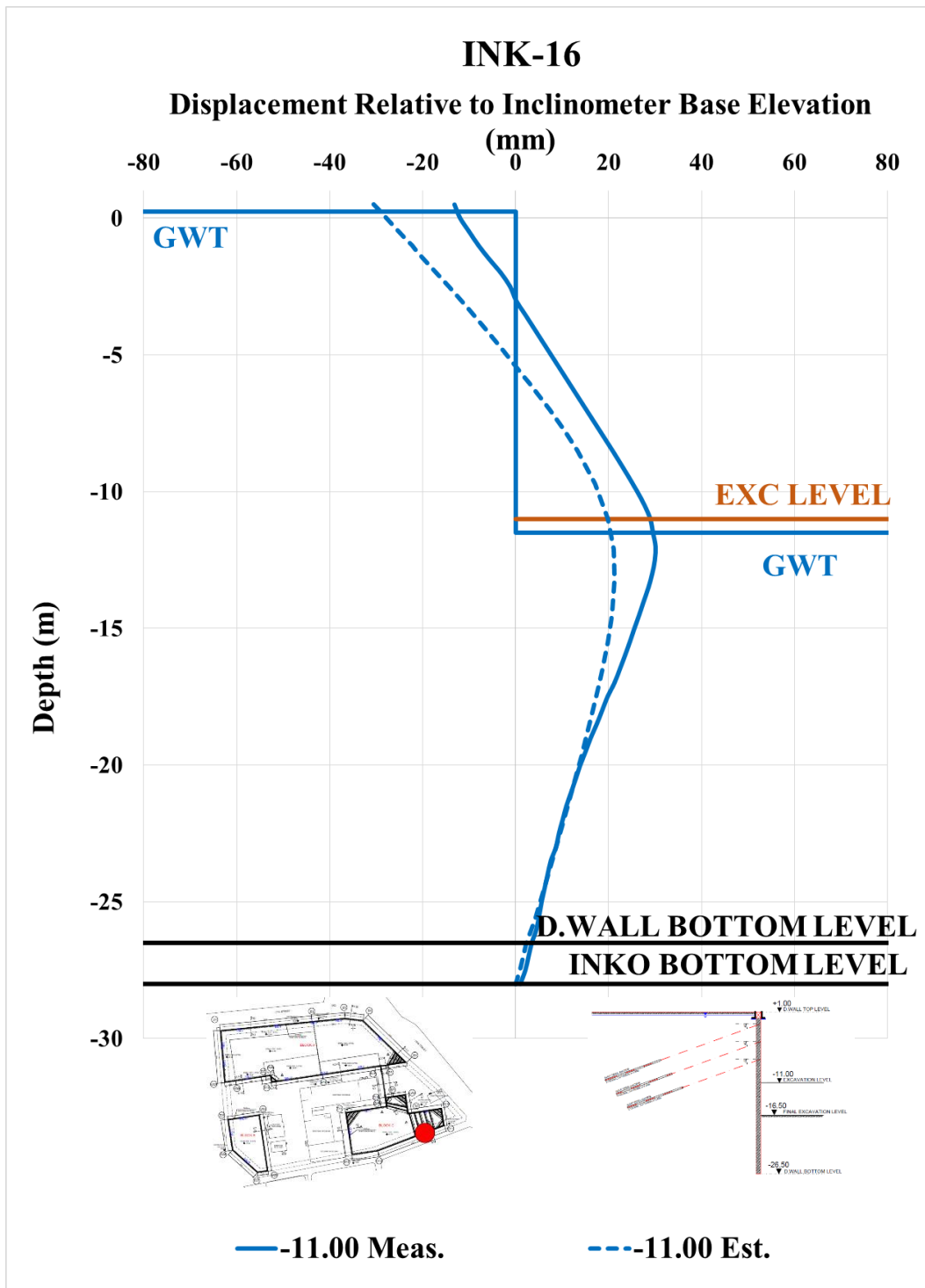
Figure A. 282. Estimated and Measured Displ. Rel. to Inc. Base Elev. at -11.00 m
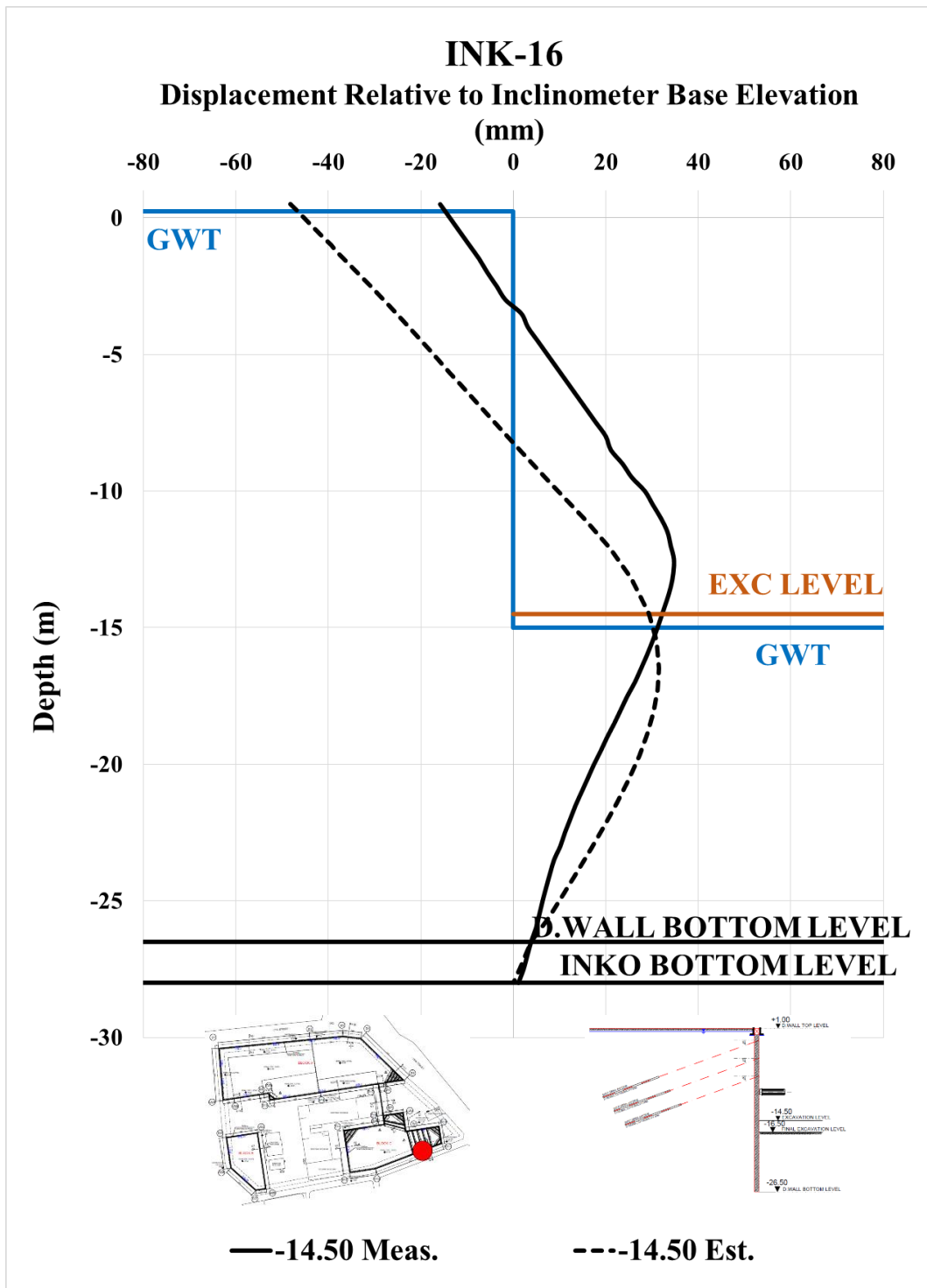
Figure A. 283. Estimated and Measured Displ. Rel. to Inc. Base Elev. at -14.50 m
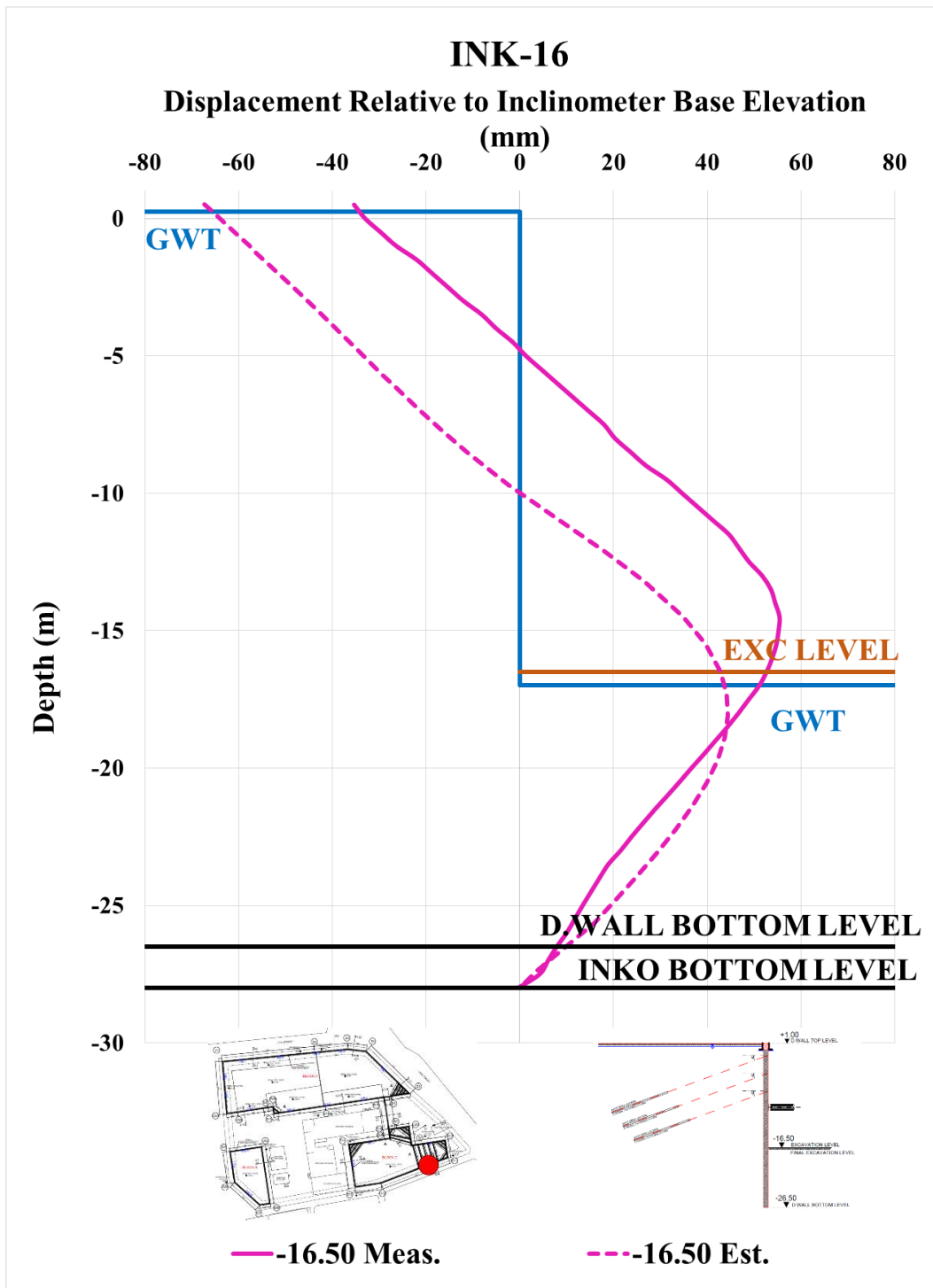
Figure A. 284. Estimated and Measured Displ. Rel. to Inc. Base Elev. at -16.50 m

Table A. 62. Internal Forces of Diaphragm Wall

INK - 16 / Section 6A-6A						
Excvation Stage	1	2	3	4	5	6
Excavation Level (m)	-2.50	-5.50	-8.50	-11.00	-14.50	-16.50
N_{max} (kN/m)	98.96	218.70	368.60	551.50	631.10	688.00
V_{max} (kN/m)	56.09	415.80	415.80	415.80	744.90	1087.00
M_{max} (kN.m/m)	98.20	753.90	988.80	1140.00	1552.00	2242.00

Legend	Excvation Stage	1. Anchor Level	2. Excavation Level	2. Anchor Level	3. Excavation Level	3. Anchor Level	4. Excavation Level	5. Excavation Level	Final Excavation Level
	Estimated Load of 1. Anchor Row (kN)	650.00	672.80	550.86	566.46	526.43	528.45	470.24	411.16
	Estimated Load of 2. Anchor Row (kN)	-	-	650.00	682.48	594.08	614.05	537.52	463.25
	Estimated Load of 3. Anchor Row (kN)	-	-	-	-	650.00	701.75	616.48	539.90
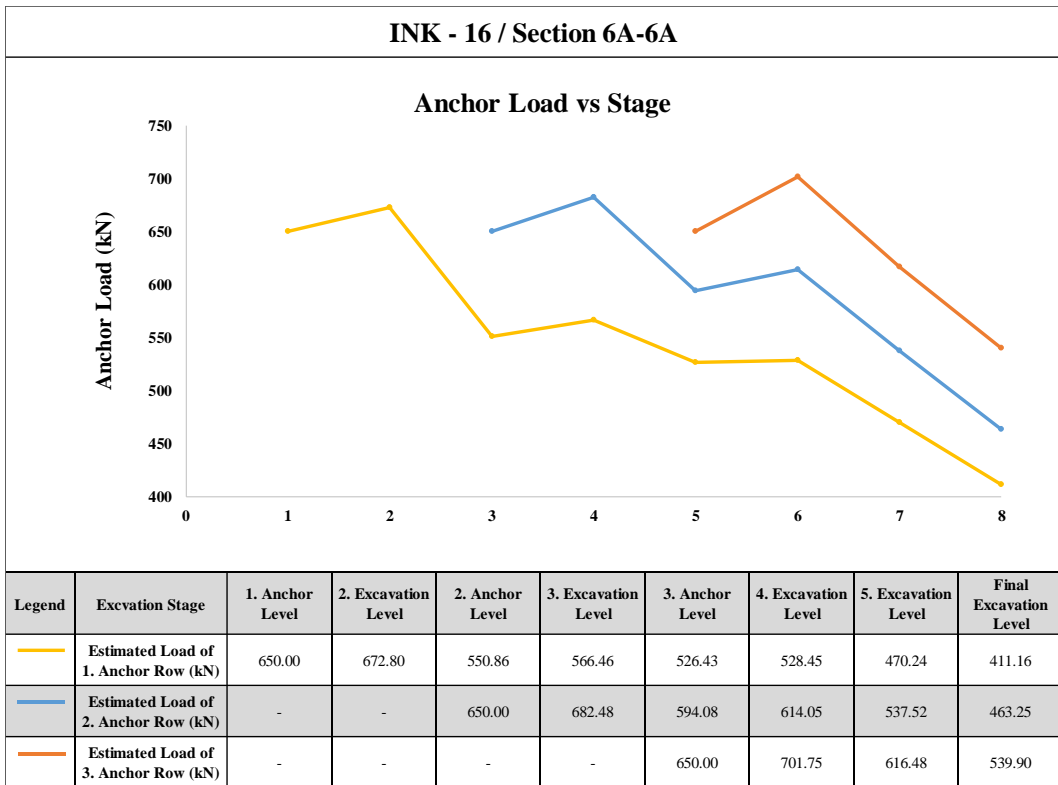
Figure A. 285. Estimated Anchor Loads

INK-17 – Estimated and Measured Displacements
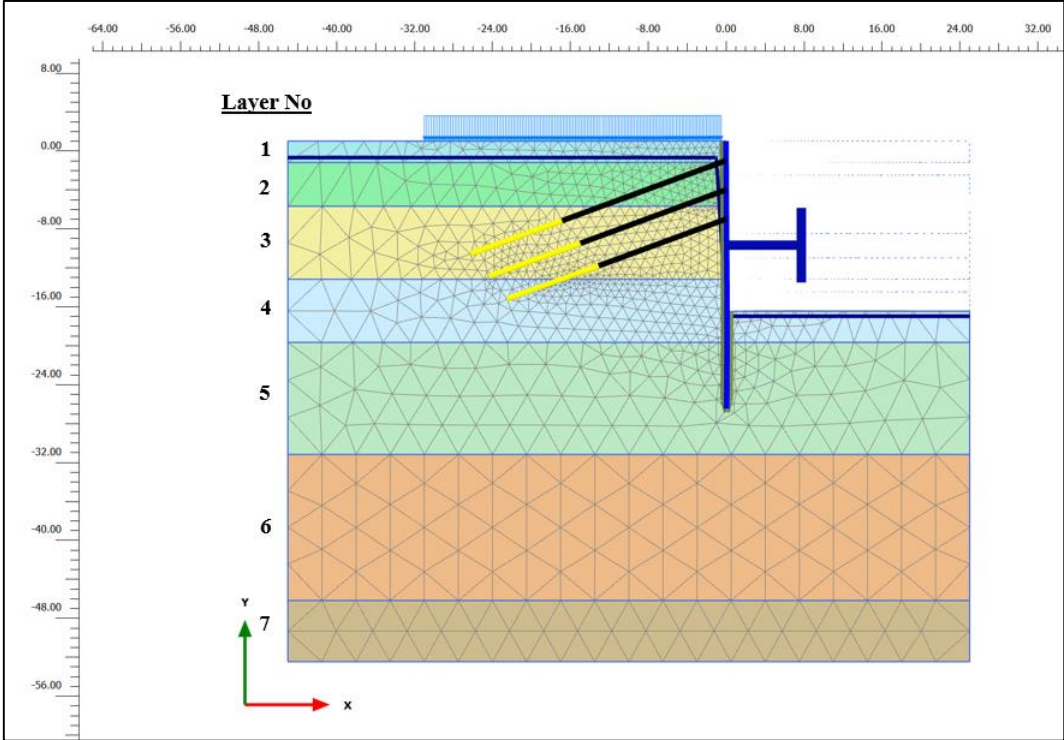
Figure A. 286. Meshed Model for INK-17
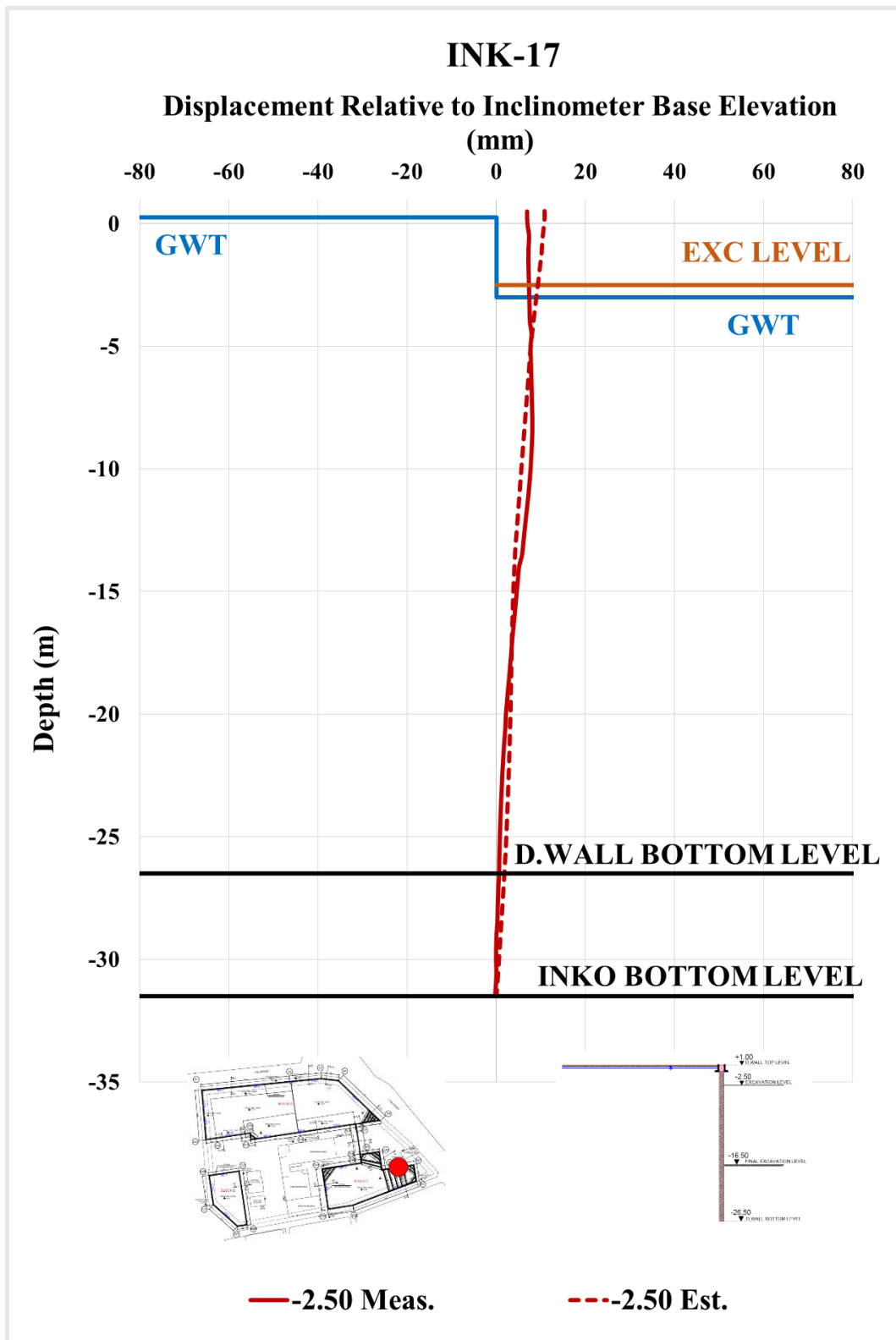
Figure A. 287. Estimated and Measured Displ. Rel. to Inc. Base Elev. at -2.50 m
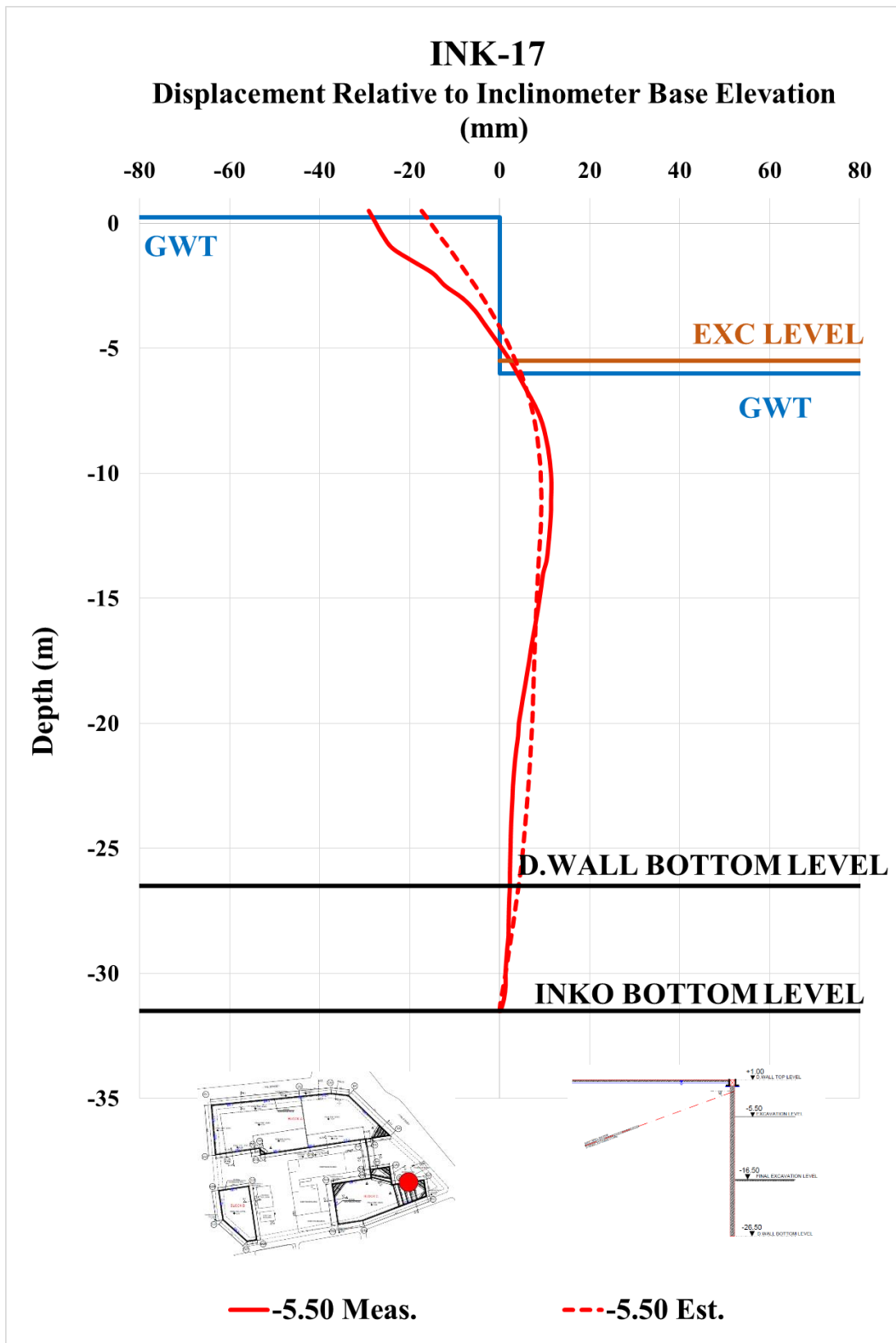
Figure A. 288. Estimated and Measured Displ. Rel. to Inc. Base Elev. at -5.50 m
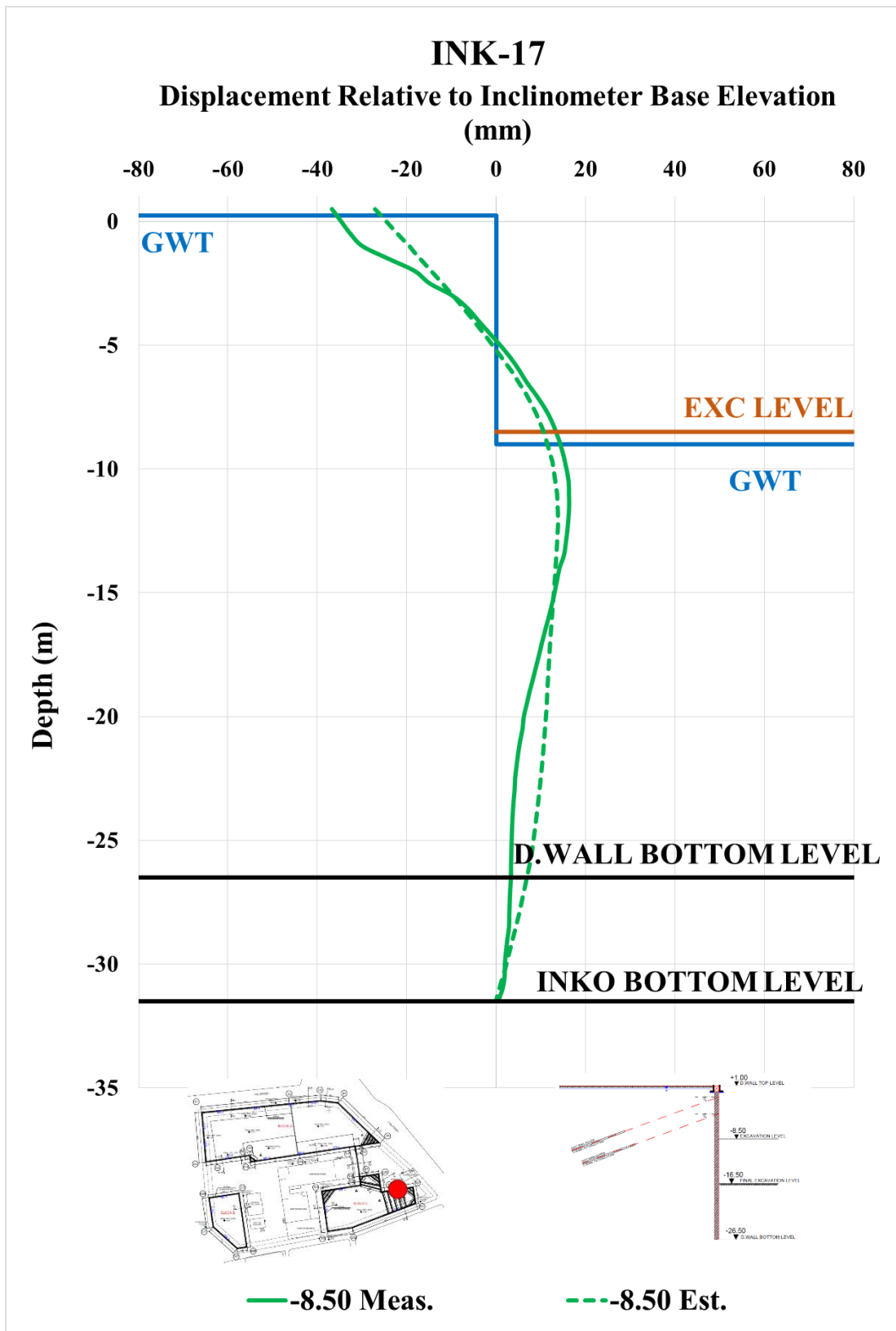
Figure A. 289. Estimated and Measured Displ. Rel. to Inc. Base Elev. at -8.50 m
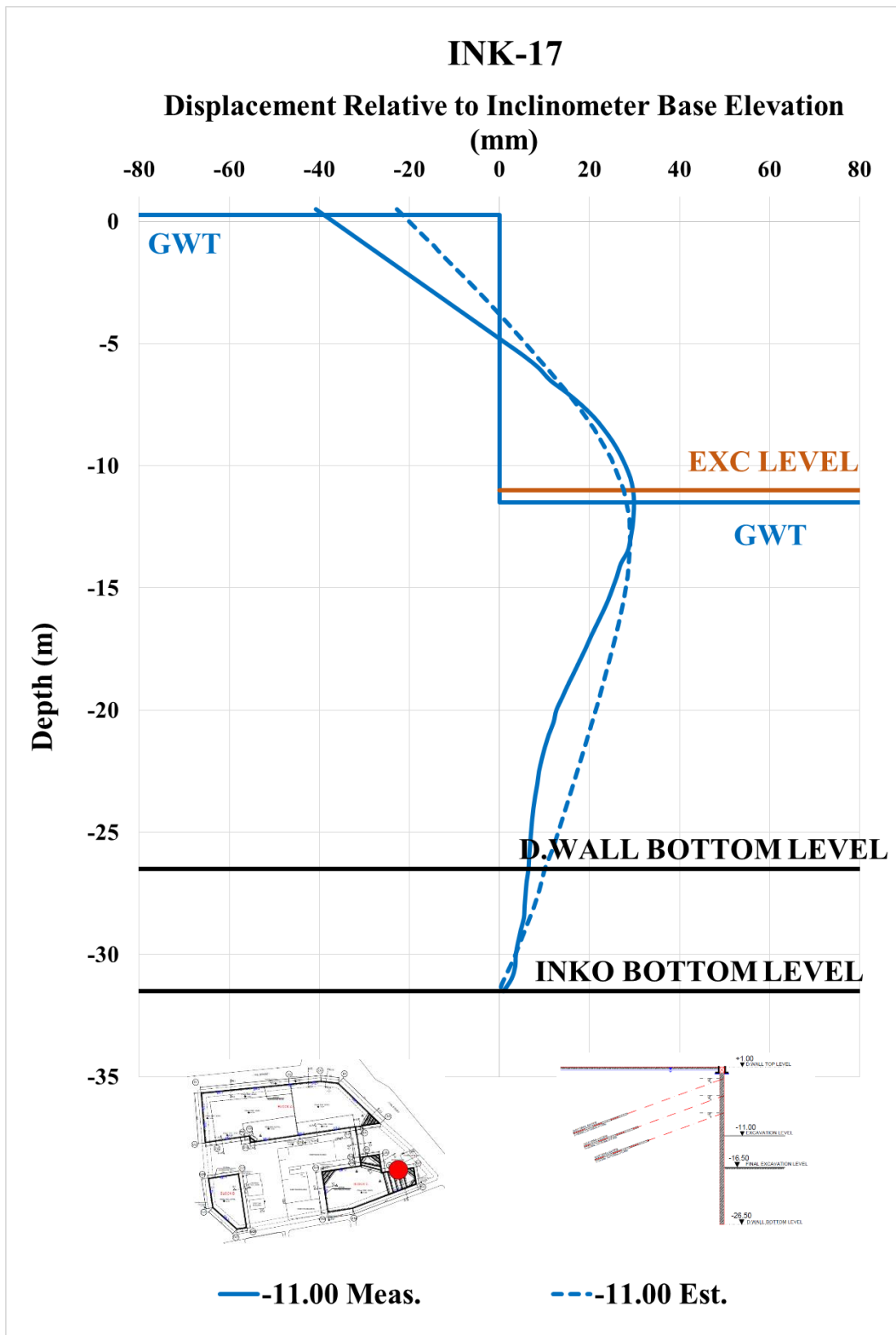
Figure A. 290. Estimated and Measured Displ. Rel. to Inc. Base Elev. at -11.00 m
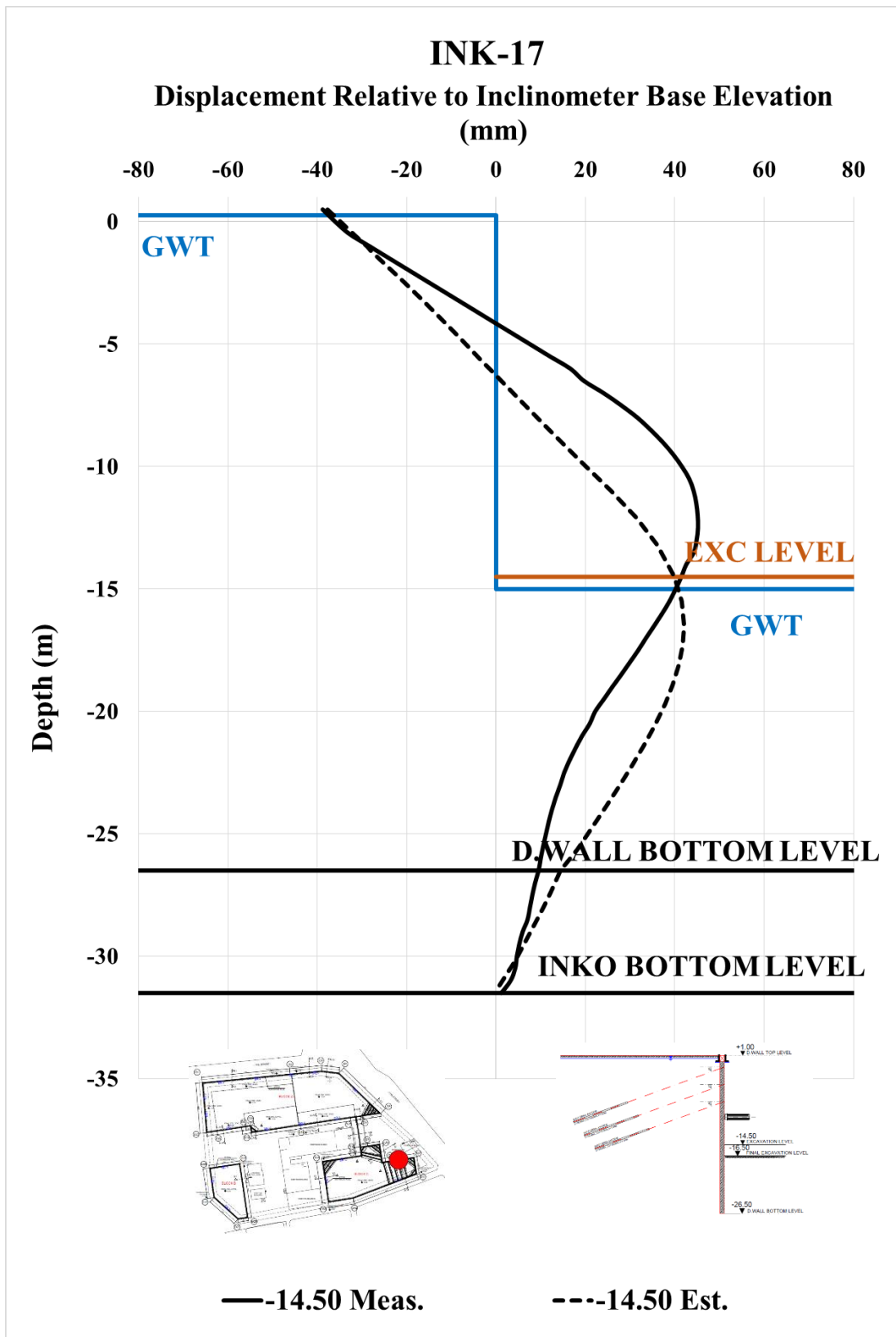
Figure A. 291. Estimated and Measured Displ. Rel. to Inc. Base Elev. at -14.50 m
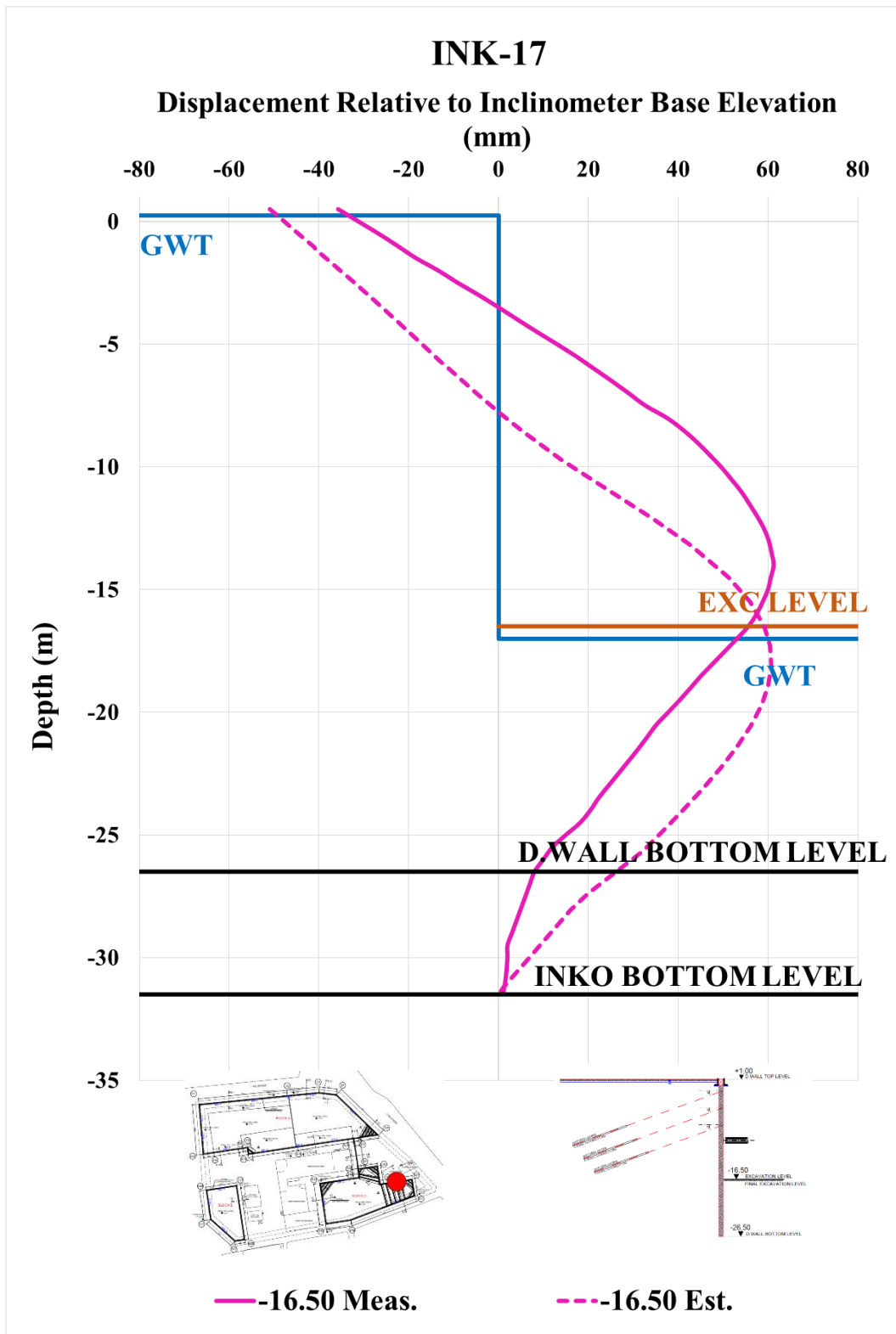
Figure A. 292. Estimated and Measured Displ. Rel. to Inc. Base Elev. at -16.50 m

Table A. 63. Internal Forces of Diaphragm Wall

INK - 17 / Section 6A-6A						
Excvation Stage	1	2	3	4	5	6
Excavation Level (m)	-2.50	-5.50	-8.50	-11.00	-14.50	-16.50
N_{max} (kN/m)	98.96	218.70	368.60	551.50	631.10	688.00
V_{max} (kN/m)	56.09	415.80	415.80	415.80	744.90	1087.00
M_{max} (kN.m/m)	98.20	753.90	988.80	1140.00	1552.00	2242.00

Legend	Excvation Stage	1. Anchor Level	2. Excavation Level	2. Anchor Level	3. Excavation Level	3. Anchor Level	4. Excavation Level	5. Excavation Level	Final Excavation Level
	Estimated Load of 1. Anchor Row (kN)	650.00	672.80	550.86	566.46	526.43	528.45	470.24	411.16
	Estimated Load of 2. Anchor Row (kN)	-	-	650.00	682.48	594.08	614.05	537.52	463.25
	Estimated Load of 3. Anchor Row (kN)	-	-	-	-	650.00	701.75	616.48	539.90
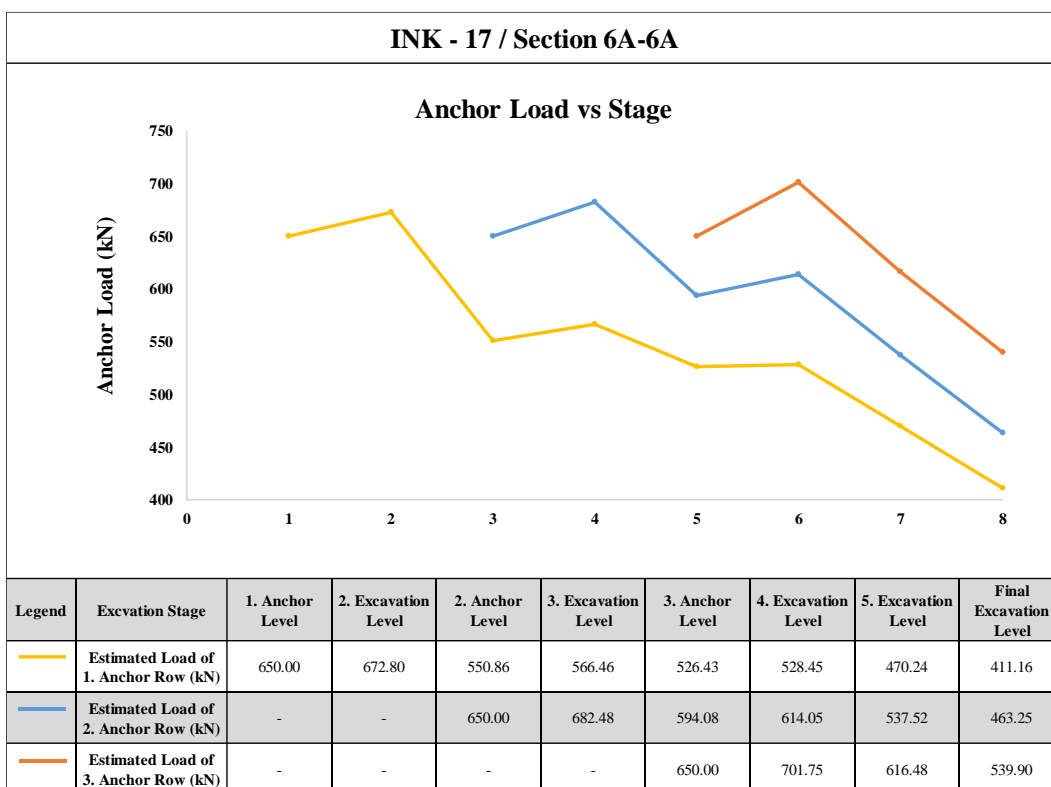
Figure A. 293. Estimated Anchor Loads

INK-16 – Calibrated, Estimated and Measured Displacements
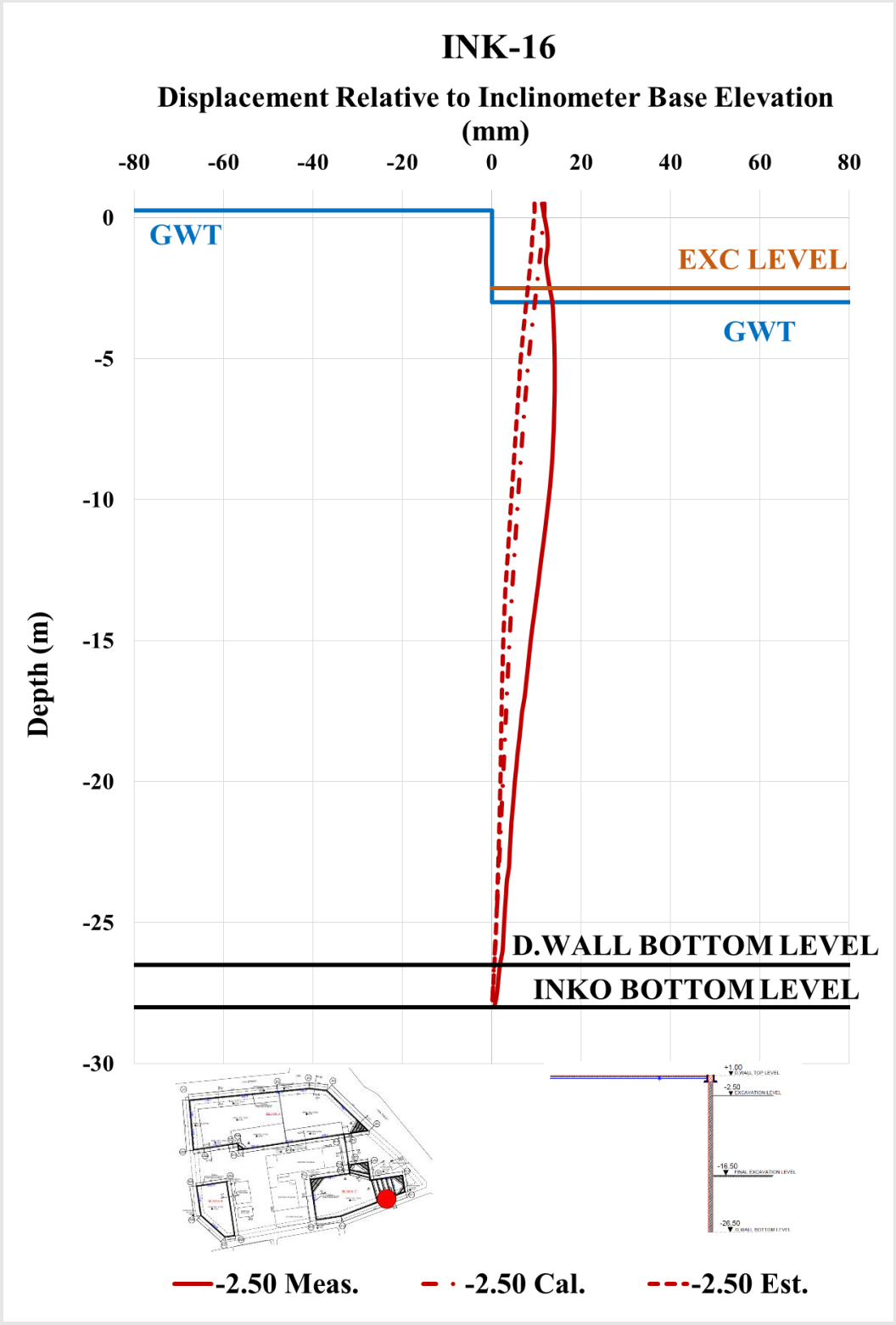
Figure A. 294. Calibrated and Measured Displ. Rel. to Inc. Base Elev. at -2.50 m
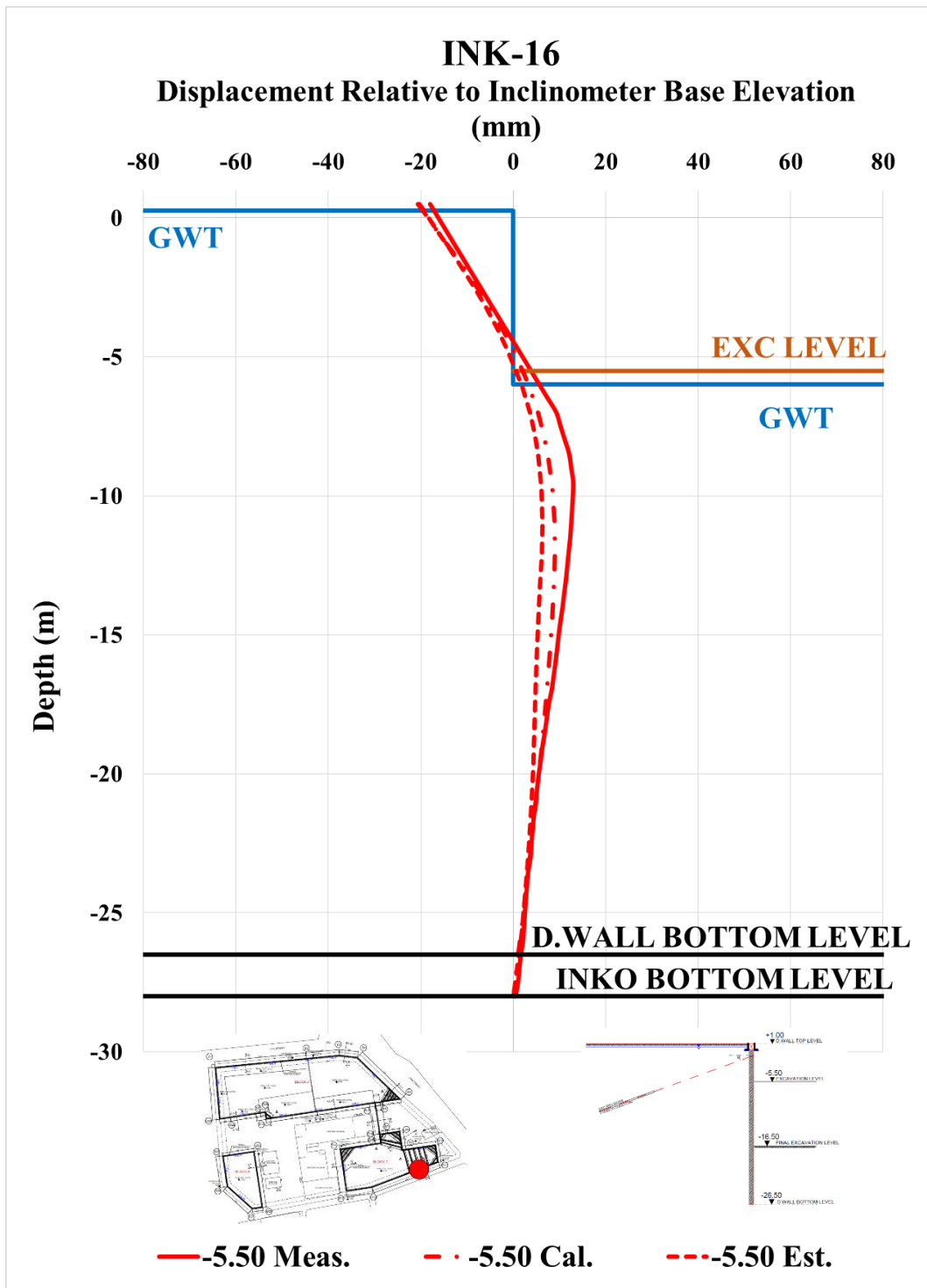
Figure A. 295. Calibrated and Measured Displ. Rel. to Inc. Base Elev. at -5.50 m
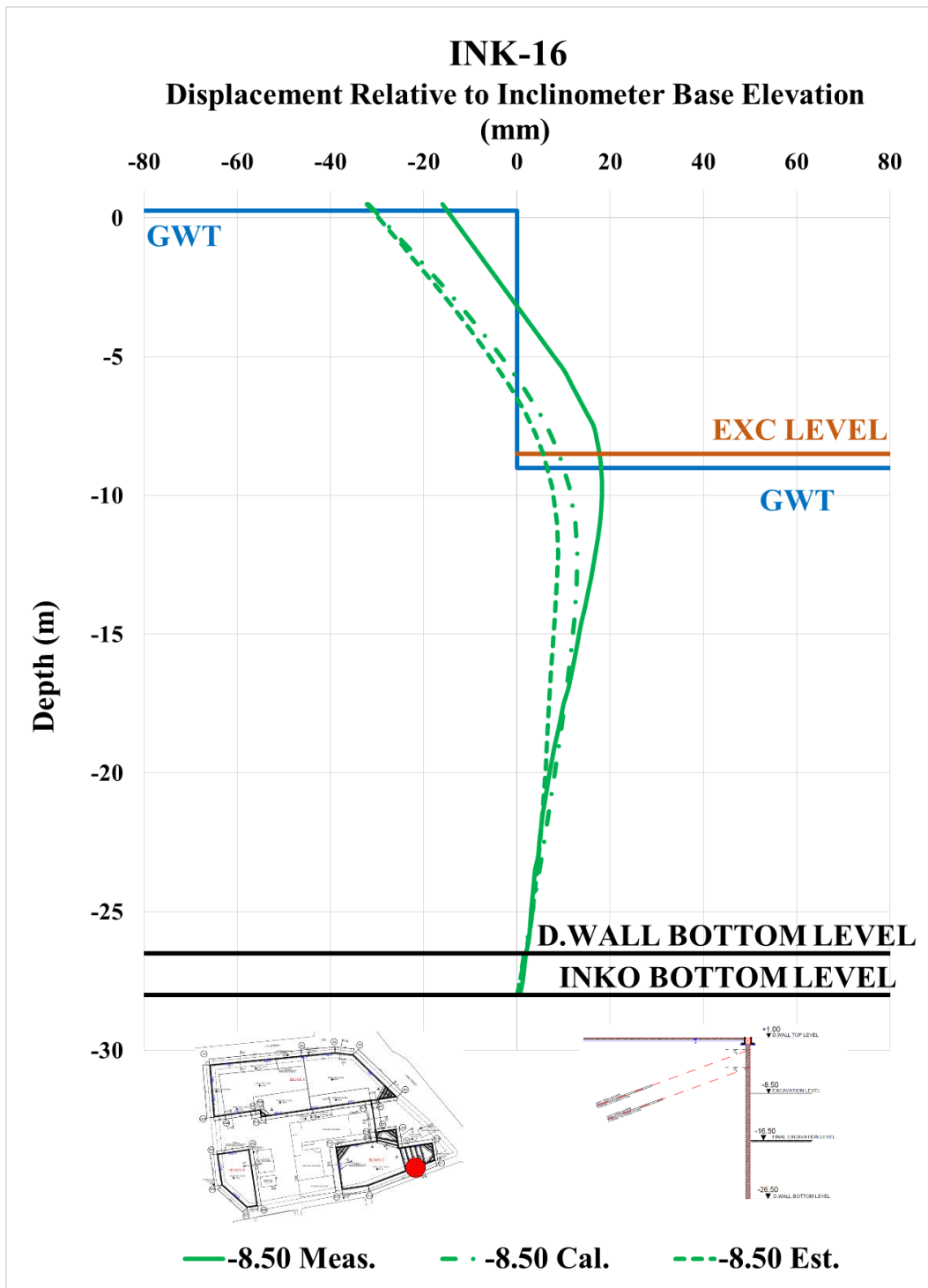
Figure A. 296. Calibrated and Measured Displ. Rel. to Inc. Base Elev. at -8.50 m
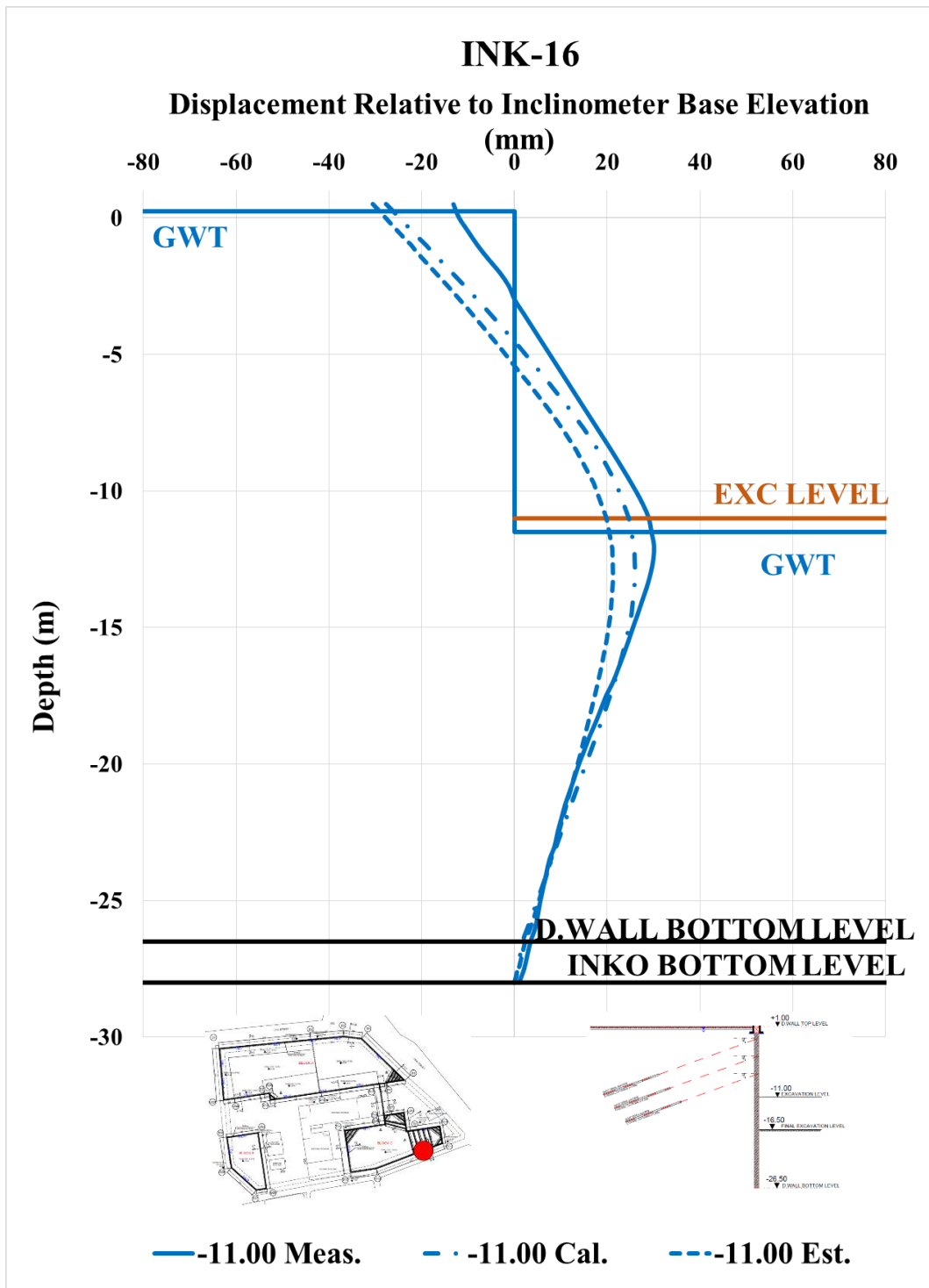
Figure A. 297. Calibrated and Measured Displ. Rel. to Inc. Base Elev. at -11.00 m
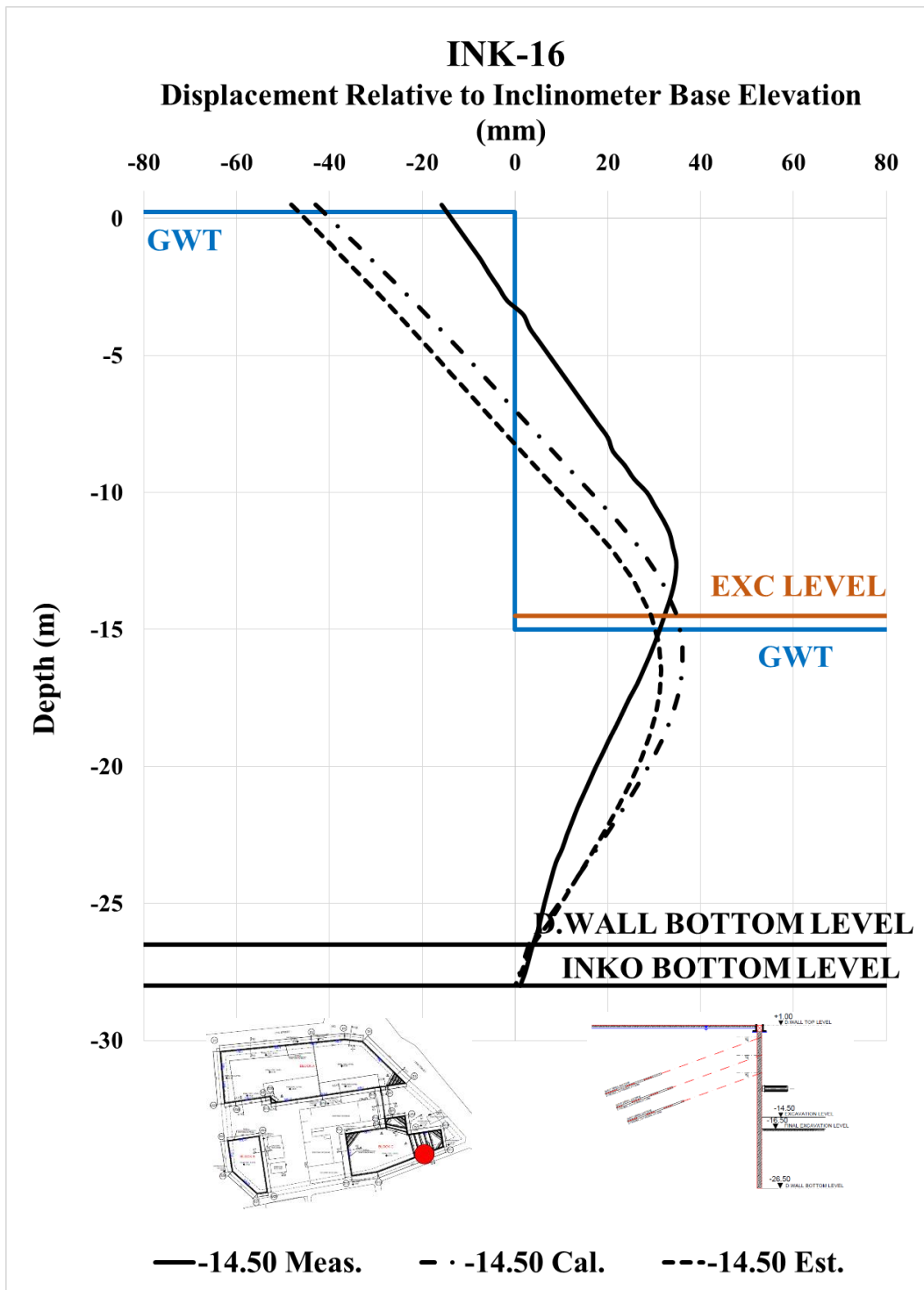
Figure A. 298. Calibrated and Measured Displ. Rel. to Inc. Base Elev. at -14.50 m
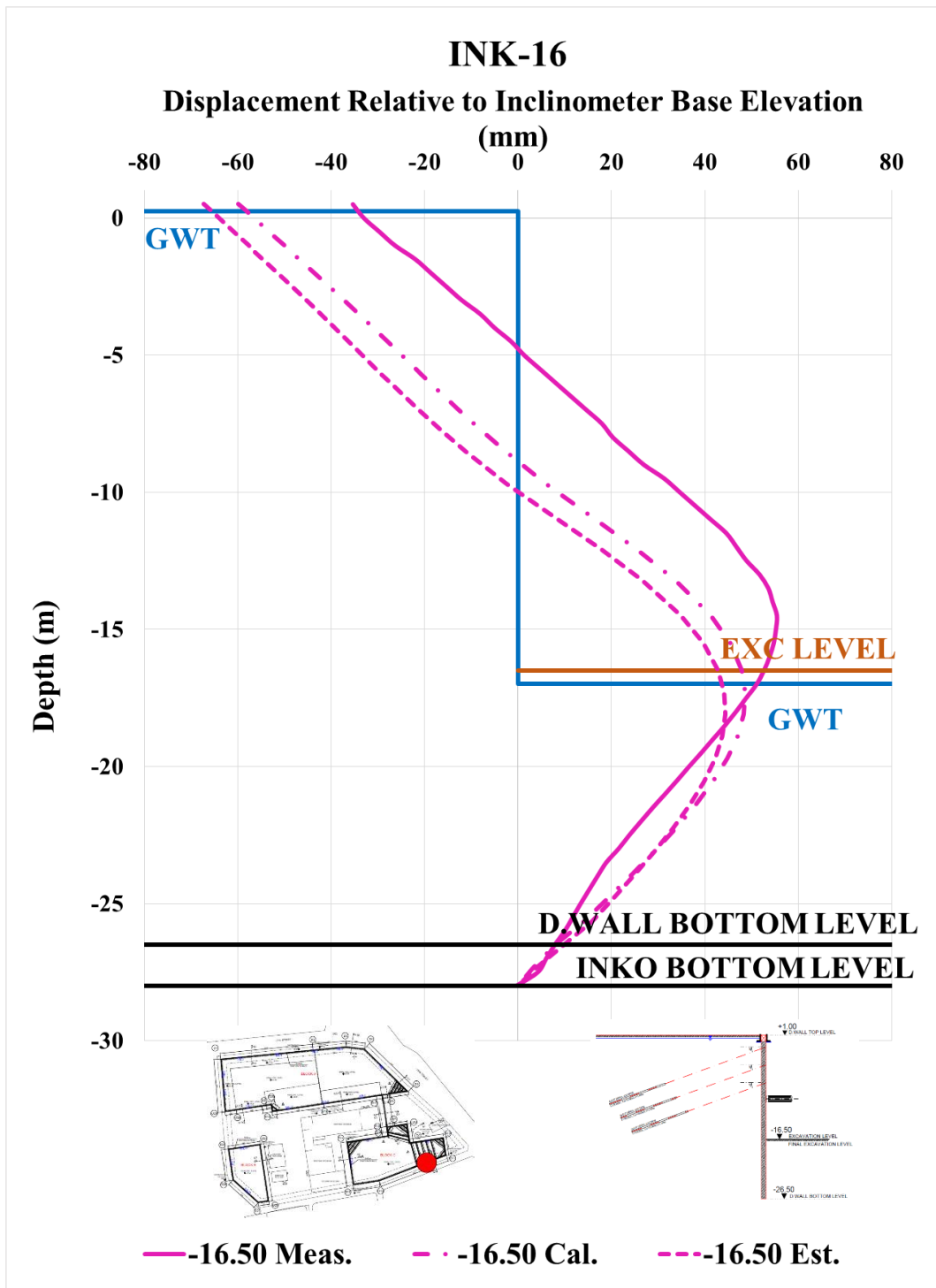
Figure A. 299. Calibrated and Measured Displ. Rel. to Inc. Base Elev. at -16.50 m

Table A. 64. Internal Forces of Diaphragm Wall

INK - 16 / Section 6A-6A						
Excvation Stage	1	2	3	4	5	6
Excavation Level (m)	-2.50	-5.50	-8.50	-11.00	-14.50	-16.50
N_{max} (kN/m)	99.10	216.00	373.50	559.40	636.00	695.70
V_{max} (kN/m)	43.10	409.60	409.60	409.60	731.50	1063.00
M_{max} (kN.m/m)	94.94	767.20	1025.00	1213.00	1635.00	2294.00

Legend	Excvation Stage	1. Anchor Level	2. Excavation Level	2. Anchor Level	3. Excavation Level	3. Anchor Level	4. Excavation Level	5. Excavation Level	Final Excavation Level
	Estimated Load of 1. Anchor Row (kN)	650.00	673.00	547.46	564.83	523.72	528.26	471.14	414.14
	Estimated Load of 2. Anchor Row (kN)	-	-	650.00	686.32	598.76	622.23	550.40	481.05
	Estimated Load of 3. Anchor Row (kN)	-	-	-	-	650.00	703.63	627.35	557.54
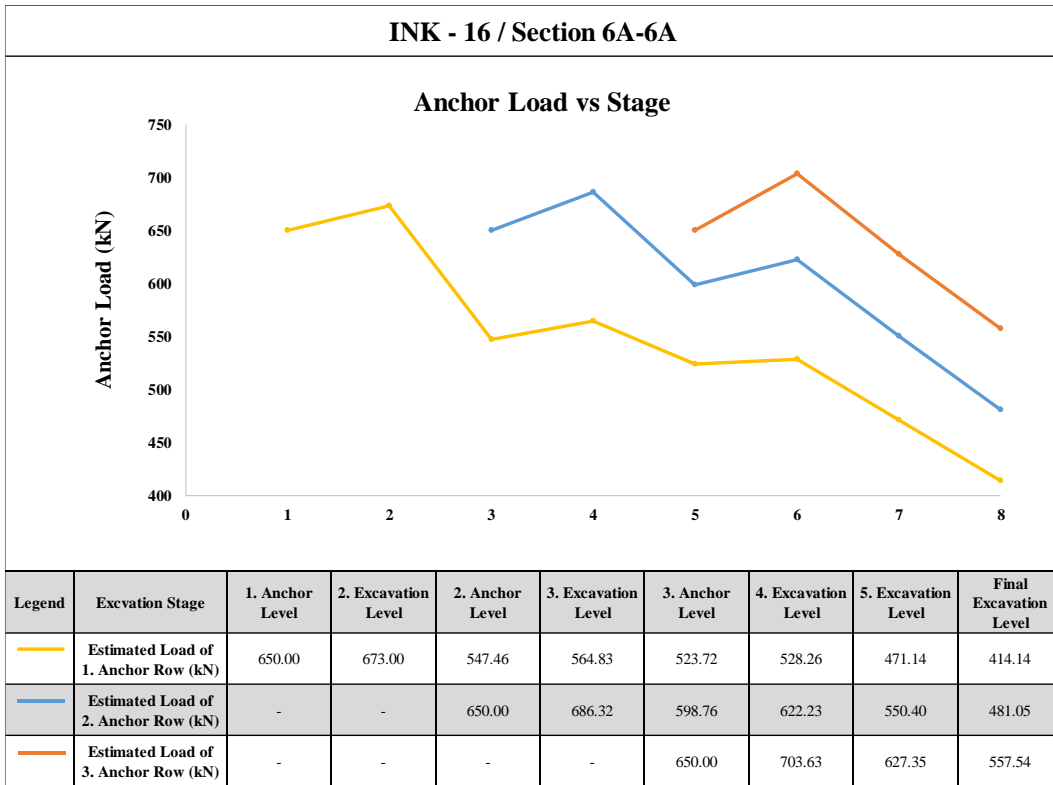
Figure A. 300. Estimated Anchor Loads

442

Table A. 65. Summary of Displacement Results of INK-16

INK - 16 / SECTION 6A - 6A

Excvation Level (m)	Excvation Depth (m)	u_{meas} (mm) Inclinometer Measurements	u_{est} (mm) Estimation with Plaxis 2D Analysis	u_{cal} (mm) Calibration with Plaxis 2D Analysis	$u_{literature}$ (mm) FHWA-IF-99-015 (1999) - Maksimum	$u_{literature}$ (mm) FHWA-IF-99-015 (1999) - Average	$u_{literature}$ (mm) Goldberg et al. (1976)	$u_{literature}$ (mm) Clough et al. (1990) - Maksimum	$u_{literature}$ (mm) Clough et al. (1990) - Average	$u_{literature}$ (mm) Long (2001)	$u_{literature}$ (mm) Long (2001) (Extraordinary cases eliminated)	$u_{literature}$ (mm) Long (2001) Cantilever System
-2.50	3.50	14.09	9.62	11.80	17.50	7.00	17.50	17.50	7.00	6.65	4.90	12.6
-5.50	6.50	12.96	6.27	8.92	32.50	13.00	32.50	32.50	13.00	12.35	9.10	-
-8.50	9.50	18.22	8.83	12.87	47.50	19.00	47.50	47.50	19.00	18.05	13.30	-
-11.50	12.50	30.09	21.31	26.08	62.50	25.00	62.50	62.50	25.00	23.75	17.50	-
-14.50	15.50	34.71	31.45	36.08	77.50	31.00	77.50	77.50	31.00	29.45	21.70	-
-16.50	17.50	55.43	44.42	48.64	87.50	35.00	87.50	87.50	35.00	33.25	24.50	-

443
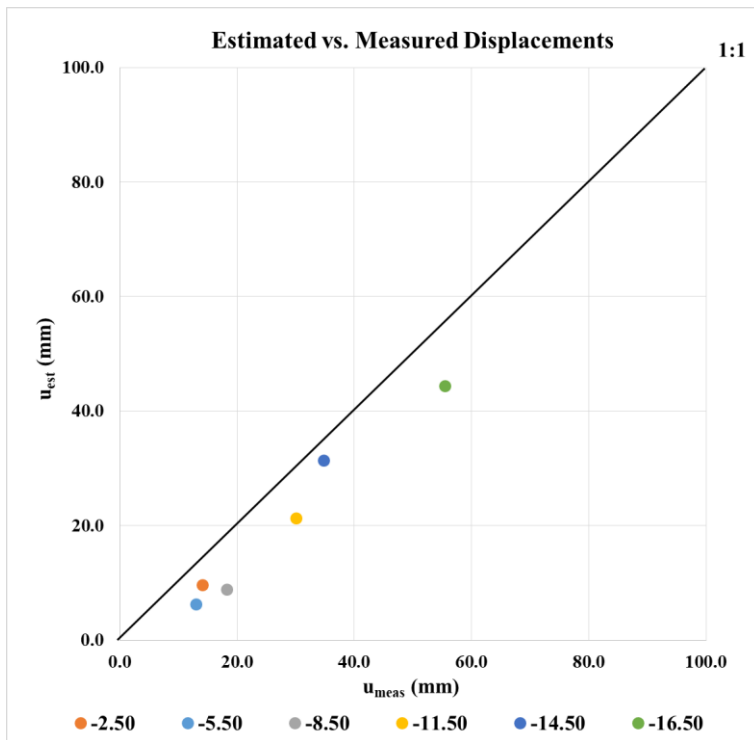
Figure A. 301. Estimated and Measured Displacements of INK - 16
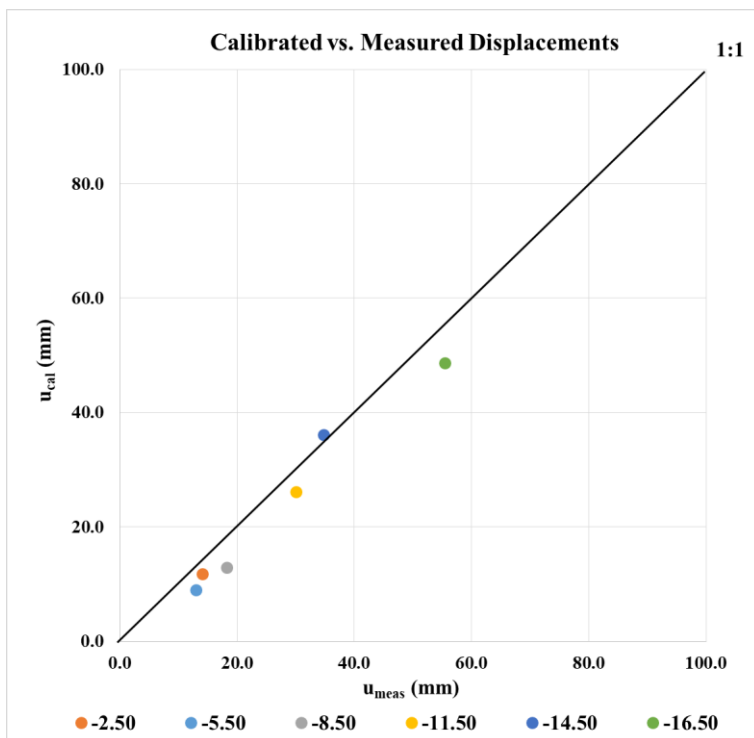
Figure A. 302. Calibrated and Measured Displacements of INK - 16

INK-17 – Calibrated, Estimated and Measured Displacements
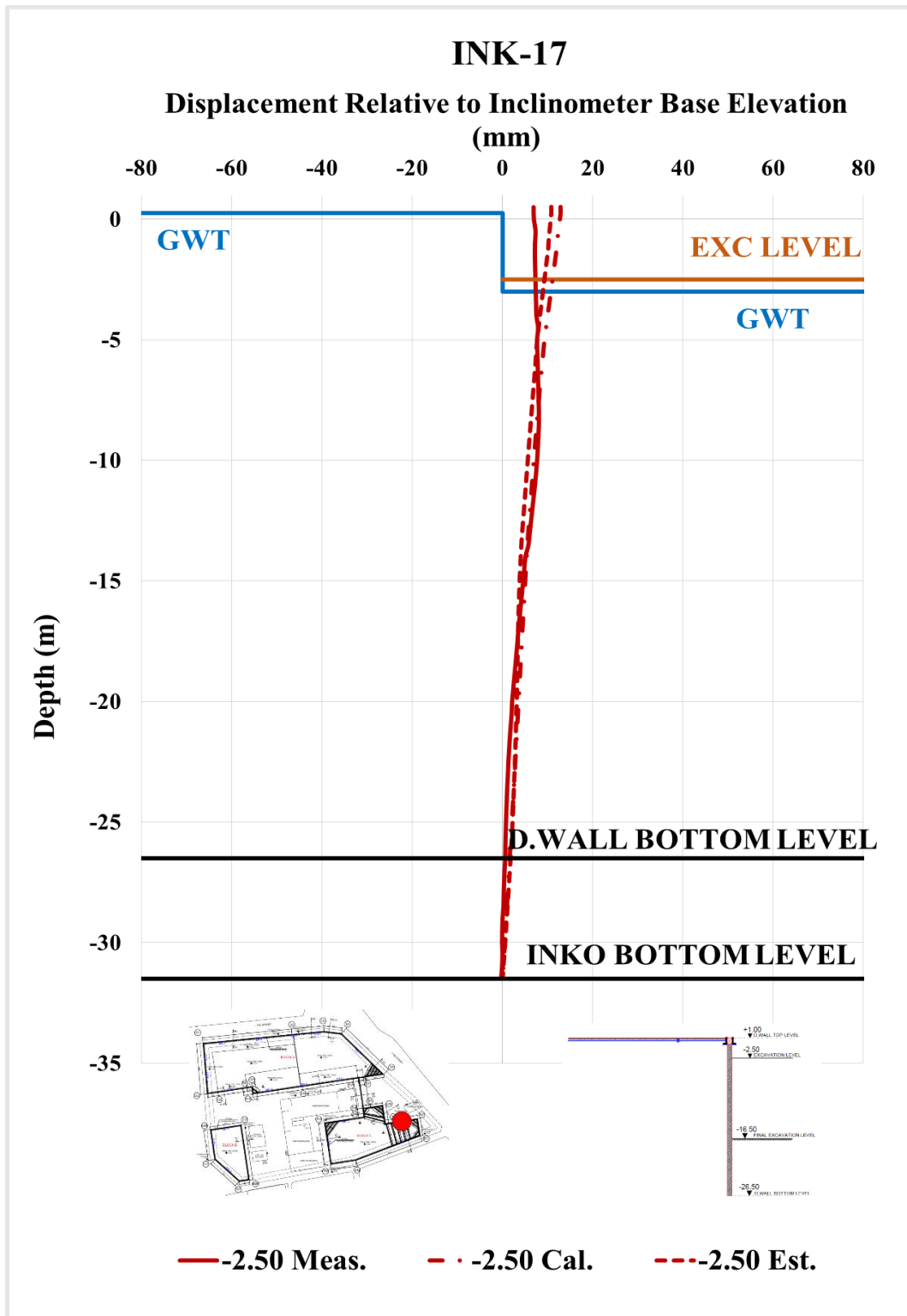
Figure A. 303. Calibrated and Measured Displ. Rel. to Inc. Base Elev. at -2.50 m
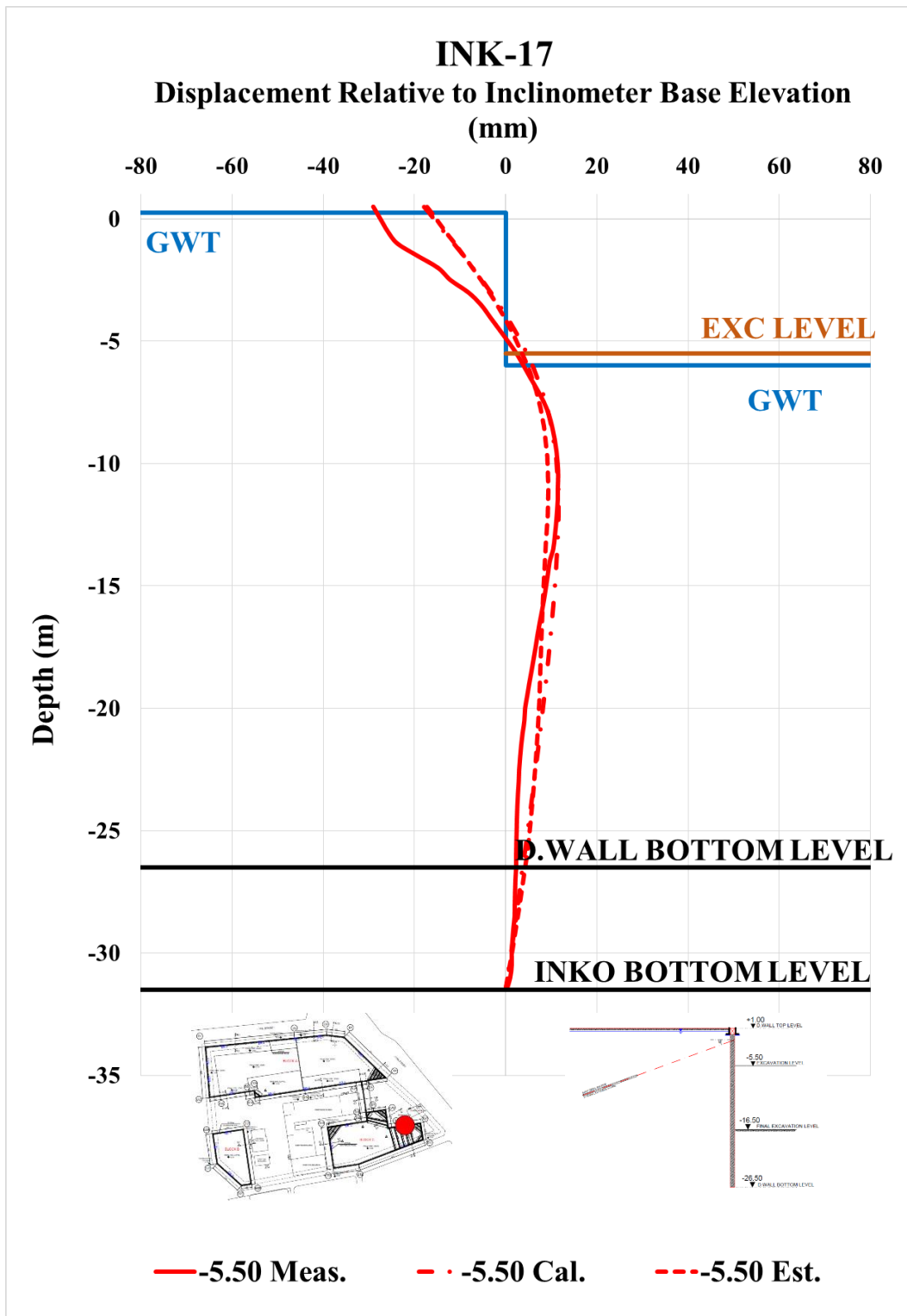
Figure A. 304. Calibrated and Measured Displ. Rel. to Inc. Base Elev. at -5.50 m
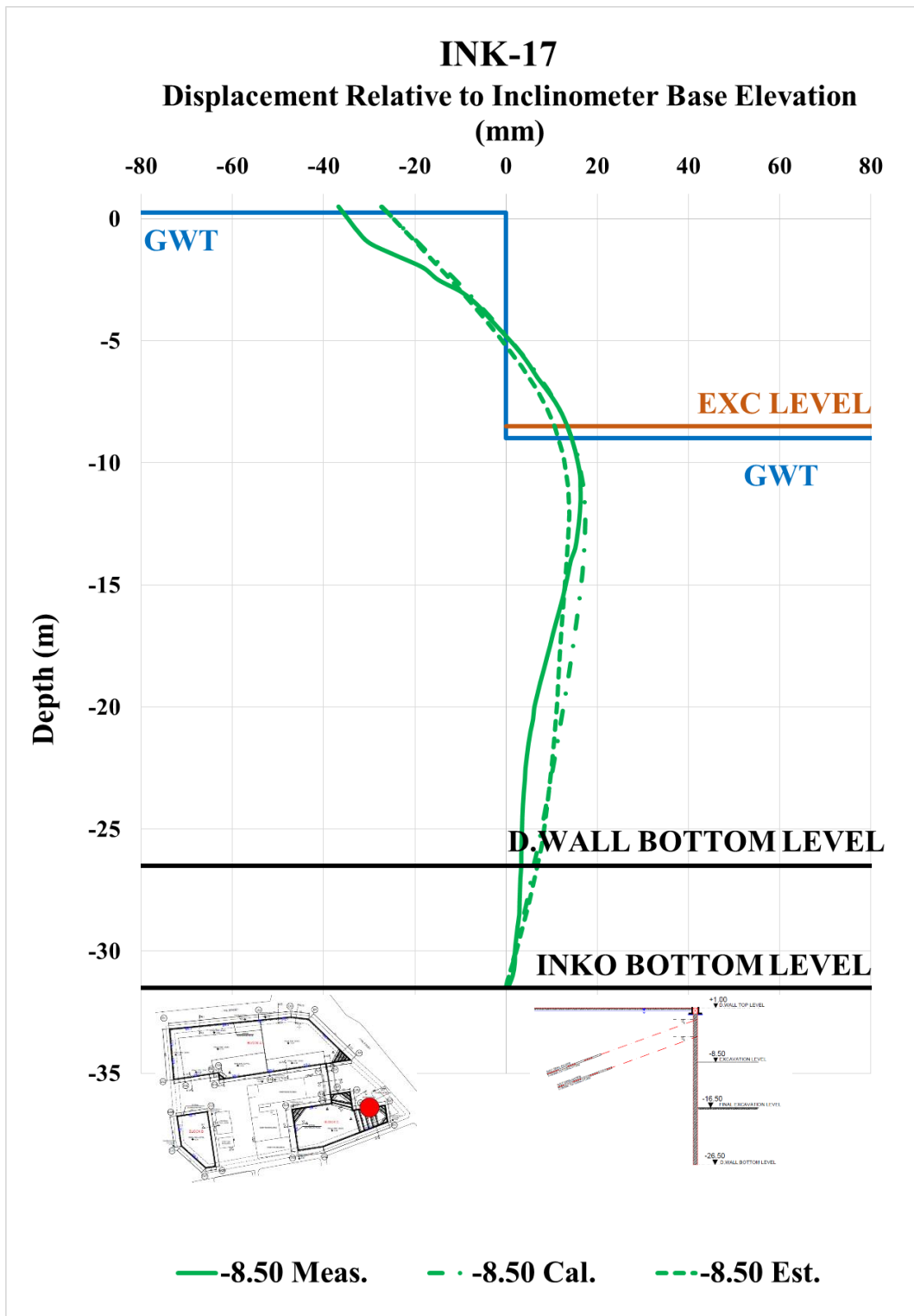
Figure A. 305. Calibrated and Measured Displ. Rel. to Inc. Base Elev. at -8.50 m
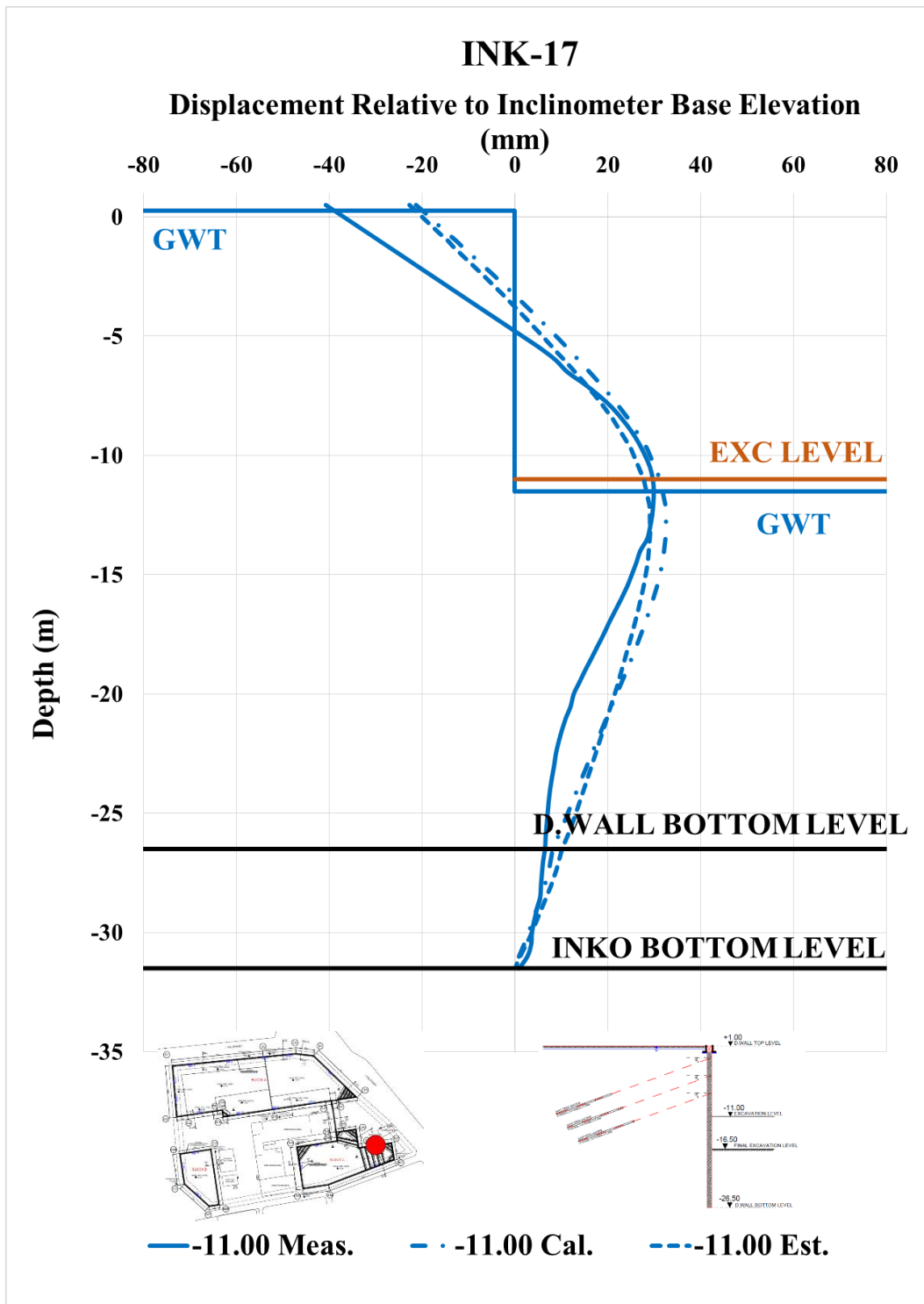
Figure A. 306. Calibrated and Measured Displ. Rel. to Inc. Base Elev. at -11.00 m
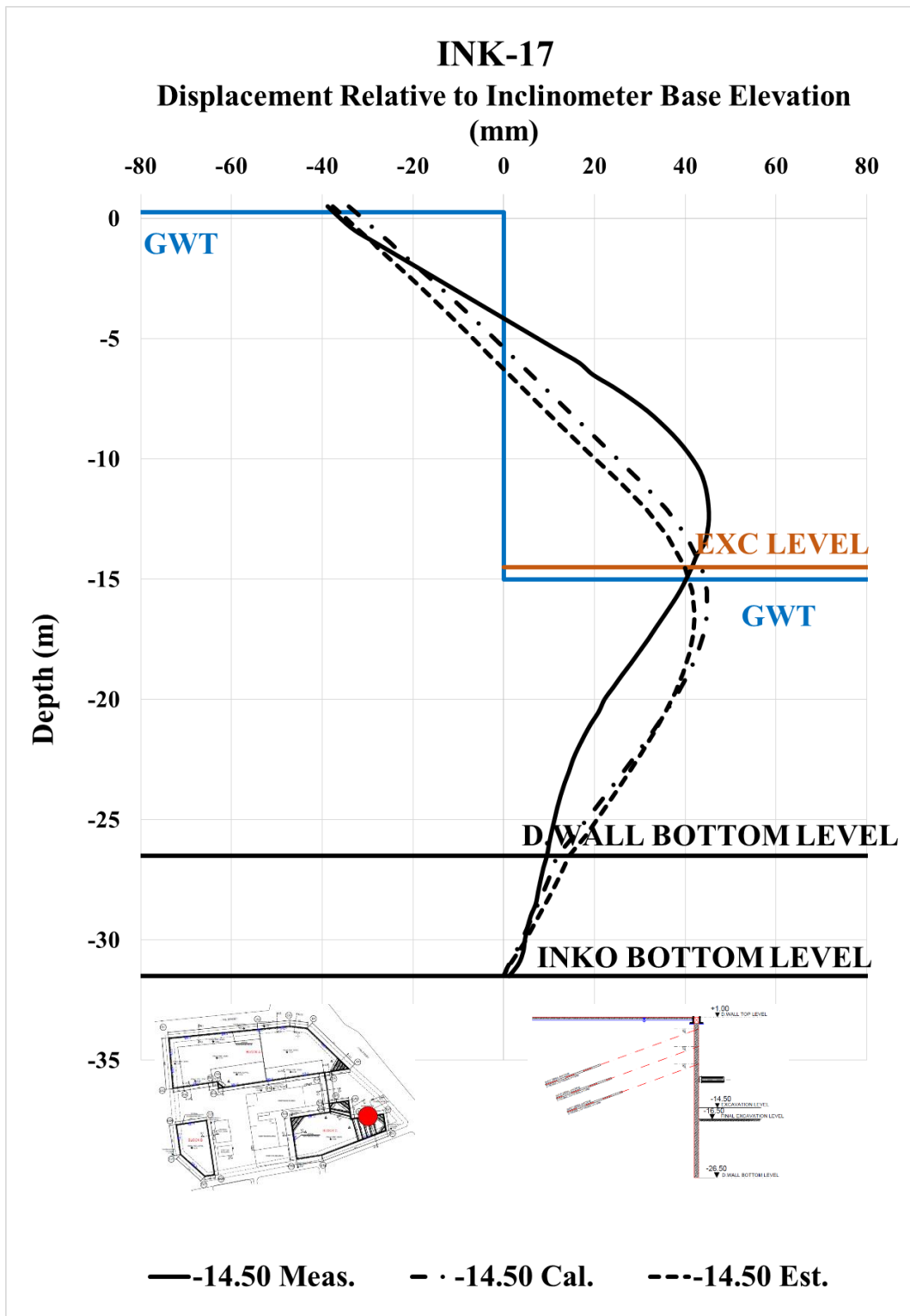
Figure A. 307. Calibrated and Measured Displ. Rel. to Inc. Base Elev. at -14.50 m
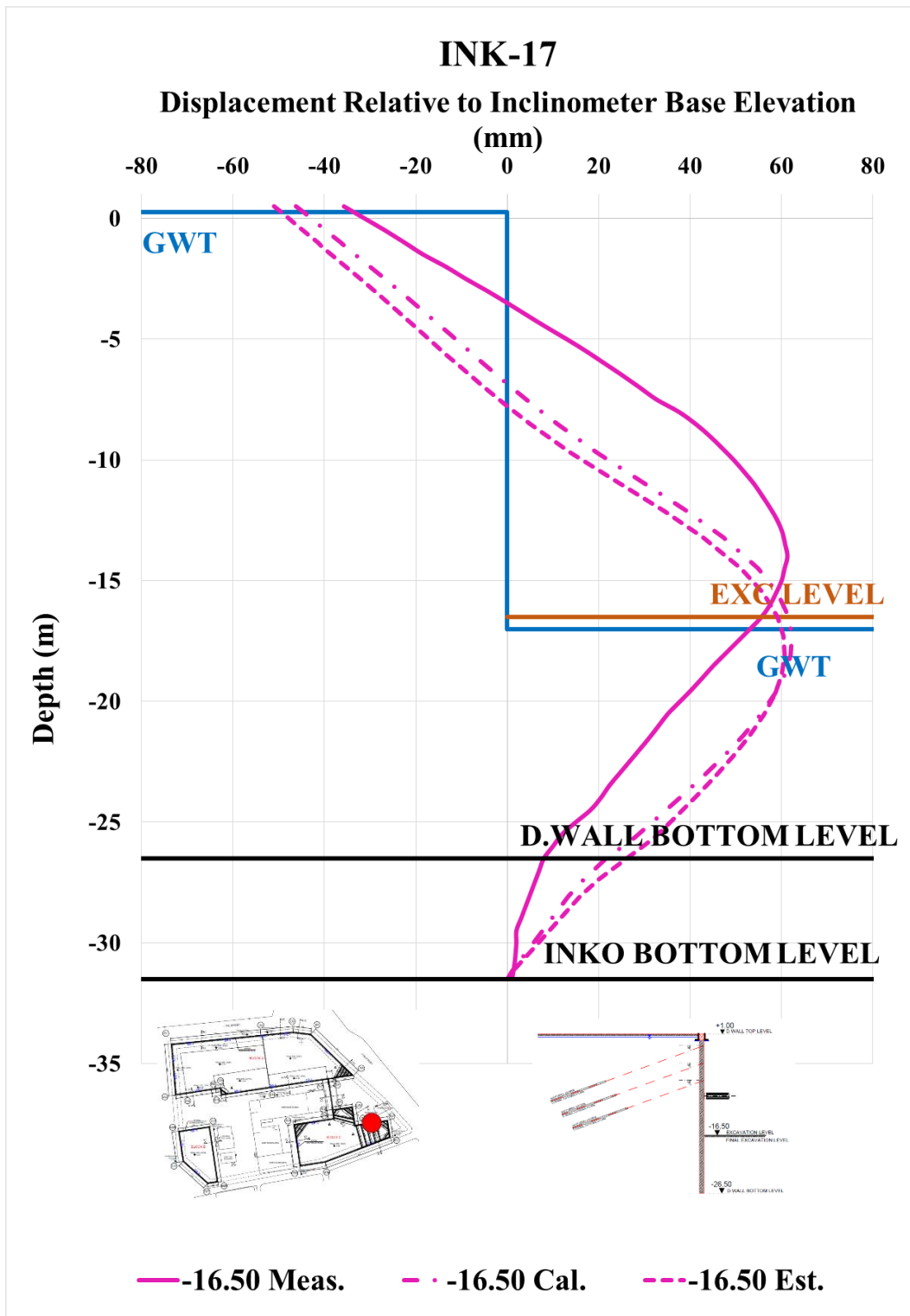
Figure A. 308. Calibrated and Measured Displ. Rel. to Inc. Base Elev. at -16.50 m

Table A. 66. Internal Forces of Diaphragm Wall

INK - 17 / Section 6A-6A						
Excvation Stage	1	2	3	4	5	6
Excavation Level (m)	-2.50	-5.50	-8.50	-11.00	-14.50	-16.50
N_{max} (kN/m)	99.10	216.00	373.50	559.40	636.00	695.70
V_{max} (kN/m)	43.10	409.60	409.60	409.60	731.50	1063.00
M_{max} (kN.m/m)	94.94	767.20	1025.00	1213.00	1635.00	2294.00

Legend	Excvation Stage	1. Anchor Level	2. Excavation Level	2. Anchor Level	3. Excavation Level	3. Anchor Level	4. Excavation Level	5. Excavation Level	Final Excavation Level
	Estimated Load of 1. Anchor Row (kN)	650.00	673.00	547.46	564.83	523.72	528.26	471.14	414.14
	Estimated Load of 2. Anchor Row (kN)	-	-	650.00	686.32	598.76	622.23	550.40	481.05
	Estimated Load of 3. Anchor Row (kN)	-	-	-	-	650.00	703.63	627.35	557.54

Figure A. 309. Estimated Anchor Loads

Table A. 67. Summary of Displacement Results of INK-17

INK - 17 / SECTION 6A - 6A

Excavation Level (m)	Excavation Depth (m)	u_meas (mm) Inclinometer Measurements	u_est (mm) Estimation with Plaxis 2D Analysis	u_cal (mm) Calibration with Plaxis 2D Analysis	u_literature (mm) FHWA-IF-99-015 (1999) - Maksimum	u_literature (mm) FHWA-IF-99-015 (1999) - Average	u_literature (mm) Goldberg et al. (1976)	u_literature (mm) Clough et al. (1990) - Maksimum	u_literature (mm) Clough et al. (1990) - Average	u_literature (mm) Long (2001)	u_literature (mm) Long (2001) (Extraordinary cases eliminated)	u_literature (mm) Long (2001) Cantilever System
-2.50	**3.50**	8.10	10.86	12.89	17.50	7.00	17.50	17.50	7.00	6.65	4.90	12.6
-5.50	**6.50**	11.51	9.33	11.59	32.50	13.00	32.50	32.50	13.00	12.35	9.10	-
-8.50	**9.50**	14.82	13.94	17.36	47.50	19.00	47.50	47.50	19.00	18.05	13.30	-
-11.50	**12.50**	29.90	29.09	32.52	62.50	25.00	62.50	62.50	25.00	23.75	17.50	-
-14.50	**15.50**	41.09	42.09	44.84	77.50	31.00	77.50	77.50	31.00	29.45	21.70	-
-16.50	**17.50**	61.30	60.72	62.25	87.50	35.00	87.50	87.50	35.00	33.25	24.50	-

452
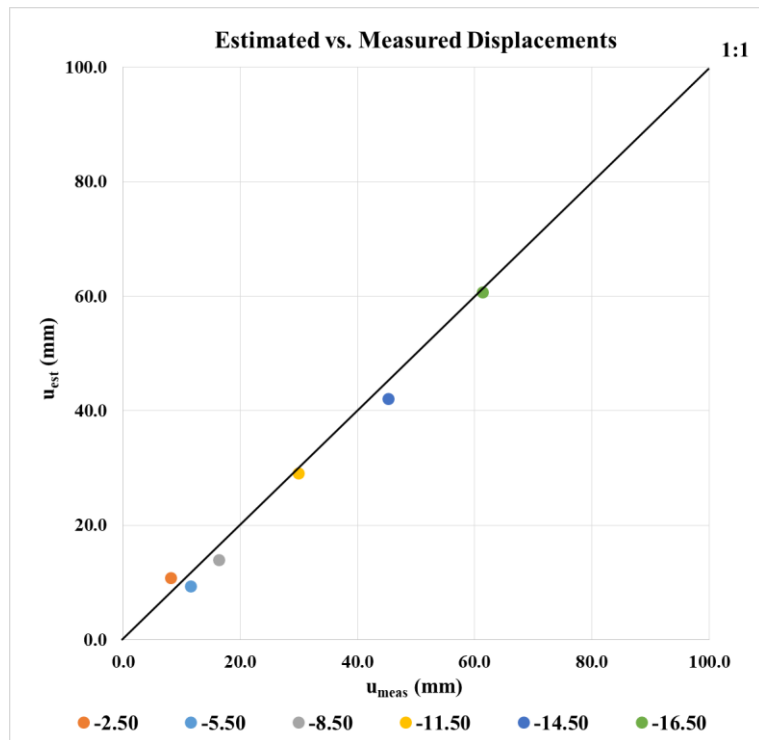
Figure A. 310. Estimated and Measured Displacements of INK – 17
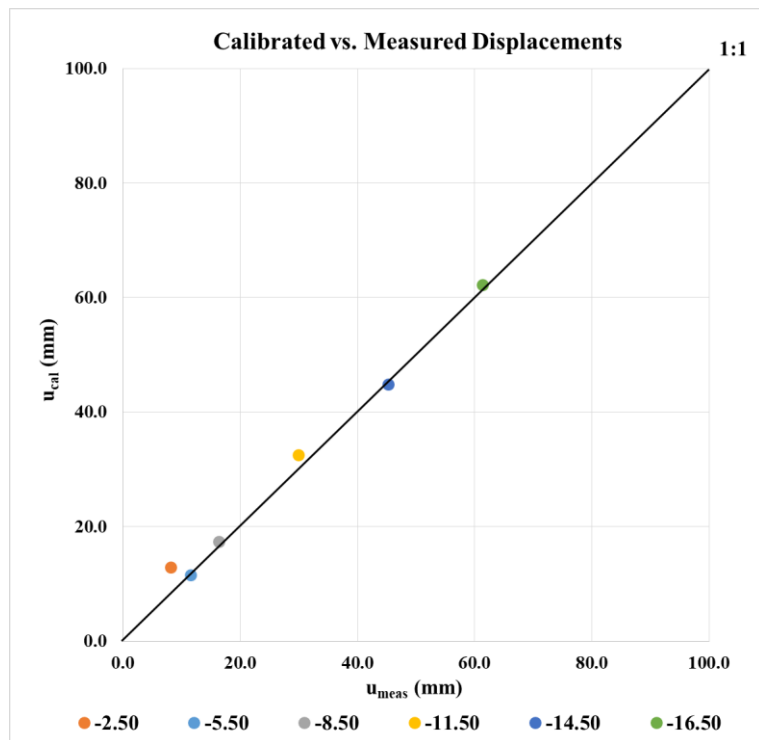
Figure A. 311. Calibrated and Measured Displacements of INK - 17